Markus Stoffel
Michelle Bollschweiler
David R. Butler
Brian H. Luckman
Editors

ADVANCES IN GLOBAL CHANGE RESEARCH 41

Tree Rings and Natural Hazards

A State-of-the-Art

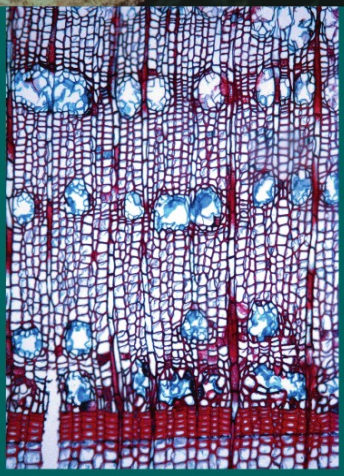

Springer

Advances in Global Change Research

ADVANCES IN GLOBAL CHANGE RESEARCH

VOLUME 41

For other titles published in this series, go to
www.springer.com/series/5588

Markus Stoffel · Michelle Bollschweiler
David R. Butler · Brian H. Luckman
Editors

Tree Rings and Natural Hazards

A State-of-the-Art

Springer

Editors
Markus Stoffel
Laboratory of Dendrogeomorphology
Institute of Geological Sciences
University of Bern
3012 Bern
Switzerland
and
Chair for Climatic Change
and Climate Impacts
Institute for Environmental Sciences
University of Geneva
1227 Carouge-Geneva
Switzerland
markus.stoffel@dendrolab.ch

Michelle Bollschweiler
Laboratory of Dendrogeomorphology
Institute of Geological Sciences
University of Bern
3012 Bern
Switzerland
and
Chair for Climatic Change
and Climate Impacts
Institute for Environmental Sciences
University of Geneva
1227 Carouge-Geneva
Switzerland
michelle.bollschweiler@dendrolab.ch

David R. Butler
Department of Geography
Texas State University
San Marcos, TX 78666-4616
USA
db25@txstate.edu

Brian H. Luckman
Department of Geography
University of Western Ontario
London ON N6A 5C2
Canada
luckman@uwo.ca

ISBN 978-90-481-8735-5 e-ISBN 978-90-481-8736-2
DOI 10.1007/978-90-481-8736-2
Springer Dordrecht Heidelberg London New York

Library of Congress Control Number: 2010926582

Cover illustration: Front cover (top to bottom): New leaders formed in tilted sub-alpine fir after snow avalanche impact (© BH Luckman); European larch destroyed by rockfall (© DM Schneuwly); Cross-section of a freshly cut European larch stem with multiple injuries (© M Stoffel); microsection of a European larch tree-ring with tangential rows of traumatic resin ducts (© M Bollschweiler). Back cover: European larch tilted by snow pressure (© M Bollschweiler).

Printed on acid-free paper

Springer is part of Springer Science+Business Media (www.springer.com)

To our families for their understanding and support during our absences over many field seasons

Foreword

Dendrogeomorphology Beginnings and Futures: A Personal Reminiscence

My early forays into **dendrogeomorphology** occurred long before I even knew what that word meant. I was working as a young geoscientist in the 1960s and early 1970s on a problem with slope movements and deformed vegetation. At the same time, unknown to me, Jouko Alestalo in Finland was doing something similar. Both of us had seen that trees which produced annual growth rings were reacting to geomorphic processes resulting in changes in their internal and external growth patterns. Dendroclimatology was an already well established field, but the reactions of trees to other environmental processes were far less well understood in the 1960s. It was Alestalo (1971) who first used the term, *dendrogeomorphology.* In the early 1970s, I could see that active slope-movement processes were affecting the growth of trees in diverse ways at certain localities. I wanted to learn more about those processes and try to extract a long-term chronology of movement from the highly diverse ring patterns.

As a graduate student in Utah I was encouraged to gain expertise in disciplines outside geology and geography with which I was comfortable. All non-biology majors in the botany course did term papers that combined some aspect of plants with their main disciplines. I wrote an original paper on plants as **geoindicators**, mainly because I had discovered in my readings that some endemic species only occur in soils developed from certain lithologies. That choice of botanical **geoindicators** as a term-paper eventually opened doors I had never dreamed of and exposed me to a diverse literature that I would normally never have read. In this research I discovered a few early papers on various surficial processes that had been studied in some fashion through use of plants. A decade later, when studying ice- and water-driven slope failures on mountain slopes in Utah, I found a slope covered with distorted trees and remembered that term paper. Then, upon trying to cut down one of the inclined trees, my small camp saw stuck irretrievably in its dense reaction wood. This annoying event wonderfully focused my mind upon the solution to two problems; how to extract my saw and how to find out what had happened to distort those trees into curved trunks, even into corkscrew spirals. We later discovered that

the geotrophic growth response in these trees curved them ever upward as they were slowly rotating as they simultaneously tipped over and were carried downslope. I needed some way to assess these processes quantitatively.

Searching the literature anew, I discovered the work of the Tree-Ring Laboratory at the University of Arizona. Discussion of my samples with Val Lamarche, Wes Ferguson and Hal Fritts convinced me that it should be possible to obtain a chronology of slope movements from my tree-ring data, although it certainly could not simply be by using simple ring-width measurements. These scientists impressed upon me the complexity of extraneous factors that can affect tree growth, and the need to identify and differentiate the desired 'signal' from the profuse 'noise'. Fritts' (1976) five basic concepts of dendrochronology became my mantra, especially the fact that robust replication was essential. Ferguson, LaMarche, and Fritts sent me home to renew my efforts on better understanding how the trees reacted to the disturbance of the soil in which they were rooted. Little by little, after examining many cores and cross sections, I saw a way to extract the particular signal I was interested in from the enormous clutter of other irrelevant tree-ring data. The event-response methodology (Shroder 1978, 1980; Giardino et al. 1984) of tree-ring dating and geomorphology emerged from this work.

In Tucson I had met Gordon Jacoby when he was working on detecting past seismicity from tree-rings and he later invited me to give a keynote presentation on dendrogeomorphology at the International Tree-Ring Conference in Tarrytown in 1986. At the same time, when he was my student, David Butler and I (Fig. 1) had frequently discussed the problems with missing and interannular ('false') rings that gave dubious chronologies to the uninitiated. I was especially concerned with published work that took unreplicated ring counts as gospel and uncritically accepted chronologies with little thought as to whether or not the ring count was correct. I had encountered this problem in New Zealand with Val LaMarche in 1974 where I tried unsuccessfully to extract the timing of debris-flow events from roots of the Southern Hemisphere silver beech (*Nothofagus menziesii*). Back in Nebraska my students and I encountered similar lack of replication in dating the roots of Ponderosa pine (*Pinus ponderosa*) in gullies in the Nebraska panhandle. Clearly more work was required. Apparently the conversion of rootwood to stemwood and development of a new callus margin over corrosion scars as roots are exposed was not straightforward. Perhaps some species reacted in predictable fashions and on an annual basis, and others did not. Interannular rings or missing rings in disturbed roots remain a significant problem that continues to need attention. Great care and rigorous replication were indicated then and are still just as important. With those experiences in mind, David Butler and I wrote the paper for Jacoby's conference (Shroder and Butler 1987).

Off and on over the next two decades I periodically revived my interest, read the newest literature, got out my increment borers, and taught my students a few old and new tricks of the trade. Avalanche-stricken trees and landslides in the La Sal Mountains of Utah (Shroder and Sewell 1985), landslides on the Pierre Shale of north-central Nebraska, conifer germination on the landforms of the Himalaya (Shroder and Bishop 1995), trees falling on railroad rights of way, terracette development in the Loess Hills of Iowa; all were fair game and chronologies were developed.

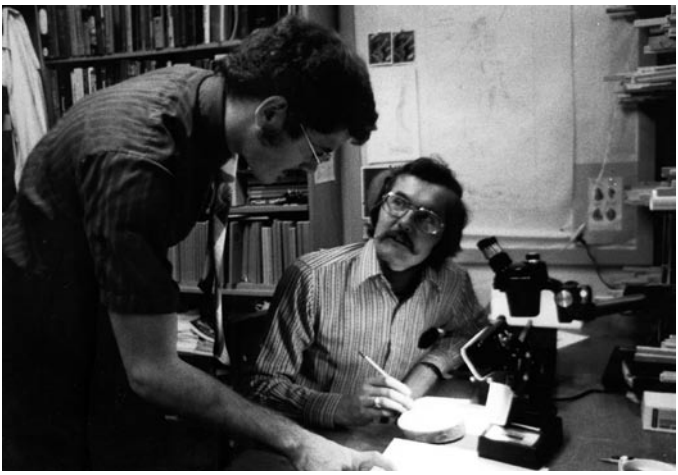

Fig. 1 Jack Shroder (seated) at the University of Nebraska at Omaha in the middle 1970s explaining some of the principles of dendrogeomorphology to David Butler while he was a student. The cross-cut tree-trunk section that Shroder is pointing to was sampled from a tree knocked flat by rapid-wet debris-flow that occurred some decades previously in the High Plateaus of Utah. Such cross sections were easy to use to explain basic principles to new students, but the preferred method of data collection was from the many multiple cores stacked on the shelves to the right, mainly because fewer trees were killed in the process of data collection

It is gratifying over these past years to see the field develop so robustly, especially when I remember sterile arguments as to whether dendrogeomorphology should ever be included in geography or geology! I considered such stultifying disciplinary debates irrelevant – all that mattered was that the science was solid and the dendrogeomorphic investigations were productive. In recent decades tree-ring laboratories have sprung up in universities across the world, the methods of dendrochronology and dendrogeomorphology have continued to be refined and real progress is being made on the use of tree-ring dating to study various environmental problems. A glance at the internet or Henri Grissino-Mayer's "Ultimate Tree-Ring Pages" certainly shows abundant new publications and on-going projects. I must admit that I am proud to have had a small part in the beginnings of this tree-ring endeavor and was humbled to be offered the opportunity to reflect upon that fact.

The science of dendrogeomorphology has come a long way in the past half century, and as long as sufficient care is used in the future assembly of tree-ring based chronologies of surficial processes and natural hazards, the methodology should continue to be a useful procedure in our geo-toolkits. Nonetheless, strong attention to the principles of Fritts (1976), especially cross dating and replication, are as germane now as they were decades ago. This new volume on **Tree Rings and Natural Hazards** contributes essential studies to ongoing hazard problems that continue to plague so many people worldwide. The history and periodicities of natural processes are critical, necessary data to reduce and evaluate future hazard.

In the absence of documentary records, relevant periodicities are best established from tree rings and this book presents studies of some of those periodicities and possibilities. This assembly of a critical collection of classic and ongoing tree-ring studies offers a wide range of examples of the study of natural hazards and possible applications to solutions to the management of those hazards.

Omaha, NE John (Jack) F. Shroder, Jr.

References

Alestalo J (1971) Dendrochronological interpretation of geomorphic processes. Fennia 105:1–140

Fritts HC (1976) Tree-rings and climate. Academic, London

Giardino JR, Shroder JF Jr, Lawson MP (1984) Tree-ring analysis of movement of a rock-glacier complex on Mount Mestas, Colorado, USA. Arct Alp Res 16(3):299–309

Shroder JF Jr (1978) Dendrogeomorphologic analysis of mass movement on Table Cliffs Plateau, Utah. Quat Res 9:168–185

Shroder JF Jr (1980) Dendrogeomorphology; review and new techniques of tree-ring dating and geomorphology. Prog Phys Geogr 4(2):161–188

Shroder JF Jr, Sewell RE Jr (1985) Mass movement in the La Sal Mountains, Utah. Utah Geol Mineral Surv Spec Stud p 63

Shroder JF Jr, DR Butler (1987) Tree-ring analysis in the earth sciences. In: Jacoby GC, Hornbeck JW, Dougherty L (eds) Proceedings of the International Symposium on Ecological Aspects of Tree-Ring Analysis. Geological Observatory & US Department of Agriculture, pp 186–212

Shroder JF Jr, Bishop MP (1995) Geobotanical assessment in the Great Plains, Rocky Mountains and Himalaya. In: Hupp CR, Osterkamp WR, Howard AD (eds) Geomorphology, special issue on biogeomorphology – terrestrial and freshwater systems, 26th Binghamton Symposium in Geomorphology 13:101–119

Contents

Part I
Tree Rings and Natural Hazards – An Introduction

European larch (*Larix decidua*) destroyed by rockfall (© D. M. Schneuwly)

Tree Rings and Natural Hazards: An Introduction

Markus Stoffel, Michelle Bollschweiler, David R. Butler, and Brian H. Luckman

1 Introduction

Each year, natural disasters claim thousands of lives and lead to economic losses of several billion US dollars worldwide. In 2008, natural disasters caused 240,500 fatalities and losses of more than US$250 billion (SwissRe 2009), making it one of the largest annual amounts ever recorded. More than 90% of people killed by catastrophic events in 2008 were during two tropical cyclones (Myanmar and Philippines) and the 7.9 moment-magnitude earthquake hitting China's Sichuan region in May 2008 (Rodriguez et al. 2009). In February 2009, severe bush fires destroyed several villages in Victoria (Australia), killing more than 90 people and leaving 700 houses in ashes (Shaban 2009).

The aim of this book is to demonstrate how tree-ring studies can further our understanding of the nature, magnitude and frequency of more frequent, smaller scale natural hazards. Although they have less spectacular impacts, floods, windstorms, volcanic eruptions, landslides, rockfall, debris flows and snow avalanches have contributed to more than 10% of hazard-related deaths over the twentieth century (e.g., Wisner et al. 2003; EMDAT 2009; Rodriguez et al. 2009). As small disasters are by

M. Stoffel (✉) and M. Bollschweiler
Laboratory of Dendrogeomorphology, Institute of Geological Sciences, University of Bern, CH-3012 Bern, Switzerland
and
Chair for Climatic Change and Climate Impacts, Institute for Environmental Sciences, University of Geneva, CH-1227 Carouge-Geneva, Switzerland
e-mail: markus.stoffel@dendrolab.ch

D.R. Butler
Department of Geography, Texas State University-San Marcos, San Marcos, TX 78666-4616 USA

B.H. Luckman
Department of Geography, University of Western Ontario, London, ON, N6A 5 C2, Canada

M. Stoffel et al. (eds.), *Tree Rings and Natural Hazards: A State-of-the-Art*, Advances in Global Change Research 41, DOI 10.1007/978-90-481-8736-2_1,

definition, more frequent than mega-events, we may be able to appreciate and examine their causes, frequency and magnitude, in both space and time (including the potential impacts of future climatic changes) and, thereby, develop a better understanding of these hazards and possibly mitigate future impacts.

A major key to the assessment of ongoing hazard is the documentation of the number and size of past events at a site. In many cases, because of the absence of documentary records, this information must be developed from natural archives or "silent witnesses" (Aulitzky 1992) that remain in the landscape after the event. In addition to the geomorphic or sedimentological evidence, key information is required on the dating and history of past events. The significant contribution of tree rings to these endeavors lies in their capacity to both preserve evidence of past events and to provide critical information on their dating with annual or sub-annual resolution. Therefore, in many climates, the tree-ring record may represent the most valuable and precise natural archive for the reconstruction and understanding of past events over the last several centuries. This book will illustrate how tree-ring analysis has been used to reconstruct natural hazards and provide information that may be used to understand potential future incidence of these events.

The book offers an overview of tree-ring based reconstructions of natural hazards that result from mass-movements, water, weather and fire. This introduction provides a brief background to hazard and disaster research and outlines the impact of these events on tree morphology, tree growth and wood anatomy. It clarifies the approaches used for the tree-ring reconstruction of past events and suggests standards and definitions. It also offers an overview of state-of-the-art principles of dendrogeomorphology and a short illustration of recent methodological developments.

2 Natural Hazards, Disasters and Risk: Some Definitions

The contributions in this edited book will deal with different types of natural hazards and the description of applications of tree rings to studies of past events. In addition, terms like risk, frequency, magnitude, recurrence intervals or return periods will be used by the authors and therefore deserve a short description here.

1. A **natural hazard** is a natural process or phenomenon that may result in the loss of life, injury or health impacts, property damage, livelihood, injury or health impacts, property damages, social and economic disruption, or environmental damage (UNISDR 2009, p. 9). Rodriguez et al. (2009) define five sub-groups of natural hazards: namely geophysical (i.e. earthquakes, volcanic activity, landslides, rockfall, avalanches and subsidence and other mass movements), hydrological (floods, flash floods), meteorological (tropical, extra-tropical, and local storms), climatological (extreme temperatures, drought, wildfires), and biological hazards (epidemics, insect infestation, animal stampede). This book focuses on the first three sub-groups and wildfires, but disregards biological hazards, extreme temperatures and drought.

2. A **natural disaster** represents a serious disruption of the functioning of a community or a society involving widespread human, material, economic or environmental losses and impacts. A natural disaster may be defined as a situation where the ability of a community or society to cope using its own resources is exceeded. Disasters normally result from a combination of an existing exposure to hazard, the presence of conditions of vulnerability and insufficient capacity or measures to reduce or cope with the potential negative consequences of an event (UNISDR 2009). Other definitions stipulate quantitative thresholds for a natural event to become a disaster. For the Centre for Research on the Epidemiology of Disasters (CRED; Rodriguez et al. 2009), at least one of the following criteria must be fulfilled: ten or more people reported killed; more than 100 people reported affected; declaration of a state of emergency or a call for international assistance.
3. The term **risk** describes the probability of an event and its negative consequences (UNISDR 2009). In contrast to popular usage, the emphasis of the word "risk" is not based on chance or probability in technical settings, but on the consequences, i.e. potential losses for a particular reason, location or time.

Natural hazard events can be characterized by their magnitude or intensity, their frequency, speed of onset, duration, and areal extent. The number of occurrences per unit time is often described as **frequency** or **temporal frequency**. The size or intensity of an event is defined as **magnitude**, allowing for a differentiation of larger from smaller incidences of the same process at the same site. Based on the analysis of frequencies and magnitudes, **return periods** – also known as **recurrence intervals** – can be derived. They represent an estimate of the average interval of time between events of a certain intensity or size. They are statistical measurements denoting the average number of occurrences relative to a period of time or number of observations (Wolman and Miller 1960).

3 Tree Rings and Natural Hazards

3.1 Basic Patterns of Tree Growth

Dendrochronology depends on the fact that trees growing in areas with strong seasonal climates can form distinct annual growth rings. In conifers (*gymnosperms*), reproductive cambium cells form large, thin-walled earlywood tracheids during the early stages of the growing season (Camarero et al. 1998; Rigling et al. 2002), which primarily serve the transport of nutrients and water. Later in the season, smaller and denser latewood tracheids are developed. These layers are darker in appearance due to thicker cell walls and serve to increase the stability of the tree. Tissue formation in broadleaved trees (also called *angiosperms* or flowering plants) is more complex and diverse than in gymnosperms. In addition to the tracheids found in gymnosperms, the dividing cambium of broadleaved trees also produces vessels. Figure 1 illustrates the appearance of tree rings in conifers (a, b) and broadleaved trees (c, d).

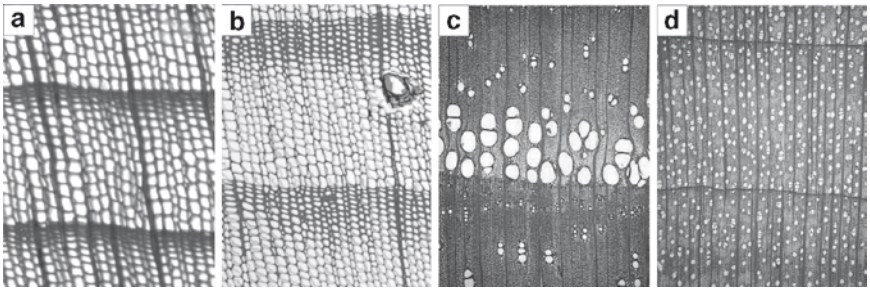

Fig. 1 Micro-sections of tree rings prepared from conifer and broadleaved trees: In (**a**) Norway spruce (*Picea abies*) and (**b**) Cembran pine (*Pinus cembra*), bands of tracheids form the individual increment rings. In broadleaved trees, tracheids and vessels are formed by the dividing cambium. Depending on the distribution of vessels in the ring, we distinguish between (**c**) ring-porous (European Ash, *Fraxinus excelsior*; photo: Schoch et al. 2004) and (**d**) diffuse-porous angiosperms (Sycamore Maple, *Acer pseudoplatanus*; photo: Schoch et al. 2004)

The width and character of each tree ring is influenced by biotic and abiotic factors. Biotic factors include the genetic makeup as well as the aging of trees and are individual for each species and each tree. Abiotic factors include a wide range of environmental factors, e.g. light, temperature, water, nutrient supply or the influence of strong wind, that are more or less common for all trees growing at a specific site (Fritts 1976). Therefore, trees growing at the same site can record the same environmental impacts and fluctuations (e.g., temperature or precipitation) in their tree-ring series. More details on tree growth can be found in Fritts (1976), Cook and Kairiukstis (1990) or Schweingruber (1996).

3.2 How Do Natural Hazards Affect Tree Growth?

In addition to site-specific information common to all trees at a location, individual trees also record the effects of mechanical disturbance caused by external processes. Trees can be injured, their trunks inclined, suffer breakage of their crown or branches, burial of the basal trunk or exposure of roots. Evidence of these events can also be recorded in individual tree-ring series. The analysis of geomorphic processes through the study of growth anomalies in tree rings is called dendrogeomorphology (Alestalo 1971). Dendrogeomorphic research is normally based on the "process–event–response" (Fig. 2) concept as defined by Shroder (1978). The "process" is represented by any geomorphic agent, e.g., debris flows or snow avalanches. Individual geomorphic "events" that affect the tree may result in range of growth "responses". These "events" and associated "responses" are illustrated in the following paragraphs.

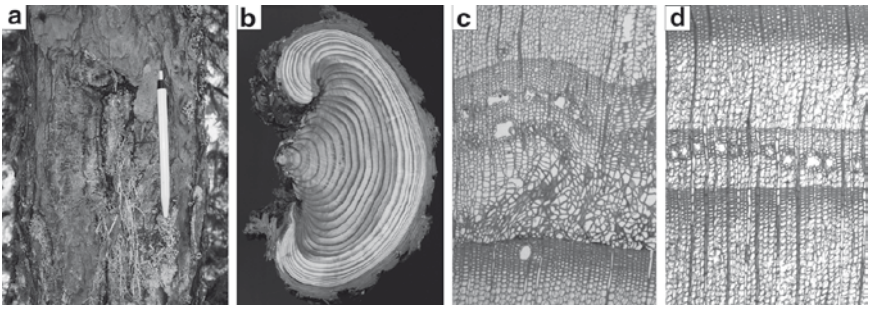

Fig. 2 Injuries in European larch (*Larix decidua*): (**a**) Injured trunk (**b**) Cross-section with overgrowth starting from the lateral edges of the injury. (**c**) Callus tissue as observed in the overgrowing cell layers bordering the injury. (**d**) Tangential row of traumatic resin ducts migrating from earlywood towards later portions of the tree ring with increasing distance from the wound (Bollschweiler 2007)

3.2.1 Wounding of Trees (Scars) and Resin-Duct Formation

Scratches on the outer bark and injuries are a very common feature in trees affected by geomorphic processes (Lundström et al. 2008). Wounds can be observed on the tree's trunk (Fig. 2a), branches or roots. When impact locally destroys the cambium, increment cell formation is disrupted and new cell formation ceases in the injured segment of the tree. In order to minimize rot and insect attacks after damage, the injured tree will (i) compartmentalize the wound (Shigo 1984) and (ii) almost immediately start production of chaotic callus tissue at the edges of the injury (Fig. 2c; Schweingruber 2001). Through the production of callus tissue, cambium cells will continuously overgrow the injury from its edges (Fig. 2b; Larson 1994; Sachs 1991) and ideally can lead to the complete closure of the wound. The extent of healing of the wound greatly depends on the annual increment rate, the age of the tree, and on the size of the scar.

Following injury, tangential rows of traumatic resin ducts (TRD) are produced in the developing secondary xylem of certain conifer species e.g., European larch (*Larix decidua*), Norway spruce (*Picea abies*) or Silver fir (*Abies alba*; Fig. 2d). They extend both tangentially and axially from the injury (Bannan 1936; Bollschweiler et al. 2008b; Nagy et al. 2000). When wounding occurs during the vegetation period of the tree, resin production will start a few days after the event and ducts emerge within 3 weeks after the disturbing event (Luchi et al. 2005; McKay et al. 2003; Ruel et al. 1998). Therefore, when analyzing cross-sections, the intra-seasonal position of the first series of TRD can be used to reconstruct previous events with monthly precision (Stoffel 2008; Stoffel and Beniston 2006; Stoffel et al. 2008; Stoffel and Hitz 2008; Stoffel et al. 2005b), provided that the incidence occurred during the vegetation period. With increasing axial and tangential distance from the impact, however, TRD tend to migrate to later portions of the tree ring,

which is why intra-seasonal dating with monthly precision has to be based on a large number of samples when working with increment cores (Bollschweiler et al. 2008a; Schneuwly and Stoffel 2008a, b; Schneuwly et al. 2009). This technique cannot be used in pines as this genus does not produce traumatic and tangential rows of resin ducts: it can produce copious amounts of resin that is unrelated to mechanical wounding (Phillips and Croteau 1999).

Depending on the impact energy and the relative size of the damage, an injured tree will concentrate the formation of tree rings to those parts essential for survival and limit growth in other segments in the years succeeding the impact (Bollschweiler 2007). This may result in missing or partial rings from certain areas of the trunk.

3.2.2 Tilting of Trunks

Tilting (or inclination) of trees may result from the sudden pressure induced directly by geomorphic impacts or by the associated deposition of material (e.g., avalanche snow, debris-flow material) as well as by the slow but ongoing destabilization of a tree through landslide activity or erosion (Lundström et al. 2007, 2008). Tilted trees are common in many areas affected by geomorphic processes (Fig. 3a) and have therefore been used in many dendrogeomorphic studies to date previous events (e.g., Braam et al. 1987a, b; Casteller et al. 2007; Clague and Souther 1982; Fantucci and Sorriso-Valvo 1999).

The trunk of a tilted tree will always try to regain its vertical position. The reaction will be most clearly visible in that segment of the tree to which the center of gravity has been moved by the inclination of the stem axis (Mattheck 1993). In the tree-ring series, eccentric growth will be visible in the cross-section after a tilting event and thus allow accurate dating of the disturbance. In coniferous trees, compression wood (also known as reaction wood) will be produced on the underside of the trunk. Individual rings will be considerably larger here and slightly darker in appearance as compared to the upslope side (Fig. 3b). The difference in color is due to the much thicker and rounded cell walls of early- and latewood tracheids (Schweingruber 2001; Timell 1986; Du and Yamamoto 2007). In contrast, trunk tilting in broadleaved trees leads to the formation of tension wood (Schweingruber 1983; Schweingruber et al. 1990; Schweingruber 1996; Westing 1965) and the eccentricity will occur on the upper side facing the tilting agent. Broadleaves trees also react upon tilting with ultrastructural modifications (e.g., a gelatinous layer oriented nearly parallel to the fibre axis) that are only visible when studied on micro-sections (Pilate et al. 2004).

In addition to the formation of different types of reaction wood, trees may also respond with reduced growth after tilting (Bollschweiler 2007). It is believed that such reductions in annual tree-ring width are related to the destruction of roots resulting from the abrupt or severe tilting. It is worthwhile to note that the growth decrease will be normally less visible on the side where the reaction wood (i.e. compression or tension wood) is being formed. Figure 3c provides an example of the appearance of differing yearly increments in a *Picea abies* tree tilted by a debris flow in 1922.

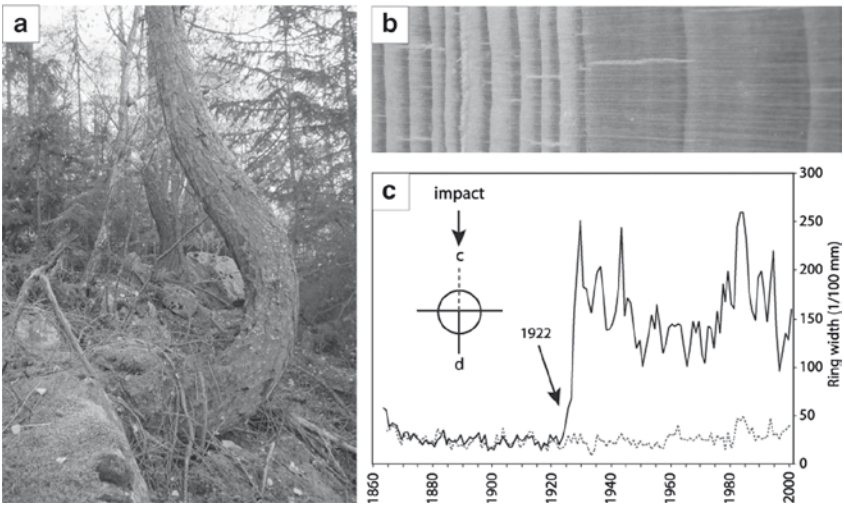

Fig. 3 (**a**) Tree morphology and (**b**) cross-sections of a tilted *Larix decidua* (D. M. Schneuwly). (**c**) Increment curves of a *Picea abies* tree tilted by a debris flow in 1922 (Stoffel et al. 2005b)

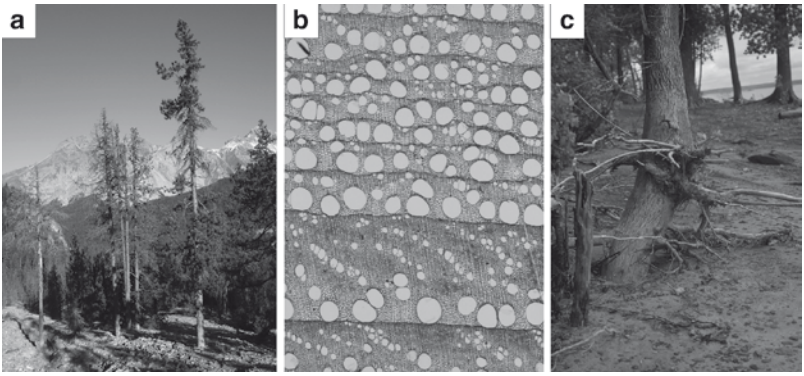

Fig. 4 (**a**) Sedimentation and subsequent die-off of trees after sedimentation. (**b**) Micro-section showing an abrupt growth decrease in Sweet Chestnut (*Castanea sativa*) following an event (F. H. Schweingruber). (**c**) Several levels of adventitious roots in Eastern Cottonwood (*Populus deltoids*) (F. H. Schweingruber)

3.2.3 Trunk Burial

Debris flows, hyperconcentrated flows, floods or landslides may bury trees by depositing material around their trunk base (Fig. 4a). Growth in these trees will normally be reduced as the supply of water and nutrients will be temporarily disrupted or at least limited (Fig. 4b; Friedman et al. 2005; Hupp et al. 1987; LaMarche 1966). Exceptionally, the burial of a trunk can cause a growth increase

if the material deposited is rich in nutrients, the water supply guaranteed and the depth of the deposited material is not too important (Strunk 1995).

If trunk burial exceeds a certain threshold, trees will die from a shortage in water and nutrient supply (Fig. 4a). According to case studies from the Italian Dolomites (Strunk 1991), *Picea abies* may tolerate a maximum burial depth of 1.6–1.9 m in environments dominated by fine-grained debris flows composed of calcareous and dolomitic material (Strunk 1997). Although there are no data available for other species or lithologies, it is believed that survivable burial depths will be (much) smaller in regions where debris flows are composed of massive and large crystalline blocks.

Occasionally, buried trees produce adventitious roots close to the new ground surface (Fig. 4c; Bannan 1941). As adventitious roots are normally formed in the first years succeeding burial (Strunk 1995), the moment of root sprouting can be used for approximate dating of the sedimentation processes, as shown by e.g., Strunk (1989, 1991) or Marin and Filion (1992). When a tree has been repeatedly buried and formed several layers of adventitious roots, it is possible to estimate the thickness of sedimentation from individual events at the location of the tree (Strunk 1997).

3.2.4 Decapitation of Trees and Elimination of Branches

Bouncing rocks and boulders, debris in flowing water, debris flows and lahars or the windblast of snow avalanches may decapitate trees (Fig. 5a) or remove branches. The loss of the crown or branches is more common in bigger trees, where trunks have lost their suppleness. Apex loss has also been observed as a result of rockfall impacts close to the ground level. In such cases, the sinusoidal propagation of shockwaves in the trunk results in the break-off of the crown. This phenomenon has been described as whiplash or "hula-hoop" effect (Dorren and Berger 2006; Stoffel et al. 2005b).

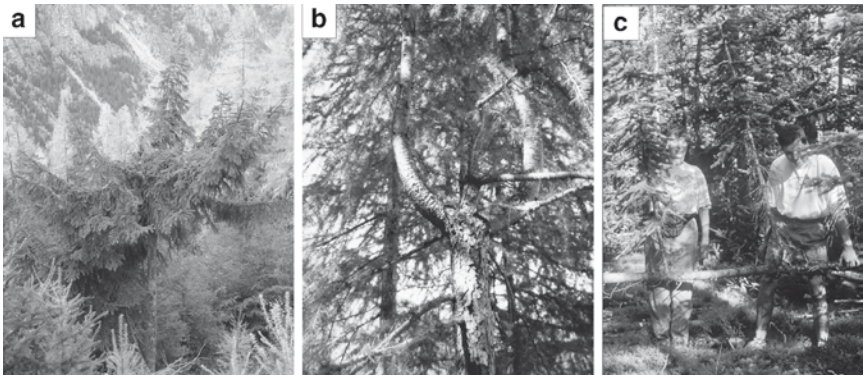

Fig. 5 (**a**) *P. abies* topped by rockfall. (**b**) Candelabra growth in *Larix decidua* following apex loss. (**c**) Engelmann Spruce (*Picea engelmannii*) with two "leaders" developed from a prostrated trunk knocked to the ground by a snow avalanche

Following decapitation, trees react with distinct radial growth suppression in the years following the impact (see Fig. 5b). One or several lateral branches will form a "leader" that replaces the broken crown, resulting in a tree morphology called "candelabra" growth (Fig. 5b; Butler and Malanson 1985; Stoffel et al. 2005c). In addition, it is not unusual that the shock of the impacting material causes injuries and provokes the formation of TRD as well (see Section 3.1). "Leaders" may also be formed from prostrated trunks knocked over by mass wasting events (Fig. 5c).

3.2.5 Root Exposure and Damage

Erosional processes and the (partial) denudation of roots may generate different growth reactions, both in the trunk and in the exposed roots. The type and intensity of the reaction(s) will depend on the nature of the erosive event, which may be instantaneous or progressive and gradual. If several roots are completely denuded during a sudden erosive event (e.g., debris flow, lahar, flood or landslide), they are no longer able to fulfill their primary functions and quickly die. The tree subsequently suffers from a shortage in water and nutrient supply, resulting in suppressed tree growth and the formation of narrow rings in the trunk (see Fig. 4b; Carrara and Carroll 1979; La Marche 1968; McAuliffe et al. 2006).

In cases where only part of a root is exposed (Fig. 6a) and its outer end remains in the ground, the root will continue to grow and fulfill its functions. In the exposed part, however, anatomical changes will occur and individual growth rings similar to those in the trunk or branches will be formed. The localization of this change in the tree-ring series may allow determination of the moment of exposure (Fig. 6b–d; see Bodoque et al. 2005; Gärtner et al. 2001). The continuous exposure of roots is usually caused by gradual processes and relatively low denudation rates, e.g. by overland

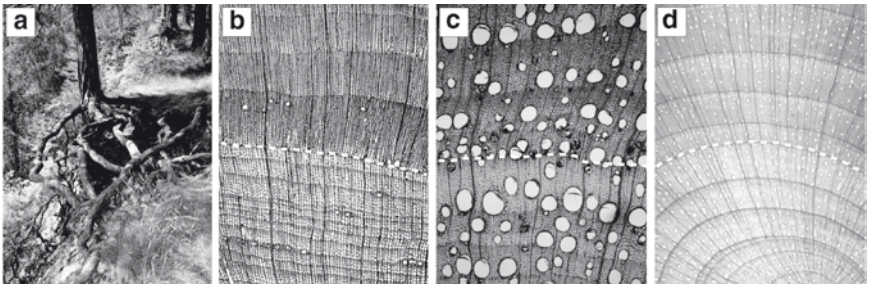

Fig. 6 (**a**) Exposed roots of Scots Pine (*Pinus sylvestris*). (**b**) Larger increment rings with distinct latewood formed in Silver fir (*Abies alba*) after sudden exposure (*dashed white line*). (**c**) Following sudden exposure, the arrangement of vessels in *Fraxinus excelsior* change from diffuse-porous to ring-porous. (**d**) In addition to cell changes, tension wood is formed in this root of *Acer pseudoplatanus* (Hitz 2008)

flow of rain water, the slow opening of cracks in soils (e.g., soil creep, landslides) and in disintegrated bedrock (e.g., preparation of rockfall, thrusts), along rivers, streams, lakes and oceans (floods, shore erosion) as well as with faulting activity and displacements in relation with earthquake activity. Provided that the roots are gradually exposed with time, it is also possible to determine the erosion rates (Carrara and Carroll 1979).

Root shearing and root damage frequently occurs in areas affected by landsliding or along earthquake faults (Allen et al. 1999; Vittoz et al. 2001). As a result of root damage, tree-ring growth will be suppressed or eventually cease (Fig. 7). Previous studies using ring-width series to determine landsliding and earthquake activity include Meisling and Sieh (1980), Lin and Lin (1998), Carrara and O'Neill (2003), or Papadopoulos et al. (2007). Rizzo and Harrington (1988) showed that periods of decreased growth of red spruce (*Picea rubens*) and balsam fir (*Abies balsamea*) trees from the northern Appalachian Mountains were significantly correlated with wind exposure and related root and crown damage variables.

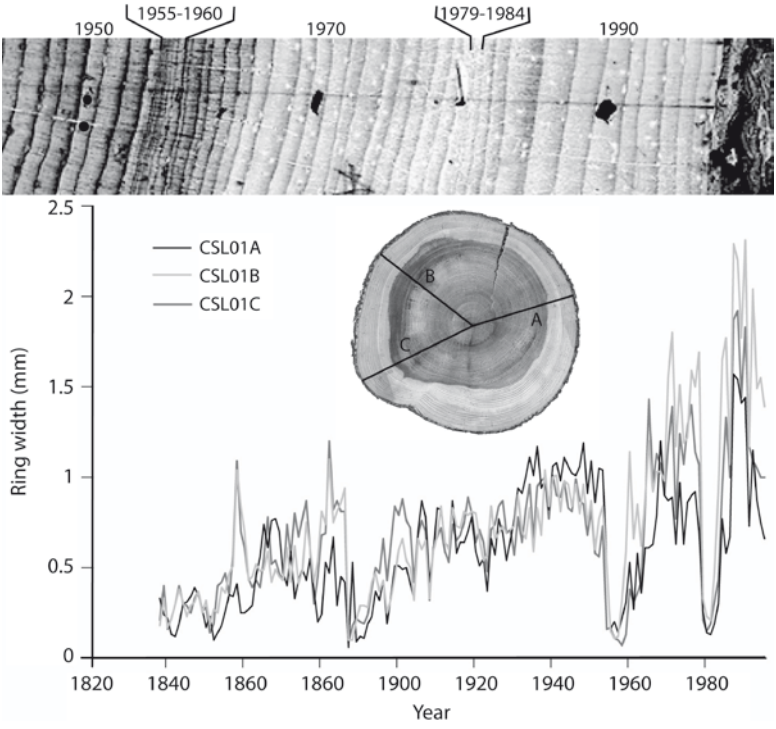

Fig. 7 Radial growth suppression caused by landsliding. This tree was growing on a slope destabilized by downwasting of Columbia Glacier, Alberta. The abrupt radial suppressions in 1887–1894, 1955–1960 and 1979–1984 are thought to result from root damage as a landslide block moved downslope three times. The tree was cut in 1996. The enlargement shows part of radius A (B.H. Luckman, unpublished data)

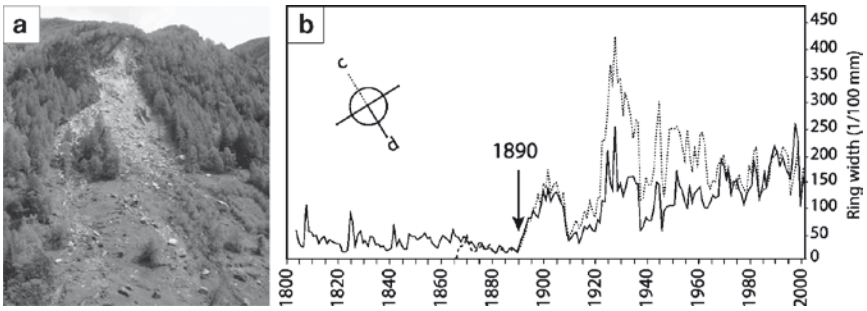

Fig. 8 (**a**) Part of this forest stand has been eliminated by a rockslide event, leaving survivor trees uninjured at both sides of the scar. (**b**) Increment curves of a survivor tree (*Larix decidua*) remaining intact after a major debris flow in 1890 (Stoffel et al. 2005b)

3.2.6 Elimination of Neighboring Trees

Geomorphic processes can also eliminate trees along channels or couloirs through uprooting and stem breakage and leave neighboring trees intact (Fig. 8a). This phenomenon can be observed with e.g., rockfalls, debris flows, lahars, extreme floods, landslides or snow avalanches (Butler 1979, 1985; Stoffel et al. 2005c).

In their new environment the uninjured survivor trees have less competition, more light, nutrients and/or water (Schweingruber 1996). As a consequence, they will start to produce larger increment rings. However, several observations indicate that this growth release in survivor trees can be delayed and therefore this reaction cannot always be used to date past destructive events with yearly precision (Fig. 8b). Nevertheless, the growth release in survivor trees can corroborate the dating of events that have been identified in other trees at the same site, e.g., from scars, tilted trunks, etc. (Stoffel et al. 2005a).

3.2.7 Colonization of Landforms After Surface-Clearing Disturbances

Many natural processes can eliminate surface vegetation including entire forest stands, leaving no direct dendrogeomorphic evidence. In such cases, germination ages of trees growing on the bare surfaces can be used to estimate the time of creation of the new landforms and/or surface-clearing disturbances to existing landforms. This approach provides a minimum age for that surface and has been used repeatedly to date landforms or assess the minimum time elapsed since the last devastating event in snow avalanche couloirs, debris-flow channels or floodplains (Bollschweiler et al. 2008a; McCarthy and Luckman 1993; Pierson 2007; Sigafoos and Hendricks 1969; Winter et al. 2002). It involves estimating the time between the exposure of the surface and the germination of the first surviving seedling on that surface. This "ecesis" estimate varies with the environment, substrate, available seed sources and several other factors. Problems of ecesis determination have been extensively discussed in studies that attempt to date the

formation of glacier moraines (see Koch 2009; McCarthy and Luckman 1993) where ecesis estimates may vary from a few years to several decades.

3.3 Sampling Design and Laboratory Analyses

3.3.1 Field Approach and Sampling Design

The types of damage to trees described in the preceding section may result from a wide variety of natural processes. Linkage between the damage and the causative process depends on a critical evaluation of the sampling site. In many cases, hazard investigations are undertaken with a specific context where the process or processes involved are known and appropriate sampling methods and sampling design may be applied. These vary considerably with the nature of the process or investigation and are best discussed in the specific context of individual processes. For example, the sampling network needed to define past earthquake activity may be very different than trying to reconstruct the history of snow avalanches and debris flows on a large debris cone.

At an individual site the choice of sampling design and selection of the trees to be sampled will depend on the purpose of the investigation and the processes or hazards being sampled. The sampled area and number of trees sampled may be very small and specific e.g. on a small landslide or may involve systematic sampling of a larger area (e.g. within a large run-out zone of a snow avalanche) or target trees damaged at the margins of an event. The choice of individual trees is based on (i) an inspection of the trunk surface (i.e. does the tree show obvious signs of past disturbance?) and (ii) the location of the trees with relation to the processes/ hazards studied i.e. is the tree located on or adjacent to the area influenced by the process studied? (e.g. a debris flow levee). A detailed description on the documentation and numbering of trees in the field is provided by Stoffel et al. (2005a).

The tree-ring record of growth disturbances created by past events is analyzed with cross-sections or increment cores. Cross-sections are normally taken at the location of the growth disturbance and provide an excellent and very complete insight into the tree's history. However, in many locations (e.g. protection forests, National Parks) felling may be prohibited or ill-advised for aesthetic or safety reasons. Most tree-ring studies therefore use cores extracted with an increment borer. Grissino-Mayer (2003) provides a technical description on the correct use of increment borers. In some cases useful information may also be obtained from the analysis of cross-sections sampled from tree stumps remaining on the slopes after logging (Hughes and Brown 1992; Swetnam 1993; Stoffel and Perret 2006).

The nature of visible growth defects observed in the tree's morphology will strongly influence the sampling height, sampling directions and the minimum number of samples to be taken per tree. In trees with visible **scars**, previous geomorphic events are most easily dated through the destructive sampling of trees and the preparation of cross-sections taken at the location where the injury is largest. This approach will facilitate an accurate and intra-seasonal identification of the onset of **callus tissue** production (and **TRD** formation in certain conifer species) and

therefore allows a reconstruction of the impacting event with a very high temporal resolution. Alternatively, wedges can be sawn from the overgrowing callus and an increment core extracted from the side opposite of the wound. In this case, the sampled tree will survive and a reconstruction of the wounding event will be possible. When cross-sections and wedges cannot be taken from the injured trees, at least two increment cores need to be extracted, one from the overgrowing callus and the other from the side opposite to the wound. Internal scars that have been completely healed over cannot be sampled with cores, except fortuitously. Special attention needs to be addressed to the sampling of cores from the overgrowing callus: Samples taken inside the overgrowing tissue will provide an incomplete tree-ring record, as wounds are closed from their edges. On the other hand, samples taken too far away from the callus growth will not show any signs of the disturbing event at all and thus prevent dating of the event. Figure 9 illustrates the recommended position for the extraction of increment cores in injured trees. In addition and in the case of certain conifer species, TRD formation will be delayed with increasing distance from the wound and improper core location may influence the intra-seasonal dating quality (Bollschweiler et al. 2008b; Schneuwly and Stoffel 2008b).

Tilted trunks are best analyzed with at least two increment cores extracted per tree, one in the direction of the tilting and the other on the opposite side of the trunk. The reaction wood will be visible on the tilted side in conifer trees (= compression wood) and on the side opposite to the tilting direction in the broadleaved trees (= tension wood). Individual cores are best extracted at the location where the tilting is strongest based on an outer inspection of the tree morphology.

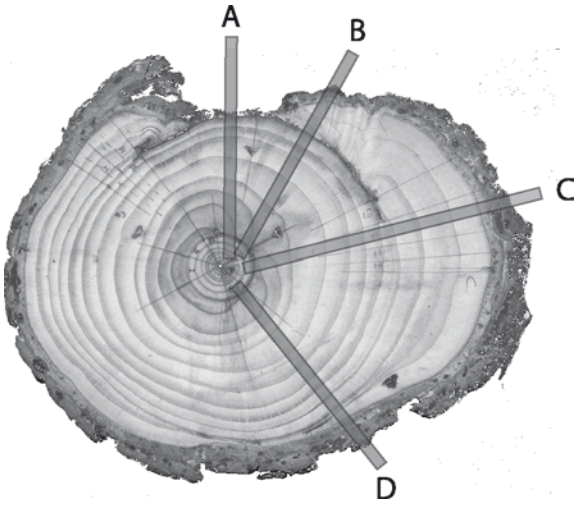

Fig. 9 When sampling injured trees, special attention needs to be addressed to the sampling position. Samples taken inside the wound (**a**) or from the overgrowing callus tissue (**b**) will provide an incomplete tree-ring record, as wounds are closed from their edges. Ideally, increment cores are extracted just next to the injury (**c**) where the presence of overgrowing callus tissue and TRD will allow accurate dating. Cores taken too far away from the wound (**d**) will not necessarily show signs of the disturbing event and thus prevent dating

In the case of **buried trunk bases**, the sampling of two increment cores in opposite directions (ideally from the upslope and the downslope side) will normally allow accurate reconstruction of the event that has led to the sedimentation of material around the trunk's base. It is best to sample these trees as close to ground level as possible (ca. 20–40 cm) to extract the maximum number of tree rings and obtain maximum information. However, the influence of roots should be avoided.

The analysis of **exposed roots** is normally based on cross-sections, as they regularly show partially or completely missing rings. The position of samples needs to be carefully noted with respect to the ground surface or the non-eroded parts of the root. Accurate notes on the position of the roots with respect to the soil level will be essential for the understanding and interpretation of continuous erosion processes and the determination of denudation rates (Bodoque et al. 2005; La Marche 1968).

The **germination of trees** on new landforms is best determined by counting the annual growth rings in increment cores taken from the root crown level. However, branches, obstacles and rot sometimes require sampling positions higher on the trunk. In these cases, an age correction factor needs to be added to compensate for the time a tree takes to grow to sampling height (McCarthy et al. 1991). A height-age correction can be achieved by dividing the tree height by the number of tree rings to get an average rate for the yearly apical increment. Thereafter, the sampling height is divided by this yearly increment so as to obtain an estimate of the number of rings between sampling height and the root crown (e.g. McCarthy et al. 1991; McCarthy and Luckman 1993; Bollschweiler et al. 2008a). In addition if the pith is not present on the core the number of rings to pith has to be estimated. This correction can be undertaken using a transparent sheet with concentric rings (Bosch and Gutierrez 1999; Gutsell and Johnson 2002). An age correction also needs to be applied for the assessment of the colonization time or ecesis, i.e. the time elapsed between the clearing or creation of the surface and the germination of pioneer trees (McCarthy and Luckman 1993; Pierson 2007; Koch 2009).

In some cases a reference tree-ring chronology may need to be developed from a nearby forest stand to assist in cross dating of trees at the sampled site to verify the age assignment of rings. The reference site should be undisturbed and the trees sampled should not show obvious signs of external injury, disease or anomalous tree-ring growth to minimize non-climatic influences on ring growth. Usually the oldest trees are selected to maximize chronology length. For reference chronologies two increment cores are extracted per tree, normally from locations > 90° apart and at breast height (≈ 130 cm). Adequate sample size varies between species and also depends on the strength of the common signal. In general, 20–30 trees are is a useful guide for most species to minimize the potential influence of geomorphic processes and hidden growth disturbances.

3.3.2 Laboratory Procedures: Sample Preparation and Analysis

In the laboratory, samples are normally analyzed and data processed following the standard procedures described in Bräker (2002) or Stokes and Smiley (1968). Normally these involve surface preparation, counting of tree rings, skeleton plots

(Schweingruber et al. 1990) plus ring-width measurements using a digital positioning table connected to a stereo microscope and computer with tree-ring analysis software. Development of a reference chronology, where needed, follows standard procedures of measurement, crossdating and standardization (see e.g. Fritts 1976; Cook 1987; Cook and Kairiukstis 1990; Vaganov et al. 2006).

Ring widths of the disturbed samples may also be measured and the series compared graphically or statistically with the reference chronology. These tools also allow for an assessment of crossdating accuracy between ring-width series of individual disturbed trees and the reference chronology. Once dating of all tree-ring series has been checked and missing rings identified, individual growth curves may be analyzed **visually** to identify the tree's response to geomorphic processes, e.g. the initiation of abrupt growth reduction or releases (Schweingruber 2001; McAuliffe et al. 2006). In the case of tilted trunks, the growth curve data may be analyzed to identify the dating of the tilt (Braam et al. 1987 a, b; Fantucci and Sorriso-Valvo 1999; Fig. 3c). In addition, the appearance of the cells (e.g. structure of the reaction wood cells) may be investigated on the samples to yield further evidence of disturbance (Wilson and Archer 1977). Other features like callus tissue overgrowing scars or the presence of tangential rows of traumatic resin ducts (TRD) formed following cambium damage can only be identified through a visual inspection of the cores and cross-sections (e.g., Stoffel et al. 2005c; Perret et al. 2006; Bollschweiler et al. 2008b). Finally, the first decade of juvenile growth should be excluded from the analysis, as tree rings in seedlings tend to be more susceptible to disturbance than larger trees.

All growth reactions identified by analysis of the samples are noted in order to identify events. Except for processes with limited volumes (e.g., single rocks or boulders involved in rockfall events; Stoffel et al. 2005b, c; Moya et al. 2010, this volume), one growth disturbance identified in a single tree is not considered sufficient evidence to identify an event. The **reconstruction of past events** needs to be based on quantitative (i.e. indices; Butler et al. 1987) or semi-quantitative (Stoffel and Bollschweiler 2008, 2009) thresholds identified from a number of trees or lines of evidence.

4 The Organization of This Book

The subsequent sections of the book address specific natural hazards, namely snow avalanches, landslides, rockfall, debris flows, floods, meteorological hazards (tornados, hurricanes, and wind storms), wildfires, earthquakes and volcanic eruptions. Each of these sections is prefaced by an introductory overview of the process dynamics and recent applications of tree rings to the analysis of the hazard, followed by two case studies and several shorter text boxes that illustrate dendrogeomorphic reconstructions of past and contemporary process activity. Although some of these contributions are new and original, most are drawn from the existing literature and have been reformatted or rewritten by the original author(s). These selections attempt to provide a comprehensive overview of the field in a single volume.

Table 1 Common damage-process associations. The table lists the major parts of the volume and the specific chapters of each part in which examples of these types of damage are discussed

	Avalanches	Landslides	Rockfall	Debris flows	Flooding	Meteorology	Wildfires	Earthquake	Volcanic activity
Part	II	III	IV	V	VI	VII	VIII	IX	X
Trunk tilting	1, 2, 3, 4, 5	1, 2, 3, 4	2	2, 3, 4	1	2, 3		1, 2, 4	1
Wounding	1, 2, 4, 5	1, 3	2, 3, 4, 5	1, 2, 3, 4, 5	1, 2, 3, 4		1, 2, 3, 4, 5	2, 4	1, 6
Decapitation	1	1	2, 4	2		3		2, 4	
Trunk burial	2	4		1, 2, 4				2	1, 2, 6
Root exposure		1		2, 4	1			2, 3, 4	
Tree death	1, 2, 4	1, 4, 5		2	1	3	1, 2, 3, 4	1, 2, 4	1, 2, 3, 5, 6

Theoretically almost all of the hazards discussed in this book may result in most of the categories of tree damage that have been discussed above. However, some types of damage are more typically associated with specific processes or process combinations. As a guide to the chapters which follow, Table 1 indicates the most common evidence used to reconstruct specific hazardous processes and identifies those sections of the book that provide examples of these specific combinations.

This book will be useful to academics and students in the geosciences, environmental sciences, engineering and biology, plus natural hazard consultants or experts in a broad range of organizations. We hope that it will enhance understanding of these hazards and the risks they present. Furthermore, we hope it may facilitate and promote the adoption of state-of-the-art tree-ring techniques into hazard and risk practices.

References

Alestalo J (1971) Dendrochronological interpretation of geomorphic processes. Fennia 105:1–139

Allen R, Bellingham P, Wiser S (1999) Immediate damage by an earthquake to a temperate montane forest. Ecology 80:708–714

Aulitzky H (1992) Die Sprache der "Stummen Zeugen". International Conference Interpraevent 1992, pp 139–174

Bannan MW (1936) Vertical resin ducts in the secondary wood of the Abietineae. New Phytol 35:11–46

Bannan MW (1941) Vascular rays and adventitious root formation in *Thuja occidentalis* L. Am J Bot 28:457–463

Bodoque JM, Diez-Herrero A, Martin-Duque JF, Rubiales JM, Godfrey A, Pedraza J, Carrasco RM, Sanz MA (2005) Sheet erosion rates determined by using dendrogeomorphological analysis of exposed tree roots: Two examples from Central Spain. Catena 64:81–102

Bollschweiler M (2007) Spatial and temporal occurrence of past debris flows in the Valais Alps – results from tree-ring analysis. GeoFocus 20:1–182

Bollschweiler M, Stoffel M, Schneuwly DM (2008a) Dynamics in debris-flow activity on a forested cone – A case study using different dendroecological approaches. Catena 72:67–78

Bollschweiler M, Stoffel M, Schneuwly DM, Bourqui K (2008b) Traumatic resin ducts in Larix decidua stems impacted by debris flows. Tree Physiol 28:255–263

Bosch O, Gutierrez E (1999) La sucésion en los bosques de Pinus uncinata del Pirineo. De los anillos de crecimiento a la historia del bosque. Ecologia 13:133–171

Braam RR, Weiss EEJ, Burrough PA (1987a) Dendrogeomorphological analysis of mass movement – a technical note on the research method. Catena 14:585–589

Braam RR, Weiss EEJ, Burrough PA (1987b) Spatial and temporal analysis of mass movement using dendrochronology. Catena 14:573–584

Bräker OU (2002) Measuring and data processing in tree-ring research – A methodological introduction. Dendrochronologia 20:203–216

Butler DR (1979) Snow avalanche path terrain and vegetation, Glacier National Park, Montana. Arct Alp Res 11:17–32

Butler DR (1985) Vegetational and geomorphic change on snow avalanche path, Glacier National Park, Montana, USA. Great Basin Nat 45:313–317

Butler DR, Malanson GP (1985) A history of high-magnitude snow avalanches, Southern-Glacier-National-Park, Montana, USA. Mt Res Dev 5:175–182

Butler DR, Malanson GM, Oelfke JG (1987) Tree-ring analysis and natural hazard chronologies: minimum sample sizes and index values. Prof Geogr 39:41–47

Camarero JJ, Guerrero-Campo J, Gutierrez E (1998) Tree-ring growth and structure of *Pinus uncinata* and *Pinus sylvestris* in the Central Spanish Pyrenees. Arct Alp Res 30:1–10
Carrara PE, Carroll TR (1979) Determination of erosion rates from exposed tree roots in the Piceance Basin, Colorado. Earth Surf Process Land 4:307–317
Carrara PE, O'Neill JM (2003) Tree-ring dated landslide movements and their relationship to seismic events in southwestern Montana, USA. Quat Res 59:25–35
Casteller A, Stöckli V, Villalba R, Mayer AC (2007) An evaluation of dendroecological indicators of snow avalanches in the Swiss Alps. Arct Antarc Alp Res 39:218–228
Clague JJ, Souther JG (1982) The Dusty Creek landslide on Mount Cayley, British Columbia. Can J Earth Sci 19:524–539
Cook ER (1987) The decomposition of tree-ring series for environmental studies. Tree-Ring Bull 47:37–59
Cook ER, Kairiukstis LA (1990) Methods of dendrochronology – Applications in the environmental sciences. Kluwer, London
Dorren LKA, Berger F (2006) Stem breakage of trees and energy dissipation during rockfall impacts. Tree Physiol 26:63–71
Du S, Yamamoto F (2007) An overview of the biology of reaction wood Formation. J Integr Plant Biol 49:131–143
EMDAT (2009) Emergency events database. www.emdat.be
Fantucci R, Sorriso-Valvo M (1999) Dendrogeomorpholigical analysis of a slope near Lago, Calabria (Italy). Geomorphology 30:165–174
Friedman JM, Vincent KR, Shafroth PB (2005) Dating floodplain sediments using tree-ring response to burial. Earth Surf Process Land 30:1077–1091
Fritts HC (1976) Tree rings and climate. Academic, London
Gärtner H, Schweingruber F, Dikau R (2001) Determination of erosion rates by analyzing structural changes in the growth pattern of exposed roots. Dendrochronologia 19:81–91
Grissino-Mayer HD (2003) A manual and tutorial for the proper use of an increment borer. Tree-Ring Res 59:63–79
Gutsell SL, Johnson EA (2002) Accurately ageing trees and examining their height-growth rates: implications for interpreting forest dynamics. J Ecol 90:153–166
Hughes MK, Brown PM (1992) Drought frequency in central California since 101 B.C. recorded in giant sequoia tree rings. Clim Dynam 6:161–167
Hupp CR, Osterkamp WR, Thornton JL (1987) Dendrogeomorphic evidence and dating of recent debris flows on Mount Shasta, northern California. US Geol Surv Prof Paper 1396B:1–39
Koch J (2009) Improving age estimates for late Holocene glacial landforms using dendrochronology – Some examples from Garibaldi Provincial Park, British Columbia. Quat Geochronol 4:130–139
La Marche VC (1968) Geomorphic and dendroecological impacts of slushflows in central Gaspé Peninsula (Québec, Canada). US Geol Surv Prof Paper 352-I
LaMarche VC (1966) An 800-year history of stream erosion as indicated by botanical evidence. US Geol Surv Prof Paper 550D:83–86
Larson PR (1994) The vascular cambium. Development and structure. Springer, Berlin
Lin A, Lin S (1998) Tree damage and surface displacement: the 1931 M 8.0 Fuyun earthquake. J Geol 106:751–757
Luchi N, Ma R, Capretti P, Bonello P (2005) Systemic induction of traumatic resin ducts and resin flow in Austrian pine by wounding and inoculation with Sphaeropsis sapinea and Diplodia scrobiculata. Planta 221:75–84
Lundström T, Stoffel M, Stöckli V (2008) Fresh-stem bending of silver fir and Norway spruce. Tree Physiol 28:355–366
Lundström T, Heiz U, Stoffel M, Stöckli V (2007) Fresh-wood bending: linking the mechanical and growth properties of a Norway spruce stem. Tree Physiol 27:1229–1241
Marin P, Filion L (1992) Recent dynamics of sub-arctic dunes as determined by tree-ring analysis of white spruce, Hudson Bay, Quebec. Quat Res 38:316–330
Mattheck C (1993) Design in der Natur. Rombach Wissenschaft

McAuliffe JR, Scuderi LA, McFadden LD (2006) Tree-ring record of hillslope erosion and valley floor dynamics: Landscape responses to climate variation during the last 400yr in the Colorado Plateau, northeastern Arizona. Global Planet Change 50:184–201

McCarthy DP, Luckman BH (1993) Estimating ecesis for tree-ring dating of moraines – a comparative study from the Canadian Cordillera. Arct Alp Res 25:63–68

McCarthy DP, Luckman BH, Kelly PE (1991) Sampling height-age error correction for spruce seedlings in glacial forefields, Canadian Cordillera. Arct Alp Res 23:451–455

McKay SAB, Hunter WL, Godard KA, Wang SX, Martin DM, Bohlmann J, Plant AL (2003) Insect attack and wounding induce traumatic resin duct development and gene expression of (-)-pinene synthase in Sitka spruce. Plant Physiol 133:368–378

Meisling K, Sieh K (1980) Disturbance of trees by the 1857 Fort Tejon earthquake. J Geophys Res 85:3225–3238

Moya J, Corominas J, Pérez Arcas J (2010) Assessment of the rockfall frequency for hazard analysis at Solà d'Andorra (Eastern Pyrenees). In: Stoffel M, Bollschweiler M, Butler DR, Luckman BH (eds) Tree rings and natural hazards: A state-of-the-art. Springer, Berlin, Heidelberg, New York, this volume

Nagy NE, Franceschi VR, Solheim H, Krekling T, Christiansen E (2000) Wound-induced traumatic resin duct development in stems of Norway spruce (Pinaceae): Anatomy and cytochemical traits. Am J Bot 87:302–313

Papadopoulos AM, Mertzanis A, Pantera A (2007) Dendrogeomorphological observations in a landslide on Tymfristos mountain in Central Greece. In: Stokes A, Spanos I, Norris JE, Cammeraat E (eds) Eco- and ground bio-engineering: The use of vegetation to improve slope stability. Springer, Berlin, Heidelberg, New York, pp. 223–230

Perret S, Stoffel M, Kienholz H (2006) Spatial and temporal rockfall activity in a forest stand in the Swiss Prealps – a dendrogeomorphological case study. Geomorphology 74:219–231

Phillips MA, Croteau RB (1999) Resin-based defences in conifers. Trends Plant Sci 4:184–190

Pierson TC (2007) Dating young geomorphic surfaces using age of colonizing Douglas fir in south-western Washington and northwestern Oregon, USA. Earth Surf Process Land 32:811–831

Pilate G, Chabbert B, Cathala B, Yoshinaga A, Leple JC, Laurans F, Lapierre C, Ruel K (2004) Lignification and tension wood. C Biol 327:889–901

Rigling A, Bräker O, Schneiter G, Schweingruber F (2002) Intra-annual tree-ring parameters indicating differences in drought stress of Pinus sylvestris forests within the Erico-Pinion in the Valais (Switzerland). Plant Ecol 163:105–121

Rizzo DM, Harrington TC (1988) Root movement and root damage of red spruce and balsam fir on subalpine sites in the White Mountains, New Hampshire. Can J Forest Res 18(8):991–1001

Rodriguez J, Vos F, Below R, Guha-Sapir D (2009) Annual disaster statistical review 2008. The numbers and trends. Centre for Research on the Epidemiology of Disasters, Jacoffset Printers, Melin, Belgium, p 33

Ruel JJ, Ayres MP, Lorio PL (1998) Loblolly pine responds to mechanical wounding with increased resin flow. Can J Forest Res 28:596–602

Sachs T (1991) Pattern formation in plant tissue. Cambridge University Press, Cambridge

Schneuwly DM, Stoffel M (2008a) Spatial analysis of rockfall activity, bounce heights and geomorphic changes over the last 50 years – A case study using dendrogeomorphology. Geomorphology 102:522–531

Schneuwly DM, Stoffel M (2008b) Tree-ring based reconstruction of the seasonal timing, major events and origin of rockfall on a case-study slope in the Swiss Alps. Nat Haz Earth Syst Sci 8:203–211

Schneuwly DM, Stoffel M, Bollschweiler M (2009) Formation and spread of callus tissue and tangential rows of resin ducts in *Larix decidua* and *Picea abies* following rockfall impacts. Tree Physiol 29:281–289

Schweingruber F (1983) Der Jahrring: Standort, Methodik, Zeit und Klima in der Dendrochronologie. Paul Haupt, Bern, Stuttgart, Wien

Schweingruber FH (1996) Tree rings and environment. Dendroecology. Paul Haupt, Bern, Stuttgart, Wien

Schweingruber F (2001) Dendroökologische Holzanatomie. Paul Haupt, Bern, Stuttgart, Wien
Schweingruber F, Eckstein D, Serre-Bachet F, Bräker OU (1990) Identification, presentation and interpretation of event years and pointer years in dendrochronology. Dendrochronologia 8:9–39
Shaban R (2009) Australia's natural disasters: The 2009 fires and floods. Australas Emerg Nurse J 12:29
Sheppard P, Jacoby G (1989) Application of tree-ring analysis to paleoseismology: two case studies. Geology 17:226–229
Sheppard P, White D (1995) Tree-ring responses to the 1978 earthquake at Stephens Pass, northeastern California. Geology 23:109–112
Shigo AL (1984) Compartmentalization – A conceptual framework for understanding how trees grow and defend themselves. Ann Rev Phytopathol 22:189–214
Shroder JF (1978) Dendrogeomorphological analysis of mass movement on Table Cliffs Plateau, Utah. Quat Res 9:168–185
Sigafoos RH, Hendricks EL (1969) The time interval between stabilization of alpine glacial deposits and establishment of tree seedlings. US Geol Surv Prof Paper 650B:B89–B93
Stoffel M (2008) Dating past geomorphic processes with tangential rows of traumatic resin ducts. Dendrochronologia 26:53–60
Stoffel M, Beniston M (2006) On the incidence of debris flows from the early Little Ice Age to a future greenhouse climate – A case study from the Swiss Alps. Geophys Res Lett 33:L16404
Stoffel M, Hitz OM (2008) Rockfall and snow avalanche impacts leave different anatomical signatures in tree rings of juvenile Larix decidua. Tree Physiol 28:1713–1720
Stoffel M, Perret S (2006) Reconstructing past rockfall activity with tree rings: some methodological considerations. Dendrochronologia 24:1–15
Stoffel M, Lievre I, Conus D, Grichting MA, Raetzo H, Gärtner HW, Monbaron M (2005a) 400 years of debris-flow activity and triggering weather conditions: Ritigraben, Valais, Switzerland. Arct Antarc Alp Res 37:387–395
Stoffel M, Lievre I, Monbaron M, Perret S (2005b) Seasonal timing of rockfall activity on a forested slope at Taschgufer (Swiss Alps) – A dendrochronological approach. Z Geomorphol 49:89–106
Stoffel M, Schneuwly D, Bollschweiler M, Lievre I, Delaloye R, Myint M, Monbaron M (2005c) Analyzing rockfall activity (1600–2002) in a protection forest – a case study using dendrogeomorphology. Geomorphology 68:224–241
Stoffel M, Conus D, Grichting MA, Lievre I, Maitre G (2008) Unraveling the patterns of late Holocene debris-flow activity on a cone in the Swiss Alps: Chronology, environment and implications for the future. Glob Planet Change 60:222–234
Stoffel M, Bollschweiler M (2008) Tree-ring analysis in natural hazards research – an overview. Nat Haz Earth Sys Sci 8:187–202
Stoffel M, Bollschweiler M (2009) What tree rings can tell about earth-surface processes. Teaching the principles of dendrogeomorphology. Geogr Compass 3:1017–1037
Stokes MA, Smiley TL (1968) An introduction to tree-ring dating. University of Chicago Press, Chicago
Strunk H (1989) Dendrogeomorphology of debris flows. Dendrochronologia 7:15–25
Strunk H (1991) Frequency distribution of debris flow in the Alps since the "Little Ice Age". Z Geomorphol Suppl 83:71–81
Strunk H (1995) Dendrogeomorphologische Methoden zur Ermittlung der Murfrequenz und Beispiele ihrer Anwendung. Roderer, Regensburg
Strunk H (1997) Dating of geomorphological processes using dendrogeomorphological methods. Catena 31:137–151
Swetnam TR (1993) Fire history and climate change in Giant Sequoia groves. Science 262:885–889
SwissRe (2009) Natural catastrophes and man-made disasters in 2008: North America and Asia suffer heavy losses. Sigma 2(09):1–41
Timell TE (1986) Compression wood in Gymnosperms. Springer, Berlin

UNISDR (2009) United Nations International Strategy for Disaster Reduction. UNISDR Terminology on Disaster Risk Reduction. www.unisdr.org
Vaganov EA, Hughes MK, Shashkin AV (2006) Growth dynamics of conifer tree rings. Images of past and future environments. Springer, Berlin, Heidelberg, New York
Vittoz P, Stewart G, Duncan R (2001) Earthquake impacts in old-growth Nothofagus forests in New Zealand. J Veget Sci 12:417–426
Wells A, Duncan R, Stewart G (1998) Forest dynamics in Westland, New Zealand: the importance of large, infrequent earthquake-induced disturbance. J Ecol 89(6):1006–1018
Westing AH (1965) Formation and function of compression wood in gymnosperms II. Bot Rev 34:51–78
Wilson BF, Archer RR (1977) Reaction wood: Induction and mechanical action. Ann Rev Plant Physiol 28:23–43
Winter LE, Brubaker LB, Franklin JF, Miller EA, DeWitt DQ (2002) Initiation of an old-growth Douglas-fir stand in the Pacific Northwest: a reconstruction from tree-ring records. Can J Forest Res 32:1039–1056
Wisner B, Blaikie P, Cannon T, Davis I (2003) At risk: Natural hazards, people's vulnerability and disasters, 2nd edn. Routledge, London
Wolman MG, Miller JP (1960) Magnitude and frequency of forces in geomorphic processes. J Geol 68:54–74

Part II
Snow Avalanches

Avalanche tracks in Jasper National Park, Canadian Rocky Mountains (© M. Stoffel)

Dendrogeomorphology and Snow Avalanche Research

Brian H. Luckman

1 Introduction

Snow avalanches are rapid downslope transfers of snow, often with great destructive power, which are significant natural hazards in areas of steep terrain. Although normally observed in mountain areas, they may occur in lowland environments where local topographic conditions are suitable (e.g. Liverman et al. 2001). Although avalanches are rarely, if ever, initiated in forested terrain, snow avalanche tracks are often a common feature of sub-alpine forests. The calendar dated tree-ring record of damage in these tracks provides a powerful archive from which to examine the nature, magnitude and frequency of past avalanche activity and has been exploited for over 40 years. It was one of the first applications of dendrogeomorphology (Potter 1969; Shroder 1980) and there are over 50 references to snow avalanches in the tree-ring literature (Grissino-Mayer 2009). In this introduction I will briefly review some of that work and comment on some of the successes and problems associated with this research field.

2 The Nature of Snow Avalanches

Snow avalanches vary in size from a few to several million cubic meters of snow ranging in character from dry powder avalanches to dense wet snow or slush avalanches. The distribution and characteristics of snow avalanche activity depend on the interaction between (i) terrain variables that control slope characteristics and

B.H. Luckman (✉)
Department of Geography, University of Western Ontario, London, ON, N6A 5 C2, Canada
e-mail: luckman@uwo.ca

M. Stoffel et al. (eds.), *Tree Rings and Natural Hazards: A State-of-the-Art*, Advances in Global Change Research 41, DOI 10.1007/978-90-481-8736-2_2,

the accumulation patterns of snow and (ii) the meteorological and climatic conditions that control the amounts, distribution, physical characteristics and stability of snow on a sloping surface. The terrain characteristics usually determine the locations within the landscape where snow can accumulate to sufficient depth on an adequate slope (usually between 25° and 55°) to generate avalanches. Ultimately however, avalanches result from the mechanical failure of the snow cover when it becomes unstable. This may be the result of direct loading during precipitation events (either snow or rain on snow), changes in the physical characteristics of the snow cover over time, or inherent instability of the snow cover due to its depositional history and stratigraphy. An overview of avalanche types and related processes is given in McClung and Schaerer (1993).

3 Location and Distribution

Most avalanche sites associated with forests occur below major gullies or couloirs linking starting zones above treeline to run-out fans on lower valley sites. The location and distribution of snow avalanche sites can be predicted and mapped based on topographic features except where changes in forest cover, e.g. following fire or logging (Germain et al. 2005) make new sites available. Year-to-year variability in the magnitude and frequency of avalanches depends on the meteorological variables that control the amounts, strength and stratigraphy of the seasonal snow cover. Avalanche activity does not necessarily depend on the absolute amounts of snow but the rate, manner and history of snow accumulation and its mechanical strength. The mix of avalanche types will depend on the climatic regime of a particular region. In maritime or heavy snowfall sites "direct action" avalanches are triggered by loading during precipitation events in response to the rate, volume and physical characteristics (i.e. density) of the snowfall. Such avalanches are relatively easily predicted and are strongly related to precipitation amounts and history. However, drier, more continental (or interior) regions may exhibit a mix of avalanche types. "Delayed action" avalanches do not usually have an immediate meteorological trigger but result from inherent instability in the snowpack due to the presence of weak layers (e.g. depth hoar or sugar snow) or sliding surfaces within the snowpack that lead to failure following a minor triggering event (a skier, rockfall, cornice collapse, etc). The number and frequency of these types of avalanches depend on the history of accumulation and subsequent metamorphism of the snowpack. Wet spring thaw related avalanches are often of this type and are particularly damaging.

Snow avalanches almost always occur during the dormant season of tree growth and the evidence for avalanche damage in trees is manifest only in the rings of the subsequent growing seasons. It is therefore impossible to differentiate multiple events within a single year as the preserved record integrates the effects of all avalanches in the preceding winter (although the results of large single avalanches may be mapped). Therefore tree-ring studies at snow avalanche sites are largely

restricted to the reconstruction of the size, magnitude and (annual) frequency of events rather than a study of process dynamics. i.e. avalanche years rather than avalanches per se. Only rarely does dendrogeomorphology provide direct evidence of avalanche processes themselves e.g. where tree shear has been used to infer avalanche pressures (e.g. Mears 1975) or the distribution of debris used to infer transport processes in the formation of avalanche plunge pools (Smith et al. 1994). Relationships between avalanche characteristics (i.e. avalanche winters) and climate variables will depend on the dominant types of avalanches. In areas where many avalanches release independently of precipitation events, there will be little relationship between avalanches and total snowfall amounts (see e.g. Germain et al. 2010, this volume).

4 Evidence of Avalanche Activity

The dendrochronological evidence used to evaluate snow avalanche activity has been reviewed many times from the classic manual of Burrows and Burrows (1976) to the most recent papers of Butler and Sawyer (2008), Stoffel and Bollschweiler (2008) and Germain et al. (2009). Most tree-ring studies occur where avalanches are initiated on open slopes above the forest cover and a well defined avalanche track and runout zone terminates within the forest. Inferences about avalanches have been made on the composition and age of vegetation within those tracks but most tree-ring studies involve examination of avalanche damage to vegetation. External evidence includes tree death or breakage (often shear scars), tilting or uprooting (e.g. Akifyeva et al. 1978), scarring and development of leaders (i.e. epicormic branches or "reiterates") where apical dominance has been lost. Tree-ring studies examine internal evidence of damage such as reaction or tension wood series to define tilting events, locally missing rings, growth eccentricity, radial suppression events or, more recently, the development of tangential rows of traumatic resin ducts (TRD) in some coniferous species. This internal evidence is usually used to date the external damage. It also may be used to determine the date of the last significant event by studies of vegetation dynamics within the site. The tree-ring data are usually from damaged trees based on multiple cores, wedges or cross sections. While the latter are preferable because of the presence of micro rings and complex growth patterns (Fig. 1), cross sectioning may not be possible for conservation, aesthetic or practical reasons (e.g. tree size) though discrete wedge cuts in scar faces may be possible. Most studies have been carried out on coniferous species where, generally, annual rings and damage (e.g. reaction wood, TRD) are more clearly defined, though studies on deciduous species are becoming available (e.g. Mundo et al. 2007; Casteller et al. 2010, this volume).

The types of tree-ring evidence used to infer avalanche impact in trees may result from a wide range of geomorphic or biotic processes e.g., rockfall, debris flow, windthrow, insect outbreaks etc. In some cases processes can be separated based on the timing of damage or anatomical details – e.g. Stoffel et al. (2006)

Fig. 1 A cross section of alpine fir (*Abies lasiocarpa*) from Parker's Ridge, Banff National Park, Canada, showing multiple avalanche scars on the upslope (1965, 1973, 1974, and 1979) and downslope (1973/1974) sides plus several reaction wood series. The tree lived from 1929 to 1982

differentiate between snow avalanche and debris flow damage by the position of TRD within the annual ring as snow avalanches (winter/spring) and debris flows (summer/ fall) occur in different seasons. Recently Stoffel and Hitz (2008) have used anatomical differences to distinguish dormant season injuries from rockfalls and avalanches. In many cases however, spatial replication (at least two well separated trees), the location within avalanche tracks and the spatial pattern of damage (and/or position on the tree) is usually accepted as sufficient evidence to identify avalanche vs. other sources of damage within the avalanche track, unless there is strong morphological evidence for multiple debris-flow or significant rockfall activity at the site. In such cases more detailed mapping, sampling and anatomical work may be necessary to distinguish the geomorphic processes causing damage.

5 Developing Avalanche Chronologies

Although many studies have used ring-width measurement alone, the most common approach to developing an avalanche history is some variant of tree-ring "event-response analysis" initially promoted by Shroder (1980). Tree-ring data are used to identify individual "damage" events (i.e. avalanches) and build up an "event chronology" for the site. External scars, reaction wood events (in conifers) and growth asymmetry have been the most frequently used data as they allow the dating and determination of multiple events from the same tree. However, all of these phenomena vary in their expression within the tree e.g. reaction wood series differ in duration, radial encompassment and degree of development. Thus the investigator must make critical decisions about these data to build the event chronology, i.e. whether to "score "data as presence or absence, above a certain threshold value or in a series of graduated classes. Similarly, where multiple lines of evidence are available, the investigator must decide how to weight different lines of evidence e.g. reaction wood vs. corrasion scars or TRD. Different studies have adopted different approaches to this problem (see Frazer 1985; Reardon et al. 2008; Germain et al. 2009 and the discussion in Butler and Sawyer 2008), most of which produce reasonable "event chronologies". The event chronologies from individual trees are then compiled into a site chronology from which the occurrence and spatial extent of avalanches can be identified. These site chronologies are often expressed as an avalanche index for each year of record. This is usually some variant of the number of trees showing a response in a given year divided by the number of records available for that year (i.e. number of trees sampled) to compensate for the decreasing replication back in time (see Butler and Sawyer 2008; Germain et al. 2010, this volume for a discussion).

Sampling strategies depend on the purpose of the investigation. Normally damaged and/or dead trees are targeted within the avalanche track but sampling may follow a systematic or random pattern. Special attention is often given to the lateral track margins and the downslope runout zone to define the maximum extent of past avalanches. Where detailed avalanche frequency data are desired, sampling tends to be more intensive, particularly targeting older trees to maximize the length of record.

Two key questions arise around sampling: what is the minimal evidence required to identify an avalanche event within a given track and what is the optimal number of trees to be sampled to characterize avalanche activity in that track? In recent studies authors have suggested that synchronous evidence of avalanche damage should be present in at least 10%, 20% or 40% of the sampled trees containing records for a given year (Butler and Sawyer 2008; Butler et al. 2010, this volume, Germain et al. 2010, this volume, Reardon et al. 2008) and at least two trees. While such thresholds may be met in the most active parts of the track, these criteria become critical when establishing dating for older/ more extensive avalanche events where poor replication (fewer older trees or limited numbers of survivor trees) reduces sample numbers below these critical thresholds and thereby shortens the usable length of the avalanche history that can be reconstructed. In some cases older avalanches may be identified from strong evidence within a single tree (e.g. Burrows and Burrows 1976;

Frazer 1985; Luckman and Frazer 2001; Stoffel et al. 2006) based on the context at the site, the strength of the evidence and the purpose of the investigation. Though not ideal, this may be necessary where the sample population is limited in either the temporal or spatial domains. There is also no easy answer for the related question of what is the minimum number of trees needed to ensure a reasonable sampling of the avalanche history of a site. Germain et al. (2010, this volume) suggest diminishing returns when sampling more than 40 trees in a track. Butler and Sawyer (2008) suggest ten "good" trees could be adequate but obviously 100 trees would be better! Clearly the optimal number depends on the nature of the investigation, the age distribution of trees sampled and the desired length of the avalanche record. Though avalanche-damaged trees provide abundant evidence and a good record within the main track, older damaged trees and trees at the margin of the track may be far more critical. Two trees with 200 years of record may be more important for the avalanche history of a track than 30 trees that are only 50 years in age. Therefore, where practical, the critical number should be defined over a common period rather than an absolute figure and may have to differ e.g., between the main track and the downslope limits.

As a result of the avalanche destruction of trees within the track most well replicated event chronologies are usually less than 100 years, though still significantly longer than observational records. Several studies have compared historically documented and tree-ring derived records (e.g. Reardon et al. 2008; Muntán et al. 2010, this volume). Such comparisons rarely show 100% correspondence indicating that, where possible, a combination of the two approaches provides the most complete chronology. However, invariably the longer tree-ring derived record provides the greatest information about former high-magnitude events. Nevertheless the differential preservation of evidence makes it difficult to establish changes in the frequency of events over periods longer than the age of most trees within the track. In many cases the problem remains as to whether reconstructed changes in avalanche frequencies are real or reflect differential preservation of the evidence. Such studies must be assessed based on the sampling strategies used and the availability of supporting evidence, e.g. from appropriate climate data.

As the field has progressed and the acceptable evidence becomes more standardized, studies have progressed from individual sites, through specific valleys to studies with a more regional focus. Many recent studies have used site or regional chronologies to define the probability or recurrence intervals of avalanches (or avalanches of a given magnitude). These data are used to map individual large avalanches, avalanche frequency, magnitude and the probability of avalanches within the track (Reardon et al. 2008). However such reconstructions must recognize that as most evidence for older events is destroyed by younger avalanches, the older parts of the reconstructed record are censored to an unknown degree and therefore represent minimum frequencies. In addition individual trees are not consistent recorders of evidence over time i.e. the propensity to record damage varies with the age (and size) of the tree. Most authors ignore the first 10–20 years of record from young small trees for obvious reasons, but major tilting or scarring events may mask the evidence of later events in the same tree and, clearly, older and larger trees tilt less easily than younger ones (but young trees may tilt and bend rather than shear!). Therefore older trees at the track margin may

record earlier but not later events of equivalent magnitude. Nevertheless, despite these difficulties these historical and magnitude-frequency data do provide conservative estimates that are sufficient for first-order planning assessments of hazard zoning or avalanche defence. Exceptional events will always occur but these data can indicate the possible consequences of such events and allow planning accordingly.

6 Final Remarks

Tree-ring studies yield important information about the magnitude and frequency of snow avalanches that provide significant contributions to studies of avalanche hazard and defence, especially at sites where little previous avalanche history is known. Although the techniques and nature of the evidence are well established, it is difficult to provide prescriptive sampling designs or sample numbers for these studies because the needs vary depending on the specific purpose of the investigation, the nature of track vegetation and avalanche history of the site. Probably the most extreme events in last few 100 years can be defined if the forest is old enough but quantitative estimates of avalanche frequency and magnitude should probably be restricted to the last 50–100 years. Studies are now being carried out in mountain areas and with new species away from the North American and Alpine sites where many of the techniques were developed. The following four contributions provide a cross section of this ongoing work. The two shorter papers show initial applications of tree-ring studies to new areas (and species) in Spain and Argentina. Casteller et al. also provide an example of the use of tree-ring data to calibrate computer models of avalanche activity (also suggested by Germain et al. 2010, this volume). The paper by Butler et al. (2010, this volume) explores the potential use of tangential rows of traumatic resin ducts (a relatively new initiative) as an indicator of avalanche activity at sites where many previous studies have been done. Finally Germain et al. (2010, this volume) discuss a wide range of methods and the building of regional chronologies of avalanche activity to develop a regional picture of avalanche history and hazard for Gaspésie in Québec. These papers all illustrate promising future directions in this research, namely; the application of standard techniques to new areas, combining tree-ring studies with modeling data to predict avalanche hazards, the exploitation and better definition of new anatomical evidence of hazard plus the attempt to expand analyses and provide regional syntheses of hazard and relationships with climate.

References

Akifyeva KV, Volodicheva NA, Troshina ES, Turmanina VT, Tushinsky GK (1978) Avalanches of the USSR and their influence on the formation of natural-territory complexes. Arct Alp Res 10:223–233

Burrows CJ, Burrows VL (1976) Procedures for the study of snow avalanche chronology using growth layers of woody plants. Arct Alpin Res Occas Paper No. 23

Butler DR, Sawyer CF (2008) Dendrogeomorphology and high-magnitude snow avalanches: a review and case study. Nat Haz Earth Syst Sci 8:303–309

Butler DR, Sawyer CF, Maas JA (2010) An examination of the presence of traumatic resin ducts in annual tree rings of two species affected by snow avalanches in Glacier National Park, Montana, USA. In: Stoffel M, Bollschweiler M, Butler DR, Luckman BH (eds) Tree rings and natural hazards: A state-of-the-art. Springer, Berlin, Heidelberg, New York, this volume

Casteller A, Christen M, Villalba R, Stöckli V (2010) Dendrochronology as a tool for validating numerical simulations of snow avalanches in the Patagonian Andes. In: Stoffel M, Bollschweiler M, Butler DR, Luckman BH (eds) Tree rings and natural hazards: A state-of-the-art. Springer, Berlin, Heidelberg, New York, this volume

Frazer GW (1985) Dendrogeomorphic evaluation of snow avalanche history at two sites in Banff National Park. M.Sc. Thesis, University of Western Ontario

Germain D, Filion L, Hétu B (2005) Snow avalanche activity after fire and logging disturbances, northern Gaspé Peninsula, Québec, Canada. Can J Earth Sci 42:2103–2116

Germain D, Filion L, Hétu B (2009) Snow avalanche regime and climatic conditions in the Chic-Chocs Range, eastern Canada. Clim Change 92:141–167

Germain D, Hétu B, Filion L (2010) Tree-ring based reconstruction of past snow avalanche events and risk assessment in Northern Gaspé Peninsula (Québec, Canada). In: Stoffel M, Bollschweiler M, Butler DR, Luckman BH (eds) Tree rings and natural hazards: A state-of-the-art. Springer, Berlin, Heidelberg, New York, this volume

Grissino-Mayer HD (2009) Bibliography of Dendrochronology. http://wsl.ch/dbdendro/index-EN. Accessed on 16 April 2009

Liverman D, Batterson M, Taylor D, Ryan J (2001) Geological hazards and disasters in Newfoundland and Labrador. Can Geotech J 38:936–956

Luckman BH, Frazer GW (2001) Dendrogeomorphic investigations of snow avalanche tracks in the Canadian Rockies. Paper presented at the international conference on the future of dendrochronology, Davos, Switzerland, 22–26 September 2001

McClung D, Schaerer P (1993) The avalanche handbook. The Mountaineers, Seattle, Washington, DC

Mears AI (1975) Dynamics of snow avalanches interpreted from broken trees. Geology 3:521–523

Mundo IA, Barrera MD, Roig FA (2007) Testing the Utility of Nothofagus pumilo for dating a snow avalanche in Tierra del Fuego, Argentina. Dendrochronologia 25:19–28

Muntán E, Oller P, Gutiérrez E (2010) Tracking past snow avalanches in the SE Pyrenees. In: Stoffel M, Bollschweiler M, Butler DR, Luckman BH (eds) Tree rings and natural hazards: A state-of-the-art. Springer, Berlin, Heidelberg, New York, this volume

Potter N Jr. (1969) Tree-ring dating of snow avalanches, northern Absaroka Mountains, Wyoming. In: Schumm SA, Bradley WS (eds) Contributions to Quaternary Research INQUA VIII. Geol Soc Am (Special Paper) 123:141–165

Reardon BA, Pederson GT, Caruso CJ, Fagre DB (2008) Spatial reconstructions and comparisons of historic snow avalanche frequency and extent using tree-rings in Glacier National Park, Montana, USA. Arct Antarc Alp Res 40:148–160

Shroder JF (1980) Dendrogeomorphology: review and new techniques of tree-ring dating. Prog Phys Geogr 4:161–188

Smith DJ, McCarthy DP, Luckman BH (1994) Snow-avalanche impact pools in the Canadian Rocky Mountains. Arct Alp Res 26:116–127

Stoffel M, Bollschweiler M (2008) Tree-ring analysis in natural hazards research – an overview. Nat Haz Earth Syst Sci 8:187–202

Stoffel M, Bollschweiler M, Hassler G-R (2006) Differentiating past events on a cone influenced by debris-flow and snow avalanche activity – a dendrogeomorphological approach. Earth Surf Process Land 31:1427–1434

Stoffel M, Hitz OM (2008) Rockfall and snow avalanche impacts leave different anatomical signatures in juvenile rings of Larix decidua. Tree Physiol 28:1713–1720

Tree-Ring Dating of Snow Avalanches in Glacier National Park, Montana, USA

David R. Butler, Carol F. Sawyer, and Jacob A. Maas

1 Introduction

Snow avalanches are major hazards to humans occupying or visiting mountain ranges around the world. Accurate dating of past high-magnitude snow avalanches is important for a better understanding of their frequency, extent, and climatic driving factors. As climates change, prediction of shifts in avalanche frequency and/or magnitude are better enabled when a thorough understanding of past avalanche occurrences exists.

Tree rings are a primary data source for the dating of past snow-avalanche occurrence. A recent development in dendrogeomorphology, the use of traumatic resin ducts in annual rings of select conifers, has shown great promise for expanding the utility of tree-ring dating of geomorphic processes such as avalanches, rockfalls, and debris flows (see below). This work has, to date, been restricted almost exclusively to the analysis of geomorphic processes in the Alps of central Europe. In this work, we seek to determine if traumatic resin duct analysis can be used to assist in the dating of snow avalanches in the mountains of western North America. We also bring together past work on tree-ring dating of snow avalanches in a major American national park, in order to more fully assess the synoptic climatic patterns associated with major avalanche winters there.

D.R. Butler (✉) and J.A. Maas
Department of Geography, Texas State University-San Marcos, San Marcos, TX 78666-4616, USA
e-mail: db25@txstate.edu

C.F. Sawyer
Department of Earth Sciences, University of South Alabama, Mobile, AL, 36688-0002, USA

M. Stoffel et al. (eds.), *Tree Rings and Natural Hazards: A State-of-the-Art*, Advances in Global Change Research 41, DOI 10.1007/978-90-481-8736-2_3,

2 Glacier National Park Study Area

Glacier National Park, Montana (henceforth GNP), and its Canadian neighbor Waterton Lakes National Park (WLNP), Alberta, collectively comprise the Waterton-Glacier International Peace Park along the 49th parallel (Fig. 1). Both Parks were extensively glaciated during the Pleistocene, creating an avalanche-prone landscape

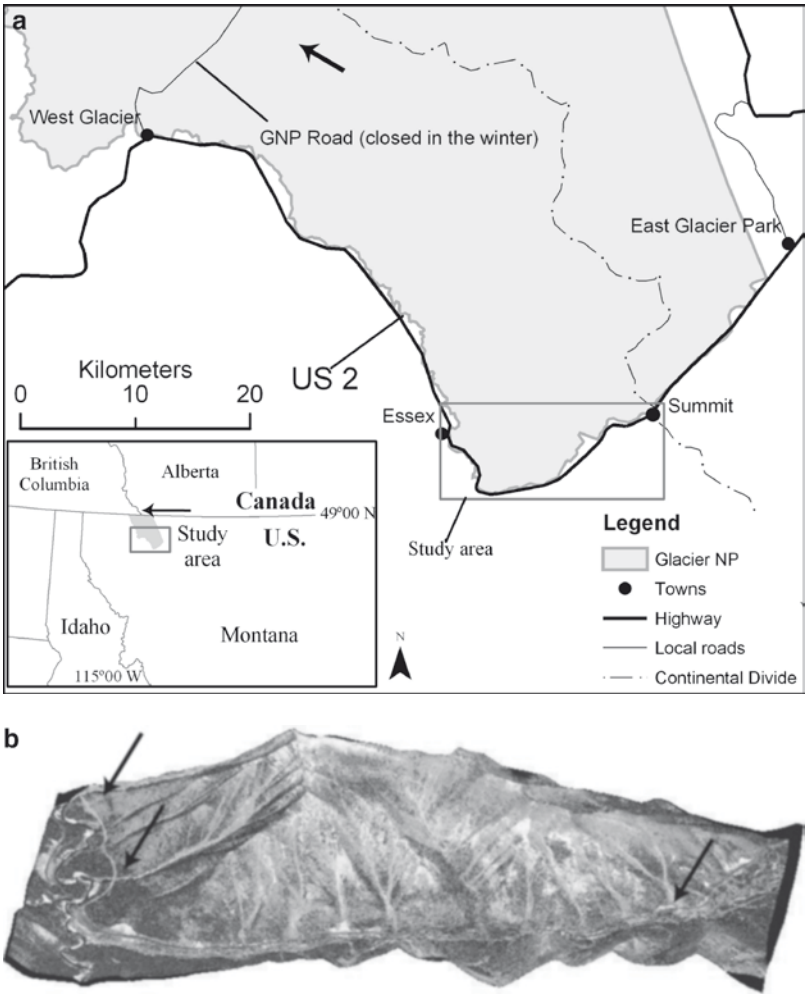

Fig. 1 (**a**) (*above*) Map of US Highway two study area along southern boundary of Glacier National Park, Montana, USA. *Arrow in inset map* points to Waterton Lakes study site in Alberta. *Arrow on main map* points to Snyder Lake study site. (**b**) (*below*) Three-dimensional view of the study area and the numerous snow-avalanche paths. *Left black arrow* points Goat Lick avalanche path, *middle black arrow* to I-Beam path, *right arrow* to Shed 7 path. Three-dimensional image is comprised of 1-m Ikonos image merged with and draped over a 10-m Digital Elevation Model

of steep mountainous slopes and deep U-shaped valleys. Elevations range from ca. 960–1,000 m asl in the glacial valleys in western Glacier Park to more than 3,000 m on the Parks' highest peaks. GNP is split approximately in half by the Continental Divide, producing differing local climatologies; the western half experiences a modified Pacific-maritime climate, with maximum precipation levels on the high western slopes near the Continental Divide. All of WLNP is east of the Continental Divide, and shares with the eastern half of GNP a more severe and windy, interior continental climate (Butler et al. 1992).

More than 1,200 avalanche paths exist in the Parks (Butler et al. 1992). Tree-ring dating of snow avalanches has been carried out in the central and southern portions of GNP (locations shown in Fig. 1) (Butler 1979; Butler and Malanson 1985; Butler and Sawyer 2008), and in 2001 a pilot study was also carried out in adjacent WLNP; those data are reported here for the first time. This latter study was initiated to determine if broad regional patterns of avalanching that have been reported from GNP (Butler 1986, 1989; Butler and Sawyer 2008; Reardon et al. 2008) extend as far north as WLNP.

Butler (1986, 1989) identified two broad-scale synoptic patterns that produce widespread avalanching in the study area: pronounced meridional flow associated with Arctic air outbreaks resulting in catastrophic avalanching caused by heavy snowfall from rapid advection of warm, moist Pacific air over the Arctic air; or strong zonal flow with frequent storms from the Pacific Ocean to the west, resulting in heavy snowfalls. Reardon et al. (2008) noted that the meridional flow pattern characterized almost all major avalanche events in John F. Stevens Canyon along the southern border of GNP, the area of the Park with the greatest avalanche hazard for human activity. Over 40 snow-avalanche paths are located within this canyon, with the paths primarily located between the towns of Essex and Summit (Fig. 1). Snow avalanches there frequently disrupt highway and rail traffic on US Highway 2 (US 2), and the Burlington Northern – Santa Fe Railroad (BNSF) that runs parallel to US 2 (Butler and Malanson 1985, 1990; Sawyer and Butler 2006; Reardon et al. 2008). The bulk of these hazardous snow avalanches originate on unmanaged slopes to the north in GNP, with some also coming from the adjacent unmanaged National Forest to the south. Although this region is sparsely populated, transportation through JFS Canyon serves as an important link between several otherwise isolated communities. When US 2 is closed by avalanches, a 300-km detour is required in order to drive from the western to the eastern side of GNP. Avalanche closure of the tracks of the BNSF creates costly interruptions and stoppages in the transport of goods between Midwestern US cities and major Pacific coast ports, and creates the potential for hazardous cargo spills in the pristine environment of the canyon.

3 Tree-Ring Features Analyzed for Dating Snow Avalanches

When snow avalanches impact forests, trees may be tilted and/or uprooted, trunks can be scarred, branches may be trimmed, surrounding trees may be removed, and material may be deposited against or around the trunk of trees.

Typical tree-ring features analyzed for the study and dating of snow avalanches include corrasion scars initiated by impact; initiation and continuation of reaction wood in response to tilting; suppression rings associated with stress caused by tilting, burial, and/or branch trimming; or release rings created as a tree responds to the removal of competing neighboring trees (Germain et al. 2005; Decaulne and Sæmundsson 2008; Casteller et al. 2008; Reardon et al. 2008; also see Butler and Sawyer 2008, and Stoffel and Bollschweiler 2008, for recent reviews of earlier papers describing dendrogeomorphic techniques employed in the study of snow avalanches). These tree-ring features allow for to-the-year identification of past snow avalanche occurrence. Most practitioners have agreed that corrasion scars and reaction wood growth provide the most unequivocal evidence for avalanche-induced trauma that can be separated from climatic variations that can also induce suppression/release ring patterns similar to those avalanching may initiate (Germain et al. 2005; Butler and Sawyer 2008; Decaulne and Sæmundsson 2008; Reardon et al. 2008).

The newest tree-ring technique that furthers the dating of snow avalanches is the use of traumatic resin ducts (TRD) in conifers scarred and tilted by avalanche activity. Larocque et al. (2001) used TRD initiated by basal stem burial, together with corrasion scars and reaction wood, to date slushflows in the Gaspé peninsula of Québec, Canada. More recently, Stoffel and associates have initiated the widespread use of TRD as a tool in dendrogeomorphology that provides to-the-year, and in some cases seasonal, dating of geomorphic process occurrences, including snow avalanches (Stoffel et al. 2006; Bollschweiler et al. 2008; Stoffel 2008; Stoffel and Bollschweiler 2008; Stoffel and Hitz 2008). TRD appear under a microscope as asymmetric, atypical cells differing in appearance from normal earlywood or latewood cells (excellent examples of TRD photomicrographs appear in Stoffel and Bollschweiler (2008)).

4 Tree-Ring Analysis of Snow Avalanches in Glacier National Park

Tree ring sampling described in this section employed standard dendrogeomorphic techniques. Species were recorded in the field for each tree; cores or cross-cut discs were collected and air-dried, and subsequently sanded; cross-dating, in accordance with the methods of Stokes and Smiley (1968), was employed; and tree-ring event responses were recorded for each year following Shroder (1978, 1980).

The first application of tree-ring analysis for the dating of past high-magnitude avalanche events was from the central portion of GNP in the Snyder Creek valley (Fig. 1) (Butler 1979). Tree rings from that study were collected in 1975, and extend back to the early twentieth Century. Butler (1979), using a relatively high minimum threshold cutoff, identified major avalanche events in the valley in 1945, 1950, 1954, 1963, 1965, 1966, 1972, and 1974. A re-examination of these data, utilizing a lower minimum threshold of 20% as advocated by Butler and Sawyer (2008), adds the winters of 1933, 1948, and 1957 to this data set (Table 1).

Table 1 Comparison of high-magnitude snow avalanche years with high SWE years

Snyder Creek	Goat Lick	I Beam	Shed 7	Waterton	High SWE[a]
	1925				
1933					
	1935		1935		
	1937				
					1939
					1943
1945	1945	1945			
		1947			1947
1948			1948		
					1949
1950	1950		1950		1950
					1951
		1952	1952		
1954		1954	1954		1954
					1956
1957	1957		1957		
		1959			
1963	1963		1963		
		1964			
1965	1965		1965		1965
1966					
					1967
			1969		
			1970	1970	
1972	1972	1972	1972	1972	1972
1974		1974	1974		1974
[b]					
			1976		
	1979	1979	1979		
	1982[c]	1982	1982	1982	
	[b]				
			1985		
		1987	1987		
				1988	
			1989		
		1991	1991	1991	1991
		1996		1996	1996
		1997			1997
				[b]	
		2002	2002		2002

[a]SWE data from Reardon et al. (2008)

[b]Last tree-ring year for Snyder Creek, 1975; for Goat Lick, 1983; for Waterton, 2001; for I Beam and Shed 7, 2002

[c]Goat Lick experienced large avalanche below level of sampled trees

Butler and Malanson (1985) created tree-ring histories of high-magnitude avalanches for the Goat Lick and Shed 7 paths in the Stevens Canyon region of GNP (Fig. 1) (all avalanche path names in Stevens Canyon are informal names used by the US Geological Survey). Those samples were collected in 1983, and the ages of the samples extend back into the 1920s (Table 1). Years of major avalanche events from these paths were broadly similar both to each other and to the Snyder Creek record from central GNP (Table 1); in 6 years all three paths experienced large avalanches, and in four additional winters one of the two southern paths matched with Snyder Creek.

Butler and Sawyer (2008) extended the Shed 7 path history to that shown in Table 1, and also created the first chronology for the I Beam path, located between the Goat Lick and Shed 7. Although the I Beam chronology was only based on a sample of ten trees uprooted by avalanching in 2002, the record cross-dated with four major avalanche winters from Snyder Creek, and with 6 from either or both Goat Lick and Shed 7.

Recently, Reardon et al. (2008) used dendrogeomorphic techniques to create a chronology of high-magnitude avalanching on another avalanche path in Stevens Canyon, Shed 10.7, located a few kilometers down canyon from Shed 7. An exact comparison of their record with the others described here is hampered by their use of a 10% minimum threshold event-response value. Nevertheless, in comparing their record to the records from Goat Lick and Shed 7, they noted that 10 years identified in their study corresponded to those at either Goat Lick or Shed 7, and 4 avalanche years (1935, 1950, 1957, and 1979) were common to all three paths (Reardon et al. 2008). It is also notable that two of these years (1950 and 1957) correspond to the record from Snyder Creek, roughly 40 km to the northwest (Fig. 1). Although the tree-ring record for Snyder Creek ends in 1975, a visit there in 1983 revealed widespread damage very probably attributable to a high-magnitude avalanche on that path in 1979 (Butler 1985) that would also match with Shed 10.7 as well as with Goat Lick, I Beam, and Shed 7.

Because the comparison of the Snyder Creek record with the Stevens Canyon records reveals such widespread temporal correspondence, a preliminary reconnaissance of an avalanche path along the Cameron Lake road in WLNP (Fig. 1) was undertaken in 2001, with ten cross-cut samples collected from damaged trees in the runout zone. Sampled trees in this pilot project were small, and the tree-ring record only extends back into the 1960s. This record only overlaps the Snyder Creek record by about 10 years, and only about 20 years for the Goat Lick record. Nevertheless, the WLNP record corresponds with every other sample path from Snyder Creek and Stevens Canyon in 1972; with every available Stevens Canyon path in 1982 and 1991; and at least one other sampled path in two of the other three recorded years of high-magnitude avalanche activity. This path did not record a 1979 event, but the sampled trees were probably simply too small (and possibly protected beneath the snowpack) to be affected by an avalanche in that year.

5 Implications for the Avalanche Climatology of the Region

Widespread avalanching during many winters, from the eastern side of the Continental Divide in WLNP to Stevens Canyon on the western side of the Divide on the southern tip of GNP, as well as at points throughout the Parks including Snyder Creek (Butler 1979, 1986) is evidence of a regional avalanche climatology covering the entire Peace Park. Reardon et al. (2008) suggested that these periods of widespread avalanching coincide with episodes of meridional flow and intrusion of cold Arctic air masses over which moist Pacific air is subsequently advected, leading to heavy snowfall and avalanching. Rainfall often accompanies this advection and acts as an additional catastrophic avalanche trigger of wet-snow avalanches (Reardon et al. 2008), a conclusion also noted previously by Butler (1986). Most years with major avalanches coincide with years in which the El Niño Southern Oscillation (ENSO) and mean January-February Pacific Decadal Oscillation (PDO) indices were neutral (Dixon et al. 1999; Reardon et al. 2008).

Reardon et al. (2008) compared their avalanche chronology of high-magnitude avalanches at Shed 10.7 with the annual 1 March snow water equivalent (SWE) snow course record from Marias Pass, located on the Continental Divide 16 km northeast of Shed 10.7 at Summit (Fig. 1). Their results demonstrated a strong correlation between positive snowpack anomalies (in excess of 10% above the long-term mean) and winters with high-magnitude avalanches. In Table 1, we tabulate

Fig. 2 Tree sampling areas on Shed seven avalanche path (*arrows*). Note downed trees on roof of railroad snowshed man stands on, and on ground beyond snowshed

these same years against our chronologies of high-magnitude avalanche winters at Snyder Creek, Goat Lick, I Beam, Shed 7, and Waterton. The results illustrate a good relationship between episodes of widespread avalanching (years 1950, 1954, 1965, 1972, 1974, 1991, 1996, and 2002) and years with high SWE anomalies, not only in Stevens Canyon but at Snyder Creek in central GNP (1950, 1954, 1965, 1972, and 1974) and in WLNP (1972, 1991, 1996).

Interestingly, the most widespread avalanching in recorded history occurred in February 1979 (Butler and Malanson 1985; Butler 1986; Sawyer and Butler 2006; Reardon et al. 2008), but that year does not coincide with a high positive SWE anomaly. Park Service officials in GNP noted that "just about every place in the park that can avalanche has avalanched yesterday and today (Butler 1986, p. 79). The catastrophic avalanching was triggered by a "Pineapple Express" of moisture-laden Pacific air flowing in from the southwest, producing widespread extended rainfall on a deep but not abnormally thick snowpack (Butler 1986).

6 Initial Observations on Traumatic Resin Ducts and Their Use for Dating Snow Avalanches in Glacier National Park

The particular benefit of TRD is their circumferential extent (on average, in almost one-fifth of the total circumference; Bollschweiler et al. 2008). This circumferential extent makes identification via increment-core sampling much easier, whereas in

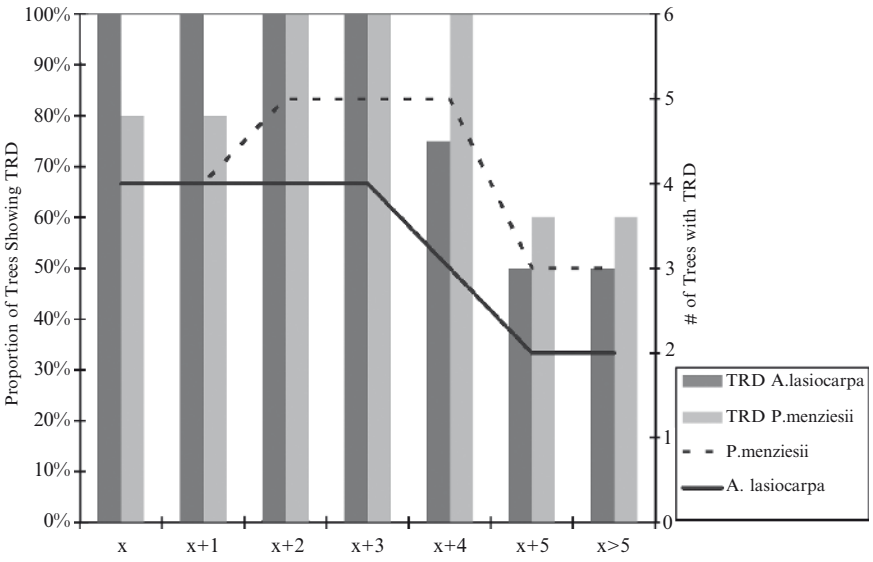

Fig. 3 Graph illustrating number of years' persistence of TRD after initiating scarring event, and percentage of samples per year illustrating presence of TRD

the past the use of cores for dating snow avalanches has been particularly challenging when trying to date onset of corrasion scar growth. The seasonality of TRD occurrence within an annual tree ring can also assist in differentiating between geomorphic processes such as snow avalanches and debris flows (Stoffel et al. 2006), or avalanches and rockfalls (Stoffel and Hitz 2008).

The aforementioned work by Larocque et al. (2001) is the only known application of TRD for dendrogeomorphic purposes in North America. The bulk of analyses of TRD (also called traumatic resin canals) in North America have focused on biotic infections as causal agents (Cruickshank et al. 2006). TRD are known to develop in North American species of the genera *Abies* (fir), *Picea* (spruce), and *Pinus* (pine), and in the species *Pseudotsuga menziesii* (Douglas fir) (Cruickshank et al. 2006).

Widespread avalanching occurred throughout the JFS Canyon region, stopping traffic on both US 2 and the BNSF, in the winter of 2001–2002. Large, mature conifers were uprooted and deposited by avalanches in the furthest reaches of individual path runout zones, outside the boundary of GNP (Fig. 2), providing an opportunity for tree-ring sampling of downed trees without sacrificing living trees within or along the margins of avalanche paths in the protected national park.

Cross sectional discs were collected from ten uprooted trees in the I Beam path and 12 trees in the Shed 7 path. Analyses of the corrasion scars and reaction wood from these discs provided the chronology of high-magnitude avalanche winters for each path described herein and by Butler and Sawyer (2008). Because of the serendipitous deposition of avalanche-damaged trees from which cross-cut samples could be extracted, we also used these samples to determine if TRD occurred in their circumferences.

We examined each of the cross-cut samples under a binocular microscope for the presence of TRD in the annual rings. The majority of the samples examined did not possess corrasion scars; these samples also did not illustrate TRD. TRD were identified, in association with corrasion scars, in five Douglas fir (*Pseudotsuga menziesii*) and four subalpine fir (*Abies lasiocarpa*) samples. We recorded the longevity (how many years duration) of TRD in every case where TRD were initiated. The angular circumferential extent of the TRD in each annual ring was also recorded. We also noted any delays in initiation of TRD between the ring in which scarring occurred and the ring in which TRD were initiated. We employed the Mann-Whitney U test, because of the small sample size, to determine if there existed any difference in the longevity of TRD between Douglas fir and subalpine fir samples; we did the same to determine if there existed any difference between the angular extent of TRD between the two species.

Every corrasion scar examined, in both species, also illustrated the initiation of TRD. In nearly every case (all but one, a Douglas fir), TRD were initiated in the same annual ring as the year in which scarring occurred (Fig. 3); the lone exception had a 2-year lag response. In all cases, TRD endured for at least 4 years (Fig. 3), after which drop-off occurred. Nevertheless, most samples showed a continuation of TRD in annual rings beyond 4 years after scarring initiated TRD production. The Mann Whitney test illustrated that no difference in TRD longevity existed between the two species under examination.

The angular extent of TRD associated with individual scars varied, depending on the size and severity of the corrasion scar. In general, year two often had the widest angular extent of TRD, followed by a relatively rapid drop-off in circumferential extent. Occasional secondary increases in extent were noted; we have no explanation for such features at this time. The Mann Whitney test illustrated no difference in the angular extent of TRD between Douglas fir and subalpine fir.

These initial observations showed the presence of TRD in association with corrasion scars from a year of known avalanching, establishing the utility of TRD in tree-ring studies of avalanching in North America. Our next step is to go back through our samples collected from 1975 to 2002, and seek out TRD to discern if we can identify previously unrecorded avalanche episodes contained therein.

7 Conclusion

This study is the first known illustration of traumatic resin ducts in avalanche-affected tree rings in western North America. TRD were identified in avalanche-affected tree rings from both Douglas fir and subalpine fir, two species with widespread distribution throughout the western cordillera of North America. The two sampled species showed virtually no difference in the form, longevity, or angular extent of TRD in affected annual rings. Given the absence of a difference in their utility, and their respective widespread distributions in the western USA and Canada, the potential exists for using TRD in annual rings of affected trees throughout the region. Future studies should also focus on examining additional widespread genera such as *Picea*, *Larix* (both certainly useful genera in studies in the Alps by Stoffel and associates), and *Pinus* to determine their possibility in dendrogeomorphic studies of snow avalanches. Attention should also be given to intra-annual variations in positioning of TRD, as described by Stoffel et al. (2006) and Stoffel and Hitz (2008), to determine if snow avalanches induce TRD at different points within an annual ring than do other geomorphic processes.

Examination of the avalanche chronologies from across GNP and an initial chronology from WLNP illustrates the widespread nature of high-magnitude snow avalanche winters in the area. Although exceptions occur, such as in the catastrophic avalanche cycle of February, 1979, the most widespread signals coincide with years of anomalously high snowpacks (SWE), and are triggered by meridional intrusions of cold Arctic air that cause advection of moist Pacific air, inducing heavy snowfall and in some cases rain-on-snow events.

Acknowledgements This research was funded by a 2002 National Science Foundation Small Grant for Exploratory Research to Butler, G.P. Malanson, S.J. Walsh, and D.B. Fagre (BSC-0234018), the US Geological Survey Global Change program (through D.B. Fagre to Butler), a Waiver of Fees from Parks Canada, a Quick-Response Grant from the Natural Hazards Research and Applications Information Center to Butler, and grants from the Burlington Northern Foundation and the Association of American Geographers to Butler and G.P. Malanson. Housing and camping fee waivers in West Glacier were provided by the US National Park Service. G.P.

Malanson, S.J. Walsh, B. Reardon, L.M. Resler, H.J.M. Sandford, S. Panciera, and W.A. Marienau assisted in sample collection. A. Sawyer assisted in the preparation of the cross sections for the TRD analysis. Figure 1b is provided courtesy of S.J. Walsh. This paper is a Contribution of the Mountain GeoDynamics Research Group.

References

Bollschweiler M, Stoffel M, Schneuwly D, Bourqui K (2008) Traumatic resin ducts in *Larix decidua* stems impacted by debris flows. Tree Physiol 28:255–263

Butler DR (1979) Snow avalanche path terrain and vegetation, Glacier National Park, Montana. Arct Alp Res 11:17–32

Butler DR (1985) Vegetational and geomorphic change on snow avalanche paths, Glacier National Park, Montana, USA. Great Basin Nat 45:313–317

Butler DR (1986) Snow-avalanche hazards in Glacier National Park, Montana: meteorologic and climatologic aspects. Phys Geogr 7:72–87

Butler DR (1989) Snow-avalanche dams and resultant hazards in Glacier National Park, Montana. Northwest Sci 63:109–115

Butler DR, Malanson GP (1985) A history of high-magnitude snow avalanches, southern Glacier National Park, Montana, USA. Mt Res Dev 5:175–182

Butler DR , Malanson GP (1990) Non-equilibrium geomorphic processes and patterns on avalanche paths in the northern Rocky Mountains, USA. Z Geomorphol 34:257–270

Butler DR, Sawyer CF (2008) Dendrogeomorphology and high-magnitude snow avalanches: a review and case study. Nat Haz Earth Syst Sci 8:303–309

Butler DR, Malanson GP, Walsh SJ (1992) Snow-avalanche paths: conduits from the periglacial alpine to the subalpine-depositional zone. In: Dixon JC, Abrahams AD (eds) Periglacial Geomorphology. Wiley, London, pp 185–202

Casteller A, Christen M, Villalba R, Martinez H, Stöckli V, Leiva JC, Bartelt P (2008) Validating numerical simulations of snow avalanches using dendrochronology: the Cerro Ventana event in Northern Patagonia, Argentina. Nat Haz Earth Syst Sci 8:433–443

Cruickshank MG, Lejour D, Morrison DJ (2006) Traumatic resin canals as markers of infection events in Douglasfir roots infected with *Armillaria* root disease. Forest Pathol 36:372–384

Decaulne A, Sæmundsson Þ (2008) Dendrogeomorphology as a tool to unravel snow-avalanche activity: preliminary results from the Fnjóskadalur test site, Northern Iceland. Norsk Geografisk Tidsskrift 62:55–65

Dixon RW, Butler DR, DeChano LM, Henry JA (1999) Avalanche hazard in Glacier National Park: an El Niño connection? Phys Geogr 20:461–467

Germain D, Filion L, Hétu B (2005) Snow avalanche activity after fire and logging disturbances, northern Gaspé, Quebec, Canada. Can J Earth Sci 42:2103–2116

Larocque SJ, Hétu B, Filion L (2001) Geomorphic and dendroecological impacts of slushflows in central Gaspé peninsula (Québec, Canada). Geogr Ann 83A:191–201

Reardon BA, Pederson GT, Caruso CJ, Fagre DB (2008) Spatial reconstructions and comparisons of historic snow avalanche frequency and extent using tree rings in Glacier National Park, Montana, USA. Arct Antarc Alp Res 40:148–160

Sawyer CF, Butler DR (2006) A chronology of high-magnitude snow avalanches reconstructed from archived newspapers. Disas Prevent Manage 15:313–324

Shroder JF Jr (1978) Dendrogeomorphological analysis of mass movement on Table Cliffs Plateau, Utah. Quat Res 9:168–185

Shroder JF Jr (1980) Dendrogeomorphology: review and new techniques of tree-ring dating. Prog Phys Geogr 4(2):161–188

Stoffel M (2008) Dating past geomorphic processes with tangential rows of traumatic resin ducts. Dendrochronologia 26:53–60

Stoffel M, Bollschweiler M (2008) Tree-ring analysis in natural hazards research – an overview. Nat Haz Earth Syst Sci 8:187–202

Stoffel M, Bollschweiler M, Hassler G-R (2006) Differentiating past events on a cone influenced by debris-flow and snow avalanche activity – a dendrogeomorphological approach. Earth Surf Process Land 31:1424–1437

Stoffel M, Hitz OM (2008) Rockfall and snow avalanche impacts leave different anatomical signatures in tree rings of juvenile *Larix decidua*. Tree Physiol 28:1713–1720

Stokes MA, Smiley TL (1968) An introduction to tree-ring dating. University of Chicago Press, Chicago

Tracking Past Snow Avalanches in the SE Pyrenees

Elena Muntán, Pere Oller, and Emilia Gutiérrez

Winter 1995–1996 was an exceptional snow avalanche season in the Pyrenees. Núria Valley, at the SE Pyrenees, registered four avalanches that reached a rack railway that runs along the valley floor. One of these avalanche paths, Canal del Roc Roig, was studied by dendrochronological means. Muntán et al. (2004) reported tree-ring evidence for two previously known snow avalanches and provided striking evidence for one undocumented event that occurred in 1929–1930. Subsequently, to unveil past avalanches more extensive research based on a higher sample density was carried out. The results of this research are outlined here.

A total of 777 samples, mostly increment cores, from 265 Mountain pine (*Pinus uncinata*) were analysed. A local reference chronology from old unaffected trees was built to date snow avalanche samples. Disturbed *P. uncinata* trees showed the following ring responses: compression wood, growth suppression, growth release, wounds, traumatic resin ducts and death of the tree. Compression wood and growth suppression were the most frequent. Resin ducts are ordinarily abundant in this species, so only very few unmistakable tangential rows of traumatic resin ducts were quantified. For the total count, the different tree-ring responses had identical weight, and disturbed trees were considered equal regardless of the number of responses per tree.

Dating of past snow avalanches was done in accordance with the following criteria. (1) High proportion of trees showing synchronic growth disturbances. (2) No similar growth disturbances in the reference chronology. (3) Coexistence of a variety of tree-ring responses. (4) Spatial concordance between in situ affected trees and avalanche trajectory. (5) Growth disturbances starting in the early earlywood.

E. Muntán (✉) and E. Gutiérrez
Department of Ecology, Faculty of Biology, University of Barcelona,
E-08028, Barcelona, Spain
e-mail: emuntan@ub.edu

P. Oller
Geological Institute of Catalonia, Balmes 209–211, E-08006 Barcelona, Spain

M. Stoffel et al. (eds.), *Tree Rings and Natural Hazards: A State-of-the-Art*,
Advances in Global Change Research 41, DOI 10.1007/978-90-481-8736-2_4,

Three documented snow avalanche seasons, on account of the damage to the railway (1971–1972, 1985–1986, and 1995–1996), showed respectively 26.3%, 16.9%, and 35.7% of trees with dendrochronological evidence (Fig. 1). In line with Butler and Sawyer (2008), who recommend tempering an index value with historical records for specific sites, after the documented 1985–1986 snow avalanche, 16% was used as the threshold to consider the occurrence of events. As a result, other avalanche seasons were identified: 1915–1916, 1929–1930, 1973–1974, 1981–1982, and 1990–1991. However, trees are scarce and younger than 75 years at the runout, and this hampered the interpretation of extent for events prior to 1925. Eventually, from a total number of eight avalanche winters for the twentieth century, five could be assessed only by dendrochronological means. These results highlight the potential of dendrogeomorphology to yield information on avalanche occurrences, provided that a high sample density fieldwork is performed.

Winters 1995–1996 and 1929–1930 held the highest proportion of growth-disturbed trees (35.7% and 42.6% respectively) corresponding to high-magnitude snow avalanches, and coming close to 40%, the index value first used by Butler and Malanson (1985). Based on the spatial distribution of trees, the extent of these major avalanches was mapped (Fig. 2). The dendrogeomorphic map of the 1995–1996 avalanche showed that the starting zone was broader than the mapped, in a winter survey, shortly after the avalanche released (see also Molina et al. 2004). Tree-ring data determined that the 1929–1930 event was a first magnitude snow

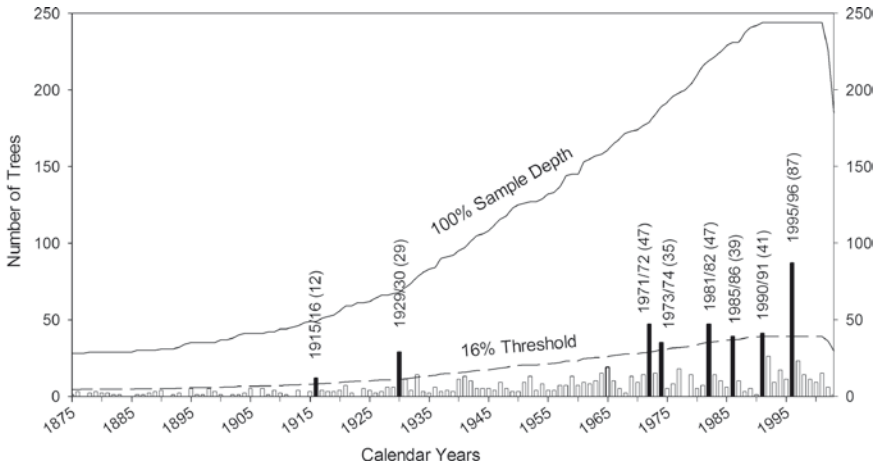

Fig. 1 Frequency histogram of trees displaying tree-ring responses to growth disturbances per year (total number of trees, 245). *Black bars* indicate the most likely years of snow avalanches. In *brackets*, number of growth-disturbed trees per avalanche season. Dead trees were omitted to enable comparison with past events, from which wood debris had already disappeared. The local reference chronology was reliable from 1875 (EPS ≥ 0.85; Expressed Population Signal, Wigley et al. 1984)

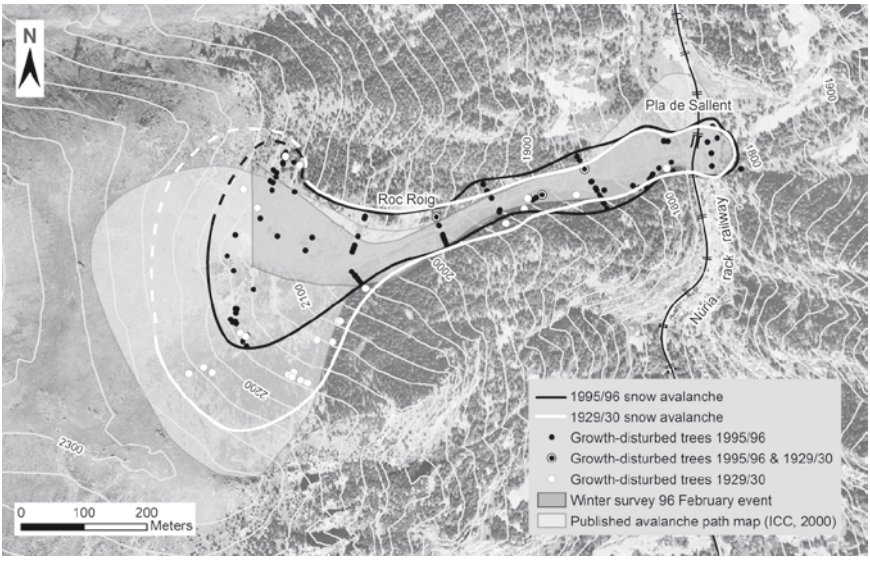

Fig. 2 Dendrogeomorphic map of major avalanches. *White lines*, 1929–1930 event and *black lines*, 1995–1996 event. The 1929–1930 avalanche was totally inferred by tree-ring features, no evidence of this event was known previously to the dendrochronological studies. The distribution of growth-disturbed trees also displays that the extent of the 1995–1996 was broader than the mapped during a winter survey. (Mapa de zones d'allaus de Catalunya 1:25000, ICC 2000)

avalanche, even wider than 1995–1996. In situ affected trees at the starting zone comprised the whole catchment. These results demonstrate that dendrogeomorphology can be used to improve maps performed by conventional techniques, and is an essential tool to map past unknown events.

Acknowledgments The Spanish Ministry of Science and Technology (project REN2002-02768/RIES) and the Cartographic Institute of Catalonia (ICC) provided financial support. Dendrochronological analyses were performed at the Department of Ecology, Faculty of Biology, University of Barcelona. Vall de Núria Tourist Resort facilitated the field tasks with transportation in the rack train and lodging.

References

Butler DR, Malanson GP (1985) A history of high-magnitude snow avalanches, southern Glacier Park, USA. Mt Res Dev 5(2):175–182

Butler DS, Sawyer CF (2008) Dendrogeomorphology and high-magnitude snow avalanches: a review and case study. Nat Haz Earth Syst Sci 8:303–309

Molina R, Muntán E, Andreu L, Furdada G, Oller P, Gutiérrez E, Martínez P, Vilaplana JM (2004) Using vegetation to characterize the avalanche of Canal del Roc Roig, Vall de Núria, eastern Pyrenees, Spain. Annal Glaciol 38:159–165

Muntán E, Andreu L, Oller P, Gutiérrez E, Martínez P (2004) Dendrochronological study of the avalanche path Canal del Roc Roig. First results of the ALUDEX project in the Pyrenees. Annal Glaciol 38:173–179

Wigley T, Briffa KR, Jones PD (1984) On the average value of correlated time series, with applications in dendroclimatology and hydrometeorology. J Appl Meteorol 23:201–213

Tree-Ring Based Reconstruction of Past Snow Avalanche Events and Risk Assessment in Northern Gaspé Peninsula (Québec, Canada)

Daniel Germain, Bernard Hétu, and Louise Filion

1 Introduction

Although frequencies of avalanches are much higher in the Canadian Cordillera, archival research, coroner's investigations and newspaper searches revealed the occurrence of many snow avalanche events in eastern Canada (Liverman et al. 2001; Hétu and Brown 2006; Hétu et al. 2008), highlighting the great destructive capacity of snow wasting even on short slopes. Historical records indicate that avalanches are the second most deadly natural hazard in the Province of Québec with over 71 victims between 1825 and 2008 (Hétu et al. 2008). Snow avalanches primarily affect backcountry recreational activities in highlands but also dwellings and transportation corridors in inhabited areas (Germain 2005; Hétu 2007; Hétu et al. 2008). It is therefore a priority to improve our knowledge of this phenomenon for better management of this deadly natural hazard, particularly regarding the following topics: (i) recognition of snow-avalanche prone areas and hazard mapping. This implies the assessment of predisposing factors (local topography, slope aspect, vegetation) in the specific context of Québec where deadly avalanches have mainly occurred on very short slopes outside mountainous areas (Hétu et al. 2008); (ii) the frequency-magnitude of snow avalanches, including extreme events like the

D. Germain (✉)
Département de géographie, Université du Québec à Montréal,
Montréal QC, H3C 3P8, Canada
e-mail: daniel.germain@uqam.ca

B. Hétu
Centre d'études nordiques, Groupe de recherche BioNord and
Département de biologie, chimie et géographie, Université du Québec à Rimouski,
Rimouski QC, G5L 3A1, Canada

L. Filion
Centre d'études nordiques and Département de géographie,
Université Laval, Québec QC, G1V 0A6, Canada

M. Stoffel et al. (eds.), *Tree Rings and Natural Hazards: A State-of-the-Art*,
Advances in Global Change Research 41, DOI 10.1007/978-90-481-8736-2_5,

avalanche event which occurred in Kangiqsualujjuaq (east of Ungava Bay) in 1999 (nine fatalities and 25 injured); and (iii) the specific climatic and meteorological conditions responsible for avalanche occurrence and variability for the last century which is critical for the understanding of present and future avalanche activity in the context of climate change (Larocque et al. 2001; Boucher et al. 2003; Dubé et al. 2004; Hétu and Bergeron 2004; Germain et al. 2005, 2006; Hétu 2007; Hétu et al. 2008; Germain et al. 2009).

In the Province of Québec, there is no structural protection nor any daily forecasting procedures to reduce avalanche risks, as compared with western Canada (Hägeli and McClung 2003), France (Jomelli et al. 2007) or Switzerland (Salm 1997), where prevention plans against avalanche initiation and snow avalanches are available and provide land-use prescriptions to minimize the impacts of avalanches. However, because backcountry recreational activities in the Chic-Chocs Mountains (Gaspé Peninsula) are growing rapidly (Boucher 2000), the Haute-Gaspésie Avalanche Center (Centre d'avalanche de la Haute-Gaspésie) now produces bi-weekly bulletins to inform backcountry users on snow conditions and avalanche risks. However, linking snow avalanche activity and weather conditions using standard forecasting methods (Laternser and Schneebeli 2002; Hägeli and McClung 2003; Jomelli et al. 2007) is a difficult task in this region because of the lack of avalanche surveys and the scarcity of weather stations providing long-term records, both at low and high elevations. On the other hand, tree-ring data from several sites spread over large areas may help in understanding the spatio-temporal variations of avalanches (Butler and Sawyer 2008; Stoffel and Bollschweiler 2008; Germain et al. 2009). In that respect, ~10 years ago we started a long-term research program on snow avalanches in the Chic-Chocs Mountains. The objectives can be stated as follows:

1. To provide a tree-ring-based chronology of snow avalanches (frequency-magnitude) in several avalanche paths, particularly high-magnitude snow avalanches
2. To outline specific conditions responsible for avalanche occurrence in low-elevation coastal valleys but also in the alpine–subalpine highlands of the Chic-Chocs Mountains, two areas with contrasting climatic conditions and vegetation cover but significant avalanche hazard
3. To establish a regional tree-ring database based on the study of several avalanche paths, which will allow the assessment of the role of regional (climate and weather conditions) versus local (topography, slope aspect, forest cover and disturbance) factors in avalanche initiation
4. To test and evaluate various sampling procedures and statistical techniques to enhance dendrogeomorphological methods for the study of snow avalanches

Tree-ring analysis has been used for the study of several geomorphic and geological phenomena (cf. Shroder 1980; Solomina 2002), but its accuracy has yet to be investigated (Butler and Sawyer 2008; Stoffel and Bollschweiler 2008), with regard to the appropriate sample size and number of tree responses needed for the recognition of past events. Our research program on snow avalanches in the Chic-Chocs Mountains has focused on appropriate sampling design and statistical methods.

Many efforts were devoted to the evaluation of different types of responses, sample sizes, and the minimum number of samples required for the recognition of past avalanche events.

After a brief description of the study area, we describe methodologies and statistics used so far and summarize results from coastal and highland sites. Subsequently we address methodological issues, stressing the contribution of each method and its usefulness for risk assessment. Problems raised by tree-ring-based studies of snow avalanches are also discussed. Finally, some areas where new developments are needed are outlined.

2 The Study Area

The Chic-Chocs highlands and the coastal valleys near Mont St. Pierre are located in the northern Gaspé Peninsula (Fig. 1). In the mountains, snow avalanches affect mainly backcountry skiing whereas in the low-elevation coastal valleys, snow avalanches may reach roads and affect the transportation system for several hours or days. Clearly there is a need for good quality data on the frequency-magnitude of snow avalanches in this context.

The climate of the Chic-Chocs Mountains is complex largely due to orographic effects and the influence of oceanic air masses on precipitation and temperature, which results in frequent thermal inversions and high cloudiness (≥70%, Gagnon 1970).

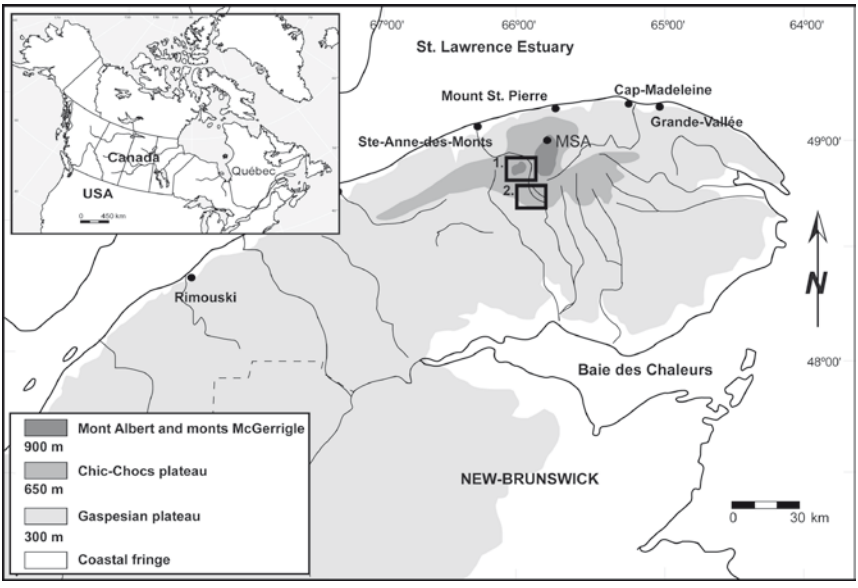

Fig. 1 Location of the study areas in the northern Gaspé Peninsula

Rain can occur in any month during the snow season, even on the highest summits. The mean annual temperature ranges from +3°C at sea level to −4°C at 1,200 m elevation (Gray and Brown 1979). The annual precipitation ranges from 800 mm at sea level to 1,600 mm in the mountains, with 40% falling as snow.

The pattern of snow accumulation is very different in the coastal valleys compared to the Chic-Chocs highlands. In the low-elevation valleys, avalanches occur on small, open patches along forested slopes: elsewhere, strong winds blowing on these scree slopes often result in snow accumulation in forest fringes, reducing the probability for an avalanche to release. Moreover, there is no possibility for snow drifting from the wooded plateau to the steep slopes (Germain et al. 2005; Hétu 2007) and for snow cornice formation in the upper rock wall. Thus, snow avalanches are climatically controlled and are primarily a response to major snow precipitation events. In the Chic-Chocs highlands, snow drifting by prevailing north-westerly winds favours avalanche activity due to deep snow accumulation and formation of cornices. These differences in the climatic controls of avalanching between coastal valleys and alpine–subalpine environment of the Chic-Chocs are favourable to high-magnitude snow avalanche activity following several weather scenarios (Germain et al. 2009).

3 Methods

Two main sectors in the northern Gaspé Peninsula, without previous records of avalanche events were investigated using tree-ring techniques. Since our objective was to build a tree-ring-based chronology of high-magnitude avalanches, we used the definition based on that provided by Germain et al. (2009, p. 147), namely "a high-magnitude snow avalanche is regarded as one of sufficient size to exceed the normal boundaries of a given avalanche path, characterized by small scattered and generally impacted trees, entering the mature forests downslope". We thus assumed that high-magnitude avalanche should result in a greater number of damaged trees and consequently a higher probability of being recorded by tree-ring techniques.

The characteristics of tree-ring sampling in the snow avalanche paths studied are presented in Table 1. It should be noted that avalanche years, e.g. 1898, denote the winter of 1897–1898.

3.1 Site Selection, Sampling Design and Laboratory Analysis

3.1.1 Site Selection

The selection of snow avalanche paths for sampling was based primarily on evidence of past large avalanche events deduced from damaged trees. Physical damage included impact scars, broken trees, tilted stems and asymmetrical branch thinning.

Table 1 Characteristics of tree-ring sampling in the snow avalanche paths studied in northern Gaspé Peninsula

Avalanche path						Tree-ring sampling							
Paths	Elevation (m)	Length (m)	Relief (m)	Slope (°)	Aspect	Sampling design[a]	Sampling location[b]	Trees (n)	Cross-sections (n)	Impact scars (n)	Reaction wood (n)	Years[c]	Year of inner rings[d]
Low-elevation coastal valleys													
T-5	375	390	325	>30.0	W	Lateral Tr.	T & R	62	112	41	300	1860	–
T-3	400	–	375	>30.0	W	Long. Tr.	T & R	20	24	0	–	1939	–
RC	400	–	350	>30.0	W	Long. Tr.	T & R	28	34	0	–	1934	–
T-9	500	700	450	>30.0	W	Dispersed	T & R	78	103	116	95	1932	1809
T-10 1	575	450	400	>30.0	SE	Dispersed	T & R	25	39	58	34	1934	1765
T-10 2	575	680	425	>30.0	SE	Dispersed	T & R	27	45	53	64	1947	1897
T-10 3	575	600	425	>30.0	SE	Dispersed	Run out	8	13	11	14	–	1943
T-10 4	575	550	425	>30.0	SE	Dispersed	Run out	5	8	9	7	–	1942
Highlands of the Chic-Chocs range													
Val-1	840	520	240	27.6	NE	Dispersed	Run out	50	78	50	41	1972	1965
Val-3	840	510	240	27.9	NW	Dispersed	Run out	27	42	25	26	1971	1958
Val-4	870	360	190	33.0	NW	Dispersed	Run out	61	82	64	85	1917	1889
Val-7	840	420	205	29.2	NW	Dispersed	Run out	20	84	26	129	1870	1756
Val-8	800	450	230	31.1	NW	Dispersed	Run out	39	82	26	56	1974	1921
MSA	1,100	670	310	27.1	N	Dispersed	Run out	62	72	77	93	1951	1913
HBN	800	665	350	30.4	NE	Lateral Tr.	T & R	62	–	35	207	1895	–
HBS	800	710	350	30.3	NE	Dispersed Lateral Tr.	T & R	243	436	207	592	1838	1760
GC	950	320	120	22.6	SE	Dispersed	Run out	10	59	17	171	1908	1813
MA	995	1125	605	23.9	NE	Dispersed	Run out	68	109	93	115	1944	1901
BLS	830	300	160	5533.2	NW	Dispersed	Run out	22	90	45	103	1896	1772
BLN	830	440	240	31.8	N	Dispersed	Run out	25	80	23	122	1938	1827
Slush flow site													
CM	710	1200	200	8.0	SE	Dispersed	T & R	111	–	–	–	–	–

[a]Sampling design: D = dispersed; Lateral Tr. = lateral transect; Long Tr. = longitudinal transect.

[b]Sampling location: R = run out zone; T = avalanche track.

[c]Years with ≥10 individuals.

[d]Oldest ring dated on the oldest tree for each path.

Some types of damage may induce sprouting of lateral buds that produce new leaders (reiterates). The sites studied included eight avalanche paths on scree slopes in the low-elevation coastal valleys of Mont St. Pierre and Rivière-à-Claude (Fig. 1), plus 12 alpine–subalpine snow avalanche paths and one subalpine slushflow site. Avalanche path accessibility was also considered given the low density of roads in the region.

3.1.2 Sampling

Most trees sampled were located in open or semi-forested run-out zones and along trimlines. At some sites, however, trees were sampled along 1-m wide lateral transects through the lower part of avalanche tracks and run-out zones and along a 1-m wide transect parallel to the long slope profile (Boucher et al. 2003; Dubé et al. 2004). The sample sizes varied from 5–243 trees (1,049 in total, Table 1). Because some study sites were located within a recreational park area, the sampling concentrated on trees showing evidence of multiple events in order to reduce the number of trees sampled. Cross-sectional discs were collected at various levels along the trunk (curve in the stem, scars, base of reiterates, etc.).

3.1.3 Laboratory Analysis

Cross-sectional discs were finely sanded and analyzed under a binocular microscope for the age determination and the dating of growth-ring anomalies. Growth-ring dating was made possible by ring counting along two or three radii. Frost rings and narrow rings were also recorded. To develop our snow avalanche chronologies, we used tilted trees with reaction wood lasting for at least 2 years and trees with impact scars, as these types of damage provided the most reliable evidence for past snow avalanches (Larocque et al. 2001; Boucher et al. 2003; Dubé et al. 2004; Germain et al. 2005, 2009). Drastic changes in the direction of reaction wood were considered as distinct snow avalanche events. Because small-diameter tree stems are highly susceptible to stem deformation on steep slopes (Johnson 1987; Dubé et al. 2004; Germain et al. 2005, 2009), the 20 innermost rings were not considered in the analysis of reaction wood.

Traumatic resin ducts and new leaders developed from dormant axillary buds on the stems or from a branch which shifted from a subhorizontal (plagiotropic) axis to a stem-like vertical (orthotropic) axis were also used tentatively at some sites, in conjunction with other types of response (Larocque et al. 2001; Dubé et al. 2004). Because traumatic resin ducts may form in response to various environmental stresses (defoliation by insects, tree dieback, etc.), they were not useful indicators for avalanche activity. Accurate dating of the initiation of leaders or radial growth release in branches transformed into stem-like structures revealed a 1–8 year time lag for surviving trees to respond to stem damage (Dubé et al. 2004).

3.2 Statistical Treatments of Tree-Ring Data Sets

3.2.1 Scree Slopes in Low-Elevated Coastal Valleys

Our approach was based on the process-event-response developed by Shroder (1978, 1980). For each year *t* at each site, the avalanche activity index (AAI; 0–100%) was calculated following Shroder's methodology, which is based on the percentage of responses in relation to the number of trees alive in year *t*:

$$\mathrm{AAIt} = \left(\sum_{i=1}^{n} \mathrm{Rt}\right) \Big/ \left(\sum_{i=1}^{n} \mathrm{Nt}\right) * 100\%$$

where R represents the response to an event for year *t* and N the number of trees alive in year *t*. For each avalanche path, event-response histograms were produced based on a combination of reaction wood and impact scars evidence. Each stand-scale chronology of high-magnitude avalanches was based on ≥10% threshold on the event-response histogram. Only years with a sample size ≥10 trees were considered in avalanche chronologies to avoid overestimation caused by low tree numbers in the event-response calculations. Avalanche tracks studied by Dubé et al. (2004) and Germain et al. (2005) were used at the stand scale.

The regional-scale chronology of high-magnitude avalanches for the low-elevation sites was based on ≥10% threshold on the event-response histogram, for the three undisturbed stands (T-5, T-3 and RC) on active scree slopes (Dubé et al. 2004). The two disturbed sites (T-9 & T-10) studied by Germain et al. (2005), which originated from fire and logging, were not considered at the regional scale.

3.2.2 Highlands of the Chic-Chocs Mountains

The tree-ring data from alpine–subalpine snow avalanche paths were analyzed using five different statistical methods (Germain et al. 2009). In this paper, however, we focus on the process-event-response developed by Shroder (1978, 1980) using combined tree responses (i.e., impact scars and reaction wood) to avalanche. For this reason, the avalanche chronology presented here differs slightly from that produced by Boucher et al. (2003) and Germain et al. (2009). Each stand-scale chronology of high-magnitude avalanches was also based on ≥10% threshold on the event-response histogram.

In order to provide an estimate of the overall avalanche activity in the alpine–subalpine zone, we developed a regional avalanche activity index (RAAI; 0–100%; Germain et al. 2009). For each year *t*, the RAAI was calculated as follows:

$$\mathrm{RAAIt} = \left(\sum_{i=1}^{n} \mathrm{AAIt}\right) \Big/ \left(\sum_{i=1}^{n} \mathrm{Pt}\right) * 100\%$$

where AAI represents the avalanche activity index for a given avalanche path for year *t* and P the number of paths that could potentially record an avalanche in year *t*, with a sample size ≥10 trees. Therefore, the AAIs calculated for all active paths were averaged over the total number of paths in a given year *t*. Because of overestimates created by low path numbers in the response calculations, only years with a sample size ≥3 avalanche paths were considered in the RAAI. In order to ensure the representativeness of the RAAI, with regard to high-magnitude avalanche occurrence, the percentage of active avalanche paths (PAAP; 0–100%) for each year was also calculated based on the number of high-magnitude avalanches recorded in year *t* divided by the number of avalanche paths that could potentially record an avalanche in year *t* (sample size ≥10 trees).

We used a binary stepwise regression model (i.e., specification of avalanche year or not with values of 1 and 0, respectively) to assess the role of regional *vs.* local factors in avalanche initiation. The regression was carried out with all weather factors until a significant determination coefficient was obtained for a given RAAI threshold value.

3.3 Return Interval and Annual Probability

Tree-ring-based avalanche records allowed us to estimate the return interval (RI) of high-magnitude avalanches for each path. The return intervals calculated are maximum values because of the decreasing sample size and the possible loss of evidence going back in time. Annual probability (AP) of widespread snow-avalanche activity was also calculated and was found to be inversely related to the return interval, as AP = 1/RI (Mears 1992). We also evaluated RI and AP at the regional-scale for both sectors studied.

4 Results

4.1 Low-Elevation Coastal Valleys

In low-elevation coastal valleys in the northern Gaspé Peninsula, two distinct snow-avalanche regimes can be recognized: (i) natural avalanches that occurred on active scree slopes and; (ii) avalanche activity on treed slopes disturbed by fire and logging.

4.1.1 Snow-Avalanche Regime on Active Scree Slopes

Of the three stands studied by Dubé et al. (2004), stand T-5 yielded the longest record of avalanches going back to AD 1860 with a sample size ≥10 individuals (Table 1). At stand T-5, years with avalanche activity index values ≥10% were

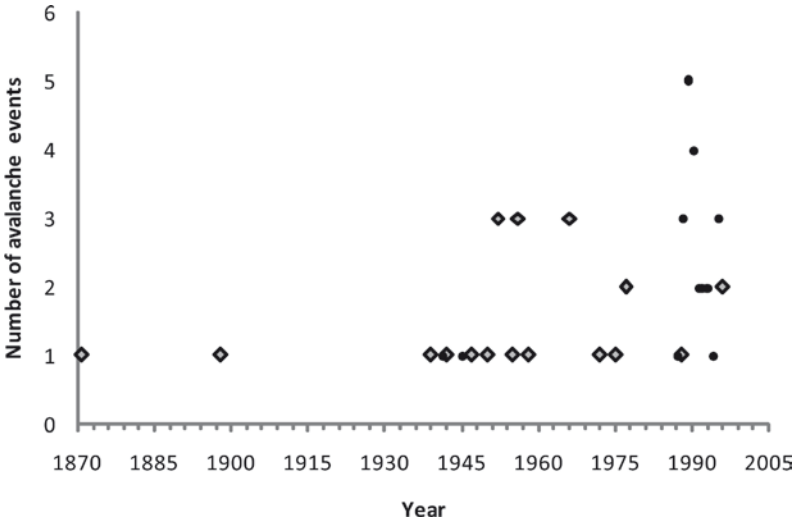

Fig. 2 Number of high-magnitude avalanche events through time on undisturbed scree slopes (*light diamonds*) and disturbed treed slopes after fire and logging (*black dots*)

1871, 1898, 1952, 1956, 1966, and 1996. At stand T-3, they were 1947, 1950, 1952, 1956, 1958, 1966, 1972, 1975, 1977, 1988 and 1996. Finally, at stand RC, the seven following years were recorded as avalanche years: 1939, 1942, 1952, 1955, 1956, 1966, and 1977. One should note that at this stand the event-response for the year 1996 was 9%, i.e., just below the threshold value. In spite of the limited temporal extent of avalanche records from T-3 and RC (1939–1997; see Table 1), these two scree slopes yielded a higher frequency of high-magnitude avalanches over the interval common to all three tracks.

At the regional scale, event-responses estimated from the 110 trees sampled in the three stands investigated showed 7 years of high-magnitude snow avalanches (≥10%): 1871, 1898, 1952, 1956, 1966, 1977, and 1996. The two oldest years were only recorded at stand T-5, which recorded six out of these seven snow avalanche years (Fig. 2). Of the 5 years after 1939, corresponding to a sample size ≥10 trees for all stands, all were recorded at stand T-3 and four at stand RC (Fig. 2).

4.1.2 Snow-Avalanche Activity on Treed Slopes After Fire and Logging Disturbances

At site T-9, the 1938 fire was dated with several fire scars and documented from historical data. This human-induced fire burned 185 ha of forests at the outer edge of the plateau and in the upper part of the slope. The forest opening created local conditions conducive to snow drifting and accumulation of large amounts of snow in the burned, vegetation-free area in the upper steep slope. The tree-ring data indicated two periods of avalanche activity (AAI ≥10%), i.e., 1941–1945, and 1989–1995 (Fig. 2).

At site T-10, where a clear cut occurred in 1986 on the plateau (~2,250 ha of forest harvested), tree-ring analysis showed high avalanche activity index for the years 1988, 1989, 1990, 1991 and 1995 for avalanche path C-1 and 1988, 1989, 1990, 1992, 1993, and 1995 for avalanche path C-2. Four of the 6 years (1988, 1989, 1990, and 1995) were recorded in both paths. Additional data from two adjacent avalanche paths (C-3 & C-4) also indicated past avalanche events in 1987, 1988, 1989, and 1990. Once again, the forest opening on the plateau created conditions conducive to snow drifting and formation of cornices, as opposed to the three undisturbed scree slopes. The avalanche window in the post-logging site was shorter (<10 years) than that of the post-fire site where avalanche activity was recorded 55 years after fire. This is an indication that avalanche activity after tree removal largely depends on the capacity of woody vegetation to reach heights and density sufficient to control snow drifting and thus avalanche activity.

4.2 Snow-Avalanche Regime in the Highlands of the Chic-Chocs Range

4.2.1 Reconstructed Tree-Ring Local Avalanche Record

The 689 trees sampled in the 12 alpine–subalpine avalanche paths provided 244 avalanche events, which correspond to 86 years. Of the 12 avalanche paths investigated, paths HBS and Val-7 yielded the longest records, going back to 1838 and 1870, respectively. The HBS and Val-7 tree-ring records showed no avalanche activity index ≥10% before 1895 in spite of sample sizes ≥10 individuals.

High-magnitude avalanches occurred 44 times corresponding to 31 years before 1950, i.e., 56% of all years between 1895 and 1950, compared to 200 times after 1950 corresponding to 49 years, i.e., 98% of all years between 1950 and 2000 (Fig. 3). This means that after 1950 at least one avalanche event was recorded each year, except 1999. Twelve of the 49 avalanche years were recorded on ≥6 avalanche paths (50% of all paths investigated, PAAP > 50%): 1969, 1971, 1977, 1981, 1984, 1986, 1988, 1990, 1991, 1993, 1994, and 1995.

On the yearly and decadal scales, the records indicated that high-magnitude avalanche events increased significantly between 1895 and 2000 ($R^2 = 0.55$; $p < 0.0001$), especially after 1950 (Fig. 3). Less than ten avalanche events per decade were recorded between 1900 and 1950 and 40 on average per decade after 1950. Avalanches were twice as frequent during the 1990s (55 occurrences) than between 1950 and 1970.

Tree-ring data from a subalpine site documented by Larocque et al. (2001) indicated the occurrence of three slushflow events in the last century: 1925, 1964, and 1988. A slushflow event was also visually documented in January 2006. The lack of synchrony between snow avalanches and slushflows for 2 years (1925 and 1964, but not 1988 where eight avalanche events were recorded in the alpine–subalpine belt)

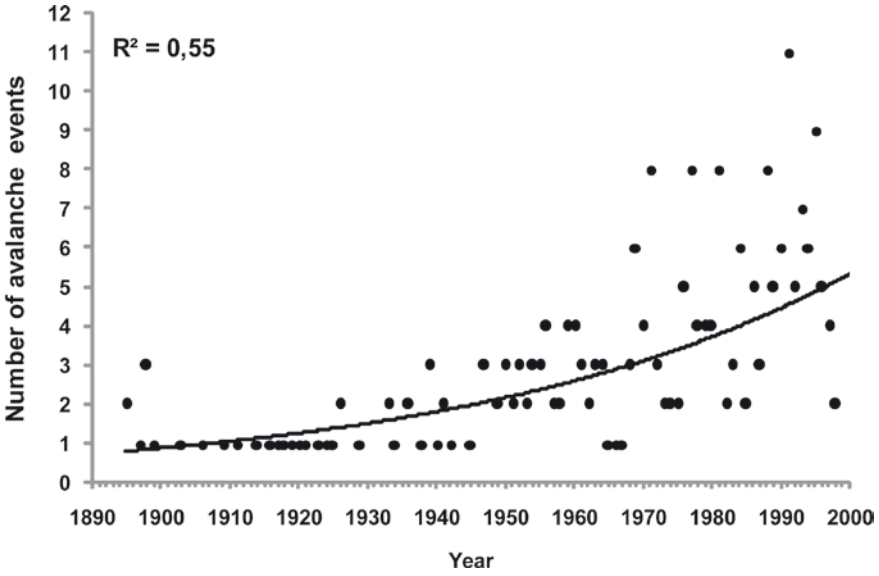

Fig. 3 Number of high-magnitude avalanche events through time in highlands of the Chic-Chocs Range

suggests a strong influence of meteorological conditions in the initiation of slushflows which usually occur in response to increased water content in the snowpack through rainfall and/or snowmelt (Larocque et al. 2001).

4.2.2 Chronology of Regional Snow Avalanche Activity

Using a RAAI ≥10% as a threshold ($R^2 = 0.67$; $p < 0.0001$) for identifying widespread, regional avalanche activity, 19 years of high avalanche activity were identified for the period between 1895 and 2000: 1898, 1936, 1939, 1941, 1965, 1969, 1970, 1971, 1977, 1981, 1984, 1987-1992, 1994, and 1995. Fifteen out of the 19 avalanche years (1898, 1936, 1969-1971, 1977, 1981, 1984, 1988–1992, 1994 and 1995) were also characterized by a high PAAP value (≥33%). The PAAP explained more than 63% ($p < 0.0001$) of the variance of the RAAI over the 1895–2000 period. Statistically, the data showed a random scatter around zero with a Durbin-Watson *d-statistic* of 2.0 ($p < 0.01$), which satisfied the assumption of constant variance and non-correlated residuals (Clark and Hosking 1986). This means that 65% of all tree anomalies (damage) were related to high-magnitude avalanche events, likely during major snow avalanche cycles as reported in the western United States (Birkeland and Mock 2001), Switzerland (Hächler 1987), Austria (Höller 2009), and France (Glass et al. 2000). Therefore, the RAAI enabled us to identify 1939, 1941, 1965 and 1987 as high-magnitude avalanche

years at the regional scale, with RAAIs of 13%, 11%, 10% and 16%, respectively, in spite of the low number of high-magnitude avalanches recorded those years at the local scale.

4.3 Risk Assessment

4.3.1 Scree Slopes in Coastal Valleys

The return intervals (RI) and annual probabilities (AP) of high-magnitude avalanches on undisturbed scree slopes are presented in Table 2, with RI of 12 years and AP of 12% on average. At stand T-3, RI was short (~5 years) with ~19% probability that avalanches occur in any 1 year. Stand T-5 had the longest estimated return

Table 2 Number of events, return interval, and annual probability (%) of high-magnitude avalanches

					1900–1949		1950–1999	
Path	N years[a]	N events	RI	AP	RI	AP	RI	AP
Low-elevation coastal valleys								
T-5	137	6	22.8	4	0	0	12.0	8
T-3	58	11	5.3	19	–	–	4.8	21
RC	58	7	8.3	12	–	–	9.6	10
T-9	68	9	7.6	13	–	–	7.0	14
T-10 1	66	8	8.3	12	–	–	6.3	16
T-10 2	53	5	10.6	9	–	–	10.0	10
Average	73	8	10.5	12	0	0	8.3	13
Highlands of the Chic-Chocs range								
Val-1	28	6	4.7	21	–	–	–	–
Val-3	29	10	2.9	34	–	–	–	–
Val-4	83	19	4.4	23	6.4	16	3.5	29
Val-7	130	31	4.1	24	16.7	6	1.8	55
Val-8	26	4	6.5	15	–	–	–	–
MSA	49	11	4.5	22	–	–	4.5	22
HBN	103	17	6.1	17	8.3	12	5.4	18
HBS	157	15	10.5	10	50.0	2	4.1	24
GC	92	42	2.2	45	3.2	31	2.2	45
MA	56	14	4.0	25	–	–	4.0	25
BLS	104	27	3.9	26	16.7	6	2.3	43
BLN	62	37	1.7	59	–	–	1.7	59
Average	81	20	5.0	29	16.9	12	3.4	34
Slushflow site								
CM	83	4	20.8	5	25	4	19.0	5

[a]Years with ≥10 individuals.

interval (~23 years) for a 137-year record. No high-magnitude avalanche was recorded during the first half of the twentieth century, but four occurred after 1950 (Table 2). RC showed intermediate values (~8 years).

At the regional scale, the return interval of high-magnitude avalanches was estimated for the period 1839–1997. Using only those events recorded at two or three stands, RI was estimated as 19 or 12 for all three or two of three sites.

The risk assessment of avalanches after forest disturbances is hard to evaluate for several reasons: (1) forest disturbances, especially fire occurrences, sizes and intensity, cannot be predicted; (2) the frequency-magnitude of avalanches on disturbed treed slopes is closely related to the capacity of woody vegetation to achieve a density and heights for efficient snow drifting control; and (3) RIs and APs may be under-estimated for heavily disturbed areas where specific land-use prescriptions do not exist, especially for logging activities.

4.3.2 Alpine–Subalpine Avalanche-Prone Areas

Depending on the location within the alpine–subalpine belt, RIs varied from 1.7 to 10.5 years in paths BLN (north slope) and HBS (south-east slope), respectively (Table 2), with an average return interval of 5 years. APs varied from 10% to 59% in paths HBS and BLN, respectively, with an average of 29% calculated for all paths.

RIs and APs for the first (1900–1949) and second halves (1950–1999) of the twentieth century were calculated for each avalanche path with an avalanche chronology ≥100 years (Val-4, Val-7, HBN, HBS, GC, BLS). RIs decreased sharply after 1950, particularly in the HBS path where only one high-magnitude avalanche event was recorded before 1950 compared to 12 after 1950, which corresponds to a shift of RI from 50 to 4.1 years (Table 2). APs increased after 1950 with values of 29%, 55%, 18%, 24%, 45%, and 43% as opposed to ~16%, 6%, 12%, 2%, 31%, and 6% before. The increase was smaller for avalanche path HBN, with values of 18% and 12% after and before 1950, respectively (Table 2). The number of years for which at least one third of the paths were active (PAAP ≥33%) also increased after 1970, indicating a significant change in avalanche activity rather than in the preservation of evidence of that activity.

The average interval between high-magnitude avalanche years at the regional-scale was 5.5 years (19 of 105 years). However, 15 (79%) of these 19 years occurred after 1950, which corresponds to a much shorter return interval of 3.3 years (15 of 50 years) and reinforces our interpretation for increased avalanche activity after 1950, both locally and regionally, in the highlands of the Chic-Chocs Range (Germain et al. 2009). Finally, with an average RI of 5 years and AP of 29%, the alpine–subalpine avalanche-prone areas showed shorter RI and higher AP than undisturbed scree slopes in the coastal valleys, with RI of 12 years and AP of 12% on average, and a slushflow subalpine site with a return interval longer than ~20 years calculated for a 83-year period (1925–2008).

5 Discussion

5.1 Comparison of Snow-Avalanche Regime Between Scree-Slopes in Low-Elevated Coastal Valleys and Alpine–Subalpine Highlands

In the absence of historical data on avalanche occurrences, our research program provided tree-ring-based records of avalanches for a mountainous region of eastern Québec where avalanches are widespread and frequent. Despite contrasted climatic conditions and vegetation cover, the two sectors studied are characterized by high-magnitude avalanches with great destructive power. In the Chic-Chocs highlands, ~65% of all trees sampled randomly were damaged during the 19 avalanche years identified (Germain et al. 2009). We calculated a RI of 5.5 years for the period between 1895 and 1999, which is very close to that calculated for the Austrian Alps (nine events in more than 50 years) (Höller 2009). This interval is also close to the interval of 5 years reported by Fitzharris (1981) and Johnson et al. (1985) for the Rocky Mountains of western Canada, and 4.9 years reported by Hebertson and Jenkins (2003) for the Wasatch Plateau, Utah (USA).

At the regional scale, no synchronism in high-magnitude avalanche occurrences was apparent between inland subalpine sites and undisturbed scree slope sites in coastal valleys, which suggests the influence of local factors on avalanche activity. The location of the starting zones in open (alpine tundra) or semi-forested (subalpine) areas in the Chic-Chocs highlands creates conditions for snow drifting and cornice formation as opposed to wooded plateaus that dominate scree slopes and vertical rockwalls in the coastal valleys. In this low-elevation environment, strong winds blowing on active scree slopes, which form small open patches along forested slopes, usually decrease the probability of an avalanche to release (Hétu and Bergeron 2004). Therefore, the return interval of avalanche events is longer (12 years) and strongly related to snowstorms and snowy winters in coastal lowlands (Dubé et al. 2004; Hétu 2007).

The number of avalanche events recorded after 1950 was much higher than during the first half of the century, at both local and regional scales (Figs. 2 and 3). High avalanche frequencies in the western USA during the second half of the twentieth century were also documented using tree-rings. For instance, on the Wasatch Plateau, Utah, Hebertson and Jenkins (2003) recorded 14 avalanche years between 1928 and 1996, ten of them (71%) after 1950. In Glacier National Park, Montana, Butler and Malanson (1985) documented an increase in avalanche frequencies after 1975, compared to the previous 25 years. In the Chic-Chocs Range, the higher frequency of snow avalanche activity seems to be related to an increased climate variability, which creates propitious conditions for snow avalanche release following several scenarios: (1) above-average total snowfall, (2) high-frequency of snowstorms, (3) major rain events and facet-crust development, (4) sequences of freezing rain and strong winds, and (5) early-season weak layers of faceted crystals and

depth hoar (Germain et al. 2009). However, given the possibility of poorer preservation of the earlier record, methodological issues and quality of the data for reconstructing chronologies of snow avalanching are discussed below.

The multi-decadal trend in increased avalanche activity in the Chic-Chocs Mountains and the anticipated climate change, which may favour increased climate variability (frequency of snowstorms, significant rise in air temperature, heavy snowfall and strong winds), should be considered more thoroughly to prevent and mitigate avalanche hazards. For instance, appropriate land management plans should identify safety margins in settlements located in avalanche-prone areas.

5.2 Methodological Issues and Quality of the Data

By utilizing evidence found in living (and, when possible, dead) damaged trees, dendrogeomorphic investigations offer a longer temporal perspective on avalanche frequency and magnitude. On the other hand, avalanches may destroy evidence of earlier events, as well as the susceptibility of a tree to record damage. Therefore, the sampling design, sample size, and tree-ring responses can impact the quality of the record, which also varies with tree species, age and size. Because the tree-ring records from both sectors showed an increased frequency of snow avalanches after 1950, it raises the question of the quality of the data, the influence of sample size, and the threshold value for the acceptance of an avalanche event.

5.2.1 Tree-Ring Reconstruction of High-Magnitude Snow Avalanches or Extreme Events?

Specification of return periods in the run-out zone is the first and most important step for avalanche hazard assessment and zoning (McClung 2000). It is therefore surprising that many studies that dealt with tree-rings for the reconstruction of past snow-avalanches did not clearly state the objectives. Because the distribution of run-out distances in space follows a Gumbel distribution (McClung and Mears 1991), the location of sampled trees may induce significant discrepancies in the evaluation of return periods. We must keep in mind that some avalanches cannot be recorded by trees because snow masses were too small to reach the run-out zone or to cause obvious damage to trees such as impact scars. Conversely, large avalanches can cause extensive damages and high mortality reducing the subsequent potential of tree-ring records (Rayback 1998).

In the Chic-Chocs Mountains, sampling covered the present run-out zone and its immediate forested peripheral area entirely so as to locate distant damaged trees and to minimize the effect of the sampling design. Past avalanche events were confirmed as high-magnitude events by analyzing the location of damaged trees. Hence, we did not focus on extreme events for which damaged trees were only to be found farther down on very gentle slope (<10°) and in mature forest stands.

5.2.2 What Are the Best Indicators of Past Snow Avalanche Activity?

To develop snow avalanche chronologies, various tree responses have been used so far. Impact scars, sequences of reaction wood, and growth release or suppression appeared the most useful responses (Burrows and Burrows 1971; Carrara 1979). In the northern Gaspé Peninsula, we used living trees with impact scars and tilted trees with reaction wood, as these tree damage types provided the most reliable evidence of past snow avalanches (Larocque et al. 2001; Boucher et al. 2003; Dubé et al. 2004; Germain et al. 2005, 2009). However, to ensure the reliability of our avalanche records, we opted for the following procedures: (i) the 20 innermost rings were not considered in the analysis of reaction wood because small-diameter tree stems are highly susceptible to stem deformation on steep slopes; (ii) we used sequences of reaction wood lasting for at least 2 years; (iii) a drastic change in the direction of reaction wood was also considered as originating from distinct snow avalanche event, and (iv) when possible, two types of responses or more were used as complementary tools for avalanche reconstruction.

Traumatic resin ducts have also been used successfully as valuable tools for documenting various geomorphic processes by Stoffel et al. (2006) and Casteller et al. (2007). In the Chic-Chocs Range, however, the formation of traumatic resin ducts seemed related to other environmental stresses, namely insect activity causing defoliation during severe epidemics. Larocque et al. (2001) showed that only a few annual rings with rows of traumatic resin ducts were related to avalanche disturbances.

Additional, less well documented tree response types (e.g. as used by Carrara 1979) consist of shoot initiation and radial growth release in branches transformed into stem-like structures, which marks a change in axis direction. However, these responses remain poorly documented. At a stand studied by Dubé et al. (2004), 12 and 11 new leaders were produced 8 and 6 years after the 1956- and 1966-avalanche events, respectively. Therefore, traumatic resin ducts shoot initiation and radial growth release in branches may be used as complementary tools to the main type of responses, namely impacts scars and reaction wood.

5.2.3 What Are the Optimum and Minimum Sample Sizes?

In a recent paper, Butler and Sawyer (2008) argued that a few damaged trees may be sufficient for the development of an avalanche chronology, but 100 such trees would be better. It is clear that the larger the sample size, the higher the probability to record past avalanche events. However, because the avalanche activity index is based on the percentage of responses in relation to the number of trees alive for a given year (following Shroder's method) a very large sample size may increase the noise and make deciphering past avalanche events even more difficult.

The cumulative distribution function (CDF) of avalanche chronologies, which describes the probability distribution of avalanche chronologies for variable sample sizes, were plotted for sites at low-elevation coastal valleys (Fig. 4a) and alpine–subalpine belt in the Chic-Chocs Range (Fig. 4b), respectively. In both cases,

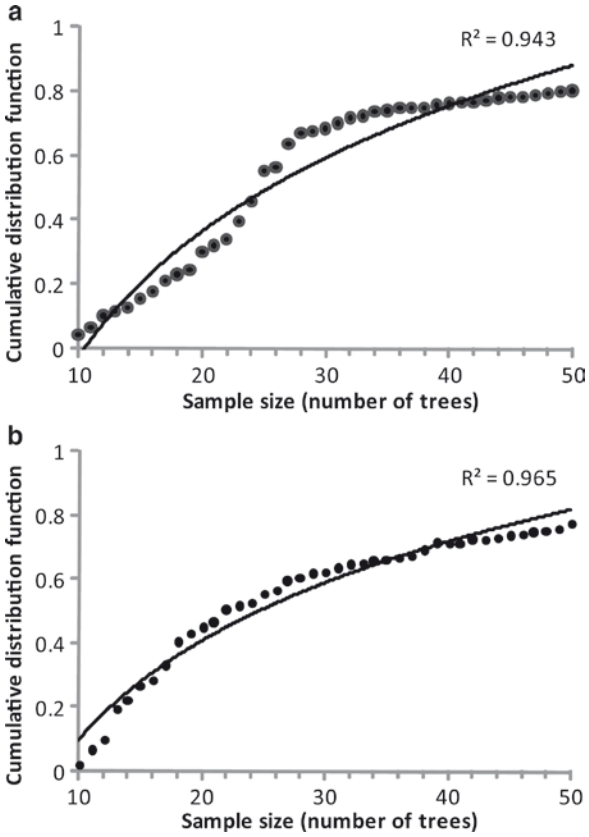

Fig. 4 Cumulative distribution function of avalanche chronologies as a function of sample size for scree slopes in low-elevation coastal valleys (**a**) and for alpine–subalpine avalanche paths in the Chic-Chocs Range (**b**)

the data follow a logarithmic law ($R^2 = 0.94$ & 0.97; $p < 0.0001$). With a sample size increasing from 10 to 25–30 trees (Figs. 4a and b), the probability to extend avalanche chronologies is high, but with sample size >40, this probability will increase only slightly, indicating that a good selection of trees for sampling is an important prerequisite for the development of avalanche chronologies. In that connection, the higher avalanche frequency calculated for the period after 1950 in the northern Gaspé Peninsula is not related to the sample size. Indeed, no significant correlations were found between the number of avalanches recorded and the length of the chronologies ($R^2 = 0.30$; $p > 0.05$) and between the number of avalanches and trees sampled ($R^2 = 0.21$; $p > 0.10$), which varied greatly from one path to another.

The sampling design is unquestionably an important issue, but also the location, dendrometric parameters (heights, diameters, presumed ages) and anomalies (damages originating from multi-events) of trees. Table 1 shows the oldest growth ring dated at each avalanche path, which indicates that tree longevity rather than

tree life expectancy in avalanche-prone areas appears to be the main limiting factor for avalanche chronology development. Obviously, the number of old trees decreases back in time, but we argue that a minimum of ten trees is required for calculation of any avalanche activity index. Burrows and Burrows (1971) and Stoffel et al. (2006) used a single tree to conclude past avalanche events. Tree responses for years with <10 trees should be considered as additional pertaining information, but not for chronology building and ensuing calculation of frequencies, return intervals, etc. A single tree is definitely not enough, particularly for risk assessment. When the sample size has to be minimized for some reasons (e.g., recreational or protected areas) sampling should be done so as to maximize the information, by collecting several discs from a limited number of trees (Stoffel et al. 2006; Germain et al. 2009).

5.2.4 What Is the Minimum Number of Tree-Ring Responses for Past Avalanche Event Identification?

One of the main difficulties in tree-ring analysis on trees showing damage from multiple events is to statistically distinguish avalanche events from other types of disturbances (slope or wind effects on stem deformation). Following the approach based on the process-event-response developed by Shroder (1978, 1980), each stand-scale chronology of high-magnitude avalanches is based on the ability to identify growth anomalies in the field, but also on a quantitative threshold value for the identification of avalanche events. Butler and Sawyer (2008) considered that 20% as a minimum number of trees needing to respond in order to invoke an avalanche event was more appropriate than 40% (Butler and Malanson 1985; Butler et al. 1987; Bryant et al. 1989) because of the small size of sampled trees (≤12) along some avalanche paths and based on data from historical records of avalanches.

In the northern Gaspé Peninsula, a 20% threshold value is not appropriate given the sample size (average >50) per avalanche path. With a 20% threshold, no avalanche events at site HBS would be recorded. Dubé et al. (2004) calculated an avalanche activity index of 9% for the year 1996 in stand RC, although the treed area devastated was over 50 m^2. Thus, it is not surprising that historical and tree-ring records of avalanches may not totally correspond (Luckman and Frazer 2001; Butler and Sawyer 2008) for several reasons: (1) the quality and reliability of surveys vary from site to site; (2) a significant change in avalanche survey may have occurred over time and; (3) local factors (slope aspect or gradient) may be responsible for differences in avalanche occurrences in two adjacent sites. Butler and Malanson (1985) indicated that knowledge of site-specific geomorphic conditions helps choosing an acceptable threshold value.

A 10% threshold value appeared appropriate for the avalanche paths studied in the northern Gaspé Peninsula (Larocque et al. 2001; Boucher et al. 2003; Dubé et al. 2004; Germain et al. 2005, 2009). Figure 5 shows that the relative number (%) of recorded avalanche years for variable threshold values follows an exponential distribution ($R^2 = 0.96$; $p < 0.0001$). Using threshold values of ≤5%, 10% and 20%,

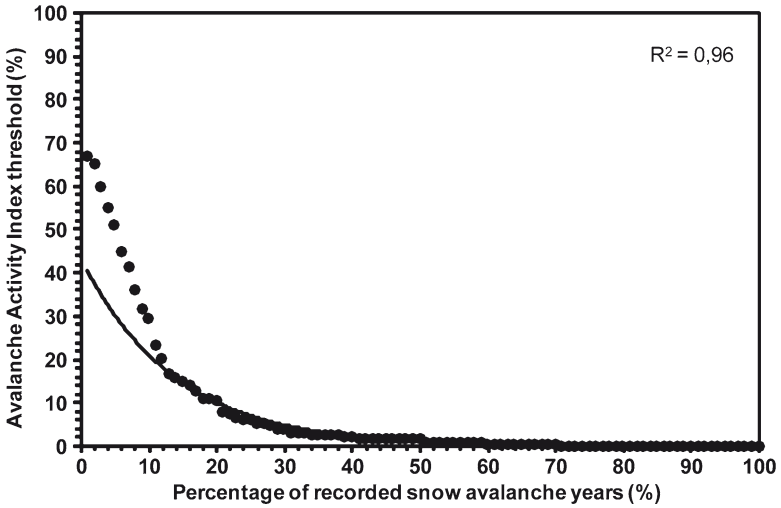

Fig. 5 Percentage of recorded avalanche years for different threshold values. The relative number of recorded avalanche years is the mean number of avalanche years for a given threshold value divided by the length of the chronology at each avalanche path

a total of 50% 20% and 10% of years were identified as avalanche years. A threshold of ≤5% may include several small avalanches, and a threshold of ≥20% may only include extreme events that cause extensive damage. The exponential distribution (Fig. 5) clearly justifies a 10% threshold, which likely corresponds to high-magnitude snow avalanches, thus excluding small events because the sampling covered the present run-out zone and its immediate forested peripheral in order to minimize the effect of the sampling design.

At the regional scale, Dubé et al. (2004) and Germain et al. (2009) used a 10% threshold value. However, for the regional chronology in alpine–subalpine highlands, this threshold was established by using a robust statistical method rather than subjectively. Indeed, Germain et al. (2009) established this value from a binary stepwise regression model which identified the minimum possible value for avalanche year identification. Avalanche years were characterized by a regional avalanche activity index statistically different from those calculated for non-avalanche years. The regional avalanche activity index takes into account the number of paths that could potentially record an avalanche for a given year, with a sample size ≥10 trees.

5.3 Risk Assessment: The Contribution of Dendrogeomorphology

Several recent papers suggest that climate change is likely to cause shifts in the magnitude and frequency of natural hazards (Jomelli et al. 2004; Germain et al. 2009), increasing the exposure of populations to severe disasters, particularly in

mountain environments. Snow avalanches should figure among the most worrying processes because of their great destruction capacity (Gürer et al. 1994; Keiler 2004). In this respect, the tragedies that occurred recently in Europe and the Canadian Cordillera (Jarry and Sivardière 2000; Campbell et al. 2007) raise the question of the accuracy of the present avalanche zoning procedures given the possible impacts of climate change. The long-term reconstruction of diachronous events still represents great interest for risk determination and mapping (Salm 1997). Indeed, the return interval of high-magnitude avalanches for a given run-out distance is still, more than ever, an essential part in land-use planning (McClung 2000).

Because the snow avalanche regime may have been altered by defence structures, forecasting and explosive control and by changes in land use during the last century (Laternser and Schneebeli 2002), historical records may provide a better identification of past events but can hardly be used for precise zoning. Conversely, dendrogeomorphic methods may help characterizing the relative degree of hazard in alpine and subalpine environments where historical records are lacking.

A tree-ring-based avalanche record allows estimation of return intervals and annual probabilities of high-magnitude avalanches at both local and regional scales. However, land managers and engineers show little interest in tree-ring data despite of their usefulness for establishing spatiotemporal variations of high-magnitude events and calculation of run-out distance. Based on extreme events, i.e., ≥50 year return interval, run-out distances are usually evaluated using physical or statistical models that need to be calibrated with historical and/or field data. Statistical run-out models known as alpha-beta (Lied and Bakkehoi 1980; McClung and Lied 1987) or runout-ratio models (McClung et al. 1989; McClung and Mears 1991) are easier to use because they are based on topographic parameters. Dendrogeomorphic methods may be very useful for the calibration of such models, but surprisingly very little attention has been paid so far to tree-ring-based avalanche records. Knowledge of avalanche frequencies at the head of run-out zones would allow theoretical estimation of effective return intervals as a function of position along a given slope (McClung 2000). Tree-ring methods thus appear as a practical tool for zoning applications when used in conjunction with run-out models.

6 Conclusion

The important points made in our long-term research program in snow avalanches in the northern Gaspé Peninsula can be stated as follows: (i) the dendrogeomorphic methods provide valuable information on the frequencies (return intervals and annual probabilities) of past snow avalanches; (ii) impact scars and tilted trees with reaction wood are the most reliable evidence of past avalanche events; (iii) the probability to extend avalanche chronologies was high with a sample size of 25–30 trees, but increased only slightly with a sample size >40; (iv) a 10% threshold value was appropriate for high-magnitude avalanche identification; and (v) the threshold value can be established using a robust statistical method rather than subjectively.

However, in spite its utility in providing data on frequency-magnitude of geomorphic processes, the accuracy of this methodology has yet to be examined, particularly in regard to distinguishing the effects of other processes, i.e., snow creep, soil creep, and wind that may contribute to noticeable impacts on the tree-rings. In this respect, the use of a statistical technique to establish a threshold value should allow us to go one step further in spatiotemporal modeling. Finally, the scarcity of investigations dealing with spatial mapping (GIS) of avalanche return periods and with tree-ring sequences and icefall activity and slushflows are promising research directions, testifying that this approach is still at the developmental stage.

Acknowledgements Our long-term research program on snow avalanches could not have been conducted without the support of several people and agencies. We are especially grateful to François Boulanger (director of the Gaspésie National Park), Dominic Boucher and Jean-Pierre Gagnon (Centre d'avalanche de la Haute-Gaspésie), Guy St-Pierre (Ministry of Transportation of Québec), Natural Sciences and Engineering Research Council of Canada (NSERC), Fonds Québécois de Recherche sur la Nature et les Technologies (FQRNT), Emergency Preparedness Canada and the Community Foundation of Gaspé and Magdalen Islands.

References

Boucher D (2000) Projet d'implantation d'un centre d'avalanche dans le parc de la Gaspésie. MRC de Denis-Riverin, Québec

Boucher D, Filion L, Hétu B (2003) Reconstitution dendrochronologique et fréquence des grosses avalanches de neige dans un couloir subalpin du mont Hog's Back, Gaspésie centrale (Québec). Géogr phys Quat 57:159–168

Bryant CL, Butler DR, Vitek JD (1989) A statistical analysis of tree-ring dating in conjunction with snow avalanches: comparison of on-path versus off-path responses. Environ Geol 9:53–59

Burrows CJ, Burrows VL (1971) Procedures for the study of snow avalanche chronology using growth layers of woody plants. Arct Alp Res Occas Paper No. 23

Butler DR, Malanson GP (1985) A history of high-magnitude snow avalanche, Southern Glacier National Park, Montana, USA. Mt Res Dev 5:175–182

Butler DR, Sawyer CF (2008) Dendrogeomorphology and high-magnitude snow avalanches: a review and case study. Nat Haz Earth Syst Sci 8:303–309

Butler DR, Malanson GP, Oelfke JG (1987) Tree-ring analysis and natural hazard chronologies: minimum sample sizes and index values. Prof Geogr 39:41–47

Campbell C, Bakerman L, Jamieson B, Stethem C (2007) Current and future snow avalanche threats and mitigation measures in Canada. Canadian Avalanche Center, Canada

Carrara PE (1979) The determination of snow avalanche frequency through tree-ring analysis and historical records at Ophir, Colorado. Geol Soc Am Bull, Part I 90:773–780

Casteller A, Stöckli V, Villalba R, Mayer AC (2007) An evaluation of dendroecological indicators of snow avalanches in the Swiss Alps. Arct Antarc Alp Res 39:218–228

Clark WAV, Hosking PL (1986) Statistical methods for geographers. Wiley, New York

Dubé S, Filion L, Hétu B (2004) Tree-ring reconstruction of high-magnitude snow avalanches in the northern Gaspé Peninsula, Québec. Arct Antarc Alp Res 36:555–564

Fitzharris BB (1981) Frequency and climatology of major avalanches at Rogers Pass, 1909 to 1977. National Research Council of Canada No. 956

Gagnon RM (1970) Climat des Chic-Chocs. Ministère des Richesses Naturelles, Service de la Météorologie, Gouvernement du Québec 36

Germain D (2005) Dynamique des avalanches de neige en Gaspésie, Québec, Canada. Ph.D. Thesis, Université Laval
Germain D, Filion L, Hétu B (2005) Snow avalanche activity after fire and logging disturbances, northern Gaspé Peninsula, Québec, Canada. Can J Earth Sci 42:2103–2116
Germain D, Filion L, Hétu B (2006) Snow avalanche frequency inferred from tree-ring in a changing climate, Chic-Chocs Range, Canada. Analele Universitatii de Vest din Timisoara Geografie 16:7–34
Germain D, Filion L, Hétu B (2009) Snow avalanche regime and climatic conditions in the Chic-Chocs Range, eastern Canada. Clim Change 92:141–167
Glass B, Huet P, Rat M, Tordjeman R. (2000) Retour d'expérience sur l'avalanche du 9 février 1999 à Montroc, commune de Chamonix. Inspection Générale de l'Environnement. France, Rapport d'expertise, 65 pp
Gray JT, Brown RJE (1979) Permafrost presence and distribution in the Chic-Chocs Mountains, Gaspésie, Québec. Géogr phys Quat 33:299–316
Gürer I, Tunçel H, Yavas O, Erenbilge T, Sayin A (1994) Snow avalanche incident in north-western Anatolia, Turkey, during December 1992. Nat Haz 11:1–16
Hächler P (1987) Analysis of the weather situations leading to severe and extraordinary avalanche situations. Avalanche formation movement and effects. IAHS Spec Publ 162:295–303
Hägeli P, McClung DM (2003) Avalanche characteristics of a transitional snow climate—Columbia Mountains, British Columbia, Canada. Cold Reg Sci Tech 37:255–276
Hebertson EG, Jenkins MJ (2003) Historic climate factors associated with major avalanche years on the Wasatch Plateau, Utah. Cold Reg Sci Tech 37:315–332
Hétu B (2007) Les conditions météorologiques propices au déclenchement des avalanches de neige dans les corridors routiers du nord de la Gaspésie, Québec, Canada. Géogr phys Quat 61(2–3):165–180
Hétu B, Bergeron A (2004) Les avalanches au Québec: analyse des conditions météorologiques et des facteurs de terrain propices au déclenchement des avalanches. Secrétariat général de Recherche et Sauvetage Canada, PCSAQ
Hétu B, Brown K (2006) Inventaire des avalanches mortelles au Québec depuis 1825. Avalanche.ca 79:56–59
Hétu B, Brown K, Germain D (2008) L'inventaire des avalanches mortelles au Québec depuis 1825 et ses enseignements. Proceedings of the 4th Canadian conference on geohazards, Université Laval, Québec, 20–24 May 2008
Höller P (2009) Avalanche cycles in Austria: an analysis of the major events in the last 50 years. Nat Haz 48:399–424
Jarry F, Sivardière F (2000) Characteristics of fatal avalanche accidents in France 1989-1999. Proceedings of the International Snow Science Workshop, Montana, pp 8–15
Johnson EA (1987) The relative importance of snow avalanche disturbance and thinning on canopy plant populations. Ecology 68:43–53
Johnson EA, Hogg L, Carlson C (1985) Snow avalanche frequency and velocity for the Kananaskis valley in the Canadian Rockies. Cold Reg Sci Tech 10:141–151
Jomelli V, Delval C, Grancher D, Escande S, Brunstein D, Hétu B, Filion L, Pech P (2007) Probabilistic analysis of recent snow avalanche activity and weather in the French Alps. Cold Reg Sci Tech 47:180–192
Jomelli V, Pech P, Chochillon C, Brunstein D (2004) Geomorphic variations of debris flows and recent climatic change in the French Alps. Clim Change 64:77–102
Keiler M (2004) Development of the damage potential resulting from avalanche risk in the period 1950-2000, case study Galtür. Nat Haz Earth Syst Sci 4:249–256
Larocque S, Hétu B, Filion L (2001) Geomorphic and dendroecological impacts of slushflow in central Gaspé Peninsula (Québec, Canada). Geogr Ann 83A:191–201
Laternser M, Schneebeli M (2002) Temporal trend and spatial distribution of avalanche activity during the last 50 years in Switzerland. Nat Haz 27:201–230
Lied K, Bakkehoi S (1980) Empirical calculations of snow avalanche run-out distance based on topographic parameters. J Glaciol 26:165–177

Liverman D, Batterson M, Taylor D, Ryan J (2001) Geological hazards and disasters in Newfoundland and Labrador. Can Geotech J. 38:936–956

Luckman BH, Frazer GW (2001) Dendrogeomorphic investigations of snow avalanche tracks in the Canadian Rockies. Paper presented at the international conference on the future of dendrochronology, Davos, Switzerland, 22–26 September 2001

McClung DM (2000) Extreme avalanche runout in space and time. Canad Geotech 37:161–170

McClung DM, Lied K (1987) Statistical and geometrical definition of snow avalanche runout. Cold Reg Sci Tech 13:107–119

McClung DM, Mears AI (1991) Extreme value prediction of snow avalanche runout. Cold Reg Sci Tech 19:163–175

McClung DM, Mears AI, Schaerer PA (1989) Extreme avalanche run-out: data from four mountain ranges. Annal Glaciol 13:180–184

Mears AI (1992) Snow avalanche hazard analysis for land-use planning and engineering, Colorado. US Geol Surv Bull 49:55

Rayback SA (1998) A dendrogeomorphological analysis of snow avalanches in the Colorado Front Range, USA. Phys Geogr 19:502–515

Salm B (1997) Principles of avalanche hazard mapping in Switzerland. In: Izumi M, Nakamura T, Sack RL (eds) Snow engineering: recent advances. Balkema, Rotterdam

Shroder JF Jr (1978) Dendrogeomorphological analysis of mass movement on Table Cliffs Plateau, Utah. Quat Res 9:168–185

Shroder JF Jr (1980) Dendrogeomorphology: review and new techniques of tree-ring dating. Prog Phys Geogr 4:161–188

Solomina O (2002) Dendrogeomorphology: research requirements. Dendrochronologia 20:233–245

Stoffel M, Bollschweiler M (2008) Tree-ring analysis in natural hazards research – an overview. Nat Haz Earth Syst Sci 8:187–202

Stoffel M, Bollschweiler M, Hassler G-R (2006) Differentiating past events on a cone influenced by debris-flow and snow avalanche activity – a dendrogeomorphological approach. Earth Surf Process Land 31:1427–1434

Using Dendrochronology to Validate Numerical Simulations of Snow Avalanches in the Patagonian Andes

Alejandro Casteller, Marc Christen, Ricardo Villalba, and Veronika Stöckli

Snow avalanches pose a considerable risk in the Patagonian Andes. Despite this, avalanche hazard maps are rare for this region. One way to reduce this risk uncertainty is to apply numerical models that predict avalanche runout. These models require that the avalanche release areas must be precisely determined (Maggioni and Gruber 2003) and the friction parameters used by the models must be adjusted to local terrain and snow conditions (Furdada et al. 2002). These parameters can be estimated by simulating avalanche events for which the extent of runout is known. Dendrochronological methods become a valuable tool for precisely defining the spatial extent of past events in the Andes where directly observed evidence is not available. Tree-ring studies are also important for reconstructing years of avalanche occurrences in such cases (Casteller et al. 2008).

Here, we present the results of a study related to the largest tragedy in the history of Argentinean mountaineering, in which nine people were killed by a slab avalanche. This occurred on 1 September 2002 at Cerro Ventana, Bariloche, in northern Patagonia (41°12′36″S, 71°22′32″W). Detailed information about the avalanche features were compiled in the field, providing the required inputs to run the avalanche models. As the lower part of the avalanche track is forested by the broadleaf Lenga beech (*Nothofagus pumilio*), we were able to examine different tree-ring indicators associated with the 2002 event and previous undocumented avalanches at the site. The tree-ring data used to estimate the maximum extent of the 2002 event are verified by the field observations.

Two sampling strategies were applied: (i) purposeful sampling of 15 trees with clear external evidence of past avalanche disturbance along the track, and (ii) systematic sampling of all 24 trees, regardless of the presence of external damage,

A. Casteller (✉) and R. Villalba
Instituto Argentino de Nivología, Glaciología y Ciencias Ambientales IANIGLA,
5500 Mendoza, Argentina
e-mail: casteller@lab.cricyt.edu.ar

A. Casteller, M. Christen, and V. Stöckli
WSL, Institute for Snow and Avalanche Research SLF,
CH-7260 Davos Dorf, Switzerland

M. Stoffel et al. (eds.), *Tree Rings and Natural Hazards: A State-of-the-Art*,
Advances in Global Change Research 41, DOI 10.1007/978-90-481-8736-2_6,

in a 28 m^2 plot located in the run-out zone of the track at 1,455 m elevation. Cross-sections were taken in all cases. In the purposeful sampling, scars from the 2002 avalanche were found in seven of the ten trees sampled between 1,440 and 1,490 m (Fig. 1); none of the five trees below 1,440 m showed damage from the 2002 event. These 15 trees also contained evidence of several earlier avalanche events. In particular, three scars, one variation in eccentricity, and seven abrupt growth changes were noted in 2000. Avalanche events in 1943, 1949, 1978, 1985 and 1991 are also suggested by limited evidence from these trees. Avalanche-damaged trees extend down to 1,380 m, indicating that the 2002 event was not the most extensive from the site. In the systematic sampling, evidence of the 2002 event was recorded in 19 of the 24 sampled trees: seven trees showed scars and 12 unscarred trees showed abrupt growth changes.

RAMMS is a numerical model for avalanche dynamics (Christen et al. 2008) and was used to simulate the 2002 event. Four simulations were conducted using the observed snow release depth of 0.6 m (release volume of 10,300 m^3) and the following coefficients: (a) $\mu = 0.47$, $\xi = 1000$ m s^{-2}; (b) $\mu = 0.42$, $\xi = 1000$ m s^{-2}; (c) $\mu = 0.38$, $\xi = 1000$ m s^{-2}; (d) $\mu = 0.40$, $\xi = 700$ m s^{-2}, where μ and ξ are the dry and viscous friction coefficients, respectively. An erodible snow layer of 0.6 m was

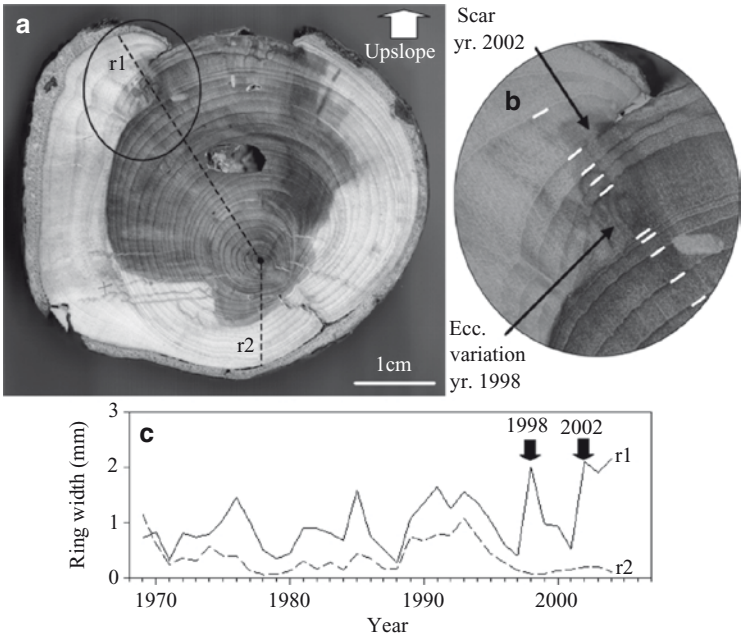

Fig. 1 (**a**) Cross section of a *Nothofagus pumilio* tree damaged by avalanche events in 1998 and 2002. (**b**) Detail of the eccentricity variation from 1998 and the 2002 scar. (**c**) Similar growth trends are recorded for both radii prior to the first avalanche impact in 1998. The 2002 avalanche produced the scar shown in (**b**)

incorporated in Simulation d, which resulted in an additional eroded snow volume of 21,000 m^3. The modeled run-out altitude in Simulation c coincides with the dendrochronologically-reconstructed value of 1,440 m, and varies between 40 m upslope and 9 m downslope for Simulations a and d, respectively (Fig. 2). Maximum avalanche velocities provided by the model range from 15.40 to 17.85 m s^{-1}; unfortunately, no recorded avalanche velocities are available for comparison.

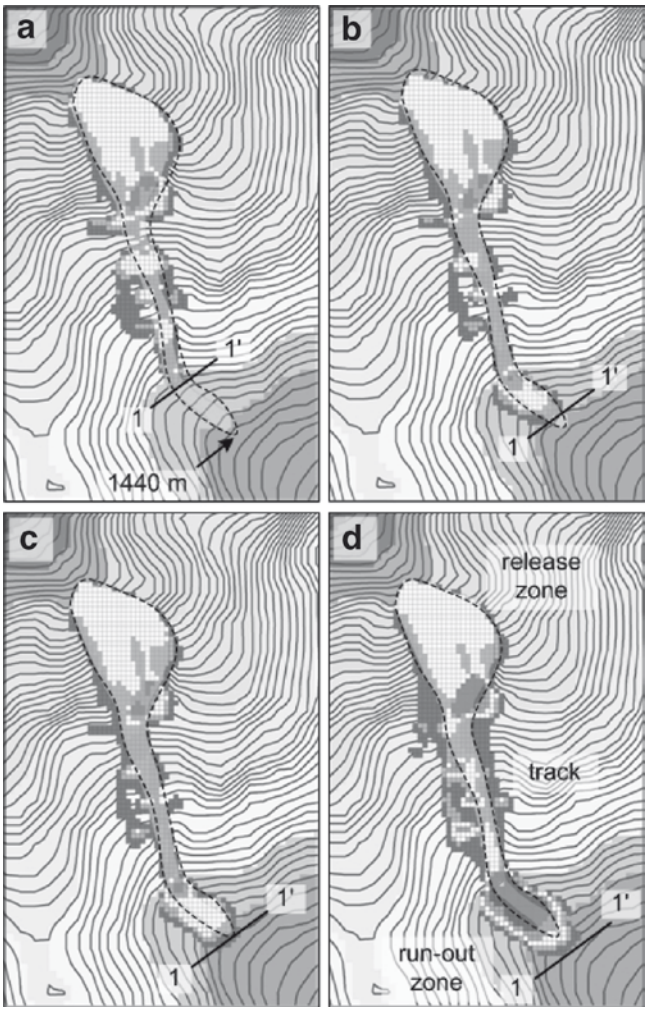

Fig. 2 Four numerical simulations of the 2002 avalanche event (for details see text). The boundary of the 2002 event is shown by a *dashed line*. The *solid lines* indicated by 1–1′ show the maximum extent of each simulated event. The extent of the observed and simulated events coincide in figure **c**. The contour interval is 10 m. The *shaded areas* within and adjacent to the avalanche track show the modeled distribution and depth of avalanche show (see Casteller et al. 2008)

The maximum simulated snow depths deposited in the track vary from 1.95 to 3.5 m (detail not shown) and are considerably lower than the 7 m observed, even with the model that includes snow entrainment (Simulation d). This limitation reflects the low resolution (30 m) of the topographical model (ASTER DEM), which does not accurately show the terrain features that funneled the avalanche along a narrow path, resulting in lower simulated snow deposition depths and a greater simulated width for the avalanche in the run-out zone.

Our results support previous studies suggesting that tree rings from *N. pumilio* can be used to date and determine the extent of past snow avalanches (Mundo et al. 2007). Also, though only a preliminary study, this paper demonstrates that tree-ring data can be used to calibrate numerical avalanche models for the Patagonian Andes. Ultimately, advances in snow avalanche modeling and in tree-ring applications will provide regional hazard maps for this mountainous area.

References

Casteller A, Christen M, Villalba R et al (2008) Validating numerical simulations of snow avalanches using dendrochronology: the Cerro Ventana event in Northern Patagonia, Argentina. Nat Haz Earth Syst Sci 8:433–443

Christen M, Bartelt P, Kowalski J et al. (2008) Calculation of dense snow avalanches in three-dimensional terrain with the numerical simulation program RAMMS. In: Gleason JA (ed) Proceedings of the International Snow Science Workshop 2006, Whistler, Canada, pp 709–716

Furdada G, Naaim M, Martinez H (2002) Calibration and application of the MN2D dynamics model to the avalanches of Las Leñas (Argentina). Nat Haz Earth Syst Sci 2:221–226

Maggioni M, Gruber U (2003) The influence of topographic parameters on avalanche release dimension and frequency. Cold Reg Sci Tech 37(3):407–419

Mundo IA, Barrera MD, Roig FA (2007) Testing the utility of Nothofagus pumilio for dating a snow avalanche in Tierra del Fuego, Argentina. Dendrochronologia 25:19–28

Part III
Landslides

Trees disturbed and destroyed by the 1959 Madison Canyon rockslide, Montana, USA (© D. R. Butler)

Dating Landslides with Trees

John J. Clague

1 Introduction

Dendrochronology is increasingly being use in natural hazard studies, especially in those concerned with estimating risk. Central to such studies are frequency–magnitude relations, which relate the size of hazardous events to their average recurrence. Frequency–magnitude curves are best established from observational data, but the historic record may be too brief to capture extreme events, or it may be otherwise non-representative of longer periods. Earth scientists thus use the recent geologic record to add depth to the observational database by estimating both the size distribution of prehistoric events and the frequency of events of different size. The latter requires knowledge of the ages of prehistoric events, which is where dendrochronology comes into play. Some past earthquakes, landslides, floods, and other events can be dated using tree rings and the ages then used to quantify relations between event frequency and magnitude. The equations that define frequency–magnitude relations, in turn, are the basis for probability-based forecasts of hazard.

The papers in this section of the book deal with landslides. Dendrochronology is particularly suited to landslide research because potentially unstable slopes in temperate and tropical environments may be treed and because the rings of trees damaged or killed by a landslide can record the age of the event.

2 Landslides

A landslide is the movement of a mass of rock, sediment, soil, or artificial fill under the influence of gravity (Fig. 1). Landslides range in volume from tens of cubic meters to tens of cubic kilometers; their velocities range from millimeters per year

J.J. Clague (✉)
Centre for Natural Hazard Research, Simon Fraser University, Burnaby BC, V5A 1S6, Canada
e-mail: jclague@sfu.ca

M. Stoffel et al. (eds.), *Tree Rings and Natural Hazards: A State-of-the-Art*, Advances in Global Change Research 41, DOI 10.1007/978-90-481-8736-2_7,

Fig. 1 Rock avalanche at Tetsa River in northeast British Columbia. Tree rings can be used to date landslides such as this (Photo by Marten Geertsema)

to more than 100 m per second. Landslides are primarily associated with mountainous terrain, but they also occur in areas of low relief, for example in roadway and building excavations, mine-waste piles, and river bluffs.

Landslides kill thousands of people each year and cause tens of billions of dollars in damage. One of the most deadly landslides on record occurred during an earthquake in Peru on May 31, 1970. An earthquake dislodged a large mass of rock and glacier ice on Nevado Huascarán, a high peak in the Cordillera Blanca. The failed rock mass rapidly fragmented, producing a debris flow that killed 20,000 inhabitants of the towns of Yungay and Ranrahirca (Plafker and Ericksen 1978). Large landslides can also block rivers, creating impoundments and causing upstream flooding. Sudden failure of landslide dams may cause devastating downstream floods. Because of the threat that landslides pose to public safety and infrastructure, research aimed at better understanding slope stability and failure has accelerated in recent years. This acceleration has been accompanied by basic research into slope failure processes, mechanisms of debris movement, and landslide history, causes, and triggers.

Landslides commonly are classified according to their velocity, type of movement, and source material (Fig. 2; Turner and Schuster 1996). Water also is important because it commonly causes or triggers slope failure and also exerts a strong

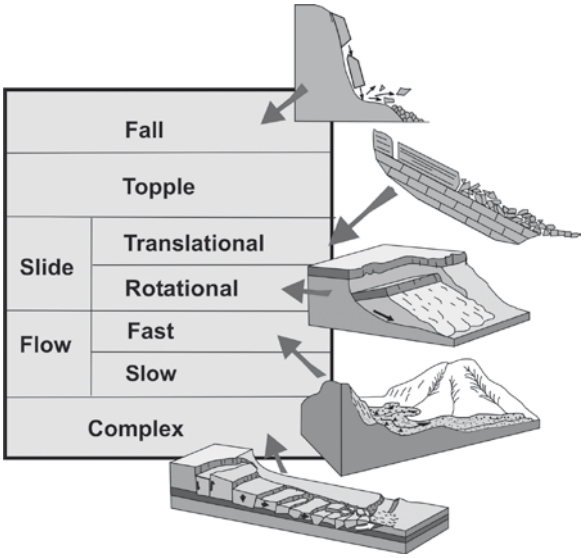

Fig. 2 Simplified classification of landslides (Clague 2007, Fig. 1)

influence on movement. The scheme shown in Fig. 2, although simplified, provides an understanding of the range and complexity of landslides. The main landslide types are briefly described below.

A fall involves rolling and bouncing of rock and, less commonly, sediment, from a cliff or down a steep slope. Failure typically occurs along steeply inclined fractures or other discontinuities in the source rock or sediment.

A topple involves the forward rotation of a large mass of rock or sediment about a pivot point under the influence of gravity. Movement occurs along steeply inclined fractures. Topples range from shallow movements to deep-seated displacements of large volumes of rock. The process operates almost imperceptibly, but a threshold of stability may be reached, whereupon the toppling block suddenly fails, producing a fall or a slide.

A slide involves movement of an intact or disintegrating mass of rock or sediment along a well defined basal failure plane. Slides are subdivided into translational and rotational types. Translational sliding takes place on planar or undulating surfaces. The slide mass commonly disintegrates as it moves downslope, but the fragments tend to retain their positions with respect to one another. Rotational sliding involves translation of rock or sediment along a concave-upward, curved failure surface, producing what is termed a slump. Movement rates range from millimeters per hour to meters per second. Many slides are complex phenomena, involving both translational and rotational movements.

Flows are a large and varied group of landslides that share one similarity – the failed material moves as fluid, commonly a non-Newtonian fluid. In wet flows,

rock fragments are partly supported by interstitial water. Debris flows are the most common type of wet flow; they consist of a mixture of water, rock fragments, and plant detritus that moves down a steep stream course or ravine as a slurry. Mudflows are similar to debris flows, but the solid fraction consists of sand, silt, and clay, with little or no gravel or coarser material. Sediment flows also happen in oceans and lakes, especially off deltas and at the heads of submarine canyons. Those that travel down submarine canyons into deep ocean waters are termed turbidity currents.

Rock avalanches (also known as sturzströme) are large, fast-moving flows of fragmented rock. Rapid flow results from the release of large amounts of energy due to particle interactions and comminution. Rock avalanches are the fastest of all landslides, in some cases achieving speeds of 100 m per second or more. They also travel long distances where unimpeded by topography. Rock avalanches are rarer than other types of landslides, but they are important and of scientific interest because of their long travel distances and because of the destruction and death they cause. One of the most famous examples is the Frank Slide, which killed about 70 people in the mining town of Frank, Alberta, in April 1903 (McConnell and Brock 1904; Cruden and Krahn 1978).

Many landslides do not fit comfortably into classification schemes. Prominent examples include sackung and lateral spreads. Sackung, a German word meaning "sag", is the deep-seated downslope movement of a large, internally broken rock mass, with no single, well defined basal failure plane. Movement is manifested at the land surface by cracks, trenches, and scarps at mid and upper slope positions, and by bulging of the lower slope. Lateral spreading involves extension of a slab of earth material above a nearly flat shear plane. The moving slab may subside, rotate, disintegrate, or flow. Lateral spreading in silts and clays is commonly progressive – failure starts suddenly in a small area, but spreads rapidly, ultimately affecting a much larger area.

Finally, many landslides, including most large ones, are complex, that is they involve more than one type of movement. A rockslide, for example, may evolve into a debris flow by entraining water or saturated sediments along its path.

3 Dating Landslides with Trees

Dendrochronologists use three general strategies to date landslides. The first strategy is to determine the age of the oldest tree living on the landslide deposit. The surface of the deposit obviously must have been colonized by trees after the landslide, thus the oldest tree provides a minimum age for the event. This strategy has been successfully used, for example, to date exceptional regional rainstorms that triggered large numbers of debris flows in British Columbia (Schwab 1998).

The assumption underpinning this strategy is that the tree became established soon after the landslide. However, trees do not immediately seed on new landslide surfaces – there is a period, termed the ecesis interval, between the time the new

surface becomes available and the time that trees become established on it. Ecesis intervals in northwest North America range from a year or two to almost 100 years, depending on the tree species, the nature of the substrate, and climate (Sigafoos and Hendricks 1969; Smith et al. 1995; Wiles et al. 1999; Luckman 2000; Lewis and Smith 2004). A correction may be applied for a specific area if the ecesis time is known in the modern environment.

A more serious problem, which commonly restricts the strategy to landslides less than 1,000 years old, is that the living trees on a landslide deposit may not be first cohort; in other words, the original cohort died and was replaced by second-growth or younger forest. In such cases, of course, the living trees provide, at best, a gross minimum age for the landslide.

A second strategy is to date trees that were affected, but not killed, by landslides. Catastrophic landslides, including rockslides and rock avalanches, remove trees along their paths, but some trees at the lateral margins and fronts of these landslides survive the trauma. Damage to the crown or root systems may produce a sudden reduction in the thickness of the annual rings, known as suppression. In other cases, landslides produce a marked increase in ring width (release) by eliminating competition from nearby trees (Paolini et al. 2005). In both cases, the landslide is easily dated by counting back from the outermost ring to the ring where tree growth changed. Trees also are scarred or tilted by landslides (e.g., Shroder 1978; Clague and Souther 1982; Bégin and Filion 1985, 1988; Braam et al. 1987a, b; Osterkamp and Hupp 1987; Corominas and Moya 1999; Fantucci and Sorriso-Valvo 1999). After the landslide, the trees repair the damage – new tissue is progressively emplaced over scars (Fig. 3), and the tilted trees may gradually right their stems to a vertical position. Conifers right their stems by adding compression wood preferentially on the down-tilted side of their trunks (Fig. 4). In both instances, the age of the landslide can be easily determined by counting back from the cambium to the first ring emplaced after the tree was damaged by the landslide. Dating is not so straightforward in the case of slow-moving earthflows and sackung. Tilted trees may archive the initiation of movement, but if the movement is continuous, the tree may never right itself. Episodic movement may leave a complex pattern of stem rings, comprising asymmetric rings formed during times of movement and symmetric ones when no movement occurred (Shroder 1978; Braam et al. 1987a, b).

A third strategy is used to date trees that were killed by the landslide. In some cases, scarred or tilted trees at the margin of the debris, although dead, still stand. Floating ring-width chronologies derived from these stems potentially can be crossdated with local or regional master chronologies derived from living trees. In other cases, where trees were overridden and destroyed by the landslide, growth-position roots and boles of trees may remain beneath the debris or exposed along the path of the landslide. Again, ring-width chronologies from the boles possibly can be crossdated with local or regional master chronologies (Bégin and Filion 1988). In still other instances, logs and stems, entrained by the landslide, occur within the debris (Filion et al. 1991). The strategy of crossdating the subfossil series into living tree-ring chronologies can be problematic. The outer-ring age of an entrained stem

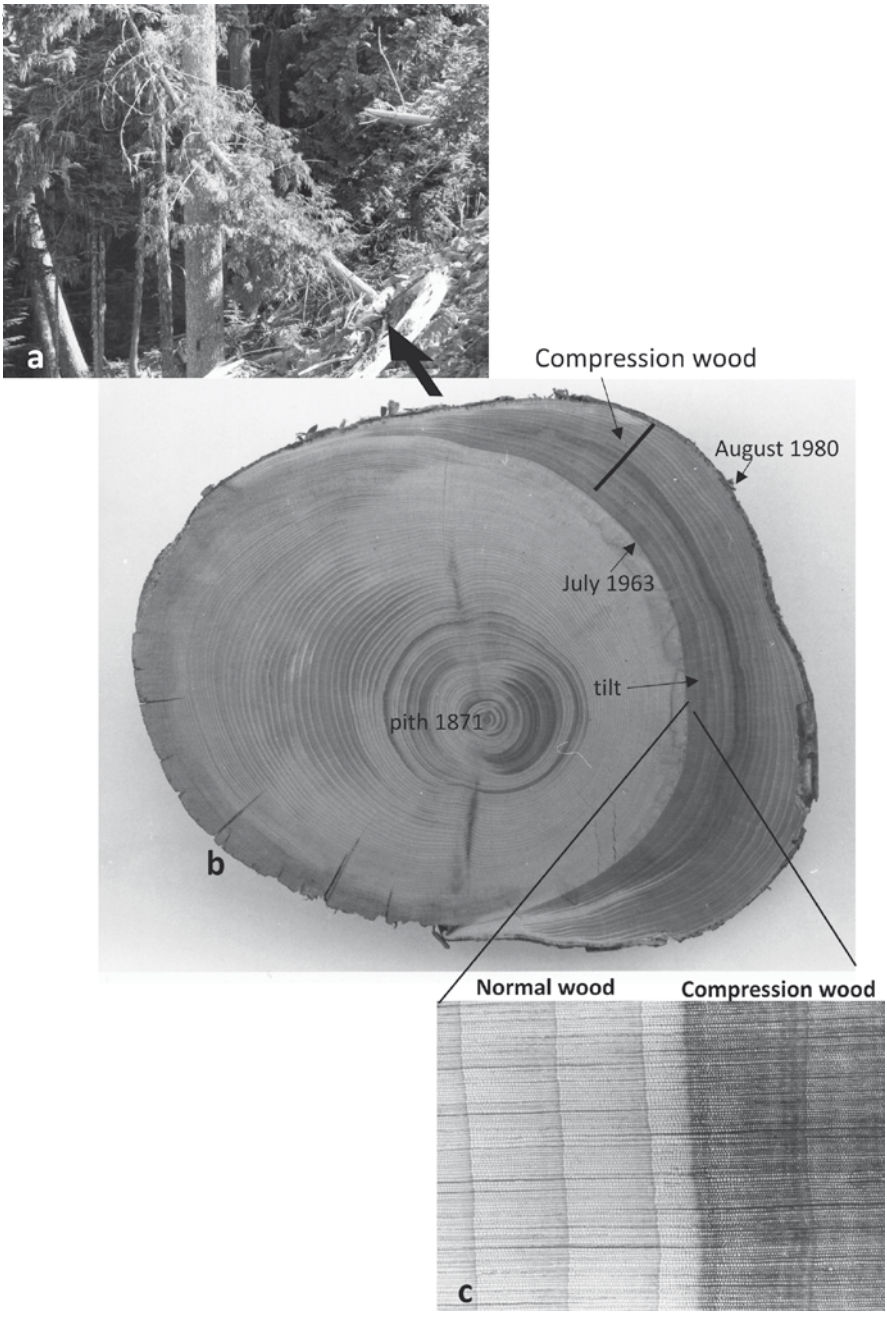

Fig. 3 Example of landslide-tilted trees (**a**) Western red cedar (*Thuja plicata*) tilted and partly buried by debris of the 1963 Dusty Creek landslide in the southern Coast Mountains of British Columbia. (**b**) Section of tilted Alaska yellow-cedar (*Chamecyparis nootkatensis*) showing change in the ring width in 1963. Compression wood, formed between 1963 and 1980, is concentrated on the lower side of the trunk. (**c**) Photographic enlargement of part of the section shown in (**b**). The beginning of the production of compression wood occurred in 1963 prior to the formation of a late-wood layer (Modified from Clague and Souther 1982, Fig. 9; reproduced courtesy of National Research Council of Canada)

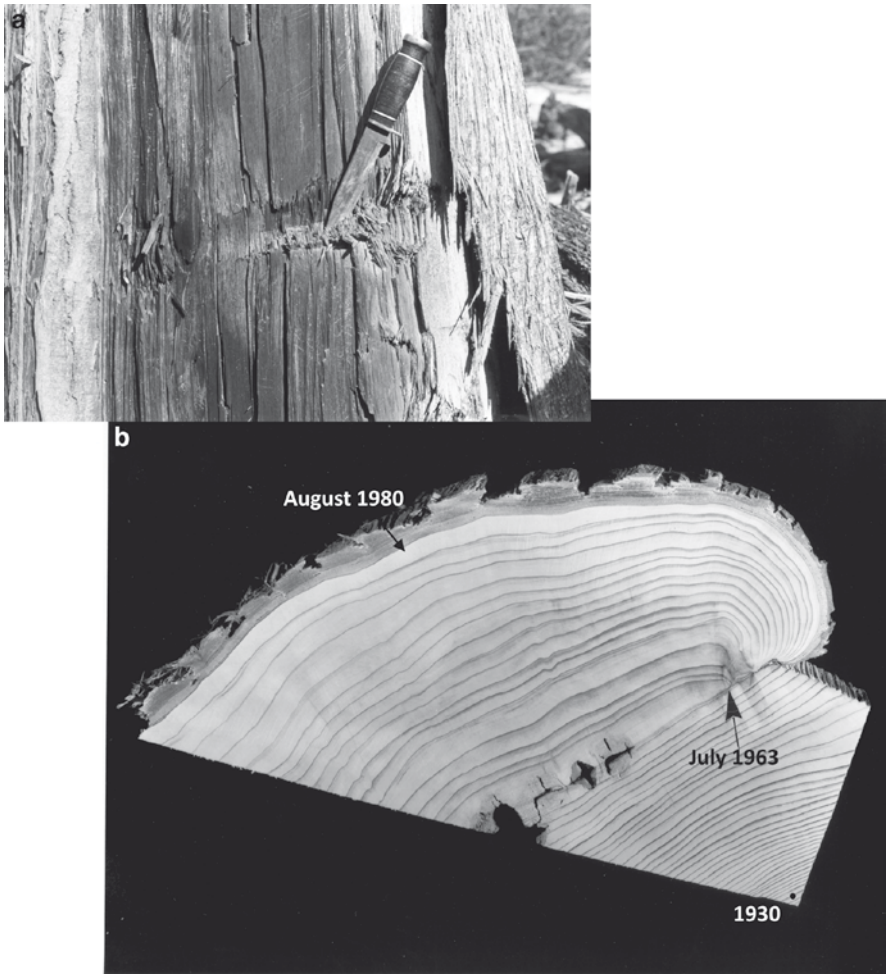

Fig. 4 Example of a landslide-scarred tree. (**a**) Scar produced by impact of airborne debris of the Dusty Creek landslide on Western red cedar (*Thuja plicata*). Wood tissue in the scar area was ripped off and sliced during impact. (**b**) Partial section of tree shown in (**a**). Note the increase in ring width after 1963. *Arrows* in (**a**) and (**b**) indicate where living tissue is advancing over the scar (Clague and Souther 1982, Fig. 10; Reproduced courtesy of National Research Council of Canada)

or in-situ root bole will coincide with the age of the landslide only if the tree was killed by the event. This assumption probably is valid in the case of overridden in-situ boles with preserved bark. However, the assumption becomes more tenuous when dealing with incorporated stems and other woody debris lacking bark. In such cases, the researcher must date many stems and also consider the possibility that deadfall was entrained by the landslide, in which case the age of the outermost ring is older than the landslide.

4 Concluding Remarks

Dendrochronology, when integrated into geomorphic and stratigraphic studies, is a powerful tool for assessing landslide hazard and risk. It is the only technique that can provide annual, even seasonal, precision on the dates of prehistoric landslides and historic landslides for which no observational data exist. It may prove particularly useful in testing the hypothesis that several landslides suspected of being seismically triggered or caused by an unusually severe storm, are, in fact, the same age. It also can be used to establish chronologies for periods of earthflow activity and stability that, in turn, can be linked to fluctuations of climate on different timescales. Dendrochronology, however, is generally limited to dating landslides that are no more than several hundred years old. Another limitation of the technique is that living trees on landslide deposits and subfossil tree stems entombed within the debris may not closely date the time of the landslide. Caution is thus required in interpreting the relation between dendro-dated trees and the landslides with which they are associated.

References

Bégin C, Filion L (1985) Analyse dendrochronologique d'un glissement de terrain dans la région du Lac á l'Eau Claire (Québec nordique). Can J Earth Sci 22:175–182

Bégin C, Filion L (1988) Age of landslides along Grande Rivière de la Baleine estuary, eastern coast of Hudson Bay, Quebec (Canada). Boreas 17:289–299

Braam RR, Weiss EEJ, Burrough A (1987a) Spatial and temporal analysis of mass movement using dendrochronology. Catena 14:573–584

Braam RR, Weiss EEJ, Burrough A (1987b) Dendrogeomorphological analysis of mass movement; a technical note on the research method. Catena 14:585–589

Clague JJ (2007) Landslides. In: McGraw-Hill yearbook of science & technology 2007. McGraw-Hill, New York, pp 127–130

Clague JJ, Souther JG (1982) The Dusty Creek landslide on Mount Cayley, British Columbia. Can J Earth Sci 19:524–539

Corominas J, Moya J (1999) Reconstructing recent landslide activity in relation to rainfall in the Llobregat River basin, Eastern Pyrenees, Spain. Geomorphology 30:79–93

Cruden DM, Krahn J (1978) Frank rockslide, Alberta, Canada. In: Voight B (ed) Rockslides and avalanches, 1; natural phenomena. Elsevier, Amsterdam, pp 97–112

Filion L, Quinty F, Bégin C (1991) A chronology of landslide activity in the valley of Rivière du Gouffre, Charlevoix, Quebec. Can J Earth Sci 28:250–256

Fantucci R, Sorriso-Valvo M (1999) Dendrogeomorphological analysis of a slope near Lago, Calabria (Italy). Geomorphology 30:165–174

Lewis DH, Smith DJ (2004) Little Ice Age glacial activity in Strathcona Provincial Park, Vancouver Island, British Columbia, Canada. Can J Earth Sci 41:285–297

Luckman BH (2000) The Little Ice Age in the Canadian Rockies. Geomorphology 32:357–384

McConnell RG, Brock RW (1904) Report on the great landslide at Frank, Alberta. Canadian Department of the Interior, Annual Report 1902–1903, 3 pp

Osterkamp WR, Hupp CR (1987) Dating and interpretations of debris flows by geologic and botanical methods at Whitney Creek Gorge, Mt. Shasta, California. In: Costa JE, Wieczorek

GF (eds) Debris flows/avalanches; process, recognition, and mitigation. Geol Soc Am Rev Eng Geol 7:157–163
Plafker G, Ericksen GE (1978) Nevados Huascaran avalanches, Peru. In: Voight B (ed) Rockslides and avalanches, 1; natural phenomena. Elsevier, Amsterdam, pp 277–314
Paolini L, Villalba R, Grau HR (2005) Precipitation variability and landslide occurrence in a subtropical mountain ecosystem of NW Argentina. Dendrochronologia 22:175–180
Schwab JW (1998) Landslides on the Queen Charlotte Islands: Processes, rates, and climatic events. In: Hogan DJ, Tschaplinksi PJ, Chatwin S (eds) Carnation Creek and Queen Charlotte Islands fish/forestry workshop: Applying 20 years of coast research to management solutions. BC Ministry of Forests, Land Management Handbook 41:41–48
Shroder JF (1978) Dendrogeomorphological analysis of mass movements on Table Cliffs Plateau, Utah. Quat Res 9:168–185
Sigafoos RS, Hendricks EL (1969) The time interval between stabilization of alpine glacial deposits and establishment of tree seedlings. US Geol Surv Prof Paper 650-B:B89–B93
Smith DJ, McCarthy DP, Colenutt ME (1995) Little Ice Age glacial activity in Peter Lougheed and Elk Lakes Provincial Parks, Canadian Rocky Mountains. Can J Earth Sci 32:579–589
Stefanini MC (2004) Spatio-temporal analysis of a complex landslide in the Northern Apennines (Italy) by means of dendrochronology. Geomorphology 63:191–202
Turner AK, Schuster RL (eds) (1996) Landslides – investigation and mitigation. Special Report 247, Transportation Research Board, National Research Council, Washington, DC
Wiles GC, Barclay DJ, Calkin PE (1999) Tree-ring-dated Little Ice Age histories of maritime glaciers from western Prince William Sound. Holocene 9:163–173

Dendrogeomorphological Analysis of a Landslide near Lago, Calabria (Italy)

Rosanna Fantucci and Marino Sorriso-Valvo

1 Introduction

Dendrogeomorphology, first introduced by Alestalo (1971) has been applied successfully in the spatial and temporal analysis of mass movements by many authors: Shroder (1978) investigated landslides in the Table Cliffs Plateau of Utah finding peak periods of mass-movement reactivation. Many authors (Terasme 1975; Shroder 1978; Hupp 1984; Strunk 1992; Denneler and Schweingruber 1993) found that trees subject to stress due to mass-movement have manifested strong and sudden decreases in ring growth. This effect on tree growth was also found by Orombelli and Gnaccolini (1972) in dating the Vajont landslide in Italy through the study of tilted conifers. Another important kind of information on the causes of landslide movement was pointed out in the papers of Jibson and Keefer (1988) and Filion et al. (1991). Those authors discovered coincidence between the dating of tree disturbances and past strong earthquakes in the Mississippi Valley and Rivière du Gouffre, respectively. Dendrochronology was used by Hupp (1984), Van Asch and Van Steijn (1991) and Strunk (1992) to evaluate the frequency of landslide activity. Kashiwaya et al. (1989) have investigated the relationship between tree-ring width and heavy rainfall in the landslide-prone area of Kobe district in Japan.

2 Study Site

The aim of this study was to investigate phases of past activity of a large-scale deep-seated gravitational slope deformation involving the part included between the Vallone Pizzotto canyon and Greci Village, of the right side slope of the torrent

R. Fantucci (✉)
Studio Geologi Associati, 01027 Montefiascone VT, Italy
e-mail: rosannafantucci@tele2.it

M. Sorriso-Valvo
CNR IRPI 87030 Roges di Rende CS, Italy

M. Stoffel et al. (eds.), *Tree Rings and Natural Hazards: A State-of-the-Art*,
Advances in Global Change Research 41, DOI 10.1007/978-90-481-8736-2_8,

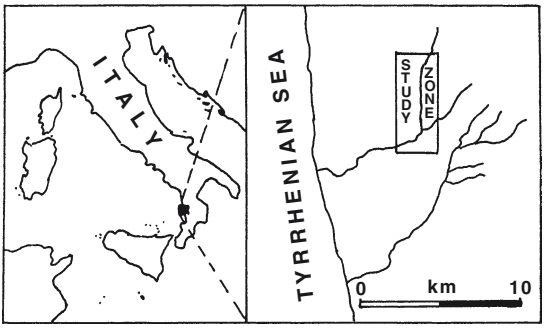

Fig. 1 Location of the study zone

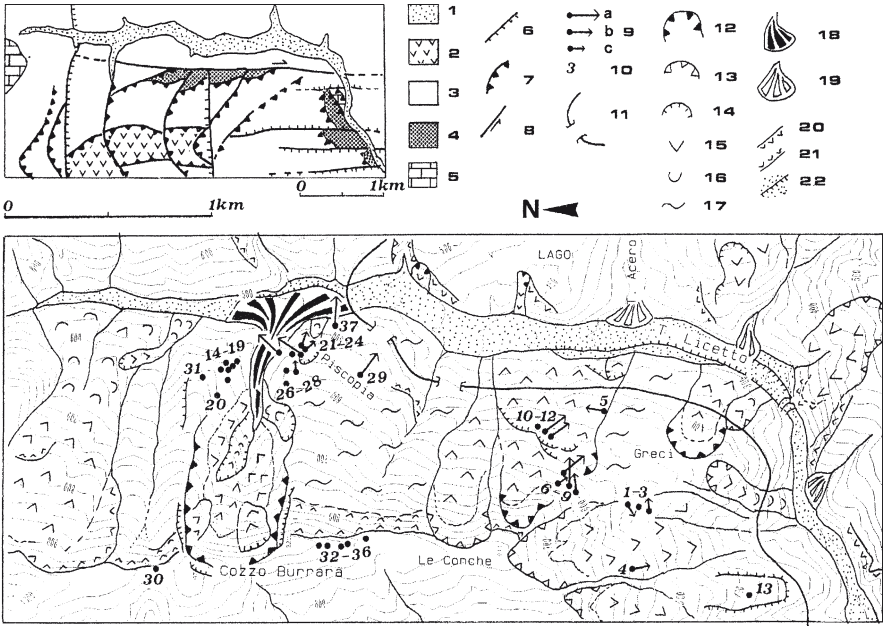

Fig. 2 Dendrochronological samples, geomorphological scheme and regional sketch map of the study area. The Vallone Pizzoto canyon landslide and fan complex East of Cozzo Burrara. Key to the symbols: 1= Holocene deposits; 2 = high-grade metamorphics; 3 = low-grade metamorphics; 4 = metabasite and metalimestones; 5 = dolostones; 6 = normal fault (tics on the down-thrown block); 7 = thrust fault (teeth on the upthrust side); 8 = strike-slip fault; *arrows* if stems are reclining by: a: > 30°; b: 10°/30°; c: 1°/9°; 10 = sample number; 11 = highway; 12 = principal landslide scarp; 13 = principal landslide scarp, non active; 14 = secondary scarp; 15 = sliding-type landslide; 16 = flow-type landslide; 17 = sackung deformation type; 18 = alluvial fan, active; 19 = alluvial fan, non active; 20 = slope convexity (teeth on the downslope side); 21 = slope concavity (teeth on the upslope side); 22 = stream erosion scarp

Elicetto, near the city of Lago, northern Calabria (Figs. 1 and 2). The deformation is of the sackung type (Zischinsky 1969) and is ca. 1,300 ha in extent. It is active, as clearly indicated by the current activity of the landslide at its upstream and downstream boundaries, and by inclinometric and topographic data (Sorriso-Valvo et al. 1996). The slope comprises essentially allochtonous terrains emplaced during the Alpine Orogeny. They consist of low- to medium-grade metamorphics represented essentially by ophiolite-bearing phyllites with metacalcarenite and quartzite bands, and by porphyroids. High-grade metamorphics (white schists and gneiss) lie over the lower-grade metamorphics, forming the top of the slope. Carbonate rocks outcrop just north of the deforming slope; they represent the basement onto which the metamorphic units are thrust. This basement outcrops extensively in a tectonic window that is geometrically protruding through the allochtonous nappes. All the rocks are very intensely jointed and faulted. Thrust faults pervasively affect the parent rocks at every dimensional scale. Only the major tectonic structures are mapped in the geo-structural scheme of Fig. 2. As the sackung activity is reflected in the activity of the overlying shallow slides, it was decided to trace back the activity stages of the shallow slides by means of dendrogeomorphic analysis. We performed this analysis essentially on the oldest white oaks (*Quercus pubescens*) scattered on the landslide area, and black pines (*Pinus nigra*) outside it. We tried to also find the causes that could have trigged the events of reactivation of the mass movement.

3 Material and Methods

3.1 Sampling Strategy

The entire Vallone Pizzotto-Greci slope was investigated through dendrogeomorphic techniques. Using an increment borer, the sampling strategy was to collect cores from the oldest trees living on the site, belonging to the same species, and displaying signs of past disturbances such as anomalies in the tree-stem morphology. In fact, many trees showed a tilting and sometimes an S shape of the stem, which is a sign of a recovered straight stem growth after a tilting event (Alestalo 1971; Braam et al. 1987). From each of the trees sampled, usually two cores were collected: one on the side opposite to the direction of tilting, and the other orthogonal to or facing the first one. For each tree sampled, we recorded: (a) its position on the topographic map; (b) the direction and degree of the stem tilting; (c) the directions of the core sampling. In total, 38 trees were sampled; 24 trees from different parts of the landslide and 14 trees from the stable surrounding zones.

3.2 Dendrochronological Analysis

All samples were subjected to standard procedures used in dendrochronological research such as samples surface preparation, skeleton plots, cross dating, and

ring-width measurement with a micrometer to construct growth curves (Stokes and Smiley 1968). The ring-width measurements were then checked with the program COFECHA (Holmes 1983). The "visual growth analysis", introduced by Schweingruber et al. (1990), was a very important tool for the identification of sudden growth decrease (suppression) or increase (release) in the cores. Most previous research on mass movements has used different species of conifer trees, while this research is based principally on deciduous oak species, as in the case of another dendrogeomorphic study developed in central Italy on a landslide by Fantucci and McCord (1995), who used trees of Turkey oak (*Quercus cerris*). Here, we used a classification of growth anomaly developed by Schweingruber et al. (1990) and added a fourth class of reduction to indicate the situations in which the growth reduction was so strong that some rings were missing (Table 1). Indeed, in some cases the suppression was so strong that it was impossible to read single rings, so the average value of growth computed for the whole period of suppression was assigned to each single ring of the strongest suppression period. This was done to have a complete growth curve for all the cores examined, even if the ring growth was estimated in the periods of strongest suppression. In order to investigate the possible causes that could have induced the growth anomalies in the trees living on the landslide, both seismic and hydrological time-series were considered. The seismic data are related to those earthquakes whose intensity in the study area had reached at least degree of VII on the Mercalli-Cancani-Sieberg (MCS) seismic intensity scale. The earthquakes that affected the study area in the period 1820–1995 are listed in Table 2.

In order to correlate the meteorological data with growth anomalies, data from the rain gauge station of Aiello Calabro were considered. This station is 5.7 km from the landslide site. Unfortunately, the daily rainfall series were not complete. To overcome this problem, the missing meteorological data were estimated using the data of the rain gauge at Fiumefreddo Bruzio, 10 km from the site. The homogeneity of the data of this station was tested with those of Aiello Calabro by means of a Mann-Kendall test (Holmes et al. 1986). The test resulted positive, thus, we could make the estimation required.

The monthly precipitation data were then grouped seasonally into winter (December to February), spring (March to May), summer (June to August) and autumn (September to November). The reason for this grouping is twofold: first, the study area lies in a Mediterranean climate zone, i.e. with strong seasonality for rainfall

Table 1 Classes of stress release and suppression (Modified from Schweingruber et al. 1990)

Class	Anomalies type	Percentage of increase or decrease
III	Strong release	>200%
II	Medium release	101–200 %
I	Light release	30–100%
I	Light suppression	40–55%
II	Medium suppression	56–70%
III	Strong suppression	>70% without missing rings
IV	Very strong suppression	>70% with missing rings

Table 2 Earthquakes that affected the study area

Date	Distance from epicenter (km)	H (km)	Io	Mk	Epicenter
12 October 1835	30	03	9	5.4	Castiglione
11 February 1854	20	04	9	5.6	Cosenza
04 October 1870	20	07	9	5.8	Cosenza
08 September 1905	50	11	10	6.5	S.Eufemia
28 December 1908	130	08	11	6.8	Calabria

h = focal depth; Io = epicentral intensity in MCS scale; Mk = magnitude (Postpischl 1985).

and temperature; second, other studies conducted in study zones relatively close to the study area demonstrated that the reactivation of deep-seated landslides is related to precipitation periods of 50–90 days preceding the landslide (Sorriso-Valvo et al. 1993). For each season, the average rainfall for the period of available data (1913–1987) was calculated. Then, all the seasons where rainfall exceeded the mean value by 1.5 times the mean square residuals were considered as extremely wet seasons. This threshold is subjective, but there are no standard values to refer to. Climatic events able to trigger mass-movement are recorded in historical chronicles. We could obtain information over a time span that extends back to the early 1800s.

4 Results

4.1 Stem Tilting

The map of direction and degree of inclination of trees sampled (Fig. 2) indicates a first important difference between the morphological characteristics of sampled trees living on the slope and those in the surrounding stable areas or on the ridge top. In fact, the latter all had straight stems without any evidence of disturbance, whereas the former were mostly affected by stem tilting, with 51.3% of trees sampled showing this feature. On the landslide body, 78% of trees sampled have a tilted stem while the remaining 22% have straight stems. The main tilting direction within the sector is NE-S, with a maximum in the ESE direction. Regarding the relationship between tilting direction and slope direction, 78% of the tilted trees lean downslope or nearly downslope (this reflects the ESE peak in tilt direction); 17% lean orthogonal to the downslope direction; 5% dip upslope (Table 3).

4.2 Tree-Growth Curves and Growth Suppression

The effects of growth anomaly can be seen in Fig. 3 comparing the ring-growth curves for the undisturbed trees with some of the most representative ring growth curves for the disturbed trees. In the cores of the disturbed trees, a sudden growth decrease is

Table 3 Classes of trees' tilting

Direction	(%)
No tilting	22
N-NE	4
NE-E	17
E-SE	30
SE-S	17
S-SW	10
SW-W	–
W-NW	–
NW-N	–

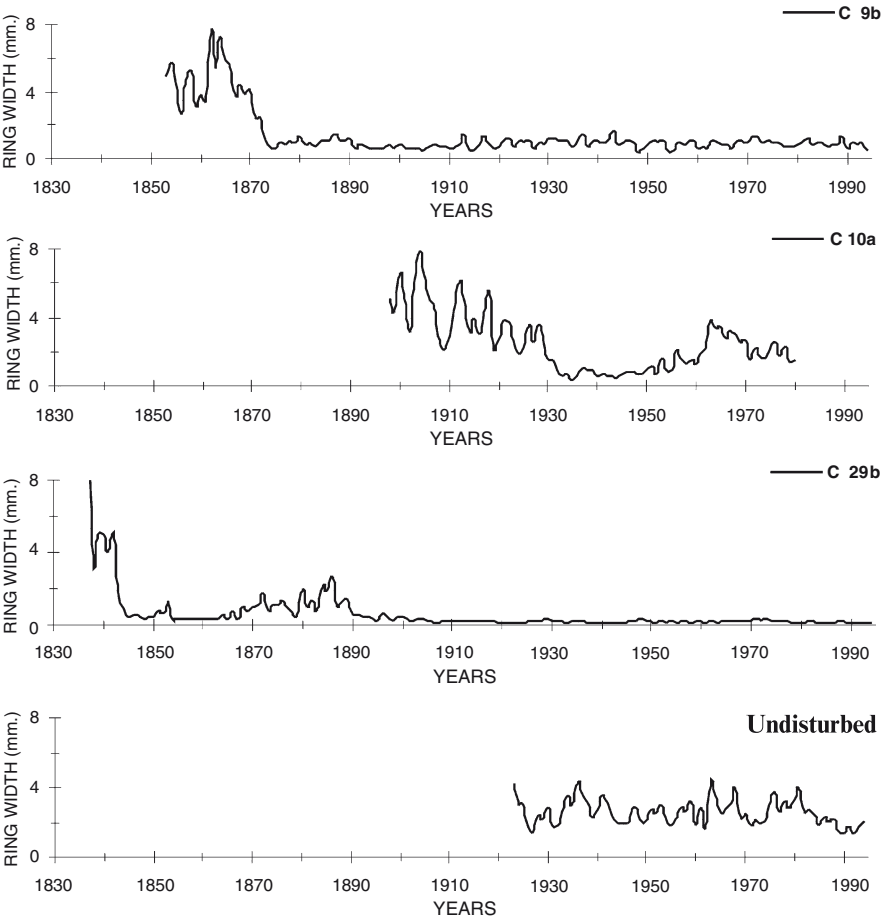

Fig. 3 Growth curves of disturbed (C9b, C29b and C10a) and undisturbed trees

clearly evident, compared to the normal growth of the undisturbed trees. Sometimes, the effect of the growth decrease was so strong that the trees never regained regular growth, as in the cases of samples C9b and C29b (respectively due to the events in 1871, 1845 and 1890). The strong suppression often caused a ring growth close to zero; in some cases the cores showed a very intense suppression after the stressing event, so that many rings were missing, or the existing ones were so narrow that they became indistinguishable. In other cases, trees regained their regular growth decades later, as was the case for sample C10a. The undisturbed ring growth curve in Fig. 3 was obtained using the mean ring width of eight trees not affected by growth anomalies.

4.3 Visual Analysis of Growth Anomaly

The visual growth analysis was made on all cores sampled on the landslide area. Then, all the anomalies found were used to create a graph based on a modified Shroder formula (Shroder 1978) to calculate the anomaly index (*It*) for each of the event-response cases. The modified *It* used was calculated considering for each year the number of observed rings affected by suppression, the intensity of suppression as expressed by a coefficient of intensity of suppression, and the total number of samples analyzed in that year. The *It* was calculated as follows:

$$\text{anomaly index } (It) = \frac{\sum_{t=1}^{n} (Sup(x)t * (Fx))}{\sum_{t=1}^{n} (Ntot)t} * 100\%$$

where Sup*(x)t* = number suppressions of each class *(x)* in year t; Fx = weight coefficient. It is expressed by integers in a rank scale from 1 to 4, according to increasing intensity of suppression (i.e. slight, moderate, strong and very strong); *(Ntot)t* = total number of samples analyzed in year *t*.

In this way, it was possible to give more emphasis to those events that had induced strong growth suppressions in trees. To construct the graph, only the growth reduction anomaly was considered, because the recovery anomalies were very few and always subsequent to the suppression anomalies, thus they were not directly related to the events. The results of the visual growth analysis are represented through the *It* graph in Fig. 4. *It* (shaded bars) is scaled on the left-hand axis. The horizontal axis indicates the period of analysis (1820–1994), the percent of disturbed samples (solid line) is scaled on the right-hand axis. The first registered disturbance occurred in 1845. The events that occurred during the period between 1860 and 1895 were stronger than those that occurred during the subsequent period, reaching 45% of the disturbed cases. Then, another period of disturbance followed between 1905 and 1950, with more than one low-intensity event that had involved a decrease in the percentage of cases from 40% to 23%. The last period, between 1951 and 1995, was the least disturbed with a percentage of disturbed cases never exceeding 16%.

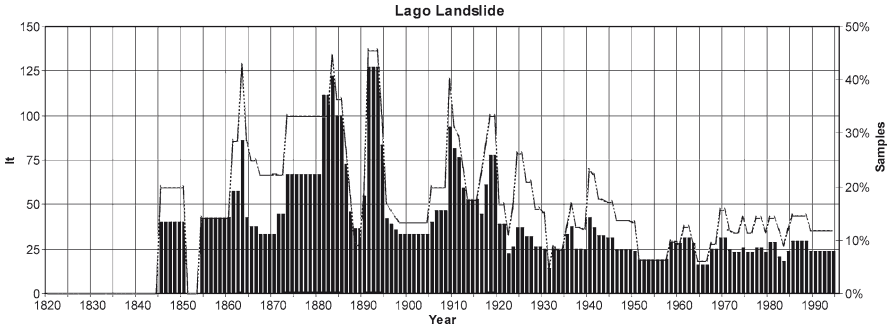

Fig. 4 Graph of visual growth anomaly index related to landslide area. *It* = anomaly index (*solid bars*); samples = percentage of disturbed samples (*line*)

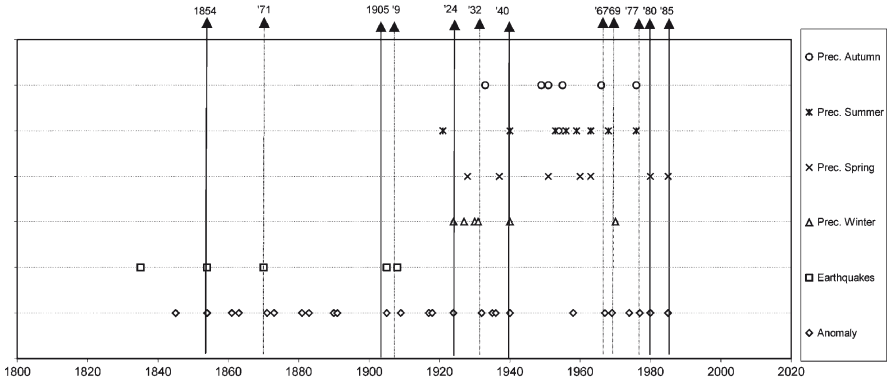

Fig. 5 Skeleton plot of the study case. *Bottom figures* are years; *top figures* with *solid triangles* are anomaly years corresponding with either seismic or rainfall events. The *solid line* means that the growth anomaly occurred in the same year of the causative event, whereas the *dotted line* means that the anomaly occurred the year following that of the causative event. Rainfall data time series began in 1913

4.4 Correlation Between Growth Anomaly Events and Geological Causes

In the study zone, such events occurred in the winters of 1863–1864, 1882, 1894, 1896, 1910, 1919, 1927, 1936, 1937; coincident with growth in 1863, 1882, 1910, 1927, and 1936, i.e., in 55% of the cases. Using the dates of the main growth anomaly events, the dates of the earthquakes and those of the seasonal precipitation values, we composed the skeleton plot shown in Fig. 5. In this figure, the dates in which the growth anomalies are related to the dates of seismic and meteorological events are marked by the lines with solid triangles.

5 Discussion and Conclusion

The method used to investigate the periods of disturbance, proved to be of great help in determining the temporal sequence of diffused slope movement in the study area, and, to a lesser extent, clarifies the possible causes of triggering events of the mass-movement activity. The trees sampled outside the slope had regular growth patterns, without evidence of tilting and distortion of stems. Available information on the geomorphology and on the deformation occurring in the study zone indicates that the slope is deforming through deep-seated creeping and landsliding (Sorriso-Valvo et al. 1996). The movement is expanding rapidly in the northern part of the slope where deformation occurs up to the top. However, the seismic profile suggests that the entire mountain is undergoing a unilateral sackung (Hutchinson 1988), with essentially translational displacement and no or very little rotational activity. On the slope, instead, leaning trees indicate that the movement is active. This agrees with inclinometric data (Sorriso-Valvo et al. 1996). Tilted trees represent 78% of the sample population (Table 3), 78% of which lean downslope, indicating that the velocity of the mass movement decreases with depth, but no toppling has been detected. One tree leans upslope, indicating a local rotation. The remaining 17% of the stems which lean orthogonal to the slope are difficult to explain. By visual inspection of Fig. 2, it seems that they are located along or in the proximity to the outcrops of the shearing surfaces of the landslide, where ground deformation is controlled by very local geometry. Dendrochronological analysis was conducted by means of visual growth analysis and an anomaly index (*It*). The visual growth analysis indicated that anomalies consisted of sudden growth decrease of the growth (suppression) induced by stress after ground disturbance, followed in some cases by sudden increase (release), induced by the high moisture content, typical of the landslide body. From the graph in Fig. 4, it is possible to infer that after a sudden increase of *It* between 1840 and 1860, there is a period of strongly oscillating values that however decrease to a stationary level around 1950. The reason for this pattern is difficult to explain. However, as historical records (Sorriso-Valvo et al. 1996) indicate that slope movement began to affect this zone soon after the 1850s, we can tentatively assume that the cause of the growth anomalies has been the landsliding, with a maximum influence in the period between 1860 and 1895. Causes of the mass-movement may be many. By comparing (Fig. 5) the time series of possible causative events (earthquake, extremely wet seasons) with that of ring-growth anomaly, it appears that 80% of the earthquake dates correspond with growth anomalies found in sampled trees. The converse is of course not true: only 15% of anomaly dates correspond with an earthquake, confirming that the reasons for an anomaly can be other than earthquakes. However, the growth anomaly in 1871 and 1909 are delayed by 1 year with respect to the date of earthquakes because they occurred during the dormant season (October 1870 and December 1908, respectively), thus the effects of the stress on the trees are recorded in the following year. The two anomalies of 1854 and 1905 are instead related to seismic events which occurred during the growing season of the same year. The meteorological data are moderately related

to mass-movement reactivation as the seismic data: indeed, considering the period for which rainfall data is available (1913–1987), only 55% of the anomaly cases can be connected to extreme precipitation values. On the other hand, correspondence between seasonal extreme values and anomaly is low (spring 28%, summer 33%, autumn 33%, and winter 50%; average 35%), but as expected higher than that for earthquakes. If information from historical records of landsliding is considered, then 55% of the recorded events correspond with an anomaly record, while 31% of the anomaly records correspond with a historical landslide record. Correspondence is nearly equal for instrumental and historical data. Conclusions based on instrumental rainfall data (after 1913) suggest that only a minority of extreme meteorological events may produce slope movement intense enough to be recorded in the tree-ring series, and that only 30% of anomalies can be explained in terms of extreme events. This weak connection is probably due to the fact that the relationship between rainfall and mass-movement activity is complex. For instance, the ca. 30 m deep, slow-moving sackung-type deformation should respond to much longer periods of increased rainfall. On the other hand, the continuous creeping of the sackung might irregularly trigger the movement of shallower landslides in non-extreme events years. Coincidence between the seismic and hydrologic-meteorologic time series can be found only for the 1908–1909 earthquake and the 1910 rainfalls. An anomaly has been found in 1910. It is only one case, and *It* cannot be used for any kind on inference. Thus nothing can be said on the combined effects of the two causes. We can conclude that we obtained a moderate degree of success in the use of the dendrochronological analysis in the identification of the temporal occurrence of causes of landslide movement. A higher degree of coincidence between disturbing causes and anomalous tree growth has been obtained using archival data for extreme rainfall periods. This might have depended on the much higher annual rainfall depth in the period from the beginning to the 1880s. On the other hand, we could successfully distinguish the dendrochronological series of trees growing in the unstable area from those outside the unstable area. In addition, the period of maximum instability could be well defined between 1860 and 1895.

Acknowledgements This paper is a part of the CEC Environment Program Project TESLEC (EV 5V-CT94-0454) “The temporal stability and activity of landslides in Europe with respect to climatic change”.

References

Alestalo J (1971) Dendrochronological interpretation of geomorphic processes. Fennia 105:1–140

Braam RR, Weiss EEJ, Burrough PA (1987) Spatial and temporal analysis of mass movement using dendrochronology. Catena 14:573–584

Denneler B, Schweingruber FH (1993) Slow mass movement. A dendrogeomorphological study in Gams, Swiss Rhine valley. Dendrochronologia 11:55–67

Fantucci R, McCord A (1995) Reconstruction of landslide dynamic with dendrochronological methods. Dendrochronologia 13:43–58

Filion L, Quinty F, Bégin C (1991) A chronology of landslide activity in the valley of Rivière du Gouffre, Charlevoix, Quebec. Can J Earth Sci 28:250–256

Holmes RL (1983) Computer-assisted quality control in tree-ring dating and measurement. Tree-Ring Bull 43:69–78

Holmes RL, Adams RK, Fritts HC (1986) Tree-ring chronologies of western North America. California, eastern Oregon and northern Great Basin, with procedures used in the chronology development works, including users manual for computer programs COFECHA and ARSTAN. Chronology Series IV. Laboratory of Tree-Ring Research, University of Arizona, Tucson

Hupp CR (1984) Dendrogeomorphic evidence of debris flow frequency and magnitude at Mount Shasta, California. Environ Geol Water Sci 6(2):21–128

Hutchinson JN (1988) Morphological and geotechnical parameters of landslides in relation to geology and hydrogeology. General report. In: Bonnard C (ed) Landslides. Proceedings of 5th ISL Lausanne Balkema Rotterdam 1:3–35

Jibson RW, Keefer D (1988) Landslide triggered by earthquakes in the Central Mississippi valley, Tennessee and Kentucky. US Geol Surv Prof Paper 1336-C

Kashiwaya K, Okimura T, Kawatani T (1989) Tree ring information and rainfall characteristic for landslide in the Kobe District, Japan. Earth Surf Process Land 14:63–71

Orombelli G, Gnaccolini M (1972) La dendrocronologia come mezzo per la datazione di frane avvenute nel recente passato. Bollettino della Societa' Geologica Italiana 91:325–344

Postpischl D (1985) Atlas of isoseismal maps of Italian earthquakes C.N.R. Quaderni de la Ricerca Scientifica 114 (2A)

Schweingruber FH, Eckstein D, Serre-Bachet F, Braker OU (1990) Identification, presentation and interpretation of event years and pointer years in dendrochronology. Dendrochronologia 8:9–38

Shroder JF (1978) Dendrogeomorphological analysis of mass movements on Table Cliffs Plateau, Utah. Quat Res 9:168–185

Sorriso-Valvo M, Agnesi V, Gullà G, Merenda L, Antronico L, Di Maggio C, Filice E, Petrucci O, Tansi C (1993) Temporal and spatial occurrence of landsliding and correlation with precipitation time series in Montalto Uffugo (Calabria) and Imera (Sicily) area. In: Falgeollet JC (ed) Temporal occurrence and forecasting of landslides in the European Community. Final report Programme EPOCH CT900025 part II vol 2, pp 823–869

Sorriso-Valvo M, Antronico L, Catalano E, Gullà G, Tansi C, Dramis F, Ferrucci F, Fantucci R (1996) The Lago study case. In: Dikau R, Schrott L, Dehn M, Hennrich K, Rasemann S (eds) The temporal stability and activity of landslides in Europe with respect to climatic change (TESLEC) Final Report 2, pp 89–151

Stokes MA, Smiley TL (1968) An introduction to tree-ring dating. University of Chicago Press, Chicago

Strunk H (1992) Reconstructing debris flow frequency in the southern Alps back to AD 1500 using dendrogeomorphological analysis. In: IAHS (ed) Erosion, debris flows and environment in mountain regions. Proceedings of the Chengdu Symposium, July, vol 209, pp 299–307

Terasme J (1975) Dating of landslide in the Ottawa river valley by dendrochronology – a brief comment. In: Mass wasting Proceedings of 4th Guelph Symposium on Geomorphology, pp 153–158

Van Asch ThWJ, Van Steijn H (1991) Temporal patterns of mass movements in the French Alps. Catena 18:515–527

Zischinsky U (1969) Über Sackungen. Rock Mech 1:30–52

Tree-Ring Analysis and Rockfall Avalanches: The Use of Weighted Samples

David R. Butler

A significant amount of dendrogeomorphic research has focused recently on the effects of isolated rockfall activity on tree growth and annual rings (reviewed in Stoffel 2006, and Schneuwly and Stoffel 2008). By comparison, however, only a few studies have used tree-ring analysis in the dating of large-scale rockfall avalanches, or *bergsturz* (see Butler et al. 1986). Butler et al. (1986, 1991, 1998) examined a number of rockfall avalanches in Glacier National Park, Montana, USA, and used tree-ring analysis of trees severely tilted and/or scarred along the margins of the rockfall-avalanche deposits to date three of those deposits – Slide Lake at 1910 (Fig. 1), Slide Pond at 1946 (Fig. 2), and Napi Point at 1954.

Recently, several dendrogeomorphic works examining snow-avalanche occurrence have advocated "weighting" tree-ring data, in some cases by concentrating only on unequivocal corrosion scar and strong reaction wood evidence (Germain et al. 2005; Butler and Sawyer 2008; Reardon et al. 2008). I suggest here that similar weighting is useful in dating the year of occurrence of rockfall avalanches.

Tree rings (Butler et al. 1986, 1991) illustrated the age of the Slide Lake rockfall avalanche as occurring in 1910; subsequent to that confirmation, previously unknown historical documents were located that confirmed the year of occurrence as 1910 (summarized in Butler et al. 1998). The tree ring evidence for 1910 was, however, only marginally stronger than was evidence for years a few years earlier (1908 and 1909) or later (1911 and 1912) (Oelfke 1984), when using all tree-ring growth responses present from trees tilted and scarred by the rockfall avalanche (corrasion scars, reaction wood onset and continuation, suppression, and release rings): 1908 had an index value (see Butler and Sawyer 2008) of 10, indicative of 10% of sampled trees illustrating response for that year (cross-cut samples from 21 trees of an original sample of 30 trees were sufficiently old to extend back to the early

D.R. Butler (✉)
Department of Geography, Texas State University-San Marcos, San Marcos, TX 78666-4616, USA
e-mail: db25@txstate.edu

M. Stoffel et al. (eds.), *Tree Rings and Natural Hazards: A State-of-the-Art*, Advances in Global Change Research 41, DOI 10.1007/978-90-481-8736-2_9,

Fig. 1 Composite photograph of the Slide Lake deposit taken in 1910 by US Geological Survey geologist M.R. Campbell (U.S.G.S. M.R. Campbell photos 891 and 892 used to create composite)

Fig. 2 Photo from helicopter taken by author in 1995, showing Slide Lake in lower right portion of photo and its damming rockfall-avalanche deposit and Slide Pond and its damming rockfall-avalanche deposit (*center left*). Note difference in revegetation on the surfaces of the 1910 Slide Lake versus the 1946 Slide Pond deposits

twentieth century); 1909, index value (IV) of 24; 1910, also an IV of 24; 1911 an IV of 10; and 1912 an IV of 14 (Table 1). Using a weighted system similar to that described for snow avalanches by Reardon et al. (2008), in which only corrasion scars and associated onset of reaction wood, or strong onset of reaction wood without scarring that lasted for a minimum of three years, were used to calculate annual index values, the Slide Lake data illustrated a much clearer picture supportive of the date of 1910 (Table 1): 1908 IV of 5, 1909 IV of 10, 1910 IV of 19, 1911 IV of 10, and 1912

Table 1 Full index number versus weighted index number for study sites

Site	Full index number	Weighted index number
	Years 1908–1912	
Slide lake	10, 24, **24**, 10, 14	5, 10, **19**, 10, 0
	Years 1944–1948	
Slide pond	9, 4, **70**, 57, 13	4, 4, **65**, 22, 4
	Years 1952–1956	
Napi point	9, 9, **83**, 17, 17	0, 0, **83**, 17, 13

Year of occurrence in bold.

IV of 0. Essentially, using the strongest data (scars and strong, long-lived onset of reaction wood) produced an Index Value almost twice as strong for 1910 as for any other year. Applying the same system (without using weighting versus using weighting), the following results emerged for the 1946 Slide Pond and the 1954 Napi Point rockfall avalanches: Slide Pond, 1944 9 versus 4, 1945 4 versus 4, 1946 70 versus 65, 1947 57 versus 22, and 1948 13 versus 4; Napi Point, 1952 9 versus 0, 1953 9 versus 0, 1954 83 versus 83 (these were excellent samples!), 1955 17 versus 17, and 1956 17 versus 13. Using only the clearest, most distinct displays of scarring and strong and continuous reaction wood clearly pinpointed the year in all three cases in which the large and potentially very hazardous rockfall avalanches occurred, and is recommended for dating of other rockfall avalanche deposits of unknown age.

References

Butler DR, Sawyer CF (2008) Dendrogeomorphology and high-magnitude snow avalanches: a review and case study. Nat Haz Earth Syst Sci 8:303–309

Butler DR, Oelfke JG, Oelfke LA (1986) Historic rockfall avalanches, northeastern Glacier National Park, Montana, USA. Mt Res Dev 6:261–271

Butler DR, Malanson GP, Oelfke JG (1991) Potential catastrophic flooding from landslide-dammed lakes, Glacier National Park, Montana, USA. Z Geomorphol Suppl 83:195–209

Butler DR, Malanson GP, Wilkerson FD, Schmid GL (1998) Late Holocene sturzstroms in Glacier National Park, Montana, USA. In: Kalvoda J, Rosenfeld C (eds) Geomorphological hazards in high mountain areas. Kluwer, Dordrecht

Germain D, Filion L, Hétu B (2005) Snow avalanche activity after fire and logging disturbances, northern Gaspé, Quebec, Canada. Can J Earth Sci 42:2103–2116

Oelfke JG (1984) The location and analysis of landslides along the Lewis Overthrust Fault, Glacier National Park, Montana. Thesis, Oklahoma State University, Oklahoma

Reardon BA, Pederson GT, Caruso CJ, Fagre DB (2008) Spatial reconstructions and comparisons of historic snow avalanche frequency and extent using tree rings in Glacier National Park, Montana, USA. Arct Antarc Alp Res 40:148–160

Schneuwly DM, Stoffel M (2008) Tree-ring based reconstruction of the seasonal timing, major events and origin of rockfall on a case-study slope in the Swiss Alps. Nat Haz Earth Syst Sci 8:203–211

Stoffel M (2006) A review of studies dealing with tree rings and rockfall activity: the role of dendrogeomorphology in natural hazard research. Nat Haz 39:51–70

Age of Landslides Along the Grande Rivière de la Baleine Estuary, Eastern Coast of Hudson Bay, Quebec (Canada)

Christian Bégin and Louise Filion

1 Introduction

Landslides are widespread in tectonically active zones, in mountains and in areas where fine-grained deposits predominate, particularly in lowlands influenced by postglacial marine transgression. Late and postglacial marine clays in Norway (Bjerrum 1954a, b) and eastern Canada (La Rochelle et al. 1970; Leroueil et al. 1983) are particularly prone to multiple rotational slips (Hutchinson 1968). Identification of causal processes involved in landslide activity has been discussed by several workers (Sharpe 1938; Terzaghi 1950; Varnes 1958; Selby 1982). In such an attempt one must be able to distinguish between direct and indirect causes. In general, the direct causes were more easily identified, as for example seismic or volcanic activity, oversteepening of slopes undercutting at the toe of a slope by stream action, fluctuations in depth of water bodies, prolonged rainfall, storm surges or rapid snow melting, and overloading of surfaces. While the inherent characteristics of deposits (lithologies, weathering states) and slope were considered as prerequisites for sliding occurrence, climate influence has been generally identified as an indirect cause.

Landslides in many regions are ancient and the conditions under which they were formed may be relict. In some areas, their presence is an indication of shifts in temperature, and in amount, distribution and intensity of rainfall during the Pleistocene and the Holocene. Identification of mode of failure and causal processes is complicated in ancient landslides, because of rapid degradation of the sliding surface (Brunsden and Jones 1972; Carson 1979), lack of geotechnical or meteorological data, and absence of archival records or eye-witness accounts. In areas with a high frequency of mass movements inducing several generations of landslides, it may be useful to establish their chronology in the context of past geomorphic, climatic and

C. Bégin
Natural Resources Canada, Québec QC, G1K 9A9, Canada

L. Filion (✉)
Centre d'études nordiques and Département de géographie, Université Laval, Québec QC, G1V 0A6, Canada
e-mail: Louise.Filion@cen.ulaval.ca

M. Stoffel et al. (eds.), *Tree Rings and Natural Hazards: A State-of-the-Art*, Advances in Global Change Research 41, DOI 10.1007/978-90-481-8736-2_10,

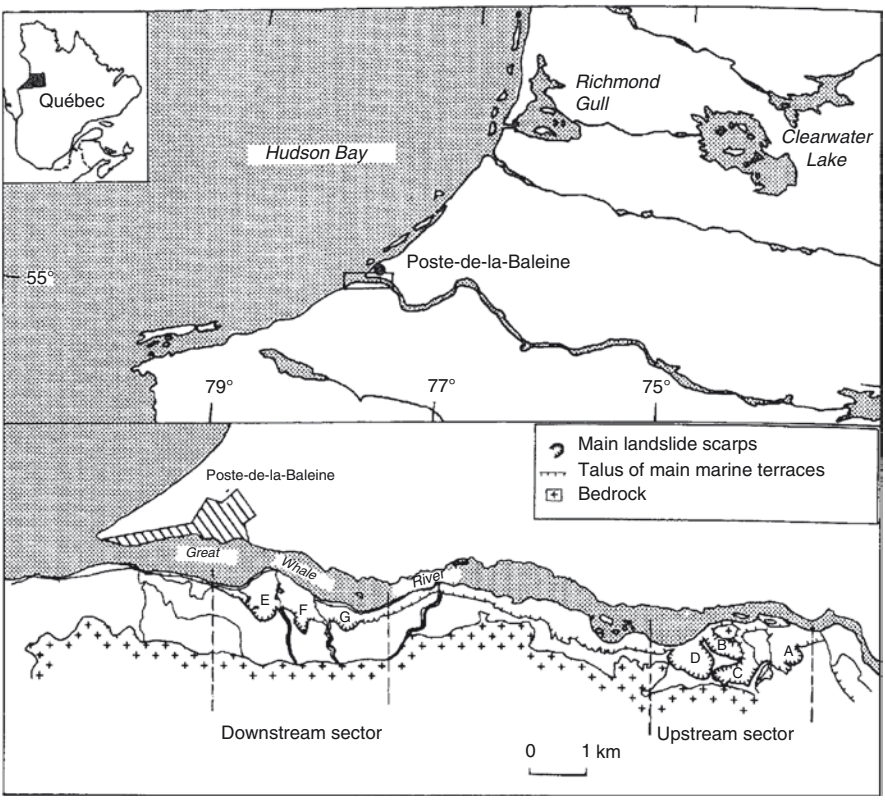

Fig. 1 Location of the study area and landslides discussed in text (A–G)

ecologic conditions. In this connection, the fluvio-marine terraces located at the mouth of the Grande Rivière de la Baleine, northern Quebec (Fig. 1), provide evidence of long-term landslide activity, as the sandy surfaces and underlying marine clay deposits were disrupted by seven major landslides (Demangeot 1974) since their formation around 3,200 BP. (Hillaire-Marcel 1976). The main objectives of this study were therefore to establish the landslide chronology along a 12 km stretch of the Grande Rivière de la Baleine estuary, and to discuss the climatic conditions prevailing at the time of their formation using recent dendroclimatic reconstructions in subarctic Quebec (Parker et al. 1981; Jacoby 1983; Payette and Filion 1985; Payette et al. 1985).

One major problem in reconstructing landslide activity over a long period of time arises from availability of datable material and use of suitable dating techniques. In a recent paper, Goulden and Sauchyn (1986) reviewed briefly some techniques that have been used to date landslides. Some provide absolute dates (radiocarbon dating), while others yield relative dates (morphological parameters, weathering-rind thickness, size and coverage of lichens on boulders exposed by landsliding, soil properties). Tree-ring dating of landslides was not mentioned by these authors, although this technique gives an accurate absolute dating as to the

year or even to the season of occurrence. Its application in geomorphological studies has been extensively discussed by Alestalo (1971) and Shroder (1978, 1973, 1975). It was successfully applied in many studies dealing with mass movements (Agard 1979; Begin and Filion 1985). In this study, we have focused on tree-ring analysis to obtain accurate dates of recent landslides, and on the ^{14}C technique for ancient ones. Landslides from the Poste-de-la-Baleine area were considered in this respect, because they developed in a forest environment where buried tree stumps and other organic material could be used in tree-ring and ^{14}C dating.

2 Study Area

The Poste-de-la-Baleine area is located along the eastern coast of Hudson Bay (Fig. 1). The geological basement is made of Precambrian granitic and gneissic rocks (Eade 1966). Deglaciation occurred around 8,000 BP. (Hillaire-Marcel 1976). Three terraces are found along the river, the uppermost being dated at 3,200 BP. According to emersion curves (Hillaire-Marcel 1976; Allard and Seguin 1985). Its surface declines in elevation toward the west, from 45 m above sea level up the river to 30 m near the mouth where it is truncated by the coastline.

The terrace stratigraphy and landslide morphology were described recently (Begin and Filion 1987). The overall stratigraphic pattern shows the following sequence, from bottom to top: morainic material, 10 m thick marine clay sediments, and 15–20 m thick fluvial and deltaic sands. The clay deposits were made of 55–70% of fines (<2 μ). The water content and liquidity limit ranged respectively between 24% and 44% and 28–57%.

Four out of seven major landslides depicted within the 12 km long terraces occurred in the upstream sector of the river, while the other three landslides were located in the downstream sector, in front of Poste-de-la-Baleine settlement (Fig. 1). Occurrence of various sliding levels, and degree of degradation and paludification of some landslide surfaces suggest that they were formed at different periods, although they all belong to the same, single or multiple rotational type (Begin and Filion 1987). This slip-flow double movement is typical of quick-clay deposits overlain by sand and it is most obvious in recent landslides near the Poste-de-la-Baleine settlement. All mass movements in the study area have eroded approximately 10% of the initial surface and about 17×106 m^3 of flow material.

3 Methods

Postulated old landslides (A–C) were dated using the ^{14}C method, and dendrochronological techniques were used for dating of recent landslides (D–G). Three ^{14}C dates were performed at Teledyne Isotopes, and three at the Laboratoire de Radiochronologie of Laval'University. The radiocarbon dates (Libby's half-life, 5,568 years) were calibrated to calendar dendroyears using tables and methods from Stuiver and Becker (1986).

Table 1 Summary of landslide chronology. Also indicated type of material and events, dating techniques, laboratory numbers and identification: 1 for samples from Teledyne Isotopes and UL from Laval University

Landslide	Type of material	Geomorphic and ecological events	Dating techniques	^{14}C dates	Calendar years
A	–	–	–	Undated	Undated
B	Buried charcoal	Burying of theoriginal surface	^{14}C	2,200 ± 80 BP (1–13,271)	405–90 BC (p = 0.99)
C	Basal peat	Peat accumulation	^{14}C	890 ± 70 BP (UL-77)	AD 1018–1260(p = 0.99)
C1	Buried organic matter	Minor movement(base of the main scarp)	^{14}C	180 ± 60 BP (UL-78)	AD 1641–1899 (p = 0.83)
C2	Buried organic matter	Minor movement(base of the main scarp)	^{14}C	260 ± 80 BP (1–13,270)	AD 1646–1703 (p = 0.67)
C3	Buried organic matter	Subsidence at theouter limit of theflowage zone	^{14}C	320 ± 80 BP (1–13,273)	AD 1428–1677 (p = 0.90)
D	Buried trees	Burying of trees	^{14}C	160 ± 60 BP(UL-147)	AD 1654–1896(p = 0.83)
D’	Buried trees	Burying of trees	Tree rings light rings	–	AD 1846 spring
E	Stumps	Development ofreaction wood	Tree rings	–	AD 1818 summer
F	Stumps	Development ofreaction wood	Tree rings	–	AD 1818 summer
G	Buried trees	Burying of trees	Tree rings light rings	–	AD 1839 spring

The calibrated AD/BC age ranges are first obtained from intercepts method and then from probability distribution (p) method. The age ranges shown on Table 1 are those with the highest probability of date occurrence within two sigma.

Landslides D–G were dated with dendrochronological techniques. The tree-ring analysis was performed on buried tree stumps found in an upright position in flowed sediments, and also on stumps located at the surface of rotated blocks. In the case of buried trees which died in the hazard, the absolute age of landslides was obtained by dating the last growth-ring year (landslides D and G). The trees found at the surface of rotated blocks have recorded sliding movements by developing reaction wood in response to stem tilting. Sometime after tilting, the trees have been cut by Indians or by the staff of the Hudson Bay Company (Delwaide and Filion 1987). In this case, the age of landslides was obtained by dating the first year of reaction wood (compression wood) on the well preserved side of the stump (landslides E and F). The eccentric growth pattern was not studied in itself because of rotten wood in the opposite direction. All the trees analyzed were white spruce (*Picea glauca*).

The growth-ring analyses were performed on discs sampled at the root collar. Nine stumps were used for dating landslides D and F, and about 20 for landslides E and G. Ring width was measured with a Henson micrometer (precision of 0.01 mm). Cross-dating was facilitated by the presence of light rings (Filion et al. 1986), i.e. annual rings mostly made of earlywood cells with one or a few layers of latewood-cells typical of a shortened growing season. Growth-ring patterns were also used in association with existing master chronologies (Parker et al. 1981; Payette et al. 1985) and a local chronology built from 15 trees growing on the upper terrace.

The age of the largest and presumably oldest trees found in landslides E, F and G was determined for an evaluation of the minimum age of each landslide. This procedure may be useful in absence of other field methods (Shroder 1978). Accordingly, 122 trees were sampled in landslide E, 150 in landslide F, and 33 in landslide G, so as to represent the flowage zone, the floor of flowbowl and the landslide scarp. The increment cores were taken as low as possible, i.e. 30 cm above the ground surface using a Pressler probe.

Archival records from Hudson Bay Company were used for historical information dealing with geomorphic and climatic proxy data. These documents belong to the Public Archives at Ottawa and to the Hudson Bay Company at Winnipeg (Canada), and spanned more or less continuously the 1744–1931 period.

4 Results

4.1 Landslides from the Upstream Sector

Landslide A is presumably the oldest landslide in the study area, because it is found at the highest altitude. The floor of the flowbowl is at 38 m above the present sea level, and the base level of the frontal slope circumscribing the flowage zone is at 30 m.

This elevation corresponded probably to the effective river level at the time of landslide formation. Because the original terrace surface has not been found, no organic material was available for dating. However, it seems likely that it occurred between c. 3,200 and 2,200 BP, i.e. between the time of the upper terrace formation and inception of landslide B located nearby at a slightly lower level (Fig. 1).

The floor of the cavity of landslide B was at a mean elevation of 33 m, about 3 m below the surface of landslide A. The base level of the frontal slope formed into the slipped masses is at 11 m above the present sea level. Landslide B was formed at about 2,200 ± 80 BP (1–13,271) (Table 1). This ^{14}C date was obtained from charcoal recovered from a buried organic horizon corresponding to the original surface of the upper terrace and it gives a maximum age for landslide occurrence. It is the oldest date for landslide formation in the study area. Several soil profiles observed at the edge of this landslide surface showed many microfaults, indicating that the upper part of the deposit was frozen at the time of sliding. This suggests that the landslide occurred probably during spring.

The surface of landslide C is at an altitude of 28 m, 5 m below the surface of landslide B. The sampling of basal peat covering the floor of the flowbowl, about 1.8 m as maximum thickness, yielded a date of 890 ± 70 BP (UL-77) (Table 1) which is an approximate but minimum age for the formation of landslide C. Sliding thus occurred between c. 2,200 (age of landslide B) and 900 BP. Additionally, three young radiocarbon dates (Table 1) were obtained from buried organic matter. Two dates (UL-78:180 ± 60 BP, and I-13,270: 260 ± 80 BP) appear to indicate minor movements at the base of the main scarp (CI and C2, on Table 1) and the last one (1–13,273: 320 ± 80 BP) subsidence of the slope at the lower limit of the flowage zone (C3, on Table 1).

A tree-ring date of AD 1846 has been determined for inception of landslide D. Cross-dating based on growth patterns and light-ring occurrences showed that the last complete ring was formed in 1845 (Fig. 2), and that sliding occurred most likely in spring 1846. A radiocarbon date of 160 ± 60 BP (UL-147) yielded AD 1654–1896 age ranges (probability distribution of 0.83 within two sigma) (D on Table 1). The outer rings were removed from the stem section to avoid contamination during dating. It is the most recent landslide to have occurred in the upstream sector and in the study area.

4.2 Landslides from the Downstream Sector

When landslides E and F occurred their flowage zones merged and the slipped material flowed into the river. At the contact zone between the two earthflows, arrangement of the ridges suggest that the landslides occurred simultaneously. Many trees survived to sliding, particularly those growing at the surface of rotated blocks, and developed reaction wood and eccentric growth pattern later on (Fig. 3a and b). In many samples, the outer portion of 1818-ring was made of compression wood suggesting a change in stem position during the growing season (Fig. 3a). Many trees that toppled over during sliding were unable to grow for the rest of the

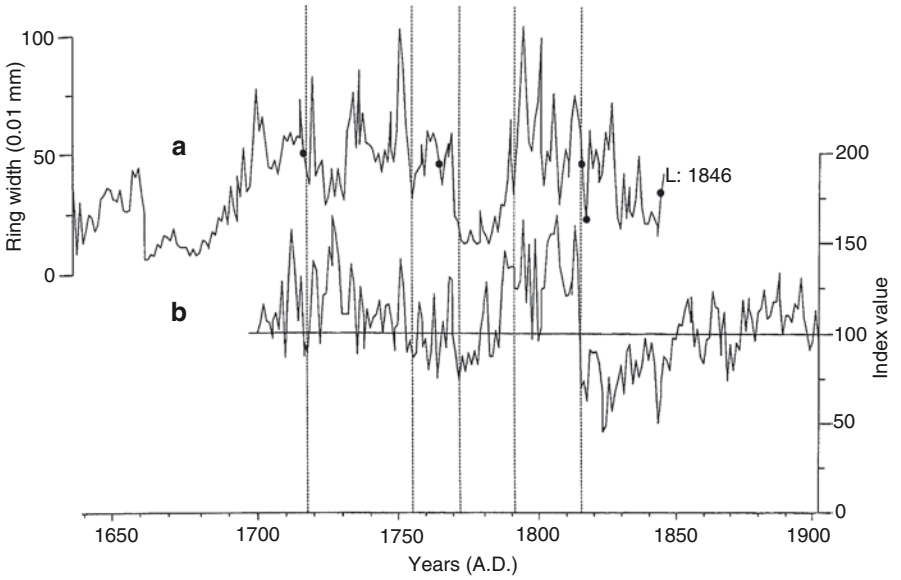

Fig. 2 Age of landslide D (L: AD 1846) using cross-dating of sample D-l (*curve* **a**) with the chronology of Parker et al. (1981) (*curve* **b**) and light-ring years (•) (Filion et al. 1986)

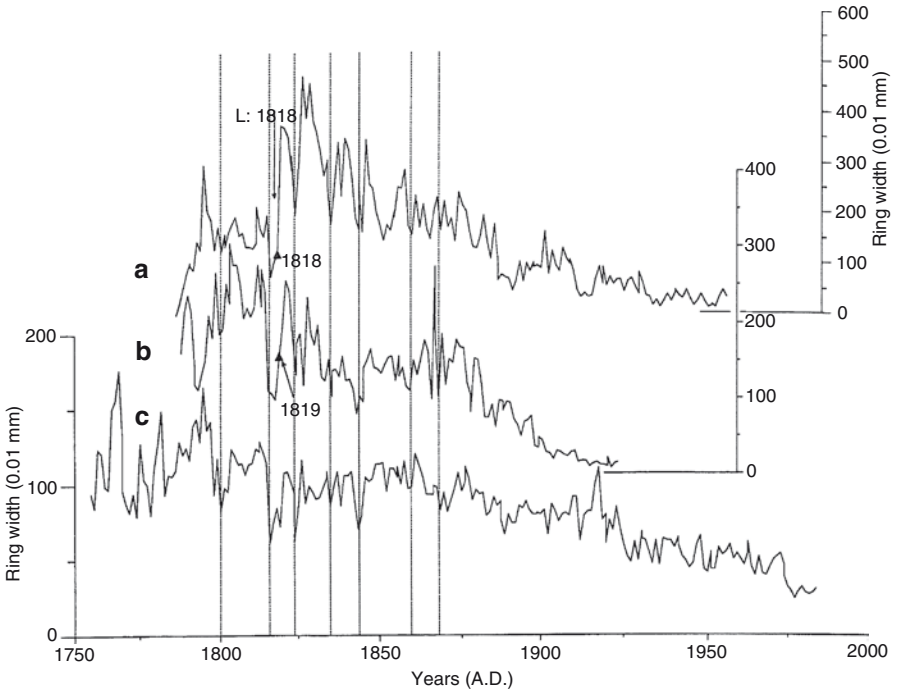

Fig. 3 Age of landslides F and E (L: AD 1818) using cross-dating of samples F-24 (*curve* **a**) and E-l (*curve* **b**) with the local chronology (*curve* **c**). *Triangle* indicates beginning of reaction wood induced by tilting (1818 on curve a and 1819 on curve b). No light rings were depicted on those samples

season, and recovery began in 1819 (Fig. 3b). Cross-dating of these tilted trees with our local chronology (Fig. 3c) allows us to show that landslides E and F occurred in 1818, probably in July (Table 1).

Landslide G occurred in AD 1839. Many trees were found in their normal position buried by landslide debris and exposed by stream erosion. The last complete ring among several sampled trees was formed in AD 1838. (Fig 4a–c), which suggests that sliding occurred in spring 1839 before the beginning of the growing season (Fig. 4a–d and Table 1).

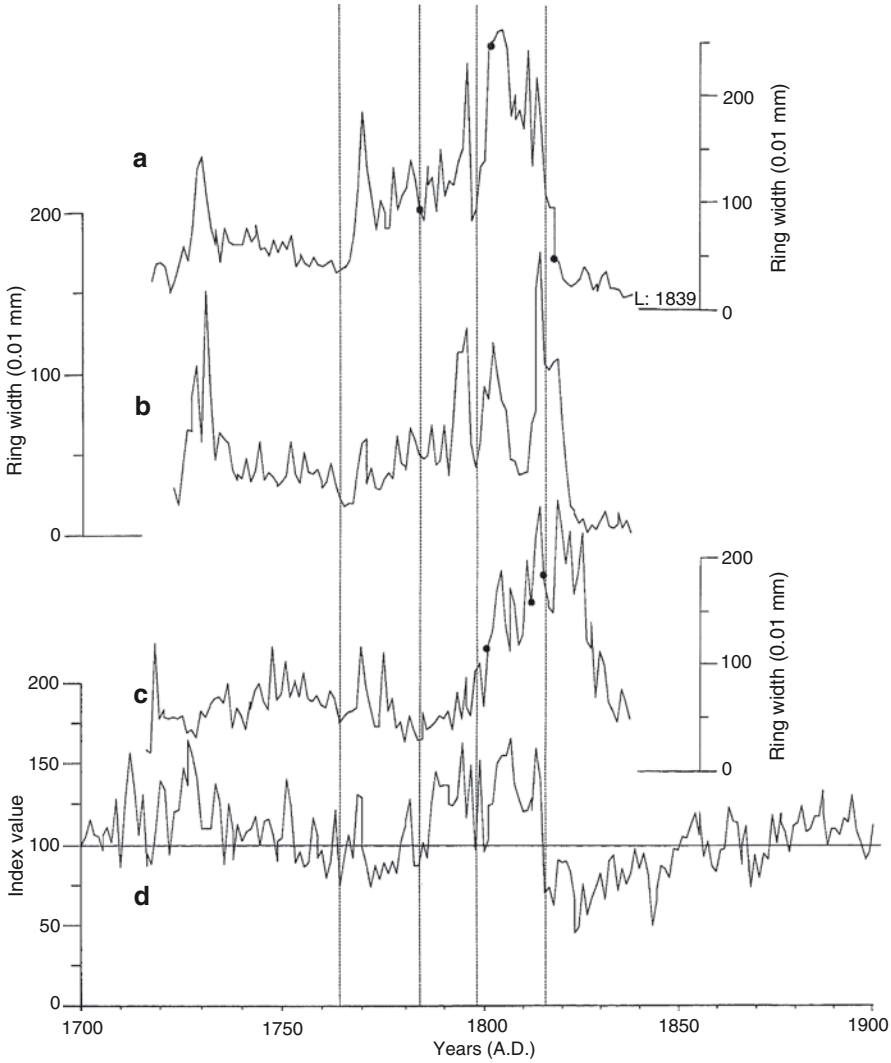

Fig. 4 Age of landslide G (L: AD 1839) using cross-dating of samples G-5 (*curve* **a**), G-7 (*curve* **b**), and G-2 (*curve* **c**) with the chronology of Parker et al. (1981) (*curve* **d**) and light-ring years (•) (Filion et al. 1986)

4.3 Tree Regeneration in Landslides E, F, and G

Age of the oldest spruces growing in landslides from the downstream sector is shown in Fig. 5 according to position in landslide, i.e. along the main scarp, on the floor of the flowbowl, and in the flowage zone. Tree regeneration started 15 years after inception of landslides F and G, and 25 years in landslide E. Spruce establishment began first at the proximity of seed-bearers, i. e. along the scarps near the undisturbed terrace edges where mature trees were growing. The floor of flowbowls were colonized lately and only superficially, because of eolian activity eroding the sandy outcrops. Finally, the flowage zones were characterized by a low potential in spruce regeneration.

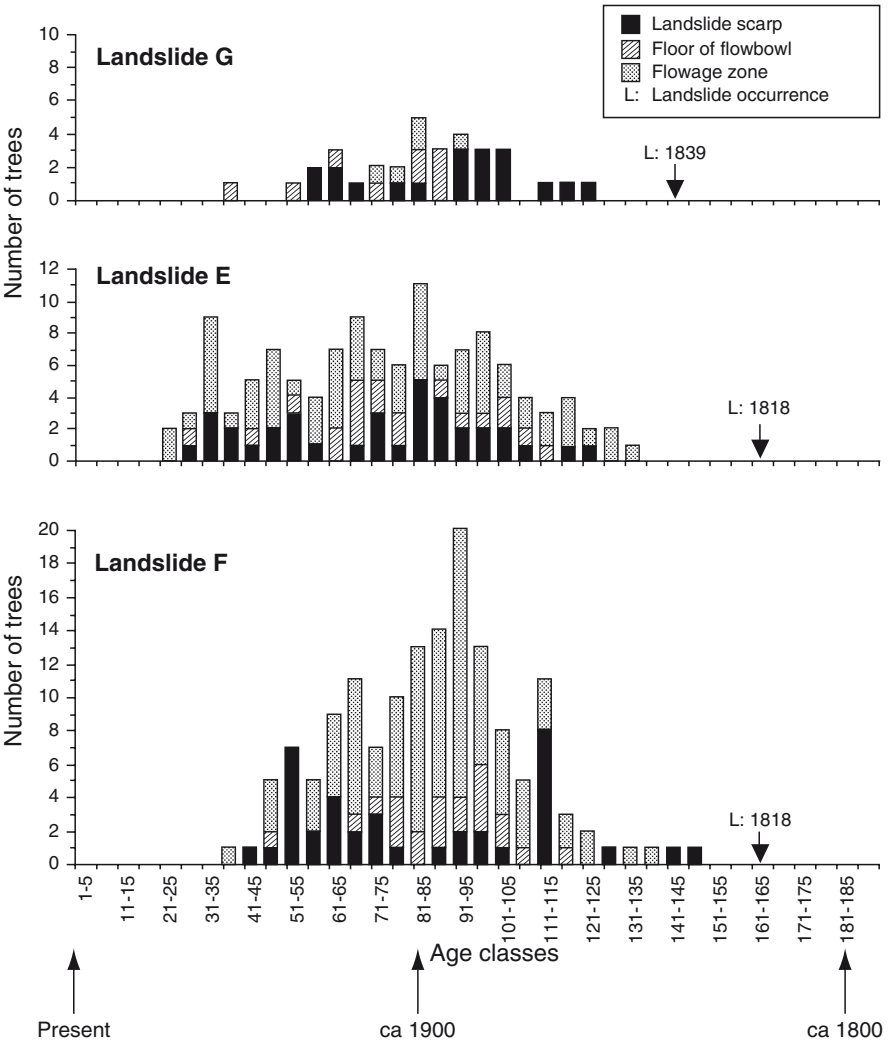

Fig. 5 Age-class frequency distribution of trees from initial establishment following the formation of landslides G, E, and F

5 Discussion

The Grande Rivière de la Baleine terraces were disturbed by seven major landslides since their formation (3,200 BP). The age of the second oldest movement (2,200 BP) gives the minimum age for landslide occurrence in the area, because the presumed oldest landslide A has not been dated. Mass movements reoccurred in the upper part of the river, ate. 900 BP (c. AD 1018–1260). From the eleventh to thirteenth to the nineteenth centuries, the area was relatively stable, showing only minor movements at the base of the main scarp and at the outer limit of the flowage zone in landslide C. The most active period in landslide activity occurred during the first half of the nineteenth century. Between 1818 and 1847 four large landslides occurred, and since that time no major disturbance was observed.

Thus, two contrasted periods appear from the chronology of landslide activity in the area. The first one lasted for a long time and included only three landslides (A–C), i. e. sometime after the inception of the estuarine terraces (3,200 BP) but before occurrence of landslide B (2,200 BP) until the beginning of the nineteenth century. The second period spanned only 30 years, but it was characterized by the occurrence of four landslides (D–G) including two synchronous events (landslides E and F). Because these recent landslides were dendrochronologically dated, it is possible to evaluate the conditions responsible for their formation and the climatic context in which they developed.

5.1 Recent Landslides

The two major landslides (E and F) located in the downstream sector occurred simultaneously in July 1818. In most of the sampled trees used for tree-ring analysis, a sharp reduction in growth was observed in 1816 and 1817. Far from being of local origin, this drop appears to be significant in all tree-ring chronologies from northern Quebec and Labrador (Cropper and Fritts 1981; Parker et al. 1981; Jacoby 1983; Filion et al. 1985; Payette et al. 1985).

Moreover, the 1816 and 1817 tree rings were identified as light rings (Filion et al. 1986), because of the absence of latewood probably caused by low temperatures in August and by an untimely stop of the growing season. These authors showed that about two thirds of the light-ring years corresponded to years (or triads) of major volcanic eruptions around the world. The 1815 Tambora eruption in Indonesia was the most important, and caused a drop in northern-hemisphere temperature of about 0.4–0.7°C (Lamb 1977; Bryson and Goodman 1980). Its influence on the northern Quebec climate lasted for 2 years, as suggested by the successive occurrence of 1816 and 1817 light rings. These two light rings were identified in more than 75% of individual spruce stems sampled in an old-growth lichen-spruce woodland at the tree line (Filion et al. 1986).

According to historical data from New England, the temperature in 1816 was 3–6°C below normal in June and July, and about 2–3°C in August (Hughes 1979;

Stommel and Stommel 1979). Information from the Hudson Bay Company's archives indicated that the Grande Rivière de la Baleine (Great Whale) trading post was abandoned in autumn 1816, and was reoccupied only in 1857. The 1816 and 1817 tree-ring characteristics showed that the climatic conditions were inimical to tree growth. Temperature was lower, which caused most likely a reduction in evaporation. The summer precipitation was probably higher, inducing water-logged ground conditions, and probably a higher river level with accelerated stream erosion. The relationship between precipitation and mass movements has been suggested and, in some cases, demonstrated convincingly by several workers (Terzaghi 1950; Nilsen and Turner 1975; Shroder 1978; Caine 1980; Rogers and Selby 1980). These particular conditions during 2 successive years culminated in July 1818 to produce the two major landslides.

The 1839 and 1846 landslides (G and D) occurred during spring, as suggested by the last complete tree ring. These 2 years are part of a long climatic sequence of reduced tree growth (Fig. 4d). The reduction in growth conditions between 1815 and 1860 appears to be general in tree-ring curves from northern Quebec and Labrador. As deduced from long tree ring records, the first half of the nineteenth century was probably one of the coldest intervals of the Little Ice Age in northern Quebec. Higher landslide incidence during this period seems to reflect the persistence of cold and humid conditions. Slope instability appeared to have been general in subarctic Quebec during this period. Several instability phases associated with slope solifluction were identified by Bégin and Filion (1985).

These climatic conditions have also largely influenced forest succession in the newly-exposed mineral surfaces. The time lag between landslide occurrence and seedling establishment was relatively long, about 15–25 years. A similar time lag was reported by Begin and Filion (1985) in a landslide at Clearwater Lake, about 175 km northeast of Poste-de-la-Baleine. The tree regeneration pattern in subarctic areas is closely associated with climatic conditions, because seed production and germination are typically sporadic (Hustich 1970; Payette and Filion 1985). Landslide dating using age of the oldest trees appears questionable in this context, because it underestimates landslide age; this technique provides at best a minimum age to sliding in subarctic environments.

5.2 Ancient Landslides

Only two radiocarbon dates were available for ancient-landslide dating. The undated landslide A occurred probably between 3,200 and 2,200 BP, as suggested by its slightly higher position relative to landslide B. The latter occurred sometime after 2,200 BP. This date gives a maximum age to landslide because it was obtained from a buried charcoal layer corresponding to the top of the original terrace surface. Landslide C would have been formed before 900 BP. This date suggests a minimal landslide age, because there is no indication about the delay in paludification of the floor after its formation.

These few dates cannot give an accurate time scale to evaluate the climatic context initiating landslide activity, as it was for recent landslides with tree-ring analysis. Lebuis et al. (1982) reported frequent landslide activity between 1,250 and 750 BP in the St. Lawrence Lowland, but this time interval overlapped both a cold period (1,600–1,000 BP) and a mild period (1,000–750 BP) in northern Quebec (Filion 1984). The only reliable indication of conditions conducive to landslide activity yet available referred to the season of occurrence. The presence of microfaults in landslide-B topsoils suggests that it was formed during spring. No such evidence was found in landslides A and C.

6 Conclusions

The landslide chronology described here shows temporal discontinuity in mass-movement activity over the last 3,200 radiocarbon years. Three landslides were formed during a period of about three millenia, while four others occurred within a 30-year period. The tree-ring analysis has been a useful dating tool for recent landslide activity. It has provided the exact date and season of landslide occurrence, as well as the short-term climatic context responsible for their inception. The higher landslide frequency recorded in the first part of the nineteenth century was associated with particular climatic conditions (cold and humid). Some landslides occurred during spring, and others during summer. The former were probably induced by snowmelt conditions, and the latter by cool and humid summer conditions. More detailed studies using dendrochronological and archival data could be helpful in determining the seasonal occurrence of a greater number of landslides. On the other hand, landslide dating by the ^{14}C technique does not provide enough information on the particular climatic conditions prevailing at the time of landslide activity, unless several dates are used to build reliable mass-movement chronologies which may be compared to existing geomorphic or ecological chronologies. Nevertheless, this dating technique gives the possibility to define the spatio-temporal sequence of landslide development during the Holocene.

Acknowledgements We are grateful to Benoit Perrier, Gilles Bordage and Francois Quinty for field assistance. This research has been financially supported by the Ministère de l'éducation (FCAR Program) of Quebec and the Department of Indian Affairs and North-Canada.

References

Agard SS (1979) Investigation of recent mass movements near Telluride, Colorado, using the growth and form of trees. M.Sc. Thesis, University of Colorado, 132 pp

Alestalo J (1971) Dendrochronological interpretation of geomorphic processes. Fennia 105:1–140

Allard M, Seguin MK (1985) La déglaciation d'une partie du versant hudsonien québécois: bassins des rivières Nastapoka, Sheldrake et à l'Eau Claire. Géogr phys Quat 39:13–24

Begin C, Filion L (1985) Analyse dendrochronologique d'un glissement de terrain dans la région du Lac à l'Eau Claire (Québec nordique). Can J Earth Sci 22:175–182
Begin C, Filion L (1987) Morphologie et interprétation des glissements de terrain de la région de Poste-de-la-Baleine (Québec subarctique). Géogr phys Quat 56:19–32
Bjerrum L (1954a) Stability of natural slopes in quick clays. Géotechnique 5:101–119
Bjerrum L (1954b) Geotechnical properties of Norwegian marine clays. Géotechnique 5:49–69
Brunsden D, Jones DKC (1972) The morphology of degraded landslide slopes in southwest Dorset. Quart J Eng Geol 5:205–222
Bryson RA, Goodman BM (1980) Volcanic activity and climatic changes. Science 207:1041–1044
Caine N (1980) The rainfall intensity. Duration control of shallow landslides and debris flows. Geogr Ann 62A:23–27
Carson MA (1979) Le glissement de Rigaud (Québec) du 3 mai 1978: une interprétation du mode de rupture d'après la morphologie de la cicatrice. Géogr phys Quat 33:63–92
Cropper JP, Fritts HC (1981) Tree-ring width chronologies from the North American Arctic. Arct Alp Res 13:245–260
Delwaide A, Filion L (1987) Coupes forestières effectuées par les Indiens et par la Compagnie de la Baie d'Hudson à Poste-de-la-Baleine, Québec subarctique. Géogr phys Quat 41:87–96
Demangeot J (1974) Les glissements de terrain de Poste-de-la-Baleine (Nouveau-Québec). Cahiers de géographie de Québec 18:463–478
Eade KE (1966) Fort George River and Kaniapiskau River (west half) Map-Areas, New Québec. Geological Survey of Canada, Department of Mines and Technical Surveys, Memoire 339, p 84
Filion L (1984) A relationship between dunes, fire and climate recorded in the Holocene deposits of Quebec. Nature 309:543–546
Filion L, Payette S, Gauthier L (1985) Analyse dendroclimatique d'un krummholz à la limite des arbres, lac Bush, Québec nordique. Géogr phys Quat 39:221–226
Filion L, Payette S, Gauthier L, Boutin Y (1986) Light rings in subarctic conifers as a dendrochronological tool. Quat Res 26:272–279
Goulden MR, Sauchyn DJ (1986) Age of rotational landslides in the Cypress Hills, Alberta-Saskatchewan. Géogr phys Quat 40:239–248
Hillaire-Marcel C (1976) La déglaciation et le relèvement isostatique sur la côte est de la Baie d'Hudson. Cahiers de géographie de Québec 20:185–220
Hughes P (1979) The year without a summer. Weatherwise 32:108–111
Hustich I (1970) On the study of the ecology of subarctic vegetation. Proceedings of the Helsinki Symposium, UNESCO, Paris, pp 235–240
Hutchinson JN (1968) Mass movement. In: Fairbridge RW (ed) The encyclopedia of geomorphology, pp 688–695. Dowden, Hutchinson and Ross Inc., Stroudsburg, PA
Jacoby GC Jr. (1983) A dendroclimatic study in the forest tundra ecotone, on the east shore of Hudson Bay. In: Morisset P, Payette S (eds) Proceedings of the northern Québec Tree-Line Conference. Nordicana 47, pp 95–99
Lamb HH (1977) Climate, present, past and future, vol 2. Climatic history and the future, 835 pp. Methuen, London
La Rochelle P, Chagnon JY, Lefevre G (1970) Regional geology and landslides in the marine clay deposits of eastern Canada. Can Geotech J 7:145–156
Lebuis J, Robert JM, Rissmann P (1982) Regional mapping of landslide hazard in Quebec. Swedish Geotechnical Institute Symposium on Slopes and Soft Clays, Report 17, pp 205–262, Linköping
Leroueil S, Tavenas F, Le Bihan JP (1983) Propriétes caractéristiques des argiles de l'Est du Canada. Can Geotech J 20:681–705
Nilsen TH, Turner BL (1975) Influence of rainfall and ancient landslide deposits on recent landslides (1950–1971) in urban areas of Contra Costa County, California. US Geol Surv Bull 1388:18

Parker ML, Jozsa LA, Johnson SG, Bramhall PA (1981) Dendrochronological studies on the coast of James Bay and Hudson Bay (Parts 1 and 2). In: Harrington CR (ed) Climatic change in Canada, pp 129–188. National Museums of Canada, Ottawa, Syllogeus 33

Payette S, Filion L (1985) White spruce expansion at the tree-line and recent climatic change. Can J Forest Res 15:241–251

Payette S, Filion L, Gauthier L, Boutin Y (1985) Secular climate change in old-growth tree-line vegetation of northern Quebec. Nature 315:135–138

Rogers NW, Selby MJ (1980) Mechanisms of shallow translational landsliding during summer rainstorms: North Island, New Zealand. Geogr Ann 62A:11–21

Selby MJ (1982) Hillslope materials and processes. Oxford University Press, Oxford

Sharpe CFS (1938) Landslides and related phenomena. Columbia University Press, New York

Shroder JF Jr. (1973) Tree-ring dating and analysis of movement of boulder deposits, High Plateaus of Utah, USA. Abstract Ninth Congress, International Union, Quaternary Research, pp 328–329. Christchurch, New Zealand

Shroder JF Jr. (1975) Dendrogeomorphic analysis of mass movement. Proceedings on the Association of American Geographers, pp 222–226

Shroder JF Jr (1978) Dendrogeomorphological analysis of mass movement on Table Cliffs Plateau, Utah. Quat Res 9:168–185

Stommel H, Stommel E (1979) The year without a summer. Sci Am 240:176–186

Stuiver M, Becker B (1986) High-precision decadal calibration of the radiocarbon time scale, AD 1950–2500 BC. Radiocarbon 28:863–910

Terzaghi K (1950) Mechanism of landslides. In: Paige S (ed) Application of geology to engineering practice, pp 83–123. Berkey Volume, Geological Society of America, New York

Varnes DJ (1958) Landslide type and processes. In: Eckel EB (ed) Highway research board, pp 20–47. Special Report 29, NAS-NRC Publication 544, Washington, DC

Rainfall Up, Mountain Down?

Leonardo Paolini and Ricardo Villalba

Climate and natural disturbances are strongly related. Several studies have shown the strong relationships between precipitation, soil-water content, and landslide occurrence (e.g. Keefer and Johnson 1983; Schwab 1983; Iverson and Major 1987; Bovis and Jones 1992; Schwab 2002).

Variability is an intrinsic characteristic of climate, which in turn alters natural disturbance regimes. Instrumental and tree-ring records show a precipitation increase during recent decades in Northwestern Argentina (NWA; Minetti and Vargas 1997; Villalba et al. 1998), which appears to be associated with changes in the regional atmospheric circulation related to global warming (Labraga and Lopez 2000; Villalba et al. 1998). If present and future climatic changes related to global warming involve increases in precipitation, could this increase in rainfall result in increased landslide frequency?

Landslides are a major component of the disturbance regimes on steep mountain slopes across the world. In the subtropical montane forests of NWA, landslides affect not only forest dynamics, but also human activities. Three major cities in NWA (total population >1.500.000 people) are located in the foothills of the mountains where landslide events impact water quality, transportation, and hydropower generation.

Dendrochronological dating was used to reconstruct landslide occurrence along a 300 km stretch of the mountain ranges of NWA during the past 50 years. We used a combination of three dendrochronological techniques to date landslide occurrence. The minimum age for a landslide was established by dating Andean alder (*Alnus acuminata*) trees growing on the landslide scar and its deposits. The age of the oldest tree growing on the new surface provides an estimate of the minimum age

L. Paolini (✉)
Instituto de Ecologia Regional, Universidad Nacional de Tucumán, 4107 Yerba Buena, Argentina
e-mail: leopaolini@gmail.com

R. Villalba
Instituto Argentino de Nivología, Glaciología y Ciencias Ambientales IANIGLA, CCT Mendoza, CONICET C.C. 330, 5500 Mendoza, Argentina

M. Stoffel et al. (eds.), *Tree Rings and Natural Hazards: A State-of-the-Art*, Advances in Global Change Research 41, DOI 10.1007/978-90-481-8736-2_11,

for the deposit. The occurrence of a disturbance can also alter the ring-width pattern of trees growing along the landslide scar, causing suppression or growth release events. The recorded changes in tree-ring patterns were also used for dating landslide events. In addition, we dated trees killed by landslides as a complement to the event chronology. The accuracy of the dendrochronological techniques used in our study was validated on landslides of known age (Fig. 1). Finally, the landslide chronologies were compared with regional precipitation records in order to establish the relationship between landslide occurrence and precipitation fluctuations over time.

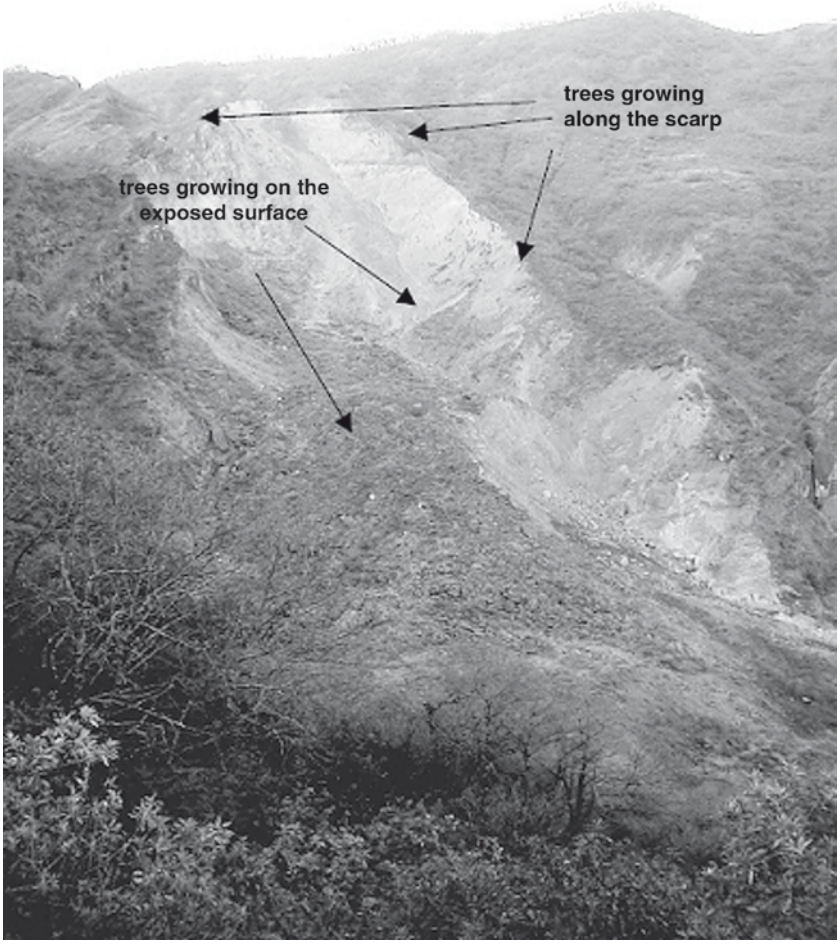

Fig. 1 Landslide in Yala, Northwestern Argentina, which occurred in the summer 1998–1999, showing the location of sampled trees on the new surface and the scarp (Photo by L. Paolini)

There is a strong agreement in the landslide dates provide by the different techniques used in the sites with landslides of known age (Fig. 2). In Yala, most trees growing on the new surface created by a landslide in 1998 established between 1999 and 2000. This observation suggests that *A. acuminata*, the dominant subalpine tree, rapidly (1 year or 2) colonizes the new exposed surfaces in NWA. In the six trees sampled along the landslide scarp, 1998 is the narrowest ring since 1990

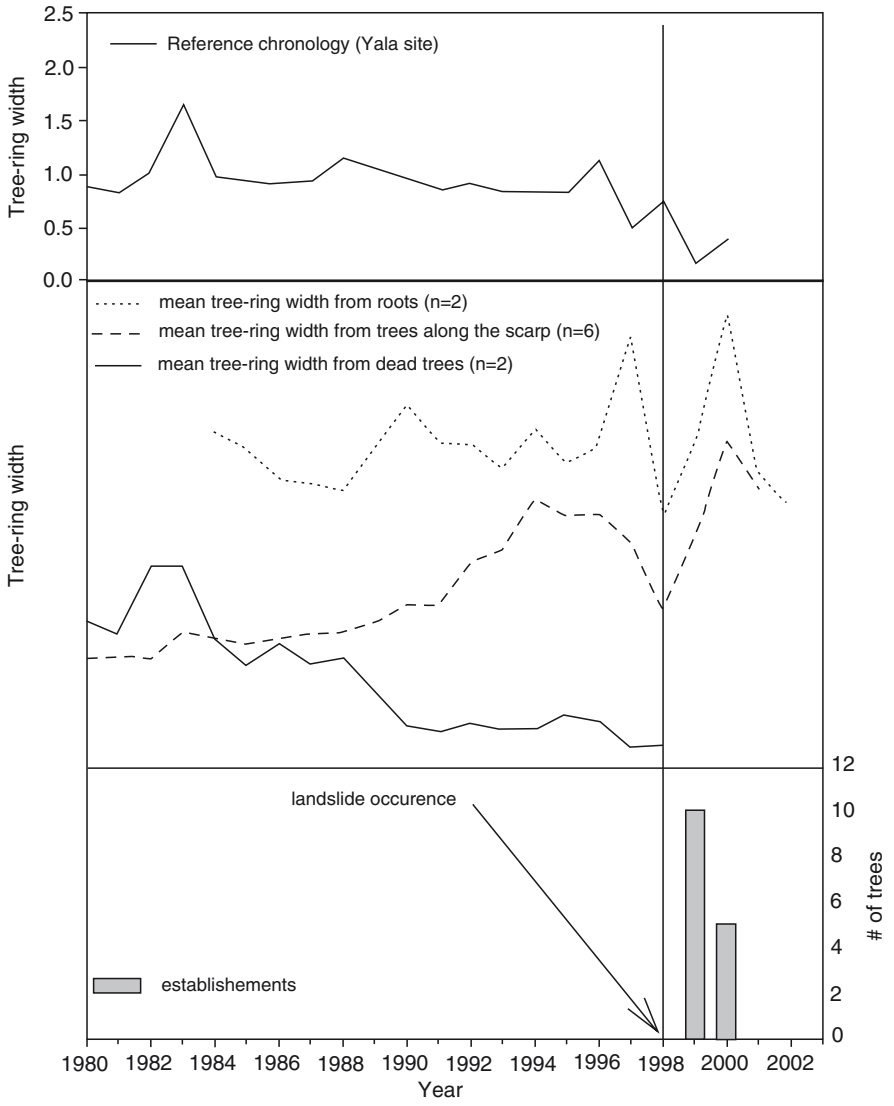

Fig. 2 Suppression and release patterns from trees growing along the scarp and establishment dates from trees on the exposed surface. Tree-ring variations for a dead tree are also shown

and was followed by a sudden release peaking in 2000. Cross-dating of dead trees indicates that the last ring in the cross-section was formed in 1998. Comparison with a control chronology, developed from trees not affected by landslides, showed that growth in 1998 was around the mean, suggesting no influence of climate on the narrow ring identified in 1998 in the trees severely affected by the Yala landslide. Due to topographic (elevation, slope) and environmental (climate, vegetation) similarities between the landslide sites, we applied the techniques previously validated to date the occurrence of 39 landslides of unknown age. For most sites (>90%), we found a good agreement between suppression-release patterns of tree growth and the ages of trees growing on the new surfaces. For the 39 landslides, the mean lag period between the oldest tree established on the landslide and the suppression and/or release signal recorded in the tree-ring pattern was 1.3 years (median 1 year), indicating, as in Yala, a good agreement between the ages provided by the different methods.

A strong relationship between landslide occurrence and precipitation variability in NWA was recorded during the past decades (Fig. 3). Thirty seven of the 42 landslides dated along the interval 1934–2001 occurred in years with above-average precipitation. Precipitation in years with landslide occurrence is significantly greater than in years without events ($t = 4.87$; $p < 0.001$). Similar results were also provided by the Superpose Epoch Analysis (SEA). Years with landslides are significantly rainier. The SEA also reveals that the occurrence of a landslide is positively and significantly related to the precipitation in the 2 years before the event, supporting the hypothesis of long-term soil water recharge before the events. The landslide chronology also shows that 75% of the landslides occurred between 1976 and 1987, the most humid period in NWA during the twentieth century (Minetti and Vargas 1997).

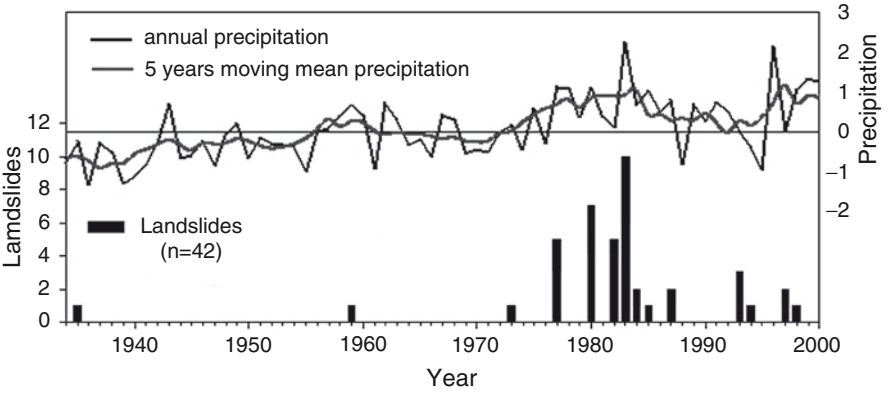

Fig. 3 Relationship between landslide events and total annual precipitation in NWA, 1934–2000

References

Bovis MJ, Jones P (1992) Holocene history of earthflow mass movements in south-central British Columbia: the influence of hydroclimatic changes. Can J Earth Sci 29:1746–55

Iverson RM, Major JJ (1987) Rainfall, ground-water flow, and seasonal movement at Minor Creek landslide, northwestern California: physical interpretation of empirical relation. Geol Soc Am Bull 99:579–94

Keefer DK, Johnson AM (1983) Earthflow, morphology, mobilization, and movement. US Geol Surv Prof Paper 1264

Labraga JC, Lopez MA (2000) Escenario de cambio climatico para la Republica Argentina: actualizacion 1999. IAI News Lett 23:16–22

Minetti JL, Vargas WM (1997) Trends and jumps in the annual precipitation in South America, south of the 15 S. Atmosfera 11:205–221

Schwab JW (1983) Mass wasting: October–November 1978 storm, Rennell Sound, Queen Charlotte Islands, British Columbia. British Columbia Ministry of Forests, Research Note 91

Schwab JW (2002) Dendrochronology of debris flows on the British Columbia north coast. In: Jordan P, Orban J (ed) Terrain stability and forest management in the interior of British Columbia. Workshop Proceedings. British Columbia Ministry of Forests Forest Sciences, Technical Report: 003–217

Villalba R, Grau HR, Boninsegna JA, Jacoby GC, Ripalta A (1998) Tree-ring evidence for long-term precipitation changes in subtropical South America. Int J Climatol 18:1463–78

Part IV
Rockfall

Open scar on European larch (*Larix decidua*) stem following rock impact, Swiss Alps (© D. M. Schneuwly)

Rockfalls and Their Hazard

Fausto Guzzetti and Paola Reichenbach

1 Introduction

Rockfalls are a type of fast mass movement common in mountain areas worldwide triggered. Natural triggers of rockfalls comprise earthquakes (Harp and Wilson 1995; Marzorati et al. 2002), freeze-thaw cycles of water (Gardner 1983; Matsuoka and Sakai 1999), melting of snow (Wieczorek and Jäger 1996) or permafrost (Gruber et al. 2004), temperature changes (Davies et al. 2001), intense rainfall (Chau et al. 2003; Cardinali et al. 2006), stress relief following deglaciation (Wieczorek and Jäger 1996), volcanic activity, and root penetration and wedging (Wieczorek and Jäger 1996). Human-induced causes of rockfalls include undercutting of rock slopes, mining activities, pipe leakage, inefficient drainage, and vibrations caused by excavations, blasting, or traffic.

An individual rockfall is a fragment of rock detached from the bedrock along new or pre-existing discontinuities (e.g., bedding, joints, fractures, cleavage, foliation, topographic surface) by creeping, sliding, toppling or falling, that falls along a cliff, proceeds down slope by bouncing and flying along ballistic trajectories, or by rolling on talus or debris slopes. When the boulder has lost enough energy in impacts or by friction, it stops on or near the foot of the slope. For primary failures, fall follows detachment immediately. For secondary rockfalls, that involve the fall of previously detached materials (e.g., by rainfall, water flow, snow avalanche, animals, vegetation, other rockfalls), the time and trigger of the fall are different from those of the detachment. A rockfall failure can involve single or multiple blocks. When multiple blocks are involved in a failure, there is little or no interaction among the individual fragments that proceed along separate trajectories. Rockfalls travel at speeds ranging from a few to tens of meters per second, and range in size from small cobbles to large boulders hundreds of cubic meters in size.

F. Guzzetti (✉) and P. Reichenbach
CNR – IRPI, 06128 Perugia, Italy
e-mail: F.Guzzetti@irpi.cnr.it

M. Stoffel et al. (eds.), *Tree Rings and Natural Hazards: A State-of-the-Art*,
Advances in Global Change Research 41, DOI 10.1007/978-90-481-8736-2_12,

Due to their high mobility, and despite their often relatively small size, rockfalls are a particularly destructive type of failure (Fig. 1), and in several areas, especially along roads and railways, they represent the primary cause of landslide fatalities (Evans 1997; Guzzetti et al. 2005). In mountain regions, where large areas can be subject to rockfall hazard, the morphological, lithological, structural, climatic and land cover settings controlling rockfalls vary considerably. For this reason, determining the location of the source areas, and predicting the trajectories, the invasion zones, and the travel velocities of rockfalls proves difficult, particularly over large areas.

Fig. 1 Rockfall triggered by the 6 April 2009 L'Aquila earthquake near Stiffe, central Italy

2 The Mechanics of Rockfalls

A rockfall is a combination of simple mechanical processes, including: (i) detachment (by creeping, toppling, or sliding), (ii) free falling (flying), (iii) bouncing (impact and rebound), and (iv) rolling (Guzzetti et al. 2002; Dorren 2003). Creeping is limited to the pre-failure stage of a rockfall and often goes undetected, unless specific monitoring is available. Toppling consists in the rotation outward or sideways from the slope of a single block or of multiple adjacent blocks. Sliding is limited to the initial stage of a rockfall, where it occurs over short distances. For large boulders sliding may also occur at impact, with significant loss of energy due to high friction. Free falling is the predominant type of motion of a rockfall. Driven by gravity, free fall occurs along ballistic trajectories at high and very high velocity.

In nature, where the motion of an individual rockfall fragment is most often by tumbling, i.e. "short bounces" forming a rapid sequence of short, low flying parabolas, a boulder rolling is rarely observed. Rolling occurs chiefly for sub-spherical, cylindrical or discoid blocks, when the velocity of the boulder is relatively low, on rectilinear or convex-upward slopes, with medium to low terrain gradient and limited surface roughness. Irregularities in the shape of the block or the terrain facilitate impact and bouncing, and prevent or interrupt rolling.

Impact is the most complex, uncertain and poorly understood phase of a rockfall. At impact, energy is lost and the direction of motion of the rockfall changes. Impact can vary from (almost) completely elastic to (almost) entirely inelastic, depending on the mechanical properties of the terrain and of the block, the impact angle, and the block shape, mass and velocity (Azzoni and de Freitas 1995; Chau et al. 2002). Upon impact, a block can break into multiple fragments that proceed along separate trajectories. In forests, collisions against trees can deflect or stop rocks (Stokes et al. 2005; Ciabocco et al. 2009; Lundström et al. 2009).

3 Rockfall Modelling and Hazard Assessment

In principle, a rockfall is a simple geomorphological process to model. Knowing the release point, the topography of the slope, the energy lost at each impact point and where a block is rolling, it should be possible to predict the location, velocity and distance to the ground of the falling block at any point along its trajectory. Reality is different, and a rockfall represents an example of a relatively simple mechanical system whose behaviour cannot be predicted exactly, even if the initial conditions and the driving forces are known. This limits our ability to ascertain rockfall hazard.

A good predictor of rockfall occurrence in an area is the evidence of previous rockfalls. Identifying and mapping rockfalls and their associated geomorphologic forms (e.g., talus slopes) provide valuable information to determine rockfall hazard. Assessing rockfall hazard involves determining: (i) where rockfalls can occur, including the identification of the detachment (source) areas, the travel zones, and

the deposition areas, (ii) the magnitude of the expected rockfalls, including the number, volume, velocity and energy of the falling blocks, and (iii) when, or how frequently, rockfalls are expected in an area, for different triggers.

To determine where a rockfall can develop, one has to locate the potential source areas of the rockfalls. When studying a single slope or an individual rockfall, the location and characterization of the unstable blocks is made in the field, through geological, geomorphological and structural mapping. For larger areas, the potential detachment zones are identified using geomorphological techniques (e.g., field observation and mapping, interpretation of aerial photographs), and GIS modelling (Frattini et al. 2008; Günther and Thiel 2009).

Where the location of the potential source areas of rockfalls is known, the travel paths and the depositional areas are ascertained through numerical modeling. Evidence for past rockfalls is valuable information to validate the numerical modeling. Software has been designed to model the rockfall trajectories adopting kinematical ("lumped mass"), dynamic and hybrid schemes (Guzzetti et al. 2002; Dorren 2003; Dorren et al. 2006). Most of the computer codes adopt a two-dimensional approach, and simulate a rockfall along pre-defined topographic profiles. To cover a large area, multiple simulations must be prepared and the results interpolated to obtain a spatially-continuous model of the rockfall process. Guzzetti et al. (2002), Crosta and Agliardi (2004) and Stoffel et al. (2006), among others, tested three-dimensional rockfall simulation software. Some of these codes have been demonstrated to perform well in small (Stoffel et al. 2006; Wieczorek et al. 2008; Agliardi et al. 2009), large (Guzzetti et al. 2003, 2004; Frattini et al. 2008), and very large (Guzzetti et al. 2002) areas, and were used successfully to ascertain hazard (e.g., Guzzetti et al. 2003, 2004; Frattini et al. 2008). Figure 2 shows the result of a spatially distributed rockfall simulation obtained using an improved version of the 3D-modelling software STONE (Guzzetti et al. 2002).

Rockfall magnitude, a proxy for destructiveness, is a function of the energy of the individual rock blocks along the falling trajectories. Adopting a simple physical model to describe a rockfall, at any given point along the trajectory the kinetic energy depends on the velocity and mass of the falling block. Velocity depends chiefly on the falling height and the gravitational acceleration. Mass depends on the volume and the bulk density of the block. The rock density is determined based on the rock type, and the falling height is obtained from topographic maps or computed from a digital representation of the topography (Guzzetti et al. 2002; Dorren et al. 2006).

Measuring the volume of an individual block, or of a few blocks, in the field is a relatively simple operation. Determining the volume of several (a few hundred to several thousands) rockfalls over a large area is impractical, and rarely performed (e.g., Wieczorek et al. 1992; Wieczorek and Snyder 2004; Luckman 2008). This limits the ability to determine rockfall hazard over large areas. To overcome this limitation, investigators have examined the statistics of rockfall volumes. Analysis of catalogues of rockfall volumes has revealed that the probability (or frequency) density of rockfall volumes exhibits a typical negative power law scaling behaviour (Brunetti et al. 2009).

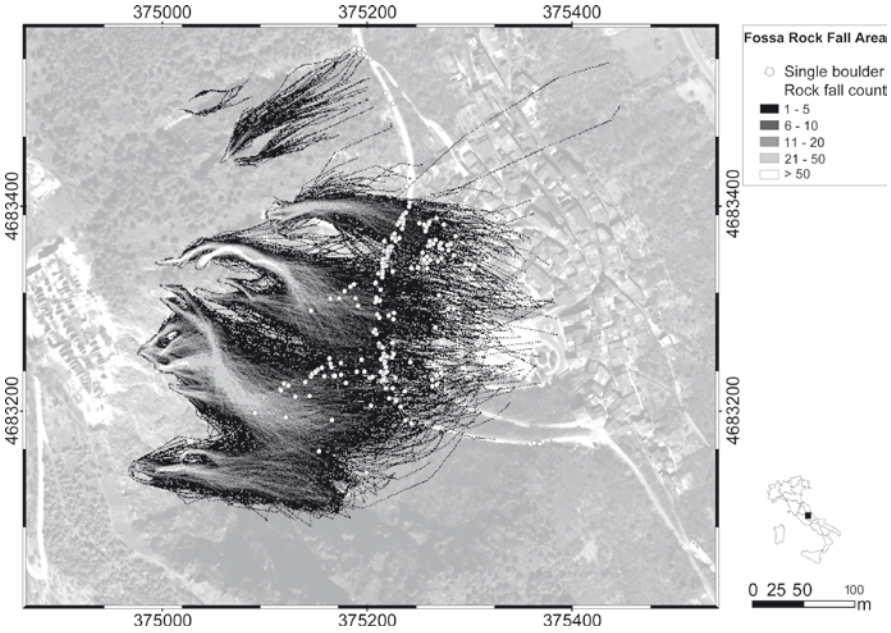

Fig. 2 Multiple rockfalls triggered by the 6 April 2009 L'Aquila earthquake at Fossa, central Italy. Rockfall source areas and individual boulders were mapped in the field studying aerial photographs and very high resolution satellite images taken shortly after the earthquake. Numerical modelling of rockfall was performed using a modified version of the code STONE (Guzzetti et al. 2002)

Establishing when or how frequently rockfalls occur is difficult. When a rockfall takes place depends on the time of the trigger (e.g., an earthquake); but daily and seasonal conditions play a role (Luckman 1976; Douglas 1980; Gardner 1983; Stoffel et al. 2005a). For a single rockfall, and assuming a simple geometry for the unstable block, the time of failure can be predicted with reasonable accuracy, where adequate monitoring is available (Zvelebil and Moser 2001). Determining how often rockfalls occur in an area is more problematic. Rockfall frequency in area depends on multiple factors, including the rate of rockfall activity and the frequency of the triggers, which are difficult to know precisely. To determine the probability of rockfall occurrence one can exploit information on past rockfall events, but constructing complete, uncensored, and accurate time series of rockfalls, covering a significant period, is difficult and time consuming.

Catalogues of rockfall events are compiled searching historical records, and through direct observation and field mapping. Wieczorek et al. (1992) prepared a catalogue of 519 rockfalls and rock slides, in the period between 1857 and early 2004, for the Yosemite Valley, California. Guzzetti et al. (2003) exploited this information to study the rate of rockfall occurrence, and to determine the annual frequency of the failures. Hantz et al. (2003) exploited a catalogue of 33 rockfalls

in the 66-year period 1935–2000 to determine the probability of rockfall failures along 120 km of escarpments in the Grenoble area, France. Luckman (2008) measured the volume of blocks deposited along an abandoned road in Jasper National Park, Alberta, in the 40-year period 1961–2000, and determined average rockfall accumulation rates. Other investigators have exploited dating techniques, including lichenometry (Luckman and Fiske 1995; McCarroll et al. 1998) and dendrochronology (Stoffel et al. 2005b; Perret et al. 2006; Stoffel 2006; Schneuwly and Stoffel 2008a, b; Moya et al. 2010, this volume) to reconstruct the history and rate of activity of rockfalls. The advantage of this approach consists in the possibility of constructing spatial-temporal catalogues spanning multiple centuries (Stoffel et al. 2005b; Perret et al. 2006; Stoffel 2006). As a drawback, the temporal resolution of the analysis is coarser.

4 Research Needs and the Potential Contribution of Tree-Ring Analysis

In mountain regions, expansion of settlements and infrastructure over dangerous areas is increasing the impact of natural hazards, including rockfalls. In several countries, this has fostered rockfall investigations. Rockfalls are studied primarily: (i) to predict where destructive events may happen, and to design adequate defensive measures ("engineering" approach), and (ii) to understand the factors and circumstances that control rockfalls and their rate of occurrence, including the temporal and geographical variations ("geomorphological" approach). Evidently, the two approaches are synergic.

From an engineering perspective, sophisticated technologies are used to design, test, construct and deploy highly efficient defensive structures to protect specific assets. In this field, research is mostly technological, and involves the innovative design and testing of new structures and new materials. Innovation is also required to improve rockfall modelling through advanced computer codes, and a better understanding of the mechanics of a rockfall; chiefly the loss of energy and fragmentation upon impact. Efforts should also be made to study the protective function of forests, and to design appropriate land management strategies.

From a geomorphological point of view, the challenge is to determine the combined geographical and temporal evolution of rockfalls. Over large areas, this has implications for sediment fluxes and erosion/accumulation studies, and for hazard assessment. To study the geographical and temporal patterns of rockfalls, historical information on past events is of paramount importance. There is a need for local, regional, national and even continental efforts to search, collect, and organize information on historical rockfall events and their consequences. Further, an agreement has to be reached on how to analyse the time series of rockfall events. When investigating a time series of natural events, the assumption is made that the series is "stationary" i.e., the rate of the process does not change significantly with time. Where a trend exists, it is assumed that the trend is known. However, a series may

be stationary (or not), depending on the length of the series. Further, in mountain areas, due to climate, environmental and socio-economical variations, the time series may be not stationary, hampering the ability to determine reliable statistics for the time series. This has implications for hazard and risk assessment, and for policy making.

The consequences of damaging natural events – including rockfalls – depend on: (i) the location, density, frequency and magnitude of the events (i.e., the hazard), and (ii) the density, relevance and fragility of the elements exposed to risk (i.e., the vulnerability). For rockfalls, efforts should be made to disentangle the two components, particularly where human impact on the environment is significant or longstanding, and to design appropriate reduction (for hazard) and strengthening (for vulnerability) strategies.

Dendrogeomorphology, the application of tree-ring dating techniques to investigate geomorphological processes (Solomina 2002), has recently emerged as a powerful tool to study rockfalls (Stoffel 2006). Where applicable, tree-ring analysis can contribute significantly to: (i) identify and date historical failure events (e.g., Stoffel et al. 2005b), (ii) reconstruct long time series of rockfall events (Stoffel et al. 2005b; Perret et al. 2006; Moya et al. 2010, this volume), (iii) determine the rates and the spatial distribution of rockfall activity (Stoffel et al. 2005b; Perret et al. 2006; Luckman 2008; Schneuwly and Stoffel 2008a), (iv) investigate the seasonal variation of rockfall occurrences (Stoffel et al. 2005a; Schneuwly and Stoffel 2008b), (v) provide long-term statistics for the geometry of rockfall trajectories in an area (Schneuwly and Stoffel 2008a), and (vi) determine the impact probability of rockfalls on trees (Moya et al. 2010, this volume), fostering our understanding of the protective role of forests (Ciabocco et al. 2009; Lundström et al. 2009). There is a clear need for similar – and other – studies, as tree-ring analysis can help advance significantly our understanding of the rockfall process, and can contribute to the production of improved rockfall hazard assessments.

References

Agliardi F, Crosta GB, Frattini P (2009) Integrating rockfall risk assessment and countermeasure design by 3D modelling techniques. Nat Haz Earth Syst Sci 9:1059–1073

Azzoni A, de Freitas MH (1995) Experimentally gained parameters, decisive for rock fall analysis. Rock Mech Rock Eng 28(2):111–124

Brunetti MT, Guzzetti F, Rossi M (2009) Power-law correlations of landslide volumes. Non Linear Process Geophys 16:179–188

Cardinali M, Galli M, Guzzetti F, Ardizzone F, Reichenbach P, Bartoccini P (2006) Rainfall induced landslides in December 2004 in South-Western Umbria, Central Italy. Nat Haz Earth Syst Sci 6:237–260

Ciabocco G, Boccia L, Ripa MN (2009) Energy dissipation of rockfalls by coppice structures. Nat Haz Earth Syst Sci 9:993–1001

Chau KT, Wong RHC, Liu J, Lee CF (2003) Rockfall hazard analysis for Hong Kong based on rockfall inventory. Rock Mech Rock Eng 36(5):383–408

Chau KT, Wong RHC, Wu JJ (2002) Coefficient of restitution and rotational motions of rockfall impacts. Int J Rock Mech Min Sci 39:69–77

Crosta GB, Agliardi F (2004) Parametric evaluation of 3D dispersion of rockfall trajectories. Nat Haz Earth Syst Sci 4:583–598

Davies MCR, Hamza O, Harris C (2001) The effect of rise in mean annual temperature on the stability of rock slopes containing ice-filled discontinuities. Permafr Periglac Process 12(1):137–144

Dorren LKA (2003) A review of rockfall mechanics and modelling approaches. Prog Phys Geogr 27(1):69–87

Dorren LKA, Berger F, Putters US (2006) Real size experiments and 3D simulation of rockfall on forested and non-forested slopes. Nat Haz Earth Syst Sci 6:145–153

Douglas GR (1980) Magnitude frequency study of rockfall in Co. Antrim, N. Ireland. Earth Surf Process Land 5:123–129

Evans SG (1997) Fatal landslides and landslide risk in Canada. In: Cruden DM, Fell R (eds) Landslide risk assessment, pp 185–196. A.A. Balkema, Rotterdam

Frattini P, Crosta GB, Carrara A, Agliardi F (2008) Assessment of rockfall susceptibility by integrating statistical and physically-based approaches. Geomorphology 94(3–4):419–437

Gardner JS (1983) Rockfall frequency and distribution in the Highwood Pass area, Canadian Rocky Mountains. Z Geomorphol N.F. 27:311–324

Gruber S, Hoelzle M, Haeberli W (2004) Permafrost thaw and destabilization of Alpine rock walls in the hot summer of 2003. Geophys Res Lett 31:L13504

Günther A, Thiel A (2009) Combined rock slope stability and shallow landslide susceptibility assessment of the Jasmund cliff area (Rügen Island, Germany). Nat Haz Earth Syst Sci 9:687–698

Guzzetti F, Crosta G, Detti R, Agliardi F (2002) STONE a computer program for the three-dimensional simulation of rock-falls. Comput Geosci 28(9):1079–1093

Guzzetti F, Reichenbach P, Ghigi S (2004) Rockfall hazard and risk assessment along a transportation corridor in the Nera Valley, Central Italy. Environ Manage 34(2):191–208

Guzzetti F, Stark CP, Salvati P (2005) Evaluation of flood and landslide risk to the population of Italy. Environ Manage 36(1):15–36

Guzzetti F, Wieczorek GF, Reichenbach P (2003) Rockfall hazard and risk assessment in the Yosemite Valley, California, USA. Nat Haz Earth Syst Sci 3(6):491–503

Hantz D, Vengeon JM, Dussauge-Peisser C (2003) An historical, geomechanical and probabilistic approach to rock-fall hazard assessment. Nat Haz Earth Syst Sci 3:693–701

Harp EL, Wilson RC (1995) Shaking intensity thresholds for rock falls and slides: Evidence from 1987 Whittier Narrows and Superstition Hills earthquake strong motion records. Bull Seismolog Soc Am 85(6):1739–1757

Luckman BH (1976) Rockfalls and rockfall inventory data; some observations from Surprise Valley, Jasper National Park, Canada. Earth Surf Process Land 1:287–298

Luckman BH (2008) Forty years of rockfall accumulation at the mount Wilcox site, Jasper National Park, Alberta, Canada. Geograph Polonica 81(1):79–91

Luckman BH, Fiske CJ (1995) Estimating long-term rockfall accretion rates by lichenometry. In: Slaymaker O (ed) Steepland geomorphology. Wiley, Chichester, pp 233–255

Lundström T, Jonsson MJ, Volkwein A, Stoffel M (2009) Reactions and energy absorption of trees subject to rockfall: a detailed assessment using a new experimental method. Tree Physiol 29:345–359

McCarroll D, Shakesby RA, Matthews JS (1998) Spatial and temporal patterns of Late Holocene rockfall activity on a Norwegian talus slope: lichenometry and simulation-modelling approach. Arct Alp Res 30:51–60

Marzorati S, Luzi L, De Amicis M (2002) Rock falls induced by earthquakes: a statistical approach. Soil Dynam Earthquake Eng 22(7):565–577

Matsuoka N, Sakai H (1999) Rockfall activity from an alpine cliff during thawing periods. Geomorphology 28:309–328

Moya J, Corominas J, Pérez Arcas J (2010) Assessment of the rockfall frequency for hazard analysis at Solà d'Andorra (Eastern Pyrenees). In: Stoffel M, Bollschweiler M, Butler DR, Luckman BH (eds) Tree rings and natural hazards: A state-of-the-art. Springer, Berlin, Heidelberg, New York, this volume

Perret S, Stoffel M, Kienholz H (2006) Spatial and temporal rockfall activity in a forest stand in the Swiss Prealps – a dendrogeomorphological case study. Geomorphology 74:219–231

Schneuwly DM, Stoffel M (2008a) Spatial analysis of rockfall activity, bounce heights and geomorphic changes over the last 50 years – A case study using dendrogeomorphology. Geomorphology 102:522–531

Schneuwly DM, Stoffel M (2008b) Tree-ring based reconstruction of the seasonal timing, major events and origin of rockfall on a case-study slope in the Swiss Alps. Nat Haz Earth Syst Sci 8:203–211

Solomina ON (2002) Dendrogeomorphology: research requirements. Dendrochronologia 20(1):231–243

Stoffel M (2006) A review of studies dealing with tree rings and rockfall activity: the role of dendrogeomorphology in natural hazard research. Nat Haz 39:51–70

Stoffel M, Lièvre I, Monbaron M, Perret S (2005a) Seasonal timing of rockfall activity on a forested slope at Täschgufer (Valais, Swiss Alps) – a dendrochronological approach. Z Geomorphol 49(1):89–106

Stoffel M, Schneuwly D, Bollschweiler M, Lièvre I, Delaloye R, Myint M, Monbaron M (2005b) Analyzing rockfall activity (1600–2002) in a protection forest – a case study using dendrogeomorphology. Geomorphology 68(3–4):224–241

Stoffel M, Wehrli A, Kühne R, Dorren LKA, Perret S, Kienholz H (2006) Assessing the protective effect of mountain forests against rockfall using a 3D simulation model. Forest Ecol Manage 225:113–122

Stokes A, Salin F, Kokutse AD, Berthier S, Jeannin H, Mochan S, Dorren L, Kokutse N, Ghani MA, Fourcaud T (2005) Mechanical resistance of different tree species to rockfall in the French Alps. Plant Soil 278:107–117

Wieczorek GF, Jäger S (1996) Triggering mechanisms and depositional rates of postglacial slope-movement processes in the Yosemite Valley, California. Geomorphology 5:17–31

Wieczorek GF, Snyder JB (2004) Historical rock falls in Yosemite National Park. US Geol Surv Open-File Report 03–491

Wieczorek GF, Snyder JB, Alger CS, Isaacson KA (1992) Rock falls in Yosemite Valley, California. US Geol Surv Open-File Report 92-0387, p 38

Wieczorek GF, Stock GM, Reichenbach P, Snyder JB, Borchers JW, Godt JW (2008) Investigation and hazard assessment of the 2003 and 2007 Staircase Falls rock falls, Yosemite National Park, California, USA. Nat Haz Earth Syst Sci 8(3):421–432

Zvelebil J, Moser M (2001) Monitoring based time-prediction of rock falls: three case-histories. Phys Chemis Earth (B) 26:159–167

Assessing Rockfall Activity in a Mountain Forest – Implications for Hazard Assessment

Markus Stoffel, Dominique M. Schneuwly, and Michelle Bollschweiler

1 Introduction

Rockfall represents the most intensely studied geomorphic process in mountainous areas. Nevertheless, very little information exists on how rockfall frequencies and magnitudes vary over time and how hazards and risks posed by rockfall could be reliably assessed. Former studies have mainly focused on short-term observations of contemporary rockfall activity (Luckman 1976, Douglas 1980), rendering it difficult to estimate long-term accretion rates. Long-term estimates of rockfall accumulation rates have, in contrast, been derived from accumulated talus volumes (Rapp 1960), but such rates may neither be representative of the present-day rockfall activities nor of those that prevailed in the past. On slopes composed of siliceous lithologies, lichenometry has repeatedly been used to evaluate the mean age or activity of talus surfaces (André 1997) or to estimate rates of rockfall accretion (Luckman and Fiske 1995).

Simultaneously, investigations of forest-rockfall interactions have tended to evolve towards the analysis of mountain forests as a means of protection against rockfall (Bebi et al. 2001, Stoffel et al. 2006). Hétu and Gray (2000) indicate that forest cover would provide effective protection in the case of low magnitude-high frequency rockfall events, but could not prevent the devastating effects of high magnitude events.

M. Stoffel (✉) and M. Bollschweiler
Laboratory of Dendrogeomorphology, Institute of Geological Sciences, University of Bern, CH-3012 Bern, Switzerland
and
Chair for Climatic Change and Climate Impacts, Institute for Environmental Sciences, University of Geneva, CH-1227 Carouge-Geneva, Switzerland
e-mail: markus.stoffel@dendrolab.ch

D.M. Schneuwly
Department of Geosciences, University of Fribourg, CH-1700, Fribourg, Switzerland

M. Stoffel et al. (eds.), *Tree Rings and Natural Hazards: A State-of-the-Art*, Advances in Global Change Research 41, DOI 10.1007/978-90-481-8736-2_13,

Although recent studies have highlighted the potential of tree rings for the analysis of spatio-temporal patterns of rockfall (Perret et al. 2006, Schneuwly and Stoffel 2008a, b), tree rings have been used only quite rarely for the reconstruction of rockfall activity and the assessment of related hazards and risks (Stoffel 2006).

It is therefore the purpose of the present contribution to illustrate the potential of tree rings to: (a) analyze the magnitude and frequency; (b) determine spatial variations; (c) derive decadal variations and (d) assess the seasonality of rockfall activity on a forested slope. In total, 564 increment cores and 270 cross-sections from 153 European larch trees (*Larix decidua*) were analyzed, documenting decadal variations in rockfall activity at Täschgufer (Valais, Swiss Alps) over more than 400 years.

2 Study Site

The area investigated is the west-facing rockfall slope "Täschgufer" (Valais, Swiss Alps). Rockfall frequently occurs on the slope, originating from the heavily disintegrated and steep (<48°) gneissic rock walls of the Leiterspitzen (3,214 m a.s.l.). Figure 1 shows that the main rockfall source areas (RSA) on the slope are located at 2,300–2,600 m a.s.l. (RSA 1) and above 2,700 m a.s.l. (RSA 2), where bedrock is highly fractured with many joints. As suggested by a locally calibrated model (Gruber and Hoelzle 2001), RSA 1 would be located on the borderline between seasonal frost and permafrost environments. The presence of contemporary permafrost is confirmed on the slope between 2,400 and 2,500 m a.s.l., where ground ice was encountered during construction works (Haeberli 1992, Fig. 2).

The volume of rockfall fragments normally does not exceed 2 m^3. Besides frequent rockfall activity, a rockslide is noted in chronicles and its minimum age was estimated with lichenometry to > 600 years (Joris 1995). The spatial extent of the rockslide deposits is given in Fig. 1b. In addition, small debris flows (<100 m^3) occur at Täschgufer, moving downslope in well-defined channels.

Forest at Täschgufer predominantly consists of *L. decidua*, accompanied by few Norway spruce (*Picea abies*) and cembran pine (*Pinus cembra*). Although timberline locally attains ~2,300 m a.s.l., continuous forest cover reaches only 1,780 m a.s.l. in the area most heavily affected by rockfall activity.

In the recent past, rockfall regularly caused damage to roads and hiking trails. On October 6, 1985, single blocks reached the valley floor, damaging agricultural buildings in the village of Täsch. As a response, five deflection dams were erected in 1988 and 1989 (Dams 1–5; Fig. 1b). In the late 1990s, two large protection dams completed the construction works on the slope (Dams 6–7, Fig. 2).

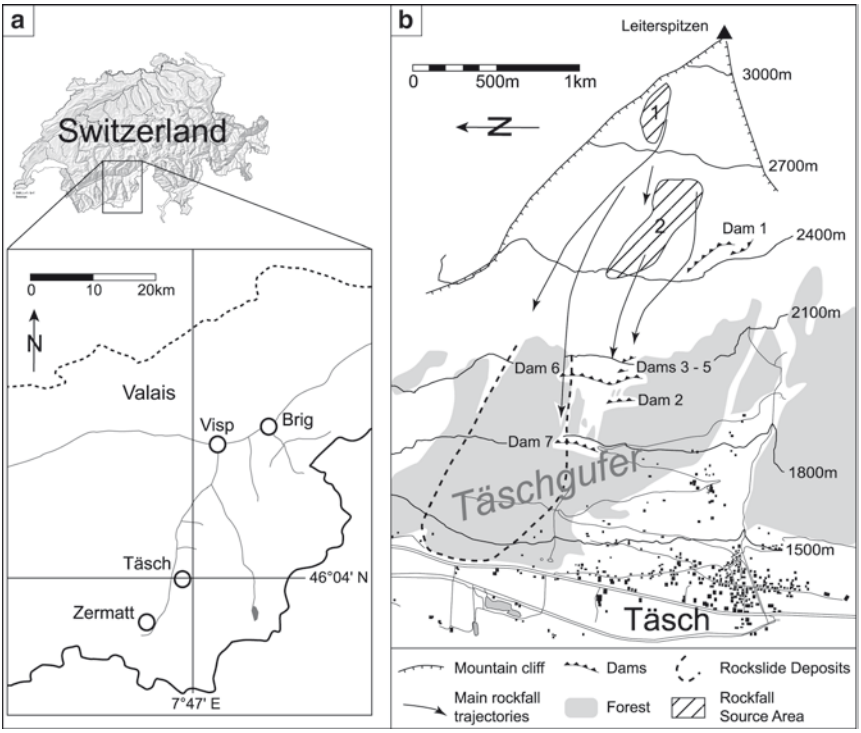

Fig. 1 Location of the study site. (**a**) The Täschgufer slope is located in the southern Swiss Alps, north-east of the village of Täsch. (**b**) The detailed sketch illustrates the rockfall slope with the main rockfall source areas and trajectories, the rockslide deposits and the dams built after 1988 (Dams 1–7)

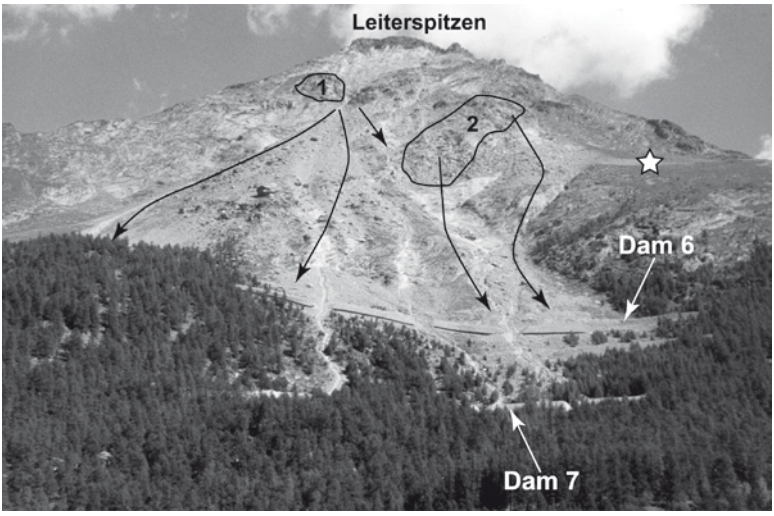

Fig. 2 View of the upper Täschgufer slope and the Leiterspitzen summit (3,214 m a.s.l.): Note the main Rockfall Source Areas (1, 2), the main rockfall trajectories (*arrows*) and the zone where ground ice has been encountered (*star*) during construction works (Photo by D. Schneuwly)

3 Methods

3.1 Sampling Strategy

In the study area covering approximately 39 ha (1,440–1,760 m a.s.l.), virtually all trees show visible damage related to rockfall activity (i.e. broken crowns or branches, scars, candelabra growth, tilted stems). We sampled severely affected trees with obvious signs of growth disturbances (GD) from both the rockslide deposits and the southern sector of the slope (Fig. 3). In contrast, we excluded a well-defined area in the southern sector influenced by both rockfall and debris-flow activity.

At least 4 cores were extracted per tree using increment borers. One core was taken upslope, one downslope and two cores perpendicular to the slope. In the case of visible scars, further samples were extracted from the overgrowing callus tissue. In addition, undisturbed reference trees were selected from a stand located south of the rockfall slope (Fig. 3). In total, we analyzed 170 *L. decidua* trees (598 cores):

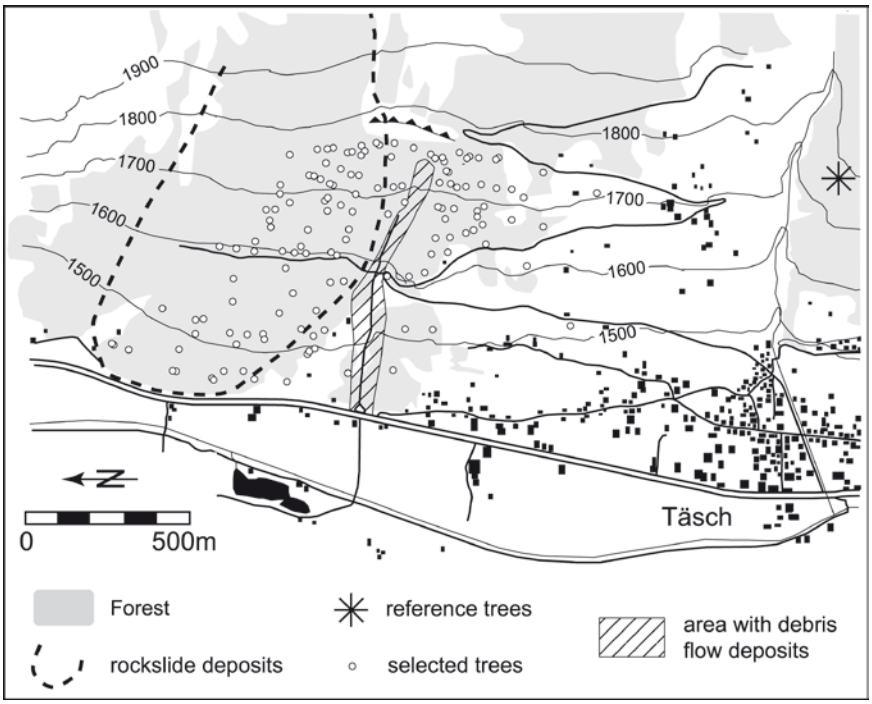

Fig. 3 Distribution of the 135 *Larix decidua* trees sampled on the Täschgufer slope (1,440–1,780 m a.s.l.). The area influenced by both debris flow and rockfall activity (*hatched surface*) has been excluded

135 trees (564 cores) from the rockfall slope and 17 reference trees (34 cores). In addition, 18 juvenile *L. decidua* trees were felled with handsaws and a total of 270 cross-sections prepared for the assessment of seasonal variations in rockfall activity.

Data recorded for each tree sampled included (1) determination of its 3D-position on the slope with compass and altimeter (x- and y-values, elevation a.s.l.); (2) sketches and position of visible defects in the tree morphology; (3) the position of the sampled cores; (4) diameter at breast height (DBH); (5) data on neighboring trees, micro-topography and/or rockfall deposits.

3.2 Tree-Ring Analysis of Trees Damaged by Rockfall

Samples were analyzed and data processed following the standard procedures described in Stoffel and Bollschweiler (2008, 2009). Single steps included surface preparation, skeleton plots and ring-width measurements using digital LINTAB positioning tables connected to a stereomicroscope and TSAP 3.0 software (Rinntech 2008). Increment curves of the rockfall trees were then crossdated with the reference chronology so as to differentiate climatically driven fluctuations in tree growth from GD caused by rockfall.

Growth curves were then used to determine the initiation of abrupt growth reduction or recovery (Schweingruber 1996). In the case of tilted stems, both the appearance of the cells (i.e. structure and color of the reaction wood cells) and the growth curve data were analyzed (Braam et al. 1987, Fantucci and Sorriso-Valvo 1999). Further focus was placed on the visual analysis of callus tissue overgrowing scars and on resin ducts. As resin ducts may result from causes other than rockfall (e.g., climate, wind, insects, fraying or browsing by ungulates), they were only considered the result of rockfall activity if they formed (a) traumatic, (b) extremely compact, (c) tangentially oriented and (d) continuous rows (Stoffel 2008, Stoffel and Hitz 2008, Schneuwly et al. 2009). In a last step, recurrence intervals were determined by dividing tree age at breast height by the number of dated GD.

3.3 Assessing Rockfall Rates

In contrast to other geomorphic processes that have a relatively large volume or surface area (e.g., debris flows, snow avalanches or floods), rockfall consists of single falling, bouncing or rolling stones which may only disturb trees along their trajectory and within a range defined by the size of the clast. Rather than using absolute values, we therefore use a rockfall rate expressed as number of rockfall events per meter width of all tree surfaces present per decade. The rate was based on the idea that thick stems expose a larger target (i.e. diameter at breast height, or DBH) to falling rocks than thin ones and so large trunks are more likely to be subject to growth disturbances (GD).

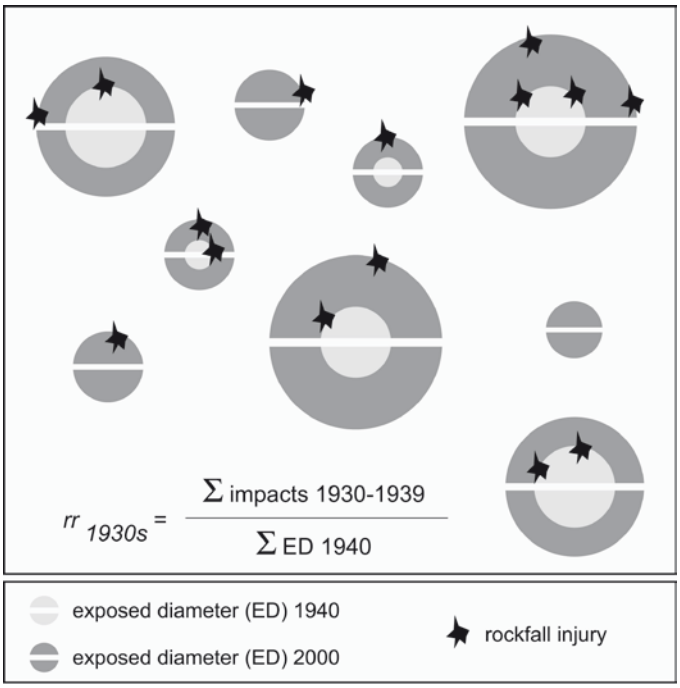

Fig. 4 The decadal rockfall rate (*rr*) represents the number of injuries identified per 1 m exposed tree diameter (ED)

The yearly DBH increment of each tree was obtained by dividing its current DBH by the number of rings between pith and sample year at breast height. This yearly DBH increment was then multiplied by the number of years a tree had existed at the beginning of a particular decade. The DBH values of all trees per decade were then summarized to comprise what is herein referred to as exposed diameter (ED; in meter). As shown in Fig. 4, the decadal sum of GD was then divided by the ED, indicating the number of GD recorded per meter ED and decade. Within this study, increment rates in trees were considered to remain constant and we willingly disregarded juvenile growth or ageing trends.

3.4 Seasonality of Rockfall

In the wider study region, highly resolved data are available on the onset and cessation of increment growth as well as on the transition from earlywood to latewood formation for several conifers (*L. decidua, P. abies, Pinus montana*; Müller 1980). Data indicates that radial growth (earlywood cells) currently starts in late May. Formation of latewood cells normally occurs by mid July and cell formation ceases in early October.

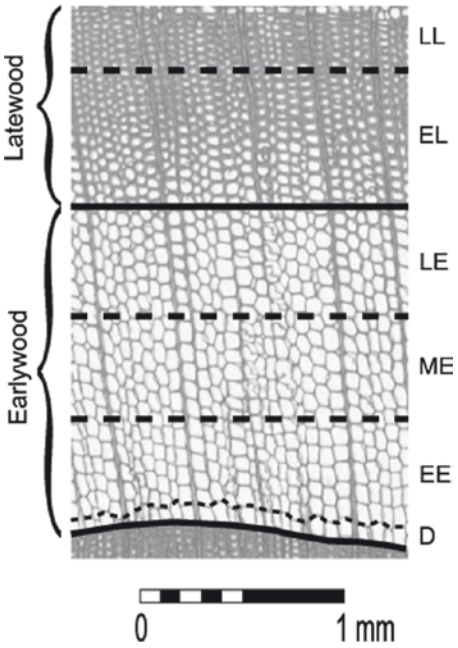

Fig. 5 Increment rings of conifers consist of thin-walled earlywood (E) and thick-walled latewood (L) cell layers. At the end of the growing season, cell division ceases and dormancy (D) occurs. When dating events with intra-annual precision, E is further subdivided into early (EE), middle (ME) and late (LE) earlywood, and L into early (EL) and late (LL) latewood

Based on the intra-ring position of 115 injuries identified on 270 cross-sections, rockfall activity on the slope was assessed with intra-annual precision (Fig. 5). In the case of rockfall injuries inflicted outside the vegetation period or within the first days of increment growth, the injury was attributed to the dormant season (D). Growth reactions within earlywood cells were subdivided into early (EE), mid (ME) and late (LE) earlywood, those in latewood into early (EL) and late (LL) latewood (see Stoffel et al. 2005).

4 Results

4.1 Age Structure of the Forest Stand

Data on the pith age at breast height indicate that the 135 sampled old-growth *L. decidua* trees are, on average, 297 years old. Over the centuries, trees gradually recolonized the slope to build up the current stand at Täschgufer. Figure 6 illustrates the spatial distribution of the age structure at Täschgufer, indicating that old trees are largely concentrated to the rockslide deposits and that the boundaries of age classes broadly correspond with its outer limits. Trees sampled in the southern sector are considerably younger and generally recolonized the slope in the first

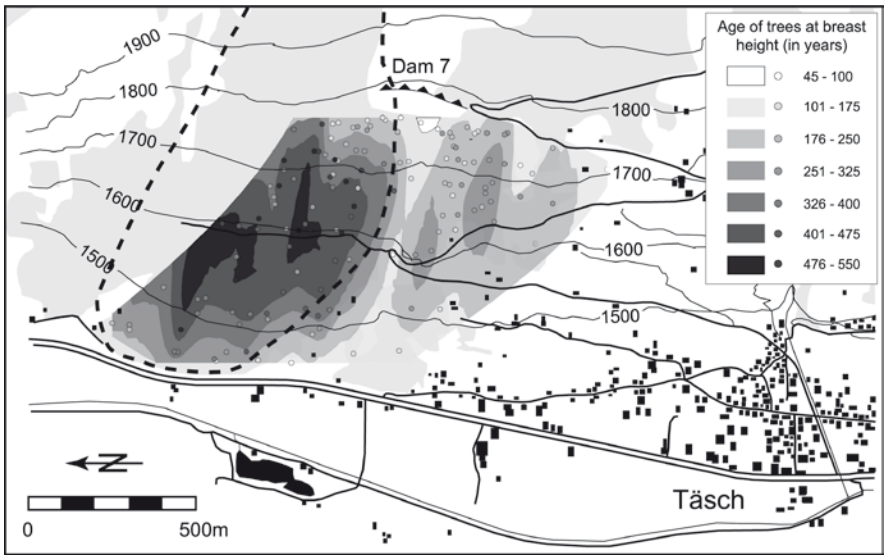

Fig. 6 Age of *Larix decidua* trees sampled on the Täschgufer slope. The patterns have been generalized based on interpolations. Ages are for tree at breast height

Table 1 Pith age at breast height of the trees sampled for analysis (in years)

Pith age at breast height	Northern sector	Southern sector
Mean	362	212
Standard deviation	141.4	75.6
Maximum	684	406
Minimum	61	45

half of the eighteenth century. The youngest trees are concentrated along the rockfall couloirs underneath Dam 7 and at the south-eastern edge of the study area (see Fig. 6).

The differences in the age structure between the two sectors also appear in Table 1. Although the trees sampled averaged 362 years on the rockslide deposits, they have an average age of "only" 212 years in the southern sector. In a similar way, the oldest sample on the rockslide attained breast height in AD 1318 and the youngest tree reached breast height in 1941. In contrast, the oldest tree from the southern sector dates to 1596 and the youngest to 1957.

4.2 Visible Defects and Growth Reactions to Rockfall Impacts

Analysis allowed for the identification of 236 visible defects on the 135 stems chosen for analysis. As illustrated in Table 2, candelabra trees largely predominate

Table 2 Different types of damage observed in the field (*left*) and growth reactions reconstructed from increment cores (*right*) at Täschgufer

Visible defects	
Broken crown	151 (64%)
Tilted stem	27 (11%)
Injuries (scars)	58 (25%)
Total	236 (100%)
Growth reactions	
Growth release	24 (3%)
Growth suppression	50 (6.5%)
Reaction wood	24 (3%)
Callus tissue	13 (1.5%)
Traumatic resin ducts	675 (86%)
Total	786 (100%)

among the visible defects. This growth feature occurs after the decapitation of the crown or part of the stem and was observed 151 times (64%). Recent or partly overgrown injuries (scars) were observed in 58 cases (25%). Finally, 27 trees (11%) were obviously tilted by rockfall impacts.

The subsequent analysis of the 564 increment cores allowed for the identification of 786 GD attributed to rockfall activity. As some rockfall impacts caused multiple GD in the same tree, the number of different rockfall events identified in the tree-ring series was reduced to 761. Table 2 shows the predominant occurrence of tangential rows of traumatic resin ducts. This feature was used in 675 cases (86%) to determine past events. Abrupt growth suppression occurred on 50 cores (6.5%), whereas abrupt growth releases and reaction wood could only be found on 24 samples each (3%). Finally, callus tissue was only rarely observed on the cores (13 cases; 1.5%).

4.3 Spatial Distribution of Growth Disturbances

On the study site, reconstructed rockfall activity varied greatly across the slope. The spatial distribution of interpolated recurrence intervals is given in Fig. 7, and shows that GD abundantly occurred in the trees located above 1,700 m a.s.l., where surfaces gradually become more sparsely forested. Similarly, GD have repeatedly been reconstructed in trees growing in the rockfall couloirs below Dam 7. Here, trees were regularly disturbed by rockfall fragments and recurrence intervals were locally <10 years. In a few century-old trees growing close to the rockslide deposits, dendrogeomorphic analysis indicates that tree growth has been disturbed almost twice a decade since the mid-nineteenth century. In contrast, very low numbers of GD are identified in trees growing on the rockslide deposits. In this part of the slope, recurrence intervals proved to be particularly high, with time elapsing between two GD regularly >150 years and individual century-old trees showing no GD at all. Not surprisingly, the spatial pattern of recurrence intervals largely

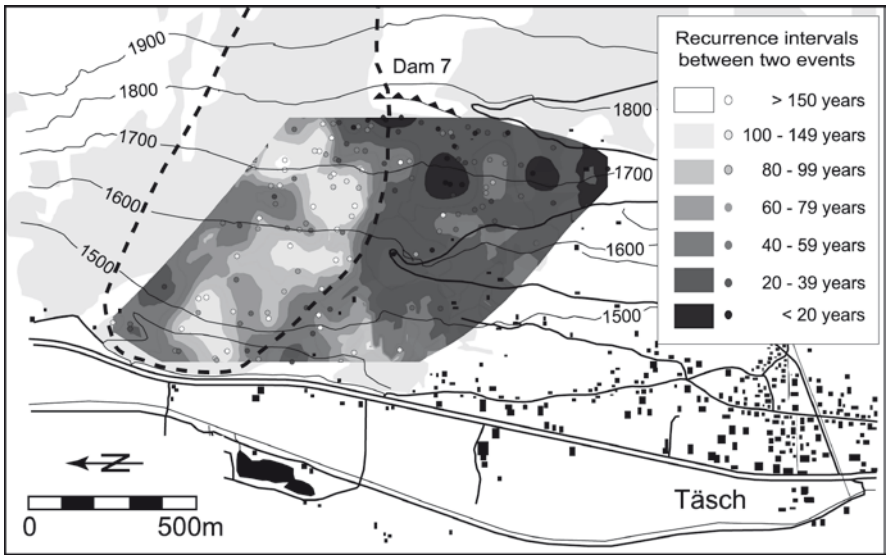

Fig. 7 Recurrence intervals of GD for the forest stand investigated. Intervals designate the number of years passing between two reconstructed growth disturbances on a single tree

coincides with the distribution of the age structure seen in Fig. 6 and oldest trees are commonly found in areas with relatively low numbers of GD. In contrast, youngest trees are largely concentrated in areas where rockfall repeatedly caused GD, leading to increased mortality and subsequently to higher recruitment rates by opening up sites for germination.

4.4 Rockfall Magnitudes and Frequencies

Throughout the last four centuries, rockfall has continuously caused GD to the trees sampled for analysis, most often in the form of low magnitude-high frequency events. Analysis of rockfall activity on the rockslide deposits starts in AD 1600, when 29 samples were taller than breast height. We disregarded 12 rockfall events occurring between 1394 and 1599, since sample size was too low for reliable analysis and the individual trees were unevenly distributed within the sector. The number of GD was thus reduced to 400 events derived from 78 trees. Due to the generally younger age of trees, the assessment of rockfall rates only starts in the 1740s in the southern sector. In total, 341 GD were dated in the 57 trees sampled.

In addition to the low magnitude-high frequency rockfall activity, tree-ring and age structure analyses also highlight one high magnitude-low frequency event, which would have destroyed the forest stand in the southern sector of the slope in 1720.

On the rockslide deposits, trees sampled were disturbed considerably by the high-magnitude rockfalls but largely survived the event. Figure 8 shows that 13

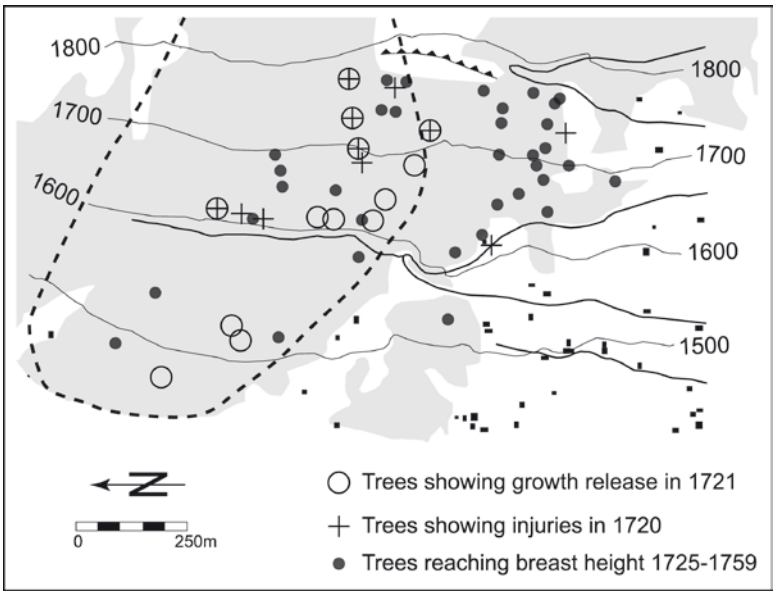

Fig. 8 Damage resulting from the 1720 rockfall. Thirteen trees have been injured (+) and eleven trees show an abrupt growth release starting in 1721 (○). The (re-)colonization of the rockfall slope (●) in the succeeding decades (1725–1759) most probably represents a reaction to the 1720 rockfall event

trees were injured by this large rockfall event. At the same time, 11 trees benefitted from improved growth conditions after the elimination of neighbors starting in 1721. GD mainly occurred in the samples located in the upper part of the forested slope (above 1,590 m a.s.l.), with 16 out of the existing 33 trees (48%) showing signs of the 1720 event. In contrast, trees sampled in the lower part of the slope mostly remained unaffected by the 1720 rockfall, scars were only present in three of the 21 existing trees (14%) and abrupt growth releases following the event were not recorded at all.

Figure 8 also illustrates that – as an indirect consequence of the high-magnitude rockfall in 1720 – trees abundantly recolonized the slope: Between 1725 and 1759, 25% of all sampled trees reached breast height (i.e. 34 trees), with most of the successor trees being located in the southern sector of the slope.

4.5 Decadal Variations in Rockfall Activity

The decadal rockfall rate on the rockslide deposits averaged 0.65 GD m ED^{-1} 10 years^{-1} over the last 400 years, but fluctuated considerably before the high-magnitude rockfall in 1720 (Fig. 9a; Table 3). As a result of the partial destruction of the forest fringe on the rockslide deposits, the highest decadal rockfall rate was noted in the

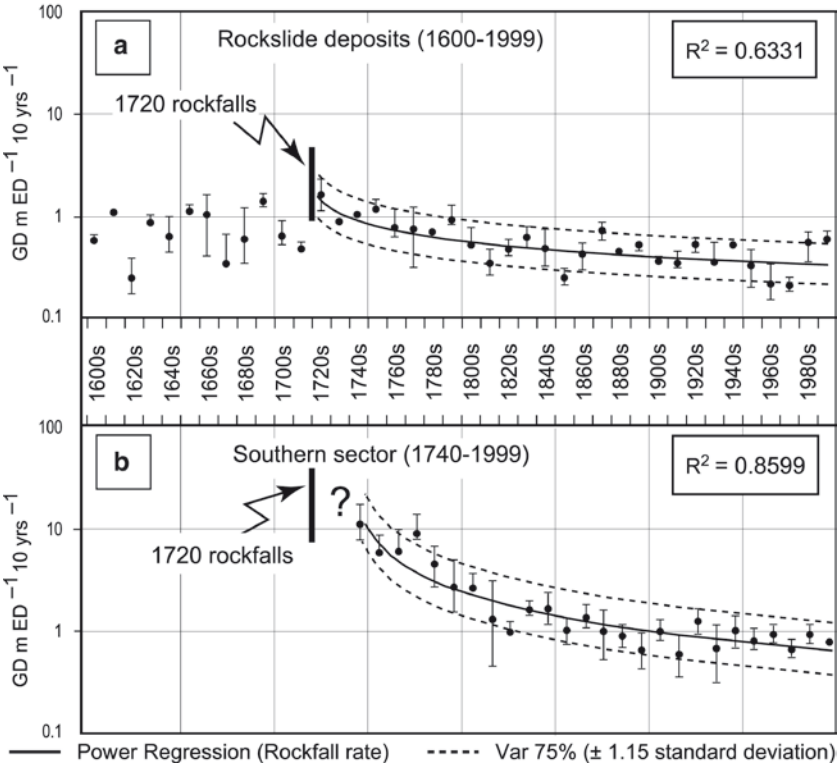

Fig. 9 Reconstructed rockfall activity measured by the rockfall rate (for explanation see text). (**a**) On the rockslide deposits, analyses cover the last four centuries (1600–1999), indicating that the large 1720 rockfalls temporarily reduced the protection afforded by the forest. (**b**) After the elimination of the forest in the southern sector by the 1720 event, the recolonizing trees permanently improved their protective function, reducing the number of rockfall impacts on the trees sampled by almost 13 times since the 1740s

Table 3 Size statistics of the trees sampled on the rockslide deposits; DBH: diameter at breast height as measured in 2002 (in cm), 10-year DBH: 10-year increment of the DBH (in cm), and rockfall "rates" (GD 1 m ED^{-1} $(10\ years)^{-1}$)

Rockslide deposits	DBH	10-year DBH	Rockfall "rates"
Mean	47.97	1.56	0.65
Standard deviation	12.62	0.97	0.34
Maximum	76.40	6.29	1.53
Minimum	17.51	0.61	0.20

1720s, causing 1.53 GD m ED^{-1} 10 $years^{-1}$. Rockfall activity continually decreased after the 1720 event, interrupted by decades with significantly low (1850s, 1960s, 1970s) and significantly high (1870s, 1990s) activity.

Table 4 Size statistics of the trees sampled in the southern sector; DBH: diameter at breast height as measured in 2002 (in cm), 10-year DBH: 10-year increment of the DBH (in cm), and rockfall "rates" (GD 1 m ED^{-1} (10 years)$^{-1}$)

Southern sector	DBH	10-year DBH	Rockfall "rates"
Mean	48.39	2.70	2.36
Standard deviation	13.89	1.58	2.70
Maximum	79.58	8.59	10.99
Minimum	25.47	0.78	0.63

Due to the generally younger age and the large amount of trees that had grown after the high-magnitude rockfall in 1720, the assessment of rockfall rates only starts in the 1740s in the southern sector. Results on decadal rockfall rates in the southern sector averaged 2.36 GD m ED^{-1} 10 years^{-1} (Table 4). Figure 9b illustrates that during the early decades following the high-magnitude rockfall of 1720, successor trees sampled for analysis were repeatedly subjected to rockfall activity. As a consequence, the most important rockfall rate was reconstructed for the 1740s with almost 11 GD identified for each meter of exposed tree surface (i.e. 10.99 GD m ED^{-1} 10 years^{-1}). Similarly to the rockslide deposits, reconstructed rates continually decreased in the southern sector after the high-magnitude event of 1720.

We also note that – after a slight decrease in rockfall activity in the 1750s and 1760s – activity considerably increased in the 1770s. For this period, the rockfall rate provides a value of 8.86 GD m ED^{-1} 10 years^{-1}, approaching that for the 1740s. This period of increased rockfall activity lasted until the 1780s or even 1790s. But in contrast to the high-magnitude rockfall of 1720s, data indicate that the considerable number of GD identified for the last 3 decades of the eighteenth century were not caused by one high-magnitude event, but rather by a series of years with increased rockfall activity (i.e. 1772, 1774, 1779, 1783, 1792). Between the 1870s and the 1940s, comparably low numbers of GD were found in the trees sampled, resulting in a considerable decrease in rockfall rates. During this period, the lowest rockfall rate of the last 260 years was reconstructed, totaling 0.63 GD m ED^{-1} 10 years^{-1} during the 1910s. In contrast to the northern sector, the rockfall rate started to increase again in the 1940s, oscillating around the calculated power regression trend line ever since.

4.6 Seasonality of Rockfall

The assessment of the intra-seasonal rockfall activity was based on 115 scars found in 18 trees. Analysis was performed on 270 cross-sections and the reconstruction covers 25 years. Data indicates years with low (1978, 1979, 1981 and 1988) and years with important rockfall activity (1985, 1994, 1995, 1999 and 2001). Even though the number of trees is too small for further interpretation, it is interesting to

note that the peaks in activity apparently coincide with observations of increased rockfall activity in 1985 and after 1993.

The intra-annual distribution of scars shows a clear predominance of rockfall activity during the dormant season of trees (D = 88%). Rocks and boulders did, in contrast, only rarely cause damage to the selected trees during the earlywood (end of May through mid-July) and latewood growth (mid-July through early October), with 5% and 7% respectively.

5 Discussion and Conclusions

In the study we report here, cores extracted from 135 living *L. decidua* trees allowed reconstruction of yearly and decadal rockfall activities on the Täschgufer slope. In addition, 270 cross-sections were prepared from 18 juvenile *L. decidua* trees so as to determine the seasonality of rockfall on the slope. In the trees sampled, tangential rows of traumatic resin ducts proved to be by far the most common reaction to rockfall impacts. Reaction wood, growth suppression or release could be identified less frequently.

On the increment cores, we identified 741 GD since AD 1600. Impacts could be found more commonly in trees located in the southern sector of the slope, where GD rockfall recurred locally more than once per decade. According to the results, we believe that rockfall activity at Täschgufer mainly consisted of low magnitude-high frequency events, considered to be typical for rockfall in alpine areas (Matsuoka and Sakai 1999). The only high magnitude-low frequency event occurred in 1720, causing considerable damage to the forest growing on the rockslide deposits. Data also suggests that the high rockfall frequency both inhibited recolonization and caused considerable damage in the juvenile trees of the southern sector thereafter.

In contrast to the analysis of geomorphic processes involving larger volumes (e.g., debris flows, avalanches or flooding), results from dendrogeomorphic investigations cannot be used immediately to illustrate yearly or decadal variations in rockfall activity. As rockfall consists of single falling, bouncing or rolling rocks and boulders, a single event may only disturb trees along its trajectory. In addition, trees were of uneven age at the study site and displayed abundant differences in their DBH as well as in decadal DBH increment. As a consequence, the number of reconstructed GD steadily increased with time, reaching maximum values for the recent past. A ratio dividing the decadal number of GD by the number of sampled trees existing at the beginning of a particular decade cannot concisely represent the importance of decadal rockfall activity, as such a ratio (i) leads to a general overestimation of past rockfall activity and as it (ii) may not represent the rockfall activity in periods without tree succession and constant sample size.

The rockfall rate presented in this paper considers the exposed diameter (ED), and proves to be a reliable indicator of past rockfall activity, as it takes account of the diameter exposed to rockfall fragments as well as the gradual change of ED with time. In addition, the rockfall rate nicely illustrates the protective function in

the two sectors: After the devastating rockfalls of 1720, the recolonizing trees could not efficiently stop rockfall fragments in the southern sector, resulting in extremely high rockfall activity during the early decades of the reconstruction (e.g., 10.99 GD m ED^{-1} 10 $years^{-1}$ in the 1740s). Compared to the 1740s, almost 13 times fewer GD are dated per 1 m ED today. On the rockslide deposits, rockfall rates persisted at a relatively low level throughout the last four centuries. Nonetheless, the high magnitude event of 1720 also left its signs in the northern sector with the highest decadal rockfall rate (1.53 GD m ED^{-1} 10 $years^{-1}$) recorded since AD 1600. The efficacy of the protective forest was temporarily reduced, resulting in higher rates until the late eighteenth century.

The assessment of intra-annual differences in rockfall activity at Täschgufer showed that a large majority (88%) of the scars was induced outside the growing period (i.e. between October and late May). Direct observations on the rockfall slope confirm these findings, indicating that rockfall is most abundant in April and May, when the active layer of locally existing permafrost starts to thaw along with the seasonal ice formed in bedrock joints (Matsuoka and Sakai 1999). In contrast, injuries occurring during the growing period are scarce and less frequent during the period of earlywood (5%) than latewood formation (7%). The release of rocks and boulders depends on many factors (Wieczorek and Jäger 1996), but it appears that (local) earthquakes and heavy precipitation would be among the predominant triggers (Schneuwly and Stoffel 2008a, b)

The two approaches outlined in this contribution clearly show that tree-ring analyses have a great potential for the study of intra- and inter-annual as well as long-term variations of rockfall activity on forested slopes. In addition, dendrogeomorphology may supply essential data on process activity and dynamics for forested areas where historical records are incomplete or completely lacking. In such situations, tree-ring records may provide researchers and administration with valuable data for the assessment of hazard and risks. In the present case, the use of dendrogeomorphology produced invaluable data on the frequency (*how often?*), volumes (*how much*?), the spatial distribution (*where*?) and reach (*how far*?) or the seasonality (*when?*) of rockfall. In addition, the protective effect of the forest stand could be quantified (*how efficient?*).

Data from dendrogeomorphic studies can thus be used for the assessment of hazards and risks in a number of ways: (i) A detailed understanding of event frequencies, magnitudes or the spatial distribution of rockfall activity considerably help a realistic realization of hazard and risk maps. (ii) In combination with data on trajectory frequencies and bounce heights, results can be used in the planning of countermeasures such as dams, barriers or restraining nets. (iii) Information on the seasonality of rockfall activity can help in a better management of risks along transportation corridors or hiking trails, allowing them to be closed during periods of enhanced activity. (iv) Tree-ring data can be used for the calibration or accuracy assessment of process-based simulation models (Stoffel et al. 2006) as well, thus contributing to the improvement of the models. (v) As an appropriate forest management and an accurate evaluation of ecosystem integrity of protection forests not only rely on data about past silvicultural treatments, but also on evidence of past

disturbances (Motta and Haudemand 2000, Berger and Rey 2004), rockfall records may largely contribute to a better understanding of the forest as a whole.

Acknowledgments The authors gratefully acknowledge Reynald Delaloye, Gion-Reto Hassler, Igor Lièvre, Maung Moe Myint, Sascha Negro, Werner Schoch and Sabine Stoffel for assistance in the field and in the lab. We also give thanks to Kilian Imboden and Leo Jörger for coring and felling permission.

References

André MF (1997) Holocene rockwall retreat in Svalbard: a triple-rate evolution. Earth Surf Process Land 22:423–440

Bebi P, Kienast F, Schönenberger W (2001) Assessing structures in mountain forests as a basis for investigating the forests' dynamics and protective function. Forest Ecol Manage 145:3–14

Berger F, Rey F (2004) Mountain protection forests against natural hazards and risks: New French developments by integrating forests in risk zoning. Nat Haz 33:395–404

Braam RR, Weiss EEJ, Burrough PA (1987) Spatial and temporal analysis of mass movement using dendrochronology. Catena 14:573–584

Douglas GR (1980) Magnitude frequency study of rockfall in Co. Antrim, Northern Ireland. Earth Surf Process Land 5:123–129

Fantucci R, Sorriso-Valvo M (1999) Dendrogeomorphological analysis of a slope near Lago, Calabria (Italy). Geomorphology 30:165–174

Gruber S, Hoelzle M (2001) Statistical modelling of mountain permafrost distribution: local calibration and incorporation of remotely sensed data. Permafr Periglac Process 12:69–77

Haeberli W (1992) Construction, environmental problems and natural hazards in periglacial mountain belts. Permafr Periglac Process 3:111–124

Hétu B, Gray JT (2000) Effects of environmental change on scree slope development throughout the postglacial period in the Chic-Choc Mountains in the northern Gaspé Peninsula, Québec. Geomorphology 32:335–355

Joris CL (1995) Der Bergsturz, ein Zufallsereignis unter vielen. In: Naturforschende Gesellschaft Oberwallis (ed) Der Bergsturz von Randa 1991, pp 43–49. Neue Buchdruckerei Visp, Visp

Luckman BH (1976) Rockfalls and rockfall inventory data: some observations from Surprise Valley, Jasper National Park. Earth Surf Process Land 1:287–298

Luckman BH, Fiske CJ (1995) Estimating long-term rockfall accretion rates by lichenometry. In: Slaymaker O (ed) Steepland geomorphology. Wiley, Chichester, pp 233–255

Matsuoka N, Sakai H (1999) Rockfall activity from an alpine cliff during thawing periods. Geomorphology 28:309–328

Motta R, Haudemand JC (2000) Protective forests and silvicultural stability – an example of planning in the Aosta Valley. Mt Res Dev 20:180–187

Müller HN (1980) Jahrringwachstum und Klimafaktoren: Beziehungen zwischen Jahrringwachstum von Nadelbaumarten und Klimafaktoren an verschiedenen Standorten im Gebiet des Simplonpasses (Wallis, Schweiz). Veröffentlichungen der Forstlichen Bundesversuchsanstalt Wien 25, Agrarverlag, Wien

Perret S, Stoffel M, Kienholz H (2006) Spatial and temporal rockfall activity in a forest stand in the Swiss Prealps – a dendrogeomorphological case study. Geomorphology 74:219–231

Rapp A (1960) Recent development of mountain slopes in Kärkevagge and surroundings, Northern Scandinavia. Geogr Ann 42:65–200

Rinntech (2008) LINTAB. http://www.rinntech.com/Products/Lintab.htm

Schneuwly DM, Stoffel M (2008a) Tree-ring based reconstruction of the seasonal timing, major events and origin of rockfall on a case-study slope in the Swiss Alps. Nat Haz Earth Syst Sci 8:203–211

Schneuwly DM, Stoffel M (2008b) Changes in spatio-temporal patterns of rockfall activity on a forested slope – a case study using dendrogeomorphology. Geomorphology 102:522–531

Schneuwly DM, Stoffel M, Bollschweiler M (2009) Formation and spread of callus tissue and tangential rows of resin ducts in *Larix decidua* and *Picea abies* following rockfall impacts. Tree Physiol 29:281–289

Schweingruber FH (1996) Tree rings and environment. Dendroecology. Paul Haupt, Bern, Stuttgart, Wien

Stoffel M (2008) Dating past geomorphic processes with tangential rows of traumatic resin ducts. Dendrochronologia 26:53–60

Stoffel M (2006) A review of studies dealing with tree rings and rockfall activity: The role of dendrogeomorphology in natural hazard research. Nat Haz 39:51–70

Stoffel M, Bollschweiler M (2009) What tree rings can tell about earth-surface processes. Teaching the principles of dendrogeomorphology. Geogr Compass 3:1013–1037

Stoffel M, Bollschweiler M (2008) Tree-ring analysis in natural hazards research – an overview. Nat Haz Earth Syst Sci 8:187–202

Stoffel M, Hitz OM (2008) Snow avalanche and rockfall impacts leave different anatomical signatures in tree rings of Larix decidua. Tree Physiol 28:1713–1720

Stoffel M, Wehrli A, Kühne R, Dorren LKA, Perret S, Kienholz H (2006) Quantifying the protective effect of mountain forests against rockfall using a 3D simulation model. Forest Ecol Manage 225:113–122

Stoffel M, Lièvre I, Monbaron M, Perret S (2005) Seasonal timing of rockfall activity on a forested slope at Täschgufer (Valais, Swiss Alps) – a dendrochronological approach. Z Geomorphol 49:89–106

Wieczorek GF, Jäger S (1996) Triggering mechanisms and depositional rates of in the Yosemite Valley, California. Geomorphology 5:17–31

Tree-Ring Based Rockfall Reconstruction and Accuracy Assessment of a 3D Rockfall Model

Simone Wehren-Perret and Markus Stoffel

Rockfall is a major threat to settlements and transportation routes in large parts of the Alps. While protective forest stands in many locations undoubtedly reduce rockfall risk, little is known about the frequency of rockfall activity in a given place. Therefore, the objective of the present study was to reconstruct rockfall events with dendrogeomorphic methods and to analyse the temporal rockfall activity in a subalpine forest stand. Analyses comprised the calculation of rockfall rates, trends in rockfall activity and the comparison of rockfall parameters with results from a three-dimensional, physically based rockfall model.

The study site is located in the runout zone of frequent, rather small rockfall events (mean rock diameter 10–20 cm) at the foot of a ca. 400-m high limestone cliff. In all, 33 stem discs from previously felled Norway spruce (*Picea abies*) trees were sampled from the Schwarzenberg forest stand located in Diemtigtal (Swiss Prealps), and a total of 301 rockfall events were identified on the basis of scars and tangential rows of traumatic resin ducts (TRD) between AD 1724 and 2002.

Figure 1 shows rockfall activity assessed through the calculation of annual *rockfall rate*s between AD 1881 and 2000. The *rockfall rate* is expressed as the number of rockfall injuries per meter of exposed tree diameter (DBH), taking into account the diameter increase of trees and the increased likelihood of a tree being hit (i.e. larger target; for details see Perret et al. 2006a and Stoffel et al. 2010, this volume).

S. Wehren-Perret
Department of Geography, University of Bern, CH-3012 Bern, Switzerland

M. Stoffel (✉)
Laboratory of Dendrogeomorphology, Institute of Geological Sciences, University of Bern, CH-3012 Bern, Switzerland
and
Chair for Climatic Change and Climate Impacts, Institute for Environmental Sciences, University of Geneva, CH-1227 Carouge-Geneva, Switzerland
e-mail: markus.stoffel@dendrolab.ch

M. Stoffel et al. (eds.), *Tree Rings and Natural Hazards: A State-of-the-Art*, Advances in Global Change Research 41, DOI 10.1007/978-90-481-8736-2_14,

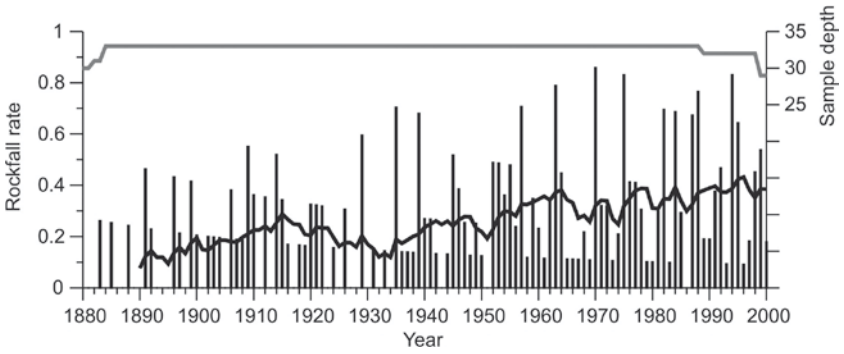

Fig. 1 Annual rockfall rate (number of injuries per 1 m exposed tree diameter) and its 10-year moving average, as well as the number of samples analysed (=sample depth)

This procedure allows for a correction of changes in the "DBH sum" over the years and the number of events recorded in each year was divided by the sum of all DBHs sampled in that year.

At Schwarzenberg, the *rockfall rate* increased over the twentieth century and the number of years without any rockfall event became less frequent. Apart from 1986, at least one rockfall event was registered in every year since 1952. The tree-ring reconstruction of rockfalls provides a good overview of activity on the slope, but it does, at the same time, not allow the distinction of single events with multiple rocks or multiple events at different times within 1 year.

In a subsequent step, we compared impact heights as well as the number of hits per tree produced by the three-dimensional process-based rockfall model *RockyFor* (Dorren et al. 2004; Stoffel et al. 2006) with field survey (i.e. impact heights from tree inventory data; Perret et al. 2006b) and dendrogeomorphic data (i.e. recurrence intervals) for 138 trees. Modeling was performed with 5,000 rocks with diameters ranging from 10–30 cm and the predicted number of tree hits corresponds well with empirical data with a root mean squared error (*RMSE*) of 0.9%. Figure 2 shows that differences in the predicted vs. observed number of impacts per tree predominantly occur in the uppermost part of the study site, where the model overestimates the number of hits in a few trees by 2.5–5%. In 93% of cases (128 trees), differences between the predicted and observed number of tree hits remain between ±2.5%. In contrast, differences can be seen with impact heights, where *RockyFor* underestimates the mean impact height by 0.46 m (*RMSE*). More details on the comparison of predicted with observed rockfall activity can be found in Stoffel et al. (2006).

Overall, this study provided an appropriate method for the initial assessment of temporal variations in rockfall activity at a given locality. The study also showed that dendrogeomorphic analyses clearly have the potential to produce detailed results for annual or decadal fluctuations of rockfall activity over a long time period and that they can help the calibration of rockfall models. However, more research is needed on the accuracy assessment of rockfall models in general and of the methods

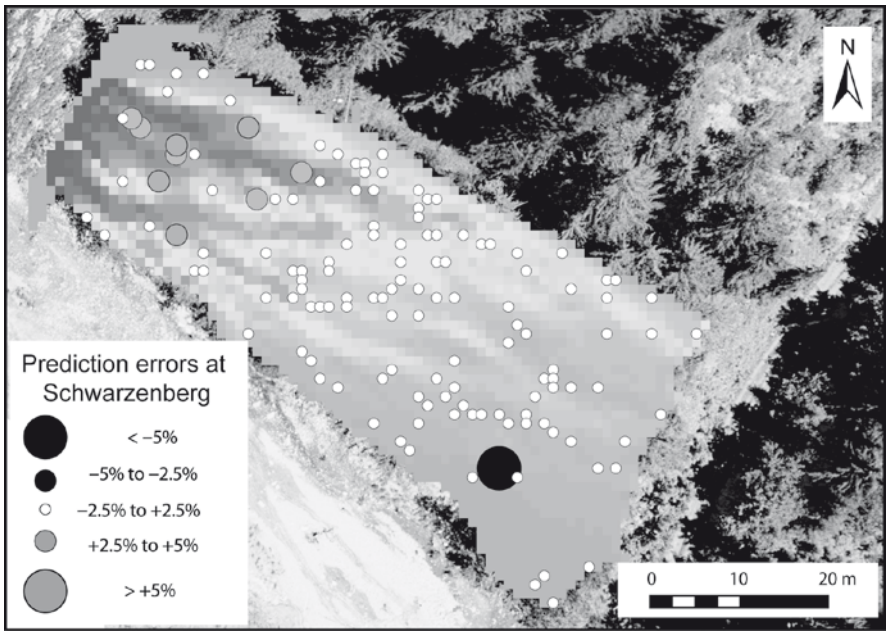

Fig. 2 Differences between simulated and observed numbers of rock impacts on trees at Schwarzenberg. The simulation was performed with 5,000 rocks with diameters ranging from 10–30 cm. *Gray circles* indicate an overestimation of tree hits by the model, *black circles* show an underestimation. The shading of the slope represents the modelled trajectory frequencies of rockfalls with darker surfaces designating areas with more rockfall activity

used to calculate rockfall rates in particular, e.g. is the probability of rockfalls hitting ten 10-cm DBH trees similar to that of rocks hitting one 1-m DBH tree as our measure assumes.

Acknowledgement Reprinted from Perret et al. 2006a and Stoffel et al. 2006 with permission from Elsevier.

References

Dorren LKA, Maier B, Putters US, Seijmonsbergen AC (2004) Combining field and modelling techniques to assess rockfall dynamics on a protection forest hillslope in the European Alps. Geomorphology 57:151–167

Perret S, Stoffel M, Kienholz H (2006a) Spatial and temporal rockfall activity in a forest stand in the Swiss Prealps – a dendrogeomorphological case study. Geomorphology 74:219–231

Perret S, Baumgartner M, Kienholz H (2006b) Inventory and analysis of tree injuries in a rockfall-damaged forest stand. Eur J Forest Res 125:101–110

Stoffel M, Schneuwly DM, Bollschweiler M (2010) Assessing rockfall activity in a mountain forest – implications for hazard assessment. In: Stoffel M, Bollschweiler M, Butler DR, Luckman BH (eds) Tree rings and natural hazards: A state-of-the-art. Springer, Berlin, Heidelberg, New York, this volume

Stoffel M, Wehrli A, Kühne R, Dorren LKA, Perret S, Kienholz H (2006) Quantifying the protective effect of mountain forests against rockfall using a 3D simulation model. Forest Ecol Manage 225:113–122

Assessment of the Rockfall Frequency for Hazard Analysis at Solà d'Andorra (Eastern Pyrenees)

José Moya, Jordi Corominas, and José Pérez Arcas

1 Introduction

Dendrochronology has been applied successfully for dating different types of slope movements, including rockfalls (Lang et al. 1999; Stoffel et al. 2005; Stoffel 2006; Perret et al. 2006). Rockfalls are downslope movements of rocks and boulders which move largely by bouncing. These characteristics cause rockfalls to leave only fragmentary and scattered evidence on the ground surface but also in trees. As a consequence, it is more difficult to obtain complete time series of events for rockfalls than for other types of slope movements.

On one hand, in areas where rockfalls are recurrent, it is hard to distinguish the area affected by a given rockfall event. Because of this, the number of rockfall events cannot be deduced from the analysis of the deposits observable on the slope surface. Moreover, a rockfall event formed by a few blocks may only impact a small number of trees. A random tree sampling probably would miss this kind of event.

On the other hand, evidence of old rockfalls visible on trees will blur with time. Wounding is the most common type of damage caused by falling rocks on trees. Older wounds remain present as internal scars, but they will not necessarily be visible on the tree surface. Depending on tree species and age, Stoffel and Perret (2006) state that between 16% and 90% of the wounds existing in a tree are masked with time and remain only as internal scars. This makes it difficult to obtain long time series of rockfalls by sampling visible injuries.

Completeness of the tree-ring record of rockfalls depends also on factors such as forest density and rockfall size. Rockfall events that did not impact trees cannot

J. Moya (✉) and J. Corominas
Department of Geotechnical Engineering and Geosciences, Technical University of Catalonia (UPC), 08034 Barcelona, Spain
e-mail: jose.moya@upc.edu

J.P. Arcas
Mekano4. 08190 Sant Cugat del Vallés, Spain

M. Stoffel et al. (eds.), *Tree Rings and Natural Hazards: A State-of-the-Art*, Advances in Global Change Research 41, DOI 10.1007/978-90-481-8736-2_15,

be dated with dendrochronology. To achieve an accurate value of the frequency of rockfalls, it is also necessary to assess the probability that falling blocks will impact trees.

This chapter presents several strategies of tree sampling in order to reconstruct complete chronologies of rockfalls from visible injuries in broadleaved trees. We show that the rockfall frequency cannot be assessed directly from a chronology of visible tree injuries, but it requires taking into account factors such as the resolution of the dating technique and the magnitude of the rockfall events in the site investigated. Finally, we present a method for the calculation of impact probability of rockfalls on trees. Strategies are illustrated through the study of rockfall frequency of a mountain area of high risk, the Solà d'Andorra (Eastern Pyrenees, Andorra Principality). The chapter summarizes the main results of an article by the authors on this topic (Moya et al. 2010).

2 The Study Site

2.1 Setting

The Solà d'Andorra is a rocky hillslope located on the northwestern slope of the Gran Valira valley (Andorra, Eastern Pyrenees; Fig. 1). The maximum altitude is reached at Carroi peak (2,332 m a.s.l.) and the valley floor is close to 980 m. The hillslope has a length of >1,000 m and is drained by steep gullies (couloirs). Bedrock is comprised of granodiorite, which shows three well developed sets of fractures. Long-term rockfall activity has produced a talus at the foot of the couloirs and of the rock walls.

The study presented here was carried out in two specific sectors of the Solà d'Andorra talus, namely the Alzina cone and the Basera Mateu talus slope (Fig. 1). The Alzina talus cone extends between 1,100 and 980 m a.s.l., and is 40–80 m wide. The cone is sustained by a steep couloir with a maximum elevation at 1,360 m a.s.l. The Basera Mateu is a rockwall, which has a face length of 420 m and a height of 380 m (Fig. 1).

2.2 Historical Record of Rockfalls

The town of Santa Coloma and part of Andorra la Vella, the capital of the country, are located in the valley floor, downslope of Solà d'Andorra. The existence of rockfall risks became obvious during the last decades, when settlement invaded the lower part of the talus. As a result, more than 30 rockfall events have been witnessed over the past 50 years. Most of the events reached the bottom of the slope and damaged

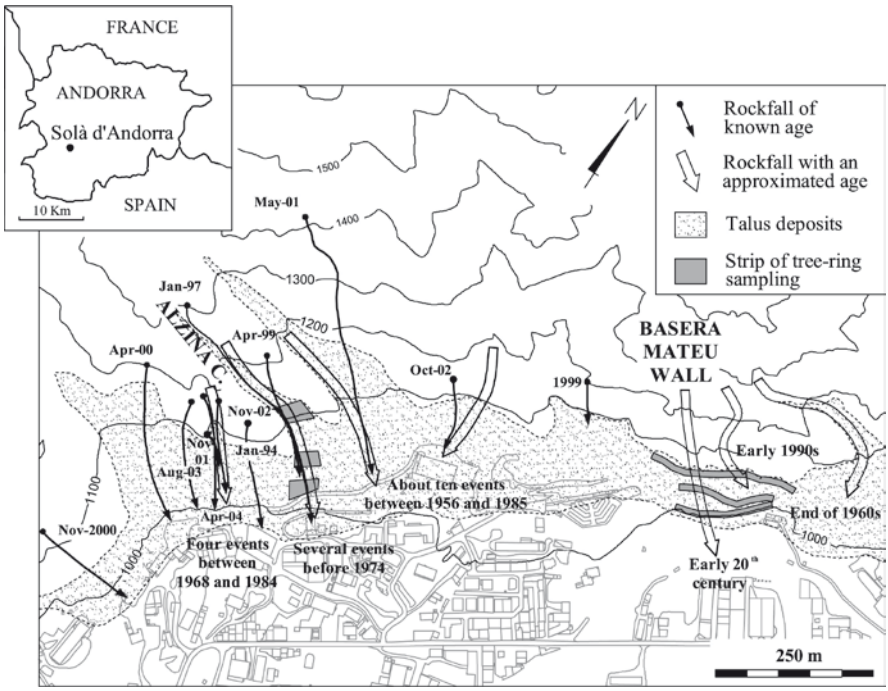

Fig. 1 Location of the Solà d'Andorra and of the historical rockfall events witnessed in the site. The transects sampled at Alzina and Basera Mateu talus for tree-ring analysis are also shown

buildings or were only stopped in their vicinity (Fig. 1). The recent rockfall events typically involved rock masses <25 m^3, and consisted of up to a few dozens of boulders. The volume of boulders ranged from 0.5–25 m^3 (Copons et al. 2005). The most dangerous rockfall occurred on January 21, 1997, when a boulder of 25 m^3 struck a building and seriously injured a person. Protective rockfall fences were installed on the lower part of the talus in 1999, and in 2002 at the outlet of the most dangerous couloirs (Copons et al. 2005; Copons and Vilaplana 2008). A quantitative assessment of the residual rockfall risk has been carried out after the construction of rockfall nets (Corominas et al. 2005).

In the Alzina talus, one of the sites investigated in this paper, two rockfall events have been witnessed in the last decades. The first event is the one of January 1997 mentioned above. A smaller event occurred in April 1999, which stopped in the lower part of the talus near the urban area; this event involved a rock mass of 5 m^3 and about 20 boulders. At Basera Mateu talus, the second site investigated, two rockfall events have been noted; the older one occurred at the beginnings of the twentieth century, and a more recent one at the beginning of the 1990s. No data on magnitude of these rockfall events is available for this talus.

2.3 Forest Characteristics

English oak (*Quercus robur*) and Holm oak (*Quercus ilex*) form 99% of the forest colonizing the talus slope of Solà d'Andorra. *Q. robur* is the dominant species usually representing >75% of the forest. The only conifer present in this environment is Scots pine (*Pinus sylvestris*) but it is only marginally present. Forest density, measured at six plots of 100–150 m^2 at the Alzina and Basera Mateu sites, ranges from 950 to 2,700 trees/ha. Diameter of trees is usually small and only averages 10 cm at breast height.

In the talus slope of the Solà d'Andorra, falling blocks injured trees in several ways, such as wounding, breakage of branches, decapitation, tree inclination and uprooting. Wounding is clearly the most dominant type of tree damage. The field investigation of the talus slope indicated that no other processes cause damage to the trees (e.g., snow avalanches, debris flows, browsing, or felling activities).

In several forest stands close to Solà d'Andorra where evidence of recent rockfalls was absent, a survey of visible growth disturbances in tree form revealed that young oaks usually have a sinuous stem with a mild to moderate leaning. This form of the stem could be related, among other causes, to phototropic processes or to a genetic malformation, although the ultimate cause remains unknown. Young oaks showing such stem shape were also present at Solà d'Andorra. Mature tilted trees were also found in the talus, but the origin of tilting is unclear. For this reason, the use of tilted trees was excluded as a criterion to date rockfalls at the site.

3 Tree Sampling Strategies

3.1 Defining a Basic Strategy for Effectively Developing a Complete Record

Obtaining a realistic value of the rockfall frequency is essential for a quantitative risk assessment. Therefore, and in order to avoid missing rockfall events, sampling should be exhaustive, especially as it is highly improbable to detect old wounds present within the stem as internal scars, in broadleaved trees. Stoffel et al. (2005) and Perret et al. (2006) used tangential rows of traumatic resin ducts to identify internal wounds. However, resin ducts are not formed in broad-leaved species and old wounds can only be found by taking multiple sets of cores at different heights in the stem or by felling the tree to obtain multiple cross-sections. The first method is very time consuming and the second one is not advisable.

The basis of the strategy applied at Solà d'Andorra consisted of a quasi exhaustive sampling of the visible tree injuries in broad strips of forest placed on the talus. The strips were arranged parallel to the contour lines, that is, perpendicular to the main direction of transport. For a given source zone, each strip was extended across the whole talus width (measured along the contour lines) in order to intercept all

possible rockfall trajectories. The width of strips (measured down the slope) ranged between 15 and 30 m.

Three sampling strategies have been applied in successively more detailed steps. The first strategy consisted of sampling damaged trees at the talus apex. This sampling was used to determine the maximum frequency of rockfalls at the base of the slope. At Alzina talus, the strip extended along the whole width of the talus apex (45 m). At Basera Mateu talus, the cross-slope strip has a length of 230 m in the central sector of the talus. Thirty-two trees were sampled at the Alzina talus and 112 trees at the Basera Mateu talus.

The second strategy of sampling was aimed at detecting changes in the frequency of rockfalls down the talus. In this case, the sampling was carried out by additional strips at increasing distances from the cliff face. Three strips, including that located at the talus apex, were sampled at both sites (Fig. 1). A total of 276 damaged trees were selected, and 294 samples were taken.

The trees sampled in this study showed visible injuries on the stem surface. Wound samples were obtained by cutting a wedge from one side of the scar. All visible wounds with a size >5 cm and located at a height <2 m above ground were sampled. Wounds located higher up in the stem were not sampled for obvious practical reason. Wounds <5 cm were considered to be the impact of very minor rock fragments (like pebbles); too small to be regarded in the frequency assessment. Decapitated trees were also occasionally sampled. Here, a cross-sectional disc was cut at the broken tip of the stem, if it was found at a height <2 m. In other cases, a diametric core was taken along the slope direction. Fieldwork included documenting the location of sampled trees on an orthophoto with the help of a compass and tape measurements, the description of the tree form, and the record of the location of the injury sampled on the tree surface. Another question to be addressed is whether the width of the strips we sampled is sufficient to obtain a complete record of the rockfalls impacting trees. The third sampling strategy was therefore addressed to clarify this question. The aim was to analyze changes in the frequency based on variations of the width of the strip sampled. To perform this analysis, all the trees showing injuries have been sampled at Alzina talus, i.e. the sampling was made of the complete talus including the areas between the strips sampled in the previous step. A total of 265 trees were sampled for this approach.

4 Frequency Assessment: Interpretation of the Chronology of Tree Damage

4.1 Determining the Number of Rockfall Events

Figure 2 shows the chronology of tree injuries observed at the apex of the Alzina talus. The time scale is expressed as seasons of dendrological years. A dendrological year includes one dormant season and the following growing season

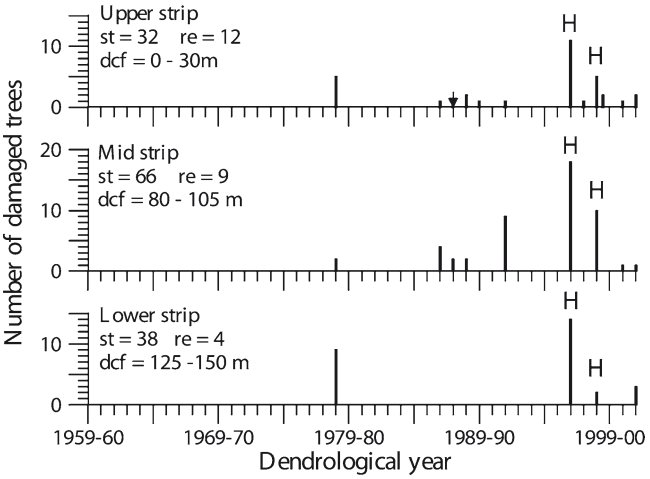

Fig. 2 Chronology of the tree injuries of transects of the Alzina talus cone. Small arrows in the chronology of a transect indicate rockfalls that have not been detected in the transect but in another one located downslope (H: historical case (witnessed), st: number of trees sampled, re: number of rockfalls, dcf: distance to the cliff foot)

(Moya and Corominas 1996). Therefore, a wound inflicted, e.g., in December 1982 can be dated to the dormant period of the dendrological year of 1982–1983.

Although the forest at Alzina consists of two species, *Q. robur* and *Q. ilex*, we found the latter not useful for dating. *Q. ilex* is a broad-leaved but evergreen species and tree rings can be easily seen in trees of this species. However, it is very difficult to precisely distinguish annual rings.

The frequency of rockfalls cannot be directly derived from a chronology of tree injuries, such as the one shown in Fig. 2. First, the relationship between the number of tree injuries that occurred in a given season and the corresponding number of rockfall events must be known. Figure 2 shows that it is usual to find several injuries in the same season, but it is not possible to distinguish if they were caused by one rockfall event or by several that occurred within the same season. A falling block may injure several trees on a strip; a greater number of injured trees can be expected in the case of rockfall events formed by several blocks.

The number of rockfall events that occurred in a given season must be interpreted from the injuries that are registered during one season. The interpretation should be based on some knowledge of the activity of rockfalls at the site. At Solà d'Andorra, most of the events witnessed and all events identified by the surveillance plan consisted of multiple blocks, ranging from a few to several dozen blocks (Copons et al. 2005; Copons and Vilaplana 2008). Moreover, the preliminary dendrogeomorphic analysis evidenced some linear tracks defined by trees injured in a same season. These tracks can hardly be formed by different rockfall events, as it is highly improbable that two events from the same source zone and in the same season will follow a similar path. Accordingly, we assume that all the injuries

caused by blocks falling from the same source zone (e.g. a couloir) and having the same age, correspond to one rockfall event. This assumption may, in some cases, entail missing some rockfall events.

In large source areas, such as the Basera Mateu rockwall, there often are two or more rockfall events during the same season, but in different parts of the area. In such cases, analyzing the tree injuries found at the talus as a whole may lead to a large underestimation of activity if only one event is considered per season. In the Basera Mateu talus a 230 m long strip was sampled (Fig. 1). To minimize underestimation, the analysis of tree injuries was carried out dividing the talus in eight sectors, each one fed by a small segment of the rock wall. Subsequently, the number of rockfall events was assessed for each sector. The result for the whole Basera Mateu is shown in Fig. 3.

A last step was used to improve the record of rockfall events. Some rockfall events may be identified in a given strip but are missed in another strip located upslope. For example, at the Alzina talus, a tree of the central strip was injured in the dormant season of 1987–1988, but no trees injured this year were found in the upper strip (Fig. 2). Considering that the talus is fed only by one couloir, and that these strips extend across the whole talus, a rockfall reaching a given strip must have travelled through any transect located upslope. Consequently, we consider that the rockfall event that occurred in the Alzina talus in 1987–1988 reached the central strip without hitting trees of the upper strip. The same has occurred in the Basera Mateu talus in other years. The events that are missed in a strip but detected in another one are indicated by small arrows in Figs. 2 and 3, and have been accounted for in the assessment of the rockfall frequency for that strip.

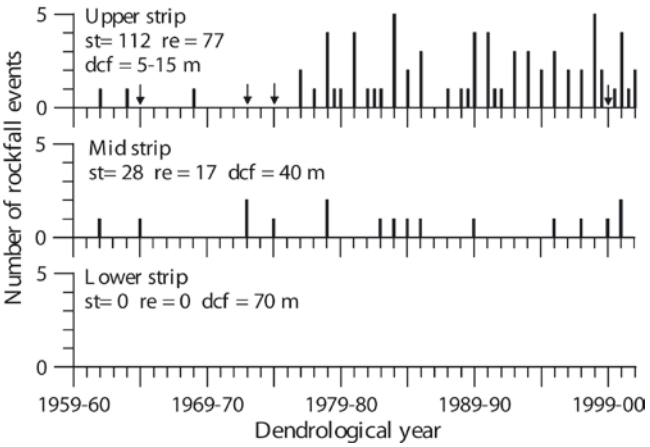

Fig. 3 Chronology of rockfall events recorded at the Basera Mateu talus slope. Small arrows in the chronology of a transect indicate rockfalls that have not been detected in the transect but in another one located downslope (st: number of trees sampled, re: number of rockfalls, dcf: distance to the cliff foot, H: historic rockfall of imprecise age)

4.2 Determining the Time Interval

The last step in the assessment of the rockfall frequency was to define the period of time to be taken into account. The oldest visible wound that we have sampled at Solà d'Andorra is 40 years old (Fig. 3). This age gives the maximum period of the dendrochronological record that is covered by visible wounds at the study site. From the analysis of Figs. 2 and 3, it is apparent that the recurrence of rockfall events recorded by visible wounds is higher since the late 1970s. At Basera Mateu, only nine of the 77 events recorded at the apex are older than 1978–1979 (Fig. 3a). In the Alzina talus no rockfall was identified before that year (Fig. 2a). This change might be due to an actual increase in the frequency of rockfalls, though it could also reflect the closure and masking of wounds with time. Actually, the masking of wounds affects the record obtained, mainly in the older part, because most of the samples correspond to visible wounds. In any case, the average number of rockfalls per year is almost constant after 1978–1979, suggesting that the record of rockfall events is less affected by the masking of wounds and that it is reasonably complete the last 24 years before sampling. Thus, the frequencies displayed in Table 1 have been calculated for this period.

5 Rockfall Frequency Down the Talus

At the two talus zones investigated, we found that the frequency of rockfalls is greater at the talus apex, as would be expected. At the Alzina talus, the two events noticed by the inhabitants in 1997 and 1999 (marked by "H" in Fig. 2) have been detected by tree-ring analysis. Rockfalls reach the apex of the Alzina talus, once every 2 years on average (Table 1). Only four of the 12 rockfall events recorded at the apex reached the lower strip; and two of them injured a significant number of trees (Fig. 2). One of these two events occurred in January 1997, which hit a building and injured one person. The other event occurred in the dormant season of the

Table 1 Frequency of rockfalls at the two talus investigated

Talus	Transect	Transect area (m^2)	Number of trees sampled	Number of events[a]	Return period (years)	Frequency (events/year)
Alzina	Upper	1,310	32	11	2.1	0.48
	Mid	980	66	8	2.9	0.35
	Lower	1,070	38	3	7.7	0.13
BaseraMateu	Upper	3,570	112	62	0.4	2.70
	Middle	2,360	28	10	2.3	0.42
	Lower	2,310	0	0	> 23[b]	<0.04

[a] Occurred after the year 1978–1979 till the year 2001–2002. The rockfall events occurred at year 1978–1979 mark the start of the period for which the frequency is assessed; these events have not been counted in the frequency assessment.

[b] When no events are recorded, the return period obtained is only a minimum one.

year 1978–1979. A large number of trees were injured by this event, but no one witnessed it, likely because the urban area was much smaller than in 1997. This fact suggests that the 1978–1979 event would have travelled farther than the lower strip, reaching the zone that now is occupied by buildings. Hence, the return period of high risk rockfall events is between 18 and 24 years.

At the talus of Basera Mateu, the frequency of rockfalls decreases downslope in a much more pronounced way than at Alzina talus. At the apex of Basera Mateu talus, 77 rockfalls have been recorded during the past 40 years, but only 17 reached the central strip, and none reached the lower one (Fig. 3). The historical record for this talus is consistent with this finding because there is only a single reference to a rockfall event during the last decades.

6 Are the Sampled Strips Wide Enough?

To address this question all the trees showing injuries in the Alzina talus have been sampled (265 trees; see Section 3). We have analyzed how the rockfall frequency increases with strip width. Three strips were defined on the talus, and the rockfall frequency was assessed with increasing width of each strip, starting from a width of 2.5 m, and making successive increments of 2.5 m up to reach 40 m. The density of the forest was also determined in a plot for each strip.

The result is similar for the three cases; the frequency increases initially with strip width until a constant value is reached, this occurs at a width of 15 m in the lower strip sampled at Alzina talus (Fig. 4). The value at which the frequency stabilizes indicates the minimum width for a strip for which no information is lost, i.e. a lower rockfall frequency will be obtained if the width of the sampled strip is smaller than this value. On the other hand, no additional rockfall events will be detected if the strip becomes wider than this value. Obviously, the minimum strip width to be sampled is case specific, because it depends on parameters

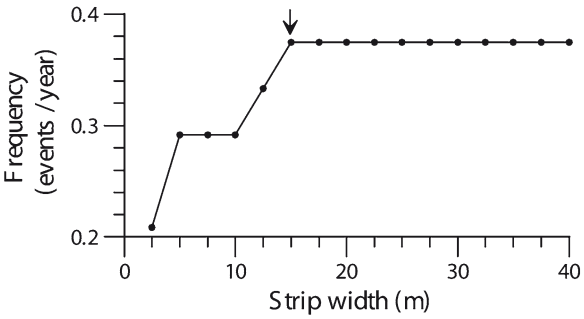

Fig. 4 Frequency of rockfalls obtained for different widths of the transect sampled. The arrow points to the transect width after which no increase of frequency is observed. Data correspond to the apex of the Alzina talus

Table 2 Minimum width of transects required to avoid miss of rockfall events. The main characteristics of the forest at each transect were measured in three plots in the Alzina talus and are also shown in the table. Forest density is shown separately for *Quercus robur*, the tree species used for dating

Plot	Tree number		Mean tree diameter (cm)	Plot area (m^2)	Forest density (trees/ha)		Minimum transect width (m)
	All species	*Quercus robur*			All species	*Quercus robur*	
Upper	12	10	9.7	124	970	800	20
Middle	33	22	10.0	152	2,100	1,450	17.5
Lower	39	22	9.0	145	2,690	1,500	15

such as the forest density, tree diameter and size of rockfalls. Table 2 shows the minimum width of strips for different densities of forest that has been determined at Alzina talus. For a forest with an average tree diameter (DBH) of about 10 cm, as was the case at this study site, the width of a strip should not be less than 15 m if the forest density is of 1,500 trees/ha, or less than 20 m if the density is lower than 800 trees/ha. The strips sampled in the first stages at Basera Mateu and Alzina talus range in width from 15 to 30 m; thus, the former results suggest that these strips are wide enough.

7 Probability of Falling Rocks Impacting Trees

7.1 Approach to the Impact Probability

Sampling in wide strips allows the development of a more complete tree-ring record of rockfalls. A chance nevertheless exists that some rockfall events may be missed merely because they have not hit trees. The impact probability has been calculated as the probability of blocks of a rockfall event hitting at least one tree of a given strip of the talus slope. This probability has been considered as conditioned by the occurrence of rockfalls reaching the strip. The conditional impact probability (CIP) depends both on the characteristics of the forest (tree location and diameter of the trunks) and on the characteristics of the rockfall event (number and size of falling blocks).

The assessment of the CIP within a sampling strip is a three-dimensional problem. However, the problem can be solved in the horizontal plane and reduced to one dimension making some simplifying assumptions:

1. We assumed that changes in the direction of falling blocks due to impact with the talus surface have a minor influence on the CIP and have considered that falling blocks move through the strip in a downslope direction, when they do not impact

with trees. Thus, in a map view, the path of a block within the strip can be represented just as a straight line down the talus. Changes in fall direction due to impact with trees do not influence the CIP because this is the measure of the probability of impacting on at least one tree. Once a block impacts a tree, the value of CIP does not change if the block subsequently impacts another tree after changing its trajectory.

2. The dendrochronological record of rockfall used to calculate the frequency only is based on impacts on the tree trunk, but not on its branches. Thus, trees can be represented only by the stem. Wounds located in branches are normally at high positions in the tree (>2 m) at the study sites and have not been sampled for practical reasons. Using the wounds located on the trunk may cause underestimation of the rockfall frequency, but this is implicitly taken into account by the CIP assessment.
3. Trees in the strip have a straight and vertical trunk; this is why the stem can be represented by a circle in the horizontal plane.
4. Any change of the trunk diameter with height and age is small enough – for the period for which rockfall frequency is calculated – to be insignificant for the CIP estimation.
5. During the period taken into account, rockfall events have not caused significant changes in the density or in the spatial structure of the forest of the strip. Thus we assumed that the forest variables have been stationary over the last 25 years.
6. We considered the forest characteristics to be homogeneous at the strip. To assess the CIP in the strip, it is necessary to measure the forest density, the tree diameter and the spatial distribution of trees within the strip. To determine this latter distribution, the location of trees must be measured, and, whether the strip is relatively large and the forest is dense (as it occurs in the sites investigated in this study) this is very time consuming. We have approached the forest characteristics of the whole strip by measuring them in a plot placed inside (the details are indicated in the following section) which has been considered as representative of the whole strip. We have also assumed that the trajectories of rockfalls distribute homogeneously in the strip.

Using the three-dimensional assumptions, the CIP can be expressed as a fraction of the length of the strip, measured along the contour lines. This can be shown regarding the trajectory of a falling block in a horizontal plan view. A falling block will hit the stem of a tree if its trajectory is closer to the trunk than half the diameter of the block (Fig. 5a). Then, given the diameter ϕ of a falling block, each tree has a circular envelope of a width of $\phi/2$, which defines a circular area of impact around the tree, that we call the *circle of impact* (Fig. 5b). A block will hit at least one tree of the strip if its path intersects a circle of impact. The path of a falling block hitting trees of a strip can be identified easily, for a given block size, using the projections of the circles of impact of the trees on the downslope boundary of the strip (Fig. 5b). For a given diameter of block, and given the location and the diameter of the trees of the strip, the CIP can be expressed as the fraction of the strip length, measured

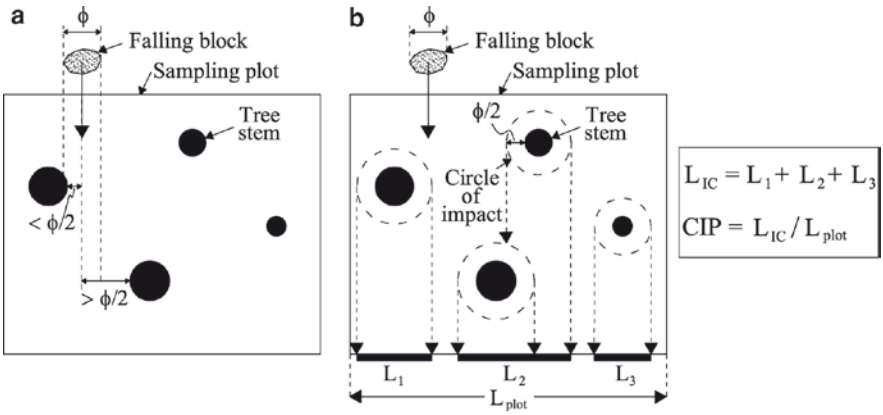

Fig. 5 Geometrical conditions used for the assessment of the conditional impact probability (CIP)

in the downslope side of the strip, which is occupied by the circles of impact (Eq. (1) and Fig. 1):

$$CIP = L_{IC} / L_{plot} \tag{1}$$

where L_{IC} is the cumulative length of the projections of the circles of impact on the downslope side of the strip, and L_{plot} is the length of the downslope side of the strip, which is arranged along the contour lines.

7.2 Calculation of CIP of the Alzina Talus

The assessment of the CIP has been carried out in the three forest strips located at Alzina talus. For each strip the forest characteristics (tree location and diameter at breast height) were measured in a plot considered representative of the whole strip (Table 3). The plots are approximately square and have an area of 125–150 m^2 (Table 3). The trees of each plot were located on an orthophoto by tape and compass measurements. Obviously, all trees placed in the plots have been measured and not only the injured ones. However, only *Q. robur* trees were taken into account for the assessment of the CIP. This species forms between 23% and 50% of the forest at Alzina talus.

The size of the rockfall events is also required for the assessment of CIP. We have used the median of block diameters identified on the talus slope to approach the average CIP. The size of blocks was measured in two plots located in the middle and lower parts of the talus, each of 50 m^2. All blocks having a length greater than 25 cm were included in the sample. A total of 176 blocks were measured. For each block, diameter was measured along three perpendicular axis, and the average used for the analysis of size distribution. We did not identify any statistically significant difference between block sizes of the two plots and no apparent sorting of the block size was observed down the talus. The median of the diameter of the blocks is 31.5 cm.

Table 3 Conditional impact probability of falling blocks on trees and corrected values of the frequency and of the return period of rockfalls at the Alzina talus. The characteristics of the forest plots used for the CIP assessment are also indicated. Forest density corresponds only to *Quercus robur* trees. The median of the block sizes measured in the talus (31.5 cm) has been the rockfall size used in the calculation

Transect	Transect width (m) (measured downslope)	Transect area (m^2)	Forest density (trees/ha)	CIP	Rockfall frequency (events/year)		Return period (years)
					Raw	Corrected by CIP	
Upper	30	1,313	800	0.68	0.48	0.70	1.4
Middle	25	982	1,450	0.87	0.35	0.40	2.5
Lower	25	1,068	1,500	0.86	0.13	0.15	6.6

The number of blocks which formed the recent rockfall events is also needed for an assessment of the CIP; but it is much more difficult to determine. The historical records indicate that the number of blocks have ranged from one to several dozens per event. But this information is not precise enough for the CIP assessment. We have followed the more conservative option and have used the CIP value corresponding to rockfall events formed by a single block, which is expressed by Eq. (1). This likely underestimates the actual CIP and it leads to a higher corrected value of the frequency of rockfalls; but it is on the safe side. The CIP values obtained for the strips of the Alzina talus are shown in Table 3. The rockfall frequency calculated previously by tree-ring analysis has been corrected by dividing it by the corresponding CIP.

Taking into account the CIP, the rockfall frequency estimated at Alzina talus experiences several changes. The most significant difference is identified at the talus apex. Here, the forest density is relatively low (800 trees/ha) which leads to a low value of the CIP (0.68% or 68%; see Table 3). This means that only two thirds of the falling blocks impact trees and are recorded in tree rings. At this part of the talus, the correction due to the CIP has raised the estimation of the rockfall frequency from 0.48 events per year (that is a recurrence of 2 years) to 0.71 events per year (a return period of 1.4 years). At the lower parts of the talus, the density of the forest is much higher (about 1,500 trees/ha) and the CIP value increases accordingly (from 0.68 to 0.87). Therefore, the value estimated of the rockfall frequency also increases here but much more moderately (Table 3). Before the CIP correction, the conclusion was that most of the rockfall events reaching Alzina talus travel to the middle-lower part of the talus; after the correction, a much more pronounced decrease of the frequency of rockfalls down the talus becomes clear.

8 Conclusions

On forested slopes, the frequency of recent rockfalls can be determined through the analysis of wounds of impacts that are visible on the tree surface. Wounding is the most common type of disturbance that is available for dating rockfalls in Solà

d'Andorra. In areas where forest consists of broad-leaved species, other types of tree responses useful for dating, such as compression wood formation or traumatic resin ducts, are not present.

The particular mode of displacement of rockfalls entails special difficulties for dating this type of slope movement by means of dendrochronology. The main sampling strategy we used in Solà d'Andorra was to sample, in an almost exhaustive way, visible tree injuries within strips located on the talus for separate source areas. The strips were arranged across the slope direction. This strategy allows a more comprehensive estimate of the occurrence of rockfalls.

Sampling of damaged trees in the talus apex provides a rockfall frequency close to that of the source area. This latter frequency can be used along with models simulating the runout distance to assess the risk of rockfall.

Sampling of multiple strips arranged down the talus has a twofold advantage. It allows identification of eventual rockfall events that are missed in strips located upslope. For example at the talus apex, where the forest may be less dense, using multiple strips allows the reconstruction of a more complete record of rockfalls. This kind of sampling also provides information about the run out of the rockfall events.

The frequency of rockfalls cannot be derived directly from the chronology of tree injuries visible on the tree surface. The two parameters required for the assessment of frequency (i.e. the number of rockfall events and the length of the time interval) can only be deduced *after interpreting* the time series of tree injuries.

In comparison to dating with internal tree scars, dating wounds visible on the tree surface makes the sampling work easier; but it also shortens the time period for which rockfalls can be dated. At Solà d'Andorra, the maximum persistence of wounds on the stem surface of *Q. robur* is 40 years. In the older part of this period the record of rockfalls is surely incomplete, due to the closure of wounds. Therefore, the frequency of rockfalls would be underestimated if this old part of the record is included in calculations. The rockfall record seems little affected by wound vanishing in the last 25 years. Though some of the small wounds may be blurred during this period, the record will remain complete as long as at least one wound is preserved for each rockfall event

The completeness of the tree-ring record of rockfalls that has been obtained at the Solà d'Andorra depends on two more factors: on the width of the strips sampled and on the probability of impact of falling blocks with trees (CIP). Our results at Alzina talus indicate that, for a forest density greater than 800 trees/ha, a strip width of 20 m is sufficient to record all rockfall events that hit trees in the strip. The CIP of a strip can be approached as a one-dimensional problem making some simplifying assumptions. Rockfall frequency assessed from tree rings should be considered as a minimum frequency when the probability of impact is not calculated.

Acknowledgements The authors gratefully acknowledge the two anonymous reviewers as well as Markus Stoffel and David R. Butler for helpful comments and suggestions that improved the manuscript. This research work has received financial support from the Safeland project funded by the European Commission and from the Big Risk project funded by the Spanish Research Council.

References

Copons R, Vilaplana JM, Corominas J, Altimir J, Amigó J (2005) Rockfall risk management in high density urban areas. The Andorran experience. In: Glade T, Anderson M, Crozier MJ (eds) Landslide hazard and risk. New York, Wiley, pp 675–698

Copons R, Vilaplana JM (2008) Rockfall susceptibility zoning at a large scale: From geomorphological inventory to preliminary land use planning. Eng Geol 102:142–151

Corominas J, Copons R, Moya J, Vilaplana JM, Altimir J, Amigó J (2005) Quantitative assessment of the residual risk in a rockfall protected area. Landslides 2:343–357

Lang A, Moya J, Corominas J, Schrott L, Dikau R (1999) Classic and new dating methods for assessing the temporal occurrence of mass movements. Geomorphology 30:33–52

Moya J, Corominas J (1996) Determination of the spatial and temporal activity of landslides based on tree analysis. In: Sennesset K (ed) Landslides. Proceedings of the Seventh International Symposium of Landslides, pp 321–326

Moya, J, Corominas J, Perez-Arcas J, Baeza C (2010) Tree-ring based frequency assessment of rockfalls at Solà d'Andorra (Andorra Principality, Eastern Pyrenees). Geomorphology doi:10.1016/j.geomorph.2010.02.007

Perret S, Stoffel M, Kienholz H (2006) Spatial and temporal rockfall activity in a forest stand in the Swiss Prealps-A dendrogeomorphological case study. Geomorphology 74:219–231

Stoffel M (2006) A review of studies dealing with tree rings and rockfall activity: the role of dendrogeomorphology in natural hazard research. Nat Haz 39:51–70

Stoffel M, Perret S (2006) Reconstructing past rockfall activity with tree rings: Some methodological considerations. Dendrochronologia 24:1–15

Stoffel M, Schneuwly D, Bollschweiler M, Lievre I, Delaloye R, Myint M, Monbaron M (2005) Analyzing rockfall activity (1600–2002) in a protection forest-a case study using dendrogeomorphology. Geomorphology 68:224–241

Reconstruction and Spatial Analysis of Rockfall Frequency and Bounce Heights Derived from Tree Rings

Dominique M. Schneuwly

Geomorphic processes continuously shape mountain regions, with rockfall being one of the most widespread and frequent events. Its unpredictable and sudden occurrence poses major threats to settlements, human infrastructure and can even lead to the loss of life (Porter and Orombelli 1981; Bunce et al. 1997; Guzzetti 2000). In recent years, anthropogenic activities increasingly expanded into marginal regions. This development results in the construction of new infrastructure and settlements in exposed areas, leading to increased risk of casualties. In order to avoid future accidents, an accurate hazard assessment and risk analysis become more and more inevitable. Besides a comprehensive understanding of the process, risk evaluation requires the knowledge of past rockfall activity in space and time. Areas where rockfall occurs have to be identified, and the frequency and magnitude of events determined. As a result, rockfall has become one of the most intensely studied geomorphic processes in the alpine environment.

However, the unpredictability of rockfall events poses major difficulties for a realistic assessment of the process. In the absence of a detailed, eyewitness history, dendrogeomorphology is the only method allowing for an adequate reconstruction of past rockfall parameters, such as rebound heights of rocks and boulders, or frequency, magnitude, and seasonality of events. Following mechanical impact, different tree species, e.g. European larch (*Larix decidua*), Norway spruce (*Picea abies*), silver fir (*Abies alba*) respond with the formation of specific growth features such as tangential rows of traumatic resin ducts, reaction wood, callus tissue, or abrupt changes in growth (Braam et al. 1987; Schweingruber 1996, 2001; Schneuwly et al. 2009). These growth features can be dated with intra-annual precision, allowing for the reconstruction of past rockfall frequencies with seasonal accuracy (Stoffel and Perret 2006). Determination of the main rockfall season and past activity patterns permits the identification of local triggers.

D.M. Schneuwly (✉)
Department of Geosciences, Geography, University of Fribourg, 1700 Fribourg, Switzerland
e-mail: dominique.schneuwly@bafu.admin.ch

M. Stoffel et al. (eds.), *Tree Rings and Natural Hazards: A State-of-the-Art*,
Advances in Global Change Research 41, DOI 10.1007/978-90-481-8736-2_16,

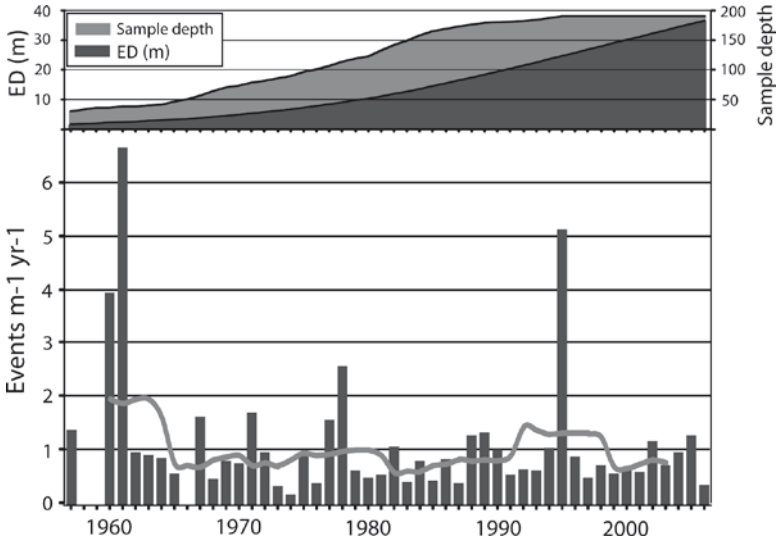

Fig. 1 Reconstructed rockfall frequency for the last 50 years with the sample depth (ED = exposed diameter). There exists an ordinary background activity during normal years with exceptional activity in event years. In 1960, a magnitude 5.3 earthquake occurred in proximity, in 1995, a heavy precipitation event triggered the outstanding activity. No long term trend (*gray line*) is detectable

A total of 191 severely injured conifer trees were sampled at a case-study slope in Saas-Balen (Valais, Switzerland). The analysis of 50 years of rockfall history unravelled an ordinary background activity during most years and severe activity during exceptional event years (Fig. 1). The intra-annual distribution of rockfall events shows a peak in activity during the dormant period (early October – late May), and lowest activity during summer. Freeze-thaw processes are identified as the main ordinary rockfall trigger. On the slope, reconstructed rockfall frequency averages 1.02 events m^{-1} $year^{-1}$. In addition, two major rockfall event years could be determined. In 1960, the rockfall rate attained 3.9 events m^{-1} and culminated in 6.6 events m^{-1} in the following year (1961). The second peak in rockfall activity is noted for 1995, when 5.1 events m^{-1} were reconstructed. Both events could be correlated with exceptional triggers. In 1960, a magnitude 5.3 earthquake (Mercalli intensity VIII) occurred 18 km away from the study site. In 1995, unusually heavy precipitation was recorded at the study site. In contrast, no long-term trend in rockfall activity could be detected. Spatial analysis of rockfall frequency revealed highest values (>4 events m^{-1} $year^{-1}$) at the lateral boundary that is oriented towards the main rockfall source area (Fig. 1b). Values at the boundaries are higher and rapidly decrease inside the stand. Investigations on injury heights reveal a mean value of 0.85 m. The maximum rebound height attains 4.5 m, but two thirds of all impacts did not surpass 1 m. Spatial analyses on rebound height indicate highest values at

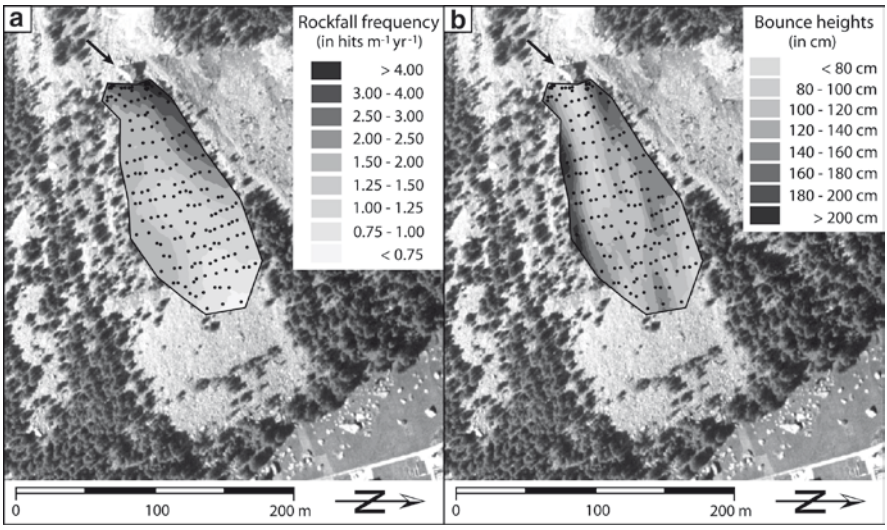

Fig. 2 Spatial analysis of the rockfall activity and the bounce heights at the study site. (**a**) Highest rockfall frequency can be found at the lateral boundary that is oriented towards the main rockfall source area. (**b**) Highest rebound heights occur at both lateral boundaries. Rapidly decreasing values inside the forest are witnessing the protection effect of the forest against rockfall. Notice the shielding effect of a big boulder in lateral top position (*black arrow*)

the lateral boundaries of the study site (Fig. 2b). Rebound heights immediately decrease inside the forest, illustrating again the deceleration effect of the trees and the dampening effect of the changed surface conditions within the stand (Schneuwly and Stoffel 2008a, b). Spatial data on rockfall frequency and rebound heights clearly demonstrate the protection effect of forest against rockfall.

Dendrogeomorphology has proven its high potential in rockfall research. Reconstructed data on rebound heights and seasonality can improve the general understanding of the process. Long-term data on frequency, magnitude as well as trigger identification substantially improves local risk assessment and allows more precise predictions on future rockfall pattern.

References

Braam RR, Weiss EEJ, Burrough A (1987) Spatial and temporal analysis of mass movement using dendrochronology. Catena 14:573–584

Bunce CM, Cruden DM, Morgenstern NR (1997) Assessment of the hazard of rock fall on a highway. Can Geotech J 34:344–356

Guzzetti F (2000) Landslide fatalities and evaluation of landslide risks in Italy. Eng Geol 58:89–107

Porter SC, Orombelli G (1981) Alpine rockfall hazards. Am Sci 69:67–75

Schneuwly DM, Stoffel M (2008a) Tree-ring based reconstruction of the seasonal timing, major events and origin of rockfall on a case-study slope in the Swiss Alps. Nat Haz Earth Syst Sci 8:203–211

Schneuwly DM, Stoffel M (2008b) Changes in spatio-temporal patterns of rockfall activity on a forested slope – a case study using dendrogeomorphology. Geomorphology 102:522–531

Schneuwly DM, Stoffel M, Bollschweiler M (2009) Formation and spread of callus tissue and tangential rows of resin ducts in *Larix decidua* and *Picea abies* following rockfall impacts. Tree Physiol 29:281–289

Schweingruber FH (1996) Tree rings and environment. Dendroecology. Paul Haupt, Bern, Stuttgart, Wien

Schweingruber FH (2001) Dendroökologische Holzanatomie. Paul Haupt, Bern, Stuttgart, Wien

Stoffel M, Perret S (2006) Reconstructing past rockfall activity with tree rings: some methodological considerations. Dendrochronologia 24(6):1–15

Part V
Debris Flows

Debris-flow material deposited against Norway spruce (*Picea abies*), Swiss Alps (© M. Bollschweiler)

State of the Art in Debris-Flow Research: The Role of Dendrochronology

Matthias Jakob

1 Introduction

Debris flows and their volcanic counterparts lahars are one of the most destructive mass movement process worldwide, being responsible for hundreds of death every year and leading to horrific multi-thousand death tolls every decade or so. Consequently, debris flows have been the focus on intensive research with hundreds of papers appearing annually on various aspects of debris flow research. For most researchers and practitioners it is difficult to keep abreast of all advances in debris flow research and to extract the most relevant publications. Several dedicated conferences have been held whose sole focus is debris flows. In 2005 a book on debris flows and related processes was published (Jakob and Hungr 2005) to offer a more systematic review of the state-of-the-art. The book was published in 2005 and thus reflects mostly knowledge up to 2003 or 2004. With that it is outdated in some fields. It is clearly impossible to replace the 2005 book and provide a comprehensive review of all significant advances in debris flow science in the space of this chapter. The author has therefore attempted to provide a short summary and highlight outstanding questions and how they can be addressed, at least in part, by application of dendrochronology.

This chapter begins with a definition of debris flows and their formation to avoid confusion in nomenclature and application in practice. It then summarizes the present state of debris flow science for select topics, the present research needs and the application of dendrochronology in helping to advance the science.

1.1 What are Debris Flows?

Debris flows are now a well-defined landslide process and nomenclature ambiguity ought to be a matter of the past. In the past, different definitions have been offered by various workers. The present author prefers a hybrid of definition by Hungr

M. Jakob (✉)
BGC Engineering Inc, D-84489 Burghausen
e-mail: mjakob@bgcengineering.ca

M. Stoffel et al. (eds.), *Tree Rings and Natural Hazards: A State-of-the-Art*,
Advances in Global Change Research 41, DOI 10.1007/978-90-481-8736-2_17,

et al. (2005) and Iverson (2009) which defines debris flows as "a flow of saturated non-plastic mineral and sometime organic debris in a steep channel that include some 50–70% solid grains by volume, can attain flow velocities in excess of 10 m/s and can range between 10 and 109 m^3 in volume. Mud flows can be contrasted by higher water content and a plasticity index of >5%." While this definition is preferred and used by the author of this chapter, in this book the term debris flow is also used for events with sediment concentration below those of true debris flows that are usually referred to as hyperconcentrated floods.

2 A Brief Summary of the State of Debris Flow Science

2.1 Debris Flow Mechanics

Debris flow mechanics are very complex, and detailed research on this topic has been conducted for over 20 years. An adequate understanding of debris flow mechanics is required to create single and multi-dimensional models that simulate debris flow motion. While it is not necessary to recreate the exact physical perturbations during the flow and deposition phases of a debris flow, an equivalent fluid needs to be formulated that behaves similar to observed debris flows and can adequately replicate runout behaviour. Accordingly, debris flow modelling has been subject to intensive research and scrutiny over the past ten years. Identification of an appropriate debris flow rheology is key to the modelling and prediction of debris flow characteristics and behaviour, which has led to a vigorous debate on the most appropriate rheological formula. Contrasting the single-rheology focus are field observations demonstrating that a single rheology is unable to completely describe debris flow behaviour. Field observations and flume experiments suggest that rheologies vary temporally, spatially and exhibit feedbacks that depend on evolving debris flow dynamics. Therefore, a single rheologic model is unattainable because non-hydrostatic forces cannot exist in steady states. More advanced models such as the Coulomb mixture theory strive to account for unsteady flow behaviour. In addition, very few workers (i.e. McDougall and Hungr 2004) have attempted to include entrainment of debris into their model regimes. Debris flow fans are understood as depositional landforms and model output is limited to fan deposition (i.e. Tekka et al. 2007), even though entrainment on debris-flow fans has been observed numerous times (see Section 2.2).

Several single and multi-dimensional debris flow runout models have been developed (MacArthur and Schamber 1986; Takahashi and Nakagawa 1989; O'Brien et al. 1993; Hungr 1995; Chen and Lee 2000; Iverson and Denlinger 2001; McDougall and Hungr 2004; Pudasaini and WangY 2005; Rickenmann et al. 2006).

One of the most prolific researchers focusing on debris flow mechanics is Dr. Iverson of the US Geological Survey. He recently provided a new depth-averaged model of debris-flow motion that is able to characterize the evolution of flow velocity,

depth, solid and fluid volume fractions and pore-fluid pressure simultaneously (Iverson 2009). This model advances beyond traditional two-phase debris-flow models that typically lack evolution of solid and fluid volume fractions and their interaction with flow dynamics. A potential downfall of the model, as admitted by Iverson, is the lack of representation of grain size segregation, which is responsible for coarse debris flow fronts, inverse grading and levees.

While progress in deciphering the "true" mechanics of debris flows is desirable and required to be translated into modelling software, it is the present author's opinion that no model will be able to fully account for random and often chaotic flow characteristics that may stem from multiphase flow with organic debris over complex terrain. This includes coarser debris lobes stalling, then being overrun by hyperconcentrated flow surges, log jams on fans leading to unpredictable avulsions, as well as spatial and temporal variability in scour within the fan reaches. For the experienced field worker, this may come as a relief as expert knowledge and judgment will always have a place in detailed debris flow hazard and risk assessments despite any future advances in debris flow physics and numerical modelling.

2.2 Scour in Colluvial Channels/Fans

Debris flow scour is one of the least understood facets in debris flow science. Debris flow scour affects the total volumes of debris flows produced, particularly if most of the material is entrained on colluvial cones or alluvial fans. Scour is also of crucial importance in the design of crossings of linear infrastructure that require burial (i.e. water/gas/oil/concentrate pipelines/fiber optics). A puncture or rupture of a mine concentrate pipeline, for example, due to debris flow scour at the pipeline crossing could result in direct economic losses of several million dollars per day plus secondary effects such as environmental losses due to pollution of heavy metal enriched concentrate. Finally, environmental pollution and contamination of water ways could result in lawsuits, retraction of mining rights and reputation loss that could amount to hundreds of millions of indirect losses. Such events provide an unacceptable risk to the owners and must be prevented at considerable expense.

Debris flow bed mobilization is likely a consequence of a combination of factors namely the transfer of momentum through solid collisions, friction and fluid thrust, often combined with reduction of effective strength of substrate due to pore pressure changes and/or strain softening (Hutchinson and Bhandari 1971; Sassa 1985). Theoretical approaches to bed stability predictions (Hungr et al. 2005) have not yielded satisfactory results for practical applications. This may be attributed to a lack of understanding of shear strength variability along a channel, the effects of vegetation on channel bank cohesion and the variability of pore pressures along the channel before and during the passage of the debris flow. Debris-flow scour is thus a multivariate problem that may only be resolved through detailed monitoring along high frequency debris flow channels and large scale flume experiments. Empirical relationships can be established that may then form the basis for mathematical formulation.

Dendrochronology may aid this science by providing some data on the depth of scour that can be expected along colluvial channel sections. Many conifers are capable to form adventitious roots if they are inundated, and thus allow the dating of inundation events but also the reconstruction of scour events. Longitudinal averaging of expected scour depth may then be used in combination with channel geometry consideration to predict potential scour. It should be pointed out, however, that this method may be prone to large error if geomorphic thresholds for catastrophic material entrainment are exceeded that are not part of the reconstructed time series. There are several such events documented in the literature and have been noted by consulting experience by the author. For example, a large alluvial fan complex in the southern Coast Mountains of British Columbia suddenly produced a debris flow in the order of 50,000 m^3 through fan channel entrainment only (Jakob et al. 1997). There had not been any such precedents in the 80 years prior that could be documented by air photo interpretation and dendrochronology.

2.3 Frequency-Magnitude Relationships

As one of the three (together with varve chronology and sclerochronology) annual dating methods, dendrochronology plays a crucial part in reconstructing debris flow activity in the past. This can be accomplished for single debris flow fans (i.e. Stoffel 2010, this volume; Bollschweiler et al. 2010, this volume), or on a regional scale (i.e. Strunk 1995; Jakob 1996; May and Gresswell 2004). This is important to answer questions of landform evolution and especially to develop reliable frequency-magnitude (F-M) relationships of debris flows that form the basis for quantitative risk assessments (QRAs).

Several countries are now calling for landslide QRAs for their existing or new developments. The development of reliable F-M relationships requires a significant effort. This book provides an example where 2,246 tree ring series were analysed from 1,102 old-growth trees (Stoffel 2010, this volume), although recent work (Stoffel and Bollschweiler 2009) has suggested that a much smaller subset of data may provide results that are still usable for frequency-magnitude relationships. Frequency estimates can and should be extended and completed from other data sources such as interviews with locals, newspaper searches, air photograph interpretation, lake sediment analysis, vegetation succession (i.e. Bollschweiler et al. 2010, this volume), lichenometry (Wilkerson and Schmid 2010, this volume) and radiometric dating (i.e. Jakob and Weatherly 2005). Dendrochronology offers the advantage of being precise and allowing a more or less continuous record over a few hundred years if performed by qualified personnel.

Dendrochronology can also support the reconstruction of debris flow volume and peak discharge. Volumes can be deciphered by mapping trees affected by the same event that may provide at least areas affected particularly for fans in densely vegetated areas that preserve the spatial pattern of debris flow inundation (Bollschweiler et al. 2007). Areas are related to volumes and can thus be used as a

volume surrogate if subsurface investigations cannot be conducted due to budget limitation, land ownership or lack of access for heavy machinery. Peak discharge can be back-calculated if tree scars along bedrock controlled sections are dated, the cross-section measured and the flow velocities calculated from empirical equations (Jakob 2005). If risk assessments need to exceed the dating range for dendrochronology because, for example, the development has a risk potential that requires modelling of several thousand year return period events, radiometric methods (standard radiocarbon and AMS dating) will need to extend the dendrochronologic record.

2.4 Debris Flow Forecasting and Warning Systems

There is an astounding body of work that has been completed on this subject. Most workers have followed Caine's (1980) approach by plotting rainfall duration against intensity for a large range of durations and plotting those events that have led to landslides or debris flows (i.e. Guzzetti et al. 2008). While this approach is a reasonable first step in identifying debris flow-producing storms, it is unsuited as a warning tool in most applications because exceedence of the lower threshold envelope would result in too many warnings to be taken seriously by residents. This calls for more sophisticated approaches that integrate antecedent conditions (e.g. Chleborad et al. 2008) or use statistical techniques to distinguish storm characteristics from storms that have produced landslides from those that have not (Jakob and Weatherly 2003; Cannon et al. 2008; Jakob 2009). Watershed conditions are typically too complex for a system based entirely on rainfall characteristics to ever yield a 100% success rate.

Unfortunately, there is little scope for dendrochronology in this field other than providing dates (years) for debris flows, which with careful analysis may be attributable to a given storm. Once verified this storm date can then be used to obtain the required hydroclimatic data.

2.5 Debris Flows and Wildfire

Devastating forest fires in the southwestern US and Europe in past few years have sparked a surge in research on the impacts of wildfires on debris flows. Debris flows are among the most hazardous consequences of rainfall on recently burned hillslopes (Cannon and Gartner 2005; Cannon et al. 2010). Removal of vegetation and impacts to soil by wildfire can change the hydrologic response to rainfall, often resulting in increased runoff and significant sediment movement (i.e. Shakesby and Doerr 2006, DeBano 2000). Most debris flows that occur in the first few years after a fire are generated through a process of progressive bulking of runoff with material eroded primarily from channels (Meyer and Wells 1997; Cannon et al. 2001; Santi et al. 2008). An abundance of fine particles from loose, burned soil, dry-ravel deposits,

and fine ash mantling the surface make burned areas particularly susceptible to this process; fine particle entrainment is thought to increase flow transport capacity and shear stress, permitting mobilization of coarser channel sediments (Gabet and Sternberg 2008). Rainfall intensity-duration conditions that trigger fire-related debris flows are significantly lower than those described for the generation of debris flows in unburned settings, and debris flows are often triggered in response to as little rainfall as that that falls in 2 year-recurrence interval storms (Cannon et al. 2008). Over longer time periods decreased rates of evapotranspiration caused by vegetation mortality and decay of root structure may result in the increased soil moisture and loss of soil cohesion necessary for failure of discrete landslide masses in burned areas (i.e. Jackson and Roering 2009).

While progress is being made in understanding the debris flow response of burned watersheds, there are still some significant gaps in our knowledge. For example, long-term (>100 years) frequency-magnitude relationships in basins with wildfire driven changes in sediment supply characteristics are still rare. Furthermore, there are only few reliable recharge relationships established from repeat channel surveys that would quantify the non-linear increase in available sediment after a wildfire.

Tree ring information, including fire scar and germination dates and age-structure data, are routinely used to establish regional and local fire histories (e.g., Covington and Moore 1994; Allen et al. 2002). Integration of data from these studies with those from alluvial fan stratigraphies that include post-fire events can be used to gain insight into the potential regional impacts of changing climates (e.g., Pierce and Meyer 2008; Pierce et al. 2004), and of basin-scale effects of the extent and severity of past fires on the geomorphic response (i.e. Bigio et al. 2005; Frechette and Meyer 2007).

2.6 Debris Flow Mitigation

Debris flow mitigation has a very long history in various mountainous regions on Earth. In particular in Austria and Japan, debris flow mitigation has advanced to a sophisticated science that addresses a range of components from source area stabilization over various intermittent channel measures to large engineered structures at the basin outlet. While rigid steel and reinforced concrete structures still prevail, there is an increasing use of dynamic debris flow defenses that allow deformation and thus absorption of kinetic energy such a debris flow nets and geo-synthetic reinforced soils (GRS). The advantage of these structures is usually lower cost than rigid systems.

The desire to construct mitigation at low cost requires a good understanding of frequency-magnitude relationships as well as debris flow intensities. Furthermore, particularly in areas frequented by tourists, large unsightly concrete structures are not always supported by local communities and may either need to be hidden from sight or replaced by more aesthetically pleasing structures.

Appropriate debris flow mitigation is based on a thorough understanding of the debris flow hazard including most of the topics included in this Chapter.

Dendrochronology can also help in the design of mitigation measures by identification of the most active fan sector and likely flow or avulsion paths. For example, Bollschweiler et al. (2010, this volume) were able to reconstruct recent activity of Grosse Graben in Switzerland and thus identify the most likely avulsion locations. It should be remembered, however, that over large (typically century) time scales, old fan surfaces can be reactivated due to episodic build up of the fan surface in recently active sectors. Accordingly, a differentiation needs to be made in the mitigation philosophy if risk reduction is aimed for decades or centuries to come. This kind of dendrochronologic investigation will also help an early recognition of shifts in fan activity and thus allow for early planning to reduce risk for fan sectors that have been unaffected for long time periods.

2.7 Debris Flows and Climate Change

Landslide response to climate change is a higher order effect of global warming that leads to higher atmospheric moisture content, which in turn will lead to higher rainfall amounts and intensities in some regions. However, the hydrologic response of debris flows to climate is complex (Jakob and Lambert 2009) and cannot be condensed to a statement that equates more rain with more or larger debris flows. Antecedent moisture conditions are an important variable in priming hillslopes to landslide susceptibility. Drier and longer summers in some areas will shift antecedent moisture thresholds later into the rainy season. Warmer temperatures may increase the elevation of significant snow accumulation that may increase both the time during which debris flows are likely (a thinning snowpack loses its capability to absorb rain) and it may lead to debris flows initiating at higher elevation. More annual rainfall may in some regions translate in more rain days, while in others, short-term rainfall intensity will be augmented. Long-term changes in the type and spatial distribution of vegetation will need to be accounted for as it changes the canopy intercept, evapotranspiration rates and perhaps even the root distribution and thus root cohesion, which affect hillslope stability in forested terrain.

Dendrochronology may help in identifying the effects of climate change through high resolution studies of debris flow frequencies (Stoffel and Beniston 2006; Strunk 1995), particularly in transport-limited watersheds where the exceedence of a given hydroclimatic threshold is very likely to trigger debris flows. An increase of debris flow frequency in those basins (in absence of human interference) may indicate that the combination of hydroclimatic parameters required to trigger a debris flow may have shifted. The related science of dendroclimatology can be used to monitor changes in moisture and/or temperature regime.

Acknowledgements Susan Cannon kindly provided materials for the debris flows and wildfire section and reviewed an early draft. Markus Stoffel and Michelle Bollschweiler provided helpful comments on a draft of this chapter.

References

Allen CD, Savage M, Falk DA, Suckling KF, Swetnam TW, Schulke T, Stacey PB, Morgan P, Hoffman M, Klingel JT (2002) Ecological restoration of Southwestern ponderosa pine ecosystems: A broad perspective. Ecol Appl 12:1418–1433

Bigio EJ, Swetnam TW, Baisan CH (2005) The integration of tree-ring and alluvial fan records of hire history at the Missionary Ridge Fire near Durango, Colorado. Geol Soc Am Abst Prog 37(7):111

Bollschweiler M, Stoffel M, Ehmisch M, Monbaron M (2007) Reconstructing spatio-temporal patterns of debris-flow activity using dendrogeomorphological methods. Geomorphology 87:337–351

Bollschweiler M, Stoffel M, Schneuwly, DM (2010) Using event and minimum age dating for the assessment of hazards on a debris-flow cone. In: Stoffel M, Bollschweiler M, Butler DR, Luckman BH (eds) Tree rings and natural hazards: A state-of-the-art. Springer, Berlin, Heidelberg, New York, this volume

Caine N (1980) The rainfall intensity-duration control of shallow landslides and debris flows. Geogr Ann 62A:23–27

Cannon SH, Gartner JE (2005) Wildfire-related debris flow from a hazards perspective. In: Jakob M, Hungr O (eds) Debris-flow hazards and related phenomena. Praxis, Springer, Berlin, Heidelberg, New York, pp 363–385

Cannon SH, Kirkham RM, Parise M (2001) Wildfire-related debris-flow initiation processes, Storm King Mountain, Colorado. Geomorphology 39:171–188

Cannon SH, Gartner JE, Wilson RC, Bowers JC, Laber JL (2008) Storm rainfall conditions for floods and debris flows for recently burned areas in southwestern Colorado and southern California. Geomorphology 96:250–269

Cannon SH, Gartner JE, Rupert MG, Michael JA, Rea AH, Parrett C (2010) Predicting the probability and volume of post-wildfire debris flows in the inter-mountain west, USA. Geol Soci Am Bull 122(1–2):127–144

Chleborad AF, Baum RL, Godt JL, Powers PS (2008) A prototype system for forecasting landslides in the Seattle, Washington area. Geol Soci Am Rev Eng 20:103–120

Chen H, Lee CF (2000) Numerical simulation of debris flows. Can Geotech J 37(1):147–160

Covington WW, Moore MM (1994) Southwestern ponderosa forest structure Changes since Euro-American settlement. J Forest 92:39–47

DeBano LF (2000) The role of fire and soil heating on water repellency in wild-land environments: a review. J Hydrol 231–232:195–206

Frechette JD, Meyer GA (2007) Episodic geomorphic impact of severe fire in ponderosa pine and mixed conifer forests of the Sacramento Mountain, New Mexico. Geol Soc Am Abst Prog 38:109

Gabet EJ, Sternberg P (2008) The effects of vegetative ash on infiltration capacity, sediment transport and the generation of progressively bulked debris flows. Geomorphology 101:666–673

Guzzetti F, Peruccacci S, Rossi M, Stark CP (2008) The rainfall intensity-duration control of shallow landslides and debris flows: an update. Landslides 5(1):3–17

Hungr O (1995) A model for the runout analysis of rapid flow slides, debris flows, and avalanches. Can Geotech J 32:610–623

Hungr O, McDougall S, Bovis MJ (2005) Entrainment of material by debris flows. In: Jakob M, Hungr O (eds) Debris-flow hazards and related phenomena. Springer, Berlin, Heidelberg, New York

Hutchinson JN, Bhandari RK (1971) Undrained loading a fundamental mechanism of mudflows and other mass movements. Geotechnique 21:353–358

Iverson RM, Denlinger RP (2001) Flow of variably fluidised granular masses across three-dimensional terrain. 2. Numerical predictions and experimental tests. J Geophys Res 106:552–566

Iverson R (2009) Elements of an improved model for debris flow motion. Invited contribution for Powders and Grains 2009. American Physical Society

Jackson M, Roering JJ (2009) Post-fire geomorphic response in steep, forested landscapes: Oregon Coast range, USA. Quat Sci Rev 28(11–12):1131–1146
Jakob M, Lambert S (2009) Climate change effects on landslides along the south-west coast of British Columbia. Geomorphology 107:275–284
Jakob M (2009) A real-time debris flow warning system for the North Shore Mountains of Vancouver, Canada. European Geosciences Conference, Vienna
Jakob M, Hungr O (eds) (2005) Debris-flow hazards and related phenomena. Springer, Berlin, Heidelberg, New York
Jakob M, Weatherly H (2005) Debris flow hazard and risk assessment. Jones Creek, Washington. In: Hungr O, Fell R, Couture R, Eberhardt E (eds) Landslide risk management. Proceedings, pp 533–542
Jakob M (2005) A size classification for debris flows. Eng Geol 79:151–161
Jakob M, Weatherly H (2003) A hydroclimatic threshold for landslide initiation on the North Shore Mountains of Vancouver, British Columbia. Geomorphology 54:137–156
Jakob M, Hungr O, Thomson B (1997) Two debris flows with anomalously high magnitude. In: CL Chen (ed) Debris-flow hazards mitigation: mechanics, prediction and assessment: Proceedings of the first International Conference, American Society of Civil Engineers, pp 382–394. American Society of Civil Engineers, New York
Jakob M (1996) Morphometric and geotechnical controls of debris flow frequency and magnitude in southwestern British Columbia. Ph.D. thesis, University of British Columbia
May CL, Gresswell RE (2004) Spatial and temporal patterns of debris-flow deposition in the Oregon Coast Range, USA. Geomorphology 57:135–149
MacArthur RC, Schamber DR (1986) Numerical method for simulating mudflows. Proceedings of the Third International Symposium on River Sedimentation, Jackson, Mississippi, pp 1615–1623
McDougall S, Hungr O (2004) A model for the analysis of rapid landslide motion across three-dimensional terrain. Can Geotech J 41:1084–1097
Meyer G, Wells SG (1997) Fire-related sedimentation events on alluvial fans, Yellowstone National Park, USA. J Sediment Res 67:776–791
O'Brien JS, Julien PY, Fullerton WT (1993) Two-dimensional water flood and mud-flow simulation. J Hydraul Eng 119(2):244–259
Pierce JL, Meyer GA (2008) Long-term fire history from alluvial fan sediments – the role of drought and climate variability, and implications for management of Rocky Mountain Forests. Int J Wildland Fire 17:84–95
Pierce JL, Meyer GA, Jull AJT (2004) Fire-induced erosion and millennial-scale climate change in northern ponderosa pine forests. Nature 432:87–90
Pudasaini SP, WangY HK (2005) Modelling debris flows down general channels. Nat Haz Earth Syst Sci 5:799–819
Rickenmann D, Laigle D, McArdell W, Huble J (2006) Comparison of 2D debris-flow simulation models with field events. Comput Geosci 10:241–264
Santi PM, deWolfe VG, Higgins JD, Cannon SH, Gartner JE (2008) Sources of debris flow material in burned areas. Geomorphology 96:310–321
Shakesby RA, Doerr SH (2006) Wildfire as a hydrological and geomorphological agent. Earth-Sci Rev 74:269–307
Sassa K (1985) The mechanism of debris flows. Proceedings of the XI International Conference on Soil Mechanics and Foundation Engineering, San Francisco, vol 1, pp 1173–1176
Stoffel M, Bollschweiler M (2009) Tree-ring reconstruction of past debris flows based on a small number of samples – possibilities and limitations. Landslides 6:225–230
Stoffel M (2010) Frequency-magnitude relationships, seasonality and spread of debris flows on a forested cone. In: Stoffel M, Bollschweiler M, Butler DR, Luckman BH (eds) Tree rings and natural hazards: A state-of-the-art. Springer, Berlin, Heidelberg, New York, this volume
Stoffel M, Beniston M (2006) On the incidence of debris flows from the early Little Ice Age to a future greenhouse climate: a case study from the Swiss Alps. Geophys Res Lett 33:L16404
Strunk H (1995) Dendrogeomorphologische Methoden zur Emittelung der Murfrequenz und Beispiele ihrer Anwendung. Roderer, Regensburg

Takahashi T, Nakagawa H (1989) Debris flow hazard zone mapping. Proceedings of the Japan–China (Taipei). Joint Seminar on Natural Hazard Mitigation, Kyoto, Japan, pp 363–372

Tekka PR, Genevois R, Deganutti AM, Armento MC (2007) Numerical modelling of two debris flows in the Dolomites (Northeastern Italian Alps). Chen and Major (eds) Fourth International Conference on Debris Flow Hazard Mitigation: Mechanics, Prediction, and Assessment. Millpress, Netherlands, pp 179–188

Wilkerson F, G Schmid (2010) Dendrogeomorphic applications to debris flows in Glacier National Park, Montana, USA. In: Stoffel M, Bollschweiler M, Butler DR, Luckman BH (eds) Tree rings and natural hazards: A state-of-the-art. Springer, Berlin, Heidelberg, New York, this volume

Using Event and Minimum Age Dating for the Assessment of Hazards on a Debris-Flow Cone

Michelle Bollschweiler, Markus Stoffel, and Dominique M. Schneuwly

1 Introduction

Debris flows are common mass-movement processes in most mountainous regions of the world, where their unpredictable and sudden occurrence represents a major threat to transportation corridors and settlements. Increased anthropogenic activity in regions exposed to debris-flow risk renders a detailed hazard assessment inevitable. As a consequence, the understanding of the debris-flow process as well as the behavior of events in space and time is crucial for the mitigation of hazards and risks (e.g. Cardinali et al. 2002; Pasuto and Soldati 2004). For many torrents in Alpine regions, however, systematic acquisition of data on past debris flows only started after the series of catastrophic events in 1987 and 1993 (Haeberli et al. 1990; Rickenmann and Zimmermann 1993; Zimmermann et al. 1997); there is still a considerable lack of knowledge about earlier events for many regions. Thus the reconstruction of past activity is essential for the understanding of current debris-flow dynamics in mountain torrents, possible future developments due to potential climatic change (Goudie 2006) and a realistic assessment of the hazards.

The most accurate method for dating past debris-flow events is the analysis of trees disturbed by geomorphic processes as described in the introductory chapter of this book (or e.g. Bollschweiler et al. 2007, 2008; Stoffel and Bollschweiler

M. Bollschweiler (✉) and M. Stoffel
Laboratory of Dendrogeomorphology, Institute of Geological Sciences, University of Bern, CH-3012 Bern, Switzerland
and
Chair for Climatic Change and Climate Impacts, Institute for Environmental Sciences, University of Geneva, CH-1227 Carouge-Geneva, Switzerland
e-mail: michelle.bollschweiler@dendrolab.ch

D.M. Schneuwly
Department of Geosciences, University of Fribourg, CH-1700 Fribourg, Switzerland

M. Stoffel et al. (eds.), *Tree Rings and Natural Hazards: A State-of-the-Art*, Advances in Global Change Research 41, DOI 10.1007/978-90-481-8736-2_18,

2008; Stoffel et al. 2008). However, particularly large or devastating debris flows may eliminate entire forest stands, rendering the reconstruction of previous events impossible with dendrogeomorphic methods. Since cleared surfaces are normally recolonized by seedlings in the years following the devastating event, germination ages of trees growing on landform surfaces have also been used in a number of studies to estimate the time of creation of new landforms or the time of surface-clearing disturbances to existing landforms (Sigafoos and Hendricks 1969; Shroder 1980; McCarthy and Luckman 1993; Winter et al. 2002). Similarly, this method can be used to date surfaces cleared by debris-flow activity.

The aim of this study was to combine dendrogeomorphic analyses with an assessment of germination dates of successor trees in order to understand the dynamics of past debris-flow events on a forested cone in the Valais Alps, Switzerland. In a first step, all forms related to debris-flow activity such as lobes, levees and abandoned debris-flow channels were mapped in a scale of 1:1000. Disturbed trees growing in these deposits were analyzed to reconstruct the debris-flow frequency and the spatial extent of previous events. For the sectors of the cone where disturbed trees are missing, unaffected trees growing in previously active debris-flow channels were sampled and their age assessed so as to approximate the minimum time elapsed since the last event. The coupling of data on events in channels with the minimum age dating allowed reconstruction of the spatial dynamics of debris-flow activity on the cone.

2 Study Site

The study of past debris-flow dynamics was conducted on the cone of the Grosse Grabe torrent, located on the west-facing slope of the Matter Valley (Valais, Swiss Alps; 46°10' N, 7°47' E; Fig. 1). The catchment area (Fig. 2a) of the torrent totals 1.5 km^2 and extends from the Breithorn summit (3,178 m a.s.l.) to the Mattervispa River (1,200 m a.s.l.). The upper part of the catchment is dominated by gneissic rocks belonging to the crystalline Mischabel unit, while in the lower part, debris originating from various gravitational processes (i.e. rockslides, rockfall) cover the bedrock (Labhart 2004). The considerable gradient between the source and the cone results in steep torrent topography (on average 25°; Fig. 2b). The debris-flow cone extends from 1,600 to 1,200 m a.s.l. and is vegetated by a forest primarily composed of European larch (*Larix decidua*) and Norway spruce (*Picea abies*; Fig. 2c). On the cone, slope gradients average 14° and deposits of past debris flows are found exclusively south of the currently active channel. In the lowermost part of the cone, a gallery was built in 1970 to protect the main road connecting Zermatt to Visp from debris flows. Archival data on past events only covers the last 13 years, with debris-flow activity noted for 1993, 1994, 1999 and 2000 (Seiler and Zimmermann 1999).

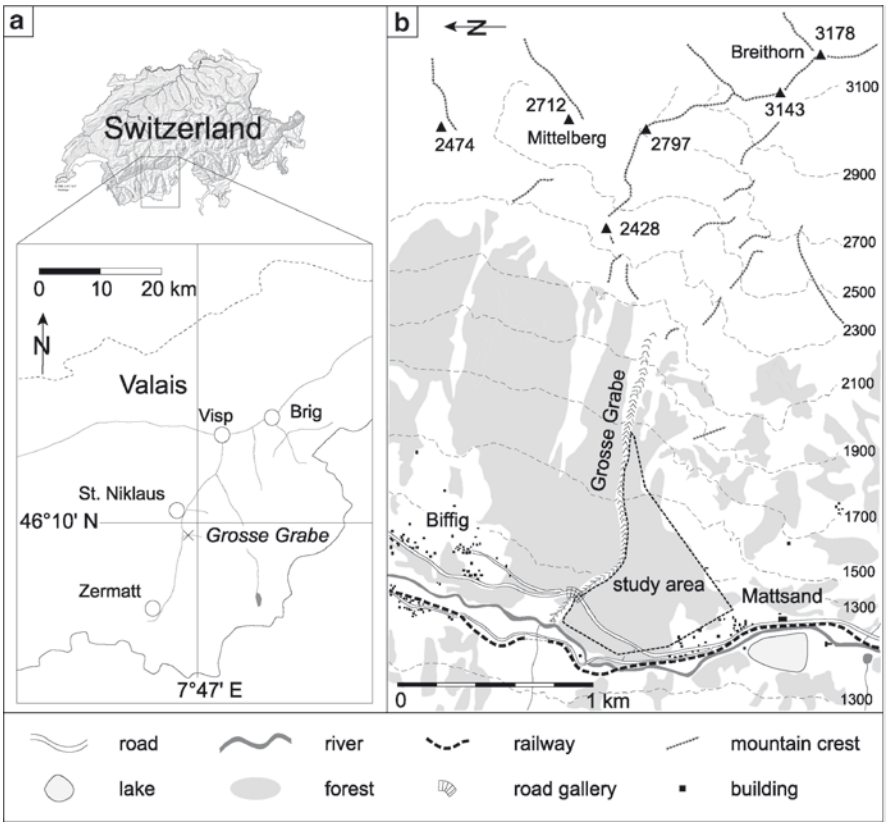

Fig. 1 (**a**) The study site in the Matter Valley close to St. Niklaus. (**b**) Sketch map of the study site with the Grosse Grabe torrent and the large debris-flow cone (= study area)

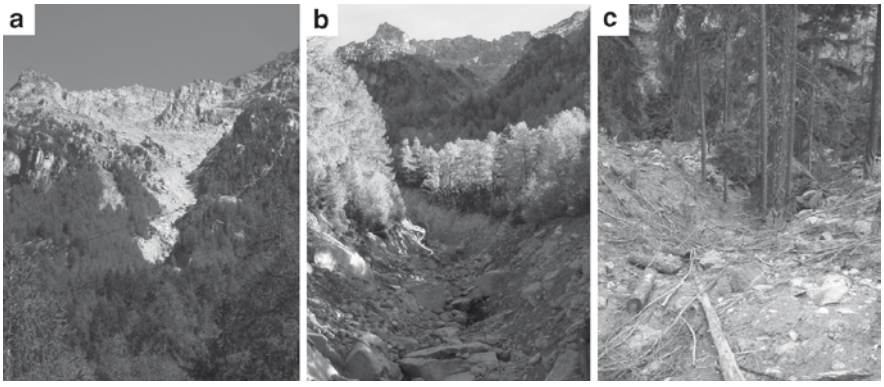

Fig. 2 (**a**) View of the upper catchment area. (**b**) The currently active debris-flow channel passes through a forest of *Larix decidua* and *Picea abies*. trees. (**c**) A formerly active channel on the debris-flow cone

3 Methods

3.1 Geomorphic Mapping and Sampling Strategy

In a first analytical step, all landforms and deposits related to previous debris-flow activity (i.e. lobes, levees or abandoned channels) were mapped on the basis of a geomorphic map at a scale of 1:1000 using compass, tape measure and inclinometer. After the mapping, 71 *L. decidua* and *P. abies* trees that had obviously been disturbed by previous debris-flow events were sampled with 150 cores using an increment borer (max. length 40 cm, 6 mm diameter). We selectively sampled trees that showed scars, candelabra growth, exposed root systems and buried or tilted stem bases resulting from the impact of past events.

Few disturbed trees are located in the channels on the southern sectors of the cone. Therefore, we sampled 72 undisturbed trees for minimum age dating in these sectors. One core per tree was extracted as close to the ground as possible to minimize the loss of rings due to sampling height. The position of all trees cored – disturbed and minimum age dating – was accurately marked on the geomorphic map.

In addition to the disturbed trees and the trees sampled for minimum age dating, we obtained two cores from each of 17 *L. decidua* and 18 *P. abies* trees outside the debris-flow cone for a reference chronology (e.g. Cook and Kairiukstis 1990).

3.2 Dating of Debris-Flow Events

The samples from the disturbed trees were analyzed using standard dendrochronological methods (see Stoffel and Bollschweiler 2008). These included surface preparation, counting of tree rings and measuring of tree-ring widths using a LINTAB measuring table and TSAP 3.0 software (Time Series Analysis and Presentation; Rinntech 2008). Tree-ring series were cross-dated with the reference chronology. Subsequently tree-ring series were analyzed visually to identify growth disturbances caused by past debris-flow events. We noted the presence of tangential rows of traumatic resin ducts as well as callus tissue bordering injuries, abrupt growth increase or decreases and the onset of compression wood. The identification of debris flow events was based on the number of samples simultaneously showing a growth disturbance and the distribution of affected trees on the cone. This spatial representation of trees affected during individual events allowed an assessment of the activity in currently inactive channels.

3.3 Minimum Age Dating

Several height-age models assume that apical growth is constant (e.g. Carmean 1972; Lenhart 1972; Schweingruber 1996) and an accurate estimate of apical growth

can be obtained from the data (McCarthy et al. 1991). Therefore, we divided tree height by the number of tree rings to get an average rate for the yearly apical increment for each tree. The sampling height was then divided by the yearly increment so as to estimate the number of rings between the root collar and coring height. The average correction factor for coring height averaged 3.3 years (min. 1; max. 9; STDEV: 2 years). In addition, the number of rings to pith was estimated whenever the pith was absent from the core. This correction was undertaken using a transparent sheet with concentric rings (Bosch and Gutierrez 1999). The missed-pith correction varied between 1 and 20 years with an average of 5.9 years per core (STDEV: 5.2 years). For samples where pith location was estimated, or where tree-rings near the pith are narrow or variable in width, this method has limited accuracy. As errors due to the presence of growth reductions are more likely to underestimate than overestimate the number of missed rings to the pith, these estimates should be considered "minimum ages" for the underlying forms and deposits.

As the tallest trees growing in a channel are not necessarily the oldest ones, we sampled, where possible, several trees per channel to minimize the risk of missing the oldest post-event tree.

We assumed that the growth of the young seedling is regular (McCarthy et al. 1991) as any sudden growth changes in the innermost rings that occur below the sampling height cannot be identified, Despite these potential errors, the minimum age dating of trees in debris-flow channels is a valuable estimate of the time elapsed since the last activity, though they may underestimate the real age of trees and, hence, the age of geomorphic forms they date.

Another factor that may influence the results is the time between channel clearing by debris flows and the recolonization of the channel by seedlings. (Pierson 2007) refers to this interval as germination lag time (GLT), while previous studies preferred the term "ecesis interval" (e.g. Desloges and Ryder 1990; McCarthy and Luckman 1993). According to Pierson (2007), this GLT for surfaces newly formed through lahars varies between 1 and 14 years. At our site, we believe that GLT are relatively short since climatic conditions are favorable for tree growth and seed sources are abundant. This assumption is supported by personal observations made on a cone formed by a rockslide at Grossgufer (see Schindler et al. 1993) in the same valley in 1991, where colonization of the cone had already started in the year following the event. As a result, we did not apply GLT corrections in our study, as it can be considered very low at the study site.

3.4 Determination of Last Date of Activity in a Channel

For the determination of the last date of debris-flow activity within abandoned channels, we sampled and dated disturbed trees. Where former channels occurred within undisturbed forested areas (i.e. no damaged or tilted trees were present) we determined the germination date of the oldest tree. The coupling of data on debris-flow events with data on minimum ages of undisturbed trees growing in

former channels allowed determination of the minimum time elapsed since the last event and therefore the assessment of spatio-temporal dynamics of past debris flows on the entire cone studied.

4 Results

4.1 Geomorphic Mapping

On the debris-flow cone of the Grosse Grabe torrent, an area of 30 ha was mapped at a 1:1000 scale and 29 abandoned channels were identified on its present-day surface. In addition, 61 segments of levees were mapped. These levees were comparably short and/or isolated and were not associated with obvious channel features. Lobate deposits are relatively scarce with only 14 forms identified on the cone. Figure 3 shows all forms mapped on the cone and the position of all trees sampled within this study. It can also be seen from Fig. 3 that the channels and their lateral levees are best developed in the upper part of the cone. Channels are less deeply incised and the debris-flow forms much smoother in the lower segments of the cone between the power line and the main road. This lower sector contains most of the lobate deposits. No deposits were mapped below the main road, because of the strong anthropogenic influence.

4.2 Growth Disturbances and Debris-Flow Frequency

The 71 heavily affected *L. decidua* and *P. abies* trees sampled on the cone allowed identification of 242 growth disturbances (GD; Table 1). In total, the analysis of GD occurring simultaneously in different trees allowed the reconstruction of 49 events between AD 1782 and 2005. Years with only one tree showing strong GD or with several trees showing moderate GD were not considered event. Figure 4 gives the reconstructed debris-flow frequency for the Grosse Grabe torrent. As can be seen from the illustration, the reconstruction yielded data for only a limited number of events in the nineteenth century. In contrast, the tree-ring records suggest several periods with increased activity during the twentieth century. Such clustering of events can primarily be identified for the periods 1905–1907, 1917–1928 and 1970–1982.

4.3 Approximation of Last Moment of Past Activity

Several of the channels shown in Fig 4 had no visible evidence of recent debris flow activity and therefore the minimum age of the last debris flow event was based on the age of the oldest trees growing in these abandoned debris-flow channels.

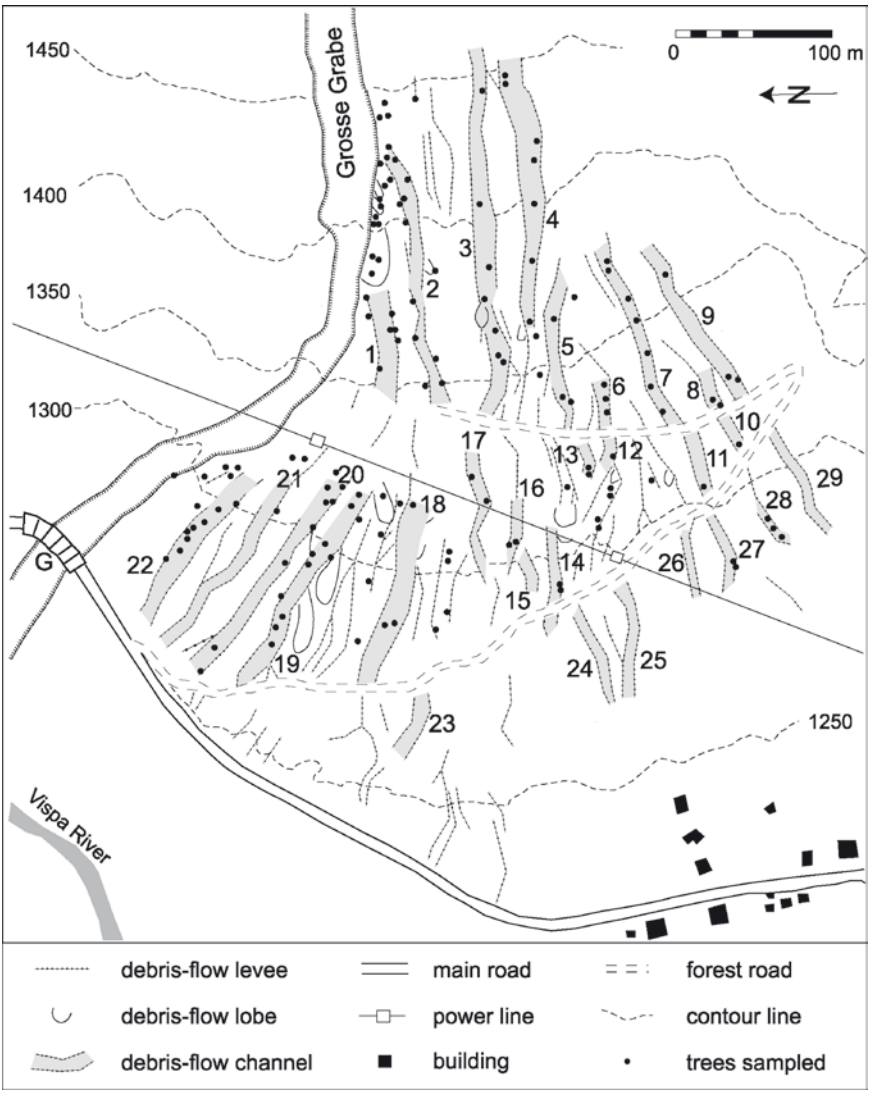

Fig. 3 Detailed geomorphic map (original scale: 1:1000) of all debris-flow landforms and deposits identified on the cone. The main road is protected by a road gallery (G). In total, 29 channels, 61 additional segments of levees and 14 lobate deposits could be identified

Table 2 gives an overview of the channels, the number of trees sampled per channel, the number of events reconstructed as well as the age of the oldest tree. A combination of all these data was then used to assess the minimum time that had elapsed since the last event.

Table 1 Types of growth disturbances identified in the 150 *Larix decidua* and *Picea abies* trees sampled

	Number	(%)
Tangential rows oftraumatic resin ducts	121	50
Compression wood	45	19
Growth increase	42	17
Growth decrease	26	11
Injuries	8	3
Total	242	100

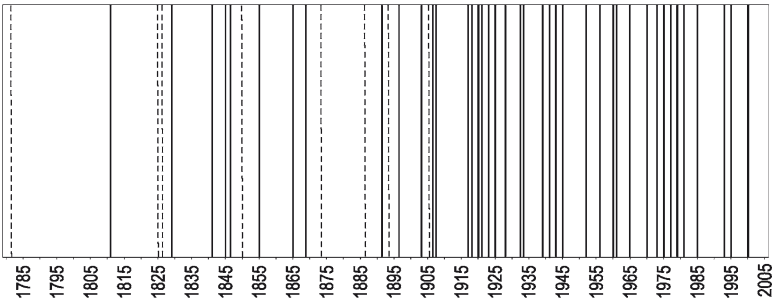

Fig. 4 Minimum debris-flow frequency for the Grosse Grabe torrent. In total, 49 events between AD 1782 and 2005 were reconstructed. Only a limited number of events could be reconstructed for the nineteenth century. Dashed lines indicate those events that were dated via the presence of growth disturbances occurring in a single tree

Figure 5a shows those channels where past debris-flow activity was dated by dendrogeomorphic methods. Here, years shown indicate the last year of activity in these channels. By way of example, it can be seen that trees in channels 16 and 17 both recorded the last event in 1925. In contrast, no event could be identified in channel 5 after 1908. The last events in the channels located next to the currently active one were dated as AD 1979 and 1985, respectively.

Figure 5b provides the age of the oldest living trees growing in channels with no sign of damage to trees by past debris-flow activity. The calendar years provide an estimate of the minimum time elapsed since the last event. Germination dates of the oldest living trees vary between AD 1817 and 1939.

Results of the two preceding investigations are summarized in Fig. 6, with calendar years indicating the last documented debris-flow activity in the channel. From our data, we observe that the time elapsed since the last debris-flow activity increases with distance from the current channel, with the last activity identified in the early 1980s close to the current channel, whereas there are no GD in trees from the southern and central sectors of the cone since the late nineteenth century.

Table 2 Dates for the last debris flow event in each track based on (1) dendrogeomorphic evidence of disturbance and (2) minimum ages of living trees in the channel. For the location of the individual channels see Fig. 3

Channel no.	No. of disturbed trees	No. of undisturbed trees	No. of events	Last event	Age of oldest tree in the channel	No event since
1	7	0	8	1979	1786	1979
2	15	0	28	1985	1735	1985
3	0	7	0	–	1912	1912
4	1	7	7	1956	1670	1956
5	1	2	2	1908	1649	1908
6	0	3	0	–	1898	1898
7	0	7	4	1939	1834	1939
8	0	2	0	–	1819	1819
9	0	3	2	1855	1841	1855
10	0	1	0	–	1866	1866
11	0	1	0	–	1834	1834
12	0	1	0	–	1894	1894
13	0	2	0	–	1879	1879
14	0	2	0	–	1909	1909
15	0	0	0	–	–	–
16	1	1	3	1975	1873	1975
17	1	1	1	1925	1752	1925
18	1	2	3	1973	1867	1973
19	8	3	9	1975	1740	1975
20	3	6	5	1945	1763	1945
21	3	0	4	1965	1875	1965
22	8	2	16	1977	1870	1977
23	0	0	0	–	–	–
24	0	0	0	–	–	–
25	0	0	0	–	–	–
26	0	0	0	–	–	–
27	0	2	0	–	1855	1855
28	0	3	0	–	1817	1817
29	0	0	0	–	–	–

5 Discussion and Conclusions

In this study, we report the reconstruction of debris-flow events on a forested cone in the Valais Alps (Switzerland) based on detailed geomorphic mapping and tree-ring analyses. Dendrogeomorphic investigations of 71 heavily affected *L. decidua* and *P. abies* trees allowed reconstruction of the frequency and the spatial extent of past debris-flow activity. In total, 49 events could be identified for the period AD 1782–2005.

The calculated debris-flow frequency represents the minimum number of events that occurred in this torrent in the recent past. The study of past events was mainly

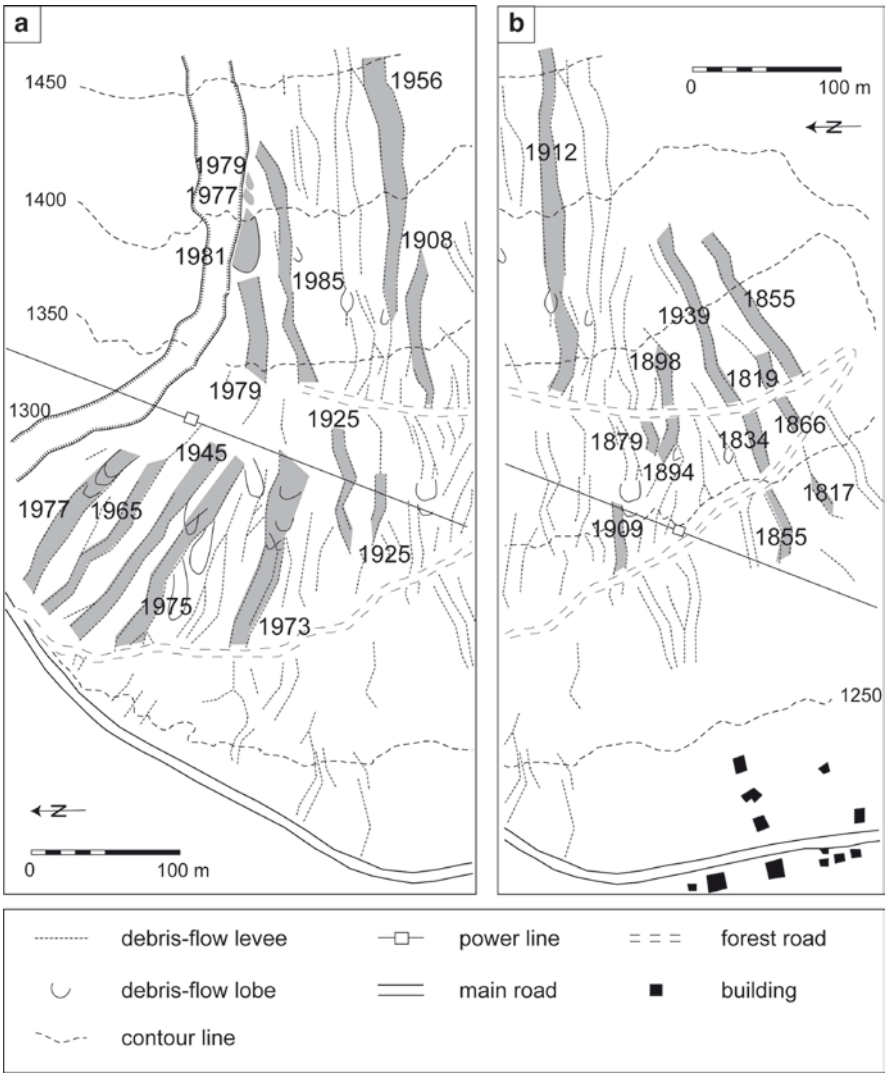

Fig. 5 (**a**) the last debris flow events in channels dated between 1908 and 1985 based on dendrogeomorphic evidence. (**b**) Minimum gages of debris flows (1817–1939) based on the oldest tree growing in the channel

limited by the age of the trees, which averaged only 140 years. As a result, the increasing number of events in the twentieth century is at least partially due to an increase in the number of sampled trees. In addition, it is possible that changing climatic conditions and the abundance of summer precipitation events at the end of the Little Ice Age and in the early twentieth century (Pfister 1999; Stoffel and Beniston 2006) may have had an effect on the release of debris flows and

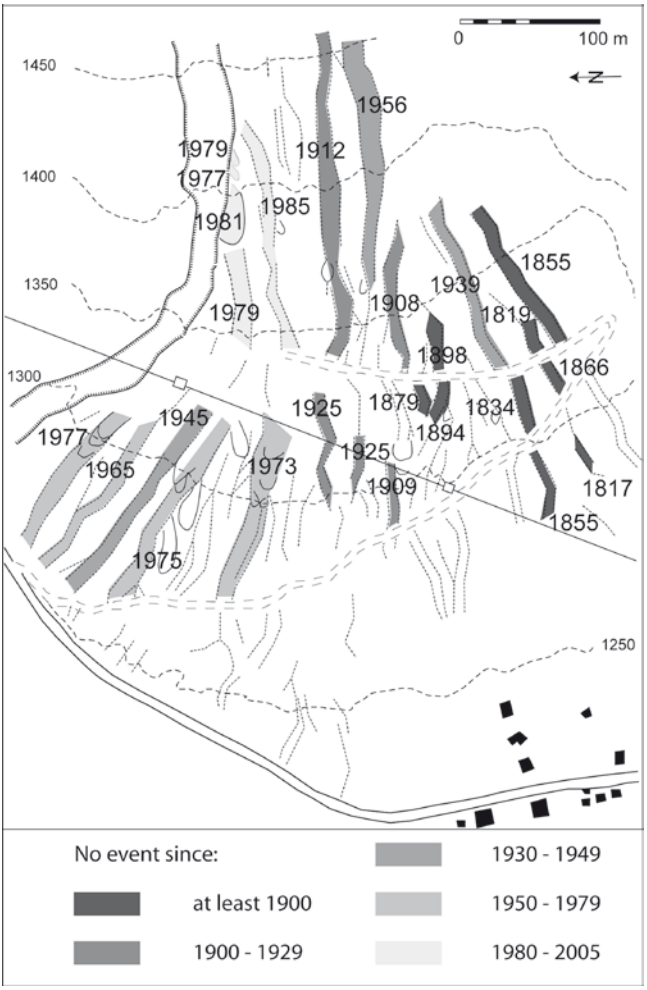

Fig. 6 Dates of the last debris flow in all channels on the Grosse Graber cone

therefore on the frequency as well. The apparent decrease in event frequency in this reconstruction in the 1980s was primarily due to bank stabilization measures, which prevented recent debris-flow surges from leaving the channel. As a result, it is probable that our tree-ring based reconstruction fails to detect recent small debris-flow surges.

Due to the absence of evidence of disturbance to trees growing in the former channels of the southern part of the cone, we selected 72 trees to provide a minimum age estimate of the last activity in these forms. The age of trees was determined through the counting of tree rings present on the increment cores and a correction factor for the missing rings due to the absence of pith on the

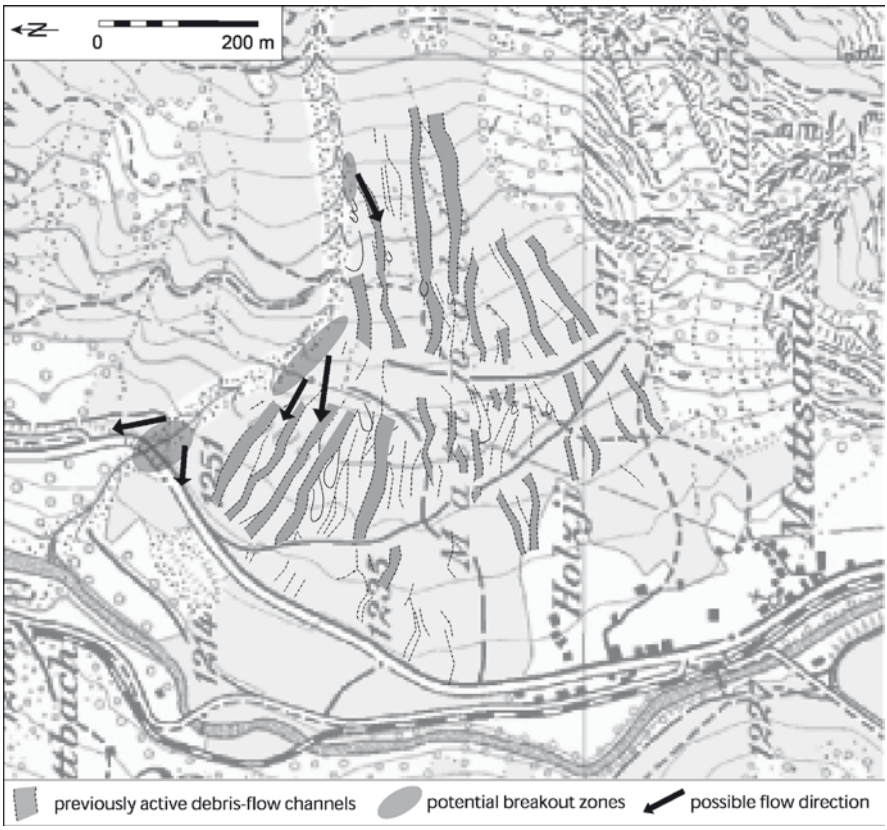

Fig. 7 Map indicating channel segments where potential breakouts could occur and re-activate abandoned channels on the forested cone of the Grosse Grabe torrent (Map reproduced by permission of swisstopo (BA071655))

cores (Bosch and Gutierrez 1999) and due to the sampling height. Even though the minimum age dating is an estimate because of pith correction, sampling height and possible variations in ecesis but we believe that ecesis is relatively short in this region and therefore the dates provided are reasonably accurate.

The coupling of tree-ring data with geomorphic mapping allowed the identification of segments along the currently used channel where overbank sedimentation or breakouts occurred during previous events. Consequently, the approach can be employed to designate sectors where breakouts and the re-activation of abandoned channels could potentially occur during future events. On the Grosse Grabe cone, the presence of three potential breakout zones could be identified (Fig. 7), with the uppermost located at 1,420–1,440 m a.s.l. Surges leaving the currently active channel in this sector would probably re-activate a channel that has regularly been used by past events. At 1,320–1,360 m a.s.l., where the active channel changes direction from east-west to southeast-northwest, breakouts could be reconstructed for several

events in the past, and are still evident today as shown by the presence of several deposits found on the cone surface. Consequently, currently abandoned channels could be re-activated at this location as well. The third potential breakout zone is located at the road gallery and could lead to sedimentation on the main road leading to the tourist resort of Zermatt. In addition, the geomorphic map provides evidence for a breakout location at the cone apex, upslope of the area investigated. Trees were not sampled in this sector because of the possible effects of snow avalanches and rockfall on tree growth would complicate the reconstruction of past debris flows.

Data obtained in this study provide an appropriate overview of the activity of channels present on the cone during the past century. Results clearly indicate that channels located close to the current channel have been occupied by regular debris-flow activity over the past decades. In contrast channels in the outermost section of the cone did not show signs of activity. Even though Fig. 6 shows a distinctive pattern of younger activity close to the current channel, this does not mean that there has been a continuous and progressive shift of activity across the cone surface. Presently inactive channels might be reactivated during future events. The information on past activity of debris-flows in the different sectors is of crucial importance for hazard assessment.

This paper demonstrates that that tree-ring analysis on forested cones can contribute to a better understanding of debris flow activity at basin-scale by reconstructing the frequency of events and the timing of the last activity in currently abandoned channels. Therefore, dendrogeomorphology is an essential component for a realistic assessment of hazards and the production of hazard maps for debris flow fans.

Acknowledgments The municipality of St.Niklaus and the Canton of Valais are warmly acknowledged for the financial support for this study. We would like to thank Simone Imseng and Sarah Gottet for the geomorphic mapping of the debris-flow cone. Reprinted from Bollschweiler et al. (2008) with permission from Elsevier.

References

Bollschweiler M, Stoffel M, Ehmisch M, Monbaron M (2007) Reconstructing spatio-temporal patterns of debris-flow activity using dendrogeomorphological methods. Geomorphology 87(4):337–351

Bollschweiler M, Stoffel M, Schneuwly DM (2008) Dynamics in debris-flow activity on a forested cone - A case study using different dendroecological approaches. Catena 72(1):67–78

Bosch O, Gutierrez E (1999) La sucésion en los bosques de *Pinus uncinata* del Pirineo. De los anillos de crecimiento a la historia del bosque. Ecologia 13:133–171

Cardinali M, Reichenbach P, Guzzetti F, Ardizzone F, Antonini G, Galli M, Cacciano M, Castellani M, Salvati P (2002) A geomorphological approach to the estimation of landslide hazards and risks in Umbria, Central Italy. Nat Haz Earth Syst Sci 2:57–72

Carmean WH (1972) Site index curves for upland oaks in the Central States. Forest Sci 18:102–120

Cook ER, Kairiukstis LA (1990) Methods of dendrochronology – Applications in the environmental sciences. Kluwer, London

Desloges JR, Ryder JM (1990) Neoglacial history of the Coast Mountains near Bella-Coola, British-Columbia. Can J Earth Sci 27(2):281–290
Goudie AS (2006) Global warming and fluvial geomorphology. Geomorphology 79(3–4):384–394
Haeberli W, Rickenmann D, Zimmermann M, Rössli U (1990) Investigation of 1987 debris flows in the Swiss Alps: General concept and geophysical soundings. IAHS Publ 194:303–310
Labhart TP (2004) Geologie der Schweiz. Ott Verlag, Thun
Lenhart DJ (1972) An alternative procedure for improving height-age data from stem analysis. Forest Sci 18:332
McCarthy DP, Luckman BH (1993) Estimating ecesis for tree-ring dating of Moraines – a comparative-study from the Canadian Cordillera. Arct Alp Res 25(1):63–68
McCarthy DP, Luckman BH, Kelly PE (1991) Sampling height-age error correction for spruce seedlings in Glacial Forefields, Canadian Cordillera. Arct Alp Res 23(4):451–455
Pasuto A, Soldati M (2004) An integrated approach for hazard assessment and mitigation of debris flows in the Italian Dolomites. Geomorphology 61(1–2):59–70
Pfister C (1999) Wetternachhersage. 500 Jahre Klimavariationen und Naturkatastrophen 1496–1995. Paul Haupt, Bern
Pierson TC (2007) Dating young geomorphic surfaces using age of colonizing Douglas fir in southwestern Washington and northwestern Oregon, USA. Earth Surf Process Land 32(6):811–831
Rickenmann D, Zimmermann M (1993) The 1987 debris flows in Switzerland: documentation and analyis. Geomorphology 8:175–189
Rinntech (2008) LINTAB – Precision ring by ring. In: www.rinntech.com/Products/Lintab.htm
Schindler C, Cuenod Y, Eisenlohr T, Joris CL (1993) Die Ereignisse vom 18. April und 9. Mai, 1991 bei Randa (VS) – ein atypischer Bergsturz in Raten. Eclogae Geol Helvetiae 86:643–665
Schweingruber FH (1996) Tree rings and environment. Dendroecology. Paul Haupt, Bern, Stuttgart, Wien
Seiler J, Zimmermann M (1999) Wildbachgefährdung durch den Grosse Grabe. Gutachten zur Gefahrenkarte. Geoplan, Steg
Shroder JF (1980) Dendrogeomorphology; review and new dating techniques of tree-ring dating. Progr Phys Geogr 4:161–188
Sigafoos RH, Hendricks EL (1969) The time interval between stabilization of alpine glacial deposits and establishment of tree seedlings. US Geol Surv Prof Paper 650B:B89–B93
Stoffel M, Beniston M (2006) On the incidence of debris flows from the early Little Ice Age to a future greenhouse climate: A case study from the Swiss Alps. Geophys Res Lett 33(16)
Stoffel M, Bollschweiler M (2008) Tree-ring analysis in natural hazards research – an overview. Nat Haz Earth Syst Sci 8(2):187–202
Stoffel M, Conus D, Grichting MA, Lievre I, Maitre G (2008) Unraveling the patterns of late Holocene debris-flow activity on a cone in the Swiss Alps: Chronology, environment and implications for the future. Global Planet Change 60(3–4):222–234
Winter LE, Brubaker LB, Franklin JF, Miller EA, DeWitt DQ (2002) Initiation of an old-growth Douglas-fir stand in the Pacific Northwest: a reconstruction from tree-ring records. Can J Forest Res 32(6):1039–1056
Zimmermann M, Mani P, Romang H (1997) Magnitude-frequency aspects of alpine debris flows. Eclogae Geol Helvetiae 90:415–420

Dendrogeomorphic Applications to Debris Flows in Glacier National Park, Montana USA

Forrest Wilkerson and Ginger Schmid

Dendrogeomorphology, the use of tree rings to determine the age of a geomorphic event such as debris flows, is a useful tool in determining the recurrence interval and to some extent, the magnitude, of potentially hazardous geomorphic events. Debris flows will damage trees as the debris moves downhill. The impact scars can be dated by counting the tree rings that have grown since the impact, or by determining the year of the onset of suppression rings or reaction wood. The following example refers to the use of dendrogeomorphology in the examination of debris flow hazards within Glacier National Park, Montana USA.

Our 10-year study of debris flows in Glacier National Park focused on forty-one separate debris flows in seven drainage basins within Glacier National Park, Montana USA (Wilkerson and Schmid 2003). We applied a combination of geomorphic techniques including dendrochronology, lichenometry, vegetation succession, event stratigraphy, and repeat photography to investigate the geomorphologic variables responsible for these debris flows (Fig. 1). The dendrogeomorphic analysis of tree cores and cross sections was critical in establishing a chronology for undocumented debris-flow events (Fig. 2).

Tree-ring records were used to delineate the age of a specific debris-flow event that had impacted or damaged a specific tree, or were used as proxy data for determining the minimum age of debris flow deposits or channel incision (McCarthy and Luckman 1993; Pierson 2007). If a tree had obvious impact damage from moving debris-flow rocks, then an absolute date for that event could be determined. If a tree was growing on either the deposits or within the debris-flow channel, then a minimum age could be determined for the event associated with that portion of the debris-flow landform. Minimum ages are less accurate than absolute ages due to the unknown time period between the debris flow event and when the debris stabilized enough to allow tree growth to begin.

Snow avalanches are common in Glacier National Park, and avalanche impact on trees can be difficult to discern from debris-flow impacts. Although a total of 39

F. Wilkerson (✉) and G. Schmid
Department of Geography, Minnesota State University, 56001 Mankato MN, USA
e-mail: forrest.wilkerson@mnsu.edu

M. Stoffel et al. (eds.), *Tree Rings and Natural Hazards: A State-of-the-Art*,
Advances in Global Change Research 41, DOI 10.1007/978-90-481-8736-2_19,

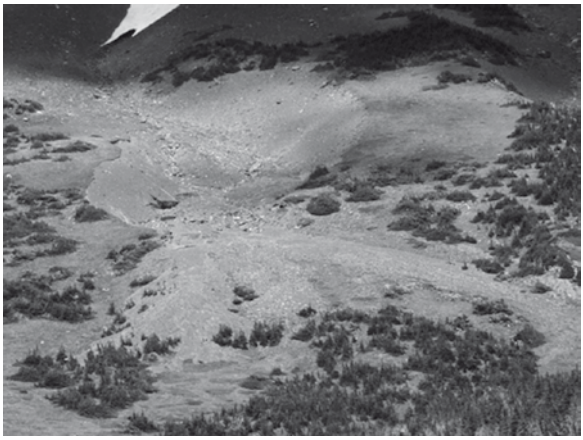

Fig. 1 The Apikuni Creek Big Red debris flow (Apikuni number 1) is evolving into a first order channel that drains the summit of Apikuni Peak. This landform has witnessed repeated debris-flow activity, with four known events since 1994. Note the impact of the channel incision on trees along the upper edges, and within the lower toe deposits

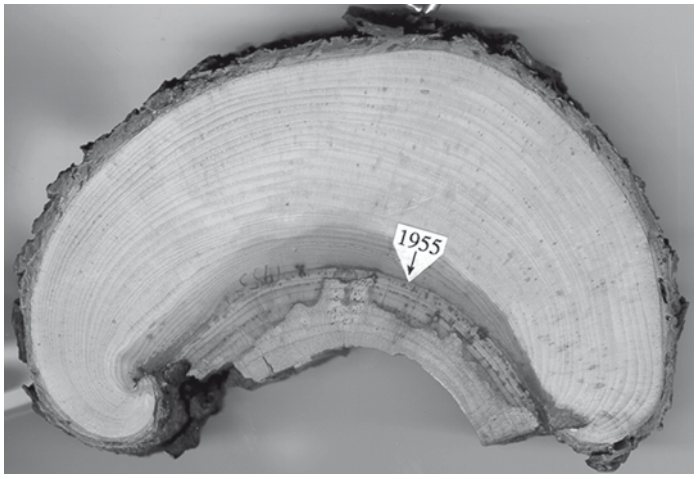

Fig. 2 An image of a cross section removed from the Windy Creek debris flow. The tree was severely damaged and partially buried by a debris flow that occurred in 1955. The damaged portion of the tree visible near the bottom of the photograph was facing upslope

tree cores and 13 cross sections were sampled for dendrochronologic analysis, only 24 cores and six cross-sections produced results that could confidently be identified as debris flow impact and not snow avalanche damage.

The results of the dendrogeomorphic event chronology are summarized in Table 1.

Table 1 Summary of dendrochronology analysis of debris flows in Glacier National Park, Montana

Drainage basin	Debris flows sampled (Year sampled)	Event chronology (c = core; xs = cross section)
Apikuni	1 (1997)	1906c, 1934c, 1956c
	2 (1997)	1930c
	3 (1997)	1898c, 1906c, 1932c
Appistoki	1 (1997)	1959c
	2 (1997)	1959c
Kennedy	1 (1997)	1984c
	2 (1997)	1955c, 1977c
	3 (1997)	1935c, 1952c, 1974c
	4 (1997, 2000)	1842c, 1857xs, 1947xs, 1964xs, 1968xs, 1979xs
Rose	1 (1994)	1904c, 1921c, 1961c
	2 (1997, 1999)	1954c, 1964c
Windy	1 (1997)	1955xs

Although the initial hypothesis behind our research was that basin-wide storm events would be identified as the trigger responsible for initiating debris flows, it can be seen from the data that storm events are not necessarily consistent within basins. Only three years have a dendrogeomorphic signal that records more than one debris flow in the same year: 1906 in the Apikuni basin, 1959 in the Appistoki basin, and 1955 in two basins sharing a common drainage divide, Kennedy and Windy.

These results are complicated by the fact that not all debris flows had trees that could be sampled and not all debris-flow events will impact the trees that are present. Despite these complications, the combination of using the tree cores along with other geomorphic techniques, led to the conclusion that the interaction of several geomorphic variables unique to each landform are responsible for the initiation of debris flows in Glacier National Park. Antecedent storm conditions (water content in the slope debris) and storm characteristics are the most important variables on the scale of each individual debris flow landform. Isolated summer thunderstorms provide enough water to initiate flows, but are highly variable in scale. Larger, basin-scale rain on snow events are also important, but are again going to be controlled by the antecedent snowpack conditions on each slope.

References

McCarthy DP, Luckman BH (1993) Estimating ecesis for tree-ring dating of moraines: a comparative study from the Canadian Cordillera. Arct Antarc Alp Res 25:63–68

Pierson TC (2007) Dating young geomorphic surfaces using age of colonizing Douglas fir in southwestern Washington and northwestern Oregon, USA. Earth Surf Process Land 32:811–831

Wilkerson FW, Schmid GL (2003) Debris flows in Glacier National Park Montana. Geomorphology 55:317–328

Frequency–Magnitude Relationships, Seasonality and Spread of Debris Flows on a Forested Cone

Markus Stoffel

1 Introduction

Debris flows repeatedly cause damage to infrastructure or even loss of life on cones or at the mouth of gullies (Jakob and Hungr 2005). With the projected greenhouse warming (Christensen and Christensen 2007), there is much debate about changes in the frequency, magnitude and seasonality of precipitation events and related flooding or mass-wasting processes (Milly et al. 2002). Before establishing any cause-and-effect relationship between global warming and the incidence of geomorphic processes, the natural variability of extreme weather events must be examined as well as detailed information obtained on past process dynamics on debris-flow cones, alluvial fans or floodplains. Sletten et al. (2003) pertinently emphasize that records of past debris-flow activity may be particularly useful in the recognition of past process dynamics and precipitation events. Individual debris flows are usually released during intense rainfall (Caine 1980; Blikra and Nemec 1998) and repetitive debris flows usually occur in sediment-rich catchments, as long as the triggering precipitation events are recurring (Zimmermann et al. 1997). In addition, debris-flow deposits have a high preservation potential on cones and can therefore be used for the analysis of spatial patterns of past events (Bollschweiler et al. 2007).

While chronostratigraphic records on past debris-flow activity exist for several case-study areas of northern Europe or the United States (e.g. Jonasson 1993; Matthews et al. 1997; Blair 1999), such reconstructions remain widely non-conclusive for the European Alps in general and for Switzerland in particular.

It is therefore the purpose of this paper to assess late Holocene debris-flow activity and process dynamics on a forested cone in the Swiss Alps using dendrogeomorphic

M. Stoffel (✉)
Laboratory of Dendrogeomorphology, Institute of Geological Sciences,
University of Bern, CH-3012 Bern, Switzerland
and
Chair for Climatic Change and Climate Impacts, Institute for Environmental Sciences,
University of Geneva, CH-1227 Carouge-Geneva, Switzerland
e-mail: markus.stoffel@dendrolab.ch

M. Stoffel et al. (eds.), *Tree Rings and Natural Hazards: A State-of-the-Art*,
Advances in Global Change Research 41, DOI 10.1007/978-90-481-8736-2_20,

methods. Through the identification of surface deposits and analysis of 2,246 tree-ring series obtained from 1,102 old-growth trees disturbed by past debris flows, this paper focuses on (i) the investigation of the frequency and timing of events, (ii) the dating and quantification of material deposited on the present-day cone surface, and on (iii) the discussion of potential effects of projected changes in climatic conditions upon the frequency and magnitude of events in a future greenhouse climate.

2 Study Area

The analysis of debris-flow dynamics and growth disturbances in century-old trees was conducted around the Ritigraben torrent (Grächen, Switzerland, 46° 11' N, 7° 49' E). Figures 1 and 2a show the torrent beginning at 2,600 m a.s.l. In its source zone,

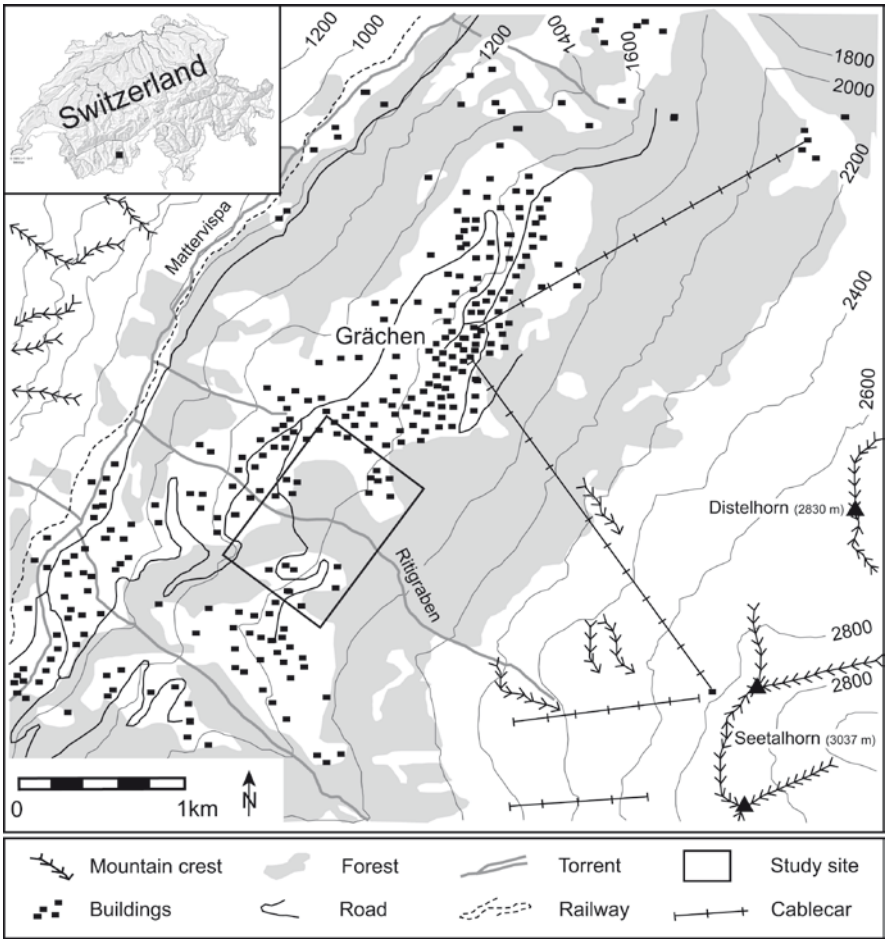

Fig. 1 The Ritigraben torrent (Valais, Swiss Alps) rises from its source at 2,600 m a.s.l. and passes through a forested cone located on a structural terrace near the village of Grächen, before converging with the Mattervispa river (1,080 m a.s.l.)

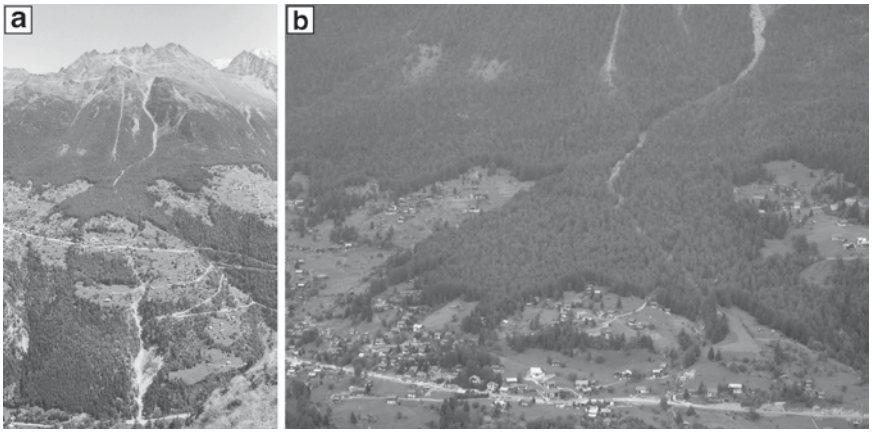

Fig. 2 (**a**) Photo of the Ritigraben debris-flow system from its source to the confluence (catchment area: 1.36 km^2, channel lengths: 3.5 km). (**b**) Detailed view of the intermediate debris-flow cone (32 ha) and its mixed conifer stand

geophysical prospecting and BTS measurements indicate the existence of contemporary permafrost (Lugon and Monbaron 1998).

On its downward course to the Mattervispa river, the torrent passes a large forested cone (32 ha; ca. 4.3×10^6 m^3) on a structural terrace (1,500–1,800 m a.s.l.), where debris-flow material affects trees within an old-growth stand comprised of European larch (*Larix decidua*), Norway spruce (*Picea abies*) and Swiss stone pine (*Pinus cembra*). Figure 2b illustrates the intermediate debris-flow cone, which is of Holocene age.

At the confluence of the Ritigraben torrent with the Mattervispa River at 1,080 m a.s.l., depositional features are lacking and debris-flow material is immediately eroded. Debris-flow material consists of heavily disintegrated, weathered metamorphic granites of Permian age partly originating from the steep source zone of the Ritigraben torrent, where an active rock glacier provides material for the initiation of debris flows. Further debris is mobilized from the channel, which is continuously recharged with fallen rocks or through bank erosion. Although mean rock sizes on the cone surface generally remain well below 2 m in diameter, there is also evidence that boulders with volumes exceeding 10 m^3 have been transported by debris flows in the past.

The high elevation of the source area currently restricts debris-flow activity in the Ritigraben torrent from June to September (Stoffel et al. 2005a; Stoffel and Beniston 2006). Present-day debris-flow activity is initiated by persistent precipitation in fall and thunderstorms in summer. The documentation of past events only covers the last 20 years, with the "largest event ever" recorded in 1993 having eleven erosive surges and an estimated volume of 60,000 m^3 (Zimmermann et al. 1997).

Geomorphic processes other than debris flows are negligible at the study site: Snow avalanches have never been witnessed on the Ritigraben cone. Similarly, the source area and bed lithology are not suitable for the formation of floods and the torrent lays dry during most of the year. Rockfall exclusively occurs in its uppermost part, which has been disregarded for analysis.

3 Material and Methods

3.1 Geomorphic Mapping of Debris-Flow Channels and Deposits

Analysis of past debris-flow activity began with a detailed mapping of all features associated with past events, such as lobes, levees or abandoned flow paths on a scale of 1:1000. Features and deposits originating from other geomorphic processes or anthropogenic activity were indicated on the map as well, so as to avoid misdating of debris-flow events. Due to the presence of a relatively dense forest cover, GPS could not be used on the cone, which is why geomorphic mapping was executed with a tape, inclinometer and compass. In addition, the mean size of blocks was measured for every individual lobe and levée (<0.5, 0.5–1, 1–2 m) and the vegetation cover present on the features was qualitatively assessed (light, medium, dense).

3.2 Sampling Design

On the intermediate debris-flow cone covering approximately 32 ha, a majority of the century-old conifers show visible growth defects related to past debris-flow activity (i.e. tilted stems, partial burying of the trunk, destruction of root mass, scars). Based on the detailed geomorphic map and on an outer inspection of the stem surface, trees obviously disturbed by past debris flows were preferably sampled.

In this investigation, at least two cores were extracted per tree using increment borers, one in the flow direction of past debris flows and the other on the opposite side of the trunk. In order to gather the greatest amount of information on the growth disturbances (GD) caused by past events, increment cores were preferably sampled at the height of the visible damage or within the segment of the stem tilted during past events. In the case of visible scars, further increment cores were extracted from the wound and the overgrowing callus tissue.

In addition to the disturbed trees sampled on the cone, undisturbed reference trees were selected from a forest stand located southwest of the cone. For every single reference tree, two cores per tree were extracted parallel to the slope direction. In total, 1,204 trees were sampled (2,450 increment cores): 539 *L. decidua*, 429 *P. abies* and 134 *P. cembra* trees (2,246 cores) from the cone as well as 102 trees (204 cores) of the same species from undisturbed reference sites. In contrast to the disturbed trees, increment cores of the reference trees were extracted at breast height (≈130 cm).

Data recorded for each tree sampled included: (i) determination of its position within levees, flow channels or on deposits; (ii) sketches and position of visible disturbances in the tree morphology such as tilted stems, partial burying of

the stem, destruction of root mass or erosion as well as scars; (iii) position of the sampled cores on the stem surface; (iv) diameter at breast height (DBH) derived from circumference measurements; and (v) data on neighboring trees.

3.3 Debris-Flow Frequency and Timing of Events

Samples were analyzed and data processed following the standard procedures described in Stoffel and Bollschweiler (2008). Single steps of sample analysis included surface preparation, skeleton plots as well as ring-width measurements using digital LINTAB positioning tables connected to a Leica stereomicroscope and TSAP 3.0 software (Rinntech 2008). Growth curves of the disturbed samples were then crossdated with the corresponding reference chronology constructed from undisturbed trees for each of the three conifer species sampled on the cone (*L. decidua*, *P. abies*, *P. cembra*), in order to separate insect attacks or climatically driven fluctuations in tree growth from GD caused by debris flows.

Growth curves were then used to determine the initiation of abrupt growth reduction or recovery (McAuliffe et al. 2006). In the case of tilted stems, both the appearance of the cells and the growth curve data were analyzed (Braam et al. 1987; Fantucci and Sorriso-Valvo 1999). Finally, the cores were visually inspected so as to identify further signs of past debris-flow activity in the form of callus tissue overgrowing abrasion scars or tangential rows of traumatic resin ducts (TRD) formed following cambium damage (Stoffel 2008; Bollschweiler et al. 2008).

As conifer trees react immediately to damage with the formation of callus tissue or TRD, the intra-annual position of these disturbances (i.e. early, mid and late earlywood as well as early and late latewood; for details see Stoffel et al. 2005b or Stoffel et al. 2010) was used to assess the timing of debris-flow activity in particular years. For the Valais Alps, highly-resolved data exist on the timing and different periods of radial growth of *L. decidua* and *P. abies* (Müller 1980), rendering dating of past debris-flow events at Ritigraben possible with monthly precision. The results obtained on the intra-seasonal timing of debris-flow events were then compared with precipitation records from a local meteorological station, operational since December 1863 (Stoffel et al. 2010), and with archival data on flooding events in rivers of the Valais Alps (Lütschg-Lötscher 1926; Röthlisberger 1991).

3.4 Dating of Deposits and Spatial Spread of Events

After the dating of GD on the increment cores, we assessed the age of lobes by attributing severe GD in the tree-ring series to the deposits in the field.

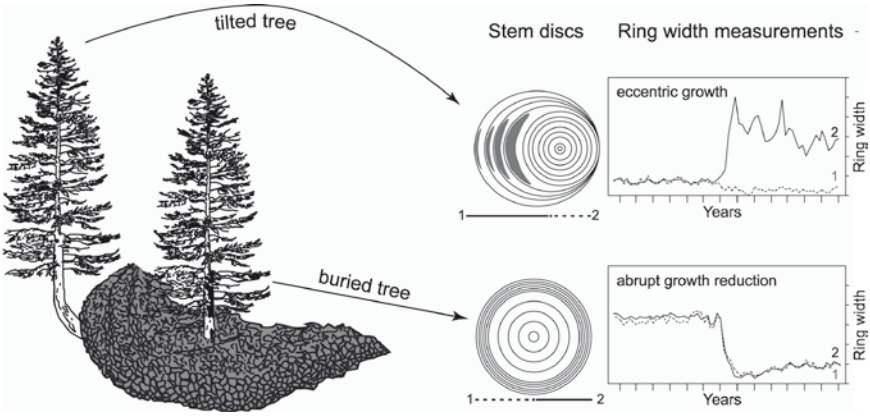

Fig. 3 Tree-ring 'signatures' used to determine the age of debris-flow deposits

As exemplified in Fig. 3, dating of a lobe was only possible if (i) a survivor tree was injured through the deposition of material (callus tissue or TRD in the growth ring); (ii) its stem base was buried by debris (abrupt growth reduction in ring widths); or (iii) if it was tilted (eccentric growth rings and presence of reaction wood).

Special attention needs to be addressed to multiple GD identified in the tree-ring series. Here, only the geomorphic features left during the most recent event could be dated. Older episodes of GD identified using dendrogeomorphic methods may have been caused either by surges that passed through without leaving material or by deposits that were later eroded or overridden by more recent debris-flow activity.

3.5 Magnitude–Frequency Relationships of Debris Flows

Magnitudes of previous events were assessed for the last 150 years based on (i) the volumes deposited during individual events, (ii) mean and (iii) maximum sizes of boulders transported, (iv) the damage caused to the vegetation (tree removal), (v) the distribution of even-aged deposits and levees on the cone, (vi) the seasonal timing of events (determining the availability of material from the active layer of the rock glacier), as well as (vii) the type, (viii) duration and (ix) severity of the precipitation event leading to the release of the debris flows (Stoffel et al. 2010). Magnitudes are given qualitatively and past incidences classed into small ($S = 10^2 - 10^3$ m^3), medium ($M = 10^3 - 5 \times 10^3$ m^3) large ($L = 5 \times 10^3 - 10^4$ m^3) and very large ($XL = 10^4 - 5 \times 10^4$ m^3) events (Stoffel 2010).

4 Results

4.1 Debris-Flow Features and Deposits

Geomorphic mapping permitted identification of 769 features relating to past debris-flow activity on the intermediate cone of the Ritigraben torrent. The features and deposits inventoried in the study area covering 32 ha included 291 lobes, 465 levees and 13 well-developed debris-flow channels. Figure 4 illustrates the features identified on the cone and provides indications of the density of the vegetation cover. Further details on the mean diameter of blocks deposited in the lobes as well as information on the vegetation cover present on the lobes are given in Table 1. The mean block size generally remains <1 m and almost half of the deposits are covered with dense vegetation. Lobes containing mostly large blocks (1–2 m) are sparsely vegetated, whereas deposits with finer rock fractions (<0.5 m) normally have a very dense vegetation cover.

The length of lateral levees varies from a few to several dozens of meters. Whereas some of these lateral levees appear quite isolated on the actual surface of the cone, others can easily be attributed to one of the twelve major channels that were in use before the erosive 1993 event and incision of the main channel.

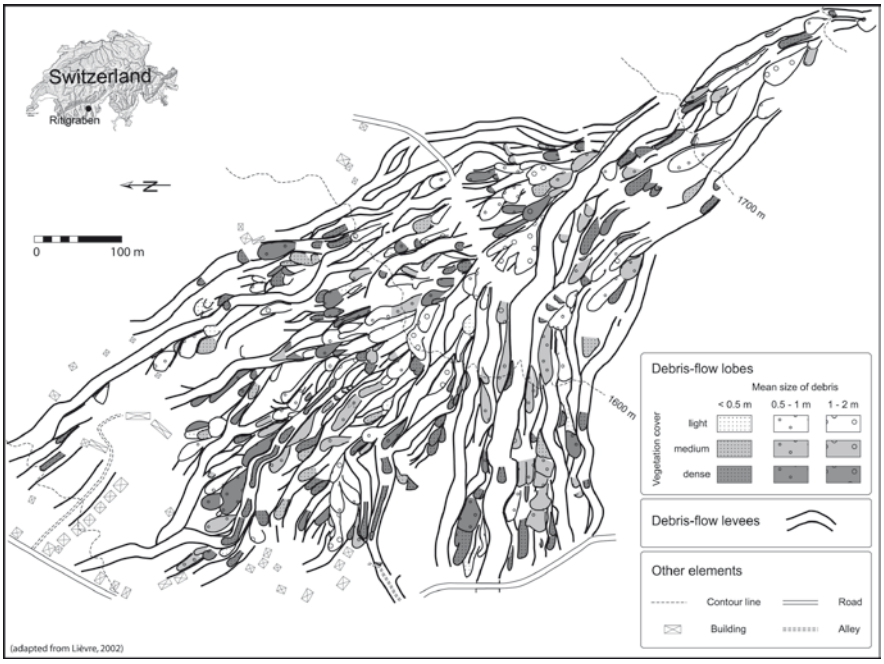

Fig. 4 Detailed geomorphological map of the intermediate debris-flow cone with lobes, levees and channels. The key indicates the density of the vegetation cover and the mean size of debris on the lobes

Table 1 Mean block size identified in and vegetation cover on the deposits

Vegetation cover	Mean diameter of blocks in deposits			
	<0.5 m	0.5–1 m	1–2 m	Total
Light	13	55	20	88 (30%)
Medium	21	47	4	72 (25%)
Dense	86	42	3	131 (45%)
Total	120 (41%)	144 (50%)	27 (9%)	291 (100%)

Table 2 Relative number of types of growth disturbances (GD) used to infer past debris-flow activity from increment cores. TRD = tangential rows of traumatic resin ducts

Growth anomaly	Number	(%)
TRD	987	43.6
Wound	118	5.2
Callus tissue	22	1.0
Reaction wood	728	32.1
Growth reduction	194	8.6
Growth release	214	9.5
Total	2263	100.0

The currently abandoned flow tracks are still clearly visible over large parts of the cone, although parts of their banks have collapsed and their beds are now filled with fallen debris and vegetation.

4.2 Age and Growth Disturbances in Trees

Data on the innermost rings of the 1,102 *L. decidua*, *P. abies* and *P. cembra* trees sampled on the cone varied from AD 1492 to 1962 with 53% of the increment cores showing more than 300 tree rings at sampling height and old trees being quite evenly spread over the cone.

Analysis of the disturbed trees allowed reconstruction of 2,263 GD caused by passing debris-flow surges or the deposition of material on the cone. Table 2 shows that signatures of past events were mainly identified on the increment cores via TRD (43.6%) or reaction wood (32.1%). Abrupt growth recovery (9.5%) or reductions (8.6%) were only occasionally found in the tree-ring series and wounds (5.2%) and overgrowing callus tissue (1%) was rarely present in the cores.

4.3 Debris-Flow Frequency and Timing of Events

In total, dendrogeomorphic analysis of the increment cores allowed reconstruction of 124 debris-flow events covering the last 440 years. The reconstructed occurrence

of debris flows is given in Fig. 5. From the data, it appears that periods of repeated debris-flow activity alternate with phases of little or almost no activity. Such clustering of events is especially obvious in the early 1870s, the 1890s and between the late 1910s and 1935.

The number of increment cores available for analysis at any one moment in the past is shown by a dotted line indicating 'sample depth' in Fig. 5. Based on the large sample depth used in the reconstruction and the distribution of old trees on the cone, it can be assumed that the GD caused by most events of the last 300 years have been recorded. Prior to this period, the decreasing number of trees available for analysis may influence the quality of the reconstructed frequency.

In Fig. 6, the reconstructed frequency is broken down into 10-year periods, with bars representing variations from the mean decadal frequency of debris flows for the period 1706–2005, when 3.26 events occurred every 10 years. Results illustrate that the frequency of events generally remained well below average during most of the classical Little Ice Age (LIA, 1570–1900; Grove 2004). Periods with increased debris-flow activity only start to emerge from the data after the last LIA glacier advance in the 1860s. This period of increased activity continued well into the early twentieth century reaching a peak between 1916 and 1935. During these 20 years, the tree-ring series indicate 14 events. Results further illustrate that this major

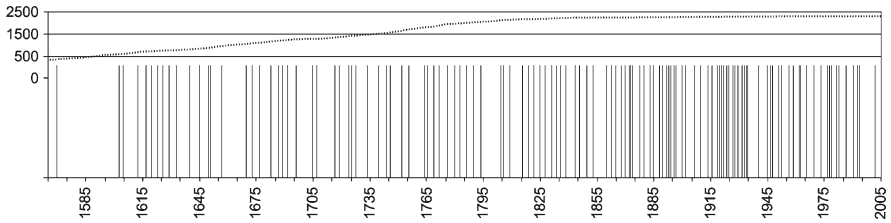

Fig. 5 Tree-ring based reconstruction of debris flow activity at Ritigraben between AD 1566 and 2005 containing 123 events. The sample depth (*dotted line*) shows the number of cores available for analysis at specific years in the past

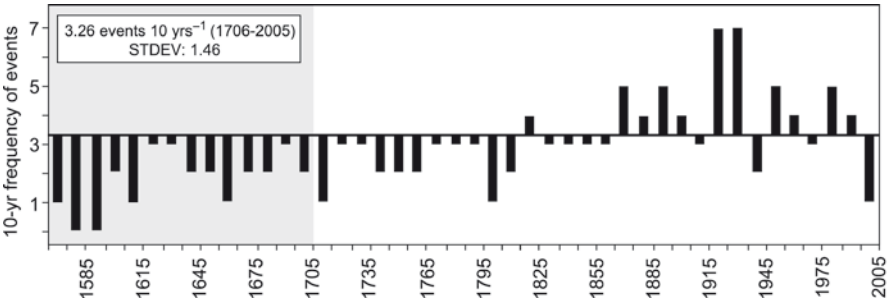

Fig. 6 Reconstructed 10-year frequencies of debris-flow events between AD 1566 and 2005. Data are presented as variations from the mean decadal frequency of debris flows of the last 300 years (AD 1706–2005). The gray surface indicates the period where sample size may influence the number of reconstructed events

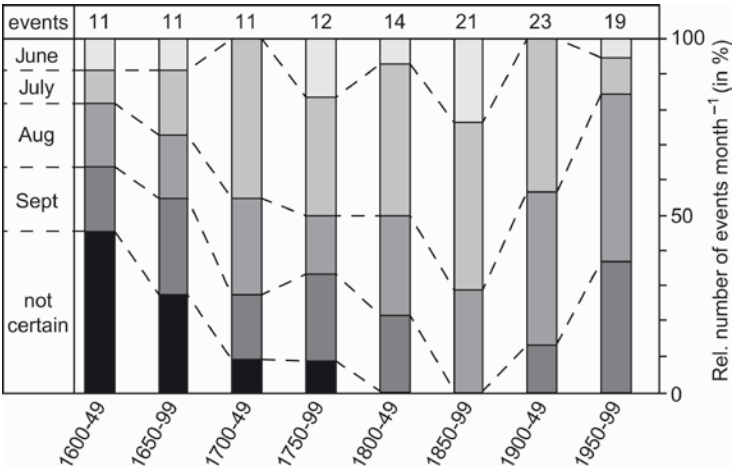

Fig. 7 Seasonality (JJAS) of past debris-flow activity as inferred from the intra-annual position of TRD in the tree ring, archival data on flooding as well as meteorological data (1863–2005)

episode of activity was followed by a decrease in debris flows, with particularly low activity over the last 10-year period (1996–2005), with only one debris-flow event recorded on August 27, 2002. The three lowest debris-flow activity periods in the last 300 years occurred in the 10-year periods of 1706–1715 and 1796–1805 and during the most recent 10 years.

The timing of past events was established by comparison of the intra-annual position of TRD in the tree rings with highly-resolved growth data of *L. decidua* and *P. abies* from the Valais Alps, meteorological records from the local MeteoSwiss station (1863–2005) and with archival data on river flooding in the Valais Alps. Results showing the timing of debris-flow activity, presented in Fig. 7, indicate that events generally occurred much earlier in summer prior to 1900. This is especially true for the period 1850–1899, when more than 70% of the reconstructed debris-flow events took place in June and July, with none in September. In the twentieth century, debris-flow activity clearly shifted towards August and September, with only one event registered in June after AD 1962. Our reconstructions suggest that snowfall and frozen ground has inhibited debris entrainment from the source zone (>2,600 m a.s.l.) during precipitation events between October and May.

4.4 Dating of Deposits and Spatial Spread of Events

The analysis of injured, buried or tilted survivor trees in deposits allowed dating of 249 out of the 291 lobes identified on the intermediate cone (86%). Attribution of GD to a specific lobe was most frequently achieved through the presence of TRD or

reaction wood in trees located close to the snout of lobes. Due to the considerable size of boulders transported by individual surges, trees located in the flow path of debris flows were normally eliminated or died as a result of excessive burying. As a consequence, buried survivor trees were less readily available on the cone and abrupt growth suppression was only occasionally identified in the tree-ring records. Dating was not possible for 42 lobes (14%), where trees were simply not present for analysis or did not show severe GD caused by past activity in their tree-ring record.

A majority of lobes that are visible on the present-day surface of the cone were deposited over the last 80 years. Although more than a third of the reconstructed debris-flow events occurred prior to 1790, only six lobes (2.4%) could be attributed to that period, with the oldest material dated on the cone to AD 1705.

Some 68 lobes (27.3%) were attributed to the period 1794–1897 and even 92 lobes (37%) were dated to the first third of the twentieth century (1897–1934). For the early decades of the twentieth century dated material is largely restricted to the southwestern part of the cone and it seems that the 1922 event considerably remodeled the morphology of the cone around 1,650 m a.s.l., leaving 26 lobes on the present-day surface. As a result, the central part of the cone was cut-off for further debris-flow activity and surges were directed to the southwestern sectors of the cone. Finally, 83 deposits (33.3%) were attributed to events that have occurred during the last 70 years (1935–1993). Selected events for the period 1916–1993 are presented in Fig. 8.

Fig. 8 Deposition of debris-flow material on the intermediate cone during selected events between 1916 and today

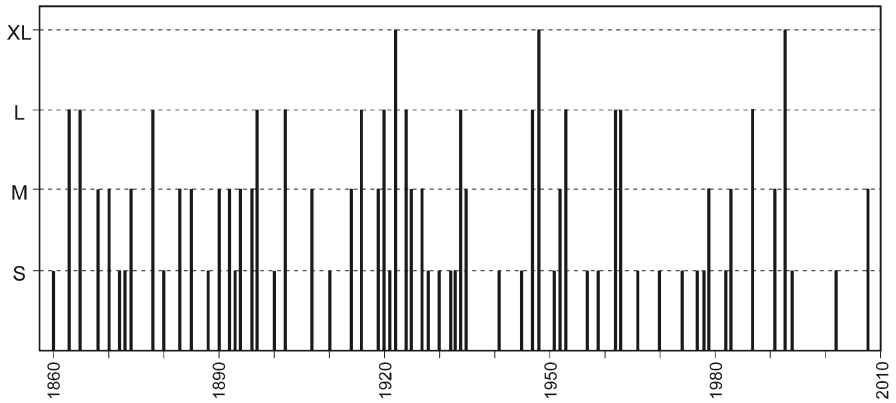

Fig. 9 Frequency distribution of debris-flow magnitudes for the last 150 years (AD 1858–2008). Note the clustering of important events in the early decades of the twentieth century and the absence of *class XL* debris flows before 1922

4.5 Frequency–Magnitude Relationships

Based on the material deposited on the cone, mean and maximum sizes of boulder, data on tree removal, the seasonal timing of events as well as the type, duration and severity of the precipitation event, magnitudes of previous events are given qualitatively as very small, small, medium, large and very large events.

Figure 9 illustrates the magnitudes of the 63 events identified in the tree-ring series for the period AD 1858–2008. From the data, it appears that 41% of the reconstructed debris-flow events were either very small or small, with volumes involved <1,000 m^3. Medium-size events transporting less than 5,000 m^3 each are identified 20 times (32%), whereas 14 debris flows (22%) are considered to have been large incidences ($5 \times 10^3 - 10^4$ m^3). During three events (5%), very large debris flows occurred at the study site, namely in 1922, 1948 and 1993. Although the event of August 1922 transported much more than 10,000 m^3, its volume remains certainly much smaller than the 60,000 m^3 transported during the 11 surges in September 1993. The importance of the September 1948 event is, in contrast, much harder to assess, as the mobilization of material on the cone has led to a strong incision of the channel, maybe comparable to that in 1993.

5 Discussion and Conclusions

In the study presented here, increment cores extracted from 1,102 living *L. decidua*, *P. abies* and *P. cembra* trees allowed reconstruction of 2263 GD belonging to 124 debris-flow events since AD 1566. In addition, 86% of the deposits identified on

the present-day surface of the intermediate cone of the Ritigraben torrent (Valais, Swiss Alps) were dated, spatial patterns of past activity identified, and frequency-magnitude relationships of debris flows assessed.

Based on the evidence presented above, it is possible to characterize climatic and meteorological factors driving debris-flow activity at the case-study site. Between the 1570s and 1860s, cool summers with frequent snowfalls at higher elevations (Pfister 1999) regularly prevented the release of debris flows. The warming trend combined with greater precipitation totals in summer and fall between 1864 and 1895 resulted in an increase in conditions favorable for the release of debris flows. Enhanced debris-flow activity continued well into the twentieth century and the reconstruction exhibits a clustering of events for the period 1916–1935, when warm-wet conditions prevailed during summer (Pfister 1999). The reconstructed frequency is also in agreement with documented data on flooding events in Alpine rivers (Lütschg-Lötscher 1926; Röthlisberger 1991), where a scarcity of flooding events is observed for most of the LIA and during the mid-twentieth century. However, floods in neighboring Alpine rivers became more frequent in the 1830s (Pfister 1999), 3 decades before activity increased at the study site.

The timing of events also underwent changes and a clear shift in debris-flow activity from June and July to August and September is observed over the twentieth century. Findings are in agreement with data from Schmidli and Frei (2005), indicating a decrease in heavy summer rainfall and a slightly positive trend in heavy fall precipitation intensities for the wider case-study area.

The assessment of magnitudes based on tree rings, superficial deposits and meteorological data has its limitations, as the release of debris flows and the ensuing magnitude of events not only depend on precipitation intensities and duration, but also on sediment availability in the source zone and the channel. In the present case, an active rock glacier delivers sediment to the departure zone and the main channel is continuously recharged with fallen rocks and material from former surges. Debris is, thus, readily available and easily entrained in the catchment and cannot therefore be considered a limiting factor under current conditions (Lugon and Stoffel 2010).

Rock-glacier dynamics in the torrent's source zone or the vegetation mantling the slopes on both sides of the channel are, however, constantly being subjected to changing climatic conditions. We therefore conclude that debris-flow activity in the Ritigraben catchment over the last ~300 years primarily depended on the presence of triggering meteorological events rather than on sediment supply. In addition, it also seems that the size of former and potential future incidences also depends on the state of the active layer of the rock-glacier body in the departure zone. We realize that very large events ($10^4 – 5 \times 10^4$ m^3) only occurred several decades after the end of the LIA and as a result of a series of exceptionally warm summers. In addition, the largest events on record were restricted to August and September, when melting of the active layer was largest and when advective precipitation events were registered. With the ongoing melting of ice of the rock-glacier body in the departure zone, the availability of sediments and the risk for a release of very large events will most probably increase in the future (Lugon and Stoffel 2010).

As for the potential evolution of climate and based on the IPCC A2 emissions scenario (Nakićenović et al. 2000), regional climate models suggest a shift in the occurrence of heavy precipitation events in the Swiss Alps from summer to spring and fall by 2100 (Beniston 2006). Spring and fall temperatures are projected to remain 4–7°C below current summer temperatures implying lower freezing levels as compared with current summers and therefore probably widespread buffering effects of snow on runoff and debris entrainment. Provided that mean and extreme precipitation events occur less frequently in summer and that wet spells will become more common in spring and fall, it is possible that debris flows will not necessarily occur as frequently in the future as they did in the past. However and as illustrated before, the magnitude of future (summer) and early fall incidences could be even greater, as warmer temperatures and higher precipitation intensities may result in greater runoff and in an increase in the transport capacity of surges leading to a greater erosive potential of debris flows.

The use of GD in tree rings for the dating of deposits on the intermediate cone of the Ritigraben torrent introduces an additional tool to aid in our better understanding of the frequency, magnitude, seasonality and spatial patterns of past events. Although overriding and erosion of older deposits are important on the cone, we are convinced that the coupling of geomorphic field surveys with tree-ring data may provide a realistic image of spatial activity for at least the twentieth century.

The apparent predominance of accumulation events on the intermediate cone should also be taken into account in risk analysis, as the banks and levees of the current channel incised by the September 1993 event have already started to collapse in some places. As a result, future debris flows could overtop the channel above 1,650 m a.s.l., reactivate abandoned flow paths and deposit material on the eastern or southwestern parts of the cone, theoretically threatening buildings and public infrastructure.

Acknowledgments The author offers sincere thanks to Delphine Conus, Michael Grichting, Igor Lièvre and Gilles Maître for all their work performed in the field and lab. We are also indebted to the Swiss Federal Office of Meteorology and Climatology (MeteoSwiss) for providing access to daily precipitation and temperature data. Michelle Bollschweiler is most warmly acknowledged for providing helpful comments on a former draft of the manuscript. This work has been undertaken partly in the context of the FP6 EU-project ENSEMBLES (no. 505539) and the SRCE-SFP RUFINE project (no. 0931030100RA/8253) projects.

References

Beniston M (2006) August 2005 intense rainfall event in Switzerland: not necessarily an analog for strong convective events in a greenhouse climate. Geophys Res Lett 33:L05701

Blair TC (1999) Sedimentology of the debris-flow dominated Warm Spring Canyon alluvial fan, Death Valley, California. Sedimentol 46:941–957

Blikra LH, Nemec W (1998) Postglacial colluvium in western Norway: depositional processes, facies and paleoclimatic record. Sedimentol 45:909–945

Bollschweiler M, Stoffel M, Schneuwly DM, Bourqui K (2008) Traumatic resin ducts in *Larix decidua* trees impacted by debris flows. Tree Physiol 28:255–263

Bollschweiler M, Stoffel M, Ehmisch M, Monbaron M (2007) Reconstructing spatio-temporal patterns of debris-flow activity using dendrogeomorphological methods. Geomorphology 87:337–351

Braam RR, Weiss EEJ, Burrough PA (1987) Spatial and temporal analysis of mass movement using dendrochronology. Catena 14:573–584

Caine N (1980) The rainfall intensity-duration control of shallow landslides and debris flows. Geogr Ann 62A:23–27

Christensen JH, Christensen OB (2007) A summary of the PRUDENCE model projections of changes in European climate by the end of this century. Clim Change 81:7–30

Fantucci R, Sorriso-Valvo M (1999) Dendrogeomorphological analysis of a slope near Lago, Calabria (Italy). Geomorphology 30:165–174

Grove JM (2004) Little ice ages: ancient and modern. Routledge, London

Jakob M, Hungr O (eds) (2005) Debris-flow hazards and related phenomena. Springer, Berlin, Heidelberg, New York

Jonasson C (1993) Holocene debris-flow activity in northern Sweden. Paläoklimaforschung 11:179–195

Lütschg-Lötscher O (1926) Über Niederschlag und Abfluss im Hochgebirge: Sonderdarstellung des Mattmarkgebietes: ein Beitrag zur Fluss- und Gletscherkunde der Schweiz. Schweizerischer Wasserwirtschaftsverband, Zürich

Lugon R, Stoffel M (2010) Rock-glacier dynamics and M–F relationships of debris-flow activity in a high-elevation watershed: Ritigraben, Swiss Alps. Global Planet Change (in press)

Lugon R, Monbaron M (1998) Stabilité des terrains meubles en zone de pergélisol et changements climatiques. Deux études de cas en Valais: Le Ritigraben (Mattertal) et la moraine du Dolent (Val Ferret). vdf Hochschulverlag, Zürich

Matthews JA, Dahl SO, Berrisford MS, Nesje A, Dresser PQ, Dumayne-Peaty L (1997) A preliminary history of Holocene colluvial (debris flow) activity, Leirdalen, Jotunheimen, Norway. J Quat Sci 12:117–129

McAuliffe JR, Scuderi LA, McFadden LD (2006) Tree-ring record of hillslope erosion and valley floor dynamics: landscape responses to climate variation during the last 400 yr in the Colorado Plateau, northeastern Arizona. Global Planet Change 50:184–201

Milly PCD, Wetherald RT, Dunne KA, Delworth TL (2002) Increasing risk of great floods in a changing climate. Nature 415:514–517

Müller HN (1980) Jahrringwachstum und Klimafaktoren: Beziehungen zwischen Jahrringwachstum von Nadelbaumarten und Klimafaktoren an verschiedenen Standorten im Gebiet des Simplonpasses (Wallis, Schweiz). Veröffentlichungen der Forstlichen Bundesversuchsanstalt Wien, Wien

Nakićenović N, Alcamo J, Davis G, de Vries B, Fenhann J, Gaffin S, Gregory K, Grübler A, Yong Jung T, Kram T, Lebre La Rovere E, Michaelis L, Mori S, Morita T, Pepper W, Pitcher H, Price L, Riahi K, Roehrl A, Rogner HH, Sankovski A, Schlesinger M, Shukla P, Smith S, Swart R, van Rooijen S, Victor N, Dadi Z (2000) IPCC Special report on emissions scenarios. Cambridge University Press, Cambridge

Pfister C (1999) Wetternachhersage. 500 Jahre Klimavariationen und Naturkatastrophen. Paul Haupt, Bern, Stuttgart, Wien

Rinntech (2008) LINTAB http://www.rinntech.com/Products/Lintab.htm

Röthlisberger G (1991) Chronik der Unwetterschäden in der Schweiz. Berichte Forschungsanstalt Wald, Schnee und Landschaft 330:1–122

Schmidli J, Frei C (2005) Trends of heavy precipitation and wet and dry spells in Switzerland during the 20th century. Int J Climatol 25:753–771

Sletten K, Blikra LH, Ballantyne CK, Nesje A, Dahl SO (2003) Holocene debris flows recognized in a lacustrine sedimentary succession: sedimentology, chronostratigraphy and cause of triggering. Holocene 13:907–920

Stoffel M (2010) Magnitude-frequency relationships of debris flows - a case study based on field surveys and tree-ring records. Geomorphology 116(1–2):67–76
Stoffel M (2008) Dating past geomorphic processes with tangential rows of traumatic resin ducts. Dendrochronologia 26:53–60
Stoffel M, Beniston M (2006) On the incidence of debris flows from the early Little Ice Age to a future greenhouse climate: a case study from the Swiss Alps. Geophys Res Lett 33:L16404
Stoffel M, Bollschweiler M (2008) Tree-ring analysis in natural hazards research – an overview. Nat Haz Earth Syst Sci 8:187–202
Stoffel M, Bollschweiler M, Beniston M (2010) Rainfall characteristics for periglacial debris flows in the Swiss Alps: past incidences – future evolutions. Clim Change (in press)
Stoffel M, Schneuwly D, Bollschweiler M (2010) Assessing rockfall activity in a mountain forest – implications for hazard assessment. In: Stoffel M, Bollschweiler M, Butler DR, Luckman BH (eds) Tree rings and natural hazards: A state-of-the-art. Springer, Berlin, Heidelberg, New York, this volume
Stoffel M, Lièvre I, Conus D, Grichting MA, Raetzo H, Gärtner HW, Monbaron M (2005a) 400 Years of debris-flow activity and triggering weather conditions: Ritigraben, Valais, Switzerland. Arct Antarct Alp Res 37:387–395
Stoffel M, Lièvre I, Monbaron M, Perret S (2005b) Seasonal timing of rockfall activity on a forested slope at Täschgufer (Valais, Swiss Alps) – a dendrochronological approach. Z Geomorphol 49:89–106
Zimmermann M, Mani P, Romang H (1997) Magnitude-frequency aspects of alpine debris flows. Eclogae Geol Helvetiae 90:415–420

High-Precision Dating of Debris-Flow Events Within the Growing Season

Ryszard J. Kaczka, Anne Deslauriers, and Hubert Morin

1 Introduction

We established and tested a new method of precise debris-flow dating using an existing model of wood formation (Deslauriers et al. 2003). The study was based on the hypothesis that scars and other wood anomalies record the stage of tree-ring development at the moment when a high-energetic impact kills the cambium, stopping further cell production. We also assumed that tangential rows of traumatic resin ducts and wood density fluctuations within the growth ring could develop soon after injury. Debris-flow sampling was carried out at four different sites located in three valleys of the Monts-Valin, north of the Saguenay River (48°40′–49°00′ N, 70°00'–71°15′ E), Québec (Canada). Fifty balsam fir (*Abies balsamea*) trees with scars dating back to 1996 were selected from a collection of 240 discs representing 12 debris-flows sites (Kaczka and Morin 2006). Major debris-flow events were recorded in the Saguenay region in 1996 as a result of severe rainstorms lasting from July 18–21 (199–202 Julian days). That known event was used to estimate the synchronism of three different proxies used in dendrogeomorphology to date debris-flow incidences, namely: (i) scars, (ii) tangential rows of traumatic resin ducts and (iii) density fluctuations.

The high-precision dating of the debris-flow event of 1996 was reconstructed by comparing the ratio of wood formed before the first appearance of the three proxies with a model of intra-annual xylem development for balsam fir for the larger study

R.J. Kaczka (✉)
Faculty of Earth Science, Department of Quaternary Paleogeography and Paleoecology, University of Silesia, 41-200 Sosnowiec, Poland
e-mail: ryszard.kaczka@us.edu.pl

A. Deslauriers and H. Morin
Laboratoire d'Écologie Végétale, Université du Québec à Chicoutimi, Chicoutimi, QC, G7H 2B1, Canada

M. Stoffel et al. (eds.), *Tree Rings and Natural Hazards: A State-of-the-Art*, Advances in Global Change Research 41, DOI 10.1007/978-90-481-8736-2_21,

region (Deslauriers et al. 2003). The ratio or percentage of wood formed before the onset of proxy formation as a result of debris-flow disturbance was obtained by comparing the number of cells in the injured and the complete parts of the 1996 tree ring. In a subsequent step, the intra-annual timing of the impact was assessed by comparing the ratio of wood formed in the scarred trees with growth data of the model of intra-annual xylem development (Fig. 1). In theory, this method allows assessing the date of previous debris-flow events with an accuracy of 1–2 weeks during the growing season (Fig. 2).

Results for the three different proxies revealed differences in the estimated timing of the debris-flow event. According to the model, scar occurred on average 5 days before the debris flow actually occurred. The underestimation of event timing based on scars is related to the collapse of cells which are not fully formed at the time of the event. Dating based on tangential rows of traumatic resin ducts and density fluctuations shows, in contrast, an overestimation of the event timing by about 10–15 days. These differences are related to the physiological processes of cell development and wood anomaly production. Similar to Silver fir (*Abies alba*; Stoffel 2008), it appears that Balsam fir would react quickly to geomorphic disturbance and that it would only require roughly 2 weeks to develop tangential rows of traumatic resin ducts in the tissues neighboring the injury.

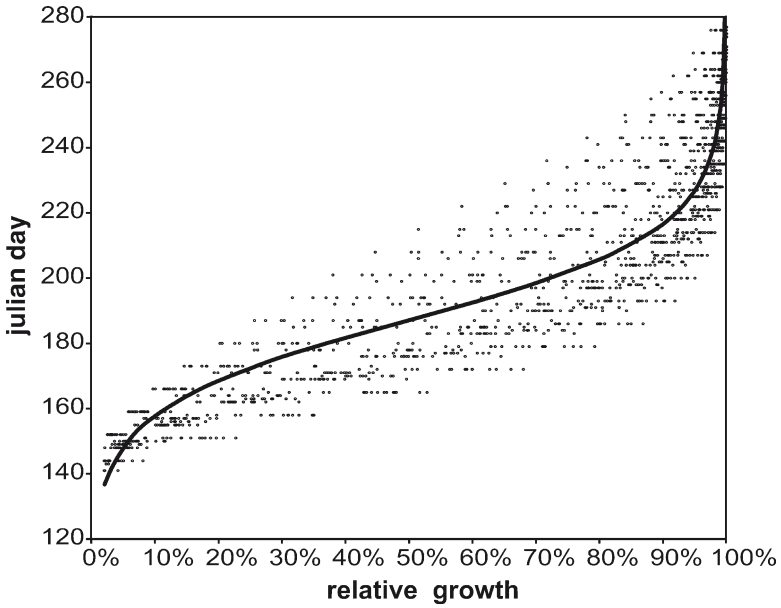

Fig. 1 Model of intra-annual xylem development expressed as relative growth, percentage of tree-ring developed during the growing season

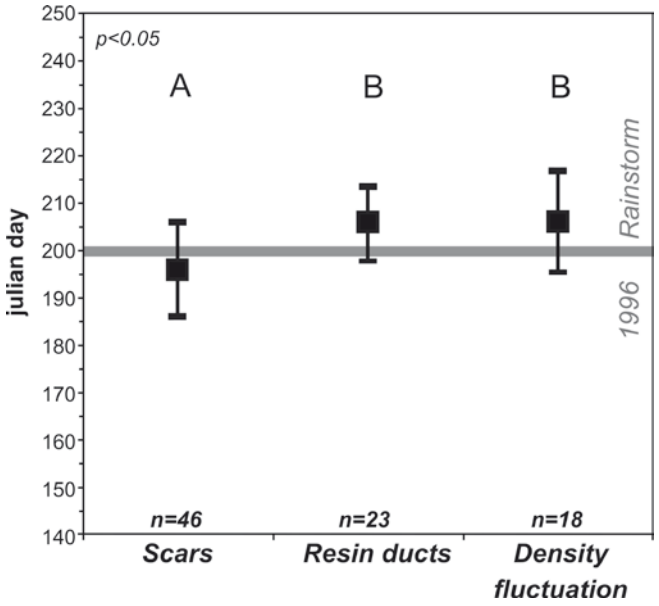

Fig. 2 Comparison of average results of the 1996 debris-flow dating using different proxies. The gray box indicates the timing of the event in July 1996

References

Deslauriers A, Morin H, Bégin Y (2003) Cellular phenology of annual ring formation of Abies balsamea in the Québec boreal forest (Canada). Can J Forest Res 33:190–200

Kaczka RJ, Morin H (2006) The dendrochronological records of debris flow activity in SE Quebec. TRACE 5:233–239

Stoffel M (2008) Dating past geomorphic processes with tangential rows of traumatic resin ducts. Dendrochronologia 26:53–60

Part VI
Flooding

Dieback of Norway spruce (*Picea abies*) following flooding, Swiss Alps
(© M. Bollschweiler)

Tree Rings as Paleoflood and Paleostage Indicators

Scott St. George

1 Introduction

Each year, floods cause enormous damage to property and kill thousands of people around the world. During the 1990s alone, freshwater flooding affected more than 1.4 billion people and caused about 100,000 deaths (Jonkman 2005). Worldwide, insured losses due to floods topped US$2 billion in 2008 (SwissRe 2009), making them the second-most expensive type of natural catastrophe (exceeded only by damages caused by tropical storms). In addition to the threats they pose to human communities, major floods are also important geological and biogeochemical agents that influence rates of erosion and sediment transport (Molnar 2001), redistribute organic matter and nutrients to downstream reaches (Velasco et al. 2006) and homogenize ecological processes and biological communities within floodplain systems (Thomaz et al. 2007).

In conventional flood science, the likelihood of floods occurring in the future is estimated from the frequency of similar floods in the past. Unfortunately, river and lake gauge records are often too short for hydrologists to make accurate predictions of the probability of large, infrequent floods (Klemeš 1989). Further-more, probabilistic flood-frequency analysis requires events to be identically distributed, independent and random through time, but real flood data usually violate these assumptions (Baker et al. 2002). Instrumental flood records are also relatively short compared to the time horizons used in the design of flood protection infrastructure and provide a limited perspective on the impact of climate or environmental change on flood risks.

S. St. George (✉)
Geological Survey of Canada, Ottawa ON, K1A 0E8, Canada
and
School of Environmental Studies, Queen's University,
Kingston ON, K7L 3N6, Canada
e-mail: sstgeorg@nrcan.gc.ca

M. Stoffel et al. (eds.), *Tree Rings and Natural Hazards: A State-of-the-Art*,
Advances in Global Change Research 41, DOI 10.1007/978-90-481-8736-2_22,

Paleoflood hydrology uses physical evidence left behind on the landscape to make inferences about past floods that were not directly observed or recorded by humans (Baker 2006). Paleoflood records based on geological and biological field evidence can span several hundreds or thousands of years and provide a prehistoric context for shorter modern flood records based on direct observations. Paleohydrological studies most commonly use geomorphic evidence of past flood stages (e.g. Baker 1987; Enzel et al. 1996; Knox 2000), but paleoflood studies can also draw upon contributions from geophysics (Pickup et al. 2002), limnology (Brown et al. 2000), archaeology (Brown et al. 2001), and dendrochronology (Yanosky and Jarrett 2002).

The argument that trees recorded evidence of past floods in their annual growth rings was first put forward by Robert Sigafoos of the United States Geological Survey in 1964. Working along the Potomac River near Washington, DC, USA, he showed that unusual growth forms in riparian trees, including vertical sprouts, partial uprooting and tilted trunks, developed in association with floods documented at nearby gauge records (Sigafoos 1964). By demonstrating that these trees represented a biological archive of past floods, this initial work created a new tool for paleoflood research that has been applied widely to hydrological problems in the subsequent four and a half decades. Dendrochronologists are now able to exploit a broad range of physical evidence preserved in tree rings to develop insights into the occurrence, extent and magnitude of floods prior to direct observations. The articles and case studies in this chapter illustrate how flood evidence from trees is being used around the world to address issues related to long-term hydrological change, the impacts of human modification of hydrological systems and future risks of extreme floods.

2 Flood Evidence in Tree Rings

Dendrochronologists use four main strategies to study past floods and high water using evidence from tree rings. Three of these approaches examine evidence created by the direct effects of flooding on inundated trees while the fourth depends on indirect connections between hydrology, climate and the growth environment of trees.

Scarring caused by abrasion or impact is the most common type of tree-ring evidence used in paleoflood research. Ice, logs, sediment or other debris rafted into riparian forests by high water can abrade or penetrate the bark and kill the underlying cambium. Trees will attempt to seal the wound by forming undifferentiated, often discoloured scar tissue (callus), which acts as a permanent record of local cambial death. Eventually, the scar will be overgrown by the cambium and disappear under newly formed wood and bark, but if the tree is subjected to repeated scarring at the same location, the cambium will not recover and the wound will remain exposed at the surface (Fig. 1). The timing of the flood can be determined by counting the number of rings between the scar and the outside ring, and the height of the

Fig. 1 Extensive scarring caused by ice jams on a plains cottonwood (*Populus deltoides*) along the bank of the Red River in Winnipeg, Canada

scar represents the minimum elevation of high water (Harrison and Reid 1967; McCord 1996; Zielonka et al. 2010, this volume). Along rivers, scarred trees are most frequent where steep gradients or channel constrictions increase stream velocity and its capacity to carry heavy debris. In nival environments, elevated lake levels can also lead to tree scarring when lake ice is pushed into onshore forests following spring break-up (Tardif and Bergeron 1997; Tardif et al. 2010, this volume).

Floods can also interfere with physiological processes that control tree growth and cause anatomical changes within a portion or the entirety of the

annual growth increment. These features are often referred to as ‘flood rings’ and have been observed most often in ring-porous trees such as ash or oak. Flood rings can be produced in low-lying trees when floodwaters reach the crown and fully or partially defoliate the tree during late spring or early summer (Yanosky 1983). If the tree is able to refoliate after flooding subsides, its growth ring will often contain a double cohort of large conductive vessels separated by one or more rows of smaller vessels. Flood rings can also be formed in flood-plain trees when the roots and trunk are subjected to prolonged inundation during the early part of the growing season (Astrade and Bégin 1997; St. George and Nielsen 2000; St. George 2010, this volume). These signatures are usually distinguished by the presence of anomalously small vessels in the earlywood of the annual ring but they can also include other anatomical features such as fibers with unusually thin cell walls and disrupted flame parenchyma. Whether caused by defoliation or inundation, flood rings are generally believed to form in response to disruptions in the normal downward flow of auxin, which partly controls the size of earlywood vessels in hardwoods (Fig. 2).

In some circumstances, floods can damage trees by tilting or partial uprooting or can uproot them completely, causing their death. When catastrophic flooding kills all trees along a reach of a river, the age of the oldest trees that colonize the fresh surface provides a minimum estimate of the flood date (Sigafoos 1964; Gottesfeld and Gottesfeld 1990). This approach requires estimates of the ecesis interval, the delay between the exposure of the new surface and the establishment of new trees. Partial uprooting can cause smaller trees to form vertical sprouts along their main stem, with the age of the sprout indicating the date of the flood that caused the change in growth habit (Sigafoos 1964). In extreme cases, trees

Fig. 2 Riparian trees inundated by the 2009 Red River flood in Manitoba, Canada

that are repeatedly damaged by flooding adopt a growth form with multiple stems that can resemble the product of coppicing. Tilting can also cause trees to form tension or compression wood (depending on whether they are deciduous or conifers) and anomalously wide or narrow rings in subsequent years (Yanosky and Jarrett 2002).

Major long-lasting shifts in regional hydrology can also create indirect evidence of their occurrence by making microsite conditions more or less favorable to tree growth. This type of analysis usually requires the presence of a water body, usually an artificial reservoir, large enough to influence aspects of the local climate such as seasonal temperature changes, evaporation rates or near-surface wind regimes. Dendrochronologists often use a suite of tree-ring indicators to compare local trees against a control population growing too far away to be affected by the reservoir. Depending on the amount of time that has passed since its construction, investigators may also examine long-lived trees to compare tree growth before and after reservoir construction. Most studies using this approach have shown that trees growing in the immediate area display a complex set of anatomical and growth-form responses that depend strongly on their position relative to the newly-created reservoir. Observed responses include but are not limited to temporary growth reductions during reservoir filling, a reduction in wood density caused by an extended growing season, an increased frequency of traumatic resin canals forced by major foliar losses and the formation of reaction wood at exposed sites due to stronger winds (Tremblay and Bégin 2005; Bégin et al. 2010, this volume).

3 Strengths, Limitations and Future Directions

The principal advantage of paleoflood studies based on tree rings is their relatively high temporal resolution and dating accuracy compared to most other methods. Dendrochronological methods can routinely date past floods to the year of their occurrence and, in rare cases, can estimate the timing of floods that occur during the growing season to within 2 weeks. This high degree of chronological control, which is surpassed only by that provided by direct observation or instrumentation, can be used to determine whether floods in separate watersheds were synchronous or offset by several years and test hypotheses that suppose linkages between extreme floods and specific forcing mechanisms. The wide geographic distribution of tree species with dateable rings combined with the broad suite of methods available to examine interconnections between floods and tree growth allow dendrochronologists to apply their style of paleoflood hydrology in many settings that are not appropriate for techniques that depend on geological evidence.

To date, paleoflood analysis based on tree rings has been restricted to describing floods that occurred during the last 500 years. Flood signatures have been reported in more ancient trees (Bernard 2003) but as yet there has not been any attempt to compile tree-ring evidence of floods that occurred prior to roughly AD 1500. Naturally, the reason that most dendrochronologically-based paleoflood studies

tend to be relatively short is because the life expectancy of trees growing in flood zones is comparatively brief. Because floods often kill trees and wash their remains downstream, it can be difficult to find evidence of floods that are older than the most recent catastrophic event and sample depth usually decreases back in time quite rapidly. It is possible to develop long paleoflood records from tree rings using samples collected from subfossil trees and historic buildings St. George and Nielsen (2000) but the success of this approach depends on the availability of ancient logs and archeological wood.

The use of tree rings to address questions related to flooding remains almost exclusively the domain of the scientific community, and there are very few examples where paleoflood evidence from trees has been formally incorporated into flood risk analysis. In part, the gap between scientific innovation and societal application is due to the fact that tree rings and other natural archives are well outside of the curriculum in civil engineering departments at most universities and, as a result, practitioners and decision-makers responsible for flood infrastructure can be unaware of the potential benefits offered by a broader geological perspective. At the same time, many lessons learned from tree rings can be difficult to apply to flood management because they do not relate to measures that are regarded as meaningful by decision-makers. Future paleoflood research involving tree rings will need to strike a balance between improving our understanding of the biological and fluvial processes that link tree growth to past floods and providing answers to questions about flood dynamics and flood hazards that are needed to safeguard people and property from future floods.

References

Astrade L, Bégin Y (1997) Tree-ring response of *Populus tremula* L. and *Quercus robur* L. to recent spring floods of the Saône River, France. Ecoscience 4:232–239

Baker VR (1987) Paleoflood hydrology and extraordinary flood events. J Hydrol 96:79–99

Baker VR, Webb RH, House PK (2002) The scientific and societal value of paleoflood hydrology, p 1–19. In: House PK, Levish DR, Webb RH, Baker VR (eds) Paleoflood hydrology. Am Geophys Union Monogr, Washington, p 385

Baker V (2006) Palaeoflood hydrology in a global context. Catena 66:161–168

Bégin Y, Sirois L, Meunier C (2010) The effects of hydroelectric flooding on a reservoir's peripheral forests and newly created forested islands. In: Stoffel M, Bollschweiler M, Butler DR, Luckman BH (eds) Tree rings and natural hazards: A state-of-the-art. Springer, Berlin, Heidelberg, New York, this volume

Bernard V (2003) North-western French Neolithic dendrochronology: prospects for a 2000 year oak chronology. Measure Sci Tech 14:1510–1515

Brown SL, Bierman PR, Lini A, Southon J (2000) 10,000 Year record of extreme hydrologic events. Geology 28:335–338

Brown AG, Cooper L, Salisbury CR, Smith DN (2001) Late Holocene channel changes of the Middle Trent: channel response to a thousand-year flood record. Geomorphology 39:69–82

Enzel Y, Ely LL, House PK, Baker V (1996) Magnitude and frequency of Holocene palaeofloods in the southwestern United States: A review and discussion of implications, pp 121–137. In: Branson J, Brown AG, Gregory KJ (eds) Global continental changes: the context of palaeohydrology, p 272. Geological Society Special Publication, Alden Press, Oxford

Gottesfeld AS, Gottesfeld LMJ (1990) Flood-plain dynamics of a wandering river, dendrochronology of the Morice River, British Columbia, Canada. Geomorphology 3:159–179
Harrison SS, Reid JR (1967) A flood-frequency graph based on tree-scar data. Proc North Dakota Acad Sci 21:23–33
Jonkman SN (2005) Global perspectives on loss of human life caused by floods. Nat Haz 34:151–175
Klemeš V (1989) The improbable probabilities of extreme floods and droughts, p 43–51. In: Starosolszky O, Melder OM (eds) Hydrology of disasters. James & James, London
Knox JC (2000) Sensitivity of modern and Holocene floods to climate change. Quat Sci Rev 19:439–458
McCord VA (1996) Fluvial process dendrogeomorphology: Reconstructions of flood events from the southwestern United States using flood-scarred trees. In: Dean JS, Meko DM, Swetnam TW (eds) Tree rings, environment and humanity. University of Arizona, Tucson, pp 689–699
Molnar P (2001) Climate change, flooding in arid environments, and erosion rates. Geology 29:1071–1074
Pickup G, Marks A, Bourke M (2002) Paleoflood reconstruction on flood-plains using geophysical survey data and hydraulic modeling. In: House PK, Levish DR, Webb RH, Baker VR (eds) Paleoflood hydrology. American Geophysical Union Monograph, Washington, DC, p 47–60
St. George S, Neilson E (2000) Signatures of high-magnitude 19th century floods in Quercus macrocarpa tree rings along the Red River, Manitoba, Canada. Geology 28:899–902
St. George S (2010) Dendrohydrology and extreme floods along the Red River, Canada. In: Stoffel M, Bollschweiler M, Butler DR, Luckman BH (eds) Tree rings and natural hazards: A state-of-the-art. Springer, Berlin, Heidelberg, New York, this volume
Sigafoos RS (1964) Botanical evidence of floods and flood-plain deposition. US Geol Surv Prof Paper 485A, p 35
SwissRe (2009) Natural catastrophes and man-made disasters in 2008. Swiss Reinsurance Company Ltd., Economic Research & Consulting, Zurich, Switzerland, p 43
Tardif JC, Bergeron Y (1997) Ice-flood history reconstructed with tree rings from the southern boreal forest limit, western Québec. Holocene 3:291–300
Tardif JC, Kames S, Bergeron Y (2010) Spring water levels reconstructed from ice-scarred trees and cross-sectional area of the earlywood vessels in tree-rings from eastern boreal Canada. In: Stoffel M, Bollschweiler M, Butler DR, Luckman BH (eds) Tree rings and natural hazards: A state-of-the-art. Springer, Berlin, Heidelberg, New York, this volume
Thomaz SM, Bini LM, Bozelli RL (2007) Floods increase similarity among aquatic habitats in river-floodplain systems. Hydrobiologia 579:1–13
Tremblay J, Bégin Y (2005) The effects of snow-packing on tree growth forms on an island in a recently created reservoir in northern Québec, Canada. Ecoscience 12:530–539
Velasco JM, Lioret J, Millan A, Marin A, Barahona J, Abellan P, Sanchez-Fernandez D (2006) Nutrient and particulate inputs into the Mar Menon Lagoon (SE Spain) from an intensive agricultural watershed. Wat Air Soil Pollut 176:37–56
Yanosky TM (1983) Evidence of floods on the Potomac River from anatomical abnormalities in the wood of flood-plain trees. US Geol Surv Prof Paper 1296, p 42
Yanosky TM, Jarrett RD (2002) Dendrochronologic evidence for the frequency and magnitude of paleofloods. In: House PK, Levish DR, Webb RH, Baker VR (eds) Paleoflood hydrology. American Geophysical Union Monograph, Washington, DC, p 77–89
Zielonka T, Holeksa J, Ciapała S (2010) A 100-year history of floods determined from tree rings in a small mountain stream in the Tatra Mountains, Poland. In: Stoffel M, Bollschweiler M, Butler DR, Luckman BH (eds) Tree rings and natural hazards: A state-of-the-art. Springer, Berlin, Heidelberg, New York, this volume

The Effects of Hydroelectric Flooding on a Reservoir's Peripheral Forests and Newly Created Forested Islands

Yves Bégin, Luc Sirois, and Céline Meunier

1 Introduction

While research shows that large water bodies can produce significant micro- and meso-climatic effects, these effects are not well documented. The flooding of large areas transforms terrestrial environments into aquatic environments, with hills becoming islands and the flooded edges dynamic shorelines. In creating these reservoirs, we expose the new shoreline forests to processes and natural hazards pertaining to lacustrine environments. The environmental transformations caused by these processes are generally limited to the immediate edges of the reservoirs. In Russia, Vendrov and Malik (1965), D'yakonov and Reteyum (1965), and Butorin et al. (1973) have shown that the effects of reservoirs in the Volga are limited to their riparian edges. Wind controls the geomorphologic activity of waves and ice delineating the shore tree line. The wind also controls the distribution of snow at the edge of the water body during the long part of the year that is covered by ice. In New Zealand, Fitzharris (1979) reviewed the effects of the planned Upper Clutha Valley hydroelectric project. The study highlighted thermal effects, i.e., a decrease in daily thermal differences at the start of summer, a

Y. Bégin (✉)
Centre Eau Terre Environnement, Institut national de la recherche scientifique, Québec QC, G1K 9A9, Canada
e-mail: yves.begin@ete.inrs.ca

L. Sirois
Université du Québec à Rimouski, Rimouski QC, G5L 3A1, Canada

C. Meunier
Centre d'études nordiques, Pavillon Abitibi-Price, Université Laval, Québec QC, G1V 0A6, Canada

M. Stoffel et al. (eds.), *Tree Rings and Natural Hazards: A State-of-the-Art*, Advances in Global Change Research 41, DOI 10.1007/978-90-481-8736-2_23,

general warming in the middle of summer, and a lengthening of the warm season in autumn. A decade earlier, in Japan, Shirata (1969) found the same effects along the shores of Lake Inawashiro. In Canada, along the banks of the Canadian-American Great Lakes, earlier studies were synthesized by Eichenlaub (1979). The principal conclusions point to the fact that large water bodies increase the mean annual temperature, reduce daily and seasonal thermal variations, delay seasons by several weeks, amplify local winds, and decrease local precipitation while increasing evaporation. Lacking a dense network of meteorological stations, most of these studies were based on estimations and theoretical models (Therrien 1981; Mysak 1993; Gooseff et al. 2005; Stivari et al. 2005). Within this context, several authors have hypothesized that the creation of vast water bodies for hydroelectric projects can have an effect on local climate (Perrier et al. 1977; Sottile and Levesque 1989). Ecological indicators on the islands and edges of large lakes in northern Québec have led several authors to stipulate that these large water bodies, particularly when frozen, may create local climates colder and more humid than those above land. These local climates create an environmental risk of transforming the ecological conditions at the peripheries of the new water bodies, as well as on their islands. To what extent are these environments exposed to disturbances that did not exist before their flooding? The development of these reservoirs creates new conditions that may cause exacerbate the intensity of natural phenomena beyond certain thresholds thus resulting in a shift of the exposed shoreline environments from one ecological state to another.

To investigate the possibility of these "anthropogenically facilitated hazards", we draw on the example of the climatic impacts resulting from the creation of large reservoirs in north eastern Canada. The creation of the La Grande hydroelectric complex in northern Québec inundated an area of 11,400 km^2, of which only 12% were previously wetlands or water bodies (Tamenasse 1980; SEBJ 1987; Fig. 1). In a study commissioned by Hydro-Québec, Météoglobe Canada (1992) estimated that the climatic effects of the reservoirs extended to a maximum of less than 25 km from their borders, a distance equivalent to the breeze created by the temperature contrast between the water body and adjacent land, that extends 1.5 times the radius of the basin according to Litynski et al. (1989). Météoglobe Canada expressed reservations about the validity of predictions of local climate effects based on models using temporally discontinuous and spatially sporadic data. We investigated the effects that the Robert-Bourassa Reservoir (also called LG-2) may have had on the forest environments of its periphery and the islands that were created by its flooding. We hypothesized that the reservoir would have a significant climatic influence on the forests, which would be observable using dendrochronological indicators. The Robert-Bourassa Reservoir (created in 1979–1980), with an area of 2,835 km^2 is the second largest reservoir in the La Grande complex after Caniapiscau (4,275 km^2). The time duration that the reservoir has been flooded (1979–1980) may be sufficient to observe how the change in climate is expressed within the regeneration, growth forms, and annual rings of new riparian trees.

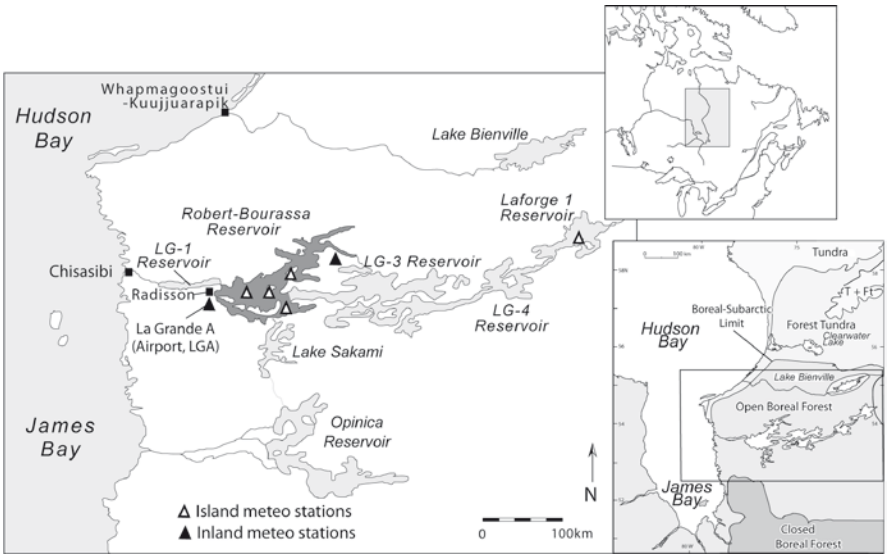

Fig. 1 Location of the Robert-Bourassa Reservoir within La Grande Rivière hydroelectric production zone in Northern Québec

2 Study Site

The drainage network of La Grande Rivière (La Grande) was, before the development of the hydroelectric complex, the fourth largest in Québec in terms of area (97,643 km^2). The Robert-Bourassa Reservoir is situated 117.5 km from the mouth of La Grande Rivière. It is the largest hydroelectric development in the world.

The study area is dominated by a cold continental climate. The influence of Hudson Bay and James Bay on the climate is very significant. During winter, the complete freezing of the bays and the gentle relief of the region allows colder conditions to develop. The mean minimum temperature in January is −23.2°C (Station LGA). In summer, warming is delayed by the presence of ice and cold currents from the peripheral seas. The mean maximum temperature for July is 13.4°C. The growing season for the region extends from mid-June to mid-September. The frost free period is very short (208 days) in the region. The annual precipitation is 679 mm, with 40% (271.6 mm) falling as snow. Snow precipitation at the start of winter is controlled by the duration of the freezing of James and Hudson Bays. The freezing of these interior seas begins towards the end of December or the beginning of January, resulting in a reduction in humidity and snow precipitation in the region. Despite the rigorous climate, winter is the sunny season of the year and the atmospheric conditions during this period are relatively stable. Snow is less abundant (~1.5 m) than in southern Québec (~2.5–3.5 m) and storms are also less frequent. Summer is short and autumn arrives early with frequent night frosts.

3 Methods

An assessment of the climate conditions over Robert-Bourassa Reservoir was made by the comparison of data collected simultaneously at four stations located on islands and at two other stations distant from the reservoir to the west and the east (Fig. 1). In order to determine the effects of temperature and wind on tree growth, a strategy was designed to sample trees on the reservoir's islands with site exposure being the principal factor considered. Results will be presented for the dominant species, namely black spruce (*Picea mariana*). Trees were selected from the shoreline forest edges of 16 islands; these are referred to as "exposed" trees and were sampled according to north, south, east, and west orientations (Fig. 2). At each island a minimum of 30 trees with diameters of less than 8 cm were sampled 30 cm from their base for a total of around 490 trees. The sampled trees were situated directly on the forest edge and thus had maximum exposure to lake effects. In addition, only trees that were isolated from neighboring trees were selected in order to avoid the influence of competition. Trees located at a distance from the forest edge were also selected and were considered as "sheltered" from the wind. These trees were sampled from band transects running perpendicular to the shore and are referred

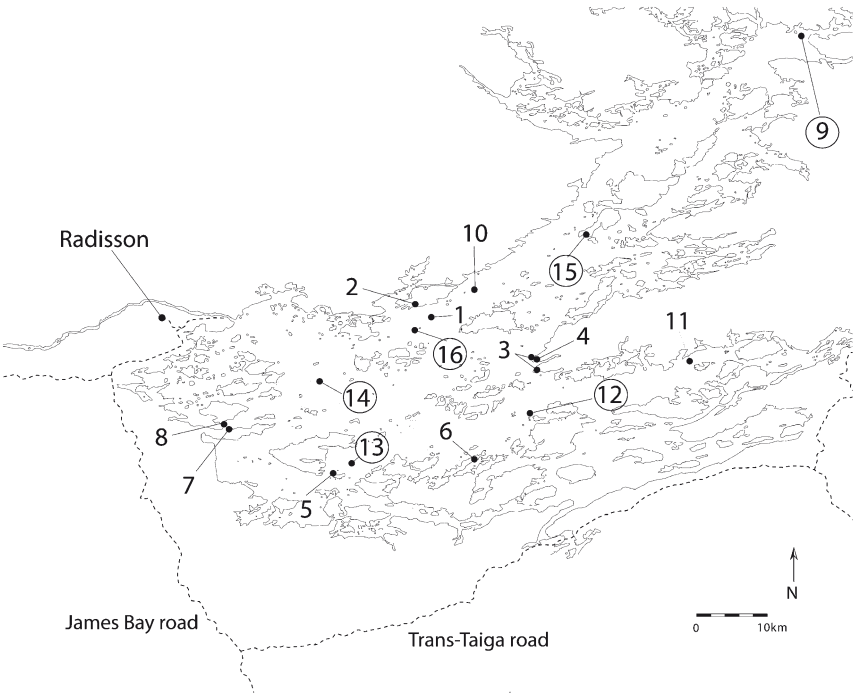

Fig. 2 Location of the sampling sites located on islands in the Robert-Bourassa Reservoir. *Circles* indicate islands where trees were sampled on hill tops for the analysis of reaction wood sequences

hereafter as north sheltered, east sheltered, etc. Only black spruce trees with a diameter of less than eight cm were sampled. Individual trees were sampled at 10 m intervals resulting in 29–31 trees per site. The maximum transect length was 300 m, with some being shorter in order to only sample sites that were homogenous in terms of topography, exposure, and forest structure and composition. In total, amongst over 900 trees sampled, 243 black spruce trees were retained for complete analysis. We systematically rejected trees that showed reaction wood sequences caused by wind destabilization. To assess the impacts of the changes in the eolian regime on the forest, we sampled mature trees situated in the open forests at the highest altitudinal points of six islands (around 15 trees per island for a total of 90 trees). These trees were the ones most exposed to the wind prior to the reservoir's creation and, by showing the development of reaction wood since its flooding, we suspected that their exposure to even stronger winds would have destabilized their original stature.

In the laboratory, in order to determine the effect of the reservoir's creation on black spruce growth, we identified and described abnormal rings (frost rings, incomplete rings, resin ducts, reaction wood), and measured the growth of annual rings using the methods of Schweingruber (1988). A densitometric analysis of a number of samples was also conducted using x-rays following the methods of Schweingruber et al. (1978). The density of earlywood, latewood, and the proportion of final wood were then analyzed for each annual ring. Finally, we investigated the effects of wind-blown snow on trees that showed intricate growth forms (Tremblay and Bégin 2005).

4 Results

4.1 The Reservoir's Effects on the Temperature and Wind Regime

The temperatures at reservoir locations differed than those outside its area of influence throughout all seasons, except winter. The mean temperature differed by 2.4°C in spring (April to June) and 0.8°C in summer. A reversal to warmer temperatures occurred in autumn, the reservoir being warmer than the hinterland (−1.5°C). No differences were observed in winter, the reservoir being covered by ice. The reservoir's continuous ice cover in winter possesses the same thermal properties as the surrounding lands. In light of these results, it is clear that the water body cools the local climate during spring and summer.

Growth degree days (GDD) were calculated as follows:

$$\sum_{i=1}^{n} (T_i \rangle 5) - 5 \tag{1}$$

where T was the mean daily temperature (°C) for each of the days of the year 'i' above 5°C and 'n' was the number of days. GDD were calculated using data from

the stations for the year 1997, which serves as a reference, as it is considered an average year for the entire record. The calculation started on the 27th of June, as all stations were functioning at that time. Island stations showed a delay compared to hinterland ones, which suggests a cooling effect caused by the reservoir. For instance, the 300 GDD level was reached the 30th of July on a reservoir island, as compared to the 25th of July at La Grande airport situated inland (a delay of 5 days). This difference increased over the course of the season. The 700 GDD marker was attained on the 28th of September at reservoir stations in 1997, 19 days later than at inland stations (9th of September). The La Grande airport station possessed an advance of around 2 weeks up until mid-September when the effect of the reservoir seemed to reverse, i.e., its cooling effect was greatly reduced. GDD decreased along the distance to water edge (Sirois et al. 1999).

We also observed a delay in the first day of frost (i.e., the first day where the mean temperature is below 0°C). Freezing at insular stations occurred about 24 days later than the inland stations.

It seems clear that thermal effects are prevalent on the islands of the reservoir. However, these effects vary with seasons and the type of weather. Indeed, the average seasonal temperature differences between the two locations (island versus hinterland) was about 3°C in spring. This difference decreased as the year progressed (2°C in summer and null or inversed in autumn and winter). According to the isotherms of Québec (data available on Environnement Canada web site, www.ec.gc.ca), the conditions prevailing on the reservoir resemble those of Inukjuak, which is situated at the northern limit of the subarctic zone (530 km farther north). The start of the growing season is delayed under these conditions. In autumn, during windless conditions, the reservoir had a slight warming effect on the local climate, in contrast with spring and summer. However, the growing season, as indicated by the GDD, is not prolonged. In winter, the thermal climate of the region was homogenous and the continuous ice cover did influence the local thermal regime.

A summary analysis of wind data comparing both sectors of the water body indicated differences that can be attributed to the reservoir. There were notable differences in the eolian regimes of the islands compared to the land. A meteo station located in the largest open water part of the reservoir recorded winds that were double the speed of those at inland stations throughout all the seasons. The acceleration of winds within the central basin also allows edge effects to penetrate more deeply into the interior of the islands' forests. Coupled with thermal effects, these factors may cause a phenological delay that extends for a greater distance from the water in the central basin than elsewhere. In winter, eolian stress may also affect wider forest fringes regardless of orientation within the central basin. A summary analysis of wind data comparing both sectors of the water body indicated differences that can be attributed to the reservoir. There were notable differences in the eolian regimes of the islands compared to the land. A meteo station located in the largest open water part of the reservoir recorded winds that were double the speed of those at inland stations throughout all the seasons. The acceleration of winds within the central basin also allows edge effects to penetrate more deeply into the interior of the islands' forests. Coupled with thermal

effects, these factors may cause a phenological delay that extends for a greater distance from the water in the central basin than elsewhere. In winter, eolian stress may also affect wider forest fringes regardless of orientation within the central basin. Depending on the configuration of the islands, snow blown by the wind may also accumulate at various distances into the forest.

4.2 Effects of the Reservoir on Tree Growth and Ring Density

A large number of the trees sampled showed growth decreases coinciding with the filling of the reservoir. Growth decreases were less than 5 years in duration and rarely irreversible. In most cases, the decrease in growth occurred a few years (1985–1986) after the transitional period of 1979–1980 when the reservoir was filled. This reaction may be attributable to the progressive deterioration (foliar loss) of the protective forest edge. Based on the orientation, the reaction of the trees appeared to be the most pronounced on the western and northern exposures, with very few reactions being observed on the south facing side of the islands. Trees with drastic and irreversible reductions in annual ring growth were rare with most of them being situated in the northern section of the central basin of the reservoir, although some were also found to the east. In summary, although undeniable effects were observed in many trees, variations in the widths of annual growth rings does not always appear to be an infallible indicator of the climatic influence of the reservoir. For example, summer 1992 was particularly cold in the Canadian subarctic, following the Pinatubo eruption. The reservoir did not exacerbate such cooling and the island trees did not show any difference in their response to climate.

Patterns of latewood characteristics for the trees situated on the islands and edges of the reservoir may be more indicative of local climate than annual tree-ring widths. Although densitometric analysis is tedious, it does provide valuable details concerning the formation of wood at the start of the growing season (earlywood) and at the end of the season (latewood). Indeed, the exposed trees displayed a net change in their densitometry profile. In general, exposure favors the development of less dense latewood (maximum density) and dense earlywood (minimum density). This reaction characterized the trees occupying the wind exposed edges of the forest islands. The densitometric profiles of sheltered trees were more variable and appeared to be dependent on the forested environments (Fig. 3).

Despite the absence of meteorological data characterizing the contrasts in the forested environments of exposed versus sheltered sites, the general trend of a decrease in ring density and an increase in the proportion of latewood suggests a delay in the growing season that involves an increase in the average density of the earlywood and a longer late growing period that allows for a greater development of latewood. The late ending of tree dormancy caused by the thermal effect of the frozen water body, along with the late autumn caused by the mitigating effects of the water body, favors the formation of a large proportion of latewood cells. The triggers for the formation of latewood in trees are still unknown. However, we do know that they appear after the foliation period.

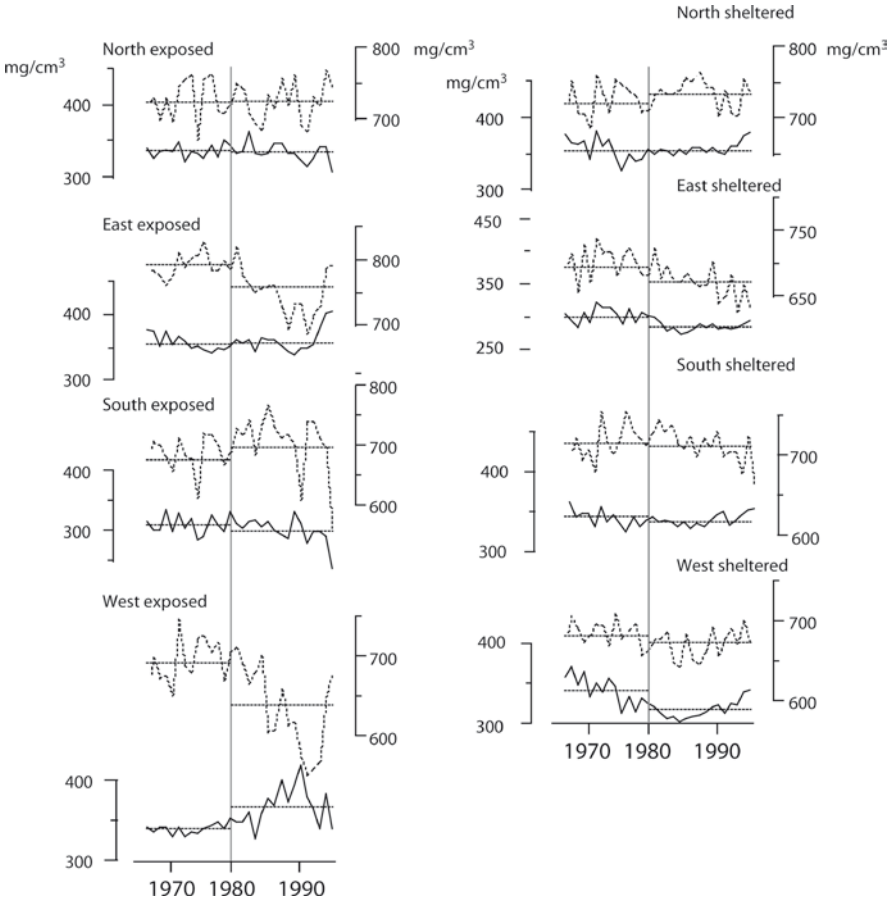

Fig. 3 Average minimum (*solid line*) and maximum (*dotted line*) densities of the tree-rings of spruce sampled on exposed and sheltered sites according to directional aspects on the 16 islands selected in the Robert-Bourassa Reservoir. Each line represents the average of about 30 trees. The vertical line refers to the year the reservoir was created

The large number of environmental factors compared to local climatic factors does not allow us to interpret the effects that the reservoir may have on different individual tree growth parameters. However, the edge effects observed around the lake shorelines and on the islands are clear. Indeed, the reduced foliar mass of the trees, their eroded growth forms, and physical damage were indicators of this influence. The study of climatic effects on the forest environment should therefore be refocused at the local scale. At the Robert-Bourassa Reservoir, the clearest border effects are related to the wind exposure of the forests and to the unequal distribution of snow cover. Similar to subarctic trees, the trees occupying the shores of the reservoir possess irregular growth forms that are indicators of hibernal erosion. This phenomenon is well documented in the literature, but its occurrence within the boreal zone is not typical. Indeed, the trees occupying the banks of large, natural

lakes in the region possess symmetrical growth forms, while those of the reservoir possess numerous dead branches that lead to the development of eroded forms (Lavoie and Payette 1997). The regression of growth forms is associated with the loss of foliar mass that occurs due to winter wind events (removal of leaves and buds by wind-blown snow crystals). The effect is not solely a winter phenomenon. Indeed, the distance to water (or ice cover) delays the bud set period despite the occurrence of milder autumn conditions. Incomplete protection of buds and needles limit their survival and, as a result of harsh winters, reduces the potential for the reconstruction of the chlorophyll apparatus over the following summers. The large number of environmental factors compared to local climatic factors does not allow us to interpret the effects that the reservoir may have on different individual tree growth parameters. However, the edge effects observed around the lake shorelines and on the islands are clear. Indeed, the reduced foliar mass of the trees, their eroded growth forms, and physical damage were indicators of this influence. The study of climatic effects on the forest environment should therefore be refocused at the local scale. At the Robert-Bourassa reservoir, the clearest border effects are related to the wind exposure of the forests and to the unequal distribution of snow cover. Similar to subarctic trees, the trees occupying the shores of the reservoir possess irregular growth forms that are indicators of hibernal erosion. This phenomenon is well documented in the literature, but its occurrence within the boreal zone is not typical. Indeed, the trees occupying the banks of large, natural lakes in the region possess symmetrical growth forms, while those of the reservoir possess numerous dead branches that lead to the development of eroded forms (Lavoie and Payette 1997). The regression of growth forms is associated with the loss of foliar mass that occurs due to winter wind events (removal of leaves and buds by wind-blown snow crystals). The effect is not solely a winter phenomenon. Indeed, the distance to water (or ice cover) delays the bud set period despite the occurrence of milder autumn conditions. Incomplete protection of buds and needles limit their survival and, as a result of harsh winters, reduces the potential for the reconstruction of the chlorophyll apparatus over the following summers. This phenomenon also characterizes the shoreline trees of large natural water bodies in this region. The spruce trees that are located at the water's edge of these water bodies generally exhibit a krummholz growth form (Lavoie and Payette 1997). The trees that are located at the edge of the reservoir differ from the natural lake ones by having been established much earlier than the reservoir was created. Their degradation thus occurred after the flooding of the reservoir.

4.3 Frost Rings and the Phenological Delay of Tree Growth on the Islands

Frost rings (Glerum and Farrar 1966) form while wood cells are still living, i.e., around 40–50 days after their development. They are formed when air temperatures drop below 0°C for 1–5 days, which causes the contents of the cells to freeze and the consequent bursting of the cells. The broken cells are sometimes sealed by resin

from the resin canals of the woody rays. The affected area in the ring is clearly visible at the macroscopic level (deformed wood cells). Frost rings may be simple (unique/singular) or double depending on the number of frost events that have affected a tree during the same growing season. They can also be continuous or discontinuous (only affecting part of the tree circumference). We observed a scarcity of frost rings after the reservoir creation. While they were frequent before 1980, they have subsequently become rare and less defined anatomically (Fig. 4). The sampled black spruce trees were all considered to be less than 50 years of age – the maximum cambial age after which frost rings cannot develop due to the protection provided by the development of thick bark. A delay in the ending of dormancy may also protect trees in the reservoir's environment from frost damage. The absence of frost rings after 1980 in the western sector is striking. This phenomenon could be related to the more pronounced cooling effects within the central basin of the reservoir.

Traumatic rings with a proliferation of resin canals have become more frequent along the reservoir islands since its flooding, even at some distance from shoreline. While the factors responsible for the development of these rings are not fully known, the most likely hypothesis is that they are a response to massive foliar loss. They are common in black spruce and their abundance is not dependent on tree age.

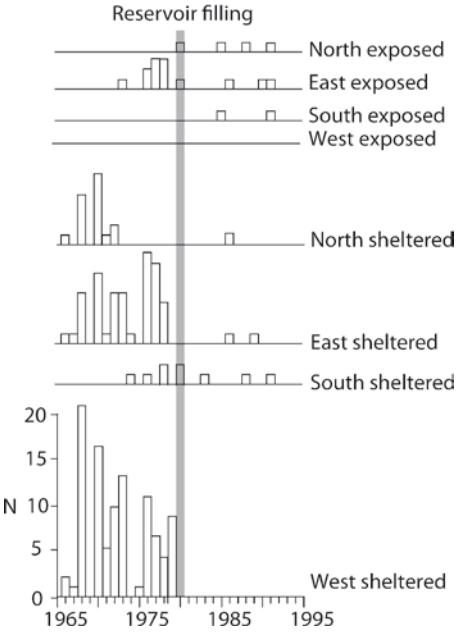

Fig. 4 Frost ring chronologies (number of frost rings amongst the sampled trees) on the islands of the Robert-Bourassa Reservoir. The *gray bar* indicates the year of flooding. The four *upper diagrams* indicate trees at the shoreline edge (exposed to the north, east, etc.); the *lower diagrams* correspond to trees sheltered from the wind (trees selected along a band transect towards the inner part of the island)

4.4 Trees Destabilized by the Wind

Although the trees occupied windy positions on the hilltops before the reservoir's flooding, their current situation on the islands that formed after flooding likely exposes them to greater winds. However, wind destabilized trees were found primarily on the shorelines and in open forests. At shoreline sites, we avoided sampling trees with leaning stems to avoid reaction wood, particularly for the densitometric analysis. Reaction wood is over-lignified wood that appears as a reaction to changes in mechanical tension that occur when a stem is destabilized (Scurfield 1973). Lignin gives wood an amber color and makes reaction wood readily identifiable. The majority of the trees showed the start of reaction wood sequences in 1980 (Fig. 5). This observation confirms that an increase in local wind force has occurred, as suggested by other work conducted on the edges of reservoirs (Arritt 1987). The presence of reaction wood and its orientation in the stems (it develops on the side where the tree is bent) are important indicators that allow wind events to be dated and delineated spatially.

4.5 The New Insular Nival Regime and Mechanical Damage to Pre-established Trees

By creating a barrier to the wind, forest edges capture powdered snow and contribute to the modification of local snow conditions. Indeed, one of the most important impacts of the reservoir was the creation of large ice surfaces over which the wind blows to create new distribution patterns of snow on the ground. Once the ice cover of the reservoir is consolidated in December, snow collected and blown by the wind

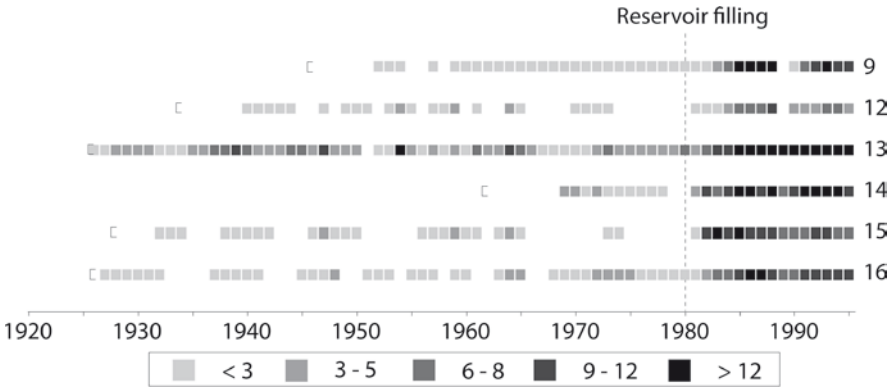

Fig. 5 Proportion of trees (in classes of three) located at the tops of islands and possessing reaction wood sequences due to destabilization by the wind before and after the reservoir's creation. Numbers on the right refer to sampling sites (Fig. 2)

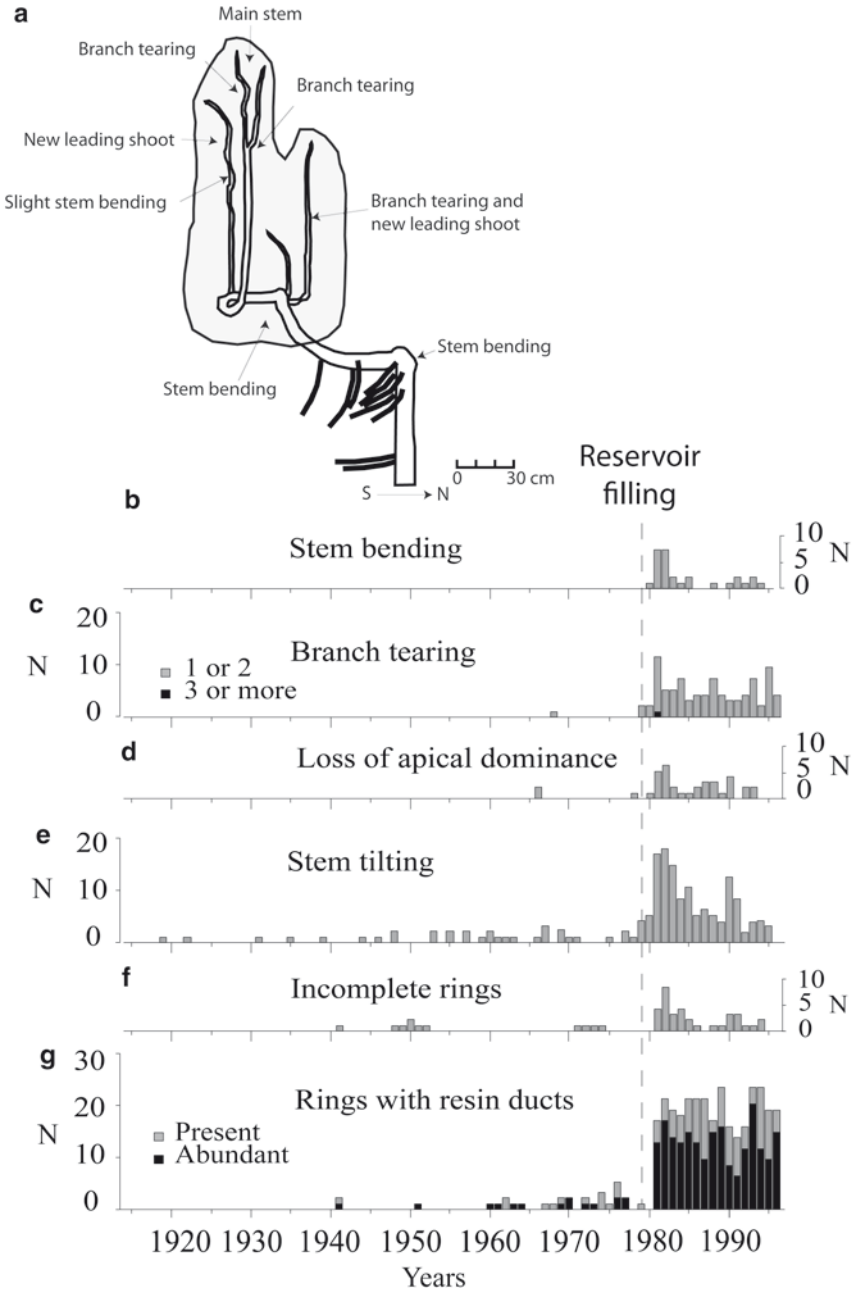

Fig. 6 (**a**) Schematic representation of a tree having experienced severe disturbances due to the over accumulation of snow on an island. (**b**–**g**) Frequency of damage to trees. The number of trees studied = 46. (**b**) Stem bending dated by the beginning of compression wood sequences and plowing scars. (**c**) Frequency of branch tearing scars. (**d**) Death of apical axis and development of a new leading stem. (**e**) Start of compression wood sequences (at least five consecutive rings) indicating stem tilting. (**f**) Incomplete rings. (**g**) Traumatic rings with alignments of resin ducts (Tremblay and Bégin 2005)

over large distance accumulates at the obstacles that are situated on the exposed southwestern banks. The islands, which were formerly hilltops that had little snow in winter due to winds, are now effective snow traps that collect up to 4 m of snow (in the past they only accumulated 1 m). The distribution pattern of snow depends on the orientation of the bank, the size and height of the island, and the forest structures present. The small islands have little effect on the wind as they are not obstacles. Their ability to accumulate snow is limited. Tall islands and those with large forest structures capture lots of snow. However, snow accumulation in the forests is highly dependent on the effectiveness of the barrier created by the foliage and branches of the first fringe of exposed trees. The progressive degradation of this fringe and/or the modification of its growth forms results in the accumulation of snow deeper and deeper within the forest to the point where damage caused by the over-accumulation of snow becomes common. This phenomenon has previously only been observed on large lakes within the subarctic zone (Boivin and Bégin 1997). Thus, it appears that the creation of the Robert-Bourassa Reservoir allows for the expression of phenomena that are generally found in the subarctic and not yet reported from lakes further south.

In order to determine the dendrochronological indicators regarding changes in the snow accumulation regime for an island in the Robert-Bourassa Reservoir, Tremblay and Bégin (2005) examined trees damaged by excessive snow. Changes in their growth forms recorded the history of damage that they experienced since the reservoir's flooding (Fig. 6a). The study revealed a gradual change in the local snow accumulation regime that corresponded with the degradation of the forest due to wind exposure. Beyond the riparian forest border that acts as an obstacle to the wind, snow accumulates towards the center of the island. Since the creation of the reservoir, trees in the shoreline forest have been subjected to various types of visible damage including stem bending, knocking over of stems, and tearing off of branches due to heavy snow loads (Fig. 6b–e). Damage to trees resulted in growth anomalies that spontaneously appeared within 3 years of the injury (Fig. 6f–g). Changes in tree growth patterns documented the degradation processes of the forest's margin. Abundant incomplete rings and traumatic rings with resin canals were found within the exposed trees at the periphery of the island, while trees situated in the interior possessed numerous scars that developed following mechanical damage related to excess snow. Damage abundance is related not only to the quantity of precipitation, but also to the reservoir's level in winter.

5 Discussion and Conclusions

The application of dendrochronology in this study relies on several fundamental principles. Firstly, although the reservoir has existed since 1980, it is possible that manifestations of the climatic effects may depend on certain events or a combination of conditions that have not yet occurred to leave obvious traces in the environment. However, the likelihood that stressful events have not occurred has

been minimized by choosing the oldest reservoir in the La Grande complex. It has already been reported that visible manifestations of the influence of large subarctic lakes only occur on their immediate edges and on their islands. By analog, we have formulated the hypothesis that the effects of the reservoir on the forest will also be restricted to the reservoir's edges and islands. Knowledge of the regional dendroclimatic signal is required to test this hypothesis. Furthermore, the temporal dichotomy offered by the key year of 1980, corresponding to when the reservoir was flooded, allows for the calibration of the dendrochronological indicators representing the reservoir's microclimatic effects with data concerning previous growth conditions.

Secondly, variations in the growth of trees that are affected by the climatic effects of large water bodies only provide an indirect and minimal measure of this influence. Trees only react to stress once a threshold has been passed and the thresholds vary according to species, tree status within the stand, age, abundance of foliage, and state of health. It is possible that the climatic influence of a lake on its surrounding environments may only affect a few sensitive individuals or cause different reactions amongst individuals. The analysis of these reactions and a clear understanding of the biological and ecological characteristics of the tree species in question are therefore fundamental. Manifestations of climatic stress, as shown by abnormal tree growth forms, only allow minimal assessments of the affected riparian strip, beyond which timber productivity and reproductive efforts can be affected by distance from the water body and exposure to the dominant westerly winds.

Thirdly, tree growth is subject to numerous ecological factors that must be distinguished from the influence of climate. Although trees can record some punctual climatic stress events (frost events during the growth season), tree rings more typically provide a signal representing the cumulative events that describe the interannual trends of the region's climatic fluctuations. Through the careful selection of trees, according to their environmental conditions and physical characteristics, these factors can become a well-controlled variable in the analysis (Fritts 1976). Finally, the microclimatic effect of the reservoir may increase or decrease through the action of macro climatic events, which, under certain conditions, favor or limit the expression of the exposed trees' reactions. We propose a third hypothesis that the expression of climate is a result of the specific ambient conditions existing at strategic moments of a tree's life and according to temporal variations in its growth and the growth season. For example, at the edge of the reservoir, the duration of the ice cover would delay and slow growth, delay the development of reproductive structures, and lead to growth anomalies. Analyzing these growth characteristics would allow the effect of the local climate to be delimited for particular moments of the year.

The creation of large reservoirs is a good example of the type of major development projects that humans are capable of constructing. While we may not have the ability to control natural hazards, we do have the ability to exacerbate them. In the context of current climate change, of which we are a cause, these vast reservoirs constitute areas where mankind's footprint will last forever.

Acknowledgements This study was financially supported by Hydro-Québec, National Sciences and Engineering Research Council of Canada, Ouranos Consortium on Regional Climatology and Adaptation to Climate Change, ArcticNet, Indian and Northern Affairs Canada, Fonds québécois de la recherche sur la nature et les technologies, and the town of Radisson. The authors thank S. Levesque (Hydro-Québec), J. Frydecki (formerly from Université Laval), L. Cournoyer (Université Laval), L. Astrade (postdoctoral fellow), S. Boivin (research assistant), and graduate students (D. Boudreault, O. Gagnon, N. Kinnard, É. Labrecque, J. Tremblay, and M. Tremblay), P. Jasinski (translation) and M. Renaud (editing) for their participation in various steps of this research. This study was conducted under the research framework of the Centre d'études nordiques, at a time when the first author was a professor at Université Laval, Québec, Canada.

References

Arritt RW (1987) The effect of water surface temperature on Lake Breezes and thermal Internal Boundary Layers. Boundary-Layer Meteorol 40:101–125

Boivin S, Bégin Y (1997) Development of a black spruce (*Picea mariana*) shoreline stand in relation to snow level variations at Lake Bienville in Northern Québec. Can J Forest Res 27:295–303

Butorin NV, Vendrov SL, Dyakonov KN et al (1973) Effects of the Rybinsk reservoir on the surrounding area. In: Ackermann WC, White GF, Worthington EB et al. (eds) Man-made lakes: their problems and environmental effects. Conference proceedings of the American Geophysical Union, Knoxville, Tennessee. Geophys Monogr 17:246–250

D'yakonov KN, Reteyum AY (1965) The local climate of the Rybinsk Reservoir. Soviet Geo 6(10):40–49

Eichenlaub VL (1979) Weather and climate of the Great Lakes region. University of Notre-Dame Press, Indiana

Fitzharris BB (1979) Climatic questions arising from Upper Clutha valley hydro development. NZ Geogr 35:64–70

Fritts HC (1976) Tree rings and climate. Academic Press, London

Glerum C, Farrar JL (1966) Frost ring formation in the stems of some coniferous species. Can J Bot 44:879–886

Gooseff N, Strzepek K, Chapra SC (2005) Modeling the potential effects of climate change on water temperature downstream of a shallow reservoir, lower Madison River, MT. Climat Change 69:331–353

Lavoie C, Payette S (1997) Late-Holocene light-ring chronologies from subfossil black spruce stems in mires of subarctic Québec. Holocene 7(2):129–137

Litynski JK, Levesque S, Gilbert R (1989) Étude d'impact sur le climat : Rivière Ashuapmushuan. Final report of a Hydro-Québec study, ENVC-89-ENV-00-024

Météoglobe Canada (1992) Étude des effets climatiques suite à la création des réservoirs. Report for Hydro-Québec Environment Service, Montréal

Mysak LA (1993) Variabilité et changement climatiques et les aménagements hydroélectriques dans le nord du Québec. Environmental assessment of the Grande Baleine Project: Synthesis document 1. Bureau de soutien de l'examen public du projet Grande Baleine

Perrier MG, Zwack P, East C (1977) Analyse du climat de la région de La Grande Rivière de la Baleine et étude préliminaire de l'impact climatique des futurs réservoirs. I : Texte et appendices. Centre de recherche en sciences de l'environnement (CERSE)

Schweingruber FH (1988) Tree rings. Kluwer, Dordrecht

Schweingruber FH, Fritts HC, Braeker OU et al (1978) The X-ray technique as applied to dendroclimatology. Tree-Ring Bull 38:61–91

Scurfield G (1973) Reaction wood: its structure and function. Science 179:647–655

SEBJ (1987) Le complexe hydroélectrique de La Grande Rivière. Société d'Exploitation de la Baie James, Chenelière, Montréal

Shirata H (1969) Thermal influence of the lake Inawashiro on the local climate in summer daytime. Sci Rep Tohoku Univ 18:213–220

Sirois L, Bégin Y, Parent J (1999) Female gametophyte and embryo development of black spruce along a shore-hinterland climatic gradient of a recently created reservoir, Northern Quebec. Can J Bot 77:61–69

Sottile M-F, Levesque S (1989) Conséquences des scénarios de changement climatique sur les infrastructures liées à la production d'hydro-électricité au Québec. Final report for the Atmospheric Environment Service, 15SD-KM351-8-S101

Stivari SMS, De Oliveira AP, Soares J (2005) On the climate impact of the local circulation in the Itaipu Lake area. Clim Change 72:103–121

Tamenasse J (1980) Connaissances du milieu dans la région de LG 2. Eau du Québec 13:16–20

Therrien N (ed) (1981) Simulating the environmental impact of a large hydroelectric project. The society for computer simulation. Simulation proceedings series, vol 9

Tremblay J, Bégin Y (2005) The effects of snow-packing on tree growth forms on an island in a recently created reservoir in Northern Québec, Canada. Écoscience 12:530–539

Vendrov SL, Malik LK (1965) An attempt to determine the influence of large reservoirs on local climate. Sov Geo 5(10):25–40

Spring Water Levels Reconstructed from Ice-Scarred Trees and Cross-Sectional Area of the Earlywood Vessels in Tree Rings from Eastern Boreal Canada

Jacques C. Tardif, Susanne Kames, and Yves Bergeron

Ice floods occurring at the time of spring break-up were reconstructed for Lake Duparquet, a large unregulated water body located at the southern fringe of the boreal forest in north-western Quebec (Tardif and Bergeron 1997). Reconstruction of the frequency and magnitude of spring floods associated with ice break-up was successfully achieved using cross-dating of ice-scars occurring along the trunk of northern white-cedar (*Thuja occidentalis*) trees exposed to drifting ice and debris during ice break-up. Maximum ice-scar height was also used as an indicator of high lake water level. Ice-scarred trees were systematically sampled on the islands and lake shore. A total of 81 *T. occidentalis* trees were collected resulting in 253 cross-sections and over 2,000 dated scars associated with 616 scarring events. All scars were dated using cross-dating within (prior and after the recorded event) and among samples. The reconstruction was also recently compared with earlywood vessel anomalies occurring in tree rings from black ash (*Fraxinus nigra*) trees growing on the lake floodplain. It was hypothesized that earlywood vessel development would be affected in *F. nigra* trees exposed to floods lasting into the early growing season thus resulting in reduced cross-sectional area of the earlywood vessels. Earlywood vessels were analyzed in twenty *F. nigra* trees from two floodplain stands. After cross-dating, the cross-sectional area of the earlywood vessels was measured in each tree-ring using WinCell Pro Ver. 2004a (Régent Instruments Inc. 2005). In the absence of long term hydrological data for Lake Duparquet, mean

J.C. Tardif (✉) and S. Kames
Centre for Forest Interdisciplinary Research (C-FIR), University of Winnipeg, Winnipeg MB, R3B 2E9, Canada
e-mail: j.tardif@uwinnipeg.ca

Y. Bergeron
NSERC-UQAT-UQAM Industrial Research Chair in Sustainable Forest Management, Université du Québec en Abitibi-Témiscamingue, Rouyn-Noranda QC, J9X 5E4, Canada

M. Stoffel et al. (eds.), *Tree Rings and Natural Hazards: A State-of-the-Art*, Advances in Global Change Research 41, DOI 10.1007/978-90-481-8736-2_24,

monthly discharge of the unregulated Harricana River, located about 100 km to the east, was used as a proxy for the lake water level.

The ice-scar chronology revealed an increase in ice-scar frequency since about AD 1870 corresponding roughly to the end of the Little Ice Age (Fig. 1a). From 1890, ice scars were most frequent in 1934, 1936, 1939, 1947, 1956, 1967, 1976–1977, 1979–1980 and 1986 (Fig. 1a and Table 1). A comparison of both cumulative ice-scar frequency distribution and *T. occidentalis* age distribution indicated that they were significantly different (Fig. 1a; Kolmogorov-Smirnov test; $p < 0.0001$) stressing that the increase in ice-activity observed in the twentieth century is not to be associated with over sampling of younger/smaller *T. occidentalis* trees (Tardif and Bergeron 1997).

For example, only 5% of the scarring events were recorded in 1870 at a time when more than 80% of the trees were present on the lake shore (Fig. 1a). On Lake Duparquet, an increase in maximum ice-scar height was also observed during the twentieth century (Fig. 1b) with maximum height being approximately 100 cm higher than during the late part of the Little Ice Age (Tardif and Bergeron 1997). In the twentieth century high flood levels at the time of ice break-up were observed in 1922, 1947, 1959, 1976, 1979 and 1984 (Fig. 1b and Table 1). Some of these years also corresponded to years with abundant scarring events (Fig. 1a). Many of the major flood years on Lake Duparquet were also reported in other regions

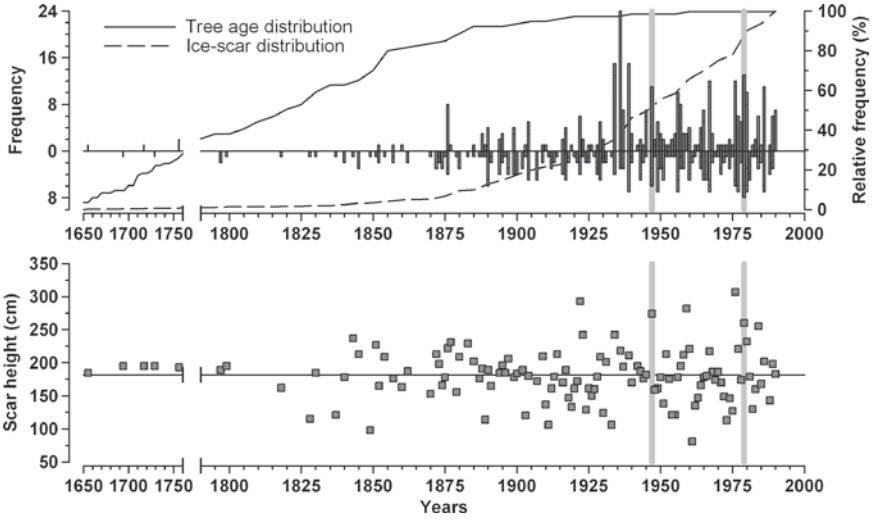

Fig. 1 *Thuja occidentalis* ice-scar chronology for the period 1655–1990 (*top figure*). Values above the zero line are from visible scars and values below the zero line are from hidden scars discovered after sectioning of the trees. Both the cumulative tree age and scar distributions are also indicated. The *bottom figure* represents the maximum ice-scar height recorded for the same period. The years 1947 and 1979 are indicated by the *gray bars* (Adapted from Tardif and Bergeron 1997)

Table 1 List of the years for which values of the cross-sectional area of earlywood vessels chronology were 1.28 standard deviation below the mean and for which both ice-scar frequency and maximum height were above 1.28 standard deviation above their respective mean value for the overlapping reference period 1890–1990. The years in **bold** correspond to those with tree-rings showing reduced earlywood vessel area that were synchronous with either scar frequency and/or scar height

Vessel area	Scar frequency	Scar maximum height
1890	1934	**1922**
1907	1936	**1947**
1909	1939	1959
1917	**1947**	1976
1922	1956	**1979**
1928	**1967**	1984
1947	1976	
1950	1977	
1960	**1979**	
1967	1980	
1979	1986	
1989		

(Payette 1980; Bégin and Payette 1988). As hypothesized, anomalies in the earlywood vessels were observed in *F. nigra* trees (Fig. 2a).

The chronology values were negatively skewed and years with lowest cross-sectional area of the earlywood vessels were 1890, 1907, 1909, 1917, 1922, 1928, 1947, 1950, 1960, 1967, 1979, and 1989 (Fig. 2). Many of these years also corresponded with years of maximum ice-scar frequency and/or ice-scar height (Table 1). An example of severe reduction in the cross-sectional area of the earlywood vessels is presented for the year 1947 (Fig. 2b), a year also corresponding to abundant ice scarring and maximum ice-scar height (Table 1). The large scale nature of the climatic events leading to high magnitude floods may be illustrated by the year 1979, a major and widespread flood year that may have been triggered by climatic conditions prevailing across all of Canada (Payette 1980). In 1979, the extent of the snow cover over North America was also maximal (Groisman et al. 1993). At Lake Duparquet, this high magnitude flood also resulted in the year 1979 being one of reduced cross-sectional area of the earlywood vessels in *F. nigra* trees exposed to flooding (Table 1).

Using the period of overlap among all chronologies (1890–1990), both ice-scar derived chronologies (frequency and maximum height) were significantly associated (Spearman $r = -0.723$, $p < 0.001$). Interestingly, the earlywood vessel chronology was negatively associated with both ice-scar frequency and maximum height (Spearman rho $r = -0.573$, $p < 0.001$ and -0.329, $p = 0.001$, respectively). The strong association between the ice-scar derived chronologies and the independently derived earlywood vessel chronology suggests that during major ice-flood years, the high water level on Lake Duparquet may persist long enough so that the earlywood vessel production of floodplain *F. nigra* trees is affected. All three chronologies were also associated with the Harricana River mean discharge for the period

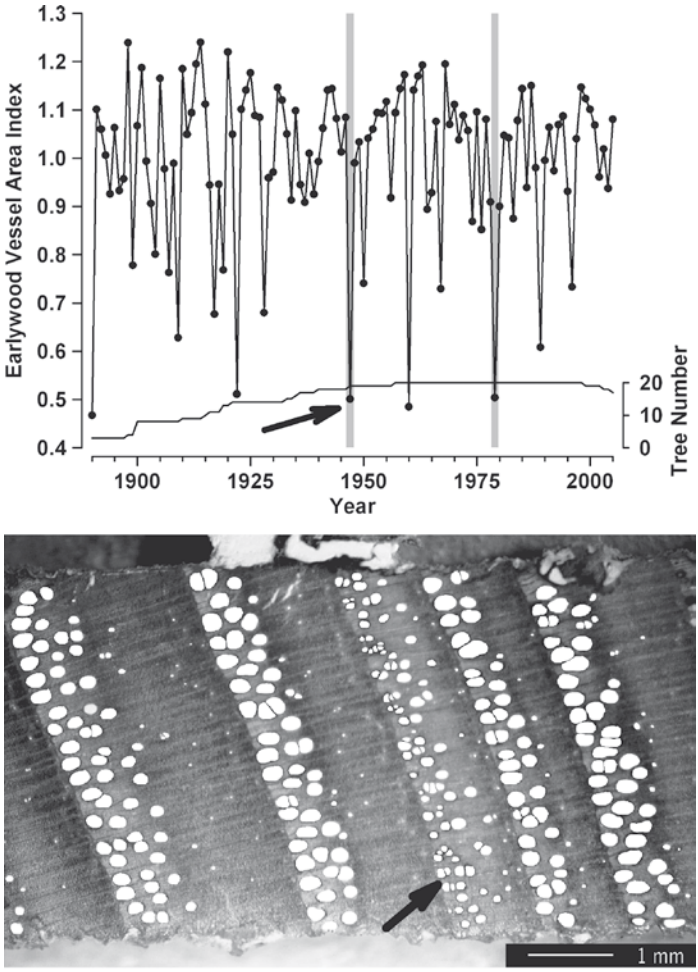

Fig. 2 Standardized mean cross-sectional area of the earlywood vessels for the period 1890–2005 from 20 *Fraxinus nigra* trees growing on the Lake Duparquet floodplain (*top figure*).The number of trees in the chronology is indicated. Tree ring sequence in *F. nigra* showing complete rings for the years 1945–1948 (*bottom figure*). The year 1947 (*black arrow*) is characterized by abnormally small cross-sectional area of the earlywood vessels. Vessel lumens were highlighted in *white* to increase contrast. Adjacent vessels were separated with *black lines*. Cracks in the wood appear white as cores were rubbed with chalk. The years 1947 and 1979 are indicated by the *gray bars*

1915–1990. The river discharge in both May and June was positively associated with ice-scar frequency (Spearman $r = 0.539$, $p < 0.001$ and $r = -0.390$, $p < 0.001$ respectively) and with maximum ice-scar height (Spearman $r = 0.380$, $p < 0.001$ and $r = -0.265$, $p = 0.021$ respectively). They were also both negatively associated with the earlywood vessel chronology (Spearman $r = -0.719$, $p < 0.001$ and $r = -0.551$, $p < 0.001$ respectively). In a context where spring flood levels have

increased since the end of the Little Ice Age, one would expect that *F. nigra* trees would also register these changes. Reduced cross-sectional area of the earlywood vessels in *F. nigra* were found to correspond to major spring floods in the twentieth century but at the moment the chronology does not extend sufficiently back in time to allow further validation of the ice-scar data. Changes in *F. nigra* stand dynamics were however documented in response to raising water levels (Tardif and Bergeron 1999). Interestingly, ice-scars are revealing flood level at the time of break-up whereas anomalies in the earlywood vessels may correspond to spring floods persisting into the early growing season. Further work on the hydrological and climatic information in earlywood vessel anomalies is currently underway. While each data set has its own specificity, the correspondence between the two can be used to provide better understanding of the historical variation in the frequency, magnitude and potential hazard associated with flooding. The correspondence of our results with those of other studies (Tardif and Bergeron 1997) and the correspondence of specific flood dates across large areas further indicated the regional nature of these events and the ability to use a large network of tree-ring chronologies to better understand changes in flood regime and climate in northern regions.

References

Bégin Y, Payette S (1988) Dendroecological evidence of lake-level changes during the last three centuries in subarctic Québec. Quat Res 30:210–220

Groisman PY, Karl TR, Knight RW (1993) Observed impact of snow cover on the heat balance and the rise of continental spring temperatures. Science 263(5144):198–200

Karl TR, Groisman PY, Knight RW, Heim RR Jr (1993) Recent variations of snow cover and snowfall in north America and their relationship to precipitation and temperature variations. J Clim 6:1327–1344

Payette S (1980) Les grandes crues glacielles de la rivière aux feuilles (Nouveau-Québec): une analyse dendrochronologique. Naturaliste Canadien 107:215–225

Régent Instruments Inc. (2005) WinCell Pro Version 2004a user manual. Québec, Québec

Tardif J, Bergeron Y (1997) Ice-flood history reconstructed with tree rings from the southern boreal forest limit, western Québec. Holocene 3:291–300

Tardif J, Bergeron Y (1999) Population dynamics *of Fraxinus nigra* in response flood-level variations, in northwestern Québec. Ecol Monogr 61:107–125

A 100-Year History of Floods Determined from Tree Rings in a Small Mountain Stream in the Tatra Mountains, Poland

Tomasz Zielonka, Jan Holeksa, and Szymon Ciapała

1 Introduction

Dendrochronological methods enable the dating of episodes with sudden disturbance events such as forest fires, tree uprooting, rockfall, and snow avalanches in time and space (e.g. Denneler and Schweingruber 1993; Fantucci 1999; Lang et al. 1999; Niklasson and Granström 2000; Storaunet and Rolstad 2004; Stoffel and Perret 2006). Tree rings have also been used to identify floods and raised water levels (Harrison and Reid 1967; Begin and Payette 1988; Hupp 1988; Gottesfeld and Gottesfeld 1990; Tardif and Bergeron 1997; Begin 2001). Information on past activity might be preserved in living trees or dead stumps, thus allowing a long-term reconstruction of past flood events (LePage and Bégin 1996; Yanoski 1999; St George and Nielsen 2003). The time window accessible using tree scars is probably wider than that achieved by dating coarse woody debris accumulated in stream channels. This seems to be especially true for small, steep mountain streams with water flow causing redistribution, fragmentation and abrasion of tree trunks shortly after their delivery to the channel.

Annual rings of various tree species record the occurrence of floods following cambium injury or death in a portion of the circumference due to mechanical abrasion. If the size of the wound is not sufficiently large for the tree to be killed, the injury is often overgrown in the years following the event to form a scar. The identification of overgrown scars can allow for a detection of the exact year of an event that

T. Zielonka (✉)
Southern Swedish Forest Research Centre, Swedish Agricultural University, SE-230 53 Alnarp, Sweden
e-mail: t.zielonka@botany.pl
and
Polish Academy of Sciences, Institute of Botany, 31-512 Kraków, Poland

J. Holeksa
Polish Academy of Sciences, Institute of Botany, 31-512 Kraków, Poland

S. Ciapała
Department of Ecology and Environmental Management, University School of Physical Education, 31-571 Kraków, Poland

M. Stoffel et al. (eds.), *Tree Rings and Natural Hazards: A State-of-the-Art*, Advances in Global Change Research 41, DOI 10.1007/978-90-481-8736-2_25,

caused the injury (Arno and Sneck 1977). Flood scars are wounds on the stems of trees growing on channel banks and in floodplains caused by impacts from objects transported with water (Gottesfeld 1996) such as floating woody debris, ice, stones and boulders. A distribution of scars on calendar-time scale permits the identification of years with flood events (Harrison and Reid 1967). There are, however, only few examples of flood event reconstructions using tree scars in Europe. Historical information about flood events is usually limited to rivers crossing inhabited areas where floods are a serious source of damage. Much less information is available from small forested catchments, such as the one identified for this research. Data generated by such a study might be very important in explaining and understanding fluvial activity of streams, geomorphological dynamics of stream channels, transportation of debris including coarse woody debris or the dynamics of riparian vegetation (McCord 1996).

Floods are among the most dangerous and unpredictable phenomena responsible for enormous losses and constituting a major threat for people. Detailed knowledge of the flood regime in the past, their frequency and intensity is important for the evaluation of potential threats for the future. Because floods are phenomena of cyclic character, it is especially important to obtain the longest possible series of observation. For this purpose, the length of dendrochronological reconstructions may significantly exceed standard series of discharge measurements or climatic records.

This study aims at (i) reconstructing a history of floods in a small mountain stream, (ii) relating these events to meteorological records, and at (iii) indicating possible combinations of extreme weather variables, which may be responsible for the occurrence of floods.

2 Study Site

The study was conducted in the Polish Tatra Mountains in the Western Carpathians and focused on the Potok Waksmundzki mountain stream (Fig. 1). The climate in this area is cool (mean annual temperature: 2–4°C, Hess 1996) and the annual precipitation at elevations of approximately 1,600 m a.s.l. reaches 1,800 mm/year. Common soils in the area are acid podzols formed on granite bedrock (Komornicki and Skiba 1996).

The Potok Waksmundzki stream originates at an elevation of 1,950 m a.s.l. and its outlet into the Białka River is located at approximately 1,000 m a.s.l. The total length of the stream is 6.6 km, the mean slope is 14.6% and the drainage basin area is 5.35 km^2. Bedrock of the valley is dominated by granite and below 1,430 m a.s.l. the stream flows through a forested area. The Waksmundzka Valley belongs to the best preserved areas in the Polish Tatra Range, as the entire valley has been declared a strict reserve in the Tatra National Park for the last 50 years, thus forest management practices and other human activity have been significantly limited.

The study was conducted along a 2.75 km-long section of the stream at an altitudinal range of 1,380–1,080 m a.s.l., where the stream flows through a natural subalpine forest.

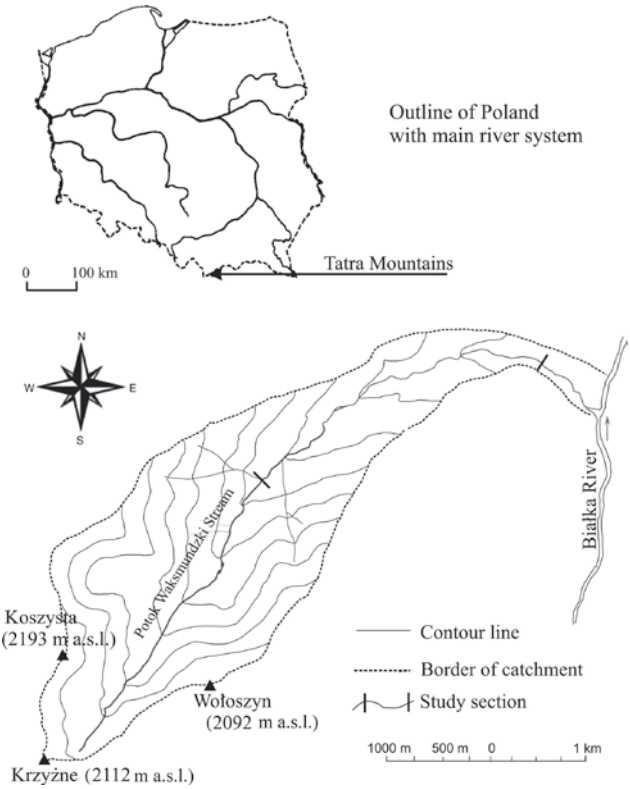

Fig. 1 Map of the study site. The catchment of the Waksmundzki stream and its location on a map of Poland

The stand covering the entire valley including the stream banks is dominated by Norway spruce (*Picea abies*). At higher elevations, dwarf pine (*Pinus mugo*) and individual stone pines (*Pinus cembra*) are present as well. Forest stands in the valley are unevenly-aged and spruces 150–200 years old dominate, however some of the oldest spruces attain up to 350 years at DBH (Zielonka 2006). The bottom of the valley near the channel is usually covered with younger tree cohorts.

3 Material and Methods

Basal parts of trees, both living and dead, were inspected on both banks of the stream for the presence of scars and the other growth anomalies. Only scars closest to the stream channel and facing the stream axis were integrated (Fig. 2). We paid attention to exclude scars formed by other factors such as the fall of neighbors from inside the forest or rot. Scars of doubtful origin were not included in the study.

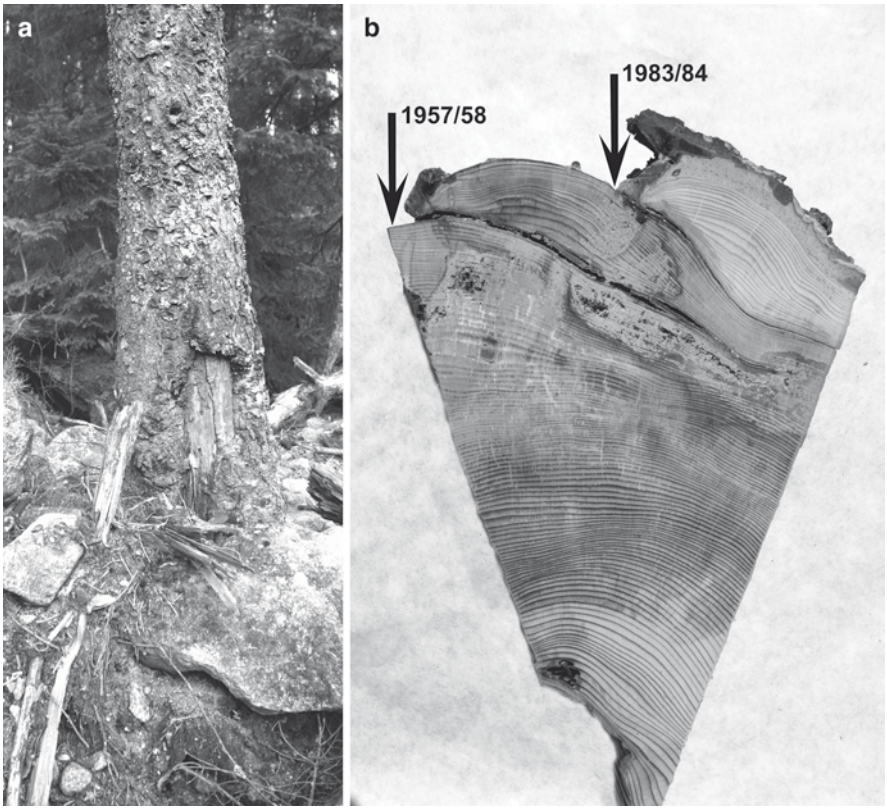

Fig. 2 A typical flood scar in a base of a spruce stem from the stream bank formed by debris transportation during a flood event (**a**). Cross-section extracted from the stem exhibits two flood scars. Dendrochronological cross-dating indicates that both scars were formed during the dormant season, namely in 1957/1958 and 1983/1984 (**b**)

In total, 48 wood samples containing scars were extracted with a saw from dead and living trees, with trees being evenly distributed along the 2.75 km-long section of the stream. While whole cross-sections were collected from dead stumps, sampling of living trees was restricted to the extraction of wedges from the scars (Arno and Sneck 1977). In the lab, samples were dried and polished with a belt sander. For the construction of a local reference chronology, 30 living spruces were chosen in the forest surrounding the stream within an altitudinal gradient between 1,100 and 1,300 m a.s.l. Selected trees belonged to the dominant layer and were free from visual signs of mechanical disturbance like broken tops or damaged branches. Each tree was cored twice perpendicular to the slope direction. Cores were glued to wooden sticks, dried and polished. Ring widths of wood samples and cores were then measured with a resolution of 0.01 mm using the LINTAB measurement devices (Rinn 1996). Before constructing the reference chronology,

the validity of tree-ring measurements was checked with COFECHA (Holmes 1983) and two measurements of each tree were averaged. So as to eliminate long-term variability, time series were indexed using a five-point moving average (Baillie and Pilcher 1973). Wood samples with scars were then cross-dated against the reference chronology using standard parameters provided by the TSAP software (Rinn 1996), before the validity of the cross-dating was verified with the sequence of pointer years (Schweingruber et al. 1990). The calendar year of scar formation was then determined (Fig. 2). We compared the years of scar formation with available climatic data recorded at the meteorological station in Zakopane, located approximately 10 km from the study area at an elevation of 820 m a.s.l. Climatic records are available for the station since AD 1900. The following weather parameters were taken into consideration: average monthly precipitation for the April-September period, average winter precipitation (December–March), the highest 24-h precipitation in a year, and the difference between average April and May temperatures (as a snow melting indicator). Variance analyses were used to test the significance of the relationship between the years of scar formation and weather parameters. As the time of scar formation was determined with yearly resolution, we assumed that weather parameters responsible for spring and early summer floods are linked with scars formed in the previous calendar year during the dormant season.

4 Results

Most of the cross-dated tree-ring series covered the entire twentieth century (Fig. 3). The oldest ring identified in the trees growing along the channel was cross-dated to 1841. In 14 samples, the first rings were formed in the nineteenth century.

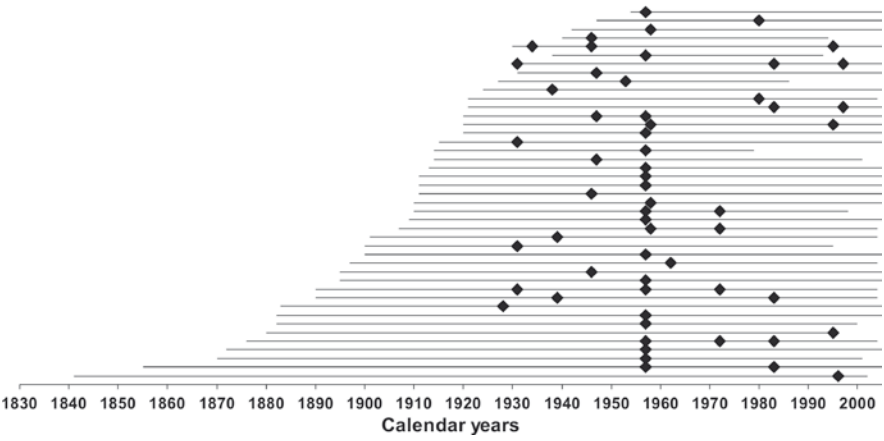

Fig. 3 Distribution of flood scars in time. *Horizontal lines* show the time span of each tree, *dots* indicate the year of scar formation in the trees sampled

However, in some cases, it was not possible to cross-date the pith due to rot in the central part of the stem.

Analyses allowed for a cross-dating of 58 scars (Fig. 3). The oldest recorded wound was induced in AD 1928. Four wood samples contained three scars, six samples contained two scars, and the rest of the trees bore just one scar (Fig. 3). For the period between AD 1928 and 2005, 17 years with scars were identified. On average, scars occurred every 4–5 years. The highest number of scars (33% of all recorded) was observed in the dormant season of 1957/1958. Numbers of scarred trees in the remaining years were much lower and did not exceed six scarred trees per year (1946/1947).

Monthly precipitation averages distinguished by both high values as well as peaks in the twentieth century overlapped with the years of scar formation (Fig. 4). This is especially true for the summer months, when precipitation was generally highest. Peaks in precipitation of July overlapped with scar formation in AD 1934, 1938, 1980 and 1997 (Fig. 4). The highest precipitation in the century occurred in June (over 300 mm in 1948, 1959 and 1972) and might be responsible for scar formation in the dormant season before cambial activity or in the beginning of cambial activity in these years. Similarly, the second highest level of precipitation during the last century, in May 1940 might have resulted in scars in the dormant season of 1939/1940. Unusually high precipitation in August 1938 (305 mm) and August 1972 (323 mm) might also have resulted in late summer floods which were responsible for scar formation. In September, which usually is much dryer than the summer months, high values of 272 mm were recorded in 1931 and 247 mm in 1996 when scars were formed. The relationship between years of scar formation and snow accumulation in winter (precipitation December–March) was not statistically significant, and no years with high winter precipitation coincides with years of scar formation (Fig. 4).

The maximal 24-h precipitation recorded in individual years does not seem to be strongly related with years of scar formation. In AD 1934, when the highest 24-h precipitation was observed (172 mm), only one scar was found in the trees (Fig. 5). During an important 24-h precipitation event in 1983 (109 mm), however, we identified five scars in the selected trees (Fig. 5).

The best explanation as to why the highest percentage of scars appeared in 1957/1958 (33%) was the extraordinary value of snow melting indicator (Fig. 6). The difference between the mean temperatures of April and May 1958 was more then twice higher than the average for the century and totaled 12.2°C (Fig. 6). This was the result of exceptionally low temperatures in April (mean 1.4°C) followed by a very warm May (mean 13.6°C) (Fig. 7). A similar situation may have occurred in 1929, when a difference between May and April temperature of 10.6°C was noted and the oldest scar found in AD 1928/1929. However, an ANOVA test for the entire series of scarred years did not confirm the significance of this relationship. In the case of the event year 1946/1947 showing the second highest number of scars, none of the analyzed parameters indicated abnormal precipitation or temperature distributions.

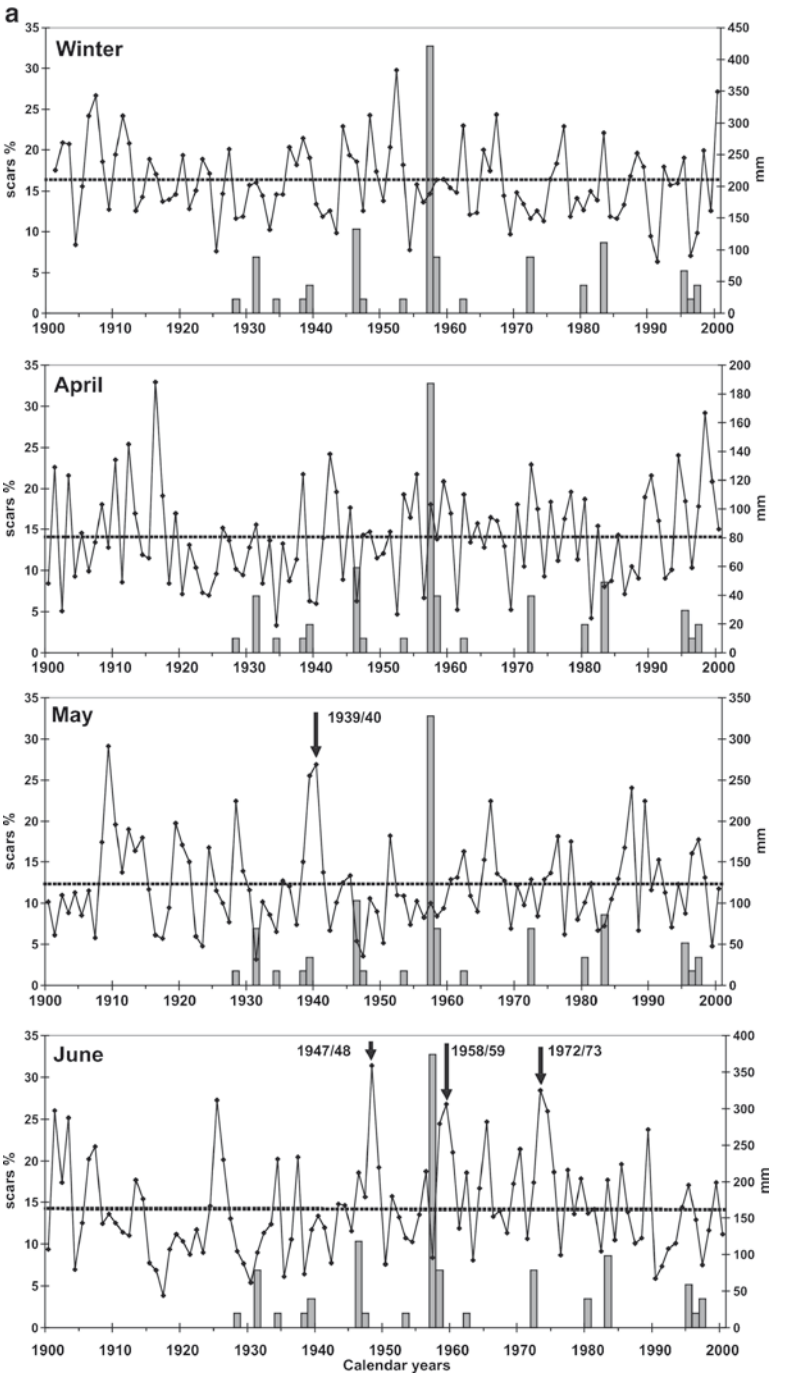

Fig. 4 Percentage of formed scars and the distribution of monthly precipitation in the twentieth century. Winter precipitation comprises precipitation in January, February, March as well as December of the previous year. *Dashed lines* show the average value for the century. *Arrows* indicate years with the highest precipitation which might be responsible for scarring

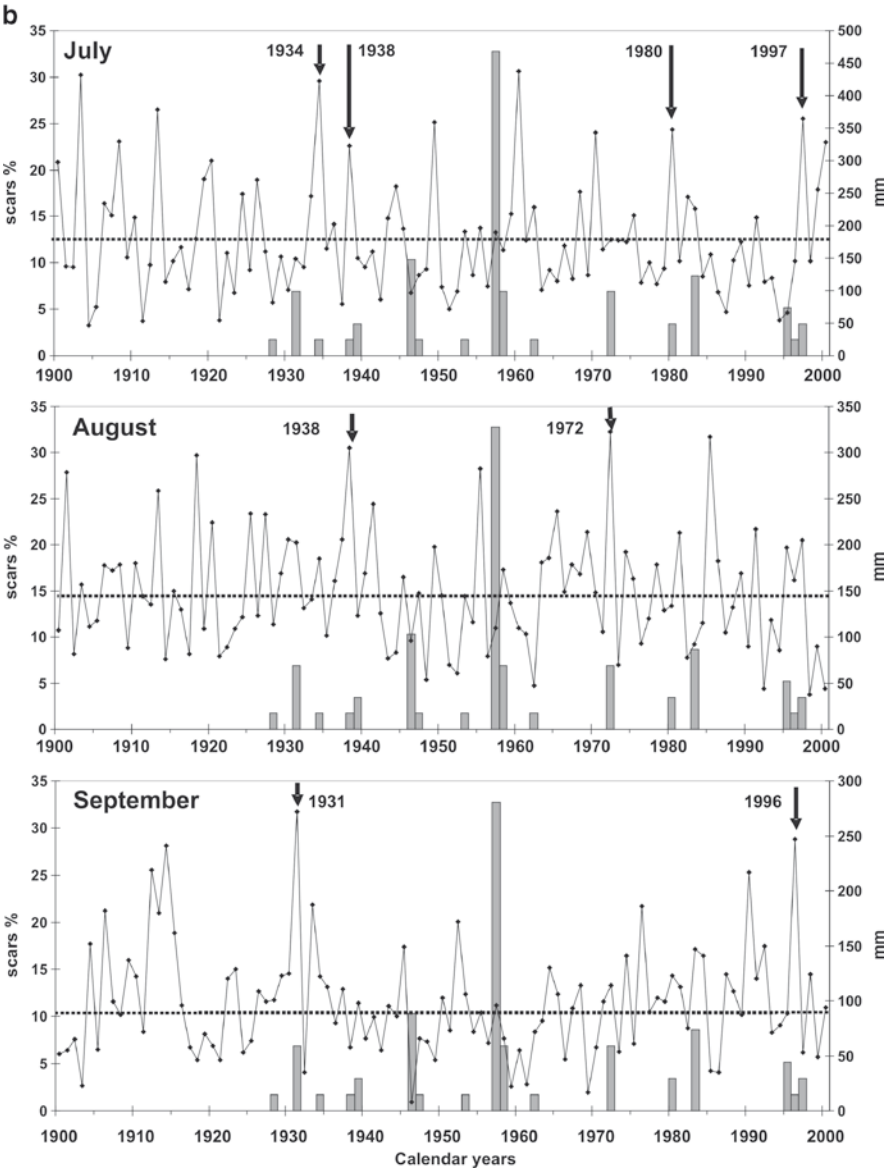

Fig. 4 (continued)

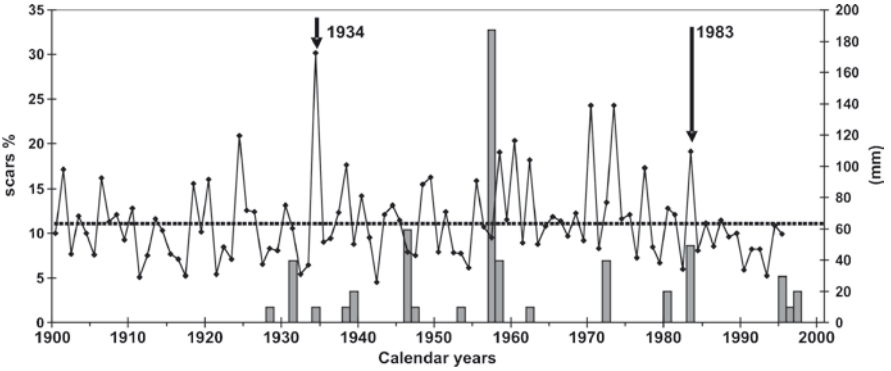

Fig. 5 Percentage of scars and the maximal 24-h precipitation recorded during a year. The *dashed line* shows the average value for the century. *Arrows* indicate years with the highest precipitation which might be responsible for scarring

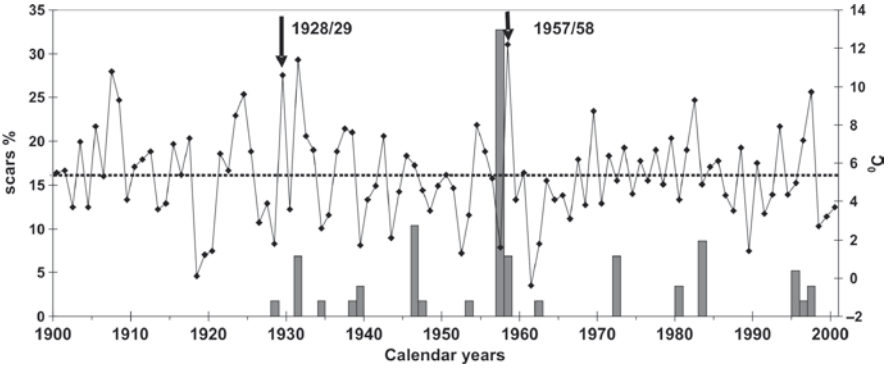

Fig. 6 Percentage of scars and snowmelt (difference between the average temperatures of April and May). The *dashed line* shows the average value for the century. *Arrows* indicate years with the highest values of the melting factor which might be responsible for scarring

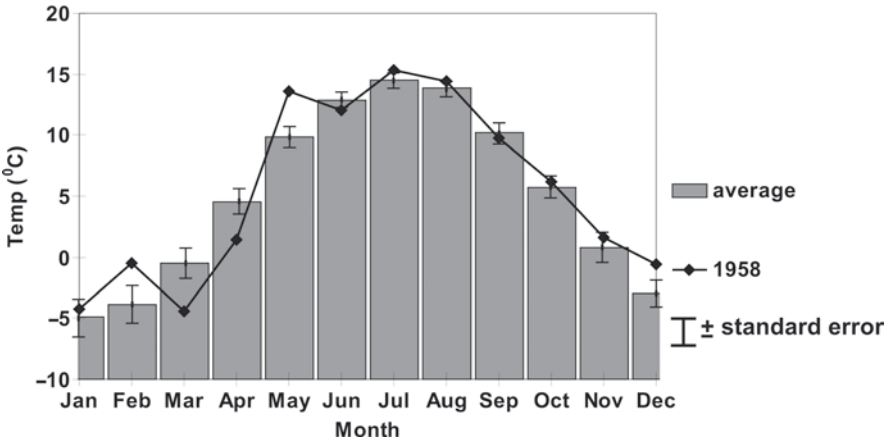

Fig. 7 Distribution of monthly temperatures, average for the whole century and for AD 1958

5 Discussion

In the Waksmundzki Potok stream, scars on trees are most likely caused by transported logs and probably also rocks and boulders. Logs of different stages of decay and various dimensions were present along the whole study section of the stream. Also, scars might be caused by granite boulders, which fill the stream channel. During fieldwork, boulders of different dimension were identified on the banks among ground vegetation, and this indicates that granite debris can be transported from and to the channel banks during floods. In contrast, floating ice, which can also be responsible for tree injuries (Begin 2001), is nonexistent in the studied stream due to the high relief and high decline of the stream channel.

According to Gottesfeld's (1996) observations, scars are easily formed on the stems of living trees by rubbing of transported logs during floods. Woody debris may hit partially submerged trees forming a wound, then rotate and continue movement downstream. Other stems may remain anchored against trees and start to rub the bark according to changes of the water level. Such a rubbing cycle may last from 10 s to several minutes with vertical movement ranging from 10 to 30 cm (Gottesfeld 1996). These mechanisms may also explain the occurrence of several scars in the same tree. After causing the first wound, a log remaining caught at the base of a living tree may cause further scars during the next flood event, thus resulting in a series of partially healed wounds (Fig. 2). On the other hand, successive and partially healed scars occurring at the same position of the tree trunk may also result from frequent impacts of debris.

The average time interval between subsequent flood events calculated for the period AD 1928–2005 was 4.5 years and shows that the Waksmundzki stream discharge can be highly variable and flood events appear very frequently. The lack of scars before AD 1928 could be caused by at least two factors. Most of the trees growing on the banks were rather young. Flow activity of the stream as a disturbance factor probably resulted in the lack or regular removal of old trees on the banks. It can also be expected that a minimal diameter is required for a tree to sustain an injury and survive. Trees of small diameters could easily be devastated by floating objects, or wounds might be too extensive to enable further growth. We can also presume that the channel was located at some distance from the present course of the stream before the late 1920s. Old, inactive channels, overgrown by vegetation and spruce regeneration were observed in the field in some flat fragments of the valley bottom.

Our results show that most probably there are two weather factors responsible for floods in the studied stream: violent mid-summer rainfall and heavy snow melting in spring. In the Tatras, the highest precipitation amounts occur in the summer months. The average July precipitation for the twentieth century was 177 mm. Rainfall in this month might be responsible for scar formation in AD 1934, 1938, 1980 and 1997. During these years, July rainfall varied from 323 to 423 mm and was more than twice as high as the mean precipitation for July. For example, at the beginning of July 1997, a large flood was recorded throughout southern Poland,

and much flood damage was reported along streams and rivers in the nearby area. August is characterized by lower average precipitation (147 mm), however, the rainfall can still be substantial in this month. In 1972, when four flood scars were formed, the highest August rainfall in the twentieth century was recorded (323 mm). Also, in AD 1938, a very wet July was followed by a rainy August.

The amount of snow fall during winter does not seem to influence the occurrence of spring floods. Irrespective of precipitation in winter, the depth of the snow cover is 0.5–1.5 m but locally may exceed 3 m in the higher elevations (Łajczak 1996). The rate of snow melting which most likely induces high water flows is more important. Many scars formed in the dormant season of 1957/1958 were most likely the result of such an intense snowmelt event in late spring of 1958. Climatic records also indicate that an unusual increase of the temperature in May occurred during this year. The monthly temperature of April was 3.1°C below average while the temperature of May was 3.8°C above average. The snow melting period, which normally lasts from April to May was limited to May in 1958. Also, the average precipitation in June 1958 exceeded considerably the average for the century. This may indicate that flooding in 1958 was a result of a coincidence of intensive snowmelt due to warm spring temperatures and high precipitation amounts in June. Such a combination of extremes, when snowmelt adds to the catchment discharge from the rainfall may cause flooding (Benestad and Haugen 2007). The flood in 1958 was also recorded in nearby Tatranská Lomnica (Slovakia), located on the other side of the mountain range (Koreň2005). Historical information also confirms a large flood in 1958 in southern Poland, described as "the largest since the Second World War" (Fal 1997). The oldest scar from 1928/1929 might also be a result of such an anomaly in AD 1929, when one of the highest differences between April and May temperatures was recorded.

The high precipitation in May and June reinforcing discharge normally caused by snowmelt may explain scar formation in 1939/1940, 1947/1948, 1958/1959 and 1972/1973, when the highest values of precipitation (>300 mm) were recorded.

The relatively small dataset collected in this study of the formation of scars during floods is to some extent accidental. The formation of a flood scar requires high flow, the presence of debris in the channel and finally an abrasive process in stems of trees growing on the bank. Thus, the flood scar indicates a flood event, but a period without scars does not have to be a period without floods. In the small scale of this study (2.75 km along a stream), a flood event may happen without leaving scars due to the lack of transported objects and therefore result in the absence of injured trees. Also scarred trees might have already disappeared from the banks. This means that the series of reconstructed flood events cannot be treated as a complete dataset. A similar problem concerns the intensity of the flood events. A high number of scars formed in the dormant season of 1957/1958 may indicate an event of relatively high intensity. In the case of the rest of the flood years when the number of scarred trees varied from one to six, the intensity of the flood can hardly be estimated. Available climatic records from Zakopane may not precisely reflect the weather conditions in the study area, where elevation is significantly higher. The use of monthly precipitation and temperature is a simplification as well,

as it might be too long a period to detect weather anomalies. For instance, the presence of six scars identified in 1946/1947 could not be explained with climatic data. This shows that stream flow in small catchments extending across wide altitudinal ranges and different hydrological zones may react very violently to abrupt local weather change, which might not be recognized with basic weather records.

6 Conclusions

Our study shows that it is possible to reconstruct flood events in the fine scale of a small mountain stream over almost one century. It is hard to point out one weather factor, which is responsible for these flood events. In the mountain area, a flood is usually linked with complex extreme meteorological events like violent rainfall and rapid snowmelt due to high spring temperatures. Small catchments of high relief and varied physiography may react very suddenly to weather extremes. Flood-scar evidence proves that the Waksmundzki Stream discharge can be highly variable. Cross-dated scars also enabled detection of past floods, which hardly could be reconstructed only with basic climatic data. The reconstruction of the flood history based on tree rings may substantially improve our understanding of this phenomenon, especially in different spatial scales when direct discharge records are lacking.

Acknowledgments This study was supported by the Ministry of Science and Higher Education (MNiSW project no. N N304 2366 33). We are grateful to Grzegorz Piątek and Piotr Malina who helped with the field and laboratory work.

References

Arno SF, Sneck KM (1977) A method for determining fire history in coniferous forests of the Mountain West. General Technical Report INT-42, US Department of Agriculture, Forest Service, Intermountain Forestry and Range Experiment Station, Ogden, Utah, pp 1–28

Baillie MGL, Pilcher JR (1973) A simple cross-dating program for tree-ring research. Tree-Ring Bull 33:7–14

Begin Y (2001) Tree-ring dating of extreme lake levels at the subarctic-boreal interface. Quat Res 55:133–139

Begin Y, Payette S (1988) Dendroecological evidence of subarctic lake-level changes during the last three centuries in subarctic Quebec. Quat Res 30:210–220

Benestad RE, Haugen JE (2007) On complex extremes: flood hazards and combined high spring-time precipitation and temperature in Norway. Clim Change 85:381–406

Denneler B, Schweingruber FH (1993) Slow mass movement. A dendrochronological study in Gams, Swiss Rhine Valley. Dendrochronologia 11:55–67

Fal B (1997) Powódź tysiąclecia? Wiedza i Życie 10 (in Polish)

Fantucci R (1999) Dendrogeomorphology in landslide analysis. In: Casale R, Margottini C (eds) Floods and landslides: integrated risk assessment. Springer, Berlin, pp 69–81

Gottesfeld AS (1996) British Columbia flood scars: maximum flood-stage indicators. Geomorphology 14:319–325

Gottesfeld AS, Gottesfeld LD (1990) Floodplain dynamics of a wandering river, dendrochronology of the Morice River, British Columbia, Canada. Geomorphology 3:159–179
Harrison SS, Reid JR (1967) A flood-frequency graph based on tree-scar data. Proc Northern Dakota Acad Sci 21:23–33
Hess M (1996) Climate. In: Mirek Z (ed) The nature of the Tatra National Park. Tatrzański Park Narodowy, Zakopane Kraków, pp 53–68 (in Polish with English summary)
Holmes RL (1983) Computer assisted quality control in tree-ring dating and measurement. Tree-Ring Bull 43:67–78
Hupp CR (1988) Plant ecological aspects of flood geomorphology and paleoflood history. In: Baker VR, Kochel CR, Patton PC (eds) Flood geomorphology. Wiley, New York, pp 335–356
Komornicki T, Skiba S (1996) Soils. In: Mirek Z (ed) The nature of the Tatra National Park. Tatrzański Park Narodowy, Zakopane Kraków, pp 215–226 (in Polish with English summary)
Koreň M (2005) Voda, vietor a oheň. Tatry ročnik XLIV 2:12-17 (in Slovak)
Łajczak A (1996) Hydrology. In: Mirek Z (ed) The nature of the Tatra National Park. Tatrzański Park Narodowy, Zakopane Kraków, pp 169–196 (in Polish with English summary)
Lang A, Moya J, Corominas J, Schrott L, Dikau R (1999) Classic and new dating methods for assessing the temporal occurrence of mass movements. Geomorphology 30:33–52
LePage H, Bégin Y (1996) Tree-ring dating of extreme water level events at Lake Bienville, Subarctic Québec, Canada. Arct Alp Res 28:77–84
McCord VAS (1996) Fluvial process dendrogeomorphology: Reconstruction of flood events from the Southwestern United States using flood scarred trees. Radiocarbon 1996:689–699
Niklasson M, Granström A (2000) Numbers and sizes of fires: long-term spatially explicit fire history in a Swedish boreal landscape. Ecology 81:1484–1499
Rinn F (1996) TSAP Version 3.0. Reference Manual. Heidelberg, Germany
Schweingruber FG, Eckstein D, Serre-Bachet F, Bräker OU (1990) Identification, presentation, and interpretation of event years and pointer years in dendrochronology. Dendrochronologia 8:9–37
St George S, Nielsen E (2003) Palaeoflood records for the Red River, Manitoba, Canada, derived from anatomical tree-ring signatures. Holocene 13(4):547–555
Stoffel M, Perret S (2006) Reconstructing past rockfall activity with rings: some methodological considerations. Dendrochronologia 24(1):1–15
Storaunet KO, Rolstad R (2004) How long do Norway spruce snags stand? Evaluating four estimation methods. Can J Forest Res 34:375–383
Tardif J, Bergeron Y (1997) Ice flood history reconstructed with tree-rings from the southern boreal forest limit, western Quebec. Holocene 7:291–300
Yanoski TM (1999) Tree ring analysis in hydrometry. In: Herschy RW (ed) Hydrometry: principles and practises. Wiley, New York, pp 265–289
Zielonka T (2006) Quantity and decay stages of coarse woody debris in old-growth subalpine spruce forests of the western Carpathians, Poland. Can J Forest Res 36(10):2614–2622

Dendrohydrology and Extreme Floods Along the Red River, Canada

Scott St. George

Spring flooding along the Red River is one of Canada's most disruptive natural hazards. In 1997, floodwaters from the Red inundated more than 2,000 km^2 in Canada and the United States and threatened communities through-out the Red River basin (Fig. 1). Dubbed the 'flood of the century' by local media, the 1997 flood caused more than CDN $500 million in damages in southern Manitoba (Manitoba Water Commission 1998) and was even more destructive upstream in Minnesota and North Dakota. The Red River breached the dikes protecting the cities of Grand Forks and East Grand Forks, caused damages in excess of USD $3.6 billion and chased several thousand people from their homes (International Joint Commission 2000). The region's largest city, Winnipeg, avoided disaster by a narrow margin. Almost half a century earlier, the Red River flood of 1950 caught the basin largely unprepared and unprotected, and displaced nearly 100,000 people from Winnipeg and other communities (Bumstead 1997).

Estimates of future flood risks are based on the frequency and magnitude of floods observed in the past (Stedinger et al. 1993). By definition, extreme floods occur infrequently, and the probability of their occurrence is often difficult to estimate from gauge records (Klemeš 1989). Moreover, a few decades of observations provides a limited perspective to judge how flooding may be influenced by factors such as climate change, low-frequency variability and land-use change. In the Red River basin, dendrochronology has provided a means to develop extended records of severe floods that span the last several hundred years.

During a severe flood, the Red River inundates trees growing within its riparian forest for several weeks between late April and early June (St. George and Nielsen 2002). Prolonged flooding causes bur oak (*Quercus macrocarpa*) to develop unusual anatomical features within its annual growth ring (Fig. 2). Flood signatures in bur oak are characterized primarily by extreme reductions in the size of conductive vessels within the earlywood (St. George and Nielsen 2000, 2003). In some cases, 'flood

S. St. George (✉)
Geological Survey of Canada, Ottawa ON, K1A 0E8, Canada
and
School of Environmental Studies, Queen's University, Kingston ON, K7L 3N6, Canada
e-mail: sstgeorg@nrcan.gc.ca

M. Stoffel et al. (eds.), *Tree Rings and Natural Hazards: A State-of-the-Art*,
Advances in Global Change Research 41, DOI 10.1007/978-90-481-8736-2_26,

Fig. 1 Flooding in the Red River basin during the spring of 1997. Photograph by Greg Brooks

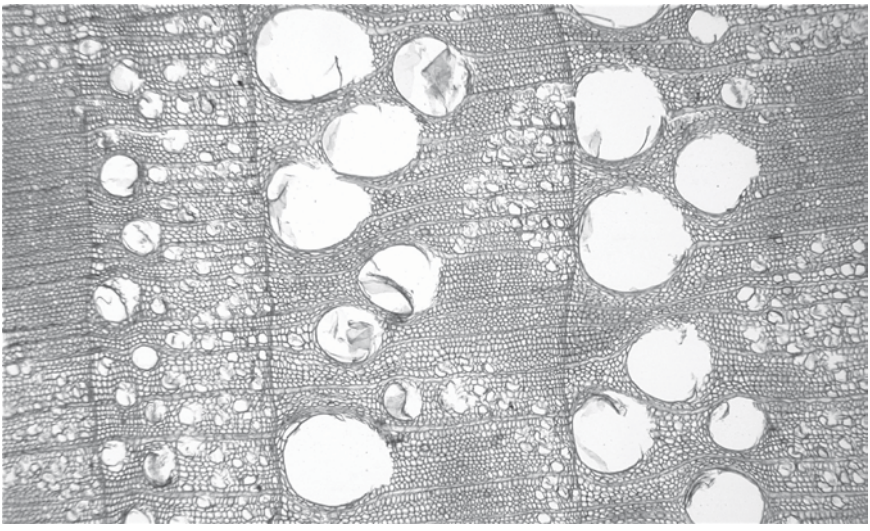

Fig. 2 Normal and flood-damaged tree rings in bur oak. The *left-most ring* was formed during 1826 and contains shrunken earlywood vessels and anomalous latewood with disrupted parenchyma and little fiber. Rings formed in 1827 and 1828 have much larger vessels and normal flame parenchyma. Photograph by Suzana Radivojevic

rings' also feature amorphous latewood with disrupted flame parenchyma and a reduced proportion of fiber. Rings formed during extremely large floods also contain low levels of Mg, Mn and Sr in their earlywood (St. George et al. 2006), but it is not clear if these anomalies represent an independent biochemical response to flooding or if they are a secondary effect caused by changes in wood anatomy.

Flood rings have proven to be an exceptional tool for studying the history of flooding in Manitoba. For the Red River, the proxy flood record developed from these signatures extends to AD 1648. During this interval, the Red River basin experienced several episodes of frequent floods: the mid-1700s, the early to mid-1800s and the latter half of the twentieth century. Conversely, there have been long periods where the Red River has been relatively quiescent, with almost a century passing between major floods. Tree-ring evidence has also been used to estimate the magnitude of past floods by comparing the relative frequency of flood rings in the regional tree-ring chronology. This analysis suggested that the largest flood in the last three and a half centuries occurred in the spring of 1826.

Paleoflood records from tree rings have provided a critical long-term perspective on flood dynamics in southern Manitoba. By documenting the occurrence of large floods during the past several centuries, tree rings have contributed to improved risk assessments for communities in the Red River basin and influenced the design of new flood measures protecting Winnipeg. These multi-centennial records have also helped clarify how climate and land-use change and geomorphic processes influence the frequency of large floods. Most importantly, tree rings preserve direct evidence of past floods that can be used to communicate flood hazards directly to those at risk.

References

Bumstead JM (1997) Floods of the centuries: a history of flood disasters in the Red River Valley 1776-1997. Great Plains, Winnipeg

St. George S, Nielsen E (2000) Signatures of high-magnitude 19th century floods in Quercus macrocarpa (Michx.) tree rings along the Red River, Manitoba, Canada. Geology 28:899–902

St. George S, Nielsen E (2002) Flood ring evidence and its application to paleoflood hydrology of the Red River and Assiniboine River in Manitoba. Géogr phys Quat 56:181–190

St. George S, Nielsen E (2003) Palaeoflood records for the Red River, Manitoba, Canada de-rived from anatomical tree-ring signatures. Holocene 13:547–555

St. George S, Outridge PM, Nielsen E (2006) High-resolution dendrochemical analysis of flood-affected oaks using laser ablation ICP-mass spectrometry. IAWA J 27:19–31

International Joint Commission (2000) Living with the Red. A report to the governments of Canada and the United States on reducing flood impacts in the Red River basin. International Joint Commission, Ottawa-Washington

Klemeš V (1989) The improbable probabilities of extreme floods and droughts. In: Starosolszky O, Melder OM (eds) Hydrology of disasters. James and James, London, pp 43–51

Manitoba Water Commission (1998) An independent review of actions taken during the 1997 Red River flood: a report to the Honourable J. Glen Cummings, Minister of Natural Resources, Government of Manitoba, Winnipeg

Stedinger JR, Vogel RM, Foufoula-Georgiou E (1993) Frequency analysis of extreme events. In: Maidment DR (ed) The handbook of hydrology. McGraw-Hill, New York, pp 18.1–18.66

Part VII
Meteorological Hazards

Windthrow in Norway spruce (*Picea abies*) stand in the Romanian Carpathians (© M. Stoffel)

Weather and Climate Extremes: Where Can Dendrochronology Help?

Martin Beniston

1 Introduction

When assessing the impacts of human activities on the climate system, it is necessary to have an insight on baseline climates where human encroachment is absent or limited, in order to determine how current and future trends may be out of the range of "natural" climate variability. In this respect, paleoclimate reconstructions have played a leading role in establishing robust estimates of baseline climates, spanning back decades to millennia, according to the proxy used (Bradley et al. 2003; Cook et al. 2002; Crowley and Lowery 2000; Esper et al. 2005; Guiot et al. 2005; Jones et al. 2001; Mann and Jones 2003; Mann et al. 1998; Villalba et al. 2003; Xoplaki et al. 2005).

Using proxy data for the analysis of extremes is, however, more problematic, in that in many cases extremes are short-lived phenomena and often on very local scales, such that many forms of paleoclimatic archives would not even register this type of event. There are other instances, however, where persistent events beyond a certain threshold (e.g., heat waves) or acting over large surface areas (droughts or extensive floods) do register in many proxy archives (e.g., Cole and Cook 1998; Cook et al. 2004; Le Quesne et al. 2006; Luckman and Wilson 2005; Luterbacher et al. 2004; Osborn and Briffa 2006; Woodhouse and Overpeck 1998). Indeed, the existence of massive droughts in the southwestern part of North America have been highlighted through dendrochronology and palynology (Cook et al. 2004; Schubert et al. 2004). Novel techniques that use information on damage to tree rings to document severe and even short-term events (e.g., Stoffel et al. 2005, 2008) are currently emerging, thereby also shedding light on the possible changes in frequency

M. Beniston (✉)
Chair for Climatic Change and Climate Impacts, Institute for Environmental Sciences, University of Geneva, CH-1227 Carouge-Geneva, Switzerland
e-mail: martin.beniston@unige.ch

M. Stoffel et al. (eds.), *Tree Rings and Natural Hazards: A State-of-the-Art*, Advances in Global Change Research 41, DOI 10.1007/978-90-481-8736-2_27,

and severity of events such as rockfall or debris flows in mountain regions, for example. Further examples of dendrochronological analyses that have been used with some degree of success include the reconstruction of tropical cyclones in the United States (e.g., Miller et al. 2006; Liu et al. 2008; Gentry et al. 2010, this volume; Grissino-Mayer et al. 2010, this volume) and even tornados (e.g., Sheppard et al. 2005, 2010, this volume).

This chapter will provide a succinct overview of extreme climatic events, what they are and where they come from, before suggesting where dendrochronology can be of key interest in the study of past, current and future extremes. Finally, a list of suggested recommendations as to future research needs linking tree-ring science and extreme weather analyses is provided.

2 What Are Extreme Events, Where Do They Come from, and Why Are They Important?

There is no single definition of what constitutes an extreme event. Extremes can be quantified inter alia on the basis of (Beniston et al. 2007):

- **How Rare They Are:** Events that occur with relatively low frequency. For example, the IPCC (2007) defines an 'extreme weather event' to be "an event that is rare within its statistical reference distribution at a particular place. Definitions of 'rare' vary, but an extreme weather event would normally be at least as rare as the 10th or 90th percentile."
- **How Intense They Are:** Events characterized by relatively small or large values (i.e. events that have large magnitude deviations from the norm). Not all intense events are rare: for example, low precipitation totals are often far from the mean precipitation but can still occur quite frequently. Note, intensity as defined here should not be confused with the definition of intensity used in the point process literature to denote the frequency/rate of events.
- **How Severe They Are:** Events that result in large socio-economic losses. Severity is a complex criterion because damaging impacts can occur in the absence of a rare or intense climatic event: for example, thawing of mountain permafrost leading to rock falls and mudslides.

It is clear that none of these definitions on their own are entirely satisfactory, and each definition corresponds to a particular situation but cannot necessarily be applied in a universal context. Understanding the mechanisms underlying various forms of climatic extremes is of interest to assess of the manner in which they may evolve in the future, under changing climatic conditions.

Extreme weather events are amplifications beyond normal levels of a particular physical process such as precipitation or winds. Such amplifications can take place within mid-latitude baroclinic waves, leading for example to strong winter wind storms, over warm tropical oceans (hurricanes), or when moisture convergence occurs over land surfaces that have been heated (severe thunderstorms).

At larger geographical scales, disturbances in normal atmospheric circulation patterns can result in heat waves, droughts, or conditions leading to large-scale flooding. Decadal-scale variability induced by phenomena such as ENSO (El Niño/Southern Oscillation) or the NAO (North Atlantic Oscillation) can result in large-scale disruptions of large-scale weather patterns (droughts and floods during El Niño events in many parts of the world; unusual heat and drought or the reverse according to the NAO mode on both sides of the Atlantic; etc.) Finally, the added thermal energy in the atmosphere forced by enhanced greenhouse-gas concentrations may already be leading to increased frequency and/or intensity of many extremes (IPCC 2007).

As climate continues to warm during the course of the twentyfirst century, it can be expected that extreme events will also increase, because the thermal energy that drives many atmospheric processes will be enhanced. Insurance statistics reveal that climate-related hazards take the heaviest toll on human life and generate some of the highest claims for insured damage. In the second half of the twentieth century, earthquakes caused 71 'billion-dollar events' globally; however, more than 170 such events were related to climatic extremes, in particular wind storms (tropical cyclones and mid-latitude winter storms), floods, droughts and heat waves. Furthermore, there is evidence that insured losses from extreme climate events have increased in recent decades (Munich Re 2002), due not only to increases in insured infrastructure – more cover, higher premiums (Swiss Re 2003) – but also to recent changes in weather and climate extremes (e.g., more storms and heat waves in the 1990s; cf., Harnik and Chang 2003; Huth et al. 2000; Siegismund and Schrum 2001). Because climatic extremes are those that generate the highest costs in terms of mortality and economic losses, compared to changes in mean climate, there is an obvious incentive for research on extreme events and the possible shifts in their frequency and intensity as climate changes in the course of the twentyfirst century.

3 How Can Tree Rings Help in Reconstructing Extreme Events?

Dendrochronology is certainly one of the key techniques that has provided extremely valuable information related to environmental and climatic change in the past. Tree-ring analyses have proven to be essential in climate and vegetation reconstruction over centuries to millenia in many parts of the world, providing data for periods when direct instrumental observation is unavailable. Tree-ring studies can also be used to determine fire histories and volcanic eruptions, stream-flow conditions using calibrated relationships between ring width and runoff amounts, as well as certain forms of extreme climatic events (Briffa et al. 2004). Dendrochronological analysis is not without problems, however, because precipitation and temperature are not the sole determinants on tree growth. Furthermore, the biological response to climate forcing may change over time (Brovkin et al. 2002; D'Arrigo et al. 2004; MacDonald et al. 2000). Carbon dioxide fertilization may also have an influence, particularly on tree species at high elevations.

Two distinct techniques provide climatic information, namely the measurement of annual ring width, and the analysis of wood density (Fritts 1976; Schweingruber et al. 1979). Ring width, when corrected for age trend, varies strongly in response to summer temperature towards polar and upper altitude tree-lines, and to summer moisture near the lower altitude tree-line in arid regions (Briffa et al. 2004; Tessier et al. 1997). In addition, the isotopic ratios (oxygen, deuterium and carbon) in tree-rings are the result of the response of the tree to complex biological and eco-physiological processes, of which climate is probably the dominant factor. Tree-ring chronologies need to be calibrated against absolutely-dated sequences and the signal-to-noise ratio has to be optimized. In this context, Hughes et al. (1982) paved the way for methodologies that treat tree-ring sequences in such a way that climate-related information (i.e., the signal) is retained while non-climatic variation (i.e., the noise) is removed (e.g., Fritts 1976; Briffa 2000; Moberg et al. 2005). In effect, the climatic factor is the only one that exhibits an annual periodicity and where the climatic anomalies are coherent over large regions. As a result, the inter-annual fluctuations of climate can be identified in the ring characteristics. Other issues such as the detection of, and distinction between, high, medium and low-frequency signals in the records need to be addressed when preparing a chronology (e.g., Briffa and Osborn 2002; Jones et al. 1997; Tessier et al. 1997).

As previously mentioned, extreme events, and not changes in mean climate, generally have the strongest bearing on environmental disruption, damage, and loss of life. This has prompted interest in modeling studies to assess the possible changes in extremes in a changing climate, to test the capability of models to reproduce past events and project these into the future, and to assess what may be some of the important non-linearities and feedbacks that are important in contributing to various extremes (e.g., Rial et al. 2004). Models are not only dependent on tree-ring data for initialization and verification purposes, but they can under certain circumstances be a powerful tool to explain the observed chronologies, particularly at the regional scale (e.g., Coe and Harrison 2002). For example, appropriate model initializations can help to simulate the atmospheric circulations, and the precipitation patterns embedded in these flows, that have resulted in particular configurations of tree-ring width and densities observed in a particular region for a given time frame (Beniston 2002). The model studies can thus provide insight as to whether the tree rings have been influenced by local, regional, or large-scale shifts in precipitation or temperature. Fine-scale regional climate models (RCMs) can also be used as "intelligent interpolators", in order to fill the gaps in sparse data and provide missing climatic information for various geographic zones. This can be particularly of interest for remote high-elevation or high-latitude sites.

At the large spatial scales, comparisons of records of past vegetation dynamics to paleoclimatic simulations by GCMs have improved the understanding of the role of climate in governing past vegetation change (Trenberth and Otto-Bliesner 2003; Webb et al. 1993). Several major findings of paleo research have guided investigations of the effects of future climate change on the Earth's biota. These include

changing seasonality, which may result in unexpected vegetation patterns (Prentice et al. 1991), rapid changes in both climate and vegetation with ecosystem-wide implications, and short-term extreme events which may impact tree population structures (Lloyd and Graumlich 1995).

Certain forms of short-lived extreme events can today be investigated with a hybrid technique known as dendrogeomorphology (Stoffel et al. 2005). This consists of looking at the damage to trees that debris flows, rock falls or other geomorphologic hazards are capable of exerting and assessing their frequency and intensity. The technique is of particular relevance in mountain regions where these hazards can be quite common and pose threats to mountain communities and disrupt communication routes. Stoffel and Beniston (2006), for example, have shown how the behavior of over 100 debris-flow events in one Swiss alpine valley is linked to climate as the primary driver, and how the study of past events can shed light on the triggering of future debris flows under much warmer conditions.

4 Conclusions: Future Research Needs

Research should continue to foster closer ties between the dendrochronology and climate modeling communities. Dendrochronology has been a key actor in the climate change debate, by providing much of the baseline climate information over the past several centuries (IPCC 2007). Tree-ring science will continue to have significant added-value for climate research, in areas that include:

- **Experimental Studies:** Dendrochronology-based information has value for fundamental understanding of various processes relevant to climate. Specific regional field studies, including transects and focusing wherever possible on regions or time horizons prone to extreme events, would allow the compilation of data sets on extremes that is still largely lacking.
- **Links to Numerical Models:** As already mentioned, tree-ring chronologies can provide essential data for initialization and inter-comparison purposes with climate models, particularly at the regional scales. The trends reconstructed from tree-ring data can be used for testing other types of model as well, such as ecosystem response models, hydrological models, and cryosphere models, enabling an integrated approach to extremes, from their underlying trigger mechanisms to the impacts that they exert on many environmental systems.

Implementation of such research, which by essence must be compatible with the long time-scales of forest dynamics anthropogenic climatic change, will help further our understanding of the fundamental processes involved. This in turn will allow the formulation of appropriate adaptation or mitigation strategies that need to be developed in order to alleviate the most adverse impacts of climatic change, namely those associated with extreme weather and climate.

References

Beniston M (2002) Climate modeling at various spatial and temporal scales: where can dendrochronology help? Dendrochronologia 20:117–131

Beniston M, Stephenson DB, Christensen OB, Ferro CAT, Frei C, Goyette S, Halsnaes K, Holt T, Jylhä K, Koffi B, Palutikoff J, Schöll R, Semmler T, Woth K (2007) Future extreme events in European climate: an exploration of Regional Climate Model projections. Clim Change 81:71–95

Bradley RS, Hughes MK, Diaz HF (2003) Climate in medieval time. Science 302(5644): 404–405

Briffa KR (2000) Annual climate variability in the Holocene: interpreting the message of ancient trees. Quat Sci Rev 19(1–5):87–105

Briffa KR, Osborn TJ (2002) Paleoclimate – Blowing hot and cold. Science 295(5563): 2227–2228

Briffa KR, Osborn TJ, Schweingruber FH (2004) Large-scale temperature inferences from tree rings: a review. Global Planet Change 40(1–2):11–26

Brovkin V et al (2002) Carbon cycle, vegetation and climatic dynamics in the Holocene: experiments with the CLIMBER-2 model. Global Biogeochem Cy 16(4):GB001662

Coe MT, Harrison SP (2002) The water balance of northern Africa during the mid-Holocene: an evaluation of the 6 ka BPPMIP simulations. Clim Dynam 19(2):155–166

Cole JE, Cook ER (1998) The changing relationship between ENSO variability and moisture balance in the continental United States. Geophys Res Lett 25(24):4529–4532

Cook ER, Palmer JG, D'Arrigo RD (2002) Evidence for a 'Medieval Warm Period' in a 1, 100 year tree-ring reconstruction of past austral summer temperatures in New Zealand. Geophys Res Lett 29(14):L014580

Cook ER et al (2004) Long-term aridity changes in the western United States. Science 306(5698):1015–1018

Crowley TJ, Lowery TS (2000) How warm was the medieval warm period? Ambio 29(1):51–54

D'Arrigo RD et al (2004) Thresholds for warming-induced growth decline at elevational tree line in the Yukon Territory, Canada. Global Biogeochem Cy 18(3):GB002249

Esper J, Frank DC, Wilson RJS, Briffa KR (2005) Effect of scaling and regression on reconstructed temperature amplitude for the past millennium. Geophys Res Lett 32(7): L021236

Fritts HC (1976) Tree rings and climate. Academic Press, New York

Gentry CM, Lewis D, Speer JH (2010) Dendroecology of hurricanes and the potential for isotopic reconstructions in Southeastern Texas. In: Stoffel M, Bollschweiler M, Butler DR, Luckman BH (eds) Tree rings and natural hazards: A state-of-the-art. Springer, Berlin, Heidelberg, New York, this volume

Grissino-Mayer HD, Miller DL, Mora CI (2010) Dendrotempestology and the isotopic record of tropical cyclones in tree rings of the Southeastern United States. In: Stoffel M, Bollschweiler M, Butler DR, Luckman BH (eds) Tree rings and natural hazards: A state-of-the-art. Springer, Berlin, Heidelberg, New York, this volume

Guiot J et al (2005) Last-millennium summer-temperature variations in Western Europe based on proxy data. Holocene 15(4):489–500

Harnik N, Chang EKM (2003) Storm track variations as seen in radiosonde observations and reanalysis data. J Climat 16:480–495

Hughes MK, Kelly PM, Pilcher JR, LaMarche VC (1982) Climate from tree rings. Cambridge University Press, Cambridge, p 223

Huth R, Kysely J, Pokorna I (2000) A GCM simulation of heat waves, dry spells, and their relationships to circulation. Clim Change 46:29–60

IPCC (2007) Climate change. The Intergovernmental Panel on Climate Change (IPCC) Fourth Assessment Report. Cambridge University Press, Cambridge

Jones PD, Osborn TJ, Briffa KR (1997) Estimating sampling errors in large-scale temperature averages. J Climatol 10(10):2548–2568

Jones PD, Osborn TJ, Briffa KR (2001) The evolution of climate over the last millennium. Science 292(5517):662–667
Le Quesne C et al (2006) Ancient Austrocedrus tree-ring chronologies used to reconstruct Central Chile precipitation variability from AD 1200 to 2000. J Clim 19(22):5731–5744
Liu KB, Lu HY, Shen CM (2008) A 1200-year proxy record of hurricanes and fires from the Gulf of Mexico coast: testing the hypothesis of hurricane-fire interactions. Quat Res 69(1):29–41
Lloyd AH, Graumlich LJ (1995) Dendroclimatic, ecological, and geomorphological evidence for long-term climatic change in the Sierra Nevada, USA. In: Dean JS, Meko DM, Swetnam TW (eds) Tree rings, environment, and humanity. University of Arizona, Tucson, AZ
Luckman BH, Wilson RJS (2005) Summer temperatures in the Canadian Rockies during the last millennium: a revised record. Clim Dynam 24(2–3):131–144
Luterbacher J et al (2004) European seasonal and annual temperature variability, trends, and extremes since 1500. Science 303(5663):1499–1503
MacDonald GM et al (2000) Holocene treeline history and climate change across northern Eurasia. Quat Res 53:302–311
Mann ME, Jones PD (2003) Global surface temperatures over the past two millennia. Geophys Res Lett 30(15):L017814
Mann ME, Bradley RS, Hughes MK (1998) Global-scale temperature patterns and climate forcing over the past six centuries. Nature 392(6678):779–787
Miller DL, Mora CI, Grissino-Mayer HD, Mock CJ, Uhle ME, Sharp Z (2006) Tree-ring isotope records of tropical cyclone activity. Proc Natl Acad Sci 103(39):14294–14297
Moberg A et al (2005) Highly variable Northern Hemisphere temperatures reconstructed from low- and high-resolution proxy data. Nature 433(7026):613–617
Munich Re (2002) Topics, an annual review of natural catastrophes. Munich Reinsurance Company Publications, Munich, 49 pp
Osborn TJ, Briffa KR (2006) The spatial extent of 20th-century warmth in the context of the past 1200 years. Science 311(5762):841–844
Prentice IC, Bartlein PJ, Webb T III (1991) Vegetation and climate change in Eastern North America since the last glacial maximum. Ecology 72:2038–2052
Rial J, Pielke RA, Beniston M, Claussen M, Canadell J, Cox P, Held H, de Noblet-Ducoulet N, Prinn R, Reynolds J, Salas JD (2004) Non-linearities, feedbacks and critical thresholds in the earth's climate system. Clim Change 65:11–38
Schubert SD et al (2004) Causes of long-term drought in the US Great Plains. J Climatol 17(3):485–503
Schweingruber FH, Bräker OU, Schär E (1979) Dendroclimatic studies on conifers from central Europe and Great Britain. Boreas 8:427–452
Sheppard PR, May EM, Ort MH, Anderson KC, Elson MD (2005) Dendrochronological responses to the 24 October 1992 tornado at Sunset Crater, northern Arizona. Can J For Res 35:2911–2919
Sheppard PR, May EM, Ort MH, Anderson KC, Elson MD (2010) Dendrochronological responses to a tornado. In: Stoffel M, Bollschweiler M, Butler DR, Luckman BH (eds) Tree rings and natural hazards: A state-of-the-art. Springer, Berlin, Heidelberg, New York, this volume
Siegismund F, Schrum C (2001) Decadal changes in the wind forcing over the North Sea. Clim Res 18:39–45
Stoffel M, Beniston M (2006) On the incidence of debris flows in the Swiss Alps since the early Little Ice Age and in a future climate. Geophys Res Lett 33:L16404
Stoffel M, Conus D, Grichting MA, Lièvre I, Maître G (2008) Unraveling the patterns of late Holocene debris-flow activity on a cone in the central Swiss Alps: chronology, environment and implications for the future. Global Planet Change 60:222–234
Stoffel M, Schneuwly D, Bollschweiler M, Lièvre I, Delaloye R, Myint M, Monbaron M (2005) Analyzing rockfall activity (1600–2002) in a protection forest – a case study using dendrogeomorphology. Geomorphology 68:224–241
Swiss Re (2003) Natural catastrophes and reinsurance. Swiss Reinsurance Company Publications, Zürich, p 47

Tessier L, Guibal F, Schweingruber FH (1997) Research strategies in dendroecology and dendroclimatology in mountain environments. Clim Change 36:499–517

Trenberth KE, Otto-Bliesner BL (2003) Toward integrated reconstruction of past climates. Science 300(5619):589–591

Villalba R et al (2003) Large-scale temperature changes across the southern Andes: 20th-century variations in the context of the past 400 years. Clim Change 59(1–2):177–232

Webb T, Bartlein PJ, Harrison SP, Anderson KH (1993) Vegetation, lake levels and climate in eastern North America for the last 18, 000 years. In: Wright HE, Kutzbach JE, Webb T III, Ruddiman WF, Street-Perrott FA, Bartlein PJ (eds) Global climates since the last glacial maximum. University of Minnesota Press, Minneapolis, MN, pp 415–467

Woodhouse CA, Overpeck JT (1998) 2000 years of drought variability in the central United States. Bull Am Meteorol Soc 79(12):2693–2714

Xoplaki E et al (2005) European spring and autumn temperature variability and change of extremes over the last half millennium. Geophys Res Lett 32:L15713

Dendrotempestology and the Isotopic Record of Tropical Cyclones in Tree Rings of the Southeastern United States

Henri D. Grissino-Mayer, Dana L. Miller, and Claudia I. Mora

1 Introduction

Tropical cyclones (TCs) (hurricanes, typhoons, and cyclones) are considered the natural hazard with the greatest potential for loss of life and destruction of property, for several reasons. First, TCs occur with greater frequency than many other destructive natural hazards, such as earthquakes and volcanic eruptions. This frequency, we are learning, depends on trends in ocean sea-surface temperatures (SSTs) (which can be monitored using the Pacific Decadal Oscillation (PDO) and the Atlantic Multidecadal Oscillation (AMO)) combined with other climatic factors, such as the presence/absence of El Niño and the extensiveness of easterly wave activity. Second, TCs disburse large amounts of energy, acting as a siphon and absorbing energy from the oceans and subsequently releasing it back to the atmosphere. Higher SSTs equate to greater amounts of latent heat and greater amounts of energy released during condensation during a tropical cyclone. Third, tropical cyclones are spatially extensive, from the eye wall of cumulonimbus clouds characterized by sustained and very damaging winds that can move in excess of 250 km/h (180 mph) to the spiral bands that can extend out hundreds of kilometers

H.D. Grissino-Mayer (✉)
Laboratory of Tree-Ring Science, Department of Geography, The University of Tennessee, Knoxville, TN 37996, USA
e-mail: grissino@utk.edu

D.L. Miller
Department of Earth and Planetary Sciences, The University of Tennessee, Knoxville, TN 37996, USA

C.I. Mora
Earth Systems Observations, Los Alamos National Laboratory, Los Alamos, NM 87545, USA

M. Stoffel et al. (eds.), *Tree Rings and Natural Hazards: A State-of-the-Art*, Advances in Global Change Research 41, DOI 10.1007/978-90-481-8736-2_28,

and capable of producing flooding rainfall. Fourth, tropical cyclones affect sub-tropical and extra-tropical locations, such as Southeastern Asia, where infrastructure is poor and there is very limited ability to provide early warnings or to evacuate human populations that often number in the millions.

Impending changes to global climate could exacerbate any of these properties. For example, an increasing trend in TC intensity and longevity has been observed for the Atlantic Ocean (Klotzbach 2006), perhaps due to increasing SSTs. Energy dissipation and therefore storm intensity of tropical cyclones may increase due to global warming, but with considerable spatial variability between hemispheres and among ocean basins (Emanuel et al. 2008). The unprecedented 2005 tropical cyclone season in the Atlantic Ocean was likely caused by abnormally high SSTs (0.9°C above the 1901–1970 normal), a major percentage attributable to global warming and not to natural variability (Trenberth and Shea 2006). TC tracks in the Atlantic Ocean are likely to shift poleward with increasing global temperatures (Jiang and Perrie 2007), thus likely affecting geographic locations not accustomed to repeated occurrences of hurricanes. A greater proportion of intense hurricanes in the last 30 years may be attributable to geographic changes in tropical cyclone source regions and therefore their subsequent tracks, highlighting a need for more carefully monitoring effects of increasing temperatures (Wu and Wang 2008). Global warming is likely to cause an increase in the size of hurricanes with a simultaneous decrease in the time it takes to reach tropical cyclone status (Jiang and Perrie 2007).

Now more than ever, a long-term perspective on TC activity is needed to place these expected changes in historical context. The use of natural archives for understanding the past history of TC activity is therefore becoming increasingly important (Fan and Liu 2008). Sand layers in near-shore sediments, bracketed by radiocarbon dates, along the Atlantic and Gulf of Mexico coasts have been particularly instructive for reconstructing TC activity (Liu and Fearn 1993, 2000; Donnelly et al. 2001; Liu et al. 2008). These are produced when overwash of coastal dunes from wave activity associated with particularly intense hurricanes is deposited in the adjacent lagoon or lake. These studies have also been carried over to Pacific Ocean coastal locations in Australia (Nott and Hayne 2001) and the South China Sea (Yu et al. 2009), in some case with decadal resolution over many thousands of years. Nyberg et al. (2007) reconstructed vertical wind shear and SSTs using luminescence intensity of banded corals growing in the Caribbean Sea and found that the frequency of hurricanes in the 1970s and 1980s was anomalously low compared to the last 270 years, and that current TC activity is not unusual (although this has been debated; see Neu 2008). The isotopic composition of speleothems that formed in subtropical locations have shown striking correspondence to TC events (Frappier et al. 2007), although the length of the current record is quite short (23 years).

Although promising, such high-resolution studies are rare, attributable to the challenges (labor, time, and finances) one faces when analyzing sediments, corals, and speleothems at high temporal resolutions. Ideally, a proxy record is needed that is spatially abundant in coastal locations, has annual or finer resolution, and can be processed relatively quickly with the proper equipment.

2 Hurricanes and Tree Rings

Tree-ring data have long been known to contain a signal of TC activity. Pillow (1931) noticed hurricanes produced reaction wood once trees were forced to lean from high winds, and Manabe and Kawakatsu (1968) were able to reconstruct past typhoons back to AD 473 using reaction wood in Japanese cedar (*Cryptomeria japonica*). Most tree-ring studies, however, have been applied to understand the effects of TCs on tree growth and forest development. For example, Henry and Swan (1974) quantified in detail the effects of the 1938 New England hurricane on forest development in the Harvard Tract of southwestern New Hampshire (USA), noting how 18 downed stems dated using tree rings all pointed in a southwesterly direction. Subsequent studies focused on hurricane effects on New England forests (Foster 1988; Dunwiddie 1991) and, more recently, on forests of the southeastern U.S. Gorham (1992) and Doyle and Gorham (1996) analyzed effects of Hurricane Camille (1969) on coastal pine forests in Alabama, Mississippi, and Louisiana, and found a hurricane signal using a combination of growth suppressions, growth releases, and establishment dates. Parker et al. (2001) found growth releases in sand pine (*Pinus clausa*) growing in the panhandle region of Florida that were coincident with past TCs dating back to the 1890s. Rodgers et al. (2006) found a hurricane signal in individual tree series of pines growing in coastal Alabama via growth suppressions and releases, which were muted when multiple series were averaged together.

Lines of evidence of past TC activity based on tree growth patterns are only indirect, however, and an improved, direct geo- or bio-marker of TC activity was needed that maintained annual precision. The goal of our study was to analyze the oxygen isotope composition of longleaf (*Pinus palustris*) and slash (*Pinus elliottii*) pine tree rings to isolate the years of landfalling hurricanes from a site in southern Georgia prone to TCs that originate in both the Gulf of Mexico and Atlantic Ocean. Previous studies have shown that TC activity produces rainfall that is depleted in ^{18}O (by as much as 10‰) when compared to typical thunderstorms (Nicolini et al. 1989; Lawrence and Gedzelman 1996; Lawrence 1998). Two basic physical factors govern $\delta^{18}O$ values in TC precipitation: (1) continued fractionation during condensation, with preferential incorporation of ^{18}O in the condensate, leads to low isotope ratios in both vapor and precipitation in systems with tall, thick clouds, and (2) diffusive isotopic exchange between falling rain and ambient vapor, which results in a ^{18}O enrichment of the falling rain and a decrease in vapor compositions. Large, organized, and long-lived storms, such as TCs, particularly amplify these isotope effects (Miyake et al. 1968; Lawrence and Gedzelman 1996; Gedzelman et al. 2003). Furthermore, this ^{18}O-depleted water can remain in the soil for weeks following a TC event (Lawrence et al. 2002), ensuring uptake by trees and incorporation of the ^{18}O-poor oxygen in the wood cellulose. Lastly, the eye of a TC event need not pass directly over the study area to be recorded because TC-related isotope depletions can be significant several hundred kilometers from the eye (Lawrence and Gedzelman 1996).

3 Study Site

Pines used in this study came from two locations in southern Georgia that were collected for a separate but related study to reconstruct past climate from the tree-ring record. Core samples from living slash and longleaf pines were collected from the campus of Valdosta State University in Valdosta Georgia from trees that were felled for building construction in the late 1990s. These trees all established in a short window of time between 1825 and 1830, indicating a disturbance-mediated (fire or wind) cohort. To extend the tree-ring chronology back in time, samples from remnant longleaf pine trees were collected from Lake Louise, about 15 km (9 mi) south of Valdosta. These samples came mostly from stumps left over from late nineteenth and early twentieth century logging related to the turpentining industry which pervaded the southeastern Atlantic coastal region between ca. 1800 and 1920. The samples represent rare old-growth longleaf pines with very slow growth rates that contained tree-ring series that were sensitive to seasonal and annual changes in rainfall amounts (Fig. 1). Standard dendrochronological techniques (Stokes and Smiley 1996; Grissino-Mayer 2001) were used to develop a continuous master chronology from 61 trees total from both locations back to AD 1421. Tree rings back to AD 1770 were analyzed in this study.

Fig. 1 Longleaf pine sample LLC 004 from the Lake Louise site in southern Georgia, with tree rings that date from AD 1542 to 1813

4 Methods

TCs are more common in late summer and fall months, when pine trees at this latitude are already forming latewood. Therefore, an isotope signal of TC activity most likely will be seen in the $\delta^{18}O$ of the latewood. We began by sectioning individual crossdated tree rings from two pine trees into earlywood (EW) and latewood (LW) components. Alpha-cellulose was isolated using modified techniques described by Loader et al. (1997) to ensure complete removal of mobile resins (Miller 2005). Approximately 100 μg of each sample were weighed and loaded into silver capsules. Oxygen isotopes were analyzed using a quantitative high temperature carbon reduction elemental analyzer (TC/EA) interfaced with a continuous flow isotope ratio mass spectrometer (Finnigan MAT Delta Plus XL IRMS). Samples were pyrolyzed at 1,450°C and CO was separated from H_2 and nitrogen-bearing gases by gas chromatography. The CO was carried in a He-stream to the mass spectrometer for measurement of $^{18/16}O$ ratios.

5 Results

The oxygen isotope time series for both EW and LW show clear decadal to multi-decadal-scale variations (Fig. 2), especially in the EW values. EW tends to be enriched in ^{18}O by 1–2‰ in comparison to LW values prior ca. 1930. After 1930, the two series become more similar in composition. Divergent compositions pre-1930 are most likely related to differences in source moisture between winter/spring rainfall (which contributes to EW formation) and summer/fall rainfall (which contributes to LW formation). The decadal-scale variations most likely reflect systematic variations in seasonal temperature or sources of normal precipitation

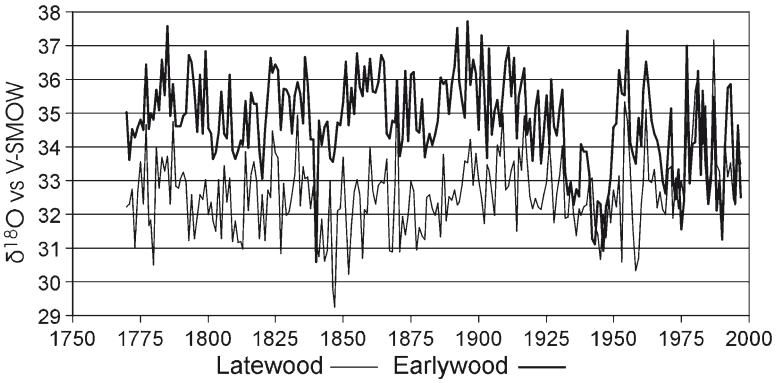

Fig. 2 $\delta^{18}O$ values for earlywood (*top*) and latewood (*bottom*) from two pines collected in southern Georgia

controlled by larger-scale climate modes, such as the AMO and North Atlantic Oscillation (NAO). For example, inspection of the EW and LW series during the twentieth century shows some similarities (and differences) with trends in the AMO. From the 1870s to early 1950s, a strong inverse relationship exists between EW and LW isotopic compositions and the AMO. From 1965 to 1990, the correlations are weaker, and positive for EW compositions, and there is no significant correlation with LW. Wavelet analysis (Torrence and Compo 1998) verified a statistically significant period at approximately 80 years (for nearly the entire record) and a near-significant period at approximately 32 years (Fig. 3), both of which could be associated with AMO activity.

The abrupt change in the relationship between the AMO and isotopic compositions coincides with a change in the predominant type of tropical cyclones, i.e., tropical or baroclinically-enhanced tropical cyclones of extratropical origin. These types of tropical cyclones form by fundamentally different mechanisms (Elsner and Kara 1999). The 1965–1990 period, in which baroclinically enhanced tropical cyclones were dominant, was one of relative quiescence for major tropical cyclones impacting the US coast. Since the mid-1990s, tropical cyclones have returned to dominance (Elsner and Kara 1999), with a greater number and greater intensity than in the previous 30 years.

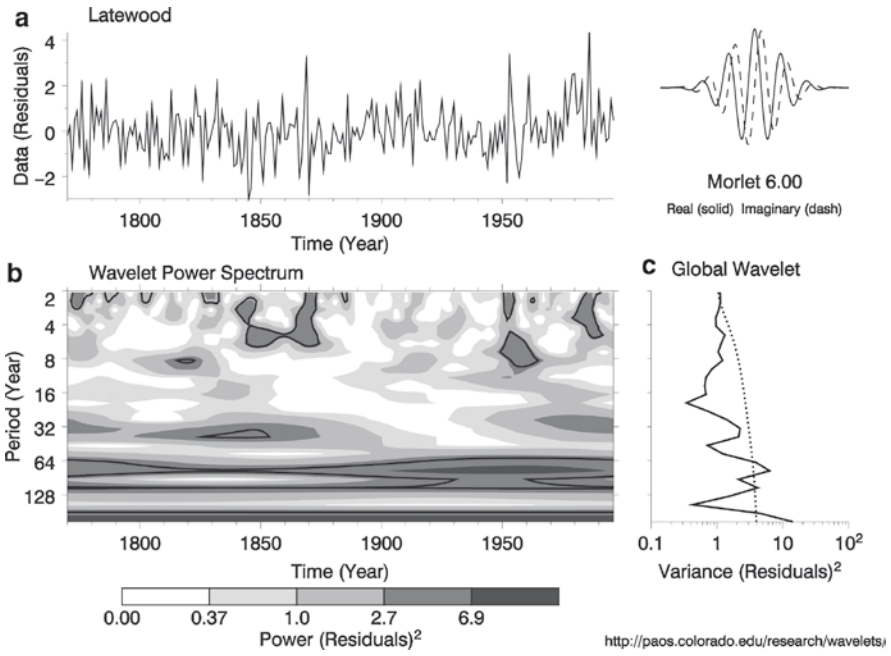

Fig. 3 (**a**) LW isotope time series along with (**b**) Morlet wavelet analysis, and (**c**) the global wavelet power spectrum (*black line*). Blackcontour in (**b**) is the 5% significance level, using a red-noise background spectrum (Torrence and Compo 1998; http:// www.ResearchSystems.com)

The low-frequency trend in the LW time series does not make apparent any relationship with TC activity, so we removed the low-frequency signal by modeling the LW series with an AR(1) process that effectively models the series as a function of itself lagged by 1 year to account for serial persistence. We used the residuals of the autoregressive model where negative values indicate low oxygen isotope compositions. We then compared the residual time series with a record of TC events recorded by instrument or historical documents that occurred within 400 km of the study area in south Georgia over the period 1851 to 1990 using the HURDAT database (Jarvinen et al. 1984; Landsea et al. 2004).

We observed that TC events coincided in years in which the residuals of the LW isotope compositions were anomalously negative (<−1.0) (Fig. 4). Using this –1 threshold, only one "false positive" (i.e., a storm detected by proxy for which there is no instrumental evidence) was noted and only three storms known to have tracked near the study area were missed ("true negatives") over the period 1855 to 1990. For example, a residual approaching –3 was found for the year 1871. In that year, no fewer than three hurricanes (Storm 4, 25–28 August; Storm 6, 6–7 September; and Storm 7, 4–6 October) affected the study area, with Storm 7 making a direct hit. In 1953, Hurricane Florence struck the panhandle of Florida as a Category 3 storm, then veered just to the north of our study site, causing large amounts of rainfall. This TC event is recorded with one of the lowest residuals in the entire record (–2.2). In 1958, Hurricane Helene stayed off the Georgia and South Carolina coasts but was still recorded with a residual of –2.0, even though local rainfall amounts from this hurricane would be considered modest (2.5 cm).

Further back in time, an unusual triad of TC events is shown in 1811, 1812, and 1813 with residuals of –1.2, –1.0, and –1.2 respectively. The years 1811 and 1813 particularly stand out because coastal areas of South Carolina were devastated in

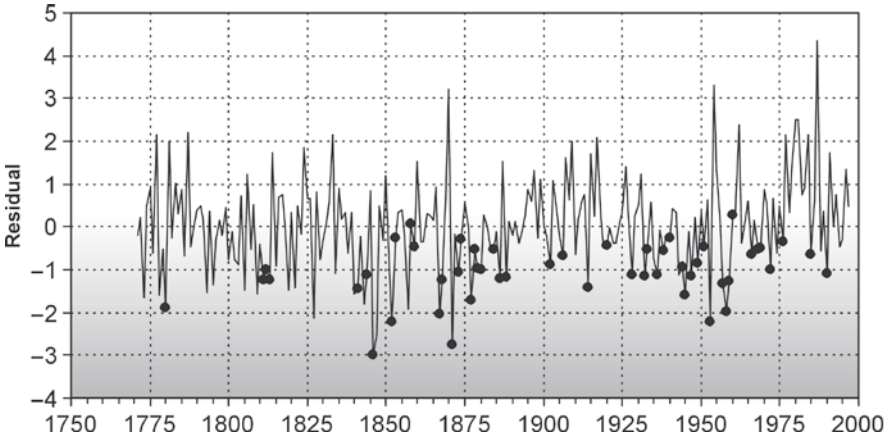

Fig. 4 Residuals (actual–predicted) created after fitting an AR(1) model to the original LW isotope time series. Documented TCs are shown as *black dots*

these years by catastrophic hurricanes (Ludlum 1989). The "Great Louisiana Hurricane of 1812" (Ludlum 1989), however, would have been a considerable distance from our study area in southern Georgia. Even further back in time, the LW residuals indicate a TC event in 1780 (–1.9) which could be showing one of the three "Great Hurricanes" that struck the Caribbean region in 1780 (Sandrik and Landsea 2003). Historical records are inconclusive whether any TC made landfall in the U.S. but a powerful hurricane (known as "Solano's Hurricane") struck the eastern Gulf of Mexico region north of Cuba between 17–22 October in 1780 (Ludlum 1989).

Although residual values ≤–1.0 strongly correlate to occurrence of a TC, TC activity is also noted for many years with residual values ≤–0.5 (Fig. 4), although using this threshold can lead to a few more "false positives." For example, residuals of –0.6, –0.7, –0.6, and –0.5 occurred in 1910, 1935, 1974, and 1988, respectively, but no known TC events occurred within 400 km of the study area during these years. For residual values >–0.5, there is no apparent relationship with TC occurrence. A TC event may or may not have occurred in those years. In some cases, residual values do not capture evidence of a storm reported to have affected the study area. For example, residuals appear to miss known storms in 1893, 1896 and 1898.

6 Discussion

The magnitude of TC-related isotopic depletions in cellulose will depend on many factors, including the size and proximity of the storm, soil type, and preexisting soil moisture conditions, and is therefore most useful as positive, rather than negative, evidence of an event, and cannot be used as a measure of TC intensity. A complicating factor concerns evaporative enrichment of oxygen isotope ratios in soil and leaf water caused by drought conditions preceding or during the growing season in which the TC event occurs, as this may affect the oxygen isotope compositions (Tang and Feng 2001). Evaporative enrichment would dampen TC isotope anomalies in the soil, causing TC events to be missed by this proxy record. For example, several well-documented TCs occurred in the 1890s, a decade that was "the busiest decade on record for the Atlantic seaboard of the United States" (Landsea et al. 2004). TCs occurred near our study area in 1893 (the "Sea Islands Hurricane" off the Georgia coast), 1896, and 1898 but were not detected in the isotope proxy record because this decade experienced mild to severe drought in the study area. A reconstruction of January–April rainfall based on longleaf pines from the Lake Louise study area showed that 14.2 in. of rainfall occurred during this interval each year during the 1890s compared to the long-term (AD 1421–1999) average of 16.2 in.

Nonetheless, examination of the temporal patterns of all residuals ≤–0.5 reveals striking patterns of increased and decreased TC activity in our study area, which may indicate broader-scale patterns of TC activity throughout the region. Five periods of increased activity are indicated: 1773–1780, 1800–1815, 1838–1852, 1867–1888,

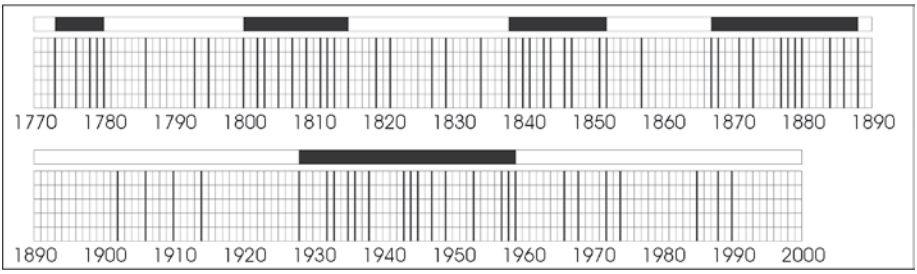

Fig. 5 Timeline of TC activity from 1770 to 1997 inferred from the residual time series (values <–0.5). *Black/white* areas above denote increased/decreased TC activity

Table 1 Periods of above- and below-average TC activity (residuals ≤–0.5)

Period of above-average TC activity	Period of below-average TC activity	Number of events (%)
1773–1780		5 (63%)
	1781–1799	3 (16%)
1800–1815		10 (63%)
	1816–1837	5 (23%)
1838–1852		9 (60%)
	1853–1866	1 (7%)
1867–1888		11 (50%)
	1889–1927	4 (10%)
1928–1959		15 (47%)
	1960–1997	7 (18%)

and 1928–1959 (Fig. 5; Table 1). Periods of decreased TC activity occurred between 1781–1799, 1816–1837, 1853–1866, 1889–1927, and 1960–1997. HURDAT records show that "the period of the 1850s to the mid-1860s was quiet, the late 1860s through the 1890s were busy and the first decade of the 1900s were quiet" (Landsea et al. 2004), which is clearly substantiated in our record. Particularly noteworthy were the decades of the 1800s (six events), 1840s (six events), 1870s (five events), 1930s (five events), and 1940s (five events).

Our isotope record may help researchers isolate unknown TC events. For example, two events are indicated in 1847 and 1857 by very low residuals (–2.5 and –1.9). No event has yet been historically documented for 1847, either on the Gulf Coast or Atlantic seaboard (Ludlum 1989), so this event could represent an unknown TC or represent a "false positive." The 1857 residual, however, may indicate a previously unknown TC event based on ongoing searches through historical documentation (Mock 2004). Efforts are currently underway by TC scientists to extend the TC record back to the 1800–1850 period and beyond, and we hope these efforts reveal TC events in such years as 1773 (–1.6), 1778 (–1.6), 1793 and 1795 (–1.5), 1805 (–1.5), 1809 (–1.6), 1819 (–1.5), 1821 (–1.4), 1827 (–2.1), 1834 (–1.1), and 1843 (–1.8). For example, in 1819 and again in 1821, TCs struck near Mobile, Alabama, 480 km from the study area, but the 1819 TC of 27–28 July was considered the worst

the residents of that part of the Gulf Coast had seen up until the 1850s (Ludlum 1989). The year 1827 saw two major hurricanes, one pushing westward across the Gulf of Mexico until eventually striking Mexico and another called the "Great North Carolina Hurricane of 1827" (Ludlum 1989). The latter may be too far removed to have affected the study area, but the former may have passed in close enough proximity to the study area. In 1834, a "small hurricane" stayed off the South Carolina coast (Ludlum 1989), but rainfall may not have made it all the way inland to the study area. In 1843, a major hurricane struck the panhandle of Florida, just 120 km southwest of our study area, near today's Newport, Florida (Ludlum 1989), which in all likelihood would have caused rainfall to occur in our study area.

A more comprehensive network of sites throughout the Gulf of Mexico and Atlantic Ocean coastal areas where the isotopic composition of pines are analyzed could provide insights on tracks and/or area affected for those TCs for which we have very little information, especially prior to 1850. For example, if several sites up the Atlantic coast from northern Florida to Cape Hatteras, North Carolina reveal ^{18}O-depleted alpha-cellulose during a particular year, this could indicate the track of a TC up the coast of the Southeastern U.S. This denser network of sites would also provide finer temporal and spatial resolution for landfalling TCs and provide critical information on TC frequency and patterns of TC activity over time, and suggest specific coastal regions that have been particularly vulnerable to repeated events. Lastly, the record of TC events can be pushed back in time, limited only by the length of the tree-ring records. We currently have well-replicated longleaf pine tree-ring chronologies for Hope Mills, North Carolina (back to AD 1503), Eglin Air Force Base, near Pensacola, Florida (back to AD 1507), eastern Texas (back to AD 1632), Sandy Island, South Carolina (back to AD 1458), St. Augustine, Florida (back to AD 1680), and Lake Louise in southern Georgia (back to AD 1421).

Another useful strategy concerns sub-sampling of the LW to improve accuracy with which TCs are detected in the isotope record. Although the phenology of longleaf pine has not been studied in detail, the phenology of other yellow pines has, including the close associate species slash pine, which is faster growing and therefore has greater economic value. Slash pine diameter growth begins approximately 2 months after budbreak (i.e. growth beginning around April or May) and ending approximately 6 months later (around October and November) (Dougherty et al. 1994). Latewood in southern yellow pines can begin forming in early summer likely caused by soil moisture reserves being largely used up (Moehring and Ralston 1967; Cregg et al. 1988) coinciding with energy expended for reproduction (emergence of male and female cones) (National Phenology Network 2009). For example, mean LW transition in loblolly pine was found to occur around day 175 (Late June) (Cregg et al. 1988). This timing encompasses the majority of hurricane season and suggests that the isotopic signal of a TC event can be masked by analysis of material representing the entire LW growth period. To overcome this limitation, the latewood, which is often abundant in longleaf pines (Fig. 1), can be sub-sampled into smaller portions. For example, Hurricane Florence struck the study area on 26 September 1953 and was recorded with a residual value of –2.2. We divided the LW evenly into early LW and late LW portions and found a 4.9‰ difference in these two samples with

the early LW residual being much lower at –3.0. Therefore, we believe that higher-resolution sampling of the LW will improve detection of the isotopic anomaly and clarify the interpretation of samples with modest (–0.5 to –1.0) LW residuals.

We also must consider additional chemical analyses of pine wood from coastal regions beyond just isotopic analyses. Advances have been made in the last 10 years for rapid and cost-effective analyses of the elemental composition of organic and inorganic materials using Laser-Induced Breakdown Spectroscopy (LIBS) (Lee et al. 2004; Cremers and Radziemski 2006; Singh and Thakur 2007). This technique uses a pulsed laser to ablate a small amount of the target material to cause constituent elements to emit light under high temperatures within the generated plasma plume. Atomic emission lines of elements within the plume can then be observed using an interfaced spectrometer with a wide spectral range, usually 170 nm (ultraviolet) to 1,100 nm (near infrared), where all elements have emission lines. LIBS has shown great utility in the environmental sciences for analyzing soil composition (Bublitz et al. 2001), contaminated sites (Theriault et al. 1998; Bousquet et al. 2008), and wood products (Moskal and Hahn 2002), for example. Coastal trees should be affected by considerable salt spray during a TC event, causing additional salt water to be added to the freshwater taken up by coastal pines. Although sodium is a macronutrient and expected in plant materials, chlorine is not and LIBS can be used to detect concentrations of dissociated chloride anions within the plant cellulose. Previous studies have shown that chlorine can be detected using LIBS (Kaski et al. 2004; Wilsch et al. 2005; Weritz et al. 2008). LIBS conducted on separated annual rings could potentially detect TC events by observing anomalous levels of chlorine in the wood cellulose and provide yet another proxy for reconstructing TC history.

References

Bousquet B, Travaille G, Ismael A, Canioni L, Pierres KML, Brasseur E, Roy S, le Hecho I, Larregieu M, Tellier S, Potin-Gauder M, Boriachon T, Wazen P, Diard A, Belbeze S (2008) Development of a mobile system based on laser-induced breakdown spectroscopy and dedicated to in situ analysis of polluted soils. Spectrochim Acta B: Atomic Spectrosc 63(10):1085–1090

Bublitz J, Dolle C, Schade W, Hartmann A, Horn R (2001) Laser-induced breakdown spectroscopy for soil diagnostics. Eur J Soil Sci 52:305–312

Cregg BM, Dougherty PM, Hennessey TC (1988) Growth and wood quality of young loblolly pine trees in relation to stand density and climate factors. Can J For Res 18:851–858

Cremers DA, Radziemski LJ (2006) Handbook of laser-induced breakdown spectroscopy. Wiley, Hoboken, NJ

Donnelly JP, Bryant SS, Butler J, Dowling J, Fan L, Hausmann N, Newby P, Shuman B, Stern J, Westover K, Webb T III (2001) 700 yr sedimentary record of intense hurricane landfalls in southern New England. Geol Soc Am Bull 113(6):714–727

Dougherty PM, Whitehead D, Vose JM (1994) Environmental influences on the phenology of pine. Ecol Bull 43:64–75

Doyle TW, Gorham LE (1996) Detecting hurricane impact and recovery from tree rings. In: Dean JS, Meko DM, Swetnam TW (eds) Tree rings, environment, and humanity. Radiocarbon 1996:405–412

Dunwiddie PW (1991) Forest history and composition of Halfway Pond Island, Plymouth County, Massachusetts. Rhodora 93:347–360

Elsner JB, Kara AB (1999) Hurricanes of the north Atlantic: climate and society. Oxford University Press, New York

Emanuel K, Sundararajan R, Williams J (2008) Hurricanes and global warming: results from downscaling IPCC AR4 simulations. Bull Am Meteorol Soc 89(3):347–367

Fan DD, Liu KB (2008) Perspectives on the linkage between typhoon activity and global warming from recent research advances in paleotempestology. Chinese Sci Bull 53(19):2907–2922

Foster DR (1988) Disturbance history, community organization and vegetation dynamics of the old-growth Pisgah Forest, south-western New Hampshire, U.S.A. J Ecol 76:105–134

Frappier AB, Sahagian D, Carpenter SJ, González LA, Frappier BR (2007) Stalagmite stable isotope record of recent tropical cyclone events. Geology 35(2):111–114

Gedzelman S, Lawrence J, Gamache J, Black M, Hindman E, Black R, Dunion J, Willoughby H, Zhang X (2003) Probing hurricanes with stable isotopes of rain and water vapor. Mon Weather Rev 131:1112–1127

Gorham LE (1992) A dendroecological study of hurricane impact and recovery along the central Gulf Coast. Thesis, Northeast Louisiana University

Grissino-Mayer HD (2001) Evaluating crossdating accuracy: a manual and tutorial for the computer program COFECHA. Tree-Ring Res 57:205–221

Henry JD, Swan JMA (1974) Reconstructing forest history from live and dead plant material–an approach to the study of forest succession in southwest New Hampshire. Ecology 55:772–783

Jarvinen BR, Neumann CJ, Davis MAS (1984) A tropical cyclone data tape for the North Atlantic Basin, 1886–1983: contents, limitations, and uses. NOAA Technical Memo, NWS NHC 22

Jiang J, Perrie W (2007) The impacts of climate change on autumn North Atlantic midlatitude cyclones. J Climat 20(7):1174–1187

Kaski S, Hakkanen H, Korppi-Tommola J (2004) Determination of Cl/C and Br/C ratios in pure organic solids using laser-induced plasma spectroscopy in near vacuum ultraviolet. J Anal Atomic Spectrom 19(4):474–478

Klotzbach PJ (2006) Trends in global tropical cyclone activity over the past twenty years (1986–2005). Geophys Res Lett 33(10):L10805

Landsea CW, Anderson C, Charles N, Clark G, Dunion J, Fernandez-Partagas J, Hungerford P, Neumann C, Zimmer M (2004) The Atlantic hurricane database re-analysis project: documentation for the 1851–1910 alterations and additions to the HURDAT database. In: Murnane RJ, Liu KB (eds) Hurricanes and typhoons: past, present and future. Columbia University Press, New York, p 177

Lawrence JR (1998) Isotopic spikes from tropical cyclones in surface waters: opportunities in hydrology and paleoclimatology. Chem Geol 144:153–160

Lawrence JR, Gedzelman SD (1996) Low stable isotope ratios of tropical cyclone rains. Geophys Res Lett 23:527–530

Lawrence JR, Gedzelman SD, Gamache J, Black M (2002) Stable isotope ratios: hurricane Olivia. J Atmos Chem 41:67–82

Lee W, Wu J, Lee Y, Sneddon J (2004) Recent applications of laser-induced breakdown spectroscopy: a review of materials approaches. Appl Spectrosc Rev 39(1):27–97

Liu KB, Fearn ML (1993) Lake-sediment record of Late Holocene hurricane activities from coastal Alabama. Geology 21(9):793–796

Liu KB, Fearn ML (2000) Reconstruction of prehistoric landfall frequencies of catastrophic hurricanes in northwestern Florida from lake sediment records. Quat Res 54(2):238–245

Liu KB, Lu HY, Shen CM (2008) A 1200-year proxy record of hurricanes and fires from the Gulf of Mexico coast: testing the hypothesis of hurricane-fire interactions. Quat Res 69(1):29–41

Loader NJ, Robertson I, Barker AC, Switsur VR, Waterhouse JS (1997) An improved technique for the batch processing of small wholewood samples to cellulose. Chem Geol 136:313–317

Ludlum DM (1989) Early American hurricanes 1492–1870, 2nd printing. American Meteorological Society, Boston, MA

Manabe D, Kawakatsu K (1968) Chronological investigations on the annual ring and typhonic patterns of the Yakushima cedar. Reports of the Kyushu University of Forestry 22:127–165

Miller DL (2005) A tree-ring oxygen isotope record of tropical cyclone activity, moisture stress, and long-term climate oscillations for the southeastern U.S. Dissertation, University of Tennessee, Knoxville, TN

Miyake Y, Matsubaya O, Nishihara C (1968) An isotopic study on meteoric precipitation. Pap Meteorol Geophys 19:243–266

Mock CJ (2004) Tropical cyclone reconstructions from documentary records: examples from South Carolina. In: Murnane RJ, Liu KB (eds) Hurricanes and typhoons: past, present, and future. Columbia University Press, Columbia, p 464

Moehring DM, Ralston CW (1967) Diameter growth of loblolly pine related to available soil moisture and rate of soil moisture loss. Soil Sci Soc Am J 31:560–562

Moskal TM, Hahn DW (2002) On-line sorting of wood treated with chromated copper arsenate using laser-induced breakdown spectroscopy. Appl Spectrosc 56(10):1337–1344

National Phenology Network (2009) *Pinus palustris*. http://www.usanpn.org/?q=Pinus_palustris

Neu U (2008) Is recent major hurricane activity normal? Nature 451:E5

Nicolini E, Jusserand C, Blavoux B, Coudray J, Eberschweiler C, Mairine P (1989) Appauvrissement en isotopes lourds des précipitations liées aux cyclones. Comptes Rendus de l'Académie des Sciences de Paris, Série II, Mécanique, Physique, Chimie, Sciences de l'univers, Sciences de la Terre 309:1255–1260

Nott J, Hayne M (2001) High frequency of 'super-cyclones' along the Great Barrier Reef over the past 5, 000 years. Nature 413:508–512

Nyberg J, Björn A, Malmgren AW, Jury MR, Kilbourne KH, Quinn TM (2007) Low Atlantic hurricane activity in the 1970s and 1980s compared to the past 270 years. Nature 447:698–701

Parker AJ, Parker KC, McCay DH (2001) Disturbance-mediated variation in stand structure between varieties of *Pinus clausa* (sand pine). Ann Assoc Am Geogr 91(1):28–47

Pillow MY (1931) Compression wood records hurricane. J For 29:575–578

Rodgers JC, Gamble DW, McCay DH, Phipps S (2006) Tropical cyclone signals within tree-ring chronologies from Weeks Bay National Estuary and Research Reserve, Alabama. J Coastal Res 22(6):1320–1329

Sandrik A, Landsea CW (2003) Chronological listing of tropical cyclones affecting north Florida and coastal Georgia 1565–1899. NOAA Technical Memorandum NWS SR-224

Singh JP, Thakur SN (eds) (2007) Laser-induced breakdown spectroscopy. Elsevier, Boston, MA

Stokes MA, Smiley TL (1996) An introduction to tree-ring dating. University of Arizona Press, Tucson, AZ

Tang K, Feng X (2001) The effect of soil hydrology on the oxygen and hydrogen isotopic compositions of plants' source water. Earth Planet Sci Lett 185:355–367

Theriault GA, Bodensteiner S, Lieberman SH (1998) A real-time fiber-optic probe for the in situ delineation of metals in soils. Field Anal Chem Tech 2(2):117–125

Torrence C, Compo GP (1998) A practical guide to wavelet analysis. B Am Meteorol Soc 79:61–78

Trenberth KE, Shea DJ (2006) Atlantic hurricanes and natural variability in 2005. Geophys Res Lett 33(12):L12704

Weritz F, Schaurich D, Wisch G (2008) Detector comparison for sulfur and chlorine detection with laser induced breakdown spectroscopy in the near-infrared-region. Spectrochim Acta B 63(12):1504–1511

Wilsch G, Weritz F, Schaurich D, Wiggenhauser H (2005) Determination of chloride content in concrete structures with laser-induced breakdown spectroscopy. Constr Build Mater 19(10):724–730

Wu L, Wang B (2008) What has changed the proportion of intense hurricanes in the last 30 years? J Climat 21(6):1432–1439

Yu KF, Zhao JX, Shi Q, Meng QS (2009) Reconstruction of storm/tsunami records over the last 4000 years using transported coral blocks and lagoon sediments in the southern South China Sea. Quat Int 195:128–137

Dendrochronological Responses to a Tornado

Paul R. Sheppard, Elizabeth M. May, Michael H. Ort, Kirk C. Anderson, and Mark D. Elson

Tree-ring responses to a historic tornado (Sheppard et al. 2005) are documented here. Little research has been published showing tree-ring responses to tornadoes, that is, long-term growth changes due to short-term, intense winds. The tornado of interest occurred at Sunset Crater Volcano National Monument, northern Arizona (Fig. 1a, b), at about 2:30 PM on 24 October 1992 (Arizona Daily Sun Newspaper, 25 October 1992; Crisp 1996). The tornado first touched ground south of Sunset Crater and then moved generally north-northwest toward O'Leary Peak (Fig. 1c) before dissipating. Many trees were uprooted and killed by the intense winds of the tornado, while other trees growing within the swaths were damaged by the tornado but survived the event and continue living today. This tornado is historically well-documented (Arizona Storms Database 2004) and thus can serve as a test case for calibrating ring-growth changes in trees that were buffeted – but not killed – by high winds. Such a calibration could serve to identify tornadoes of the past within tree-ring records.

The study area is located about 25 km northeast of Flagstaff, Arizona (Fig. 1b) at an elevation of about 2,200 m asl. Field sampling was done in the summer and fall of 2004, about 12 years after the tornado. Living trees were increment cored in the three areas damaged by the tornado (Fig. 1c). All sampled trees were ponderosa pine (*Pinus ponderosa*) and were living in 1992 as well as at the time of fieldwork.

Field procedures followed typical methods of dendrochronology (Phipps 1985). Trees were selected based on their extent of damage by the tornado: some had

P.R. Sheppard (✉) and E.M. May
Laboratory of Tree-Ring Research, University of Arizona, Tucson, AZ 85721, USA
e-mail: sheppard@ltrr.arizona.edu

M.H. Ort
Departments of Environmental Sciences and Geology, Northern Arizona University, Flagstaff, AZ 86011, USA

K.C. Anderson
Bilby Research Center, Northern Arizona University, Flagstaff, AZ 86011, USA

M.D. Elson
Desert Archaeology, Inc., Tucson, AZ 85716, USA

M. Stoffel et al. (eds.), *Tree Rings and Natural Hazards: A State-of-the-Art*,
Advances in Global Change Research 41, DOI 10.1007/978-90-481-8736-2_29,

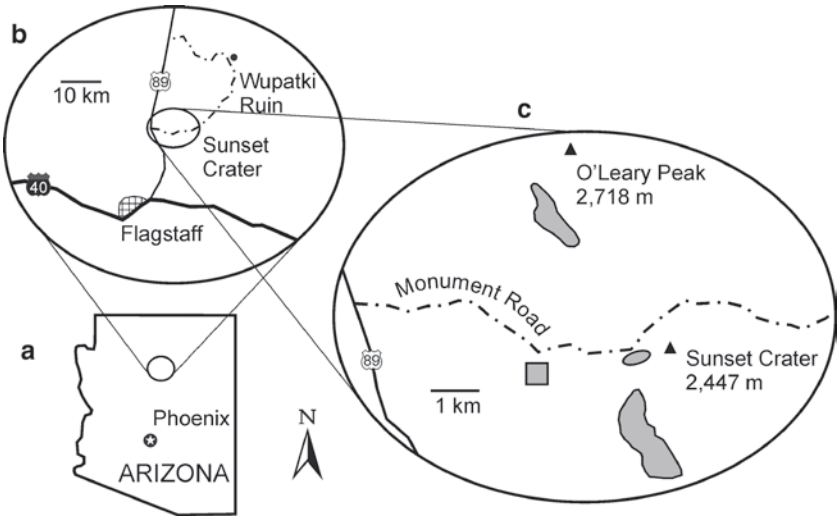

Fig. 1 Site maps. (**a**) The state of Arizona, (**b**) regional detail north of Flagstaff, and (**c**) site detail near Sunset Crater. *Filled irregular polygons* denote the tornado swath areas

crowns damaged or broken, others were completely knocked over but still living, and others showed no apparent damage. Laboratory treatment of the samples also followed typical methods of dendrochronology (Swetnam et al. 1985). Samples were visually crossdated by matching patterns of wide and narrow rings across trees (Douglass 1941). To demonstrate tree-ring responses to the tornado, ring growth was compared pre- and post-event in trees affected by the tornado.

Eighty-three living trees were sampled within the tornado swaths, 47 of which (57%) show one or more dendrochronological responses to the 1992 tornado. These event-response trees are mostly young and/or small, averaging 60 years in age and 17 cm in diameter.

Ring-growth responses to the tornado include four different changes:

- Growth Release: 57% of response trees show a release in radial growth (wider rings) beginning with 1993 and continuing to 2004 (Fig. 2a).
- Reaction Wood: 28% of response trees show reaction wood in the form of discolored tissue beginning with 1993 and continuing to 2004. Half of these trees show reaction wood for the full rings (Fig. 2b), while the other half show reaction wood only in the latewood portions and/or for only the first couple of rings after the tornado (Fig. 2c).
- Suppressed Growth: 6% of response trees show some varying degree of suppressed growth after the tornado. One of these trees has just four unusually narrow rings, from 1993 to 1996 (Fig. 2d). Another tree shows highly suppressed ring growth from 1993 until at least 2004 (Fig. 2e).
- Reduced Latewood: 45% of response trees show unusually thin latewood for just the 1993 ring (Fig. 2f).

Multiple dendrochronological signals are possible for identifying past tornadoes within tree-ring records.

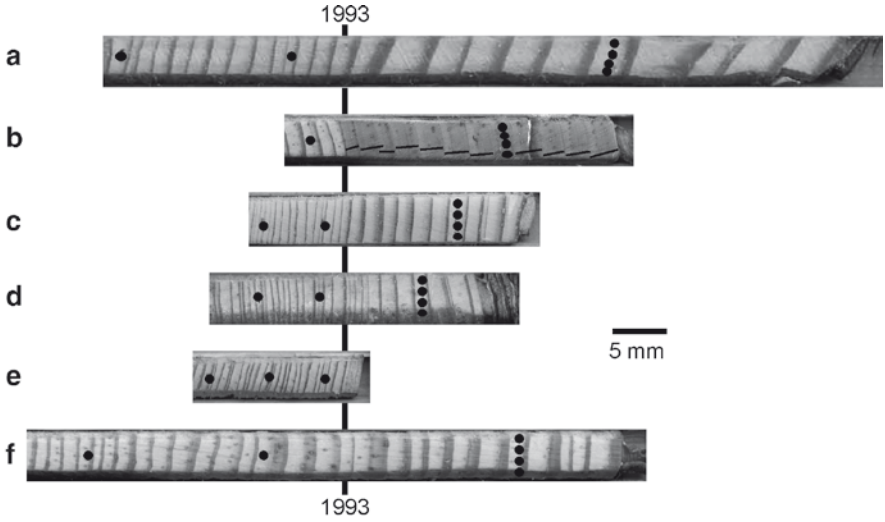

Fig. 2 Examples of Sunset Crater ring-width responses to the 1992 tornado. (**a**) Increasing ring widths, (**b**) classic reaction (compression) wood for entire rings, (**c**) reaction (compression) wood evident only in the latewood portions of each ring, (**d**) temporary ring-width suppression followed by a return to normal growth, (**e**) permanent ring-width suppression, (**f**) thin latewood width relative to total ring width. *Dots* on the sample indicate decadal years, with the quadruple dots indicating the AD 2000 year

Acknowledgments Staff from the Coconino National Forest and the Sunset Crater National Monument assisted this research. Víctor Peña and Robert Jones assisted in the field, and Frank Telewski assisted with interpretation of results. This research was funded in part by the National Science Foundation, Petrology and Geochemistry.

References

Arizona Daily Sun Newspaper (October 25, 1992) Twisters, hail shake up area

Arizona Storms Database (2004) Available online from http://ag2.calsnet.arizona.edu/cgi-bin/storms.cgi

Crisp DL (1996) Monitoring of Penstemon clutei A. Nels. on tornado salvage. In: Maschinksi J, Hammond HJ, Holter L (eds) Southwestern rare and endangered plants: proceedings of the second conference. US Department of Agriculture, Forest Service, General Technical Report RM-GTR-283, pp 243–246

Douglass AE (1941) Crossdating in dendrochronology. J Forest 39(10):825–831

Phipps RL (1985) Collecting, preparing, crossdating, and measuring tree increment cores. US Geological Survey Water Resources Investigations Report, pp 85–4148

Sheppard PR, May EM, Ort MH, Anderson KC, Elson MD (2005) Dendrochronological responses to the 24 October 1992 tornado at Sunset Crater, northern Arizona. Can J Forest Res 35:2911–2919

Swetnam TW, Thompson MA, Sutherland EK (1985) Using dendrochronology to measure radial growth of defoliated trees. USDA Forest Service Agricultural Handbook 639

Dendroecology of Hurricanes and the Potential for Isotopic Reconstructions in Southeastern Texas

Christopher M. Gentry, Daniel Lewis, and James H. Speer

1 Introduction

Hurricanes affect much of the lower to mid latitudes around the world. Hurricane season is during autumn when ocean waters have warmed from the summer, providing enough energy to maintain these large storms. Hurricanes cause severe damage when they make landfall with torrential rains and high wind speeds. Past occurrence of hurricanes can be documented through sediment analysis (Liu and Fearn 1993) but dendrochronological documentation of past hurricanes is a relatively new application that is just now being developed. This paper will present some recent research around the effects of Hurricane Rita and examine the potential for future dendrochronological reconstructions of hurricanes.

On September 24, 2005, Hurricane Rita made landfall approximately 50 km from the Big Thicket National Preserve in eastern Texas. As a category three hurricane, Rita made its way north along the Texas-Louisiana border. The path of the hurricane passed with 20 km of the Angelina National Forest. Hurricane Rita maintained at least a category one status until it was more than 150 km onto land. The Texas forest service estimated that the winds from Hurricane Rita damaged more than 3.8 billion board-feet of timber at an estimated value of $833 million dollars (Fig. 1).

C.M. Gentry (✉)
Department of Geosciences, Austin Peay State University, Clarksville, TN 37044, USA
email: gentryc@apsu.edu

D. Lewis
Department of Geography, The University of Tennessee, Knoxville, TN 37996, USA

J.H. Speer
Department of Geography, Geology, and Anthropology, Indiana State University, Terre Haute, IN 47809, USA

M. Stoffel et al. (eds.), *Tree Rings and Natural Hazards: A State-of-the-Art*, Advances in Global Change Research 41, DOI 10.1007/978-90-481-8736-2_30,

Fig. 1 Turkey Creek Unit showing trees downed by Hurricane Rita which made landfall on September 24, 2005 (Photo taken on December 13, 2005)

The Big Thicket National Preserve is an excellent location to study the effects of hurricanes on tree growth and to examine the potential for hurricane reconstruction. Between 1865 and 2007, 19 hurricanes passed within 100 km of the city of Kountze in southeastern Texas near our study areas (Fig. 2). Included in these 19 hurricanes are five which were category three or greater when reaching landfall. The most active period was a 25-year span from 1938 to 1963 which saw six hurricanes make landfall in this area. These hurricanes alter the structure of ecosystems by the removal of standing biomass, but they also bring large quantities of precipitation (albeit, for only a short duration).

Reconstructing hurricane events is difficult using standard dendrochronological techniques. However, a new technique may allow for high-resolution reconstruction of past hurricane events. Analyzing the $\delta^{18}O$ ratio of tree ring α-cellulose has proven a useful tool for characterizing hurricane events, and may provide pertinent information regarding hurricane frequency prior to instrumental records (Miller 2005; Miller et al. 2006).

In this paper we will present the results from a dendroecological analysis of the effects of Hurricane Rita. The current state of the art in dendrochronology has not provided robust reconstructions of past hurricane events, but ecological signals of past documented events are leading us to a clearer picture of the effect hurricanes have on succession in subtropical forests. Great potential exists for the use of stable isotopes to reconstruct past hurricane events and we will end with a discussion of the current state of that research and provide some suggestions on how to proceed with hurricane reconstructions.

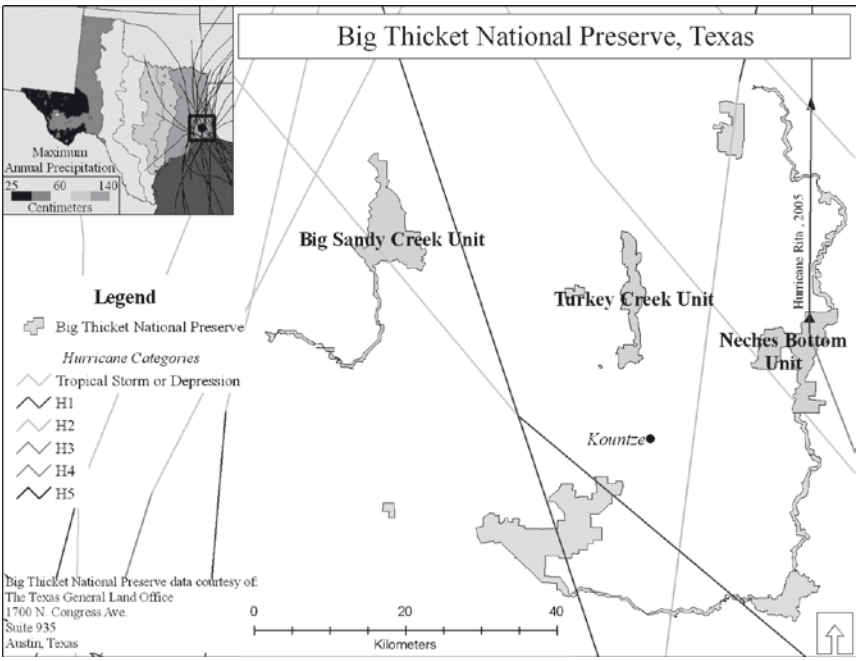

Fig. 2 Location of Big Thicket National Preserve sites with lines representing hurricane tracks and the hurricanes' category as it passed the field sites

2 Study Site

Established in 1974, the Big Thicket National Preserve has been an area of biological interest since Parks and Cory performed a biological survey in 1936. Numerous studies and surveys have been performed in and around the Big Thicket to measure vegetation dynamics (Harcombe and Marks 1977; Harcombe et al. 2002; Watson 2006). The Big Thicket National Preserve is comprised of 12 disjointed units that include the majority of the plant associations in this region. Because of this great biological diversity, the United Nations, Education, Scientific, and Cultural Organization (UNESCO) designated the 97,000 acre Big Thicket National Preserve as an International Biosphere Reserve in 1981.

Three units of the Big Thicket National Preserve (Turkey Creek, Neches Bottom, and Big Sandy Creek) were selected for this research. The Turkey Creek North site is dominated by Longleaf pine (*Pinus palustris*) and is situated on the Kirbyville-Niwana soil series (KgA). This series is located on nearly level (0–3% slopes with a 1% average) upland forest slopes. They are well to moderately well-drained with a seasonal water table of 0.6 m (UDSA SSURGO 2008). The elevations at the sampling site ranged from 42.0 to 42.6 m above sea level (a difference of 0.6 m) (Fig. 2). The Neches Bottom Unit, is at an elevation of only 9.1 m above sea level and a variability of less than 0.1 m, the site is seasonally inundated with water. These poorly drained soils have a forest canopy dominated by red maple

(*Acer rubrum*), american sweetgum (*Liquidambar styraciflua*), and oaks (*Quercus* spp.) on the slight upland flats, and by flood-resistant species such as Water tupelo (*Nyssa aquatic*) and bald cypress (*Taxodium distichum*) in the sloughs. The understory is a mix of shade-tolerant species such as ironwood (*Carpinus caroliniana*), pop ash (*Fraxinus caroliniana*), and holly (*Ilex* spp.) (Hall and Harcombe 2001). The Big Sandy Creek site is dominated by *P. palustris* and is located on Pinetucky fine sandy loam soils (PfB). The soils are well-drained with a seasonal water table of >2 m. Elevation at the sample site is approximately 75 m above sea level. All of these sites are relatively low-lying without much topographic variability and their proximity to the coast (approximately 100 km) makes them very susceptible to inundation from the heavy rains associated with hurricanes.

3 Material and Methods

3.1 Dendroecology

Dendroecological analyses were undertaken in order to identify an ecological signature for hurricane events and to determine if *P. palustris* is using meteoric precipitation as its primary source of water. Two projects were completed that can provide ecological information on the past occurrence of hurricanes. First we completed a stand-age analysis of two 20 × 20 m plots in the Neches Bottom Unit of the Big Thicket National Preserve to quantify changes in forest structure. All living and dead trees in the plots were sampled. The seven species dated in these two plots were *A. rubrum*, *F. caroliniana*, *N. aquatic*, American sycamore (*Platanus occidentalis*), *Q. lyrata*, *Q. nigra*, and *T. distichum*.

Second we selectively cored *P. palustris* trees in the Turkey Creek Unit of the Big Thicket National Preserve to determine their response to climate and see how hurricane events changed their response. Two increment cores were taken from each selected tree on opposite sides of the bole across the slope. One core was taken at breast height (approximately 140 cm above the forest floor) and the second was taken near the base (to maximize age) using an increment borer with a 5.15 mm interior core diameter. All cores and cross-sections were sanded with progressively finer grit sandpaper (ANSI 120-grit (105–125 μm) to ANSI 400-grit (20.6–23.6 μm)) and then hand sanded with up to 9 μm sanding film (Orvis and Grissino-Mayer 2002). All cores and cross-sections were visually cross-dated using a combination of skeleton plotting (Stokes and Smiley 1968) and memorization method (Douglass 1941) and each tree-ring was assigned to its exact year of formation.

After the cross-dating was complete, the individual rings from each sample were measured (earlywood (EWR), latewood (LWR), and total ring width (RWL)) using a Velmex measuring system with 0.001 mm precision. Measurements and cross dating were checked with the program COFECHA (Holmes 1983; Grissino-Mayer 2001). The EVENT program was used to perform a superposed epoch analysis

examining the effect of drought and precipitation on the radial growth of *P. palustris*. This program compares one record (in this case radial growth) to the punctuated events that are defined by the user (in this case either drought years or hurricane events). Hurricane events were identified based on a hurricane track being within 92 km of Hardin County, Texas using data from the National Oceanic and Atmospheric Administration (NOAA), Coastal Services Center.

3.2 Dendroecological Results

Sites in the Turkey Creek Unit from the Big Thicket National Preserve on the Texas Gulf Coast had an interseries correlation of 0.587 demonstrating that these trees crossdate well. Using factor analysis of climate variables (precipitation, temperature, and drought), approximately 30% of the growth in *P. palustris* was explained by the previous year's evapotranspiration and current summer precipitation. These dry conditions could well be amplified in Texas due to the elevated summer temperatures combining with the lowest average monthly precipitation during the year (Fig. 3).

The superposed epoch analysis found a significant decrease in radial growth in the year of a drought in both the latewood and total ring width chronologies (Fig. 4). With regards to hurricane years, hurricane derived precipitation had a significantly positive effect on radial growth in the year of a hurricane in both the latewood and total ring-width chronologies (Gentry 2008).

This research also found that numerous trees of many different species had establishment dates in the Neches Bottom that coincided with historical hurricane events (Fig. 5). The majority of the establishment dates occurred during six separate hurricane events between 1879 and 1963. A large number of species (25.0%) established during hurricanes in 1949 and 1957 (Hurricane Audrey). The majority of the species identified in these establishment pulses were shade-tolerant or late successional species such as *A. rubrum*, *F. caroliniana*, and *T. distichum*.

In addition to the trees which had establishment dates coinciding with hurricane events, we were also able to identify increases in radial growth at the time of the hurricane where advanced regeneration was able to acquire canopy dominance after the hurricane removed many or most of the mature trees on the site (Fig. 5). The majority of these species were *A. rubrum* and *F. caroliniana*. None of the dated species which established the year of the hurricane or could be attributed to advanced regeneration were pioneer species.

3.3 Dendroecological Indicators of Past Hurricane Activity

Tree rings provide a biological proxy with annual (to sub-annual) resolution that has the ability to record changes in climatic patterns back centuries, even millennia.

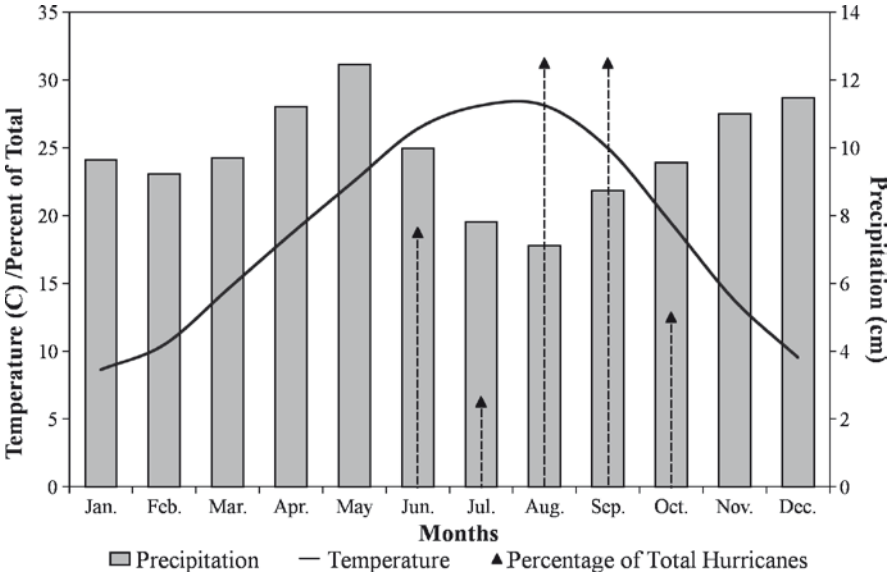

Fig. 3 Percentage of total hurricanes (*dotted arrows*) occurring by month compared to the Texas Climate Division 4 climograph. The Hurricane data is from NOAA for hurricanes that have tracked within 92 km of the field area

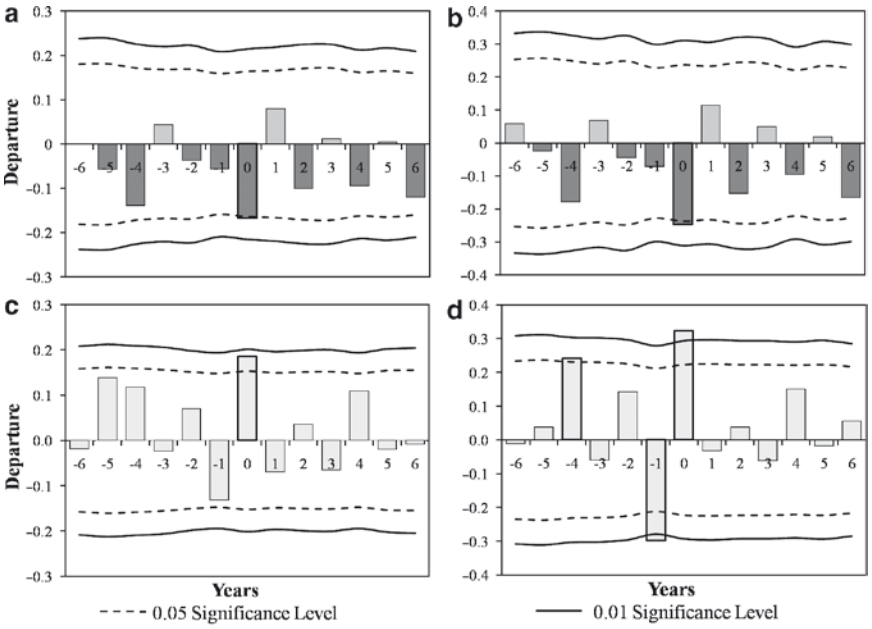

Fig. 4 Results from the superposed epoch analysis. Year zero represents drought years compared to radial growth in *Pinus palustris* as measured by total ring width (**a**) and latewood width (**b**). Figures **c** and **d** compare radial growth the year of a hurricane event with total ring width (**c**) and latewood width (**d**)

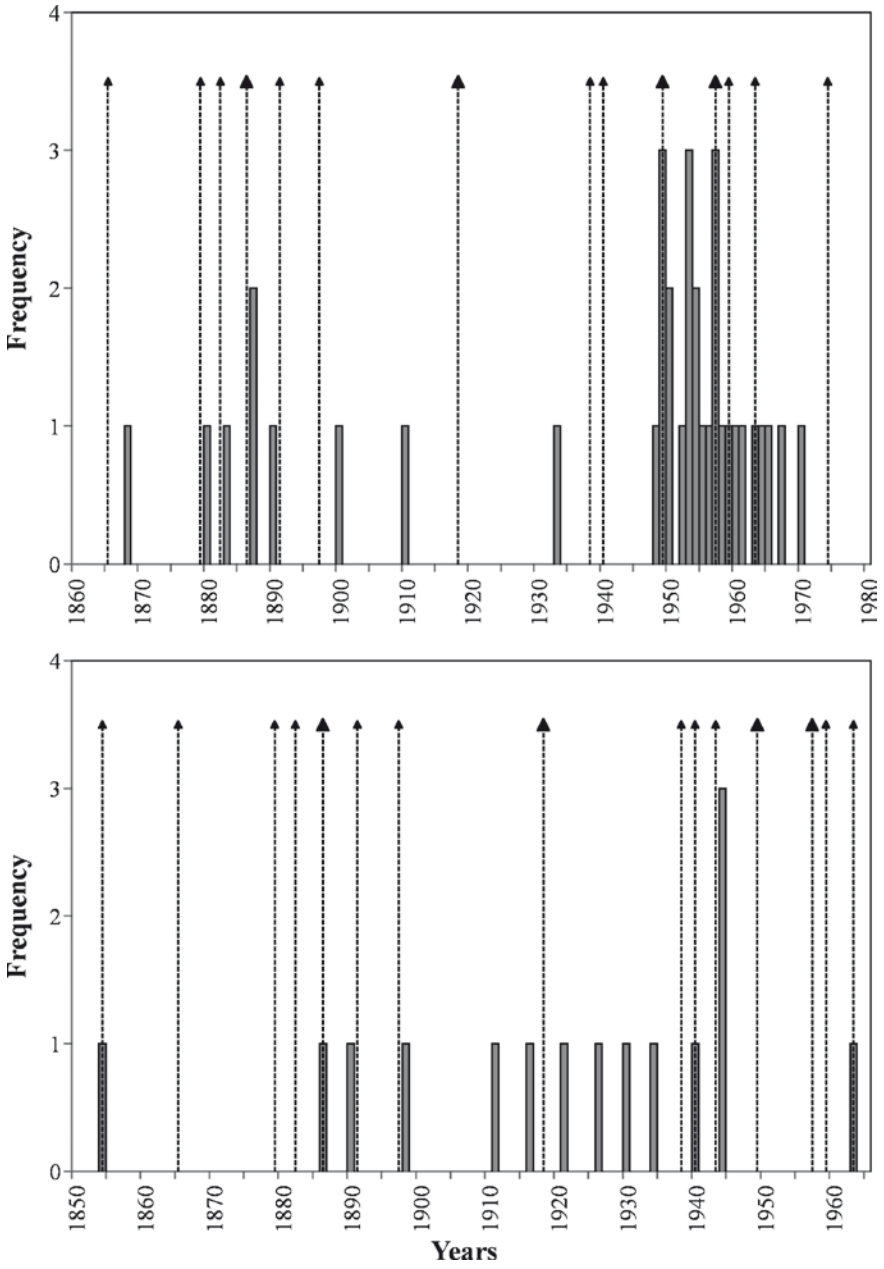

Fig. 5 Establishment dates for trees at Neches Bottom (*above*) and Weir Woods (*below*). The y-axis shows the number of trees that established in each year. The hurricanes events are marked with triangles along the top of each graph with stronger hurricanes denoted with a larger triangle. The differences in *shades of gray of the bars* represent the different species

The dendroecological study presented here documents the distinct response of species to hurricane events, where large trees are removed from the canopy and suppressed species in the understory usually grow to fill the gap. Shade-tolerant tree species usually thrive when the canopy is removed, because those trees have been surviving in the understory until the time when competition for light has been removed.

Foster and Brooks (2001) also found that summer precipitation is one of the primary factors controlling radial growth in *P. palustris*. They compared transitional to xeric sites and found that moisture parameters had a strong influence on tree growth. Overall, they found that 17.5% of the variance in growth patterns was explained by their climatic parameters (monthly temperature, monthly precipitation, mean monthly PDSI, and monthly flow) compared to our analysis that had 30% variance explained. Generally tree-ring growth in the southern Atlantic and Gulf Coastal Plain is slowed by summer moisture deficits and dry conditions (Cook et al. 1988). This is the time period when rains brought by hurricanes may greatly increase growth especially in the latewood of the trees. We hypothesize that this increase in latewood width along with an establishment pulse may be strong ecological indicators of past hurricane events. More studies on other sites should examine these indicators to determine their reliability in reconstructing past hurricane events.

Tree-ring oxygen isotope chronologies may have a greater potential to develop high-resolution hurricane records that may provide crucial information regarding the long-term variability of hurricane frequency prior to instrumental records.

3.4 The Potential Development of Hurricane Reconstructions from Stable Isotope Studies

Trees are useful candidates for stable isotopic analysis because they are stationary and record the environment at a given location over time. Trees obtain water primarily from soil moisture. Shallow-rooted conifers, such as *P. palustris*, primarily use soil moisture derived from meteoric precipitation rather than tapping into the water table (Anderson et al. 2002). A portion of the oxygen isotope signal in these trees will therefore reflect the oxygen isotopic composition of meteoric precipitation (Anderson et al. 1998; Roden et al. 2000; Anderson et al. 2002; Waterhouse et al. 2002; McCarroll and Loader 2004).

Tropical cyclone systems produce rainfall with an oxygen isotope signal 10–20‰ lower than normal precipitation (Gedzelman and Arnold 1994; Lawrence and Gedzelman 1996; Lawrence 1998). The influx of precipitation from tropical cyclone events will replace or mix with existing soil waters. Uptake and assimilation of these waters into tree-ring cellulose results in a lighter isotopic signature in the tree rings. The North Atlantic hurricane season generally lasts from June to November, generally coinciding with the latewood portion of the annual growth ring.

By separating each annual growth ring into its seasonal component, the ^{18}O-depleted rainfall events associated with tropical cyclones may be identified (Miller 2005; Miller et al. 2006).

Most researchers use the cellulose extraction methods outlined by Green (1963) with later modifications by Loader et al. (1997) for small-batch processing. New techniques are being developed that increase the speed of analysis enabling researches to include more replication from different samples and allow them to conduct their analysis with smaller quantities of wood. The oxygen isotope ratio of tree-ring α-cellulose can be rapidly analyzed using a continuous-flow isotope ratio mass spectrometer (IRMS). Cellulose samples are typically converted to CO gas using high-temperature degradation (pyrolysis). The oxygen isotope ratio ($\delta^{18}O$) is reported in per mil (‰) notation, where $\delta^{18}O = (R_{sample}/R_{standard} - 1) \times 1000$. Here, R_{sample} is the ratio of the rare isotope over the abundant isotope ($^{18}O/^{16}O$), and $R_{standard}$ is the standard (V-SMOW for oxygen).

Several potential problems exist when using stable oxygen isotopes in tree rings to characterize hurricanes. First, hurricanes are dynamic systems, and the magnitude of isotopic depletion may vary widely across a single storm (Lawrence et al. 2002; Gedzelman et al. 2003). Secondly, location and intensity of precipitation are variable inside the storm (Gedzelman et al. 2003), so that rainfall is not spread evenly across the affected area. These issues may have marked effects in the amount of depletion and amount of moisture received by trees during an event. If precipitation is not significantly depleted compared to normal meteoric precipitation, or if minimal rainfall is received, then the ^{18}O-depleted signal may not appear in the tree-ring cellulose.

The initial oxygen isotope composition of the soil water prior to a hurricane event may also influence the ability of trees to record the storm. Detailed analyses of the oxygen isotopic composition of hurricane rainwater have yet to identify the amount of precipitation required to sufficiently alter the $\delta^{18}O$ of existing soil moisture. Tang and Feng (2001) noted that depleted rainwaters from hurricane events can remain in the soil for several weeks following the event, but the initial soil moisture characteristics preceding the hurricane events were not noted. It is possible that drought events may enrich the soil water $\delta^{18}O$ such that it is impossible for the ^{18}O-depleted precipitation from a hurricane to alter the isotopic composition of the soil water significantly (Miller 2005; Miller et al. 2006).

Tree-ring isotope records of hurricane events are still few. The first record developed for the southeastern U.S. (Miller 2005; Miller et al. 2006) spanned 220 years using living and remnant *P. palustris* samples from southern Georgia. The resulting oxygen isotope series recorded all hurricanes in the area with only one false positive event when compared to instrumental hurricane track and precipitation data from 1940 to 1990. The record also highlighted periods of increased and decreased hurricane activity, likely tied to long-term ocean/atmospheric oscillations patterns known to affect Atlantic Basin hurricane frequency.

Similar techniques are currently being applied to develop long-term hurricane records from the Florida Gulf Coast (Pensacola), South Carolina (Sandy Island), and the Texas Gulf Coast (Big Thicket National Preserve, Big Sandy Creek Unit)

(Nelson 2008, Lewis unpublished data). These studies are not complete as of yet, but initial results indicate that trees in these areas are capable of yielding long-term hurricane chronologies, although 100% accuracy of the records is unlikely.

The combination of stable isotopic analysis with stand-age structure analysis may be able to provide confirmation of past hurricane events. Many different factors can cause establishment pulses in deciduous forests or an increase in latewood thickness in *P. palustris*. But these changes, coupled with a significant decrease in stable isotopic composition are likely to only be due to a hurricane. Due to ongoing research in this area (see Grissino-Mayer et al. 2010, this volume), we expect these techniques to be strengthened so that dendrochronological hurricane reconstruction can become more common in the next 10 years.

References

Anderson WT, Bernasconi SM, McKenzie JA (1998) Oxygen and carbon record of climatic variability in tree ring cellulose (*Picea abies*): an example from central Switzerland (1913–1995). J Geophys Res 103(D24): 31, 625–631, 636

Anderson WT, Bernasconi SM, McKenzie JA, Saurer M, Schweingruber F (2002) Model evaluation for reconstructing the oxygen isotopic composition in precipitation from tree ring cellulose over the last century. Chem Geol 182:121–137

Cook ER, Kablack MA, Jacoby GC (1988) The 1986 drought in the southeastern United States: how rare an event was it? J Geophys Res 93:14, 257–214, 260

Douglass AE (1941) Crossdating in dendrochronology. J Forest 39(10):825–831

Foster TE, Brooks JR (2001) Long-term trends in growth of Pinus palustris and Pinus elliottii along a hydrological gradient in central Florida. Can J Forest Res 31:1661–1670

Gedzelman SD, Arnold R (1994) Modeling the isotopic composition of precipitation. J Geophys Res 99:10455–10573

Gedzelman S, Hindman E, Zhang X, Lawrence J, Gamache J, Black M, Black R, Dunion J, Willoughby H (2003) Probing hurricanes with stable isotopes of rain and water vapor. Mon Weather Rev 131(6):1112–1127

Gentry CM (2008) Analyzing the effect of hurricanes on structure and growth in Southeast Texas Forests. Ph.D. Dissertation, Indiana State University, 302 pp

Green JW (1963) Wood cellulose. In: Whistler RL (ed) Methods of carbohydrate chemistry, III. Academic, New York, pp 9–21

Grissino-Mayer HD (2001) Evaluating crossdating accuracy: a manual and tutorial for the computer program COFECHA. Tree-Ring Res 57:205–221

Grissino-Mayer HD, Miller DL, Mora CI (2010) Dendrotempestology and the isotopic record of tropical cyclones in Tree Rings of the Southeastern United States. In: Stoffel M, Bollschweiler M, Butler DR, Luckman BH (eds) Tree rings and natural hazards: A state-of-the-art. Springer, Berlin, Heidelberg, New York, this volume

Hall RBW, Harcombe PA (2001) Sapling dynamics in a southeastern Texas floodplain forest. J Veg Sci 12:427–438

Harcombe PA, Marks PL (1977) Understory Structure of a Mesic Forest in Southeast Texas. Ecology 58(5):1144–1151

Harcombe PA, Bill CJ, Fulton M, Glitzenstein JS, Marks PL, Elsik IS (2002) Stand dynamics over 18 years in a southern mixed hardwood forest, Texas, USA. J Ecol 90:947–957

Holmes RL (1983) Computer-assisted quality control in tree-ring dating and measurement. Tree-Ring Bull 43:69–78

Lawernce JR, Gedzelman SD, Gamache J, Black M (2002) Stable isotope ratios: hurricane Olivia. J Atmos Chem 41:67–82

Lawrence JR (1998) Isotopic spikes from tropical cyclones in surface waters: opportunities in hydrology and paleoclimatology. Chem Geol 144:153–160

Lawrence JR, Gedzelman SD (1996) Low stable isotope ratios of tropical cyclone rains. Geophys Res Lett 23:527–530

Liu KB, Fearn ML (1993) Lake-sediment record of late Holocene hurricane activities from coastal Alabama. Geology 21(9):793–796

Loader N, Robertson I, Barker AC, Switsur R, Waterhouse JS (1997) An improved technique for the batch processing of small wholewood samples to alpha-cellulose. Chem Geol 136:313–317

McCarroll D, Loader NJ (2004) Stable isotopes in tree rings. Quat Sci Rev 23:771–801

Miller DL (2005) A tree-ring oxygen isotope record of tropical cyclone activity, moisture stress, and long-term climate oscillations for the southeastern U.S. Ph.D. Dissertation, The University of Tennessee, Knoxville

Miller DL, Mora CI, Grissino-Mayer HD, Mock CJ, Uhle ME, Sharp Z (2006) Tree-ring isotope records of tropical cyclone activity. Proc Natl Acad Sci 103(39):14294–14297

Nelson WL (2008) Oxygen isotope ratios of longleaf pines as a proxy of past hurricane activity along the Atlantic Seaboard. Ph.D. Dissertation, The University of Tennessee, Knoxville, 287 pp

Orvis K, Grissino-Mayer HD (2002) Standardizing the reporting of abrasive papers used to surface tree-ring samples. Tree-Ring Res 58:47–50

Roden JS, Lin G, Ehleringer JR (2000) A mechanistic model for the interpretation of hydrogen and oxygen isotopes in tree-ring cellulose. Geochim Cosmochim Ac 64(1):21–35

Stokes MA, Smiley TL (1968) An introduction to tree-ring dating. University of Arizona Press, Tucson, AZ

Tang K, Feng X (2001) The effect of soil hydrology on the oxygen and hydrogen isotopic compositions of plants' source water. Earth Planet Sci Lett 185:355–367

USDA SSURGO (2008) The United States Department of Agriculture, Natural Resources Conservation Service – Soil Survey Geographic (SSURGO) Database. Soil Survey Staff, Natural Resources Conservation Service, United States Department of Agriculture. Soil Survey Geographic. http://soildatamart.nrcs.usda.gov

Waterhouse JS, Switsur VR, Barker AC, Carter AHC, Robertson I (2002) Oxygen and hydrogen isotope ratios in tree rings: how well do models predict observed values? Earth Planet Sci Lett 201:421–430

Watson GE (2006) Big thicket plant ecology: an introduction, 3rd edn. University of North Texas Press, Denton

Part VIII
Wildfires

Ground fire damages trees in Grand Canyon National Park, U.S. (© P. Z. Fulé)

Wildfire Hazard and the Role of Tree-Ring Research

Henri D. Grissino-Mayer

1 Introduction

In February 2009, wildfires raged across 3,900 km^2 in southern Victoria near Melbourne in southeastern Australia, killing over 200 people and destroying more than 1,800 homes, the worst wildfire tragedy in the country's history and worst ever natural disaster (Callinan 2009). Wildfires in Australia are in fact common. The vegetation of the region is well-adapted to frequent fire, suggesting a long history of fires that stretches back for millennia, well before human presence, but the severity with which these series of wildfires struck caught the country (and scientists alike) by surprise. Although several arsonists were arrested and charged, some speculate that climate change contributed to the severity and spatial extent of these wildfires, although this is still a highly debatable topic (Sullivan 2009).

In October 2003, San Diego County in southern California (USA) witnessed three simultaneous wildfires that were the largest and deadliest in the state's history. Sixteen people were killed, 2,400 homes were destroyed, and 1,520 km^2 were scorched. In October 2007, San Diego County found itself again inundated by nine simultaneous wildfires that required the evacuation of 300,000 people and caused the loss of more than 1,800 homes. Nine people lost their lives, 1,500 km^2 were charred, with an estimated cost of over US$ 80 million (San Diego Wildfires Education Project 2009). Up to 2008, the year 2006 is the worst year on record for wildfire activity (not counting prescribed or wildland fire use fires) for the United States when 39,150 km^2 burned (National Interagency Fire Center 2009).

H.D. Grissino-Mayer (✉)
Department of Geography, Laboratory of Tree-Ring Science, The University of Tennessee, Knoxville, TN 37996, USA
e-mail: grissino@utk.edu

M. Stoffel et al. (eds.), *Tree Rings and Natural Hazards: A State-of-the-Art*, Advances in Global Change Research 41, DOI 10.1007/978-90-481-8736-2_31,

These events underscore the importance of research that provides background information on the history of wildfires so that land management agencies can develop more informed fire management policies and guidelines that take into account the longer-term perspective available via paleofire reconstructions (Kipfmueller and Swetnam 2001; Willis and Birks 2006). Several means exist that provide this perspective on past wildfires, such as analyzing temporal sequences of charcoal (microscopic and macroscopic) from lake, wetland, and pond sediments (Horn and Sanford 2002; Whitlock et al. 2008) and from soil (Gavin et al. 2007; Hart et al. 2008) coupled with radiocarbon dates. Tree-ring studies also have provided a wealth of information on past wildfires, taking advantage of the ubiquity of potential tree species that record wildfires in their tree rings coupled with the annual and sub-annual resolution available from the tree-ring record.

2 The Tree-Ring Record of Wildfires

The record of wildfires in the tree-ring record has long been recognized as an important contribution to ecosystem studies (Clements 1910; Leopold 1924). In their book *Plant Ecology*, Weaver and Clements (1938) observed that "The time of fire may be determined by counting the number of rings of wood put down since the burn scar was formed. Sometimes the burn scar may be double or even triple and thus give the dates of successive fires." Later studies by Spurr (1954) in Minnesota, Weaver (1959) in Oregon, and McBride and Laven (1976) in California, among others, further laid the groundwork for investigating wildfires based on fire scars. The incorporation of crossdated tree-ring records added a level of accuracy that helped advance the quantification of tree-ring based fire history data in both Europe and the U.S. (Zackrisson 1977; Madany et al. 1982; Swetnam 1983). Another major milestone was the introduction of composite fire interval analysis that used crossdated fire scars from numerous trees in a study site to evaluate the spatial dynamics of wildfires (Dieterich 1980, 1983). Later, Thomas W. Swetnam and the Fire History and Ecology Group at the Laboratory of Tree-Ring Research (University of Arizona) would greatly advance our knowledge of fire regimes in North America and elsewhere (Baisan and Swetnam 1990; Swetnam 1993, 1996; Grissino-Mayer and Swetnam 2000).

Field and laboratory techniques for analyzing wildfires from tree-ring dated fire scars have been documented in many publications (Zackrisson 1977; Baisan and Swetnam 1990; Grissino-Mayer 1999; Kipfmueller and Swetnam 2001). Obtaining dates for past wildfires back centuries and even millennia with annual precision is itself a major accomplishment, but the next revolution occurred in the 1990s with the quantification of fire regimes from tree-ring data. Statistical descriptors of fire activity (such as the Mean Fire Interval) were then already commonplace and important for managing fire-prone ecosystems, but more information was needed on the historical range of wildfire activity (Morgan et al. 1994; Brown et al. 2000). Using

more advanced modeling of the fire-free interval data available from tree rings, we now can provide improved descriptors of fire activity in the past, such as the Weibull Median Probability Interval (which is a better measure than the Mean Fire Interval) and the Lower and Upper Exceedance Intervals, which help define the historical range of variation in fire regimes (Grissino-Mayer 1999, 2001; Fulé et al. 2003; McEwan et al. 2007).

Another major advance in tree-ring studies of wildfire activity actually has a long history in dendroecology. Fire scars are found most often in ecosystems where low-severity fires are common. A moderate to higher severity wildfire could kill most or all trees in a stand, especially in ecosystems where wildfire is less common (such as in boreal and subalpine forests) causing a cohort of trees to establish after the fire. Early studies used the age structure of trees to reconstruct the history of fire disturbance in forest stands (Heinselman 1973; Tande 1979). Tree-ring dating can determine (with some small degree of uncertainty) when these trees established, thus allowing a more complete reconstruction of wildfire activity across a broader spectrum of fire severities (Ehle and Baker 2003; Brown and Wu 2005).

Important contributions of tree-ring based fire history analyses concern linkages now being discovered between wildfire activity and climate, especially broad-scale atmospheric-oceanic teleconnections such as the Pacific Decadal Oscillation (PDO), the Atlantic Multidecadal Oscillation (AMO) and the El Niño-Southern Oscillation (ENSO). In the American Southwest, Swetnam and Betancourt (1990) showed that positive phases of the ENSO correlate significantly with a greater percentage of trees scarred. Grissino-Mayer and Swetnam (2000) found that fires were more frequent but less widespread during the Little Ice Age (ca. AD 1400–1800), but less frequent and more widespread during the warmer period that followed. Synchronous positive phases of PDO and ENSO were found to contribute to more widespread fires in northeastern California (Norman and Taylor 2003). In the Pacific Northwest, fires occur more often in dry summers and during positive phases of the PDO, while the percentage of trees scarred showed a significantly positive relationship with ENSO (Hessl et al. 2004). Brown (2006) found that wildfires in South Dakota and Wyoming were synchronous during La Niñas coupled with positive PDO and AMO phases. These and other studies point to clear interdecadal to century-scale forcing of fire activity by climate.

3 Fire History in an Uncertain Future

New challenges face researchers who investigate fire history from the tree-ring record. The first concerns the quickening disappearance of suitable samples for fire history analyses. Ever expanding and intensifying wildfires today are actually destroying the very evidence we need to understand their history. Superimposed on this tragedy is the expanding use of controlled burns (whether prescription or

naturally set fires) to help restore degraded ecosystems, which also destroy valuable evidence. Within this backdrop is the steady decay of suitable samples over time. In summer 2009, I revisited a site I had sampled in 1991 in El Malpais National Monument of New Mexico and was astounded how easily the fire history samples we wished to sample crumbled in our hands even before using a chain saw.

Second, we must ask whether restoration of ecosystems is a viable management option given the changing nature of our environment. Many dendroecologists use as one of their justifications the importance of tree-ring based fire history studies for helping land management agencies restore degraded ecosystems where fire has long been purposely excluded. Fire exclusion beginning in the early twentieth century has changed the successional trajectory of nearly all temperate forests and woodlands (sometimes now called "novel ecosystems," Hobbs et al. 2006), to the point that reintroduction of fire could have detrimental (high-intensity stand-destroying fires) rather than beneficial (lower intensity stand maintenance fires) effects. Restoration begs the question: "What are we restoring to?" Environmental conditions seen in 1880? 1600? 1491? Restoration further may not be viable given that future environments will be responding to and evolving in a world dominated by increasing global temperatures, with no guarantee that ecosystem processes (such as wildfire) will operate as they once did (Westerling et al. 2006; Fauria and Johnson 2008).

Third, climate change means change in our forests and ecosystems and the vital processes that operate to shape and maintain them. Many studies have clearly linked changes in past climate with changes in past wildfire activity, including changes in fire frequency, seasonality, severity, and spatial extent (Clark 1988; Balling et al. 1992; Swetnam 1993). What remains uncertain are the fire regimes that could be expected in the twenty-first century given increasing temperatures and the likely accompanying changes in precipitation patterns, as well as the expected but uncertain changes in spatial patterns of rainfall, temperature, and drought across the Earth's surface. Vegetation ranges certainly will not change with the rapidity with which climate is changing, meaning that forests and the disturbance processes that operate within them (including wildfires) will have to accommodate an evolving disequilibrium that could prove detrimental to the health of these forests. For example, fewer fires in western and eastern U.S. ecosystems will cause fire-intolerant species to become more dominant, a successional trajectory we see happening today (Camp 1999; Schoennagel et al. 2004; DeWeese 2007; Nowacki and Abrams 2008).

Curiously, as we head into a more uncertain future, the value of tree-ring based research on fire history and ecology becomes greater, promoting a growing field of inquiry that has increasingly important implications for land management. Between 1920 and 1970, only 30 published studies had investigated the use of tree rings to make inferences on past fire activity. By 1980, this number had more than doubled to 72 studies, to 176 by 1990, and to 433 by 2000. Furthermore, dendroecologists that specialize in fire history are being very efficient at training the next generation of tree-ring scientists, ensuring that this field of inquiry will thrive and continue to benefit society.

References

Baisan CH, Swetnam TW (1990) Fire history on a desert mountain range: Rincon Mountain Wilderness, Arizona, USA. Can J For Res 20:1559–1569

Balling RC Jr, Meyer GA, Wells SG (1992) Climate change in Yellowstone National Park: Is the drought-related risk of wildfires increasing? Clim Change 22:35–45

Brown PM (2006) Climate effects on fire regimes and tree recruitment in Black Hills ponderosa pine forests. Ecology 87:2500–2510

Brown PM, Wu R (2005) Climate and disturbance forcing of episodic tree recruitment in a southwestern ponderosa pine landscape. Ecology 86:3030–3038

Brown PM, Ryan MG, Andrews TG (2000) Historical surface fire frequency in ponderosa pine stands in research natural areas, central Rocky Mountains and Black Hills, USA. Nat Areas J 20:133–139

Callinan R (2009) Horror and tragedy in Australia's worst wildfires. Time.com 09 Feb 2009. http://www.time.com/time/world/article/0,8599,1878114,00.html

Camp AE (1999) Age structure and species composition changes resulting from altered disturbance regimes on the eastern slopes of the Cascades Range, Washington. J Sustain Forest 9:39–67

Clark JS (1988) Effect of climate change on fire regimes in northwestern Minnesota. Nature 334:233–235

Clements FE (1910) The life history of lodgepole burn forests. USDA For Serv Bull 79:1–56

DeWeese GG (2007) Past fire regimes of Table Mountain pine (Pinus pungens Lamb.) stands in the central Appalachian Mountains, Virginia, USA. Ph.D. Dissertation, University of Tennessee, Knoxville, TN

Dieterich JH (1980) The composite fire interval-a tool for more accurate interpretation of fire history. In: Stokes MA, Dieterich JH (eds) Proceedings of the fire history workshop. USDA Forest Service General Technical Report RM-81:8–14

Dieterich JH (1983) Fire history of southwestern mixed conifer: a case study. For Ecol Manage 6:13–31

Ehle DS, Baker WL (2003) Disturbance and stand dynamics in ponderosa pine forests in Rocky Mountain National Park, USA. Ecol Monogr 73:543–566

Fauria MM, Johnson EA (2008) Climate and wildfires in the North American boreal forest. Philos Trans R Soc B-Biol Sci 363:2317–2329

Fulé PZ, Crouse JE, Heinlein TA, Moore MM, Covington WW, Verkamp G (2003) Mixed-severity fire regime in a high-elevation forest of Grand Canyon, Arizona, USA. Landscape Ecol 18:465–485

Gavin DG, Hallett DJ, Hu FS, Lertzman KP, Prochard SJ, Brown KJ, Lynch JA, Bartlein P, Peterson DL (2007) Forest fire and climate change in western North America: insights from sediment charcoal records. Front Ecol Environ 5:499–506

Grissino-Mayer HD (1999) Modeling fire interval data from the American Southwest with the Weibull distribution. Int J Wildland Fire 9:37–50

Grissino-Mayer HD (2001) FHX2 - Software for analyzing temporal and spatial patterns in fire regimes from tree rings. Tree-Ring Res 57:115–124

Grissino-Mayer HD, Swetnam TW (2000) Century-scale climate forcing of fire regimes in the American Southwest. Holocene 10:213–220

Hart JL, Horn SP, Grissino-Mayer HD (2008) Fire history from soil charcoal in a mixed hardwood forest on the Cumberland Plateau, Tennessee, USA. J Torrey Bot Soc 135:401–410

Heinselman ML (1973) Fire in the virgin forests of the Boundary Waters Canoe Area, Minnesota. Quatern Res 3:329–382

Hessl AE, McKenzie D, Schellhaas R (2004) Drought and Pacific decadal oscillation linked to fire occurrence in the inland Pacific Northwest. Ecol Appl 14:425–442

Hobbs RJ, Arico S, Aronson J, Baron JS, Bridgewater P, Cramer VA, Epstein PR, Ewel JJ, Klink CA, Lugo AE, Norton D, Ojima D, Richardson DM, Sanderson EW, Valladares F, Vila M,

Zamora R, Zobel M (2006) Novel ecosystems: theoretical and management aspects of the new ecological world order. Glob Ecol Biogeogr 15:1–7
Horn SP, Sanford RL (2002) Holocene fires in Costa Rica. Biotropica 24:354–361
Kipfmueller KF, Swetnam TW (2001) Using dendrochronology to reconstruct the history of forest and woodland ecosystems. In: Egan D, Howell EA (eds) The historical ecology handbook: a restorationist's guide to reference ecosystems. Island Press, Washington DC
Leopold A (1924) Grass, brush, timber, and fire in southern Arizona. J For 22:1–10
Madany MH, Swetnam TW, West NE (1982) Comparison of two approaches for determining fire dates from tree scars. Forest Sci 28:856–861
McBride JR, Laven RD (1976) Scars as an indicator of fire frequency in the San Bernardino Mountains, California. J For 74:439–442
McEwan RW, Hutchinson TF, Long RP, Ford DR, McCarthy BC (2007) Temporal and spatial patterns in fire occurrence during the establishment of mixed-oak forests in eastern North America. J Veg Sci 18:655–664
Morgan P, Aplet GH, Haufler JB, Humphries HC, Moore MM, Wilson WD (1994) Historical range of variability: a useful tool for evaluating ecosystem change. J Sustain Forest 2:87–111
National Interagency Fire Center (2009) Fire information – wildland fire statistics. http://www.nifc.gov/fire_info/fires_acres.htm. Accessed 26 June 2009
Norman SP, Taylor AH (2003) Tropical and north Pacific teleconnections influence fire regimes in pine-dominated forests of north-eastern California, USA. J Biogeogr 30:1081–1092
Nowacki GJ, Abrams MD (2008) The demise of fire and "Mesophication" of forests in the eastern United States. Bioscience 58:123–138
San Diego Wildfires Education Project (2009) San Diego State University Foundation. http://interwork.sdsu.edu/fire/index.htm. Accessed 26 June 2009
Schoennagel T, Waller DM, Turner MG, Romme WH (2004) The effect of fire interval on post-fire understorey communities in Yellowstone National Park. J Veg Sci 15:797–806
Spurr SH (1954) The forests of Itasca in the nineteenth century as related to fire. Ecology 35:21–25
Sullivan R (2009) Future shock: Warming world to fan more Australian wildfires. USA Today, 11 Feb 2009
Swetnam TW (1983) Fire history of the Gila Wilderness, New Mexico. M.Sc. thesis, University of Arizona, Tucson, AZ
Swetnam TW (1993) Fire history and climate change in giant sequoia groves. Science 262:885–889
Swetnam TW (1996) Fire and climate history in the Central Yenisey region, Siberia. In: Goldhammer JG, Furyaev VV (eds) Fire in ecosystems of boreal Eurasia. Kluwer, The Hague/The Netherlands
Swetnam TW, Betancourt JL (1990) Fire-Southern Oscillation relations in the southwestern United States. Science 249:1017–1020
Tande GF (1979) Fire history and vegetation pattern of coniferous forests in Jasper National Park, Alberta. Can J Bot 57:1912–1931
Weaver H (1959) Ecological changes in the ponderosa pine forest of the Warm Springs Indian Reservation in Oregon. J For 57:15–20
Weaver JE, Clements FE (1938) Methods of studying vegetation: ring counts and burn scars. In: Plant ecology. McGraw-Hill, New York
Westerling AL, Hidalgo HG, Cayan DR, Swetnam TW (2006) Warming and earlier spring increase western U.S. forest wildfire activity. Science 313:940–943
Whitlock C, Marlon J, Briles C, Brunelle A, Long C, Bartlein P (2008) Long-term relations among fire, fuel, and climate in the north-western US based on lake-sediment studies. Int J Wildland Fire 17:72–83
Willis KJ, Birks HJB (2006) What is natural? The need for a long-term perspective in biodiversity conservation. Science 314:1261–1265
Zackrisson O (1977) Influence of forest fires on the north Swedish boreal forest. Oikos 29:22–32

Mesoscale Disturbance and Ecological Response to Decadal Climatic Variability in the American Southwest

Thomas W. Swetnam and Julio L. Betancourt

1 Introduction

Climatic variables such as radiation, temperature and precipitation determine rates of ecosystem processes from net primary productivity to soil development. They predict a wide array of biogeographic phenomena, including soil carbon pools, vegetation physiognomy, species range, and plant and animal diversity. Climate also influences ecosystems indirectly by modulating the frequency, magnitude, and spatial scales of natural disturbances (Clark 1988; Overpeck et al. 1990; Swetnam 1993).

Disturbance is any discrete event that results in the sudden mortality of biomass on a time scale significantly shorter than that of its accumulation (Huston 1994). A broader definition would include any abrupt event that disrupts community structure and changes the physical environment, resources, or availability of space (White and Pickett 1985). Much of the focus in disturbance ecology has been on the patch dynamics produced by resetting of succession within portions of an ecosystem (so-called "gap disturbances"). Emphasis has shifted from how disturbances produce landscape mosaics to how these mosaics in turn predispose the landscape to further disturbance. Both spatial and temporal scales enter the discussion about whether disturbance helps to maintain or prevent ecosystems from ever reaching equilibrium.

The current paradigm favors a nonequilibrium perspective, but steady states may be scale dependent. Theoretically, if areas affected by disturbance are sufficiently small, then a self-reproducing steady state can exist as an average condition over

T.W. Swetnam (✉)
Laboratory of Tree-Ring Research, University of Arizona, Tucson, AZ 85721, USA
e-mail: tswetnam@ltrr.arizona.edu

J.L. Betancourt
U.S. Geological Survey, Desert Laboratory, Tucson, AZ 85745, USA

M. Stoffel et al. (eds.), *Tree Rings and Natural Hazards: A State-of-the-Art*,
Advances in Global Change Research 41, DOI 10.1007/978-90-481-8736-2_32,

relatively larger areas (Sousa 1984; Rogers 1996; Turner et al. 1993). A regional steady state is unlikely wherever mesoscale disturbances (104–106 km^2) recur on time scales shorter than the successional cycles necessary to reach and maintain equilibrium across a region (Romme 1982; Barden 1988; Sprugel 1991; Swetnam 1993; Turner et al. 1993). One such place is the American Southwest, where rates of plant and population growth are sluggish; soil properties accumulate only gradually (103–105 years) and are usually in disequilibrium with current climate and vegetation; meager soil water and organic matter cannot buffer climatic extremes; and episodic mortality from drought, insect outbreaks, and fire is often synchronized and broadscale.

In this paper, we explore the effects of climatic variability and mesoscale disturbance on non-riparian ecosystems of the American Southwest. We emphasize decadal and regional scales for three reasons. First, the mean generation times of most of the woody perennials that dominate from the lowland deserts to upland forests are from 15 to 50 years; hence these are the minimal time spans to observe their population dynamics. Second, there is ample evidence for climate behavior on decadal scales (15–30 year period) in both the instrumental (Cayan et al. 1998; Dettinger et al. 1998; Cayan and Webb 1992; Webb and Betancourt 1992) and tree-ring records of the American Southwest (Fritts 1991; Stahle et al. 1993; Dettinger et al. 1998; Grissino-Mayer 1996). Lastly, local and shorter time frames have dominated empirical and experimental work in ecology, as well as resource management, while regional and historical perspectives have been neglected (Ricklefs 1987; Brown 1995). Experimentation is valuable for clarifying mechanisms, but is generally impractical or impossible at regional or decadal to centennial time scales. In the Southwest, long-term perspectives on ecosystem response to climate and disturbance are abetted by a long tradition of vegetation monitoring (Goldberg and Turner 1984; Turner 1990; Martin 1986; Avery et al. 1976; Brown and Heske 1990; Pake and Venable 1995), and the ability to cross-date and map past climatic variations, disturbances, and tree demography at interannual resolution using tree rings (Fritts and Swetnam 1989).

Our goals in this paper are to: (1) explore the complexity of climate-disturbance relationships; (2) demonstrate the synchroneity and spatial extent of fires and drought-related plant mortality (and establishment); and (3) use extreme episodes such as the 1950s drought and the post-1976 climatic shift to illustrate the impacts of decadal-scale climate on ecosystems and the present challenge of disentangling natural and cultural factors.

2 Disturbance Climates of the American Southwest

2.1 Seasonal Variability

In the American Southwest, seasonal precipitation is characterized by a highly-variable winter-early spring (November–March), an arid late spring and foresummer

(April–June), monsoonal rains in July and August, and a dry autumn (September–October; Fig. 1). In general, cool season precipitation recharges soil moisture and controls woody plant growth, whereas summer rains drive the annual grass production

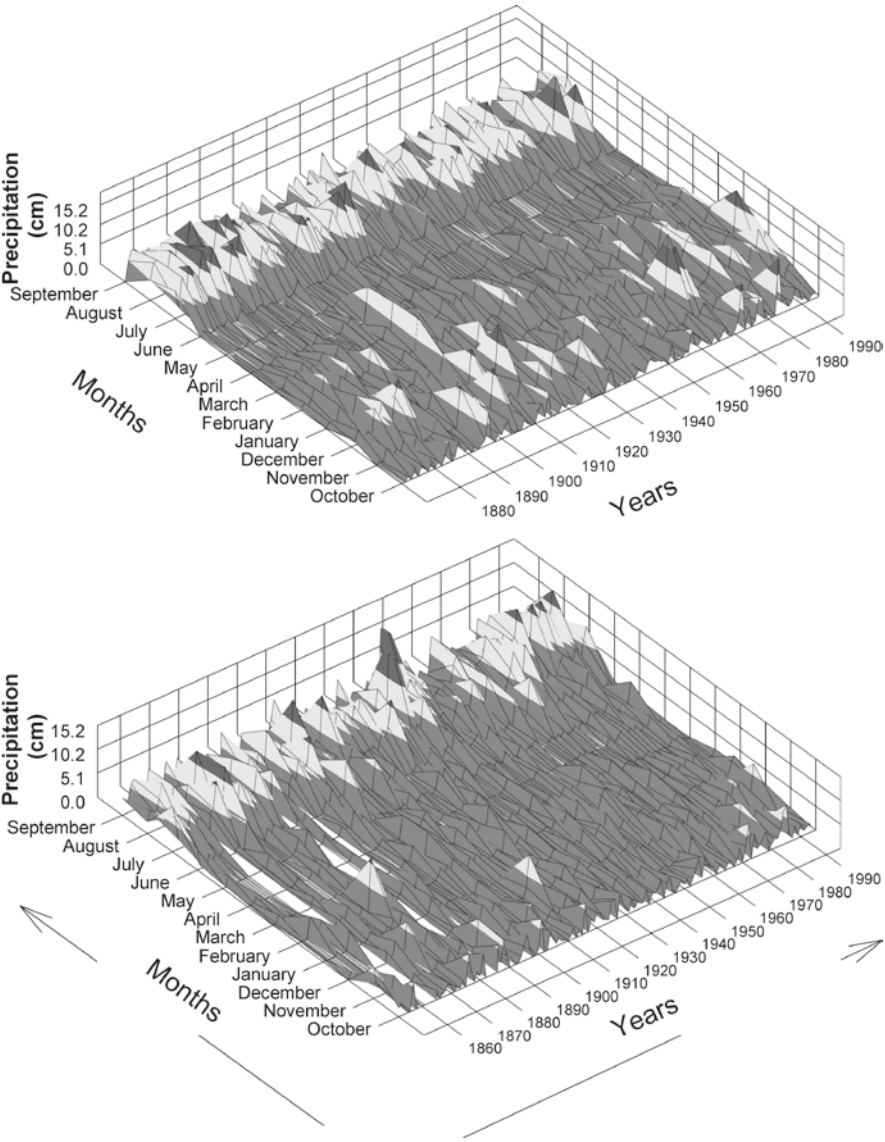

Fig. 1 Three-dimensional time series plots of monthly precipitation totals from Tucson, Arizona, 1870–1995 (*upper plot*) and Las Cruces, New Mexico, 1853–1995 (*lower plot*). Note the persistence of winter and summer drought in Las Cruces during the 1950s, and the post-1976 increase in cool season precipitation in both Tucson and Las Cruces

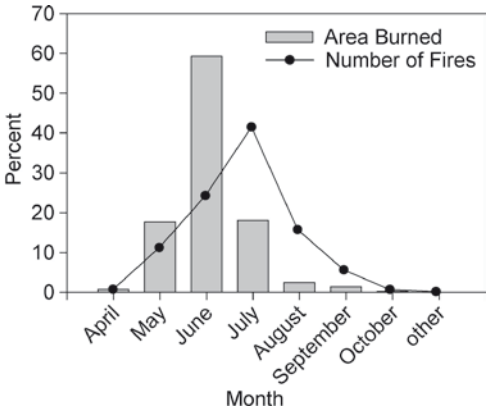

Fig. 2 Monthly distribution of numbers and area burned by lightning fires in Arizona and New Mexico National Forests, 1940–1974 (Barrows 1978)

that supports the livestock industry. Synergism between seasonal precipitation and lightning activity yields a vigorous fire regime in late spring/early summer. During the arid foresummer (Fig. 1) fuels are dry, convective storms begin to generate lightning, and the maximum area is burned in June. Subsequently, full development of the monsoonal pattern in July leads to a maximum in numbers of lightning-ignited fires, but increasing fuel moisture results in reduced area burned (Fig. 2).

Although the influence of seasonal climatic variability on wildland fires is intuitively obvious – droughts are correlated with fire – the predictive aspects of this association are poorly understood. Recently, there has been a surge of interest and research in fire climatology, driven in part by recognition of ENSO teleconnections and concern over potential impacts of future climatic change on wildfire activity (Simard et al. 1985; Swetnam and Betancourt 1990; Balling et al. 1992; Flannigan and Van Wagner 1991; Johnson and Wowchuck 1993; Larsen and MacDonald 1995; Knapp 1995; Price and Rind 1994). In contrast to traditional emphasis on short-term and local weather (temperature, relative humidity, and wind speed) effects on fire (Rothermel 1983), more recent studies focus on relatively large spatial and long temporal scales, i.e., regional to continental, and seasonal to decadal.

In the Southwest, plant communities experience episodic recruitment and mortality of seedlings and adults (Betancourt et al. 1993). To survive its first year, a new seedling must endure frost and seasonal drought. If winter is dry, there may be insufficient soil moisture for fast growth in the spring/early summer. If summer rains fail, the arid foresummer extends into the hottest time of the year, and even the hardiest of seedlings will wither and die. One outcome of seasonal or longer droughts is a lull in plant recruitment. Conversely, wet and/or warm conditions favor above-average seed germination and survival of seedlings leading to recruitment pulses. These pulses may be dominated by single-year events, such as the year 1919 in many

Southwestern ponderosa pine (*Pinus ponderosa*) stands (Pearson 1950; Savage et al. 1996), or they may be clustered in favorable decades (White 1985).

2.2 Interannual and Interdecadal Climate Variability

Interannual variability in southwestern precipitation is linked to shifts in the upper-air westerlies and ENSO. During the warm SO phase, warm waters in the eastern Pacific provide the necessary energy for development of troughs along the west coast of North America; the warm waters also weaken the tradewind inversion, resulting in stronger subtropical westerlies. Although there appears to be no single canonical response in the polar jet stream, the middle-latitude winter storm track is usually displaced southward during El Niño episodes. In general, an expanded circumpolar vortex, with strengthened westerly winds centered about 30°N and positive 700-mb height anomalies at higher latitudes, prevails during decades when the Southern Oscillation approaches a biennial cycle (Cayan and Webb 1992; Webb and Betancourt 1992; Cayan et al. 1998). In the Southwest, El Niño (La Niña) conditions are associated with wetter (drier) winters and springs (Andrade and Sellers 1988) and drier (wetter) summers in Year +1 after the onset of El Niño (Harrington et al. 1992).

Teleconnections between the tropical Pacific and American Southwest have been shown by correlations between indices such as SOI, equatorial sea surface temperatures, and Line Island rainfall against southwestern precipitation (Douglas and Englehart 1984; Cayan and Webb 1992), streamflow (Cayan and Webb 1992; Webb and Betancourt 1992; Kahya and Dracup 1994), and annual area burned in Arizona and New Mexico (Swetnam and Betancourt 1990; Price and Rind 1994). These teleconnections tend to be lagged, promising some predictive capability a season or more in advance. Although linear regressions provide weak predictive capability (about 25–30% of the variance) for precipitation, streamflow, and fire, the mesoscale responses to extreme phases of the SO are highly consistent. This predictability, for example, allows managers to schedule control fires or to improve fire readiness depending on the onset of El Niño or La Niña conditions, respectively (Swetnam and Betancourt 1990). For example, based on La Niña conditions in fall 1995 and NOAA forecasts (Climate Prediction Center) for a dry Southwestern winter and spring, emergency funds were obtained and used to combat a heavy 1996 fire season (*Albuquerque Journal*, April 14, 1996 and *The New York Times*, May 11, 1996).

Evidence for climate behavior on interdecadal scales (15–30 year period) has been demonstrated empirically from historical climate data sets (Namias et al. 1988; Rasmusson et al. 1990; Halpert and Ropelewski 1992; Xu 1993; Latif and Barnett 1994; Trenberth and Hurrell 1994; Miller et al. 1994; Mann et al. 1995; Cayan et al. 1998; Dettinger et al. 1998) and high-resolution (annual) climate proxies including tree rings, corals, marine and lake sediment varves, and ice cores (Ebbesmeyer et al. 1991; Diaz and Pulwarty 1994; Dunbar et al. 1994; Meko et al. 1993; 1995;

Slowey and Crowley 1994; Stocker and Mysak 1992; Fritts 1991; Stahle et al. 1993). In the American Southwest, three different tree-ring reconstructions of the Southern Oscillation suggest that the frequency and amplitude of the SO, and/or the strength of its teleconnections with winter precipitation in this region, has varied on decadal to multidecadal timescales (Lough and Fritts 1985; Michaelsen and Thompson 1992; Stahle and Cleaveland 1993). During the twentieth century, decadal trends are evident in time series of monthly mean sea level pressure in the North Pacific and SOI (Trenberth and Hurrell 1994). In the Southwest, twentieth century climatic trends stemming from the interdecadal behavior of the westerlies and the tropical Pacific include wet winters in the early part of the century (1905–1930), a mid-century dry period (1942–1964), and warm, wet winters and erratic summers since 1976 (Fig. 1).

In sections to follow, we illustrate and discuss a range of ecological responses to interannual and interdecadal climatic variability in the American Southwest.

3 Regionally-Synchronized Insect Outbreaks

Outbreaks of phytophagous insects are one of the most dramatic and poorly-understood mesoscale ecological phenomena (Barbosa and Schultz 1987). The cyclical or aperiodic eruption of insect populations – sometimes from rare, endemic levels, to broadscale outbreaks covering 104–105 km^2 – has been known at least since biblical times (e.g., locust plagues), and associated anecdotally with drought. The drought connection was formalized by White (1976) in the "stress" hypothesis, which stated that moisture and heat-stressed plants have a higher food quality than non-stressed plants. Highly variable and sometimes contradictory results of both observational and experimental studies, however, have fostered continued debate about insect, plant, and drought interactions (Larsson 1989; Martinat 1987; Price 1991; Mopper and Whitham 1992). Part of the difficulty in identifying the role of climatic fluctuations in outbreak dynamics has been the lack of sufficiently long and large-scale records of climate or insect populations. This is particularly true for major forest defoliators, such as the western spruce budworm (*Choristoneura occidentalis*), and the eastern North American species (*Choristoneura fumiferana*), which have repeatedly erupted over regional areas at frequencies of only four or fewer outbreaks in the twentieth century (Sanders et al. 1985).

Tree-ring reconstructions of multi-century length budworm outbreak histories are possible because past defoliation of host trees by the budworm larvae cause distinctive growth reductions in tree-ring width series of surviving trees (Blais 1962). When non-host tree species (pines) are sampled in nearby sites and their ring series examined in comparison with the host tree species (firs and spruces), effects of climatic variation can be distinguished from the host-specific defoliation effects (Swetnam and Lynch 1993). These approaches have yielded 300-year reconstructions of budworm outbreaks in the Central and Southern Rockies of Colorado and New Mexico (Swetnam and Lynch 1993; Hadley and Veblen 1993; Weber and

Schweingruber 1995) and the Blue Mountains of eastern Oregon (Swetnam et al. 1995). Independently derived tree-ring reconstructions of June Palmer Drought Severity (PDSI) from non-host tree species, show that, over the past three centuries, budworm outbreaks generally coincided with wet periods, whereas low budworm population levels corresponded to droughts (Fig. 3). These tree-ring reconstructed patterns are supported by similar comparisons between twentieth century time series of defoliated area (from aerial and ground measurements) and meteorological data in the twentieth century (Swetnam and Lynch 1993).

The positive association between precipitation or drought indices and budworm population proxies over such a long period and large spatial scale supports a "vigor" rather than a "stress" hypothesis (Price 1991). This finding is supported by experimental results showing that, in the case of some leaf or bud feeding insects, food

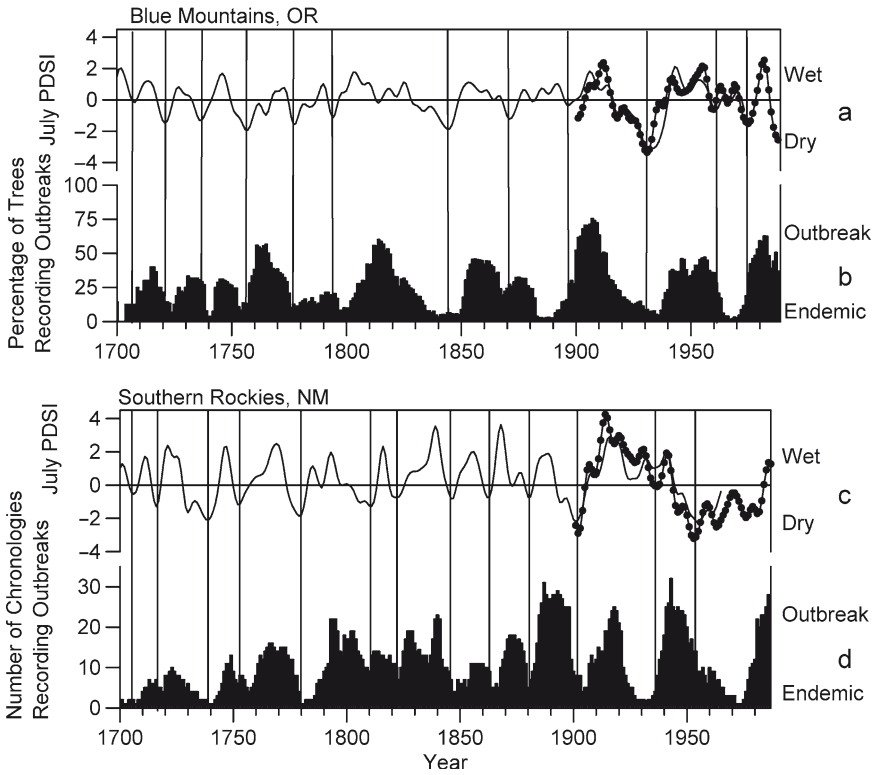

Fig. 3 Tree-ring reconstructed histories of western spruce (*Picea glauca*) budworm outbreaks in Oregon (**b**) and the Southern Rockies (**d**) compared to tree-ring reconstructed July PDSI (**a** and **c**) from the same regions. The lines with *solid circles* during the twentieth century in a and c are divisional PDSI values from Karl et al. (1983). The PDSI series are smoothed with a 13-weight low pass, gaussian filter. The *vertical lines* show approximate correspondence between drought periods and periods of endemic (low) budworm activity; the lines are centered on the lowest years of the smoothed PDSI

quality and quantity may be enhanced by increased moisture (Larsson 1989). In contrast, drought inhibits the resin production that defends a tree against cambium feeders (e.g., bark beetles) (Craighead 1925; Lorio 1986). For example, bark beetle outbreaks were associated with broadscale tree mortality during the 1986–1992 drought in the Sierra Nevada (Ferrell 1996).

Increasing drought stress and susceptibility due to increasing leaf area is touted as the leading cause of declining "forest health" in the Mountain West (e.g., Langston 1995; Rogers 1996), but clearly, there can be a variety of responses by mesoscale disturbance agents, to both wet and dry periods. Another layer of complexity is added when we consider that insect outbreaks also influence subsequent fire activity by increasing highly flammable dead leaves and woody fuels (Stocks 1987). Although these synergisms are widely noted, their temporal and spatial dynamics are virtually unexplored and unknown.

4 Regionally-Synchronized Wildfires

In most terrestrial ecosystems, fire is a keystone process that is heavily influenced by climatic variability. Seasonal to interdecadal variability in precipitation, temperature, wind, and lightning regimes determine fuel dynamics and ignition rates. The role of climate is most evident in the recurrence of regionally-synchronized wildfires during particular years. No other factor can explain the prevalence and synchroneity of such unusual fire activity.

The American Southwest has the longest and most detailed records of drought and fire history in the world. Multi-century networks of ring-width and fire-scar data allow assessment of fire-climate relations at seasonal to century scales, as well as estimation of the magnitude, extent and frequency of regional, synchronous fires. For our analyses we used 13 grid-point reconstructions of June Palmer Drought Severity Indices (PDSI) extending back to 1700. These reconstructions were derived from more than 100 ring-width chronologies (Meko et al. 1993; Cook et al. 1996) from throughout the region. Sixty-three fire-scar chronologies, specifying dates of fires during the last 400 years, have been compiled from ponderosa pine, mixed-conifer, and pine-oak woodlands in 27 mountain ranges (Fig. 4) (Swetnam and Baisan 1996). Dates were determined by obtaining cross-sections from ten or more fire-scarred trees in each stand of 10–100 ha, crossdating ring-width patterns, and determining the year of fire-scar formation of heat-caused lesions with the xylem tissue. Fire-scar dates from more than 900 trees are included in this data set.

The composite fire-scar record across the Southwest shows that regionally-synchronous fires have recurred for centuries (Fig. 5). Fire frequency within individual sites averaged about one fire per 7.5 years from 1700 to 1900. At this frequency, strictly by chance, we would expect about one coincidence of the same fire date in 21 of the 63 sites (one-third) in about a 35,000 year period. Yet, 15 different years met or exceeded this criterion in the 201 year period (Fig. 5). The probability of 41 of 63 sites recording the same fire date by chance, as in 1748, is astronomically low

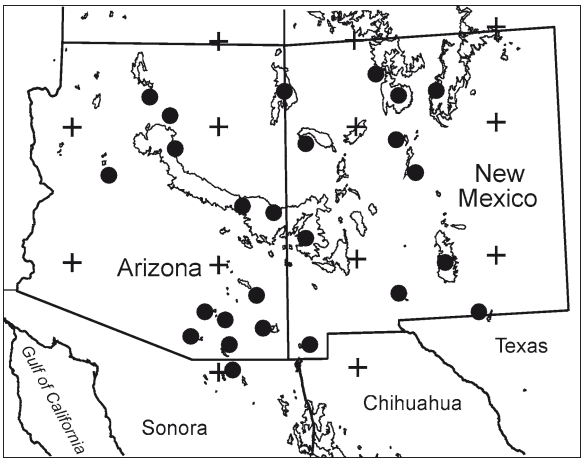

Fig. 4 The Southwestern U.S. showing fire-scar collections (*filled circles*, indicating approximate location of one or more fire-scar chronologies) and PDSI reconstruction grid points (crosses, Cook et al. 1996). The range of ponderosa pine forest type is shown by irregular outlines

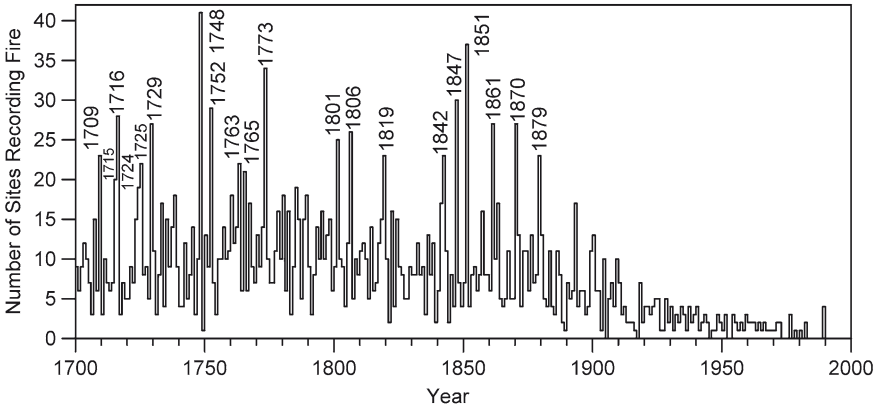

Fig. 5 Number of fire-scar sites (chronologies) in the Southwest recording fire dates in each year, 1700 to present, out of a total of 63 sites. Note the regionally-synchronous fire years (labeled), and the decrease in recorded fires after ca. 1900, reflecting livestock grazing affecting fine fuels, and subsequent fire suppression by government agencies

(one chance in billions)! As in 1910 (Fig. 6), this synchroneity of fires across such a large region must reflect regional to subcontinental-scale drought for one or more seasons. Direct comparison of the fire-scar records with independent PDSI reconstructions confirms the importance of extreme drought in synchronizing fire activity across the region (Fig. 7).

The drought-fire association also involves lags with antecedent moisture conditions. We used "super-posed epoch analysis" (SEA; Lough and Fritts 1987; Swetnam 1993)

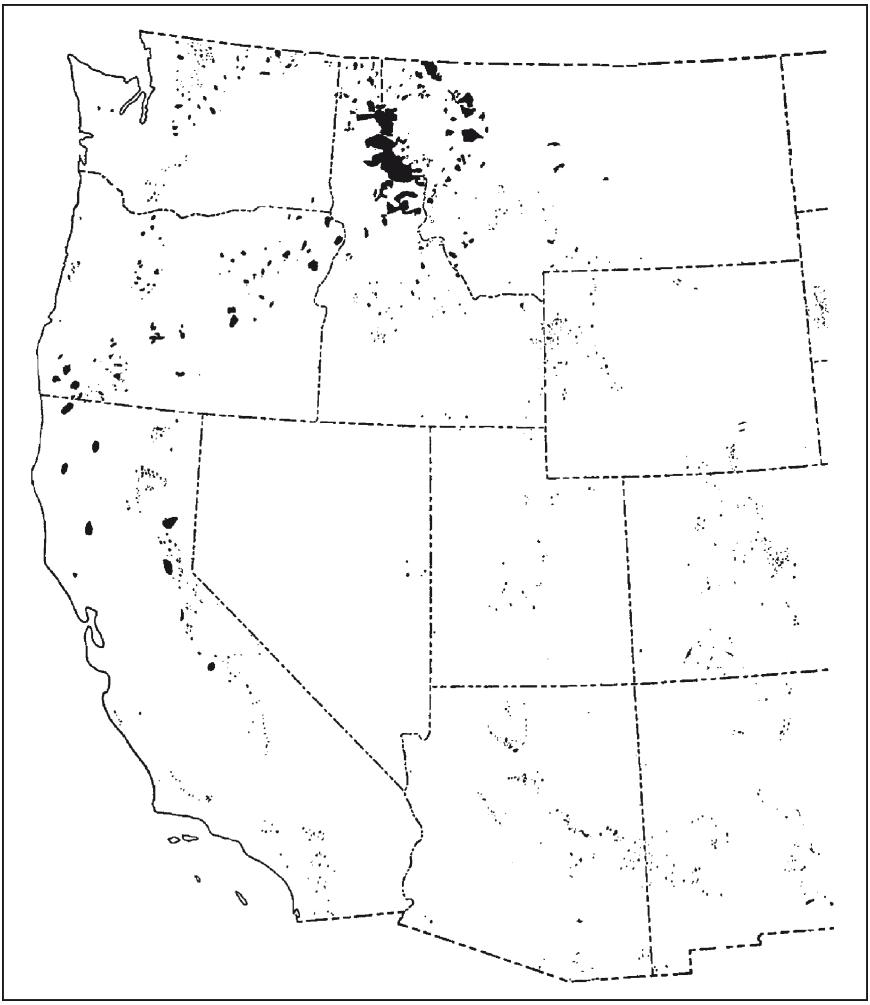

Fig. 6 Areas burned during 1910, the largest fire year of the twentieth century, on National Forest Lands in the western U.S. (Plummer 1912). Enormous fires occurred in all western States, with more than two million hectares burned on National Forest Lands. The total area burned was actually much larger, since these statistics do not include areas burned on other federal, state, and private lands. At the scale of this map the burned areas in Arizona and New Mexico appear as small specks, yet these areas totaled more than 145,000 ha

to compute the mean PDSI values during the 20 largest and 20 smallest fire years from 1700 to 1900 (derived from the composite fire-scar record; Fig. 5), and the ten largest and ten smallest events from 1920 to 1978 (derived from regional fire statistics; Swetnam and Betancourt 1990; Swetnam and Baisan 1996). The mean PDSI values also were computed for each of the 5 years (Years −1 to −5) before and 2

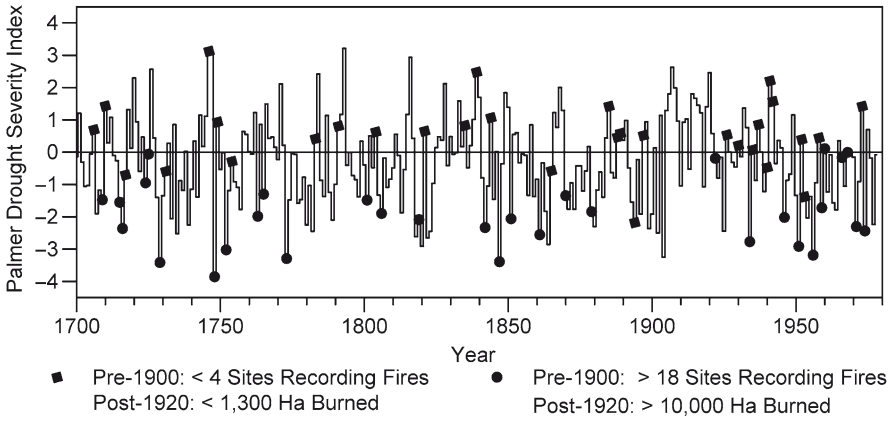

Fig. 7 Tree-ring reconstructed June–July–August Palmer drought severity indices, averaged from the 13 grid point reconstructions shown in Fig. 4. The *circles* and *squares* show the largest and smallest fire years in the regional fire-scar network (1700–1900, 20 years each) and the largest and smallest fire years in the area burned per year record from all National Forests lands in Arizona and New Mexico (1920–1978, 10 years each)

years (Year 1 and 2) after each event. A Monte Carlo simulation was used to estimate confidence intervals around the observed mean values (Mooney and Duvall 1993).

The SEA results show that extreme June drought in Year 0 is the primary factor in determining the severity of the fire year (i.e., a high percentage of sites with fire scars between 1700–1900, or large areas burned from 1920 to 1978) (Fig. 8a). Conversely, wet conditions (positive PDSI values) correspond with low fire activity. Lags are only significant in open ponderosa pine forests, where antecedent wet conditions affect fine fuel (e.g., grass) production in Years −1 to −3 prior to large fire years (Fig. 8b). This phenomenon may involve both the increased production of fine fuels during wet years prior to large fire events, and fewer fuels during dry years before small fire events (Fig. 8a). One-year lags may reflect grass production in open, ponderosa pine parklands; 2–3-year lags could indicate buildup of needle litter. Ponderosa pine needles are typically retained for 3–5 years before they are abscised and fall to the forest floor. In mixed-conifer forests, the lack of significant lags (Fig. 8b) could be explained by the deeper soils, greater persistence of snow pack into the spring, and unimportance of fine fuels in fire dynamics. Lags were also insignificant in fire statistics between 1920 and 1978 (Fig. 8a). This could reflect the many vegetation types and varying fire ecologies included in National Forests, or changing fire regimes in the twentieth century due to fire suppression, grazing, logging, and other human activities.

Changes in the strength of interannual wet-dry cycles and drought-fire relations are evident in the high frequency components of the reconstructed records (Fig. 9). The greatest amplitude of interannual switching from wet to dry occurred from 1747 to 1748, possibly indicating an extreme El Niño followed by a severe La Niña.

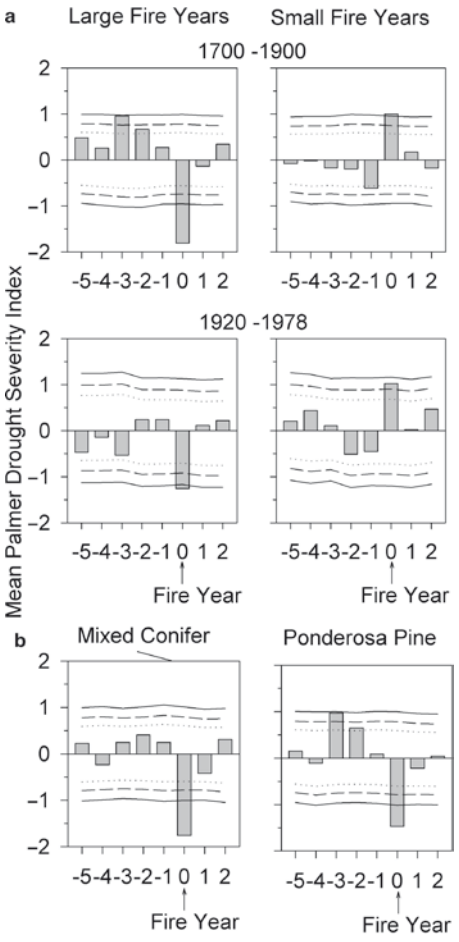

Fig. 8 Results of superposed epoch analysis showing mean June–July–August Palmer drought severity indices during the largest and smallest fire years (lag year 0), and during lagged years preceding the fire years (lag years –5 to –1), and following the fire years (lag years 1 and 2). The *horizontal solid, dashed, and dotted lines* are the 95%, 99%, and 99.9% confidence intervals, respectively, computed by Monte Carlo simulation. The *upper* two sets of plots (**a**) show the climate-fire patterns for all fire-scar sites (1700–1900) and National Forest area burned statistics (1920–1978). The large and small fire years used in this analyses are the years with *filled circles and squares*, respectively, in Fig. 7. The *lower* set of plots (**b**) show the climate-fire patterns for large fire years in mixed conifer sites compared to ponderosa pine sites (1700–1900)

The largest single regional fire year happened in 1748, with two thirds of all sampled sites (41) recording a fire during that year. Quinn and Neal's (1992) compilation from archival documents lists 1747 as a strong El Niño year. Coral records from the Galapagos show a conspicuous discontinuity at about this time (1749), suggesting dieback in warm waters (Dunbar et al. 1994). This dieback may have resulted in the loss of the 1747 and/or 1748 coral bands.

Secular variations are evident in correlations between the regional fire-scar and ring-width records. High correlations (r = 0.7 to 0.9) are obtained during the high amplitude periods of 1740–1780 and 1830–1860. Low fire-climate correlations occur in the period between 1780–1830, coincident with a decrease in amplitude of 2–4-year band-width oscillations in the regional fire-scar record (Figs. 10 and 11). This parallels similar changes in dominant oscillatory modes in Pacific coral records (Dunbar et al. 1994), tree rings, and ice cores (Stahle and Cleaveland 1993;

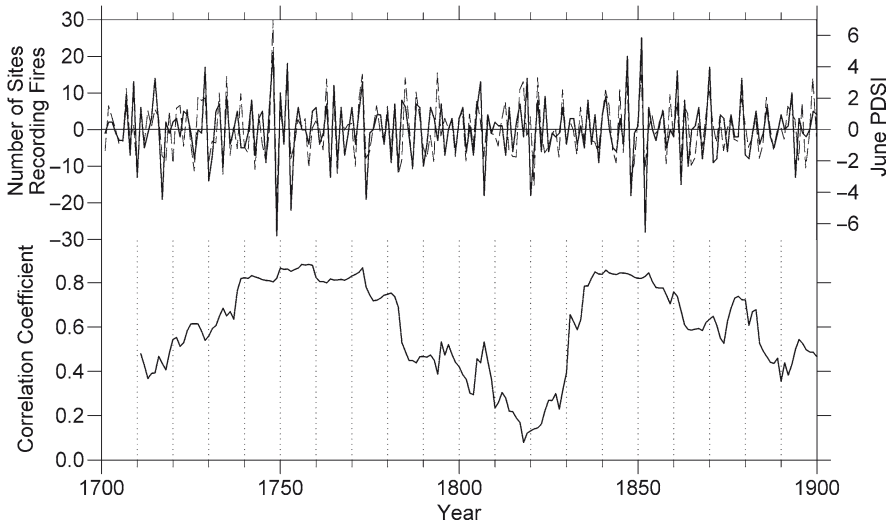

Fig. 9 Correlation of tree-ring reconstructed regional fire-scar chronology and June-July-August PDSI time series from the Southwest. The upper plot shows the first differences (year [t] − year [t−1]), which emphasize the year-to-year, high frequency changes in the two time series. Note that the PDSI is plotted inverse relative to the fire time series; negative changes in PDSI (drying condition) correspond with positive changes in fire activity (increased numbers of sites recording fire scars). The lower plot shows the 21-year moving correlation coefficients for the two time series plotted on central years

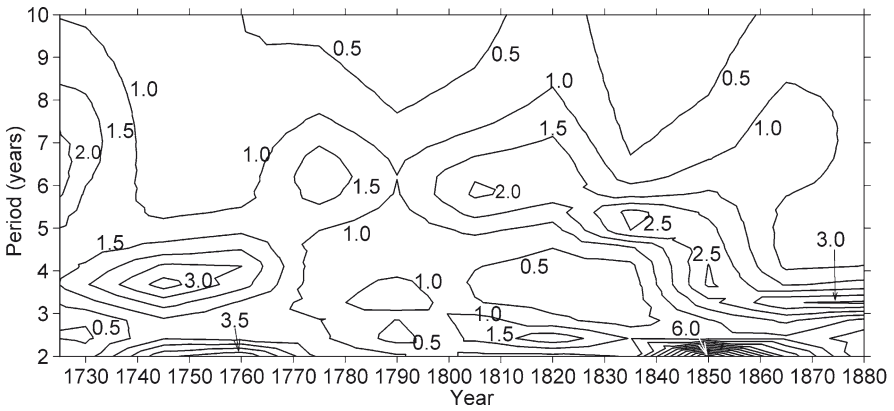

Fig. 10 Evolutionary spectrum of the Southwestern U.S. fire-scar time series, 1700–1900. Maximum entropy spectral analysis (Marple 1987) was used to compute spectra for frequency bands 0.5 to 3.3 cycles/year (2–10 year periods) for 30-year episodes overlapped by 15 years. Contours of spectral estimates in standardized units versus time are shown. Biennial oscillations (i.e., ca. 2-year period) and ca. 3–4-year oscillations dominated during the mid-century periods, but were weak during the late 1700s to early 1800s

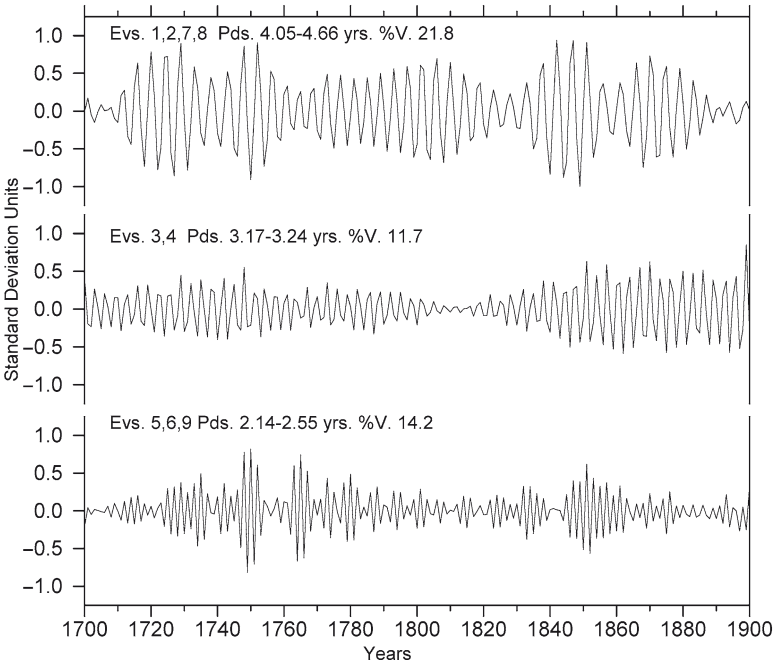

Fig. 11 Dominant waveforms of the Southwestern U.S. fire-scar time series, 1700–1900 derived from singular spectrum analysis (Vautard and Ghil 1989). These are the sums of the reconstructed components from the nine most important eigenvectors; these clustered in the three waveforms with periods varying from about 2.14 to 2.55 years (lowermost plot), 3.17 to 3.24 years (*middle plot*), and 4.05 to 4.66 (*upper plot*). A reduced amplitude period is common to all three waveforms during the early 1800s. The eigenvector numbers, range of periods, and variance explained in the original time series by the waveforms are shown on the plots

Michaelsen and Thompson 1992) and suggests that ENSO-fire teleconnections occur at both interannual and interdecadal scales. Variances of both SO and fire activity were high during 1740–1780 and 1830–1860 but low from 1780–1830. The early 1800s were notable for cool summers at high, northern latitudes (D'Arrigo and Jacoby 1992; Jacoby and D'Arrigo 1993; Luckman 1996; Shiyatov et al. 1996), and wet winters/springs in the Southwest (Meko et al. 1993; Fritts 1991). More than half of the fire-scar chronologies show lower fire frequencies during the 1780–1830 period. Although apparently less variable, the exact nature of 1780–1830 climate in the tropical Pacific or in the American Southwest is uncertain. If this was a time of average SSTs in the tropical Pacific, then wet winters in the American Southwest, normally attributed to ENSO, could be explained by persistence of a positive PNA pattern (a more sinuous and southerly-displaced polar jet stream) decoupled from ENSO.

Secular variations in fire-climate relations may be confounded by anthropogenic effects. Extreme fire years in the early twentieth century (e.g., 1910; Fig. 6) catalyzed

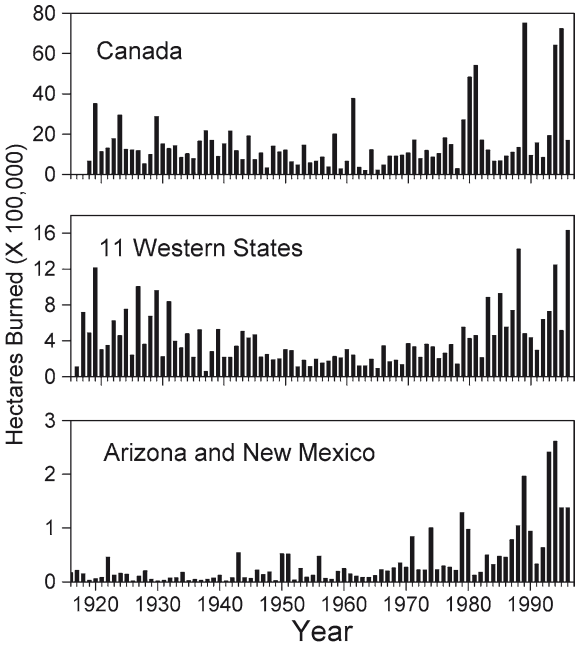

Fig. 12 Annual area burned by wildfires in Canada, the 11 American states west of the Mississippi River, and in Arizona and New Mexico. The data are from all land categories (state, private and federal), 1916–1996. Increasing area burned during the late twentieth century may be due to a combination of factors, including accumulated fuels since effective fire suppression began in the early part of the century (but probably not in Canada), and changing climatic patterns. Possible trends in the Canadian data (i.e., increased frequency of large fire years) may be an artifact of more complete data during the late twentieth century

an aggressive national program in fire suppression, which has resulted in accumulated fuels and pervasive changes in forest structure and composition. Synergism between long-term fire suppression (accumulated fuels) and a shift in climate could explain recent increases in annual area burned in Canada (Van Wagner 1988; Auclair and Carter 1993) to the southwestern U. S. (Sackett et al. 1994) (Fig. 12). In the American Southwest, for example, annual area burned is on the rise despite relatively wet winters since 1976. This rise could be due to more frequent, dry summers, to increased frequency of human ignitions, and/or to greater accumulation of both fine and coarse fuels, with wetter winters and long-term fire suppression, respectively. Greater annual area burned elsewhere in the West may be equally complex, attributed to prolonged drought, accumulated fuels with fire suppression, and higher fire frequency and extent with historic cheatgrass (*Bromus tectorum*) invasion into the expansive shrublands of the Intermountain West.

The annual cost of suppressing these increased wildfires is now approaching one billion dollars, not including losses in timber and property, as well as soil erosion and other watershed effects. The cost is significantly higher during extreme years,

hence the need to understand regionally-synchronous fires with a historical perspective on climate variability and the antecedent effects of land use on forest composition and structure. A research challenge is to determine the extent to which increasing insect outbreaks and area burned since the mid-1970s reflect long-term land-use and policy effects on forests versus decadal-scale climatic trends (Auclair and Bedford 1994).

5 Demographic Consequences of Catastrophic Drought: The 1950s Dieback

Tree mortality and autopsy traditionally have been the domain of plant pathologists and entomologists. Not surprisingly, the prevailing view is of drought as an indirect, or secondary factor that predisposes plants to disease or insect outbreaks (Mattson and Haack 1987; Waring 1987). For various reasons, disturbance ecologists have resisted the idea of physiological stress causing tree death directly. When European and North American forests began to decline during the 1980s, air pollutants were implicated, from acid rain to ozone (Hinrichsen 1987). As research progressed through the late 1980s, it became evident that climatic factors (e.g., winter freezes or desiccation) were at least partly involved in tree decline and death (Auclair 1993; Innes 1993). In general, disturbance ecologists have ignored the direct impact of catastrophic drought on mesoscale diebacks, with some notable exceptions (Jane and Green 1983; Barden 1988; Betancourt et al. 1993; Elliott and Swank 1994; Savage 1994; Villalba and Veblen 1997). Although not well understood, tree death may occur with extensive rootlet mortality, diminished water transport, and prolonged xylem cavitation during droughts.

A possible scenario for physiological dieback is as follows. In the summer after a severe winter-spring drought, reduced evaporation (soil moisture) increases the sensible heat flux, which in practice means warmer surface temperatures locally. The incident solar radiation that is normally spent towards evaporating soil moisture heats up the soil instead, and the elevated soil temperatures cause rootlet mortality across the stand (e.g., Redmond 1955). Trees with severely damaged roots translocate water poorly (Greenidge 1953) and sapwater tends to collect in the lower boles, creating a sump-like condition (Auclair 1993). As the dry, hot summer progresses, tracheids and/or vessels in the xylem become filled with air, further impeding xylem transport (Tyree and Sperry 1989), and the tree dies from prolonged cavitation, or secondarily from the additional stress of beetle attack.

In the Southwest, these conditions occur whenever the average number of degree days above some threshold temperature is exceeded by a factor of two or more in a dry year. Drought years in which this happened include 1904, 1925, 1954, 1956, and 1989. In 1989, regional diebacks occurred across southern and central Arizona in deserts (e.g., *Cercidium* ssp.), chaparral (Emory oak (*Quercus emoryi*), *Arctostaphylos* ssp.), and woodland conifers (single-leaf Pinyon (*Pinus californiarum* var. *fallax*) and *P. ponderosa*). Dieback in 1989, though conspicuous across the landscape,

was greatly exceeded by the catastrophic mortality during the multi-year drought of the 1950s.

The period 1951–1956 constitutes one of four major droughts in the U.S. during the twentieth century (1899–1904 in the southern U.S.; 1930s or Dust Bowl in the Midwest; and 1980s in the Northwest) (Namias 1955; Thomas 1962; Norwine 1978; Karl and Heim 1990). In the Southwest, it was the worst drought of the century (Fig. 13). The 1950s drought was embedded in a generally dry period between 1942 and 1956, bracketed by the strong ENSO episodes of 1940–1941 and 1956–1957.

Dry winters during the 1950s drought were a consequence of a less sinuous and more northerly polar jet stream, a weakened subtropical jet stream, and a lull in the frequency of El Niño events. Hot, dry summers were common in the late 1940s, and followed dry winters in 1951, 1953, 1954, and 1956. Namias (1955, 1988) attributed these dry summers to the anomalous development and positioning of an upper-level

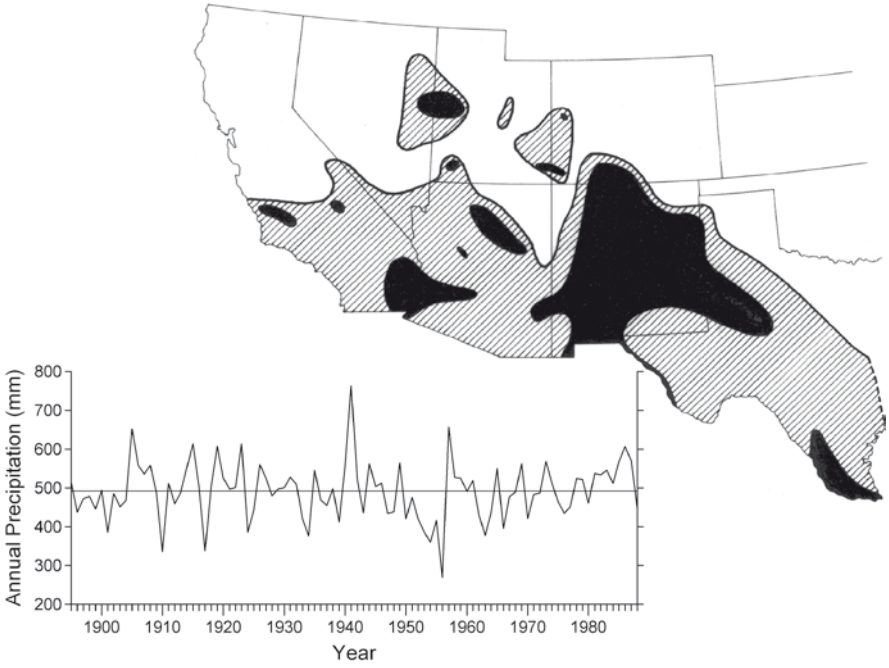

Fig. 13 The map shows areas in the Southwest where precipitation was less than 85% of the record mean as of 1941 for 8 or more years (*hatched areas*) and for 10 or more years (*black areas*) during the period 1942–1956 (after Thomas 1962). The time series is the areally-weighted annual average precipitation over the Southwest, 1895–1988. These data are the monthly climatic averages compiled by the National Climate Data Center of NOAA for each of the 50 climatic divisions in the Southwest (included in the map area, except the northern halves of the five northern states). These monthly averages were summed for each calendar year by climatic division, and then weighted by the ratio of the divisional area to the total land area in the divisions. The weighted values were then averaged to obtain annual average precipitation over the entire area. Note the depth and duration of the 1950s drought

anticyclone over the southern United States. Summers in the 1950s also were extremely warm. For example, on the Jornada Experimental Range north of Las Cruces, New Mexico, maximum daily temperature equaled or exceeded 38°C on 45 days in 1951, compared to the long-term average of 8 days a year (Herbel et al. 1972).

Dendroclimatologists have recognized the uniqueness of the mid-century drought since Schulman (1956). In the southern United States, the period 1951–1956 was the most severe, continuous drought episode since 1700 (Stahle and Cleaveland 1988; Meko et al. 1993). Millennial-long chronologies from the middle Rio Grande Basin in central New Mexico show that the 1950s drought was last exceeded during 1575–1595 (D'Arrigo and Jacoby 1991; Grissino-Mayer 1996).

In the Southwest and northern Mexico, massive vegetation dieoffs occurred from the lowland deserts well into the conifer woodlands of the uplands, testimony that the stress tolerance of most species, even drought-adapted ones, was overwhelmed by the drought. Among the species that suffered broadscale mortality were range grasses (Young 1956; Lohmiller 1963; Herbel et al. 1972; Neilson 1986), mesquite (Carter 1964), cacti (Schulman 1956; Turner 1990), and conifers (Marshall 1957; Betancourt et al. 1993).

The drought altered the composition and age structure of pinyon-juniper woodlands in central and southern New Mexico (Fig. 14). In some areas, these dieoffs contributed to shifts in ecotonal boundaries along moisture (elevational) and edaphic gradients (Marshall 1957). In addition, the 1950s drought may have played a major role in accelerating shrub invasion of grasslands (Lohmiller 1963; Herbel et al. 1972; Neilson 1986; Grover and Musick 1990).

Although modern human impacts, specifically livestock grazing and fire suppression, may have exacerbated the ecological consequences of the 1950s drought, widespread tree mortality conceivably was matched or exceeded during the sixteenth century drought. Evidence suggesting a major dieoff of conifers during this period derives from a compilation of earliest tree-ring dates from 143 sites in the Southwest (Fig. 15). These data are from tree-ring collections obtained over the past century by several generations of dendrochronologists working at the Laboratory of Tree-Ring Research in Tucson. They are composed of the oldest, most climatically sensitive trees that could be found during decades of diligent searching (Swetnam

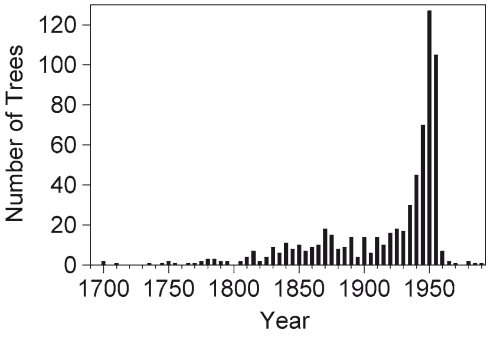

Fig. 14 Death dates of pinyon trees (*Pinus edulis*) on two plots covering approximately 28 ha in Sevilleta Long Term Ecological Research area, Los Pinos Mountain New Mexico. A total of 1,138 trees are included

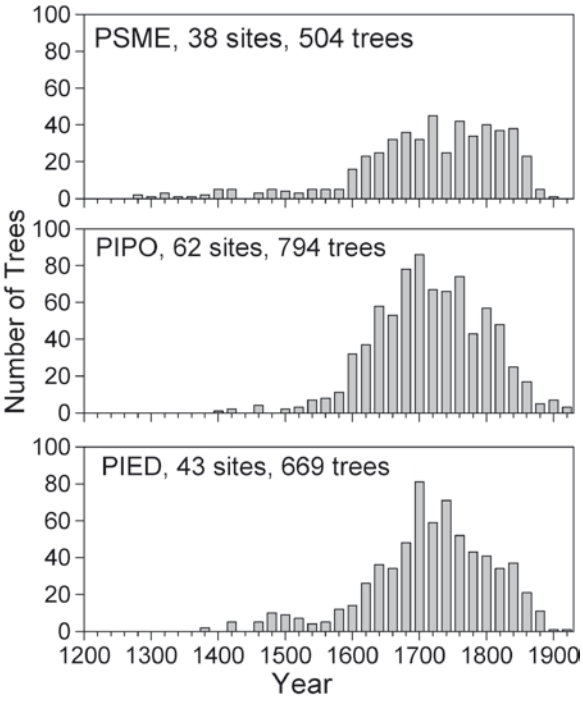

Fig. 15 Innermost ring dates of old-age conifer trees sampled for climate reconstructions in the Southwest (from data archives at the Laboratory of Tree-Ring Research). These dates are grouped in 20-year increments because the innermost rings from measured specimens did not often include the pith (or approximate establishment date of the tree), but generally were within 10–20 years of the pith. The species codes shown on the plots are: PSME = Douglas-fir (*Pseudotsuga menziesii*); PIPO = ponderosa pine (*Pinus ponderosa*); PIED = pinyon (*Pinus edulis*)

and Brown 1992). Thus, these data are an intensive sampling of the maximum-aged trees in the Southwest. Although the resolution of this age structure data set is low (plus/minus approximately 10–20 years), there is a noticeable decrease in the numbers of surviving trees that recruited into these stands before the late 1500s. Increased numbers of trees entering the data set during the early 1600s may relate to a generally cooler/wetter period that occurred during the 1600s to 1640s (D'Arrigo and Jacoby 1991; Grissino-Mayer 1996). A previous drop-off in recruitment dates occurred approximately during the late 1200s, corresponding to a drought made famous by its association (albeit controversial, see Dean 1994) with the Anasazi abandonment of settlements in the Four Corners region of the Southwest.

Clearly, the 1950s drought left a strong imprint on southwestern ecosystems, as well as regional economies (Regensberg 1996). Although the magnitude was similar to the Dust Bowl years, the drought received much less attention because the agricultural impact was buffered by irrigation from groundwater; the overall economic impact was mitigated by the influx of Eastern capital for urban growth during the 1950s.

Even so, dryland farming and ranching in the Southwest suffered losses in the billions of dollars. The 1950s drought inspired advancements in range hydrology and water conservation measures, and seemingly justified conversion of pinyon-juniper woodland to grassland to improve water yield. An appropriate sensitivity experiment of any model simulating sustainable use of water, range and forest resources would be to pit current resource demands against the backdrop of 1950s climatic conditions.

6 Ecological Consequences of the Post-1976 "Wet" Period

The importance of interdecadal variability is underscored by climatic trends since 1976, when the Southern Oscillation locked into the negative, warm (El Niño) phase (Ebbesmeyer et al. 1991). This trend culminated in the most recent El Niño (1991–1995), which was longer than the prolonged 1911–1915 and 1939–1942 events. Based on time series modeling, Trenberth and Hoar (1996) suggest that the unusual string of El Niños since 1976 and the protracted 1991–1995 event should occur only once every 1,000 years. In the Southwest, this period produced a string of wet winters and springs, but summer rainfall has been erratic. The erratic summer precipitation offsets the effect of wetter winters and springs in the areally-weighted annual averages shown in Fig. 13. However, new 1,000-year tree-ring chronologies from New Mexico and Arizona, which are primarily sensitive to cool season precipitation, show an unprecedented ramp in tree growth beginning in the mid-1970s (Fig. 16). All of the sites included in Fig. 16 are very isolated with harsh growing conditions (shallow, poor soils, rocky slopes, located on cliffs or in lava flows) where direct human-related impacts, such as logging or livestock grazing, have not occurred. This trend compares with another 1,000-year chronology from western Tasmania (Cook et al. 1991), in which increasing tree-growth since 1965 has been attributed to anomalous warming. Although CO_2 enrichment cannot be ruled out (LaMarche et al. 1984; Graybill and Idso 1993), another reason for the enhanced growth in the Southwest might be mild, wet winters and springs associated with El Niño events. Warmer winter or growing season temperatures might be indicated in these cases because most of these sites are at higher elevations (>3,000 m), where temperature tends to be more important to tree growth, than at lower elevations (Fritts 1991). Other Southwestern chronologies from lower elevations do not show the post-1976 surge in ring growth.

The expected outcome of wetter winters/springs for tree demography is accelerated recruitment and improved survivorship into the niches made available by 1950s tree mortality. However, seedling recruitment and age-specific seedling mortality are poorly understood and seldom monitored. More importantly, not enough time has elapsed since 1976 to evaluate long-term survivorship. For example, in our demography plots from the Sevilleta LTER, we dated the year of establishment for several hundred pinyon seedlings and saplings. A pulse of recruitment since approximately 1976 might be interpreted from these data (Fig. 17). However, since only surviving

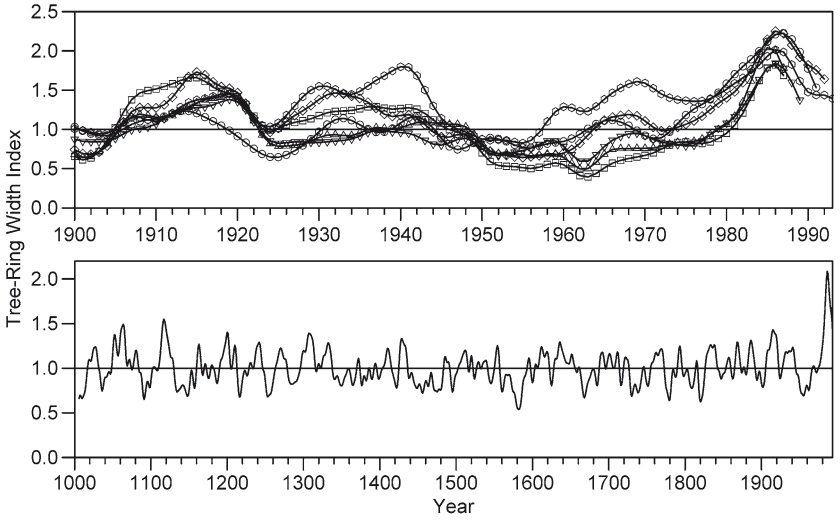

Fig. 16 Millennia-length tree-ring width index chronologies from the Southwest showing an anomalous post-1976 growth surge. The *upper plot* shows the smoothed (13-weight, low pass filter) ring-width growth in six sites in New Mexico and Arizona from a variety of species, 1900 to 1993 (*squares*: Cabresto Canyon, NM, Douglas-fir; *circles*: Mount Graham, AZ, southwestern white pine (*Pinus flexilis* var. *reflexa*); *hexagons*: Sandia Crest, NM, limber pine (*Pinus flexilis*); up triangle: Elephant Rock, NM, limber pine; *down triangle*: Italian Canyon, NM, limber pine; diamonds: El Malpais, Douglas-fir). The *lower plot* is a simple average of these six chronologies; the post-1976 growth increase is unprecedented during the past 1,000 years

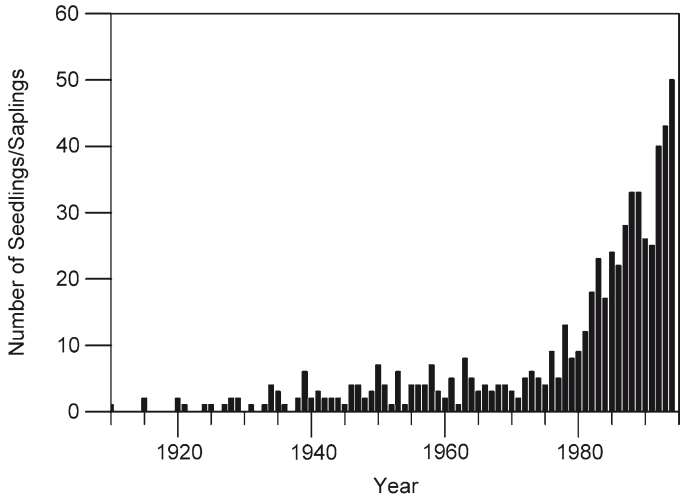

Fig. 17 Innermost ring dates (i.e., approximate germination dates) of pinyon seedlings and saplings sampled in five 0.5 ha plots in the Sevilleta Long Term Ecological Research area, Los Pinos Mountains, NM. A total of 600 seedlings and saplings were dated, 1900 to 1993. Presently, we cannot ascertain that the rise in number of seedlings after 1976 reflects normal survivorship of younger age classes, exclusion of cattle after this area was fenced, or an unusual pulse in recruitment due to wetter conditions

trees were sampled and mortality rates for seedlings are unknown, these data cannot be evaluated in a long-term perspective because similar survivorship curves are unavailable for comparison with earlier periods in the twentieth century.

The post-1976 climatic change also complicates interpretation of recent vegetation trends. For example, ongoing shrub invasions of southwestern grasslands have been attributed to drought (Herbel et al. 1972; Grover and Musick 1990; Neilson 1986), overgrazing/fire suppression (Archer et al. 1995), and even CO_2 enrichment driving C3 shrubs into C4 grasslands (Idso 1992; Mayeux et al. 1991; for opposing view see Archer et al. 1995). The debate is confounded by the fact that progressive range deterioration since 1870 has been inferred from historical data (Bahre and Shelton 1993), while long-term monitoring indicates substantial range improvement with better management and wetter conditions following the 1950s drought (Fig. 18; McCormick and Galt 1994). Such ambiguities in disentangling climatic from land use effects will continue to plague ecosystem research and management in the region.

Lastly, climate appears to be regulating the invasion of exotic plants in the Southwest. Wetter winters since 1976 have encouraged the spread of red brome (*Bromus rubens*), a winter annual, in the upper Sonoran Desert of central and southern Arizona. Consequently, fine fuels have accumulated and large fires have become chronic in desert communities that burned rarely only 20 years ago (McLaughlin and Bowers 1982). Many desert plants, such as saguaros (*Carnegiea gigantea*), grow slowly and recruit episodically; on decadal timescales, desert fires have

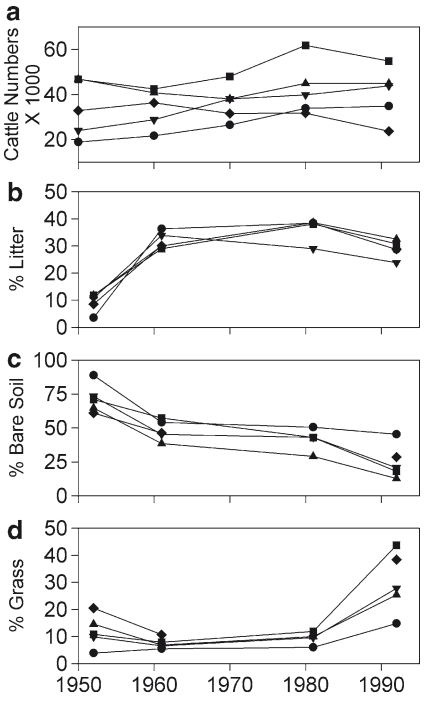

Fig. 18 Summary of (**a**) cattle numbers, (**b**) percent litter, (**c**) percent bare soil, and (**d**) percent perennial grass at 46 study sites in six southern New Mexico counties from 1952 to 1992. These sites are monitored by the Bureau of Land Management to determine range condition trends (McCormick and Galt 1994). The greatest improvement in range condition occurred during the last decade in large part due to recovery of precipitation after range deterioration during the 1950 drought

irreversible consequences. A shift to drier winters and wetter summers might slow the red brome invasion, while encouraging exotic summer annuals like African buffel grass (*Cenchrus ciliare*), which becomes flammable in the fall. It is unclear what remedies can be applied, if any. One could propose an aggressive program of fire suppression in the Sonoran Desert. This might be viewed as inconsistent by a ranching community that is increasingly accepting fire as an ecological processes capable of holding shrub invasion of grasslands at bay.

7 Conclusions

An appropriate start for studying climatic effects on ecosystems is to quantify spatial and temporal variability as a function of scale, particularly where scales of variation match (Levin 1992). Understandably, the larger spatial and temporal scales of ecosystem behavior show the greatest variations, and these should be well correlated to climate (McGowan 1990). For example, the strongest correlations between ENSO and area burned emerge from aggregation of fire occurrence data sets from all National Forest lands in Arizona and New Mexico, rather than with any particular forest (Swetnam and Betancourt 1990). The more synchronous the fires across a region, the stronger the climate signal. Likewise, climatic trends may not be reflected in the age structure of a single forest or woodland, but should be evident in a summary of tree births and deaths across a region. No matter how problematic, this regional climatic signal should be extracted before variations in ecosystem components can be attributed to other causes, be they intrinsic, in the case of competition and predation, or extrinsic, in the case of human land use.

Climatic variability can amplify or mute anthropogenic effects. Exponential increases in tropical biomass burning in the Amazon Basin coincided with both colonization and drier conditions that were associated with the decadal shift to the negative SO-phase in the 1970s. Conversely, anthropogenic effects can confound climatic relations. Both numbers of fires and area burned are on the increase in the Southwest and Pacific Northwest, even though interannual and decadal climate variability generally are in opposite phase in these two regions (Dettinger et al. 1998). This may reflect historical fire suppression and the concomitant buildup of woody fuels in both regions. Fuel loads are now far out of equilibrium with natural fire regimes, compounding the effects of the occasional drought (Auclair and Bedford 1994).

The similar trends of increased area burned in the late twentieth century in both the Northwest and Southwest, in the face of opposing climatic trends, could also be due to opposite responses of regional fire regimes to climatic variability. Persistent or frequent droughts in relatively productive Northwestern forests may be sufficient to increase fire size and severity. In contrast, large fire years in the less productive forests of the semi-arid Southwest may be stimulated by sequences of extreme wet seasons followed by average or drier than average seasons. Fine fuels, such as grasses and tree leaves, accumulate during wet spells, while subsequent dry events

favor fire ignition and spread. Even during wet decades in the Southwest, such as the post-1976 period, the arid foresummers are often sufficiently dry for some large fires to occur. When an extremely dry winter-spring event eventually follows a wet spell, such as in 1989, exceptionally large areas burn during the following summer (Fig. 12). Compilations of fire-scar records and fire statistics from the Northwest, and detailed comparisons with similar Southwestern data sets, are needed to evaluate these changing temporal and spatial patterns over the past several centuries.

Naturalists and ecologists have long noted the severe impacts of mesoscale droughts on plants and animals. Charles Darwin (1855) himself witnessed the aftermath of a great drought – "El Gran Seco" – in the Argentinean Pampas, where cattle died in the millions after grasslands failed between 1827 and 1830. Ecological study of mesoscale disturbances such as the Gran Seco, however, remains anecdotal. Part of the problem is that historical and regional phenomena are less accessible to experimentation than local processes (i.e., predation and competition) in ecological time (Ricklefs 1987; Brown 1995). With the exception of hurricanes and volcanic eruptions, ecologists have failed to take advantage of mesoscale disturbances as "natural experiments." When it happened, the 1950s drought offered the opportunity to directly study cross-scale and long-term successional processes, but until very recently the drought failed to inspire the appropriate research in the American Southwest. Similarly, prolonged drought during the 1980s caused widespread tree mortality across the Pacific Northwest (Wickman 1992), but there has been no regional effort to study this drought or future succession. The Southwest is experiencing unusually wet winters since 1976, yet no one is poised to project the ecological consequences 10–20 years from now. These missed opportunities suggest that ecologists should pay more attention to mesoscale responses of ecosystems to climatic variability, and specific climatic events, such as drought. Climatologists can play a key role in the multidisciplinary process by focusing on extreme events, and by customizing analytical approaches to match the scales of ecosystem process and variability.

One lesson from our mesoscale aggregations and comparisons of disturbance and climate times series is that ecosystem responses are more variable and complex than is often assumed. These responses are sometimes surprising, and sometimes they offer opportunities for prediction. For example, mesoscale fire activity does not simply correlate with drought; wet conditions and lagging relations between climate and fuels are also involved. These lagging relations, and improved seasonal weather forecasts based on ENSO patterns, suggest that quantitative, seasonal fire hazard forecasting tools could be constructed. Outbreaks of North America's most widespread and economically important defoliating insect – the spruce budworm – generally do not occur during droughts, but instead coincide consistently with wet periods. Tree demographic and disturbance responses to climatic variations are confounded by human impacts, but disentangling these influences is possible with comparative analyses of mesoscale data sets.

Our examples of ecological responses to climate in the Southwest underscore the importance of reconstructing, observing, and assessing ecological processes and patterns at the appropriate scales, i.e., mesoscales and centuries. Ecological synchroneity at these scales is the hallmark of climatic effects on ecosystems and

is a key to separating cultural from natural causes of environmental change. Improved understanding of changing climatic and human controls of keystone ecological processes, such as fire, will require parallel development and comparison of well-dated networks of climatic and ecological time series. In general, ecologists have a great deal to learn from the time series and spatial analytical approaches used by climatologists.

Finally, all ecosystems are historically contingent systems, whose structure and dynamics reflect continuous modification of preexisting systems (Brown 1995). Ecosystem management, then, should be predicated on understanding disturbance processes, ecosystem structures, and history in the context of past, present and future climate variability.

Acknowledgments The authors acknowledge financial and logistical support from the USDA Forest Service, Rocky Mountain Forest and Range Experiment Station (Middle Rio Grande and Borderlands Ecosystem Programs), the Pacific Northwest Forest Experiment Station, the Nature Conservancy, the Southwest Parks and Monuments Association, the U. S. Geological Survey's Global Change Program (WRD and BRD), and the Sevilleta LTER, which is funded by NSF and managed by the University of New Mexico. For field and laboratory assistance, we especially thank Rena Ann Abolt, Chris Baisan, Shelly Danzer, Paulette Ford, Mark Kaib, Ana MacKay, Henri Grissino-Mayer, Kiyomi Morino, Jim Parks, Jim Speer, and Margot Wilkinson. We also appreciate discussions with Craig Allen, Chris Baisan, Jim Gosz, Jerry Gottfried, Esteban Muldavin, Ann Lynch, Bob Parmenter, Dean Urban and Boyd Wickman.

References

Andrade ER Jr, Sellers WD (1988) El Niño and its effect on precipitation in Arizona and western New Mexico. J Climatol 8:403–410

Archer S, Schimel DS, Holland EA (1995) Mechanisms of shrubland expansion: land use, climate or CO_2? Clim Change 29:91–99

Auclair AND (1993) Extreme climatic fluctuations as a cause of forest dieback in the Pacific Rim. Water Air Soil Poll 66:207–229

Auclair ND, Bedford J (1994) Conceptual origins of catastrophic forest mortality in the western United States. J Sustain Forest 2:249–265

Auclair ND, Carter TB (1993) Forest wildfires as a recent source of CO_2 at northern latitudes. Can J Forest Res 23:1528–1536

Avery CC, Larson FR, Schubert GH (1976) Fifty-year records of virgin stand development in southwestern ponderosa pine. USDA Forest Serv General Techn Report RM-22, 71 pp

Bahre C, Shelton ML (1993) Historic vegetation change, mesquite increases and climate in southeastern Arizona. J Biogeogr 20:489–504

Balling RC Jr, Meyer GA, Wells SG (1992) Relation of surface climate and area burned in Yellowstone National Park. Agric For Meteorol 60:285–293

Barbosa P, Schultz JC (eds) (1987) Insect outbreaks. Academic Press, San Diego, CA, p 578

Barden LS (1988) Drought and survival in a self-perpetuating *Pinus pungens* population: equilibrium or nonequilibrium? Am Midl Nat 119:253–257

Barrows J (1978) Lightning Fires in Southwestern Forests. Unpublished report to USDA Forest Service, Northern Forest Fire Laboratory, under cooperative agreement 16-568 CA with Rocky Mountain Forest and Range Experiment Station, Fort Collins, CO, p 154

Betancourt JL, Pierson EA, Aasen-Rylander K, Fairchild-Parks JA, Dean JS (1993) Influence of history and climate on New Mexico pinyon-juniper woodlands. Proceedings: Managing Pinyon-Juniper ecosystems for sustainability and social needs; April 26–30, Santa Fe,

New Mexico. In: Aldon EF and DW Shaw (eds) General Technical Report RM-236, Fort Collins, CO, USDA Forest Service, Rocky Mountain Forest & Range Exp. Station, pp 42–62
Blais JR (1962) Collection and analysis of radial-growth data from trees for evidence of past spruce budworm outbreaks. Forest Chron 38:474–484
Brown JH (1995) Macroecology. University of Chicago Press, Chicago
Brown JH, Heske EJ (1990) Temporal changes in a Chihuahuan Desert rodent community. Oikos 59:290–302
Carter MG (1964) Effects of drought on mesquite. J Range Manage 17:275–276
Cayan DR, Webb RH (1992) El Niño/Southern Oscillation and streamflow in the western United States. In: Diaz HF, Markgraf V (eds) El Niño: Historical and paleoclimatic aspects of the Southern Oscillation. Cambridge University Press, Cambridge, pp 29–68
Cayan DR, Dettinger MD, Diaz HF, Graham N (1998) Decadal variability of precipitation over western North America. J Climatol 11(12):3148–3166
Clark JS (1988) Effect of climate change on fire regimes in northwestern Minnesota. Nature 334:233–235
Cook ER, Bird T, Peterson M, Barbetti M, Buckley B, D'Arrigo R, Francey R, Tans P (1991) Climatic change in Tasmania inferred from a 1089-year tree-ring chronology of Huon Pine. Science 253:1266–1268
Cook ER, Meko DM, Stahle DW, Cleaveland MK (1996) Tree-ring reconstructions of past drought across the coterminous United States: tests of a regression method and calibration/verification results. In: Dean JS, Meko DM, Swetnam TW (eds) Tree rings, environment, and humanity, 17–21, May 1994, Tucson, Arizona. Radiocarbon, pp 155–169
Craighead FC (1925) Bark-beetle epidemics and rainfall deficiency. J Econ Entomol 18:577–586
D'Arrigo RD, Jacoby GC (1991) A 1000-year record of winter precipitation from northwestern New Mexico, USA: a reconstruction from tree-rings and its relation to El Niño and the southern oscillation. Holocene 1:95–101
D'Arrigo RD, Jacoby GC (1992) Dendroclimatic evidence from Northern North America. In: Bradley RS, Jones PD (eds) Climate since A.D. 1500. Routledge, London, pp 296–311
Darwin C (1855) Journal of researches into the natural history and geology of the countries visited during the voyage of H.M.S. Beagle under the command of Capt. Fitz Roy, R.N., Vol. 2. Harper & Brothers, London, p 324
Dean JS (1994) The Medieval warm period on the Southern Colorado plateau. Clim Change 26:225–241
Dettinger MD, Cayan DR, Diaz HF, Meko DM (1998) North-south precipitation patterns in western North America on interannual-to-decadal time scales. J Climatol 11(12):3095–3111
Diaz H, Pulwarty RS (1994) An analysis of the time scales of variability in centuries-long ENSO-sensitive records in the last 100 years. Clim Change 26:317–342
Douglas AV, Engelhart P (1984) Factors leading to the heavy precipitation regimes of 1982–83 in the United States. Proceedings of the 8th Annual Climate Diagnostics Workshop, pp 42–51
Dunbar R, Wellington GM, Colgan MW, Glynn PW (1994) Eastern Pacific sea surface temperature since 1600 A.D.: the $d^{18}O$ record of climate variability in Galapagos corals. Paleoceanogr 9:291–316
Ebbesmeyer CC, Cayan DR, McLain DR, Nichols FH, Peterson DH, Redmond KT (1991) 1976 step in the Pacific climate: forty environmental changes between 1968–1975 and 1977–1984. In: Betancourt JL, Tharp VL (eds) Proceedings of the seventh annual Pacific Climate (PACLIM) Workshop, April 1990, California Department of Water Resources. Interagency Ecological Studies Program Technical Report 26, pp 115–126
Elliott KJ, Swank WT (1994) Impacts of drought on tree mortality and growth in a mixed hardwood forest. J Veg Sci 5:229–236
Ferrell GT (1996) The influence of insect pests and pathogens on Sierra Forests. In: Sierra Nevada Ecosystem Project: final report to Congress. University of California, Centers for Wildland Resources, Davis, pp 1177–1192
Flannigan MD, Van Wagner CE (1991) Climate change and wildfire in Canada. Can J For Res 21:66–72

Fritts HC (1991) Reconstructing large-scale climatic patterns from tree-ring data: a diagnostic analysis. University of Arizona Press, Tucson
Fritts HC, Swetnam TW (1989) Dendroecology: a tool for evaluating variations in past and present forest environments. Adv Ecol Res 19:111–189
Goldberg DE, Turner RM (1984) Vegetation change and plant demography in permanent plots in the Sonoran Desert. Ecology 67:695–712
Graybill DA, Idso SB (1993) Detecting the aerial fertilization effect of atmospheric CO_2 enrichment in tree-ring chronologies. Global Biogeochem Cycles 7:81–95
Greenidge KNH (1953) Further studies on birch dieback in Nova Scotia. Can J Bot 31:548–559
Grissino-Mayer HD (1996) A 2,129-year reconstruction of precipitation for northwestern New Mexico, USA. In: Dean JS, Meko DM, Swetnam TW (eds) Tree rings, environment, and humanity, 17–21, May 1994, Tucson, AZ, Radiocarbon, pp 191–204
Grover HD, Musick B (1990) Shrubland encroachment in southern New Mexico, U.S.A.: an analysis of desertification processes in the American Southwest. Climat Change 17:305–330
Hadley KS, Veblen TT (1993) Stand response to western spruce budworm and Douglas-fir bark beetle outbreaks, Colorado Front Range. Can J For Res 23:479–491
Halpert MS, Ropelewski CF (1992) Surface temperature patterns associated with the Southern Oscillation. J Climatol 5:577–593
Harrington JA Jr, Cerveny RS, Balling RC (1992) Impact of the Southern Oscillation on the North American southwest monsoon. Phys Geogr 13:318–330
Herbel CH, Ares FN, Wright RG (1972) Drought effects on a semidesert grassland range. Ecology 53:1084–1093
Hinrichsen D (1987) The forest decline enigma: what underlies extensive dieback on two continents? Bioscience 37:542–546
Huston MA (1994) Biological diversity: the coexistence of species on changing landscapes. Cambridge University Press, Cambridge, p 681
Idso SB (1992) Shrubland expansion in the American Southwest. Climate Change 22:85–86
Innes JL (1993) Forest health: its assessment and status. CAB International, Wallingford, Oxon
Jacoby GC, D'Arrigo R (1993) Secular trends in high northern latitude temperature reconstructions from tree rings. Clim Change 15:163–177
Jane GT, Green TGA (1983) Vegetation mortality in the Kaimai Ranges, North Island, NZ. Pac Sci 37:385–389
Johnson EA, Wowchuck DR (1993) Wildfires in the southern Canadian Rocky Mountains and their relationship to mid-tropospheric anomalies. Can J For Res 23:1213–1222
Kahya E, Dracup JA (1994) The influences of Type 1 El Niño and La Niña events on streamflows in the Pacific Southwest of the United States. J Climatol 7:965–976
Karl TR, Heim RR Jr (1990) Are droughts becoming more frequent or severe in the United States. Geophys Res Lett 17:1921–1924
Karl TR, Metcalf LK, Nicodemus ML, Quayle RG (1983) Statewide average climate history. National Climate Data Center, Asheville
Knapp PA (1995) Intermountain west lightning-caused fires: climatic predictors of area burned. J Range Manage 48:85–91
LaMarche VC, Graybill DA, Fritts HC, Rose MR (1984) Increasing atmospheric carbon dioxide: tree-ring evidence for growth enhancement in natural vegetation. Science 225:1019–1021
Langston N (1995) Forest dreams, forest nightmares: the paradox of old growth in the Inland West. University of Washington Press, Seattle
Larsen CPS, MacDonald GM (1995) Relations between tree-ring widths, climate, and annual area burned in the boreal forest of Alberta. Can J For Res 25:1746–1755
Larsson S (1989) Stressful times for the plant stress-insect performance hypothesis. Oikos 56:277–283
Latif M, Barnett TP (1994) Causes of decadal climate variability over the North Pacific and North America. Science 266:634–637
Levin SA (1992) The problem of pattern and scale in ecology: the Robert H. MacArthur Award lecture. Ecology 73:1943–1967

Lohmiller RG (1963) Drought and its effect on condition and production of a desert grassland range. M.Sc. thesis, New Mexico State University, Las Cruces, p 57
Lorio PL Jr (1986) Growth-differentiation balance: a basis for understanding southern pine beetle-tree interactions. Forest Ecol Manage 14:259–273
Lough JM, Fritts HC (1985) The southern oscillation and tree rings: 1600-1961. J Appl Meteorol 24:952–966
Lough JM, Fritts HC (1987) An assessment of the possible effects of volcanic eruptions on North American climate using tree-ring data, 1602 to 1900 A.D. Clim Change 10:219–239
Luckman BH (1996) Dendrochronology and global change. In: Dean JS, Meko DM, Swetnam TW (eds) Tree rings, environment and humanity, Radiocarbon, pp 3–24
Mann ME, Park J, Bradley RS (1995) Global interdecadal and century-scale climate oscillations during the past five centuries. Nature 378:266–270
Marple SL Jr (1987) Digital spectral analysis with applications. Prentice Hall, Englewood Cliffs
Marshall JT Jr (1957) Birds of pine-oak woodland in southern Arizona and adjacent Mexico. Cooper Ornithological Society, Pacific Coast Avifauna 32
Martin SC (1986) Eighty years of vegetation change on a semidesert range in southern Arizona, U.S.A. and evaluation of causes. In: Ross PJ, Lynch PW, Williams OB (eds) Rangelands: a resource under siege, Proceedings of Second International Rangeland Congress, Canberra, Australia, Sydney, Australia. Cambridge University Press, Cambridge
Martinat PJ (1987) The role of climatic variation and weather in forest insect outbreaks. In: Barbosa P, Schultz JC (eds) Insect outbreaks. Academic Press, New York, pp 241–268
Mattson WJ, Haack RA (1987) The role of drought in outbreaks of plant-eating insects. Bioscience 37:110–118
Mayeux HS, Johnson HB, Polley HW (1991) Global change and vegetation dynamics. In: James LF, Evans JO, Child RD (eds) Noxious range weeds. Westview Press, Boulder, CO, pp 62–64
McCormick JC, Galt HD (1994) Forty years of vegetation trend in southwestern New Mexico. Proceedings of the Hot Desert Symposium, July 1994, Phoenix, AZ. Society for Range Management, pp 184–203
McGowan JA (1990) Climate and change in oceanic systems: the value of time series data. Trends Ecol Evol 5:293–299
McLaughlin SP, Bowers JE (1982) Effects of wildfire on a Sonoran Desert plant community. Ecology 63:246–248
Meko DM, Cook ER, Stahle DW, Stockton CW, Hughes MK (1993) Spatial patterns of tree-growth anomalies in the United States and southeastern Canada. J Climatol 6:1773–1786
Meko DM, Stockton CW, Boggess WR (1995) The tree-ring record of severe sustained drought. J Am Water Resour Assoc 31:789–801
Michaelsen J, Thompson LG (1992) A comparison of proxy records of El Niño/Southern Oscillation. In: Diaz HF, Markgraf V (eds) El Niño: historical and paleoclimatic aspects of the Southern Oscillation. Cambridge University Press, Cambridge, pp 323–348
Miller AJ, Cayan DR, Barnett TP, Graham NE, Oberhuber J (1994) Interdecadal variability of the Pacific Ocean: model response to observed heat flux and wind stress anomalies. Clim Dyn 9:287–302
Mooney CZ, Duvall RD (1993) Bootstrapping: a nonparametric approach to statistical inference. Series: Quantitative Applications in the Social Sciences, Number 07-095, Sage, London
Mopper S, Whitham TG (1992) The plant stress paradox: effects on pinyon sawfly sex ratios and fecundity. Ecology 73:515–525
Namias J (1955) Some meteorological aspects of drought, with special reference to the summers of 1952-54 over the United States. Mon Weather Rev 83:199–205
Namias J (1988) The 1988 summer drought over the Gret Plains- a classic example of air-sea-land interaction. Trans Am Geophysical Union 69:1067
Namias J, Yuan X, Cayan DR (1988) Persistence of north Pacific sea surface temperature and atmospheric flow patterns. J Climatol 1:682–703
Neilson RP (1986) High-resolution climatic analysis and southwest biogeography. Science 232:27–34

Norwine J (1978) Twentieth-century semi-arid climates and climatic fluctuations in Texas and northeastern Mexico. J Arid Environ 1:313–325
Overpeck JT, Rind D, Goldberg R (1990) Climate induced changes in forest disturbance and vegetation. Nature 343:51–53
Pake CE, Venable DL (1995) Is coexistence of Sonoran desert annuals mediated by temporal variability in reproductive success? Ecology 76:246–261
Pearson GA (1950) Management of ponderosa pine in the Southwest. USDA Forest Service, Agriculture Monograph 6
Plummer FG (1912) Forest fires: their causes, extent and effects, with a summary of recorded destruction and loss. USDA Forest Serv Bull 117
Price PW (1991) The plant vigor hypothesis and herbivore attack. Oikos 62:244–251
Price C, Rind D (1994) The impact of a 2 X CO_2 climate on lightning-caused fires. J Climatol 7:1484–1494
Quinn WH, Neal VT (1992) The historical record of El Niño events. In: Bradley RS, Jones PD (eds) Climate since 1500. Routledge, Chapman & Hall, London, pp 623–648
Rasmusson EM, Wang X, Ropelewski CF (1990) The biennial component of ENSO variability. J Mar Syst 1:71–96
Redmond DR (1955) Rootlets, mycorrhiza, and soil temperatures in relation to birch dieback. Can J Bot 33:595–672
Regensberg A (1996) General dynamics of drought, ranching, and politics in New Mexico, 1953–1961. N M Historical Rev 71(1):25–49
Ricklefs RE (1987) Community diversity: relative roles of local and regional processes. Science 235:167–171
Rogers P (1996) Disturbance ecology and forest management: a review of the literature. USDA Forest Service, Intermountain Forest and Range Experiment Station, General Technical Report INT-GTR-336
Romme WH (1982) Fire and landscape diversity in subalpine forests of Yellowstone National Park. Ecol Monogr 52:199–221
Rothermel RC (1983) How to predict the spread and intensity of forest and range fires. USDA Forest Service, Intermountain Forest and Range Experiment Station, General Technical Report INT-143
Sackett S, Haase S, Harington MG (1994) Restoration of Southwestern ponderosa pine ecosystems with fire. In: Covington WW, DeBano LF (technical coordinators) Proceedings: Sustainable ecological systems: implementing an ecological approach to land management, July 12–15, 1993, Flagstaff, Arizona. USDA Forest Service, Rocky Mountain Forest and Range Experiment Station, General Technical Report RM-247:115–121
Sanders CJ, Stark RW, Mullins EJ, Murphy J (eds) (1985) Recent advances in spruce budworms research. Proceedings of the CANUSA spruce budworms research symposium, Bangor Maine, 16–20 September 1984. Canadian Forestry Service, p 527
Savage M (1994) Anthropogenic and natural disturbance and patterns of mortality in a mixed conifer forest in California. Can J For Res 24:1149–1159
Savage M, Brown PM, Feddema J (1996) The role of climate in a pine forest regeneration pulse in the southwestern United States. Ecoscience 3:310–318
Schulman E (1956) Dendroclimatic changes in semi-arid America. University of Arizona Press, Tucson
Shiyatov SG, Mazepa VS, Vaganov EA, Schweingruber FH (1996) Summer temperature variations reconstructed by tree-ring data at the polar timberline in Siberia. In: Dean JS, Meko DM, Swetnam TW (eds) Tree rings, environment and humanity. Radiocarbon, pp 61–70
Simard AJ, Haines DA, Main WA (1985) Relations between El Niño/Southern Oscillation anomalies and wildland fire activity in the United States. Agric For Meteorol 36:93–104
Slowey NC, Crowley TJ (1994) Interdecadal variability of Northern Hemisphere circulation recorded by Gulf of Mexico corals. Geophys Res Lett 22:2345–2348
Sousa WP (1984) The role of natural disturbance in natural communities. Annu Rev Ecol Syst 15:353–391

Sprugel DG (1991) Disturbance, equilibrium and environmental variability: what is "natural vegetation" in a changing environment? Biol Conserv 58:1–18
Stahle DW, Cleaveland MK (1988) Texas drought history reconstructed and analyzed from 1698 to 1980. J Climatol 1:59–74
Stahle DW, Cleaveland MK (1993) Southern oscillation extremes reconstructed from tree rings of the Sierra Madre Occidental and Southern Great Plains. J Climatol 6:129–140
Stahle DW, Cleaveland MK, Cook ER (1993) Secular variability of the ENSO teleconnection to northern Mexico and the southern Great Plains reconstructed with tree-ring data since A.D. 1699. Proceedings of the Seventeenth Annual Climate Diagnostics Workshop, NOAA, Norman Oklahoma
Stocker TF, Mysak LA (1992) Climatic fluctuations on the century time scale: a review of high resolution proxy data and possible mechanisms. Clim Change 20:227–250
Stocks BJ (1987) Fire potential in the spruce budworm-damaged forests of Ontario. Forest Chron 63:8–14
Swetnam TW (1993) Fire history and climate change in giant sequoia groves. Science 262:885–889
Swetnam TW, Baisan CH (1996) Historical fire regime patterns in the Southwestern United States since AD 1700. In: Allen CD (technical editor) Fire effects in Southwestern forests, Proceedings of the Second La Mesa Fire Symposium, Los Alamos, New Mexico, March 29–31, 1994. USDA Forest Service, Rocky Mountain Forest and Range Experiment Station, General Technical Report RM-GTR-286, pp 11–32
Swetnam TW, Betancourt JL (1990) Fire-Southern Oscillation relations in the southwestern United States. Science 24:1017–1020
Swetnam TW, Brown PM (1992) Oldest known conifers in the southwestern United States: temporal and spatial patterns of maximum age. In: Moir W, Kaufmann MR (eds) Proceedings of the workshop on old-growth forests in the rocky mountains and Southwest: the status of our knowledge, Portal, AZ, March 9–13, 1992. USDA Forest Service, Rocky Mountain Forest and Range Experiment Station, General Technical Report RM-GTR-213, pp 24–38
Swetnam TW, Lynch A (1993) Multi-century, regional-scale patterns of western spruce budworm history. Ecol Monogr 63:399–424
Swetnam TW, Wickman BE, Paul GH, Baisan CH (1995) Historical patterns of western spruce budworm and Douglas-fir tussock moth outbreaks in the Northern Blue Mountains, Oregon since A.D. 1700. USDA Forest Service, Pacific Northwest Forest Experiment Station, Research Paper PNW-RP-484
Thomas HE (1962) The meteorological phenomenon of drought in the Southwest: drought in the Southwest, 1942–1956. US Geol Surv Prof Paper 342A
Trenberth KE, Hoar TJ (1996) The 1990–1995 El Niño-Southern Oscillation event: longest on record. Geophys Res Lett 23:57–60
Trenberth KE, Hurrell JW (1994) Decadal atmosphere-ocean variations in the Pacific. Clim Dyn 9:303–319
Turner RM (1990) Long-term vegetation change at a fully protected Sonoran desert site. Ecology 71:464–477
Turner MG, Romme WH, Gardner RH, O'Neill RV, Kratz TK (1993) A revised concept of landscape equilibrium: disturbance and stability on scaled landscapes. Landscape Ecol 8:213–227
Tyree MT, Sperry JS (1989) Vulnerability of xylem to cavitation and embolism. Ann Rev Plant Biol 40:19–38
Van Wagner CE (1988) The historical pattern of annual burned area in Canada. Forest Chron June 1988:182–185
Vautard R, Ghil M (1989) Singular spectrum analysis in nonlinear dynamics, with applications to paleoclimatic time series. Physica D 35:395–424
Villalba R, Veblen TT (1997) Regional patterns of tree population age structures in northern Patagonia: climatic and disturbance influences. J Ecol 85:113–124
Waring RH (1987) Characteristics of trees predisposed to die. Bioscience 37:569–574

Webb RH, Betancourt JL (1992) Climatic variability and flood frequency of the Santa Cruz river, Pima County, Arizona. US Geol Surv Water-Supply Paper 2379

Weber U, Schweingruber FH (1995) A dendroecological reconstruction of western spruce budworm outbreaks (Choristoneura occidentalis) in the Front Range, Colorado, from 1720 to 1986. Trees 9:204–213

White TCR (1976) Weather, food, and plagues of locusts. Oecologia 22:119–134

White AS (1985) Presettlement regeneration patterns in a southwestern ponderosa pine stand. Ecology 66:589–594

White PS, Pickett STA (1985) Natural disturbance and patch dynamics: an introduction. In: Pickett STA, White PS (eds) The ecology of natural disturbance and patch dynamics. Academic Press, New York, pp 3–13

Wickman BE (1992) Forest health in the Blue Mountains: the influence of insects and diseases. USDA Forest Service, Pacific Northwest Research Station General Technical Report PNW-GTR-310

Xu J (1993) The joint modes of the coupled atmosphere-ocean system observed from 1967 to 1987. J Climatol 6:816–838

Young VA (1956) The effects of the 1949–1954 drought on the ranges of Texas. J Range Manage 9:139–142

Wildfire Risk and Ecological Restoration in Mixed-Severity Fire Regimes

Peter M. Brown

Wildfire risk to ecosystems and human communities varies considerably depending on the severity of fire behavior that occurs during burning. Fire severity, in turn, is dependent on fuel amount, arrangement, and horizontal and vertical continuity, which – in forests – is often broken into broad categories of surface and canopy fuels. Fire scars – areas of cambial mortality caused by low-severity surface burning – recorded in cross-dated tree-ring sequences have proven extremely useful for documenting that frequent surface fires occurred in many mid-elevation forests in western North America, especially those dominated by ponderosa pine (*Pinus ponderosa*). These fires burned mainly in surface fuels and rarely killed mature trees because of their thick bark and high crowns. Fire cessation in these forests began in the middle to late nineteenth century because of Euro-American settlement, initially as a result of widespread livestock grazing that removed surface fuel biomass and followed later in the twentieth century by active fire suppression by land management agencies. Fire exclusion has resulted in unchecked tree establishment, increased stand densities, a lowering of stand-level canopy base heights, increased numbers of small trees, deeper layers of needle litter, and an overall increase in crown fire potential in current forests. Conversely, canopy fuels have always dominated in upper-elevation subalpine forests, where fires are generally less frequent but much higher severity during which large areas of forest are killed.

Understanding such spatio-temporal variations in fire behavior is important for predicting where fuel management or ecological restoration will be most effective in reducing fire risk. As a general rule, ecological restoration is best suited for ecosystems that experienced surface fires, where modification of fuels or forest structure can play a significant role in reducing both the likelihood of crown fire

P.M. Brown (✉)
Rocky Mountain Tree-Ring Research, Ft Collins, CO 80526, USA
e-mail: pmb@rmtrr.org

M. Stoffel et al. (eds.), *Tree Rings and Natural Hazards: A State-of-the-Art*,
Advances in Global Change Research 41, DOI 10.1007/978-90-481-8736-2_33,

and the potential economic and ecological damage caused by a catastrophic wildfire. However, a question arises in ecosystems that experienced what is often called mixed- or variable-severity fire behavior, in which crown and surface fires occurred during individual fires or during different fires at the same location (e.g. Baker et al. 2007). It is not as clear in these forests that fuel modification or ecological restoration either is warranted or will be potentially effective in reducing the risk of a catastrophic wildfire.

Tree-ring data from ponderosa pine forests of the Front Range of the Rocky Mountains in Colorado and the Black Hills in southwestern South Dakota document that mixed-severity fires were present in some areas prior to Euro-American settlement (Brown et al. 1999; Brown 2006; Sherriff and Veblen 2007). The presence of denser stands and crown fires historically has led some to conclude that large-scale forest thinning or reintroduction of surface fires as means for ecological restoration is not appropriate across many of these forests (Veblen 2003; Baker et al. 2007). However, a major question that must be asked about this conclusion is how often crown fires occurred and how big an area they covered relative to surface fire in the historical forests. For example, a recent dendroecological study at Mount Rushmore National Memorial in the Black Hills – home of the world-famous Mount Rushmore sculpture – used dates and locations of fire scars and tree recruitment to estimate that crown fires burned only about 3.3% of the total area burned between 1529 and 1893 (Brown et al. 2008). The rest of the area burned as surface fire. Other fire history studies have shown that typical sizes of crown fire patches in the past were likely on the order of hectares to tens of hectares at most (Brown et al. 1999; Brown 2006). This strongly contrasts with recent mixed-severity fires, in which areas of crown mortality were orders of magnitude larger, including an area of almost 25,000 ha of almost complete overstory mortality that occurred during the 2002 Hayman Fire in central Colorado (Graham 2003). The scale of crown mortality that occurred not only in the Hayman Fire but also during other recent fires in the Front Range and Black Hills appears to be completely unprecedented relative to all available historical reconstructions, suggesting that forest stand and landscape structures are well outside of their historical ranges of variability. These larger areas of crown fire appear to be a direct result of fire cessation that has led to more contiguous, denser stands across landscapes. Thus, simply to conclude that past fire behavior was mixed- or variable-severity does little either to characterize fire as an ecological process or to provide direction for fuel management or ecological restoration efforts in these forests.

One approach to the question of how mixed-severity fire regimes may have changed from historical to current forests is to focus on the underlying dynamics of fire as a disturbance process and how individual species respond to spatiotemporal variations in fire behavior. Falk (2006) has suggested restoration efforts should focus on the ecological processes that sustain and characterize ecosystem function rather than concentrating solely on local ecosystem patterns produced by those processes. Viewed from a process-centered perspective, the local fire history may be seen as only one realization of multiple stochastic and deterministic processes that affected a particular configuration we see or reconstruct today (*sensu* Lertzman et al. 1998).

The true focus for restoration ecology and fuel and forest management in general should be to characterize underlying ecosystem dynamics that affected both the specific realization that we are able to reconstruct as well as the range of variation possible within a particular ecosystem type.

A process-centered restoration approach defines and uses historical dynamics in both biotic and ecosystem processes as central foci for restoration design and implementation (Falk 2006). In ponderosa pine forests throughout their range, the central ecological theme is that of episodic, frequent, surface fires. Although some ponderosa pine forests, such as those of the Front Range and Black Hills, apparently experienced areas of crown fires of varying sizes in the past, the relative scale of crown to surface burning is often based on questionable evidence, difficult to quantify even when adequate evidence is available, and, perhaps more critically, difficult to address in restoration programs. Furthermore, crown and mixed-severity fires will undoubtedly continue to occur in future wildfires. Funding and management policies for landscape-scale restoration programs are currently not in place, and large areas of dense stands of trees that are highly susceptible to crown fires will undoubtedly continue to persist in most ponderosa pine landscapes well into the future. Yet what is currently missing from virtually all ponderosa pine forests throughout its range in western North America are surface fires, especially those that are allowed to burn across large areas. We know with great certainty from tree-ring evidence that such fires occurred with regularity in the past. Restoration of surface fires and forest structure will not only restore longer-term function and resilience to ponderosa pine ecosystems throughout their range, but also substantially reduce the risk and adverse effects of future wildfires on human communities and natural resources across the region.

References

Baker WL, Veblen TT, Sherriff RL (2007) Fire, fuels, and restoration of ponderosa pine-Douglas-fir forests in the Rocky Mountains, USA. J Biogeogr 34:251–269

Brown PM (2006) Climate effects on fire regimes and tree recruitment in Black Hills ponderosa pine forests. Ecology 87:2500–2510

Brown PM, Kaufmann MR, Shepperd WD (1999) Long-term, landscape patterns of past fire events in a montane ponderosa pine forest of central Colorado. Landscape Ecol 14:513–532

Brown PM, Wienk CL, Symstad AJ (2008) Fire and forest history at Mount Rushmore. Ecol Appl 18:1984–1999

Falk DA (2006) Process-centered restoration in a fire-adapted ponderosa pine forest. J Nature Conserv 14:140–151

Graham RT (technical editor) (2003) Hayman Fire Case Study. USDA Forest Service General Technical Report RMRS-GTR-114. USDA Forest Serv, Fort Collins, CO

Lertzman K, Fall J, Dorner B (1998) Three kinds of heterogeneity in fire regimes: at the crossroads of fire history and landscape ecology. Northwest Sci 72:4–22

Sherriff RL, Veblen TT (2007) A spatially explicit reconstruction of historical fire occurrence in the ponderosa pine zone of the Colorado Front Range. Ecosystems 9:1342–1347

Veblen TT (2003) Key issues in fire regime research for fuels management and ecological restoration. In: Fire, Fuel Treatments and Ecological Restoration: Conference Proceedings; 2002 16–18 April; Fort Collins, CO: U.S, pp 259–276. Department of Agriculture, Forest Service, Rocky Mountain Research Station

Wildfire Ecology and Management at Grand Canyon, USA: Tree-Ring Applications in Forest Fire History and Modeling

Peter Z. Fulé

1 Introduction

Wildland fire has been a key selective force through evolutionary time, influencing the development of characteristic adaptations of forest trees ranging from the serotinous cones of lodgepole pine (*Pinus contorta*) to the vigorous sprouting of Canary Island pine (*Pinus canariensis*) (Keeley and Zedler 1998). In the semi-arid southwestern United States, forest fires play complex ecological and social roles. Ecologically, the southwestern U.S. encompass forests adapted to severe, stand-replacing fires, those adapted to frequent surface fires, and forests with a mixture of fire intensities. Overlaid on this natural mosaic, however, modern industrial society has consistently sought to suppress fire (Pyne 1982). An unintended consequence of fire exclusion, however, is the accumulation of fuel horizontally across contiguous tree canopies and vertically through the crowns of small understory trees. Coupled with warming climate, more droughts, less snow, and longer fire seasons, there is little doubt that severe fires will increase (Westerling et al. 2006). For forest ecosystems not adapted to severe burning and already stressed by non-native species, human impacts, and climate change, the likelihood of substantial irreversible degradation appears high (Savage and Mast 2005; Strom and Fulé 2007). Early proponents of taking an ecological approach to fire, such as Leopold (1924) and Weaver (1951), were lonely voices in their time. Today, however, the attention of scientists and forest managers is focused on the restoring of the naturally fire-resilient characteristics of native ecosystems (Falk 2006). In order to have a chance to accomplish this goal, it is vital that we have the best possible

P.Z. Fulé (✉)
Ecological Restoration Institute and School of Forestry, Northern Arizona University, Flagstaff, AZ 86011, USA
e-mail: Pete.Fule@nau.edu

M. Stoffel et al. (eds.), *Tree Rings and Natural Hazards: A State-of-the-Art*, Advances in Global Change Research 41, DOI 10.1007/978-90-481-8736-2_34,

understanding of historical forest characteristics: fire regimes, forest structure, species composition, and dynamics.

Tree-ring analysis is a powerful technique for developing reliable knowledge about forest history and change. The theme of this chapter is the use of tree rings for the following goals: (1) determine historical fire regimes across the elevational gradient of forest ecosystems; (2) measure changes in forest structure, composition, fuels, and simulated fire behavior; and (3) apply these data for testing management alternatives for ecological restoration and conservation.

2 Study Region

Grand Canyon National Park, in northern Arizona, USA, is a world heritage site preserving the deep canyon of the Colorado River and the surrounding ecosystems, including high-elevation coniferous forests on canyon rims. The Park is famous for its stunning rock formations but the high forests should be recognized for their own merits: Grand Canyon preserves the largest never-harvested forest in Arizona, covering an elevational gradient from woodlands to subalpine forests. In the canyon, the Colorado River runs below high escarpments which reach approximately 2,800 m in elevation on the Kaibab Plateau (North Rim) and 2,300 m on the Coconino Plateau (South Rim). Soils are derived from limestone substrates (Warren et al. 1982). Weather data are from the Western Regional Climate Center (www.wrcc.dri.edu), Bright Angel station, elevation 2,560 m, North Rim and cover the period 1925–2008. Average temperature was –2.7°C in January and 16.8°C in July; annual precipitation averaged 645 mm. Forest types include ponderosa pine (*Pinus ponderosa*), often with a substantial component of Gambel oak (*Quercus gambellii*), at elevations around 2,200 m. At higher elevations and on northern aspects, mixed conifer forests (ponderosa pine, Douglas-fir (*Pseudotsuga menziesii*), and white fir (*Abies concolor*), and aspen (*Populus tremuloides*) dominate. At the highest elevations, up to 2,700 m, forests of aspen, spruce (*Picea engelmannii* and *Picea pungens*), and subalpine fir (*Abies lasiocarpa*) are interspersed with meadows.

3 Tree-Ring Reconstruction of Historical Fire Regimes

Field sampling began in 1997, when we established study sites that eventually covered 6,565 ha stretching from the canyon rims to the highest elevations on both the North and South Rims. Sites were selected to represent the elevational gradient from ponderosa pine to mixed conifer, spruce-fir and aspen forests (Fig. 1).

Fire-scarred trees were sampled to inventory fire dates based on tree-ring analysis (Swetnam and Baisan 1996). The study sites were systematically surveyed along parallel transects to search 100% of the area, except at the large high-elevation site (4,400 ha) where fire-scarred trees were encountered predominantly on ridge tops

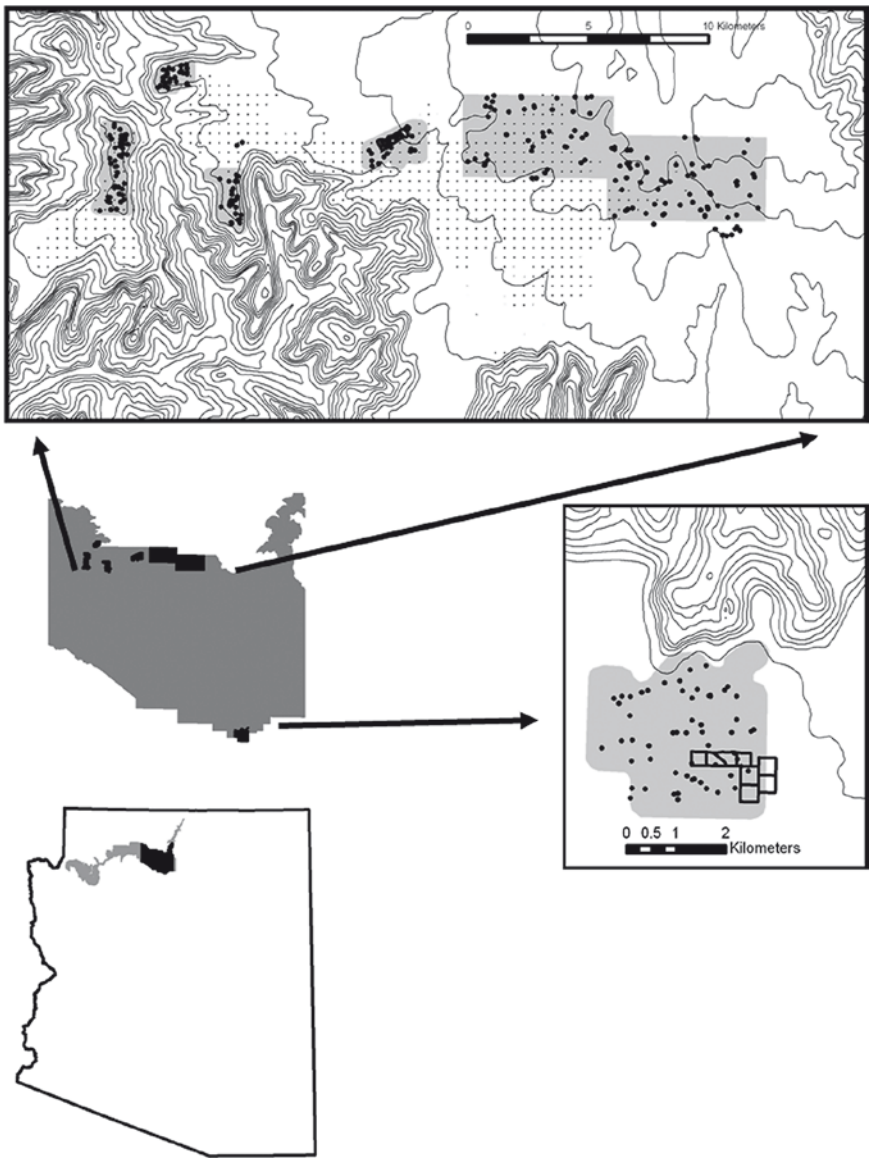

Fig. 1 Study sites in the region of Grand Canyon National Park, Arizona, USA. *Shaded* areas are the extent of systematic grids of forest sampling plots. *Dots* indicate the locations of fire-scarred trees and polygons outline forest restoration experimental sites. Stippled shading on the North Rim indicates the extent of wildfires managed by the National Park Service for resource benefits in 2003

and SW-S-SE aspects. Trees with the longest and most complete fire records were preferentially targeted for sampling. Samples were mapped when collected and were well-distributed throughout the study areas (Fig. 1).

In the high-elevation forest where stand-replacing fires were expected to be most common, we attempted to identify even-aged, homogenous stands that originated after fire. However, the landscape was highly diverse and we were not able to distinguish even-aged stands through remotely sensed data or field reconnaissance. At the finer scale of the permanent plots, however, we detected differences associated with effects of fires of differing severity. Fire-initiated and non-fire-initiated plots were characterized by age and species composition data, similar to Murray et al. (1998). The term "fire-initiated" is used here to separate groups of trees that originated following a stand-replacing fire. All age cohorts within each plot were taken into consideration but the greatest weight was given to the oldest trees. When the oldest tree or trees were the fire-resistant species *Pinus ponderosa* or *Pseudotsuga menziesii*, the plot was classified as non-fire-initiated. When the oldest trees were the fire-susceptible species *Populus tremuloides*, *Abies lasiocarpa*, or *Picea* spp., the plot was classified as fire-initiated. *Abies concolor* was considered intermediate in fire resistance; they were classified as non-fire-initiated when accompanied by uneven-aged *Pinus* or *Pseudotsuga*, and as fire-initiated when accompanied by approximately equal-aged *Populus*.

Fire-scarred samples were mounted on wood backing and surfaced with sandpaper until cells were clearly visible under magnification. Tree rings were visually crossdated (Stokes and Smiley 1968) and dating of measured rings was checked with the Cofecha software (Holmes 1983). The season of fire was estimated based on the relative position of fire injury within the annual ring (Baisan and Swetnam 1990).

Fire scar data were analyzed with FHX2 software (Grissino-Mayer 2001) beginning with the first fire year having an adequate sample depth, 10% or more of the total sample size of recording trees (Grissino-Mayer et al. 1995). "Recording" trees are those with fire scars or other wounds (e.g., lightning scars) that make them susceptible to repeated scarring by fire. Comparing data between study sites that differ in area could be biased because more scars recording small fires are likely to be included in larger study sites (Swetnam and Baisan 1996). Proportional filtering of the data set provides a useful basis of comparison by removing small fires that scarred only one or a few trees (Van Horne and Fulé 2006). Our filters were, first, all fire years, even those represented by a single scar. Then only those fire years were included in which respectively 10% or more, and 25% or more, of the recording samples were scarred.

The relationship between climatic fluctuations and fire occurrence was evaluated with superposed epoch analysis (SEA) (Grissino-Mayer 2001). The SEA superimposes all fire years and mathematically summarizes the climate data for fire years, as well as a window of several preceding and succeeding years. Bootstrapped distributions of climate data in 1,000 random windows were used to create confidence intervals. We developed a local tree-ring chronology to serve as a proxy for climate. The chronology was significantly correlated with reconstructed Palmer Drought Stress Index ($r = 0.67$) for grid point 31 in northern Arizona, A.D. 1694–1978 (Cook et al. 1996).

Results of the fire-scar analysis showed that frequent surface fires occurred throughout the ponderosa pine and mixed conifer forests of Grand Canyon, changing to lethal fires predominantly in the cooler, north-facing aspects at higher elevations (Table 1).

Table 1 Summary of fire regime reconstruction data from Grand Canyon National Park. All sites are on the North Rim except where indicated

Study site	Forest type	Elevation[a] (m)	Area (ha)	Fire type (multiple types by area)	Firefrequency[b] (year)	Source
Tusayan[c] (South Rim)	Pinyon-Juniper/ Ponderosa	2,039	770	Surface (30%)/ lethal (70%)	11.6[d]/±340	Huffman et al. (2008)
Grandview[c] (South Rim)	Ponderosa pine-Gambel oak	2,264	810	Surface	9.5	Fulé et al. (2003b)
Powell Plateau	Ponderosa pine	2,296	315	Surface	9.2	Fulé et al. (2003b)
Rainbow Plateau	Ponderosa pine	2,320	225	Surface	7.8	Fulé et al. (2003b)
Fire Point	Ponderosa pine	2,338	135	Surface	6.4	Fulé et al. (2003b)
Galahad Point	Ponderosa pine	2,350	410	Surface	6.8	Fulé et al. (2003a)
Walhalla Plateau	Ponderosa pine	2,350	~283	Surface	4.8–8.9	Wolf and Mast (1998)
Swamp Ridge	Mixed conifer	2,482		Surface	9.0	Fulé et al. (2003b)
Little Park	Mixed conifer, spruce-fir, aspen	2,700	4,400	Surface (40%)/ lethal (60%)	31.0/±100	Fulé et al. (2003a)
The Basin	Ponderosa, spruce, aspen	2,715	~141	Surface	11.9	Wolf and Mast (1998)

[a]Elevation shown is mid-point of range for each site.
[b]Fire statistic is mean fire interval for surface fires scarring 25% or more of samples/fire rotation for lethal fires. Frequency is shown prior to the time of European settlement, circa 1880.
[c]Study sites located on Kaibab National Forest adjacent to the Park (Tusayan site) or include both the National Forest and National Park (Grandview).
[d]Fires scarring 10% or more of samples.

The surface fire regimes all had composite mean fire intervals <10 years, calculated with the filtering criterion of fire years in which 25% or more of the sample trees were scarred. The only exception was a slightly longer interval (11.6 years) in the lowest-elevation site, a ponderosa/woodland ecotone, and increasing intervals (11.9–31.0 years) in the portions of high-elevation sites where surface fires occurred. Tree groups on nearly 60% of the high-elevation landscape plots were initiated by severe fire and were dominated by spruce or aspen; the oldest appeared to have originated after severe fires in 1782 or 1785. In 1880, the onset of general fire exclusion, all fire-initiated groups were less than 100 years old and nearly 25% of the groups were less than 20 years old. In contrast, non-fire-initiated groups at high elevation were significantly older, dominated by *Pinus ponderosa*, *Pseudotsuga menziesii*, or *Abies concolor*, and occurred preferentially on S and W slopes. The interspersion of fire-initiated patches of different ages and strong topographic association with fire type, creating a mixed-severity mosaic over the landscape, suggested that severe fires on the North Rim were smaller than those previously reported in spruce-fir forests of the Southwest or Rocky Mountains (Aplet et al. 1988; Grissino-Mayer et al. 1995). Patchy lethal fires also characterized the lower forest ecotone, where pinyon-juniper woodlands are dissected by drainages that support ponderosa pine (Huffman et al. 2008).

Fire occurrence was synchronized by climate across the large landscapes of Grand Canyon: five major regional fire years (1735, 1748, 1773, 1785, and 1879) burned over all or most of the North Rim study sites, an area of at least 300 km^2. Fire years were significantly dry (Fulé et al. 2003a, b), as measured by Palmer Drought Severity Index, and the years prior to fire were significantly wet in five of six study sites, patterns similar to those observed across the Southwest (Swetnam and Betancourt 1998). Fires ceased at most sites around the time of European settlement; the last year of widespread fire on the North Rim was 1879 and on the South Rim was 1887, although Wolf and Mast (1998) reported additional fires into the early twentieth century. In contrast to the general exclusion of fire after European settlement at Grand Canyon and across the southwestern U.S., three of the studied landscapes – Powell Plateau, Rainbow Plateau, and Fire Point – had two or three large, spreading surface fires since 1880, as well as several smaller fires. These remote, never-harvested forests are useful analogues for near-natural conditions prior to recent fire regime disruption.

Fire regimes reconstructed from fire scars should in theory be calibrated against modern records, providing a gauge of the accuracy, precision, and spatial fidelity of reconstructed fire histories (Baker and Ehle 2001). Calibration would be a test of the uniformity principle of dendrochronology, the concept that the factors governing tree-ring width today operated in the same way in the past. Unfortunately, it is difficult to carry out modern calibration because records were not kept when fires were common (pre-twentieth century) and most regions of the southwestern U.S. have not burned, or burned only rarely, during the recent period when records exist. At Grand Canyon, however, we found the unusual circumstance that a number of fires had occurred in the studied landscapes in the twentieth century, both wildfires and managed fires, and fire records had been maintained since 1924.

Fire scars were accurate in identifying historical fires: all of the 13 recorded fires larger than 8 ha since 1924 were identified from fire scars (Fulé et al. 2003a, b). The proportion of scarred trees was generally related to recorded fire size, a useful test of the hypothesis that higher levels of scarring can serve as a "filter" for separating larger and smaller fires (Swetnam and Baisan 1996). The high accuracy of fire-scar data in reconstructing the modern Grand Canyon fire history, coupled with similar recent findings from Saguaro National Park in Arizona (Farris et al. 2003) and studies on fire-scar sampling methodology in Arizona (Van Horne and Fulé 2006) and New Mexico (Falk 2004) show that surface fire regimes reconstructed from fire scars in southwestern ponderosa pine forests, using standard sampling methods (Swetnam and Baisan 1996) are highly reliable.

4 Tree-Ring Analysis for Forest and Fuel Structure

Over the same landscapes as in the fire history studies described above, we measured forest and fuel characteristics on grids of systematically spaced permanent plots. Sampling plots were 0.1 ha (20 × 50 m). Dendrochronological sampling was used to measure age structure and forest change. We tagged trees and measured species, condition, diameter at breast height (DBH, 1.37 m), height, and crown base height. We distinguished between trees established prior to circa 1880, when European-American settlers introduced livestock and interrupted fire disturbance regimes (Cooper 1960), and those that established later (White 1985). All living trees meeting the pre-settlement criteria were considered potentially pre-1880 trees and were cored. A random 10% sample of all other trees was also cored. Coring height was 40 cm above ground level to meet two objectives: first, to measure tree age, and second, to measure growth between the fire regime disruption date and the present (needed for the forest reconstruction).

Canopy cover was recorded with a vertical densitometer along the 50-m sidelines of each plot, every 0.3 or 3 m. Forest floor and woody debris were measured along four 15.2 m planar intersect transects (Brown 1974). Litter and duff (fermentation plus humus layers) depths were measured every 1.52 m along each transect, and woody debris was recorded by time-lag classes of 1 h (0–0.6 cm diameter), 10 h (0.6–2.5 cm), 100 h (2.5–7.6 cm), and 1,000 h (>7.6 cm).

Tree increment cores were surfaced and visually crossdated. Rings were counted on cores that could not be crossdated, mostly younger trees. Additional years to the center were estimated with concentric circles matched to the curvature and density of the inner rings for cores that missed the pith. Forest structure in 1880 was reconstructed using dendroecological methods (Fulé et al. 1997) as follows: tree size at the time of fire exclusion was reconstructed by subtracting twice the radial growth measured on increment cores since 1879. We developed local species-specific relationships between tree diameter and basal area increment (r^2 = .45 to .90) and applied these relationships to estimate past size for trees without increment cores (dead or rotten centers). For dead trees, the date of death was estimated based on

tree condition class using diameter-dependent snag decomposition rates (Thomas et al. 1979). Local tests have shown the death-date model to be reasonably accurate (Waskiewicz et al. 2007).

We modeled changes in forest structure, canopy fuels, and potential fire behavior as outlined in the schematic in Fig. 2. Forest change was simulated on a per-plot basis at 10-year intervals using the Forest Vegetation Simulator (FVS, Van Dyck 2000), Central Rockies variant. This model is a highly precise statistical model for forest simulation (Edminster et al. 1991). Simulations were initialized with reconstructed 1880 conditions. Actual regeneration data by species and decade were added to each plot and increased by 40%, an empirically determined value, to account for density-dependent mortality. Canopy biomass was estimated with diameter-based allometric equations for foliage and fine twigs, the canopy fuels that are available for burning in crown fires. Canopy volume was estimated on a per-plot basis by the maximum tree height (top of the canopy) minus crown base height (bottom of the canopy). Canopy bulk density was calculated as canopy biomass divided by canopy volume.

Fire behavior was modeled with the Nexus Fire Behavior and Hazard Assessment System (Scott and Reinhardt 2001). Nexus combines a deterministic model of surface fire behavior with models of crown fire transition and crown fire spread.

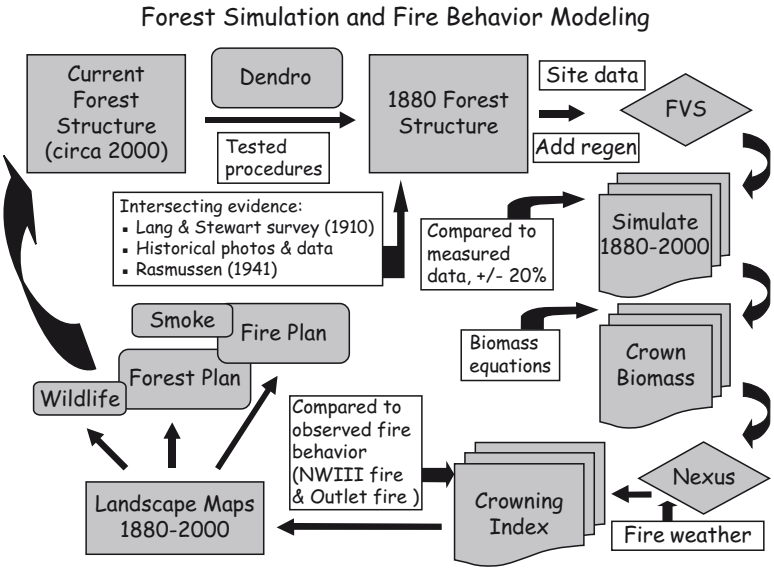

Fig. 2 Schematic of forest data and modeling process, beginning with data collection on contemporary forest structure (*upper left*), dendroecological reconstruction of forest structure in 1880, simulation modeling with FVS (Forest Vegetation Simulator, *upper right*), crown fuel modeling, fire behavior modeling with Nexus (*lower right*), and development of fire hazard maps (*lower left*) that provide information for forest and fire planning. In turn, management actions based on these plans affect forests on the Grand Canyon landscape (From Fulé et al. 2004)

Foliar moisture content was set at 100% (Agee et al. 2002). Hot and dry weather inputs were used to simulate fire behavior under extreme conditions. Fire weather extremes representing the 90th and 97th percentiles of low fuel moisture and high temperature were calculated for 1970–2001 at the Bright Angel weather station using the FireFamily Plus program (Bradshaw and Brittain 1999). Values were calculated for June, historically the month with the most severe fire weather (Table 2), because severe fires spread out of control under such conditions. Fire behavior fuel models (Anderson 1982) used were 9 (sites below 2,500 m elevation) and 10 (sites above 2,500 m elevation). We focused the analysis on crown fire behavior as measured by the crowning index (CI), defined as the windspeed at which active canopy burning could be sustained (Scott and Reinhardt 2001).

Results of tree-ring assessment of forest change indicated that forest structure since the time of European settlement and fire exclusion, circa 1880, changed substantially in fire-excluded study sites but much less in those that continued to burn. Basal area of ponderosa pine forests increased an average of 238% from 9.1–20.5 m^2 ha^{-1} at the onset of European settlement and fire regime disruption, circa 1880, to 22.9–31.4 m^2 ha^{-1} in contemporary forests (Table 2). Changes in tree density were even more dramatic: 140–160 trees ha^{-1} to 389–955 trees ha^{-1}, an average of 448%. While these increases are large, Grand Canyon forest densities actually increased less than most southwestern ponderosa forests. Densities reported in a number of forest reconstruction studies and early historical forest inventories averaged 79 pines ha^{-1} (see list in Covington and Moore 1992), whereas the current average ponderosa pine density across the state of Arizona is approximately 619 pines ha^{-1} (O'Brien 2002). At Grand Canyon, the sites where fire regimes were not completely disrupted had the smallest post-settlement increases in pine density reported to date in the Southwest, averaging 64 pines ha^{-1} or 42% (Table 2). Densities of other trees jumped, especially *Quercus* and *Robinia*, but pines continued to dominate, making up an average of 90% of basal area. We suggested that the continued presence of surface fire, even at much longer than natural intervals, was the most likely reason for maintaining relatively open forests at the remote points and plateaus (Fulé et al. 2002). The specific reasons for density change are typically difficult to untangle because livestock grazing, fire suppression, and past logging affected most southwestern forests in overlapping ways (Belsky and Blumenthal 1997), but the Grandview site and never-harvested forests of the G. A. Pearson Natural Area in Arizona (Covington et al. 1997) and Monument Canyon Natural Area in New Mexico (Falk 2004) provide examples where logging was absent but pine density increases on the order of 1,000% were observed after fire exclusion.

Forest density increases were greatest in mixed conifer and spruce/fir/aspen forests at the highest elevations of the Park. The highest basal area of any contemporary forest was reached in mixed conifer at Swamp Ridge, 41.3 m^2 ha^{-1}, and the large Little Park site averaged 31.9 m^2 ha^{-1} (Table 2). The Swamp Ridge site had had the highest basal area in 1880 as well (28.5 m^2 ha^{-1}), but ponderosa pine dropped from 75% of basal area in 1880 to only 48% today as the species composition shifted to *Abies* and *Pseudotsuga*. The high-elevation Little Park site was very

Table 2 Summary of forest reconstruction and contemporary data from never-harvested forests in Grand Canyon National Park

Study site	Post-1880 fire regime[a]	Pine/Total Basal Area 1880(m^2 ha^{-1})	Pine/Total Basal Area Current (m^2 ha^{-1})	Pine/Total Density 1880 (trees ha^{-1})	Pine/Total Density Current (trees ha^{-1})	Source
Grandview[b] (South Rim)	Exclusion since 1870	7.9/9.1	16.8/22.9	65/140	646/955	Fulé et al. (2002)
Powell Plateau	Large fires in 1892, 1924, 1987	17.8/17.9	24.4/26.3	152/157	249/638	Fulé et al. (2002)
Rainbow Plateau	Large fires in 1900, 1985, 1993	16.8/17.0	21.8/27.2	156/160	209/936	Fulé et al. (2002)
Fire Point	Large fires in 1923, 1931, 1999	20.5/20.5	30.5/31.4	151/153	193/389	Fulé et al. (2002)
Swamp Ridge	Exclusion	21.3/28.5	19.9/41.3	132/246	157/941	Fulé et al. (2002)
Little Park	Exclusion	3.5 /12.2	4.3/31.9	43/208	52/1011	Fulé et al. (2003a)

[a] Fire regime refers to predominant post-1880 pattern. At least one small fire occurred in each site since 1880.
[b] Only National Park (Grandview).

open in 1880 (12.2 m^2 ha^{-1}), likely as a result of severe fires in 1851 and 1879, but had become dense by 2000 with *Abies*, *Picea*, and *Populus*.

Assessing the accuracy of tree-ring forest reconstructions was facilitated by a thorough inventory of the Kaibab Plateau (North Rim) carried out by Lang and Stewart (1910). They reported an average in ponderosa pine forest of 128 pines >15.2 cm DBH ha^{-1}. For comparison, the Powell Plateau, Fire Point, and Rainbow Plateau sites averaged 141, 136, and 125 pines >15.2 cm DBH ha^{-1} in the 1880 reconstruction and 141.2, 148.5, and 147.8 pines >15.2 cm DBH ha^{-1} in the contemporary forest, nearly no change in pine density over approximately 120 years (Fulé et al. 2002). In higher elevation forests, the Lang and Stewart (1910) averages for several conifer species were also very close to reconstructed densities. Across the 4,400-ha Little Park study site, reconstructed 1880 average densities for *Abies*, *Pseudotsuga*, and *Picea* (trees >15.2 cm DBH) were within 2 tree ha^{-1} of the averages reported by Lang and Stewart (1910). Only ponderosa pine was more variable, about 25% or 11 trees ha^{-1} lower in density (Fulé et al. 2003a). On the South Rim at Grandview, reconstructed pine densities fell within ranges surveyed by Woolsey (1911) (Fulé et al. 2002). In addition to quantitative data, the early forest surveyors also noted that "forest fires have been the cause of incalculable losses […]. Vast denuded areas, charred stubs and fallen trunks and the general prevalence of blackened poles [illustrate] their frequency and severity long before this country was explored by white men […]. Evidence indicates light ground fires over practically the whole forest, some of the finest stands of yellow pine show only slight charring of the bark and very little damage to poles and undergrowth" but at higher elevations "old fires extended over large areas at higher altitudes, amounting to several square miles on either side of Big Park [now called DeMotte Park, N of our Little Park study site]" (Lang and Stewart 1910:18–19). These descriptions are consistent with our tree-ring-based fire regime and forest reconstructions across the elevational gradient.

Modeling results indicated that fuels and fire hazard increased over time as the forest density increased and species composition changed on the North Rim. Canopy biomass, which serves as the fuel for severe fires, increased at all sites. The average increase was only 122% at the low-elevation ponderosa pine sites, consistent with the minimal post-settlement alteration observed in these areas, but 279% at the high-elevation Little Park site (Fulé et al. 2004). The high fuel load and spatial contiguity of the Little Park site were consistent with the findings of White and Vankat (1993) in the adjacent Thompson Canyon watershed. The intermediate-elevation Swamp Ridge site, a mixed conifer forest, had the highest canopy biomass in 1880 but the smallest increase by 2040 (39%). Canopy bulk density increased in proportion with biomass. Species composition of canopy fuels remained consistent at low elevation (*Pinus ponderosa*) but shifted strongly to mesic species at higher elevations. Potential crown fire behavior forecast in terms of crowning index (CI), the minimum wind speed required for active canopy burning, decreased (i.e., the hazard of severe wildfire increased) by 23–80% over the modeled period. Canopy fuel and CI values were extrapolated across the entire North Rim landscape. At a threshold wind speed of 45 km/h, only 6% of the landscape was susceptible to active

crown fire in 1880 but 33% was susceptible by 2000 (Fulé et al. 2004). Empirical evidence of forest susceptibility to severe fire was shown by the Outlet Fire in 2000, which burned over 5,260 ha, about 35% complete overstory mortality (Bertolette and Spotskey 2001).

5 Applications to Management

Tree-ring analyses of fire regimes and forest structure carried out in these interlinked research studies have supported a wide array of ecological interpretations and management decisions. We applied tree-ring methods to reconstruct the fire disturbance regime and forest structure over the past 100–400 years. We assessed the accuracy of the findings using intersecting lines of evidence from historical and modern records. And we used vegetation and fire behavior simulation models to characterize changes in fuels and fire hazards over a 160-year period. In this section, I describe two examples of the application of this information for restoration and conservation of Grand Canyon's forest ecosystems: (1) setting ecological reference conditions and (2) supporting fire management decisions.

Ecological reference conditions: Several studies have taken advantage of the ecological value of the remote points and plateaus of the North Rim, rare never-harvested forests with surface fire regimes continuing to the present. Leopold (1941) referred to reference conditions (also, range of natural variability, range of historical variability; see Swetnam et al. 1999, Landres et al. 1999) as the "base datum" of ecology. Even when there is considerable uncertainty about the variability among alternative ecological states or the linearity and predictability of successional trajectories, reference data on ecosystem structure and process are highly valuable (Cortina et al. 2006). Modern reference sites are especially useful for assessing transitory, dynamic aspects of the ecosystem, such as herbaceous plants, wildlife, or soil nutrients, which generally do not leave enduring evidence.

Herbaceous plant communities provide over 90% of the vascular plant diversity in southwestern ponderosa pine forests, as well as critical habitat for invertebrates and vertebrates, forage for domestic livestock, and fuel to sustain the surface regime (Korb and Springer 2003). Past overgrazing, drought, introduction of non-native species, fire exclusion, and increased forest density have degraded herbaceous plant communities. The remote North Rim sites have been protected from livestock since the late 1930s. Gildar et al. (2004) contrasted plant communities across two years between two reference sites (Powell Plateau and Rainbow Plateau) and Galahad Plateau, where fire exclusion had occurred since 1880. The unburned site had significantly higher coarse woody debris and duff depth, but species richness was influenced more by inter-annual precipitation than by fire history. Moving to the landscape scale, however, Laughlin et al. (2005) modeled overstory-understory relationships over the full elevational gradient on the North Rim. In this context, the North Rim reference sites stood out because species richness was associated with lower pine basal area and inversely related to time since fire. Laughlin and Grace

(2006) used structural equation modeling to investigate potential mechanisms for the fire-richness relationship. Model results suggested that important processes included a post-fire stimulation of germination, a decline in understory abundance with time since fire, and an increase over time in pine abundance (which indirectly leads to reduced richness) in the absence of fire. The hypothesis that surface fire played a role in maintaining diverse plant communities was tested in a case study at Fire Point, which burned in 1999. After the fire, the plant community shifted toward higher compositional similarity with the reference plots at Powell and Rainbow Plateaus (Laughlin et al. 2004).

Fire management: In 2003, Grand Canyon National Park managed four naturally ignited wildfires for resource benefits, ultimately burning nearly 8,000 ha (Fulé and Laughlin 2007). The fires burned over and between our existing plot network (Fig. 1), permitting an empirical assessment of the utility of fire use in restoring historical ecosystem patterns. After the fires burned out, we remeasured 82 permanent plots burned by the fires plus 43 plots on unburned companion sites in the first 2 years following fire. Across the elevational gradient, the fires burned in a manner consistent with the evidence of the pre-settlement fire regime: predominantly surface fire behavior in ponderosa pine forest (Fig. 3), with fire intensity increasing up through the mixed conifer and spruce-fir. The maximum basal area killed on any plot was 13.7 m^2 ha^{-1}, the equivalent of 58% of the pre-fire plot basal area. At mid-elevation on Swamp Ridge, over 40% of the plots had >10 m^2 ha^{-1}; maximum

Fig. 3 Open forest dominated by mature trees at Powell Plateau, Grand Canyon National Park, is resistant to intense fire behavior because of light surface fuels and high canopy base height. Photo by P. Fulé (From Stephens and Fulé 2005)

mortality was 32.4 m^2 ha^{-1}, equal to 83% of pre-fire basal area. At the highest elevation plots in Little Park, 56% of plots exceeded 10 m^2 ha^{-1} mortality and 11% had complete overstory mortality. Tree mortality occurred primarily in smaller trees and mesic species (*Abies*, *Picea*), which had undergone the greatest increase since fire exclusion. Non-metric multiscale ordination showed that the fires reversed the shift away from reference conditions. Understory plant communities appeared resilient even to intense burning, although the non-native cheatgrass (*Bromus tectorum*) increased (Laughlin and Fulé 2008). Even after a long fire-free period (1880–2003), fire effects were mostly consistent with restoration of historical conditions. Fires simultaneously reduced living, dead and ladder fuels. These effects make the forests more resistant under warmer climate conditions that are expected to increase fire size and severity in the twenty-first century (McKenzie et al. 2004).

The future of Grand Canyon forests is uncertain, given current forecasts of severe drying in the Southwest (Seager et al. 2007). However, these ecosystems have unusual advantages compared to others in the region because they conserve the genetic and structural diversity of old trees and native species. The extensive burning carried out by managers since the 1980s has extracted a cost in terms of escaped fires and unwanted public attention, but it has also provided an increasing safety cushion for further burning. Managers in the Kaibab National Forest to the north and south of Grand Canyon also collaborate to burn and thin to create defensible boundaries. Fires at Grand Canyon provided the opportunity to test the modern calibration of the fire-scarred tree-ring record; it is now encouraging to watch the number of scars increase closer toward historical levels as more of the landscape is being burned more often. Fire and climate shaped these ecosystems through evolutionary and ecological time. Perhaps fire use can help preserve a significant part of the forest even as climate changes more rapidly.

Acknowledgments The author gratefully acknowledges the work of numerous ecologists and students from Northern Arizona University in the field and lab, as well as support from Grand Canyon National Park and the USDA Forest Service.

References

Agee JK, Wright CS, Williamson N, Huff MH (2002) Foliar moisture content of Pacific Northwest vegetation and its relation to wildland fire behavior. Forest Ecol Manage 167:57–66

Anderson HE (1982) Aids to determining fuel models for estimating fire behavior. Gen Tech Rep INT-69, U.S. Forest Service Intermountain Forest and Range Experiment Station. Ogden, Utah

Aplet GH, Laven RD, Smith FW (1988) Patterns of community dynamics in Colorado Engelmann spruce-subalpine fir forests. Ecology 69(2):312–319

Baisan CH, Swetnam TW (1990) Fire history on a desert mountain range: Rincon Mountain Wilderness, Arizona, USA. Can J Forest Res 20:1559–1569

Baker W, Ehle D (2001) Uncertainty in surface-fire history: the case of ponderosa pine forests in the western United States. Can J Forest Res 31:1205–1226

Belsky AJ, Blumenthal DM (1997) Effects of livestock grazing on stand dynamics and soils in upland forests of the Interior West. Conserv Biol 11(2):315–327

Bertolette D, Spotskey D (2001) Remotely sensed burn severity mapping. In: Harmon D (ed) Crossing Boundaries in Park Management: Proceedings of the 11th Conference on Research and Resource Management in Parks and on Public Lands, pp 45–51

Bradshaw L, Brittain S (1999) FireFamily Plus. Software available from USDA Forest Service, Rocky Mountain Research Station, Missoula MT

Brown JK (1974) Handbook for inventorying downed woody material. General Technical Report INT-16. U.S. Forest Service Intermountain Forest and Range Experiment Station. Ogden, Utah

Cook ER, Meko DM, Stahle DW, Cleaveland MK (1996) Tree-ring reconstructions of past drought across the conterminous United States: tests of a regression method and calibration/verification results. In: Dean JS, Meko DM, Swetnam TW (eds) Tree rings, environment, and humanity: Proceedings of the International Conference, Radiocarbon. Department of Geosciences, The University of Arizona, Tucson, pp 155–170

Cooper CF (1960) Changes in vegetation, structure, and growth of southwestern pine forests since white settlement. Ecology 42:493–499

Cortina J, Maestre FT, Vallejo R, Baeza MJ, Valdecantos A, Pérez-Devesa M (2006) Ecosystem structure, function, and restoration success: Are they related? J Nature Conserv 14:152–160

Covington WW, Moore MM (1992) Post-settlement changes in natural disturbance regimes: implications for restoration of old-growth ponderosa pine ecosystems. In: Old-growth forests in the Southwest and Rocky Mountain Region. Proceedings of the symposium. USDA Forest Serv General Techn Report RM-213, pp 81–99

Covington WW, Fulé PZ, Moore MM, Hart SC, Kolb TE, Mast JN, Sackett SS, Wagner MR (1997) Restoration of ecosystem health in southwestern ponderosa pine forests. J Forestry 95(4):23–29

Edminster CB, Mowrer HT, Mathiasen RL, Schuler TM, Olsen WK, Hawksworth FG (1991) GENGYM: a variable density stand table projection system calibrated for mixed conifer and ponderosa pine stands in the Southwest. USDA Forest Service Research Paper RM-297

Falk DA (2004) Scaling rules for fire regimes. Ph.D. Dissertation. University of Arizona, Tucson

Falk DA (2006) Process-centred restoration in a fire-adapted ponderosa pine forest. J Nature Conserv 14:140–151

Farris CA, Baisan CH, Swetnam TW (2003) A comparison of fire regime characteristics reconstructed from fire scar data and mapped fires in a frequently burned Arizona wilderness. Second International Wildland Fire Ecology and Fire Management Congress, 16–20 Nov 2003. Orlando, FL

Fulé PZ, Laughlin DC (2007) Wildland fire effects on forest structure over an altitudinal gradient, Grand Canyon National Park, USA. J Appl Ecol 44:136–146

Fulé PZ, Moore MM, Covington WW (1997) Determining reference conditions for ecosystem management in southwestern ponderosa pine forests. Ecol Appl 7(3):895–908

Fulé PZ, Covington WW, Moore MM, Heinlein TA, Waltz AEM (2002) Natural variability in forests of Grand Canyon, USA. J Biogeogr 29:31–47

Fulé PZ, Crouse JE, Heinlein TA, Moore MM, Covington WW, Verkamp G (2003a) Mixed-severity fire regime in a high-elevation forest: Grand Canyon, Arizona. Landscape Ecol 18:465–486

Fulé PZ, Heinlein TA, Covington WW, Moore MM (2003b) Assessing fire regimes on Grand Canyon landscapes with fire scar and fire record data. Int J Wildland Fire 12(2):129–145

Fulé PZ, Crouse JE, Cocke AE, Moore MM, Covington WW (2004) changes in canopy fuels and potential fire behavior 1880–2040: Grand Canyon, Arizona. Ecol Model 175:231–248

Gildar CN, Fulé PZ, Covington WW (2004) Plant community variability in ponderosa pine forest has implications for reference conditions. Natural Areas J 24(2):101–111

Grissino-Mayer HD (2001) FHX2—Software for analyzing temporal and spatial patterns in fire regimes from tree rings. Tree-Ring Res 57(1):115–124

Grissino-Mayer HD, Baisan CH, Swetnam TW (1995) Fire history in the Pinaleño Mountains of southeastern Arizona: effects of human-related disturbances. USDA Forest Service General Technical Report RM-GTR-264, p 399–407

Holmes RL (1983) Computer-assisted quality control in tree-ring dating and measurement. Tree-Ring Bull 43:69–78
Huffman DW, Fulé PZ, Pearson KM, Crouse JE (2008) Fire history of pinyon-juniper woodlands at upper ecotones with ponderosa pine forests in Arizona and New Mexico. Can J Forest Res 38(8):2097–2108
Keeley JE, Zedler PH (1998) Evolution of life histories in Pinus. In: Richardson DM (ed) Ecology and biogeography of pinus. Cambridge University Press, Cambridge
Korb JE, Springer JD (2003) Understory vegetation. In: Friederici PG (ed) Ecological restoration of Southwestern Ponderosa pine forests: a sourcebook for research and application. Island Press, Washington
Landres P, Morgan P, Swanson F (1999) Overview of the use of natural variability in managing ecological systems. Ecol Appl 9:1279–1288
DM, Stewart SS (1910) Reconnaissance of the Kaibab National Forest. Unpublished report on file at Northern Arizona University, Flagstaff
Laughlin DC, Fulé PZ (2008) Wildland fire effects on understory plant communities in two fire-prone forests. Can J Forest Res 38:133–142
Laughlin DC, Grace JB (2006) A multivariate model of plant species richness in forested systems: old-growth montane forests with a long history of fire. Oikos 114:60–70
Laughlin DC, Bakker JD, Stoddard MT, Daniels ML, Springer JD, Gildar CN, Green AM, Covington WW (2004) Toward reference conditions: wildfire effects on flora in an old-growth ponderosa pine forest. Forest Ecol Manage 199:137–152
Laughlin DC, Bakker JD, Fulé PZ (2005) Understorey plant community structure in lower montane and subalpine forests, Grand Canyon National Park, USA. J Biogeogr 32:2083–2102
Leopold A (1924) Grass, brush, timber, and fire in southern Arizona. J Forestry 22:1–10
Leopold A (1941) Wilderness as a land laboratory. Living Wilderness 6:3
McKenzie D, Gedalof Z, Peterson DL, Mote P (2004) Climatic change, wildfire, and conservation. Conserv Biol 18:890–902
Murray MP, Bunting SC, Morgan P (1998) Fire history of an isolated subalpine mountain range of the Intermountain Region, United States. J Biogeogr 25:1071–1080
O'Brien RA (2002) Arizona's forest resources, 1999. USDA Forest Serv Res Bull RMRS-RB-2
Pyne SJ (1982) Fire in America. A cultural history of wildland and rural fire. Princeton University Press, Princeton
Savage M, Mast JN (2005) How resilient are southwestern ponderosa pine forests after crown fire? Can J Forest Res 35:967–977
Scott JH, Reinhardt ED (2001) Assessing crown potential by linking models of surface and crown fire behavior. USDA Forest Serv Res Paper RMRS-RP-29
Seager R, Ting MF, Held IM, Kushnir Y, Lu J, Vecchi G, Huang HP, Harnik N, Leetmaa A, Lau NC, Li C, Velez J, Naik N (2007) Model projections of an imminent transition to a more arid climate in southwestern North America. Science 316:1181–1184
Stephens SL, Fulé PZ (2005) Western pine forests with continuing frequent fire regimes: possible reference sites for management. J Forestry 103(7):357–362
Stokes MA, Smiley TL (1968) An introduction to tree-ring dating. University of Chicago Press, Chicago
Strom BA, Fulé PZ (2007) Pre-wildfire fuel treatments affect long-term ponderosa pine forest dynamics. Int J Wildland Fire 16:128–138
Swetnam TW, Baisan CH (1996) Historical fire regime patterns in the southwestern United States since AD 1700. In: Allen CD (Ed) Proceedings of the 2nd La Mesa Fire Symposium. USDA Forest Service General Technical Report RM-GTR-286, pp 11–32
Swetnam TW, Betancourt JL (1998) Mesoscale disturbance and ecological response to decadal climatic variability in the American Southwest. J Climatol 11:3128–3147
Swetnam TW, Allen CD, Betancourt JL (1999) Applied historical ecology: using the past to manage for the future. Ecol Appl 9(4):1189–1206
Thomas JW, Anderson RG, Maser C, Bull EL (1979) Snags. In: Wildlife habitats in managed forests – the Blue Mountains of Oregon and Washington. USDA Agriculture Handbook 553, pp 60–77

Van Dyck MG (2000) Keyword reference guide for the Forest Vegetation Simulator. USDA Forest Service Forest Management Service Center, Fort Collins, CO
Van Horne ML, Fulé PZ (2006) Comparing methods of reconstructing fire history using fire scars in a southwestern USA ponderosa pine forest. Can J Forest Res 36(4):855–867
Warren PL, Reichardt KL, Mouat DA, Brown BT, Johnson RR (1982) Vegetation of Grand Canyon National Park. National Park Service, University of Arizona, Contribution No. 017/06
Waskiewicz JD, Fulé PZ, Beier P (2007) Quantifying the deterioration of ponderosa pine snags in northern Arizona. Western J Appl Forestry 22(4):233–240
Weaver H (1951) Fire as an ecological factor in the southwestern ponderosa pine forests. J Forestry 49:93–98
Westerling AL, Hidalgo HG, Cayan DR, Swetnam TW (2006) Warming and earlier spring increase western U.S. forest wildfire activity. Science 313:940–943
White AS (1985) Presettlement regeneration patterns in a southwestern ponderosa pine stand. Ecology 66(2):589–594
White MA, Vankat JL (1993) Middle and high elevation coniferous forest communities of the North Rim region of Grand Canyon National Park, Arizona, USA. Vegetatio 109:161–174
Wolf JJ, Mast JN (1998) Fire history of mixed-conifer forests on the North Rim, Grand Canyon National Park, Arizona. Phys Geogr 19(1):1–14

Wildfire Risk and Hazard in Northern Patagonia, Argentina

Thomas T. Veblen

Extreme wildfire events and upward trends in areas burned since the early 1980s are now well documented for many tropical and temperate forest and woodland ecosystems. Wildfire events of large extent and extreme severity are often believed to be driven either by past land-use practices that have altered fuel types (e.g. logging or fire exclusion) or by climate changes that make fuels more prone to burning, or by a combination of both. The recent trend towards increased area burned in extreme wildfires is illustrated by recent events in the mid-latitude (c. 38–43°S) Andes. In the Patagonian-Andean region of *Nothofagus* (southern beech trees) forests, in the late 1990s and early 2000s wildfires occurred that were more extensive and more severe than any fires in recent memory (Veblen et al. 2008). For example, in Chile during the austral summer of 2001–2002 large, severe fires burned in the region of *Araucaria* forests (c. 38–39°30′ S) which were believed to be the most extensive fires in this region for at least the past 50 years. Likewise, in the nearby Nahuel Huapi NP (Argentina, c. 40°S) more area burned in 1998–1999 than in any previous fire season in the 50-year documentary record (Veblen et al. 2008). Although documentary records of fire and instrumental climate records inform our understanding of changes in fire occurrence and their potential relationships to climatic variation over the past c. 100 years, assessment of the relative contributions of land-use changes and climate variation to contemporary wildfire behavior requires longer-term data for which tree-ring methods are well suited.

The mid-latitudes of the southern Andes are characterized by a strong west-to-east precipitation gradient from mean annual precipitation of 3,000 to 5,000 mm in Chile on the western side of the Andes to less than 800 mm just 50 km east of the Andean summit. Thus, the regional vegetation pattern consists of temperate rainforests and mesic *Nothofagus* forests in Chile extending c. 30 km eastwards of the Andean

T.T. Veblen (✉)
Department of Geography, University of Colorado, Boulder, CO 80309, USA
e-mail: Veblen@colorado.edu

M. Stoffel et al. (eds.), *Tree Rings and Natural Hazards: A State-of-the-Art*,
Advances in Global Change Research 41, DOI 10.1007/978-90-481-8736-2_35,

crest into Argentina which are bordered by xeric open woodlands dominated by the Andean mountain cypress (*Austrocedrus chilensis*) and the Patagonian steppe of small shrubs and bunchgrasses. Fires in the mesic forests, whether ignited by lightning or by humans, are high-severity crown fires that spread through the canopy as well as through dense understories dominated by tall bamboos and other woody species. Fire spread is not limited by lack of woody fuels, and fuel-defined hazard (*sensu* Hardy 2005) of a high-severity fire is always high. However, ignition and spread are limited by the infrequent occurrence of sufficiently dry, warm conditions required for fire spread in an otherwise moist forest environment so that fire risk (probability of ignition and spread) is typically low. The natural fire regime of these mesic *Nothofagus* forests consists of extensive, high severity fires that occur infrequently in association with exceptionally dry, warm conditions. Tree-ring data (Veblen et al. 1999) have shown that many mesic forest sites may not experience any fire for one or several centuries because of the relative infrequency of extreme drought. In contrast, eastwards near the ecotone between *Austrocedrus* woodlands and the dry Patagonian steppe the typically warm dry summers desiccate fuels so that ignition and fire spread is possible in most years. Thus, fire risk is inherently high. However, fuel discontinuities and especially lack of woody fuels result in a fire regime that historically was characterized by relatively frequent low-severity fires that mostly burned herbaceous fuels. The limitation of fine fuel quantity on fire spread in this habitat is reflected by tree-ring data that show that years of more widespread fire tend to occur one to a few years after wet cool years that promote the growth of grass fuels (Kitzberger et al. 1997; Veblen et al. 1999).

The fuel-limited fire regime of the xeric *Austrocedrus* woodlands is inherently susceptible to alteration by land-use practices of both Native American and European origin. Prior to permanent European settlement in the 1890s, fires occurred relatively frequently in this habitat (Fig. 1) and were ignited by both lightning and Native Americans. Although years of widespread fire correspond with weather conditions conducive to fire spread, areas of greatest use by Native American hunters who used fire to drive game had the highest frequency of fires (e.g. N LIM1 and N LIM2 in Fig. 1). The tree-ring record of fire in *Austrocedrus* woodlands near the steppe ecotone shows a marked reduction in fire occurrence after c. 1900 (Fig. 1). Survival of the fire-recording trees as well as eye-witness accounts from the nineteenth century indicate that previous fires were low-severity fires that mainly burned grass and small shrub fuels (Veblen et al. 2008). Fire frequencies declined dramatically at these sites after c. 1900 due to a combination of factors: (1) few fires were set by the Native American population that declined dramatically about 1900; (2) growth of the livestock population reduced the quantity of grass fuels; and (3) fires were actively suppressed, especially, after the 1940s. The decline in fire frequency coincides with a substantial increase in the density of woody vegetation in this ecosystem (Fig. 2) which mainly reflects enhanced juvenile tree survival permitted by longer fire-fire intervals. Thus, fuel-defined hazard of fire severity increased during the twentieth century.

Tree-ring based fire history studies indicate a high level of current vulnerability of people and property to wildfire in the habitat of *Austrocedrus* woodlands for

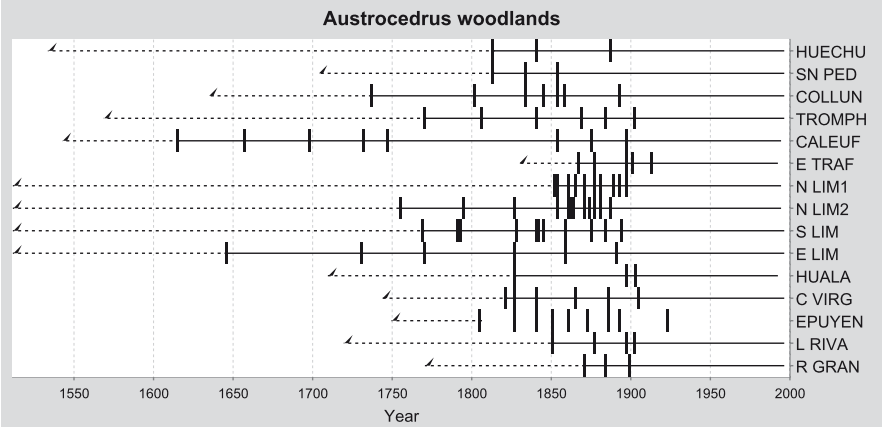

Fig. 1 Composite fire scar records indicating years in which at least 10% of the recorder trees (minimum two scars) recorded fire at sample sites in *Austrocedrus* woodlands in the Argentine Lake District. Each horizontal line represents a different site indicated by the codes to the right, for which dates of fire scars are indicated by short vertical lines. Dashed lines indicate years prior to the occurrence of the first scar on that tree. Sites are arranged from north to south, and site codes are defined in Veblen et al. (1999)

several reasons (Veblen et al. 2008). First, the tree-ring fire record shows that weather-related fire risk is inherently high in this habitat. Second, formerly frequent low-severity fires have declined dramatically in frequency so that woody fuels have accumulated to the point that many *Austrocedrus* sites now can support high-severity crown fires. Third, Native Americans historically were a significant source of ignitions in this habitat so that the current trend towards greater human presence through recreation and exurban development is also likely to contribute significantly to fire risk. In fact, fire frequency during the late twentieth century has been higher in areas near urban settlements. In addition, fuel-defined fire hazard has been further increased by extensive planting of exotic conifers in this fire-prone habitat. In these areas of formerly open vegetation types near the ecotone with the steppe, both woody encroachment since the early 1900s and planting of exotic conifers since the 1970s have increased the hazard of crown fires.

Fire risk in northern Patagonia in both the *Austrocedrus* habitat and in mesic *Nothofagus* forests appears to be increasing under the regional trend towards warmer temperatures and increased lightning ignitions (Veblen et al. 2008). The widespread burning of mesic forests in the 1998–1999 fire season, which was the peak year in area burned in Nahuel Huapi NP, coincided with the driest calendar year (1998) and the warmest spring (Oct–Nov 1998) in the c. 90-year instrumental climate record in the Park. Analyses of fire-climate relationships based on tree-ring reconstructions for the period 1740–1995 indicate the importance of infrequent dry, warm years linked to broad-scale ocean-atmosphere anomalies in creating conditions similar to those of the 1998–1999 fire season under which ignition and fire spread are possible in the wet forest environment (Kitzberger et al. 1997; Veblen

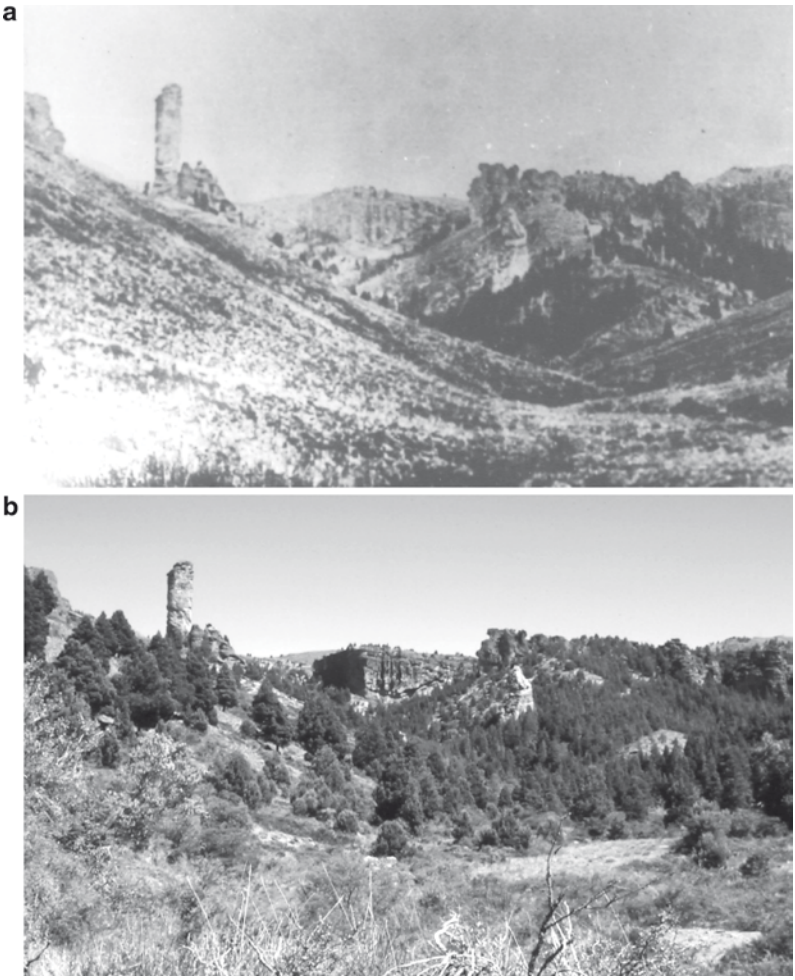

Fig. 2 Matched historical and modern photographs at the steppe and *Austrocedrus* woodland ecotone in Nahuel Huapi NP in (**a**) 1896 and (**b**) 1985. Woody encroachment into the bunchgrass and small-shrub dominated steppe has been by the native conifer *Austrocedrus chilensis* and small trees/shrubs *Schinus patagonicus* and *Discaria articulata* (Photographs: F.P. Moreno 1896 and T.T. Veblen 1985)

et al. 1999). Variability in the regional climate and fire occurrence in this region are strongly associated with variations in El Niño-Southern Oscillations (ENSO) and high latitude circulation patterns. Tree-ring records of the past c. 300 year indicate that natural variability in the regional climate creates exceptional droughts of one to a few years at intervals typically of several decades or more and that during these droughts large areas of mesic forests and even Andean rainforests burn.

Under conditions of continued warming, which is most evident in this region since c. 1976 and is consistent with hemispheric and global trends, fire risk in the wet Andean forests is likely to continue to increase.

References

Kitzberger T, Veblen TT, Villalba R (1997) Climatic influences on fire regimes along a rain forest-to-xeric woodland gradient in northern Patagonia, Argentina. J Biogeogr 24:35–47

Veblen TT, Kitzberger T, Raffaele E, Mermoz M, González ME, Sibold JS, Holz A (2008) The historical range of variability of fires in the Andean-Patagonian *Nothofagus* forest region. Int J Wildland Fire 17:724–741

Veblen TT, Kitzberger T, Villalba R, Donnegan J (1999) Fire history in northern Patagonia: The roles of humans and climatic variation. Ecol Monographs 69:47–67

Part IX
Earthquakes

Trees displaced along the fault scarp of Hebgen Lake Earthquake in 1959 (© M. Bekker)

Tree Rings and Earthquakes

Matthew F. Bekker

1 Introduction

The lithosphere, earth's rigid outer shell comprising crust and upper mantle rock, is broken into about 14 tectonic plates (Christopherson 2009) that move a few centimeters per year over superheated, pliable rock underneath. Forces within earth's interior push, pull and twist the plates in different directions, producing three types of plate boundaries: convergent (colliding with one another), divergent (moving away from one another) and transform (sliding past one another). Earthquakes occur when plates become locked together, building strain between and within them that is suddenly released, sending a burst of seismic waves that cause shaking and displacement of the surface. Nearly 95% of earthquakes are due to movement along plate boundaries, particularly convergent boundaries surrounding the Pacific Ocean and a mix of transform and convergent boundaries extending southeast from the Mediterranean region of Europe to Indonesia (Wicander and Monroe 2009) (Fig. 1). However, faults can also develop within plates, and intraplate earthquakes strong enough to affect humans and to be recorded in tree rings have occurred (e.g. Sheppard and White 1995; VanArsdale et al. 1998; Carrara 2002; Bekker 2004).

Plate boundaries can occur between any combination of dense oceanic or less dense continental crust, producing six potential combinations of crust type and plate boundary (Table 1). Subduction zones develop when dense oceanic crust collides with and is forced underneath less dense continental crust or another plate comprised of oceanic crust. The plates are in contact with each other from the surface to a depth of several hundred kilometers, thus earthquakes can be centered near the

M.F. Bekker (✉)
Department of Geography, Brigham Young University, Provo, UT 84602, USA
e-mail: matthew_bekker@byu.edu

M. Stoffel et al. (eds.), *Tree Rings and Natural Hazards: A State-of-the-Art*,
Advances in Global Change Research 41, DOI 10.1007/978-90-481-8736-2_36,

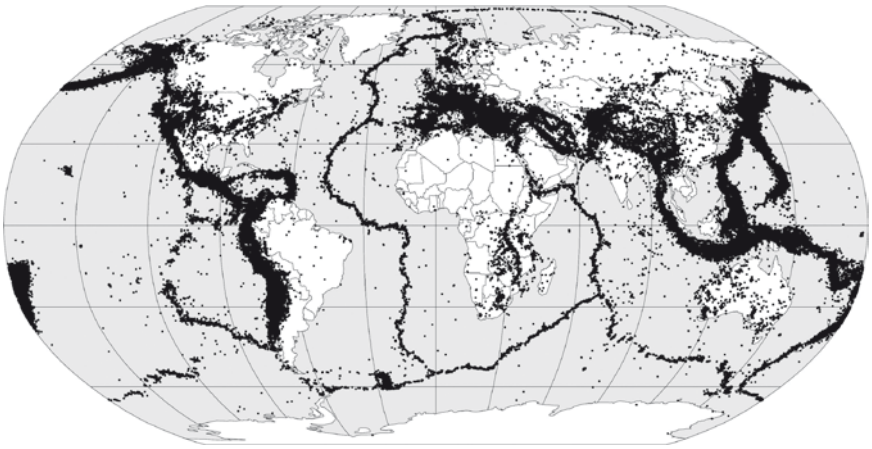

Fig. 1 Location of epicenters for all earthquakes recorded between 1963 and 1998. Lowman et al. 1999. Public domain

Table 1 Seismic features and hazards associated with tectonic plate boundaries

Boundary type	Crust type	Features and seismic activity
Convergent	Continental–continental	Mostly shallow-focus earthquakes; e.g. Himalayas
–	Continental–oceanic	Subduction zones; shallow and deep-focus earthquakes; e.g. NW USA; western S. America
–	Oceanic–oceanic	Subduction zones; shallow and deep-focus earthquakes; e.g. western Pacific Ocean
Divergent	Continental–continental	Shallow-focus earthquakes from offsetting transform faults; e.g. Iceland; E. Africa
–	Continental–oceanic	Nonexistent or short-lived (quickly becomes oceanic-oceanic)
–	Oceanic–oceanic	Shallow-focus earthquakes from offsetting transform faults; e.g. middle Atlantic Ocean
Transform	All	Shallow-focus earthquakes; e.g. southern California, USA, southern Mediterranean; western India

surface (shallow-focus) or deeper underground (deep-focus). In contrast, earthquakes along transform plate boundaries always occur near the surface (shallow-focus). A shallow-focus earthquake typically causes more damage than a deep-focus earthquake of the same magnitude because the energy is less dissipated when it reaches the surface (Wicander and Monroe 2009). At divergent boundaries the plates are not actually in contact with each other, but new crust is being formed between them as they spread apart. Earthquakes occur near these boundaries because of small, offsetting transform faults and thus are also shallow-focus.

Although millions of earthquakes occur annually, about 98% of them have a magnitude less than 3 on the Richter scale (Smith and Petley 2009), too small to be

felt by humans or to be recorded in tree rings. The modified Mercalli scale measures earthquake intensity indirectly by assessing the impact on various structures, including trees, on a scale ranging from I to XII. At level V trees are 'shaken slightly,' at VI 'slightly to moderately,' at VII 'moderately to strongly' and at VIII 'strongly,' including broken branches or trunks. For comparison, at level VIII shaking is strong enough to overturn very heavy furniture, break stone walls, and do "considerable" damage to unreinforced buildings, including wooden homes (Wood and Newman 1931, 279–280).

2 Application of Tree-Ring Research to Earthquakes

Earthquakes can produce a variety of tree-ring responses in trees (see Jacoby 2010, this volume). Previous studies have used tree rings to date known modern or historical earthquakes, most of them from sites at tectonic plate boundaries, including convergent (e.g. Jacoby and Ulan 1983; Veblen et al. 1992; Yadav and Kulieshius 1992; Kitzberger et al. 1995; Allen et al. 1999; Vittoz et al. 2001), and transform boundaries (e.g. Page 1970; LaMarche and Wallace 1972; Meisling and Sieh 1980). Others have found evidence for known earthquakes from intraplate faults (Ruzhich et al. 1982; Stahle et al. 1992; Sheppard and White 1995; Van Arsdale et al. 1998; Lin and Lin 1998, 2010, this volume; Carrara 2002; Carrara and O'Neill 2003, 2010, this volume; Bekker 2004).

Tree rings can contribute to a better understanding of earthquake hazards and the reduction of their impacts by identifying unknown events, and by clarifying the magnitude, epicenter location, timing, or amount of displacement for known but poorly-understood historical events (Jacoby et al. 1988; Jacoby 1997, 2010, this volume). Such "paleoseismic" studies are rare, but a prominent example is the identification of a previously unknown, major earthquake and associated tsunami along the Cascadia Fault in northwestern North America in AD 1700 (Atwater et al. 2005). This quake induced coastal subsidence and produced a tsunami that struck both the Pacific coast of North America and Japan. This discovery required a combination of: (1) tree-ring data, including death dates, growth rates prior to death, and ring-width changes (Atwater and Yamaguchi 1991; Jacoby et al. 1995; 1997; Yamaguchi et al. 1997); (2) geologic evidence, including radiocarbon dates and the preservation of plants in growth position in North America. (e.g. Atwater and Yamaguchi 1991; Atwater et al. 1991); and (3) historical, written evidence of a tsunami in Japan (Satake et al. 1996). This work demonstrated the potential for very large earthquakes, probably greater than Richter magnitude 9 (Yamaguchi et al. 1997; Atwater et al. 2005) to occur in the region, for which no information was available through historical records.

In another paleoseismic study, Wells et al. (1999) used ^{14}C to date several prehistoric earthquakes along a transform plate boundary in New Zealand. The most recent event was dated between 1665 and 1840. Tree-ring data showed strong and synchronous ring-width suppressions at several sites along the fault that were

initiated between AD 1717 and 1719. Noting that 1–2 year delays between the timing of damage and physiological response are not uncommon, they suggested that the most recent earthquake occurred after the 1716 growing season but before the end of the 1717 growing season.

3 Future Research Needs and Challenges

One of the principal challenges in using tree rings to identify earthquakes is finding trees that have recorded the event. Many studies have focused on "event-response" trees, which exhibit obvious damage and are located within a few meters of a fault scarp. This technique may increase the probability of finding a response in a given tree, and certainly makes it easier to attribute the response to an earthquake rather than some other factor. However, Bekker (2004) studied spatial variation in tree-ring responses to the 1959 Hebgen Lake (Montana) earthquake and found that: (1) trees that recorded a response in their rings did not always show external damage; (2) distance from the fault scarp, up to 58 m, had little effect on the proportion of trees recording a response; (3) trees below the scarp, on the downthrown block, were much more likely to record a response than those on the stationary block above the scarp; and (4) larger (mean 74 cm DBH) and older (mean 259 year) trees were more likely to record a response regardless of their position above or below the scarp (Fig. 2). These results suggest that dendroseismological studies can benefit from a research design that includes sampling over broader areas (at least tens of meters from a scarp), recording the position of trees relative to scarps, and sampling a range of tree sizes and ages. Such a design would require greater care to identify control trees, but would increase the likelihood of finding trees with a response and may reveal details about block movement for an unknown quake.

Another potential way to expand the identification of earthquakes through tree-ring analysis is by examining the effects of seismologically-induced landslides (Carrara and O'Neill 2003, 2010, this volume). Landslides can be triggered hundreds of kilometers from an earthquake's epicenter, and can damage trees over a much more extensive area than that produced by shaking alone. This method does, however, require independent evidence of a synchronous earthquake, and care to rule out climatic or other potential triggers of landslides.

It is well known that a tree may respond differently to an earthquake around its circumference, as with the formation of reaction wood when trees are tilted. Hamilton (2010, this volume) notes that trees may also show differing responses vertically on the stem. He found evidence of the 1700 Cascadia and 1959 Hebgen Lake earthquakes by sampling several meters above the ground, where trees are more likely to be directly damaged by acceleration and whiplash. LaMarche and Wallace (1972) also noted that dating leaders on a broken stem could precisely date the timing of such damage from an earthquake. Sampling trees in this way may reveal responses that are not recorded near the ground.

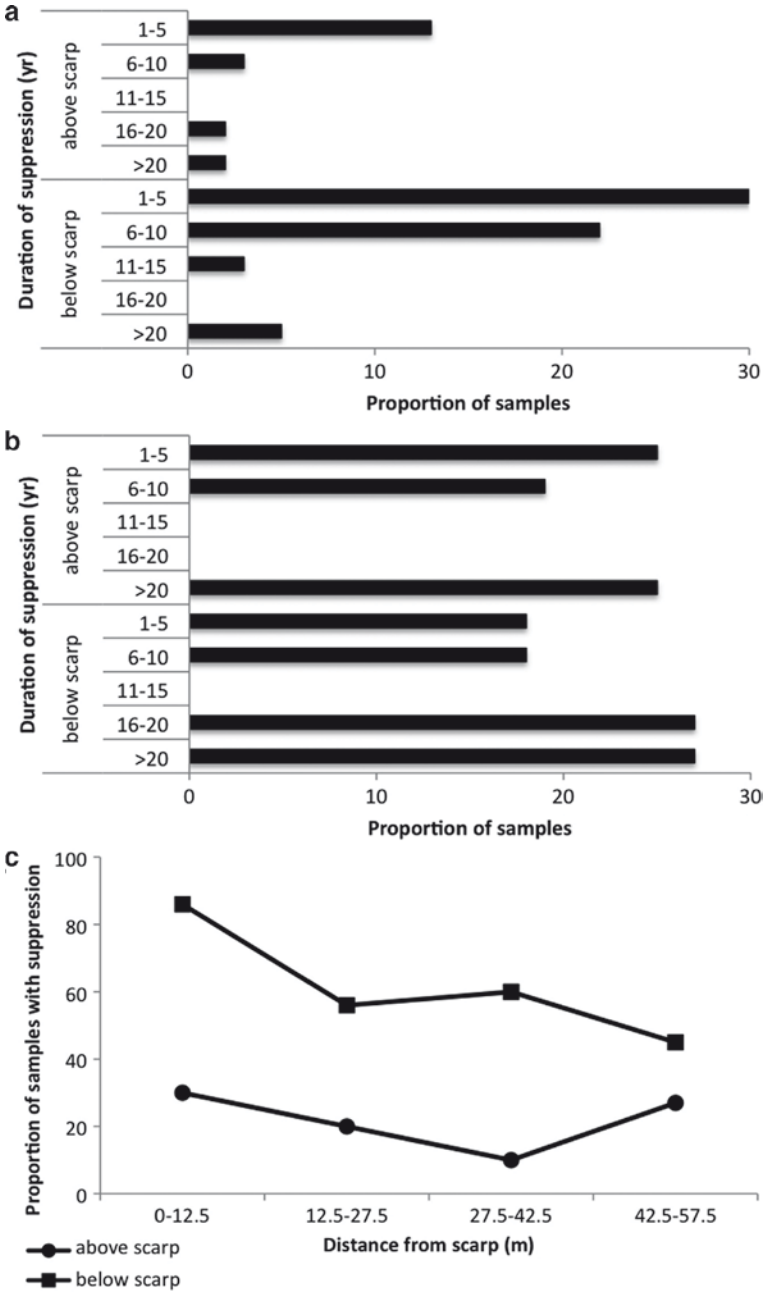

Fig. 2 Data from a dendroseismological study of the 1959 Hebgen Lake, Montana earthquake showing (**a**) higher number of growth suppressions below than above the fault scarp for all tree ages and sizes; (**b**) more even number of suppressions above vs. below the scarp for the largest and oldest trees; and (**c**) weak effect of distance from the scarp (up to 58 m) on the proportion of trees recording a suppression (Redrawn from Bekker 2004)

Most studies of tree-ring responses to earthquakes have appropriately been conducted along plate boundaries, where most earthquakes occur and human population densities are high. However, major intraplate quakes threaten large populations near several faults in China, the Wasatch Fault in Utah, and the New Madrid Fault in the Midwestern U.S. among others. Recurrence probabilities for earthquakes along intraplate faults are also difficult to estimate because the forces behind them are usually poorly understood and movement is less consistent than at plate boundaries. Thus, dendroseismological studies may be particularly valuable in clarifying the behavior of intraplate faults.

References

Allen RB, Bellingham PJ, Wiser SK (1999) Immediate damage by an earthquake to a temperate Montane forest. Ecology 80:708–14

Atwater BF, Stuiver M, Yamaguchi DK (1991) Radiocarbon test of earthquake magnitude at the Cascadia subduction zone. Nature 353:156–158

Atwater BF, Musumi-Rokkaku S, Satake K, Tsuji Y, Ueda K, Yamaguchi DK (2005) The orphan tsunami of 1700. US Geol Surv Prof Paper 1707

Atwater BF, Yamaguchi DK (1991) Sudden, probably coseismic submergence of Holocene trees and grass in coastal Washington State. Geology 19:706–709

Bekker MF (2004) Spatial variation in the response of tree rings to normal faulting during the Hebgen Lake Earthquake, southwestern Montana, USA. Dendrochronologia 22:53–59

Carrara PE (2002) Response of Douglas Firs along the fault scarp of the 1959 Hebgen Lake earthquake, southwestern Montana. Northwest Geol 31:54–65

Carrara PE, O'Neill JM (2003) Tree-ring dated landslide movements and their relationship to seismic events in southwestern Montana, USA. Quat Res 59:25–35

Carrara PE, O'Neill JM (2010) Tree-ring dated landslide movements and seismic events in southwestern Montana, U.S.A. In: Stoffel M, Bollschweiler M, Butler DR, Luckman BH (eds) Tree rings and natural hazards: A state-of-the-art. Springer, Berlin, Heidelberg, New York, this volume

Christopherson RW (2009) Geosystems: an introduction to physical geography, 7th edn. Pearson Prentice Hall, New Jersey

Hamilton WL (2010) Seismic damage in conifers from Olympic and Yellowstone National Parks, United States. In: Stoffel M, Bollschweiler M, Butler DR, Luckman BH (eds) Tree rings and natural hazards: A state-of-the-art. Springer, Berlin, Heidelberg, New York, this volume

Jacoby GC (1997) Application of tree ring analysis to paleoseismology. Rev Geophys 35:109–124

Jacoby GC, Ulan LD (1983) Tree ring indications of uplift at Icy Cape, Alaska, related to 1899 earthquakes. J Geophys Res 88:9305–9313

Jacoby GC, Sheppard PR, Sieh KE (1988) Irregular recurrence of large earthquakes along the San Andreas fault: evidence from trees. Science 241:196–198

Jacoby GC, Carver G, Wagner W (1995) Trees and herbs killed by an earthquake 300 yr ago at Humbolt Bay, California. Geology 23:77–80

Jacoby GC, Bunker DE, Benson BE (1997) Tree-ring evidence for an A.D. 1700 Cascadia earthquake in Washington and northern Oregon. Geology 25:999–1002

Jacoby GC (2010) Application of tree-ring analysis to paleoseismology. In: Stoffel M, Bollschweiler M, Butler DR, Luckman BH (eds) Tree rings and natural hazards: A state-of-the-art. Springer, Berlin, Heidelberg, New York, this volume

Kitzberger T, Veblen TT, Villalba R (1995) Tectonic influences on tree growth in northern Patagonia, Argentina: the roles of substrate stability and climatic variation. Can J Forest Res 25:1684–96

LaMarche VC, Wallace RE (1972) Evaluation of effects on trees of past movements on the San Andreas Fault, northern California. Geol Soc Am Bull 83:2665–2676
Lin A, Lin S (1998) Tree damage and surface displacement: the 1931m 8.0 Fuyun earthquake. J Geol 106:751–757
Lin A, Lin SJ Lin (2010) Tree ring abnormality caused by large earthquake: an example from the 1931 M 8.0 Fuyun earthquake. In: Stoffel M, Bollschweiler M, Butler DR, Luckman BH (Eds) Tree rings and natural hazards: A state-of-the-art. Springer, Berlin, Heidelberg, New York, this volume
Lowman P, Yates J, Masuoka P, Montgomery B, O'Leary J, Salisbury D (1999) A digital tectonic activity map of the earth. J Geosci Ed 47:428–437
Meisling KE, Sieh KE (1980) Disturbance of trees by the 1857 Fort Tejon earthquake, California. J Geophys Res 85:3225–3238
Page R (1970) Dating episodes of faulting from tree rings: effects of the 1958 rupture of the Fairweather Fault on tree growth. Geol Soc Am Bull 81:3085–3094
Ruzhich VV, San'kov VA, Dneprovskii YI (1982) The dendrochronological dating of seismogenic ruptures in the Stanovoi Highland. Soviet Geol Geophys 123:57–63
Satake K, Shimazaki K, Tsuji Y, Ueda K (1996) Time and size of a giant earthquake in Cascadia inferred from Japanese tsunami records of January 1700. Nature 379:246–249
Sheppard PR, Jacoby GC (1989) Application of tree-ring analysis to paleoseismology: two case studies. Geology 17:226–229
Sheppard PR, White LO (1995) Tree-ring responses to the 1978 earthquake at Stephens Pass, northeastern California. Geology 23:109–12
Smith K, Petley DN (2009) Environmental hazards: assessing risk and reducing disaster, 5th edn. Routledge, New York
Stahle DW, VanArsdale RB, Cleaveland MK (1992) Tectonic signal in baldcypress trees at Reelfoot Lake, Tennessee. Seismol Res Lett 63:439–448
VanArsdale RB, Stahle DW, Cleaveland MK, Guccione MJ (1998) Earthquake signals in tree-ring data from the New Madrid seismic zone and implications for paleoseismicity. Geology 26:515–518
Veblen TT, Kitzberger T, Lara A (1992) Disturbance and forest dynamics along a transect from Andean rain forest to Patagonian shrubland. J Veg Sci 3:507–520
Vittoz P, Stewart GH, Duncan RP (2001) Earthquake impacts in old-growth *Nothofagus* forests in New Zealand. J Veg Sci 12:417–426
Wells A, Yetton MD, Duncan RP, Stewart GH (1999) Prehistoric dates of the most recent Alpine fault earthquakes, New Zealand. Geology 27:995–998
Wicander R, Monroe JS (2009) Essentials of physical geology, 5th edn. Brooks-Cole, Belmont, CA
Wood HO, Newman F (1931) Modified Mercalli intensity scale of 1931. Bull Seismol Soc Am 21:277–283
Yadav RR, Kulieshius P (1992) Dating of earthquakes: tree-ring responses to the catastrophic earthquake of 1887 in Alma-Ata, Kazakhstan. Geogr J 158:295–299
Yamaguchi DK, Atwater BF, Bunker DE, Benson BE, Reid MS (1997) Tree-ring dating the 1700 Cascadia earthquake. Nature 389:922–923

Application of Tree-Ring Analysis to Paleoseismology

Gordon C. Jacoby

1 Introduction

Knowledge of the seismicity for a region is one of the keys to estimating earthquake hazards. Unfortunately, historical records are generally inadequate for evaluations of seismicity. Paleoseismology addresses this problem using various techniques for determining the times and locations of earthquake disturbances. Trees, with widespread geographical distribution, identifiable annual-growth increments, and sensitivity to environmental changes, can provide an almost unique tool for dating past earthquake events. Geomorphic and hydrologic changes and dynamic stress resulting from earthquakes can cause a variety of effects in trees and communities of trees. Tree-ring analysis can (1) produce the actual year and sometimes the season for disturbance events and (2) establish synchronicity for events that may be beyond the range of absolute calendar dating. Tree-ring dating or dendrochronology is used to establish exact dates based on patterns of annual-ring variations through time. Mere counting of rings is inadequate and may lead to errors in assigning dates to rings because of possible missing, micro, or false rings. Trees ranging in age from 300–500 years grow in many places and can be used to identify previously unknown seismic events or to better define events that are partially known. Longer time spans can be covered in some instances. Earthquakes may be more precisely located in space and time or have their magnitudes and displacements better estimated by analysis of tree rings. A number of studies have established the validity

G.C. Jacoby (✉)
Tree-Ring Laboratory, Lamont-Doherty Earth Observatory, Columbia University, Palisades, NY 10964, USA
e-mail: druid@Ldeo.columbia.edu

M. Stoffel et al. (eds.), *Tree Rings and Natural Hazards: A State-of-the-Art*, Advances in Global Change Research 41, DOI 10.1007/978-90-481-8736-2_37,

of tree-ring application to paleoseismology but only a few studies have contributed new information to the paleoseismic record. A review of the application of tree-ring analysis to paleoseismology is in Jacoby (1997). The science should now move from the discovery phase to a wider application phase. Successful applications will add important information to the records of seismicity and the evaluation of earthquake hazards.

Although there are accurate dates of earthquakes in some ancient writings, the detailed record of earthquakes is very sparse, incomplete and short for most of the world. Even in the last two centuries when records are more complete (e.g. Gu 1983), adequate information to accurately determine depths, intensities, and extent of deformation or surface rupture of earthquakes is lacking. Approximate estimates of intensities barely extend to the early 1800s in the United States (Coffman and von Hake 1973). Instrumental records of seismic events began only in the last hundred years (Lee et al. 1988). Paleoseismology is contributing greatly to the regional seismicity record and is providing improved estimates of potential earthquake hazards (Prentice et al. 1994; Atwater et al. 2003).

Various geochronological dating methods have been applied to earthquake-disturbed materials to obtain paleoseismic information (e.g. Crone and Omdahl, 1987; Prentice et al. 1994). However, most of these dating techniques have substantial uncertainties and lack annual resolution. The ability of tree-ring analysis to yield the actual or relative year and sometimes even the season of an earthquake is almost unequaled. The phrase "tree-ring analysis" is used herein, rather than dendrochronology, to emphasize that the application to paleoseismology goes beyond dating of rings to the analysis of the rings and micro-anatomy to determine what may have actually damaged the tree. The longevity of some tree species is such that absolute dates can be determined for events during recent centuries to millennia (Jacoby 1987). Relative tree-ring dating between samples from different locations can show whether events were simultaneous (within the same year or possibly season) even if the events are beyond the time limits of absolute tree-ring dating. Such synchronicity of disturbance can aid in inferring a single cause like earthquake. Sampling of living trees can be done non-destructively using hollow increment borers to obtain 5 or 12 mm diameter cores for analysis.

Tree shaking and damage to trees are mentioned often in early observations of earthquakes (e.g. Lawson 1908; Fuller 1912; Jepson 1923; Louderback 1947; Gu 1983). Some criteria of the Mercalli scale for classification of earthquake severity are based on the degree of tree disturbance (Wood and Neumann 1931). The concept that trees can provide information related to earthquakes dates back at least to the 1800s when Lyell (1849) concluded that earthquakes such as the New Madrid series, 1811–12, had not occurred for many years because he did not see older dead trees similar to those killed by the earthquakes. Later McGee (1892) attributed tree-establishment ages to the New Madrid earthquakes. He used simple ring counting to estimate ages of trees growing on uplifted and drained land raised by the earthquakes.

2 Radiocarbon Measurements and Tree-Ring Dating

Radiocarbon dating of wood should not be confused with tree-ring dating and analysis. Radiocarbon measurement, especially high-precision measurement, is an extremely useful dating tool for paleoseismic studies (e.g. Sieh et al. 1989; Fumal et al. 1993). High-precision measurements from mass spectrometers coupled with the improved calibration curves (Stuiver et al. 1998) can sometimes determine the ages of organic material, including tree rings, within a range of decades. Radiocarbon dating and tree-ring analysis can complement one another when the radiocarbon analyses guide the tree-ring analyses toward a limited temporal span in which to look for a tree-ring crossdate or when tree-ring analysis can show a disturbance in, or death of, an old tree placed in time by radiocarbon dating. There are parts of the radiocarbon calibration curve where there is a narrower range of dates spanned by the calibration of a radiocarbon-dated sample (Stuiver et al. 1998). If a wood sample has enough rings, a carefully selected second ring or set of rings can be radiocarbon dated to try to narrow the range of calendar dating for the second sample. Two ^{14}C dates from different parts of the same specimen a specific number of rings apart can be used to cross-validate the radiocarbon results (e.g., Jacoby et al. 1992). The phrase "tree-ring dating" or variations thereof should be reserved for exact tree-ring crossdating, either absolutely to calendar years or relatively between samples. Radiocarbon dating of a wood sample is not a tree-ring date.

3 Background

Tree-ring analysis is potentially useful in paleoseismology at any location where surface rupture, geomorphic or hydrologic disturbance, or accelerations and displacement due to an earthquake can affect tree growth. Individual trees and sites can confirm and date an earthquake. A network of disturbed trees or sites could provide information about the size of an earthquake or rupture length. The degree and type of tree disturbance will be in response to the depth, magnitude, geologic setting of the earthquake, and its location relative to the tree site. Earthquakes can directly cause surface rupture, elevation change, accelerations, and displacement. They also cause secondary effects such as altered hydrology, tsunami, landslides, and liquefaction. Trees can occupy areas of potential liquefaction or other unstable locations such as steep slopes and unconsolidated deposits. Large earthquakes, even centered at considerable distance, can disrupt these unstable growth sites and induce change in the normal growth-ring patterns. Tree-ring analysis can date the timing of these effects but usually needs supporting lines of evidence to establish an earthquake as the cause.

The tree-ring dating of earthquake-induced, land-surface changes is essentially applying tree-ring analysis to geomorphology and hydrology. Alestalo (1971) first described most of the fundamental types of tree response to geomorphic processes.

Building on these ideas and others, Shroder (1980) introduced the concept of "process-event-response" systems in relation to effects of geomorphic events on trees. The systems can be equated to the concept of earthquake causing dynamic stress and/or geomorphic and hydrologic change, and the ensuing response of trees. Detection of the tree-recorded earthquake signal calls for (1) understanding of the possible local and regional dynamics and types of geomorphic or hydrologic changes that occurred, (2) dating and quantification of changes in growth-ring patterns or tree growth, and (3) knowledge of growth-ring variations or tree growth in undisturbed trees (preferably the same species) in the same region as the disturbed site for comparison.

A variety of earthquake-induced effects can be recorded by trees. Table 1 evolved from previous publications (Alestalo 1971; Shroder 1980; Sheppard and Jacoby 1989) and depicts the principle ways earthquakes can affect trees. There can be direct physical breakage of tops, trunks and roots due to acceleration, displacement, and root-zone compression or extension. If the damage is severe, there are changes in the growth rings that are different from normal growth variations due to other causes, primarily climate. Earthquake-induced changes in land surface can disturb tree growth sites by causing tilting; burial; damming of rivers to flood forests; uplift to create, improve or damage growth environments; subsidence to cause drowning or deterioration of growth environments; corrasion or scarring of trees by rockfall or landslide debris; and other physical damage by earthquake-activated geologic materials. Alestalo (1971) also introduces the idea that geomorphic events can change the age structure or species composition of tree communities. As examples: (1) increased mortality due to disturbance could affect larger, overstory trees that are more vulnerable to toppling from acceleration and displacement, leaving a community of smaller, more resilient, mostly younger trees; (2) transient flooding could change species composition as only more tolerant species survive. In these cases the effects in Table 1 are applied to whole stands of trees rather than a few individuals.

The longevity of trees permits extension of the seismic record. There are several species throughout the world that live 800–1,000 years or more. A partial list of common names includes bristlecone pine (*Pinus aristata, longavea, balfouriana*), baldcypress (*Taxodium distichum*), Douglas fir (*Pseudotsuga menziesii*), mountain hemlock (*Tsuga mertensiana*), Alaska or yellow cedar (*Chamecyparis nootkatensis*), juniper (*Juniperus*), larch (*Larix*), lodgepole pine (*Pinus contorta*), limber pine (*Pinus flexilis*), sequoia, coast redwood (*Sequoia sempervirens)*, eastern white cedar (*Thuja occidentalis*), and red cedar (*Thuja plicata*) in North America; alerce (*Fitzroya cupressoides*) and *Araucaria* in South America; huon pine (*Lagarostrobos franklinii*) in Tasmania; and several other trees such as juniper (often "Sabina" in Asian papers) in Asia where tree-ring analysis has only recently been extensively undertaken. Some of these species, such as sequoia and huon pine, are restricted in distribution so their use in paleoseismology is unlikely. Species in the 300–500 year age range are more widely distributed and are most likely to be used in paleoseismologic studies. In addition to longevity, use of subfossil and relict trees and wood can be crossdated with living trees to extend the records.

Table 1 Trees as indicators of seismic disturbance

Change in trees[a]	Physical change	Possible cause
Physical damage (unusually narrow or missing rings, abnormal cells)	Top, major limb, trunk, or root system broken off	Violent shaking and/or local earth movement
	Corrasion, scarring impacting tree	Seismically-activated material e.g. landslide, seiche, tsunami
Growth rate change		
Increase (wider rings)	Improved growth environment, nutrient supply, or site hydrology	Change of site into more favorable conditions, loss of competitors
Decrease (narrower rings)	poorer growth environment, nutrient supply, or site hydrology	Change of site into less favorable conditions
Variation increase (ring width change inconsistently)	Some damage, some competitors felled, surface disturbed	Disturbance overrides normal growth trends
Reaction wood[b]	Ground surface tilted or tree pushed over, partial flooding	Surface rupture, landslide, tilting minor subsidence
Traumatic resin canals[c]	Partial flooding	Minor subsidence
Tree growth initiated (date of first ring)	Barren surface stabilized, or newly available	Uplift, change in base level, landslide, or other catastrophic event
Tree growth terminated (date of terminal ring)	Surface covered burying trees	Rapid sedimentation, landslide or other catastrophic event
	Surface inundated	Subsidence, drainage blocking

[a] Some of these changes can be caused by biological, climatic, or other factors that must be considered when making interpretations. Accurate dating and sampling from a number of appropriate locations are the means to confirm interpretations. Changes should be compared to undisturbed growth in the same region.

[b] Reaction wood is defined here to mean the geotropic (gravity-influenced growth) response by an inclined tree to regain its vertical stance and strengthen its lower trunk (Low 1964; Scurfield 1973; Shroder 1980; Timmell 1986). In conifers the darker, thicker-walled cells are called compression wood. Similar appearing cells can also be caused by partial flooding.

[c] Traumatic resin canals are open vertical pores surrounded by abnormal cells. The canals are caused by various trauma including partial flooding (Kozlowski et al. 1991).

4 Types of Earthquake Events That Can Imprint the Tree-Ring Record

4.1 Dating of Surface Ruptures and Disturbances

One of the most straightforward effects of earthquakes on trees is the direct physical damage to trees growing on a surface rupture or in a zone of distributed shear. The displacement and accelerations of the substrate can crush or rip apart the root systems,

snap off major limbs or tops of the trees, cause internal stresses, and tilt trees away from vertical. The top, or crown, usually contains the major portion of the photosynthetic surface producing carbohydrates for tree growth and the buds in the crown produce essential growth regulating substances (Kozlowski 1971, 104–105). Roots absorb water and minerals, and also seasonally store reserves for later growth (Kramer and Kozlowski 1979). Trauma to crown or roots can result in abrupt decrease in ring widths, missing rings, or even death. Damaged trees reallocate resources to replace roots and crown which are much more essential to tree survival than radial growth of the trunk (Gordon and Larson 1968).

Study of Jeffrey pine and white fir trees growing on the San Andreas Fault near Wrightwood, California showed dramatic decrease in growth and missing rings due to trauma in some of the most severely-damaged trees (Fig. 1; Jacoby et al. 1988). If only ring counting had been used, missing rings and/or barely-visible micro-rings in some trees after the trauma would have led to placing the disturbance in different years in different trees and decades later than it was. The primary method of dating was crossdating the rings prior to the event with a control chronology based on undamaged trees away from the fault zone. Then the outer rings were dated independently. This crossdating placed the first rings showing trauma at 1813 for the fault-zone trees. The 1812 rings were fully formed and showed no unusual growth

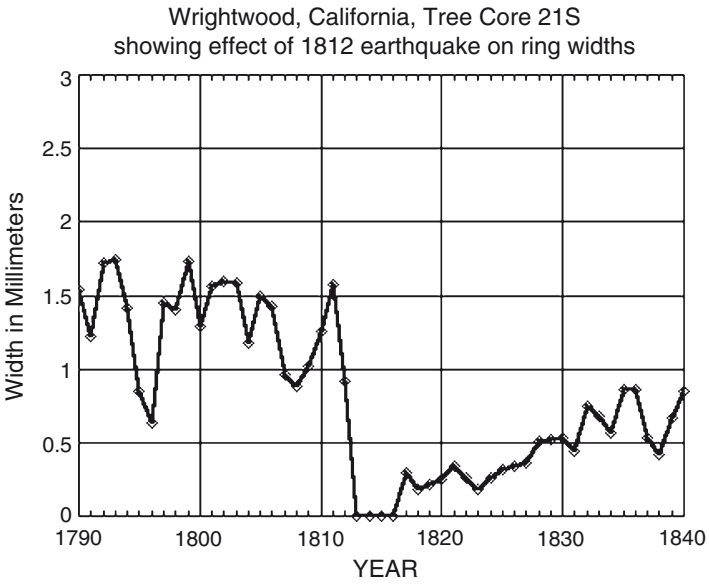

Fig. 1 Plot of ring-widths of a core sample from a tree disturbed by the 1812 earthquake on the San Andreas Fault in California. Note there was no radial growth shown in this core for 4 years after the earthquake and by 1840 it had barely recovered its previous growth rate, The roots of this tree were in the zone of distributed shear from the surface rupture and the tree must have experienced strong accelerations and displacement during the earthquake

so the disturbance must have occurred after the growing season of 1812 and before the start of cambial growth in 1813. The tree-ring analyses were combined with historical records from Spanish missions on the coast to deduce that there was a rupture along the San Andreas fault in December of 1812 (Jacoby et al. 1988). There are also narrow rings in the trees due to drought but the effects of droughts are restricted to one or two rings whereas the earthquake caused an immediate reduction in ring width and gradual recovery to normal growth over several years to decades (Fig. 1). The restriction of damaged trees to a narrow zone along the fault is also key to the interpretation (Jacoby et al. 1988).

Younger trees are more resilient and less affected by accelerations and displacements. The older, usually larger, trees with greater inertia and more extensive root distribution show more damage. Thus trees may not be responsive to, or record, earthquake disturbance at their earliest stages of growth. An old tree may have experienced an earthquake without discernible damage during its early years.

Tilting of trees at a fault rupture can leave a clear signal of disturbance in trees by the formation of reaction wood in response to the inclination. Trees have a built-in geotropism which causes them to seek upright growth after tilting. The mechanism for restoring vertical growth is to form reaction wood to push or draw the tree back to a vertical orientation (Kramer and Kozlowski 1979; Timell 1986). In conifers (gymnosperms) the reaction is to grow compression wood of wider rings on the downward side of the tree trunk to help restore vertical growth. This wood is easily recognized by its darker color and thicker-walled cells. Reaction wood can be initiated in some species by a tilt of only 2° and can start to form within weeks of the tilting (Low 1964; Panshin and de Zeeuw 1970; Scurfield 1973; Timell 1986). Conifers exhibit two types of reaction wood. Reaction wood can occur as thick-walled cells with the same appearance as normal latewood only in an unusual wider band (Panshin and de Zeeuw 1970). It can also have a distinct yellowish to reddish color. The two types can occur within the same ring. In broadleaf trees (angiosperms) the reaction wood is termed tension wood and forms on the upward side of the tree. Tension wood is usually more difficult to recognize. The initiation year of reaction wood can be found by crossdating. Once the beginning of the reaction wood ring is located, the year or possibly even time of year for formation of the first reaction wood cells can be determined.

Effects of an earthquake can vary even within one tree. Figure 2 shows the ring-width variations of three cores from the same tree at the edge of the San Andreas Fault in California. Two radii show reaction wood, distorted cells, and substantial growth increase. In the third radius reduced growth is not very different from normal growth variations. Multiple cores from different directions are essential for thorough sampling and analyses.

Broken tops, root damage, tilting, and reaction wood can also be caused by windstorm, erosion or landslide of non-seismic origin. A nearby control chronology is essential to see if there was widespread damage or tilting of trees at locations away from the fault zone at the same time. An essential part of an analysis must be the geographic distribution of disturbed trees in relation to geologic features. An interpretation of seismic cause is supported if the disturbance is confined to trees in close proximity (within a few tens of meters) to the surface rupture.

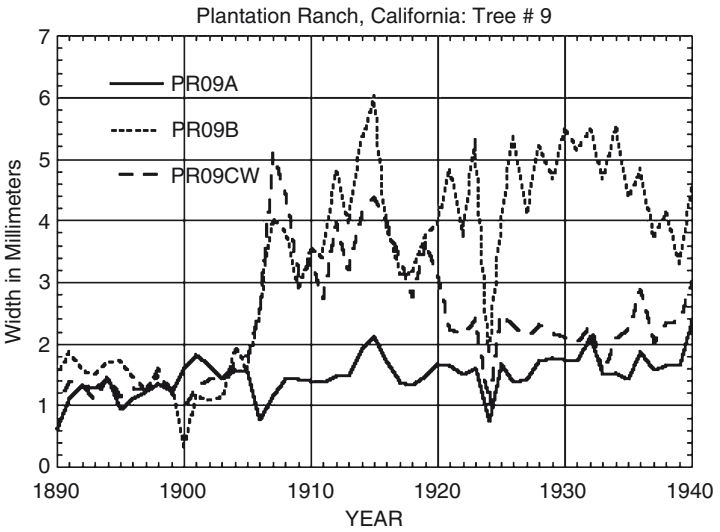

Fig. 2 Plot of ring widths of three core samples from a coastal redwood growing at the edge of a surface rupture due to the 1906 earthquake on the San Andreas Fault in California. One radius shows little effect but the other two have dramatically increased growth and reaction wood formed as a result of tilting. One core also has distorted cell structure from strain within the tree. A few normal cells formed in early 1906 before the earthquake so the tree recorded the event as early spring 1906

4.2 Dating of Earthquake-Induced Elevation or Base-Level Changes

Two related surficial changes that can affect tree growth in coastal or lowland areas are uplift to provide a new growth area and subsidence to cause inundation of trees. In the first case, the minimum age of the surface can be determined by the age of the oldest trees established on the new surface. In the second case, the actual year or possibly even season of the inundation can be established by tree-ring dating of the last growth ring before death or damage. If the dead trees cannot be crossdated with other tree-ring chronologies of known age, the date can be estimated by ^{14}C analyses. The dead trees can be crossdated with each other to learn whether the deaths were sudden and simultaneous or gradual over time. A rapid progression of death would indicate an abrupt event like an earthquake rather than a gradual rise in sea level (e.g. Jacoby et al. 1995).

Several factors can affect age estimates of a newly-uplifted surface. The first is ecesis or the germination and survival of trees. Time necessary for ecesis can range from a growing season to many years depending on the presence of a nearby seed source, suitable bedding substrate, and climatic conditions favorable for seedling survival. Next is the problem of finding the oldest trees at the location of uplift. Many trees may have to be sampled for confidence that the oldest trees have been found.

Then there is the problem of obtaining the innermost, oldest ring. Coring at ground level and hitting the exact center or first ring of the tree are difficult. All of these factors tend to give less than the true age of the trees or surface. Thus the age of such samples and trees should usually be regarded as a minimum age for the surface under study.

Another extremely important factor in using trees to date an uplifted surface is whether the trees are truly the first generation of trees. Trees tend to have a certain longevity according to species and environment. Past this age they will die and be replaced. Eventually the maximum ages will be due to longevity and not to the time of original afforestation. Lack of soil development and/or relict debris from dead trees can indicate the likelihood of the trees being the first generation and thus dating the surface.

The presence of driftwood can either help or hinder the dating of uplifted coastal areas. There is considerable driftwood in many coastal areas and if not recognized as driftwood it could be mistakenly dated as the oldest tree on a surface, either by ^{14}C or tree-ring dating. Usually abrasion of roots and limbs or mode of emplacement can help distinguish driftwood from *in situ* trees. On some raised coastlines, if nonforested because of harsh climate, lack of seed source, or unsuitable substrate; the age of the outer rings of the most recent driftwood above high tide levels can be used to estimate the minimum age of the uplift. However, one must be careful of emplacement of post-event driftwood above normal high tides by extreme storms.

In the situation of trees killed by inundation, the timing can usually be established more definitively. If the immersion is deep enough, trees can suffocate in a matter of weeks. If the root zone is flooded, soil becomes anoxic (Sanderson and Armstrong 1978) and respiration and water absorption are reduced (Kramer and Kozlowski 1979; Levitt 1980). Counter-intuitively, the upper tree dries out and leaves wither or even abscise. Submergence of the entire tree causes even quicker demise. The anatomy of the last-formed cells may help reveal when during the annual growth cycle the tree died. Cambial-cell division or radial growth in mid-latitudes may extend from spring through early fall. In the far north and at high elevations, the season of cambial-cell division may be only a few weeks in mid-summer (Burns and Honkala 1990). Cell development cannot show when during the dormant season a tree was disturbed or killed but cell anatomy and number could place an event within a month or less during the radial-growth season. With deep submersion and complete death of a tree, dendrochronological dating of the last cells formed gives the year of the event. An event during the non-growing season is dated to that season although the season includes parts of two calendar years in the northern hemisphere.

If submersion is relatively shallow, trees may take some time to expire and they may even survive if new higher roots can be developed to sustain the tree (Kramer and Kozlowski 1979). In general terms, trees typically survive if their roots are inundated in freshwater for less than half of the growing season but there is substantial variation between species (Gill 1970). In low coastal areas, subsidence of about a meter could produce periodic submergence at high tides and gradual salinization of the soil. These factors could result in a gradual death of low-lying trees

over several seasons (Jacoby et al. 1995). In areas around Cook Inlet that subsided during the 1964 Alaska earthquake, numerous trees were killed by inundation and soil salinization. Some at slightly higher or more favorable growth sites were severely damaged but, with the rebound since the earthquake, have recovered to near normal growth. That event and similar events can be dated by the death of the most severely affected trees (Yamaguchi 1991) or by the first year of damage to slightly more inland or higher survivors. Inland spruce trees near Girdwood, Alaska show tilting and reaction wood in 1964 and have now recovered to normal growth. Dating by year of death or damage must take into consideration the trees' ability to store photosynthates and growth hormones for subsequent growth. Trees have no central nervous system and portions can cease growth while other parts of the tree continue to function. We have all seen dead branches or large portions of a tree devoid of life while other parts continue to grow. This phenomenon must be considered in dating events such as shallow inundation or partial burial.

Earthquake-caused drainage blocking, while not an elevation change, can raise local base level and cause similar inundation effects in trees. The rate of inundation must be considered in the blocking of drainage by earth movement. Study or estimates of local streamflow and area of inundation will help to determine the rate of submersion. Higher sites in a valley could take several years to become flooded and give a later date for the event. Lake Waikaremoana, a landslide-dammed lake in New Zealand, took an estimated 10 years to fill (Adams 1981). The position of the trees is thus an important consideration. In the vicinity of sag ponds or blocked drainages, soil moisture can increase greatly even if actual drowning of trees does not take place. Events that substantially change the level of the water table can influence tree rings (Tonglin 1983 and unknown).

Decay is a very important factor in all year-of-death studies. Sapwood, comprising the outer sap-conducting rings in trees, is generally much more susceptible to decay than the inner heartwood (Panshin and de Zeeuw 1970). Metabolic processes of many tree species emplace extractive substances (some with fungicidal or bactericidal properties) in the heartwood causing its usually darker color. Heartwood formation varies greatly between species and even within species. The heartwood/sapwood boundary sometimes follows ring boundaries. Where the sapwood has decayed away, a smooth outer heartwood ring can give the appearance of being the outer ring of a tree. In the case of drowned trees in Lake Washington, Seattle, Washington, about 45 sapwood rings have been decayed away on all specimens not protected by partial burial in the sediments where sapwood and bark were preserved (Jacoby et al. 1992). Misinterpretation and dating of the outer heartwood rings as the outer rings of the trees would have placed the event about 45 years too early and would not have shown the simultaneous events.

The above sources of error must be taken into consideration in any study of trees on seismically uplifted, subsided or inundated surfaces. With the proper sampling and adjustment of ages for newly established trees, a limit can be placed on the minimum age of uplift. Seismically-induced changes in site hydrology can be dated if moisture supply to the tree is significantly changed. Subsidence and blocked drainages can damage or kill trees, leaving evidence in the survivors or time of

death information in relict trees, stumps or even roots. Geomorphic and hydrologic analyses are essential supplements to the tree-ring analysis to produce the best interpretation of cause and timing for these types of events.

4.3 Tsunami and Landslides

Dating of landslides can contribute important information to the paleoseismic record even though most landslides are not related to earthquakes. As in other situations, there must be supportive evidence for the inference of a seismic cause. Landslides can (1) directly damage trees by corrasion, (2) bury trees, (3) dam streams resulting in flooding and drowning of trees, and (4) carry trees into a unfavorable environment causing reduced growth or death. Landslide debris can provide a new surface for tree establishment.

Rapid burial by landslide or tsunami can preserve trees or parts of trees for tree-ring analysis and dating of the events. Geologists working in the coastal Pacific Northwest have identified many probable tsunami deposits (e.g. Atwater and Moore 1992 and Bucknam 1994). At a site near Seattle, Washington, part of a tree was incorporated in a tsunami deposit with the outer rings and bark intact. Crossdating showed that the tree from the tsunami site died at the same season of the same year as trees drowned by landslides at three sites into Lake Washington, Seattle, about 23 km away (Jacoby and Williams 1994). Although not dated to calendar year, the relative crossdating establishing simultaneous burial or drowning supports the inferred seismic cause for the tsunami and landslides leading to the tree deaths (Jacoby et al. 1992).

4.4 Liquefaction

Liquefaction results from many types of earthquakes. Liquefaction can be responsible for part or all of the subsidence related to an earthquake. If the subsidence is enough to inundate trees deeply or lethally, the year of death dates the event as discussed above. Liquefaction can destabilize loose wet sand in which trees may be rooted or it can disrupt competent soil above loose sand. Either process can cause tilting of trees that will be marked by the onset of reaction wood. Because there can also be tilting and downthrown trees due to high winds at unstable sites, evidence of liquefaction must be seen in the sediments to support the inference of a seismic event.

In the New Madrid region there are numerous sites of liquefaction. At some sites there are buried trees where initial burial appears to be by erupted sand layers from a source below the level of the original tree. The trees may have been killed or just damaged by the additional layer of sediment suffocating the root systems. Subsequent sedimentation helped to preserve the lower portion of the tree. The challenge here is to determine the year(s) of death or damage and to see if sites can be crossdated to show the geographic extent of simultaneous effects (Van Arsdale 1998).

4.5 Other Seismic Effects

Trees grow on many unstable substrates. On such sites, they are vulnerable to disturbance primarily due to storm but also due to accelerations from local or distant earthquakes. The estimated 800 km rupture length of the Alaska earthquake of 1964 was great enough to cause strong accelerations and elevation changes over a wide area (Plafker 1969). At Cape Suckling, Alaska 240 km from the epicenter but eastward along the rupture zone, Sitka spruce (*Picea sitchensis*) trees growing on an unconsolidated-sand beach ridge were shaken and tilted toward the sea. The roots were also disturbed in the loose sand. Narrow rings followed by reaction wood clearly marked the event in the rings of the trees (Sheppard and Jacoby 1989). The signal was also very directional in some trees. They showed response on the downward or seaward side of the tree but almost no indication on the opposite or landward side of the tree. Nearby trees from more solid substrate gave no indication of the event.

The Chilean earthquake of 1960 caused many landslides in Chile. To the east in Argentina, there were fewer landslides but the strong accelerations may have caused tree deaths and affected growth rings in some surviving trees (Veblen et al. 1992). The distance from the Chilean coast to the area of affected trees is less than 200 km. Veblen et al. (1992) attribute increased growth in some trees to loss of competitors leveled by the seismic accelerations. The Alaskan and Argentinean cases indicate that great subduction earthquakes at convergent plate margins can disturb trees and leave a signal over wide regions.

Blind faults do not reach the ground surface yet can cause many of the surficial changes described above that disturb trees; e.g. elevation changes, liquefaction, slumping, landslides, and tsunami that damage trees. Meter-scale surficial fractures and small local land slips can cause tilting of trees. Relatively minor surficial changes resulting from an earthquake on a blind fault can alter the water table or water levels in wetlands. These changes can cause responses ranging from drowning of trees to creating a new, drier substrate for afforestation. In between these two extremes there can be increased or decreased ring widths depending on the individual changes in the tree's environment. With minor elevation changes, certain species like eastern hemlock (*Tsuga Canadensis*) and bald cypress (*Taxodium distichum*) can respond to small (less than a meter) changes in groundwater levels.

Earthquakes such as Loma Prieta (1989) and Northridge (1994) in California caused damage to trees over a wide area. Some of the damage may have been severe enough to leave a signal in the tree rings or even fell trees. A reconnaissance of trees damaged due to Loma Prieta showed only a scattered and heterogeneous distribution of damaged trees over an area of tens of kilometers in different directions from the epicenter. Two felled or broken trees had so much root rot and decay, respectively, that the next high wind could have produced the same result. Much of the other tree damage was minor and not likely to cause significant change in the annual growth rings. If the earthquake had been unknown, it would have been extremely challenging to determine that the observed tree damage was earthquake

induced and not due to other natural causes. Much larger earthquakes would lead to more severe and widespread damage that might be easier to interpret as described above and following.

4.6 Information that May Be Developed From Tree-Ring Analysis: Event, Location, Time, Estimated Magnitude, and Displacement

Obviously trees damaged by surface rupture along a fault and by movement in the zone of distributed shear precisely locate these disturbances. There is some correspondence between the extent of surface rupture and magnitude of earthquake (Wells and Coppersmith 1994). Mapping the extent of disturbed trees or sites could be used as a minimum length of rupture and thus an index to minimum magnitude of an event.

Trees indirectly damaged by accelerations, seismic-induced landslides and geomorphic and hydrologic changes altering the growth environment, can help locate zones of disturbance. A network of disturbed trees could to help locate the event, similar to a compilation of historical reports in a region. As noted above, the 1964 Alaska earthquake affected trees over a wide area. Trees from Kodiak Island (Kaiser and Kaiser-Bernhard 1987) showed decreased growth and the trees at Cape Suckling, about 600 km to the northeast of Kodiak, were also disturbed (Sheppard and Jacoby 1989). These indicators along with the drowned trees around Cook Inlet would be interpreted as evidence of a massive earthquake even if it had not been a documented event. Thus the network of damaged and killed trees would have helped in estimating the size of the event. A challenge to the application of tree-ring methodology is to find such evidence in the prehistoric record.

Tonglin (1983 and unknown) reviewed some principles of tree-ring analysis and its use in paleoseismic and landslide studies. His studies show that in areas near Dangxiong, Tibet, cypress trees growing near normal faults decreased ring widths on the upthrown side and increased ring widths on the downthrown side just after a series of about ten estimated magnitude 5 events occurring in 1951–1952. He attributed these changes in growth to altered soil moisture and groundwater levels after the events; the uplifted side becoming drier and the down-dropped side becoming wetter. He noted the importance of control sampling to establish that climate effects are not responsible for the changes in ring widths and includes plots to demonstrate this point. By using growth to size relationships for the region, an estimate is made using the largest trees growing in the fault zone that the site was not disturbed for about 500–600 years. From historical documents, the interpretation was that the site was last disturbed by recorded earthquakes on 29 September 1411, estimated magnitude 8.0 with a strong foreshock and aftershock.

In northwest China the local displacement of the 1931 Fuyun earthquake was determined by measuring the distance between the parts of a circular shrub that straddled the fault surface-rupture (Lin 1998).

In 1988 tree-ring analysis established that an earthquake had occurred on the San Andreas Fault during the non-growing season of 1812–1813 (Jacoby et al. 1988). As described above, further sampling and analysis of the trees in the same southern California region previously studied by Meisling and Sieh (1980) revealed an unusual disturbance in nine trees, along a 12 km length of the fault, beginning with the 1813 ring (Fig. 1). The extent of disturbed trees along the fault was limited by the absence of trees below the elevation of the lower forest border as it reaches the desert. Two December 1812 earthquakes were known but previously were assigned to offshore or coastal locations based on historical observations.

Approximate ages of trees were used to estimate dates for raised terraces at Icy Cape, Alaska (Beavan et al. 1979). The ages were interpreted as indicating four earthquakes since about AD 1300 and extremely high uplift rates for the area. This interpretation was controversial and the question has not been resolved. At this location, wider annual rings after 1899 were cited by Jacoby and Ulan (1983) as evidence that earthquake uplift had shifted the shoreline in one of these events, 1899, and improved the growth environment for the trees at this coastal site. There was also post-event establishment of trees on the newly-uplifted surface after the 1899 event. This study indicated that uplift extended farther to the west than previously thought.

The Cascadia Subduction Zone (CSZ) is of increased recent interest as scientists try to assess seismic risks for the northwestern United States and southwestern Canada. There is evidence of subsidence in several areas along the coast from northern California to Vancouver Island (Atwater et al. 1995). At the southern end of the CSZ in northern California, just north of the Mendocino triple junction, an earthquake about 300 years ago caused subsidence in the vicinity of Humboldt Bay (Carver et al. 1992). There are no actual trees left on the sunken lands but major roots attached to stump fragments of former trees have been preserved. These roots have annual-ring structure although there is much distortion typical of root growth. The ring-width patterns in the roots were sufficient to establish crossdating between roots from the same and different "trees". Results of this dating established that the roots all died within four growing seasons, consistent with rapid subsidence (Jacoby et al. 1995). Supportive evidence of rapid subsidence at the site came from herbaceous plants entombed in the growth position. This is the type of subsidence that was produced by subduction earthquakes in Alaska in 1964 and Chile in 1960. Some of the subsidence could be partially due to liquefaction.

At the northern end of the CSZ along the Oregon and Washington coasts, there are locations with evidence of subsidence. At some of these locations there are relict trees evidently killed by drowning from earthquake-induced subsidence. There is enough remaining of the trees to use tree-ring analysis along with radiocarbon measurements to determine timing and circumstances of the tree deaths. Near Copalis and Nehalen, Washington, Atwater and Yamaguchi (1991) found western red cedar (*T. plicata*) trees drowned by subsidence. High-precision radiocarbon dates indicate an event about 300 years ago (Atwater et al. 1991) between 1680 and 1720. Earlier tree-ring analysis placed the event after 1687 (Yamaguchi et al. 1989). A first tentative date from analyses of living trees on subsided sites was

1699–1700 (Benson et al. 1997). Further analyses found evidence of inundation and other disturbance in more trees at the same dated period. Satake et al. (1996) analyzed historical information about a large tsunami striking Japan on 26 January 1700. Their analyses suggested that the most likely source for the tsunami was a large earthquake (est. magnitude 9) along the entire Cascadia Subduction Zone. With this information, the analyses of all the samples from coastal Oregon and Washington coasts were reviewed and finalized. In addition to the previously found tree-ring evidence it was noticed that there was an increase in traumatic resin canals starting in 1700. Traumatic resin canals are a response to flooding (Kramer and Kozlowski 1979). A compilation of these tree-ring analyses, including 1699 dating the outer ring of a dead marsh-edge tree, placed the event in the non-growing season of 1699–1700 (Jacoby et al. 1997) in agreement with the tsunami hypothesis of Satake et al. (1996). With this information, a number of stumps from subsidence-killed trees were excavated from a tidal marsh and their analyses further confirmed the 1700 date for the event (Yamaguchi et al. 1997).

In the Seattle, Washington, region several studies involving trees indicate a major earthquake about 1,000 years ago on the Seattle Fault (Bucknam et al. 1992). The times of several landslides in the region were determined by radiocarbon dating of wood samples. Two studies used tree-ring dating to establish simultaneous events, thus supporting the hypothesis of a common seismic cause (Atwater and Moore 1992; Jacoby et al. 1992). The key finding was that at two locations about 23 km apart, trees died in the same season of the same year. At one location a tree was entombed and preserved in a tsunami deposit (Atwater and Moore 1992) and at the other location a landslide carried a forested hillside down into Lake Washington and drowned and preserved the trees (Jacoby et al. 1992). Subsequent investigation showed that drowned trees at two locations in other parts of Lake Washington also died in that same season in the same year (Jacoby and Williams 1994).

Acknowledgments Some of the research has been supported by the National Science Foundation under grants EAR 88-05058 and EAR 90-04350 and U. S. Geological Survey grants 1434-93-G2366, 1434-93-G2367 and 1434-94-G2451. The following participated in the field research and/or analyses during the original studies: Atwater B, Benson B, Buckley B, Bunker B, Carver G. Sheppard PR, Sieh KE, Ulan, LD, White L, and Williams P. Lamont-Doherty Earth Obs. contribution number 0000.

References

Adams J (1981) Earthquake-dammed lakes in New Zealand. Geology 9:215–219

Alestalo J (1971) Dendrochronological interpretation of geomorphic processes, Fennia 105, Helsinki, 1–140

Atwater BF, Stuiver M, Yamaguchi DK (1991) Radiocarbon test of earthquake magnitude at the Cascadia subduction zone. Nature 353:156–158

Atwater BF, Yamaguchi DK (1991) Sudden, probably coseismic submergence of Holocene trees and grass in coastal Washington State. Geology 19:706–709

Atwater BF, Moore AL (1992) A tsunami about 1000 years ago in Puget Sound, Washington. Science 258:1614–1617

Atwater BF, Nelson AR, Clague JJ, Carver GA, Yamaguchi DK, Bobrowsky PT, Bourgeois J, Darienzo ME, Grant WC, Hemphill-Haley E, Kelsey HM, Jacoby GC, Nishenko SP, Palmer SP, Peterson CD, Reinhart MA (1995) Summary of coastal geologic evidence for past great earthquakes at the Cascadia subduction zone. Earthquake Spectra 11(1):1–18

Atwater BF, Tuttle MP, Schweig ES, Rubin CM, Yamaguchi DK, Hemphill-Haley E (2003) Earthquake recurrence inferred from Paleoseismology. Devel Quat Sci 1:331–350

Beavan J, Bilham R, Mori J, Wesnousky S, Winslow M (1979) Tree rings reveal Gulf of Alaska earthquakes in 1300, 1390, 1560 and 1899, (abstr). Eos, Transactions of the American Geophysical Union, Fall Meeting Supplement 60, 46: 884–85

Benson BE, Grimm KA, Clague JJ (1997) Tsunami deposits beneath tidal marshes on northwestern Vancouver Island, British Columbia. Quat Res 48:192–204

Bucknam RC (1994) Puget Sound seismicity, NEHRP Summ Tech Rep XXXV, 260-62, USGS Open File Report 94-176

Bucknam RC, Hemphill-Haley E, Leopold EB (1992) Abrupt uplift within the past 1700 years at southern Puget Sound, Washington. Science 258:1611–1614

Burns RM, Honkala BH (1990) Silvics of North America, Conifers. Agriculture Handbook 654, USFS, Washington

Carver GA, Stuiver M and Atwater BF (1992) Radiocarbon ages of earthquake-killed trees at Humboldt Bay, California (abstr). Eos, Transactions of the American Geophysical Union, Fall Meeting Supplement 73: 398

Coffman JL, von Hake CA (eds) (1973) Earthquake history of the United States. US Department of Commerce NOAA, Washington DC

Crone AJ, Omdahl EM (1987) Directions in paleoseismology, US Geol Surv Open-File Report 87-673, 456 p

Fuller ML (1912) The New Madrid earthquake. US Geol Surv Bull 494, 119 p

Fumal TE, Pezzopane SK, Weldon RJ, Schwartz DP (1993) A 100-year average recurrence interval for the San Andreas Fault at Wrightwood, California. Science 259:199–203

Gill CJ (1970) The flooding tolerance of woody species-a review. Forest Abstr 31:671–687

Gordon JC, Larson PR (1968) Seasonal course of photosynthesis, respiration, and distribution of ^{14}C in young Pinus resinosa trees as related to wood formation. Plant Physiol 43:1617–1624

Gu Gongxu (1983) Catalog of Chinese earthquakes. Science Press, Beijing, China, 872 p. (translated 1989, Science Press, Beijing.)

Jacoby GC (1987) Potentials and limits for dating prehistoric earthquakes using tree-ring analysis. In: Crone AJ, EM Omdahl (eds) Directions in Paleoseismology, pp 18–22. US Geol Surv Open-File Rep 87-673, 456 p

Jacoby GC (1997) Application of tree ring analysis to paleoseismology. Rev Geophys 35: 109–124

Jacoby GC, Bunker DE, Benson BE (1997) Tree-ring evidence for an A.D. 1700 Cascadia earthquake in Washington and northern Oregon. Geology 25:999–1002

Jacoby GC, Carver G, Wagner WS (1995) Trees and herbs killed by an earthquake 300 yr ago at Humboldt Bay, California. Geology 23:77–80

Jacoby GC, Sheppard PR, Sieh KE (1988) Irregular recurrence of large earthquakes along the San Andreas fault: evidence from trees. Science 241:196–199

Jacoby GC, Ulan LD (1983) Tree-ring evidence for uplift at Icy Cape, Alaska, related to 1899 earthquakes. J Geophys Res 88:9305–9313

Jacoby GC, Williams PL (1994) Landslides in Lake Washington, Seattle; Coincidence intra-lake and correlation with regional seismic events In: NEHRP Summary of Technical Report XXXV, US Geol Surv Open-File 94-176, pp 387–388

Jacoby GC, Williams PL, Buckley BM (1992) Tree-ring correlation between prehistoric landslides and abrupt tectonic events in Seattle, Washington. Science 258:1621–1623

Jepson WL (1923) The trees of California, 2nd edn. University of California, Berkeley, California

Kaiser KF, Kaiser-Bernhard C (1987) The Katmai eruption of 1912 and the Alaska earthquake of 1964 as reflected in the annual rings of sitka spruces on Kodiak Island. Dendrochronologia 5:111–125

Kozlowski TT (1971) Growth and Development of Trees. II Cambial Growth, Root Growth, and Reproductive Growth. Academic Press, New York
Kramer PJ, Kozlowski TT (1979) Physiology of Woody Plants. Academic Press, New York, 811 p
Louderback GD (1947) Central California earthquakes of the 1830's. Seismol Soc Am Bull 37:33–74
Lawson AC (1908) The California Earthquake of April 18, 1906, Report of the State Earthquake Investigation Commission, Carnegie Institution of Washington, Washington DC Publication 87(1)
Lee WHK, Meyers H, Shimazaki K (eds) (1988) Historical seismograms and earthquakes of the World. Academic Press, New York
Levitt J (1980) Response of plants to environmental stresses, II Water, radiation, salt, and other stresses. 2nd ed., Academic Press, New York
Lin A (1998) Tree damage and surface displacement: The 1931 M 8.9 Fuyun Earthquake. J Geol 106(6):751–758
Low AJ (1964) Compression wood in conifers: a review of the literature, Parts I and II, Forestry Abstracts 25:xxxv-li
Lyell C (1849) A second visit to the United States of America, II John Murray, London
McGee WJ (1892) A fossil earthquake. Geol Soc Am Bull 4:411–414
Meisling KE and Sieh KE (1980) Disturbance of trees by the 1857 Fort Tejon earthquake. J Geophys Res 85, B6: 3225–3238
Panshin AJ, de Zeeuw C (1970) Textbook of wood technology. McGraw-Hill, New York
Plafker G (1969) Tectonics of the March 27, 1964, Alaska earthquake US Geol Surv Prof Paper 543-I: 47 p
Prentice CS, Schwartz DP and Yeats RS (Eds) (1994) Proceedings of the Workshop on Paleoseismology. US Geol Surv Open-File Rep 94-568
Sanderson PL, Armstrong W (1978) Soil waterlogging, root rot and conifer windthrow: oxygen deficiency or phytotoxicity? Plant Soil 49:185–190
Satake KK, Shimazaki K, Tsuji Y, Ueda K (1996) Time and size of a giant earthquake in Cascadia inferred from Japanese tsunami records of January 1700. Nature 379:246–249
Scurfield G (1973) Reaction wood: its structure and function. Science 79:647–655
Sheppard PR, Jacoby GC (1989) Application of tree-ring analysis to paleoseismology: two case studies. Geology 17:226–229
Shroder JF Jr (1980) Dendrogeomorphology: review and new techniques of tree-ring dating. Prog Phys Geogr 4(2):161–188
Sieh KE, Stuiver M, Brillinger D (1989) A more precise chronology of earthquakes produced by the San Andreas Fault in Southern California. J Geophys Res 94:603–623
Stuiver M, Reimer PJ, Bard B, Beck JW, Burr GS, Hughen KA, Kromer J, McCormac G, van der Plicht J, Spurk M (1998) INTERCAL98 Radiocarbon age calibration, 24, 000–0 cal BP. Radiocarbon 40(3):1041–1083
Timell TE (1986) Compression Wood in Gymnosperms. Springer, New York
Tonglin Han (unknown) Applications of tree rings in the study of active tectonics in Tibet: introduction of dating active tectonics using tree ring methods, (in Chinese, translated by Jishu Deng, Lamont-Doherty Earth Obs., Palisades NY, 1995)
Tonglin Han (1983) The dendrochronological method-a new method for determining the ages of seismic deformational belts in Damxung of Xizang (Tibet). Bulletin of the Chinese Academic Geological Sciences 95-104 (in Chinese) (translated by Yantao Shi. Lamont-Doherty Earth Obs., Palisades, NY 1996)
Van Arsdale R (1998) Earthquake signals in tree-ring data from the New Madrid seismic zone. Geology 26:515–518
Veblen TT, Kitzberger T, Lara A (1992) Disturbance and forest dynamics along a transect from Andean rain forest to Patagonian shrubland. J Veg Sci 3:507–520
Wells DR, Coppersmith KJ (1994) New empirical relationships among magnitude, rupture length, rupture width, rupture area, and surface displacement. Bull Seismol Soc Am 84:974–1002

Wood HO, Neumann F (1931) Modified Mercalli intensity scale of 1931. Bull Seismol Soc Am 21:277–283

Yamaguchi DK (1991) Tree-ring record of the 1964 great Alaska earthquake: implications for Cascadia paleoearthquake studies (abstr). Eos, Transactions of the American Geophysical Union, Fall Meeting Supplement 72: 313

Yamaguchi DK, Woodhouse CA and Reid MS (1989) Tree-ring evidence for synchronous rapid submergence of the southwestern Washington coast 300 years B.P. (abstr). Eos, Transactions of the American Geophysical Union, Fall Meeting Supplement 70: 1332

Yamaguchi DK, Atwater BF, Bunker DE, Benson BE and Reid MS (1997) Tree-ring dating the 1700 Cascadia earthquake. Nature 389:922–923

Tree-Ring Abnormality Caused by Large Earthquake: An Example From the 1931 M 8.0 Fuyun Earthquake

Aiming Lin and Su-Juan Lin

Large earthquakes of magnitude >6–7 with shallow focus depths can produce distinctive co-seismic surface ruptures and cause strong ground deformation, which frequently damages trees or alters their environment along pre-existing active faults (e.g. Jacoby et al. 1997; Lin and Lin 1998). Trees along active fault zones, therefore, are potential sources of information on paleoseismic faulting. Such evidence could lead to improved estimates of the recurrence interval of large magnitude earthquakes, characteristic displacements and seismic hazards in areas with no historical record.

Co-seismic surface ruptures and ground deformation often kill and split stumps along active faults, or affect trees growing in or immediately adjacent to the rupture zone during large earthquakes such as the 1931 M 8.0 Fuyun (China) earthquake (Lin and Lin 1998), 1995 Ms 7.2 Kobe earthquake, Japan (Lin and Uda 1998), 1935 M 8.0 Haiyuan and 2008 Ms 8.1 Wenchuan (China) earthquakes. A representative example of split and damaged trees is observed on the Fuyun fault zone in northwest China (Lin and Lin 1998). Field observations reveal that a 180-km-long surface rupture zone occurred along the pre-existing Fuyun fault zone where a shrub of *Sabina pseudosabina* was displaced dextrally for 10.8 m along the surface rupture located near the epicenter of the 1931 M 8 Fuyun earthquake (Fig. 1a). Offsets observed along the rupture zone were generally less than 10 m, with a maximum offset of 14.8 m (Deng et al. 1986). Yeats et al. (1997) report that maximum offsets along an individual surface rupture generated by large interplate

A. Lin (✉)
Graduate School of Science and Technology, Shizuoka University, Ohya 836, Japan
e-mail: slin@ipc.sizuoka.ac.jp

S.-J. Lin
Department of Biological Science, Faculty of Life and Environmental Science, Shimane University, Matsue 690-0823, Japan

M. Stoffel et al. (eds.), *Tree Rings and Natural Hazards: A State-of-the-Art*, Advances in Global Change Research 41, DOI 10.1007/978-90-481-8736-2_38,

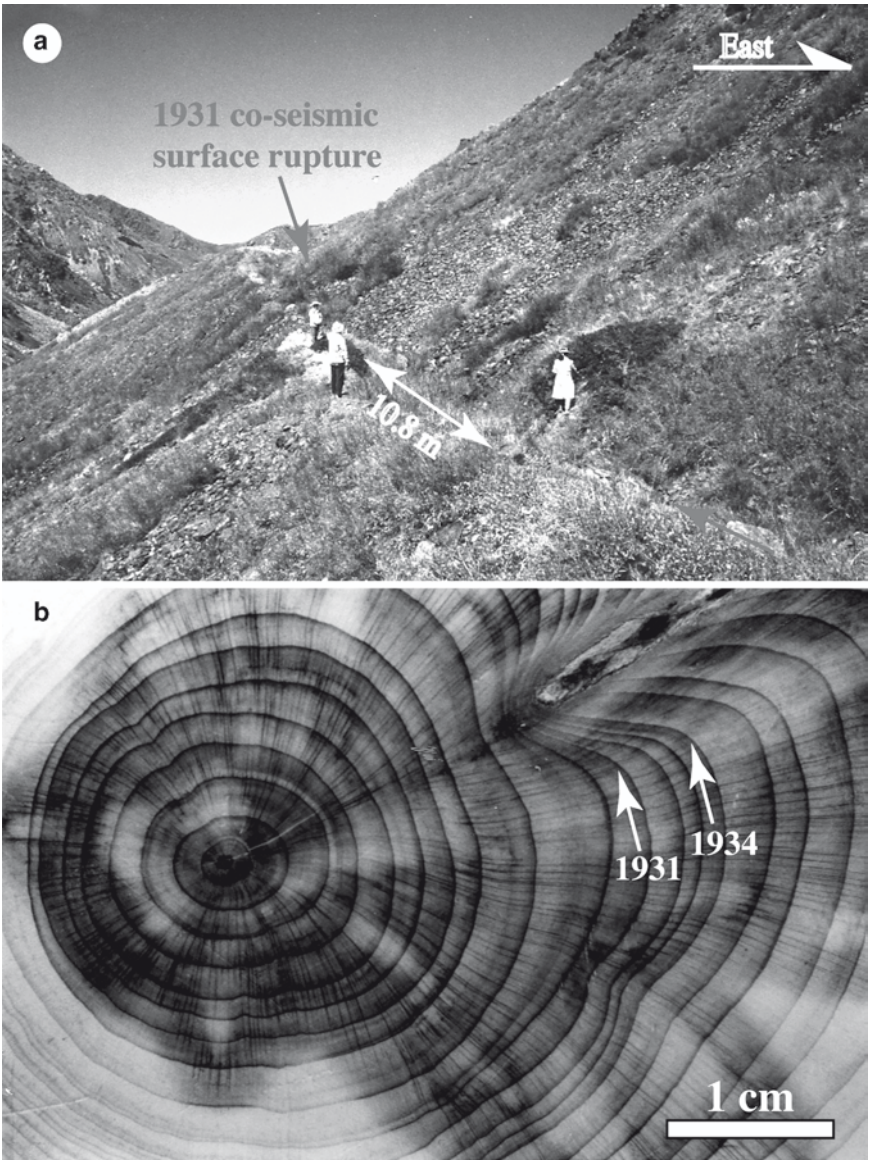

Fig. 1 Photographs showing (**a**) the surface rupture caused by the 1931 M 8.0 Fuyun earthquake and (**b**) tree ring characteristics of a *Sabina pseudosabina* sample taken from the offset tree shown in (**a**). Note that the sampled trees were dextrally displaced 10.8 m (photo **a**). There is sharp change in ring width between rings formed during 1931–1934 and those formed during the years before 1931 and after 1934 (photo **b**) (Modified from Lin and Lin 1998)

earthquakes of M >7–8 are generally less than 10 m. Therefore it is possible that the large offsets of 10–15 m observed along the Fuyun fault zone may have been generated by multiple earthquakes rather than the single 1931 seismic event.

To investigate this possibility a damaged circle scrub, displaced 10.8 m along the surface rupture zone of the 1931 earthquake (Fig. 1a), was sampled and its rings analyzed.

Tree ring analysis indicates a sharp change in ring width in 1931. The 1931–1934 rings are much narrower than those formed immediately before 1931 and after 1934 (Figs. 1b and 2). There are many potential causes for changes in ring growth, including climatic fluctuations, local changes of groundwater level, landslides and soil erosion or sedimentation. Variation in ring width of woody plants generally reflects the control of water and temperature on plant growth and, in this dry environment, rings are generally thicker when formed in years of plentiful rainfall and thinner in dry years. However, there is no obvious abnormal change in average temperature or rainfall over the 1931–1934 period (Seismological Bureau of Xinjiang Uygur Autonomous Region, 1985), so that it is improbable that this sharp change of tree-ring growth resulted from climate changes. The sampling site is located on a gentle slope dipping west of the mountains (Fig. 1) and therefore it would be difficult to form this rupture from a landslide dipping east and extending more than several hundred meters across the slope. It also would be difficult to account for the sharp change in ring width due to erosion or sedimentation. Trees often suffer damage during large earthquakes due to strong shaking and rupturing of the ground surface from associated faults. Such surface rupturing probably damaged the roots of trees and affected the transmittal of water and nutrients thus hindering tree-ring growth, and may also result in temporary asymmetric growth and reduction in the width of annual growth rings. It is therefore concluded that the

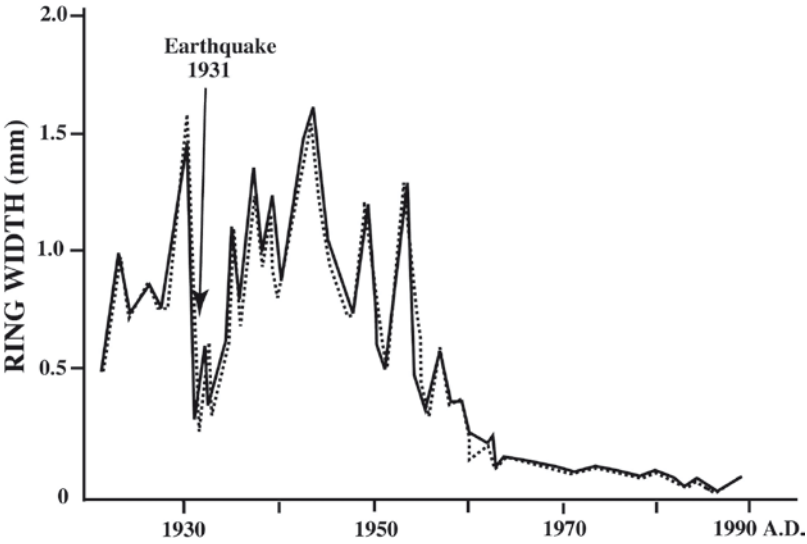

Fig. 2 Growth curves for tree rings in the displaced shrubs. The solid and dotted lines show the ring width of samples taken from the western side and eastern sides, respectively of the surface rupture shown in Fig. 1a. There is a sharp change in ring width in 1931 (After Lin and Lin 1998)

displacement of 10.8 m between the two semicircular scrubs on either side of the rupture was caused by the 1931 earthquake. This also indicates that the displacements of 10–15 m along the Fuyun surface rupture zone near the sampling location were caused by the 1931 seismic faulting and not the result of multiple events.

This study is a specific example of the use of tree-ring analysis to estimate the maximum amount of offsets along a co-seismic surface rupture zone produced by a large strike-slip earthquake, and also indicates that tree rings can be used as a specific indicator for the dendrochronologic study of seismological and geomorphological processes along active faults.

References

Jacoby GC, Bunker DE, Benson BE (1997) Tree-ring evidence for an A.D. 1700 Cascadia earthquake in Washington and northern Oregon. Geology 25:999–1002

Lin A, Uda S (1998) Morphological characteristics of the earthquake surface ruptures occurred on Awaji Island, associated with the 1995 Southern Hyogo Prefecture Earthquake. The Island Arc 5:1–15

Lin A, Lin S (1998) Tree damage and surface displacement: the 1931 M8.0 Fuyun earthquake. J Geol 106:749–755

Seismological Bureau of Xinjiang Uygur Autonomous Region (1985) The Fuyun Earthquake Fault Zone in Xinjiang (edited by Ding, G). China Sesimological Press, Beijing

Yeats RS, Sieh K, Allen CR (1997) The geology of earthquake. Oxford University Press, Oxford

Tree-Ring Dated Landslide Movements and Seismic Events in Southwestern Montana, USA

Paul E. Carrara and J. Michael O'Neill

1 Introduction

Because many tree species can live for several centuries or longer (Brown 1996), tree-ring analysis can be a valuable tool to date geomorphic events such as landslides, earthquakes, and avalanches in regions lacking long historical records. Typically, a catastrophic landslide will destroy all trees on the landslide, but trees on slower moving landslides may survive. For example, the Slumgullion earthflow, in southwestern Colorado, moves 0.5–5.5 m annually, yet is covered by aspen (*Populus tremuloides*) and conifers (Baum and Fleming 1996). Trees that survive such movements undoubtedly suffer damage, such as topping, tilting, impact, or root breakage. This damage is commonly recorded in the tree-ring record and analysis of this record can be used to reconstruct past landslide activity.

This study discusses the results of tree-ring analyses at three sites on landslides in the Gravelly Range of southwestern Montana and the relationship between landslide movement and regional seismicity. These landslides are subject to occasional incremental movement that may be as much as several meters per event.

The Gravelly Range is underlain in part by the 1.8-2.0 m.y. Huckleberry Ridge Tuff, which is in turn underlain by poorly-consolidated Tertiary sediment. These sediments consist of poorly bedded, tuffaceous mudstone that locally includes thin beds of arkosic sandstone and lenses of granule to pebble conglomerate (Luikart 1997). Beneath the tuff along the southeast slopes of the Gravelly Range, the

P.E. Carrara (✉) and J.M. O'Neill
U.S. Geological Survey, Denver Federal Center, Denver, CO 80225, USA
e-mail: pcarrara@usgs.gov

M. Stoffel et al. (eds.), *Tree Rings and Natural Hazards: A State-of-the-Art*,
Advances in Global Change Research 41, DOI 10.1007/978-90-481-8736-2_39,

Tertiary sediments thicken and the topographic relief is nearly 1,100 m. Numerous faults cut the tuff throughout the area, suggesting that as much as 700 m of displacement has occurred in the Quaternary (O'Neill et al. 1994). Well-defined fault scarps indicate ongoing tectonic activity.

A zone of landslides extends for nearly 25 km along the southeastern flank of the Gravelly Range (O'Neill et al. 1994), part of which is shown on Fig. 1. The landslides range from small, less than 0.1 km^2, to large rotational slumps and translational landslides that exceed 5 km^2. These landslides are confined to areas where the mechanically rigid, densely welded Huckleberry Ridge Tuff is underlain

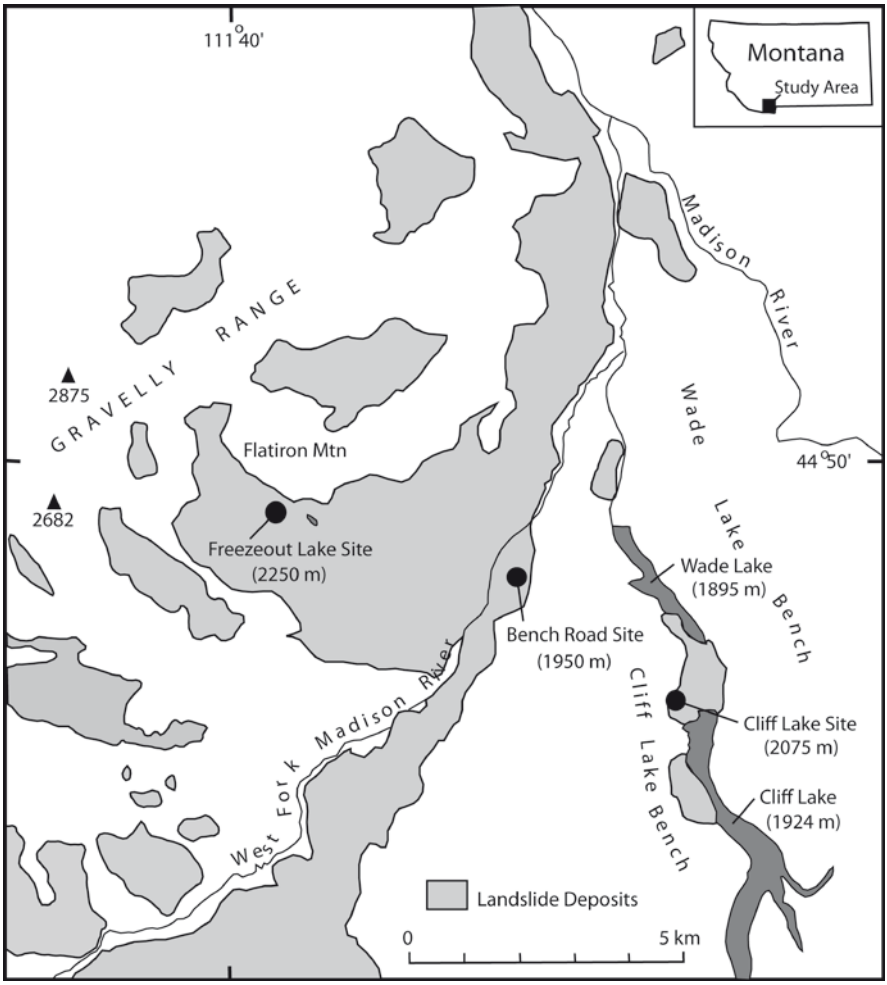

Fig. 1 Generalized map of landslides in the southeastern Gravelly Range (after O'Neill et al. 1994) and location of study sites

by the poorly consolidated Tertiary sediments (O'Neill et al. 1994). The landslides are characterized by hummocky topography containing blocks of the tuff, closed depressions containing bogs and ponds, and mud springs near the toes of the landslides that are saturated. The landslides were probably initially formed in the late Pleistocene; however, numerous tilted and deformed trees on parts of these landslides indicate that they have been subject to recent movement.

2 Dating Landslide Movement by Tree-Ring Analyses

Tree-ring analysis has been used to date landslides and other events in several ways. The ages of the trees themselves supply important information. For instance, the oldest undisturbed tree on a landslide provides a minimum age of movement (McGee 1893; Fuller 1912; Jibson and Keefer 1988; Logan and Schuster 1991).

One of the first investigators to use tree-ring analysis to date landslides was McGee (1893). On landslides near Reelfoot Lake, Tennessee, displaced by the New Madrid earthquakes of 1811 and 1812, McGee (1893) noted that trees 200 or more years old were inclined from base to crown and that the trunks of trees 100–150 years old were inclined, whereas the upper parts were vertical. He concluded that undisturbed, vertical trees that were 70 or 75 years old established a minimum age for the landslide movement. Similarly, Fuller (1912) studied the ages of upright and tilted trees on landslides also displaced by the New Madrid earthquakes. He determined that "the greater part of the upright growth on the disturbed surfaces is fairly uniform and a little less than 100 years of age, trees of greater age being in general tilted and partly overthrown."

A more complex analysis of landslide movement involves the interpretation of the annual rings in disturbed trees. Shroder (1978) used tree-ring analysis to date recurrent movement on a rock glacier-like deposit on the Table Cliffs Plateau, Utah. Reeder (1979) used tree-ring analysis to date landslide movement in the Anchorage, Alaska, area and correlated these movements with regional earthquakes. Jensen (1983) dated episodic movement in the upper Gros Ventre landslide in Wyoming by tree-ring analysis. Finally, Williams et al. (1992) investigated four landslides near Seattle, Washington using tree-ring analysis and concluded that the landslides were seismically induced.

In the studies cited above, several types of tree-ring anomalies were associated with landslide movement: (1) an abrupt reduction in annual ring width, (2) the formation of reaction wood, and (3) scars. Disturbance in the tree-ring record in a specific year indicates that the tree was subjected to damage between the end of the previous growing season and the growing season of that specific year. For instance, the tree-ring record of Douglas firs (*Pseudotsuga menziesii*) within several meters of the Hebgen Lake fault scarp, about 30 km east of the study area, exhibit a marked reduction in annual ring width or reaction wood formation beginning in 1960

(Carrara 2002; Bekker 2004). The main shock of the Hebgen Lake earthquake, occurred on August 18, 1959, after the growing season. Hence, the 1959 annual rings are of normal width and the disturbance in the tree-ring record began with the 1960 annual rings.

2.1 Reduction in Annual Ring Width

A reduction in annual ring width for several years or more can be the result of injury due to a geomorphic event, such as a landslide, earthquake, or avalanche (Shroder 1978; Carrara 1979; Meisling and Sieh 1980). Damage to the root system, loss of a major limb, or topping can all result in an abrupt reduction in annual ring width.

Effects from damage may be rather subtle. For example, in a study of the effects of the 1959 Hebgen Lake earthquake on Douglas firs growing along the fault scarp, most (13 of 15) trees were found to exhibit a reduction in annual ring width beginning in 1960 (Carrara 2002). Despite the fact that the sampled trees were only several meters from the scarp and showed obvious physical damage, in most trees (9) the response consisted of the formation of narrow annual rings for 1–3 years (Fig. 2). However, one tree produced narrow annual rings from 1960 to 1983, the last complete year of growth prior to sampling (Carrara 2002). In a similar, but more comprehensive study along this same fault scarp, Bekker (2004) found that a reduction in annual ring width was the most common response to this earthquake. Furthermore, he was able to document this response at a distance as great as 58 m from the scarp.

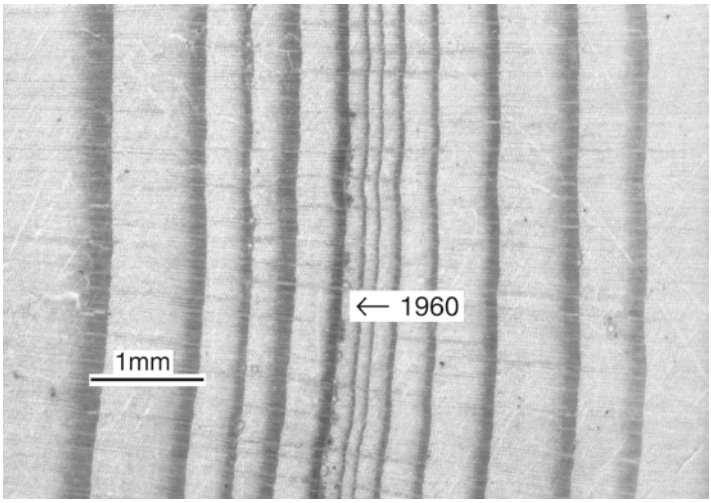

Fig. 2 Photomicrograph of cross section of Douglas fir showing a band of narrow annual rings that began formation in 1960 in response to the 1959 Hebgen Lake earthquake. Center of tree is to the left

2.2 Reaction Wood Formation

Reaction wood is formed on the underside of a tilted conifer (Fig. 3). Tilting of a conifer will often result in asymmetric growth, such that wide annual rings of reaction wood are formed on the underside of the tilted tree and narrow or discontinuous annual rings are formed on the upper side of the tree (Panshin and de Zeeuw 1970). Reaction wood in conifers is similar in appearance to latewood but is generally darker and denser and is usually characterized by a reddish-yellow color and small, thick-walled cells. Tracheids (the vertically oriented cells with thick walls) in reaction wood are shorter and have more rounded cross sections in contrast to normal tracheids, which are longer and have more angular cross sections (Panshin and de Zeeuw 1970).

In most cases the initial year of reaction wood closely dates the time of tilting; however, in some instances formation of reaction wood may be delayed for several years. For example, in the Hebgen Lake area, reaction wood was observed in Douglas firs that were tilted by the 1959 earthquake (Carrara 2002). In most trees, reaction wood formation was initiated in 1960. However, several severely damaged trees formed narrow annual rings on both the upper and underside of the tree as an initial response to the damage. Reaction wood was formed after a recovery period of 3 to as many as 9 years.

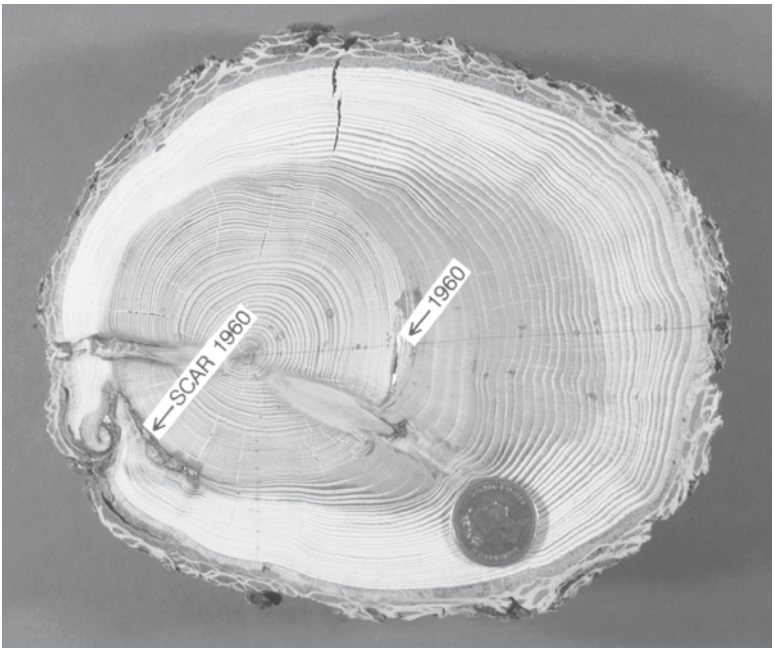

Fig. 3 Photograph of cross section of Douglas fir from the Cliff Lake site. The tree was tilted and impacted as a result of the 1959 Hebgen Lake earthquake. Eccentric growth was initiated in 1960 with reaction wood forming on the side displaying greater growth (underneath side). Note the associated scar caused by impact, which is grown over. Coin is about 20 mm in diameter

2.3 Scars

Scarring on trees (Fig. 3) can be caused by several mechanisms, including fire, gnawing by animals, and impacts from dislodged boulders or falling trees. For example, a dislodged boulder may wound a tree by removing the bark and underlying cambium tissue. Initially, the tree will be unable to form annual rings in the wound area but over time the cambium will encroach from the wound edges and overlap the damaged area forming a scar. On older scars, wound healing may have progressed to such an extent that the scar is entirely overgrown and impossible to detect at the surface. An increment borer could miss a healed scar because a core includes only a narrow radius of the tree, whereas the scar is easily recognized in a cross section.

3 Study Sites

Three sites on landslides along the southeastern flank of the Gravelly Range were chosen for tree-ring investigations: Bench Road, Cliff Lake, and Freezeout Lake (Fig. 1). Tilted and deformed trees are common at these sites.

3.1 Bench Road

The Bench Road site (1950 m asl) is located on a landslide near the West Fork of the Madison River (Fig. 1). Numerous large tilted trees are present at this site (Fig. 4). Eleven tilted Douglas firs were either cored (4) or cross-sectioned (7) at this site in August of 1993 and 1994, and their tree-ring records analyzed for signs of disturbance. The trees were sampled in an area that extends 30 m across the slope and 20 m downslope. The oldest tree had a pith date of 1790, five other trees had records extending back to 1850 or earlier. A dead standing tree was cross-dated to other trees at this site, and found to have a pith date of 1846.

3.2 Cliff Lake

The Cliff Lake site (2075 m asl) is located on the steep eastern edge of Cliff Lake Bench near the head of a large landslide separating Wade and Cliff Lakes (Fig. 1). The site contains many extensional fractures 1–2 m wide and one m deep that extend across the slope as much as 30 m. A Douglas fir forest covers the site, although along the top of the bench lodgepole pine (*Pinus contorta*) dominates.

Fig. 4 Photograph of Bench Road site showing numerous tilted Douglas firs. The road was established in 1977 (D. Reger, 2002, personal communication); most movements recorded in the tree-ring record at this site are pre-1977

At this site nine tilted or deformed Douglas-firs were cross-sectioned and one was cored in August of 1994 and 1995. The trees were sampled within an area that extended 30 m across the slope and 20 m downslope. The oldest tree had a pith date of 1878, two other trees had records extending back to 1890 or earlier. A dead standing tree was cross-dated to other trees at this site and found to have a pith date of 1893. During the 1959 Hebgen Lake earthquake boulders of Huckleberry Ridge Tuff were dislodged from the hillside and killed two people at the campground at the toe of this landslide (O'Neill et al. 1994).

3.3 Freezeout Lake

The Freezeout Lake site (2,250 m asl) is located near the head of a large landslide along the southern edge of Flatiron Mountain (Fig. 1). Eleven tilted or deformed trees, including Douglas-fir (*Pseudotsuga menziesii*) (7), subalpine fir *(Abies lasiocarpa*) (1), limber pine (*Pinus flexilis*) (1), and lodgepole pine (*Pinus contorta*) (2) were either cored (2) or cross-sectioned (9) in August 1993 and 1995. The trees were sampled within an area that extended 30 m on either side of a U.S. Forest Service road. The oldest tree had a pith date of 1855, and another four trees had records extending back to 1880 or earlier.

4 Methods

A total of 32 trees, mainly Douglas-firs, were sampled at the three sites. Trees ranged between 5 and 35 cm in diameter, and three to 30 m in height. Trunks of all sampled trees were noticeably tilted; angles of tilt ranged from 10° to 80°. Samples consisted of cross sections and cores that were collected with a 5-mm-diameter increment borer. For those trees sampled by an increment borer, a core was taken through the tree from the upper side to the lower side of the tilt, usually about 30 cm above the ground surface.

The cores and cross sections were prepared using standard procedures (Stokes and Smiley 1968) and then inspected under a binocular microscope (6 to 25X) for signs of disturbance in the tree-ring record. The cores and cross sections were cross-dated using a skeleton-plot (Stokes and Smiley 1968; Fritts 1976) for the undisturbed parts of the tree-ring record. Particularly distinctive narrow annual rings that were useful for cross-dating are: A D 1872, 1889, 1901, 1919, 1934, 1936, 1966, and 1989. False annual rings were noted in several samples and were distinguished from annual rings because the cells composing the latewood in the false annual rings grade to the inside and outside into porous tissue. In true annual rings the transition from the latewood of 1 year to the earlywood of the next year is abrupt (Panshin and de Zeeuw 1970).

In this study, significance (i.e. disturbance) was assigned to the initial year of a marked reduction in annual ring width, either for a single year or for a prominent band of narrow annual rings comprising a number of years, such that the width of the first narrow annual ring was 50% or less of the width of the annual ring of the previous year (Fig. 2). Reductions in annual ring width averaged about 5 years and ranged from 1 year to as many as 40 years. Significance was also assigned to the initial year of reaction wood formation, either for a single year or for a prominent lens of reaction wood encompassing a number of years. However, reaction wood formed in the early years of the tree and thought to be associated with early growth (Panshin and de Zeeuw 1970) was ignored. Reaction wood formation averaged about 6 years and ranged from 1 year to 54 years. In two trees formation of reaction wood was delayed for several years. For instance, one tree began formation of reaction wood in 1962 in response to the Hebgen Lake earthquake. This was preceded by an abrupt decrease in annual ring width around the entire circumference of the tree beginning in 1960. Therefore, the date of disturbance was assigned to 1960. Although scars were identified in only two trees in this study, one scar is clearly associated with damage sustained during the 1959 Hebgen Lake earthquake because it had healed over a wound that occurred between the 1959 and 1960 annual rings (Fig. 3). In this study, significance was assigned to the initial year of a scar.

5 Summary of Disturbance in the Gravelly Range Tree-Ring Record

The initial year of narrow annual ring, reaction wood, or scar formation are presented on Fig. 5. Because the number of trees with a record for a given year decreases with time, and because a given tree might not have a useful record for a

certain period (a tree may already be forming a narrow band of annual rings such that a subsequent disturbance would not be detected), the data are plotted as the percentage of trees with a useful record for a given year. As can be seen there are many disturbances for individual years that are recorded by about 10–20% of the trees at a given site (Fig. 5). Some of these smaller peaks may be related to minor landslide movements; however, some may simply be related to random events in

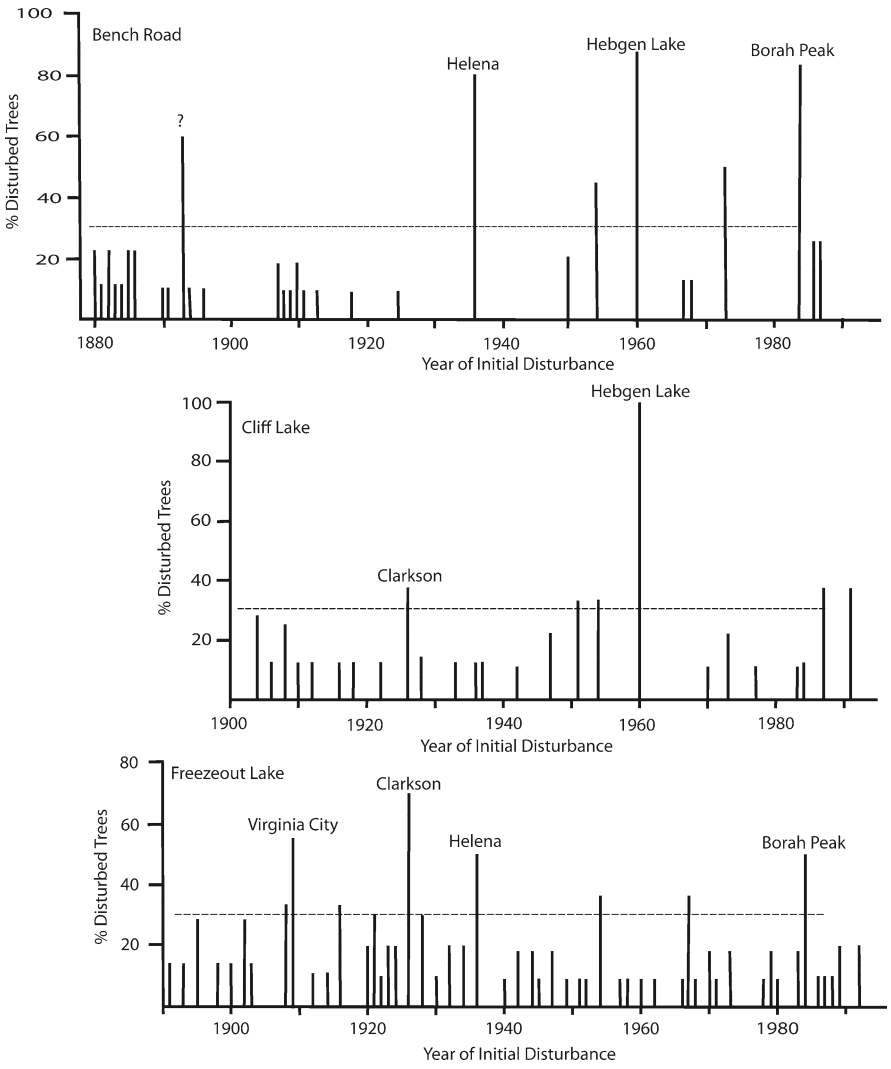

Fig. 5 Plots showing percentages of trees at the study sites indicating disturbance (movement) in a given year, and earthquake that may have initiated movement. Dashed horizontal lines indicate the level (30%) of disturbed trees. Values below these lines are considered to include random "noise" that is probably not related to seismic events

the life of the tree (insect infestation, animal disturbance). To avoid this possible "noise," significance was assigned only to those disturbances that were recorded in 30% or more of the trees at a site.

Data from the individual sites, including the number of trees displaying a marked reduction in annual ring width or the formation of reaction wood are summarized in Table 1. At the Bench Road site, six episodes of movement are indicated by disturbance in the tree-ring record of 30% or more of the sampled trees: 1984, 1973, 1960, 1954, 1936, and 1893. At the Cliff Lake site, six episodes of movement are indicated by disturbance in the tree-ring record: 1991, 1987, 1960, 1954, 1951, and 1926. At the Freezeout Lake site eight episodes of movement are indicated by disturbance in the tree-ring record: 1984, 1967, 1954, 1936, 1926, 1916, 1909, and 1908.

Disturbances in the tree-ring record of the trees sampled at the three sites are interpreted to have been caused by incremental movement of the landslides, and not by other factors, such as climatic stress, insect infestation, or fire for several reasons. First, as previously stated, the sampled trees were all tilted, an effect not

Table 1 Occurrence of narrow annual rings and reaction wood for years in which more than 30 % of sampled trees at a site showed evidence of disturbance

Site	Year[a]	NR[b]	RW[c]	TWR[d]	% Disturbed[e]
Bench Road	1984	5	0	6	83
(7 cross sec.)	1973	4	0	8	50
(4 cored)	1960	6	1	8	88
	1954	4	0	9	44
	1936	6	2	10	80
	1893	4	2	10	60
Cliff Lake	1991	0	3	8	38
(9 cross sec.)	1987	3	0	8	38
(2 cored)	1960	7	7	9	100
	1954	2	1	9	33
	1951	2	1	9	33
	1926	2	1	8	38
Freezout Lake	1984	5	0	10	50
(9 cross sec.)	1967	2	2	11	36
(2 cored)	1954	3	1	11	36
	1936	0	5	10	50
	1926	5	2	10	70
	1916	2	1	9	33
	1909	1	4	9	56
	1908	0	3	9	33

[a] Year (AD) of initial disturbance in the tree-ring record.
[b] Number of trees that formed narrow annual rings beginning in listed year.
[c] Number of trees that formed reaction wood beginning in listed year.
[d] Total number of trees with a useful record for listed year.
[e] Percent of trees with a useful record displaying evidence of disturbance in the tree-ring record beginning in listed year.

associated with these other factors. Second, the fact that the tilted trees are growing on landslides strongly suggests that the damage was caused by movement. Third, the damage observed in the tree-ring record is typical of the response of trees that have suffered physical damage and is not typical of climatic stress. Trees that exhibit a reduction in annual ring widths caused by climatic factors have a more uniform response, hence these trees generally recover at about the same year and such a response should occur over a broad region. As previously mentioned, in this study reductions in annual ring widths averaged about 5 years and ranged from as little as 1 year to as many as 40 years. Similar differences in the tree-ring response between earthquake disturbed trees and trees subject to climatic stress were noted by Jacoby et al. (1988). In addition, reductions in annual ring width in some trees at a site were also accompanied by reaction wood formation in other trees at the same site, which supports a physical disturbance as opposed to a climatic response.

6 Are the Landslide Movements Seismically Induced?

The study area is within the Intermountain Seismic Belt, a zone of pronounced seismic activity that extends from southern Nevada to northwestern Montana (Smith and Sbar 1974; Stickney and Bartholomew 1987). The largest historic earthquake recorded in this region, magnitude 7.5 Ms (surface wave magnitude) (Doser 1985), occurred on August 18, 1959 in the Hebgen Lake region, about 30 km east of the study area. It triggered a large rockslide that overran a campground and killed 26 people, burying them under an estimated 21 million cubic meter of debris (Witkind and Stickney 1987). This rockslide dammed the Madison River and formed Earthquake Lake. Other landslides in the region, including those in the Gravelly Range, may have also been initially triggered by large earthquakes.

6.1 Correlation of Landslide Movement with Significant Seismic Events

In a study of landslides caused by historical earthquakes Keefer (1984) investigated several factors including the minimum earthquake magnitudes and intensities known to have triggered landslides of various types, and the maximum distance from the epicenter that seismically triggered landslides are known to have occurred. Landslides of various types were found to have threshold magnitudes ranging from 4.0 ML (local magnitude) to 6.5 Ms and threshold Modified Mercalli intensities between IV and V (Keefer 1984). The initiation of the types of landslides in this study (rotational slumps and translational slides) have threshold magnitudes of about 5.0 ML and threshold Modified Mercalli intensities of about V (Keefer 1984).

In general, Keefer (1984) found that the larger the earthquake the greater the distance landslides were triggered from the epicenter. For instance, in the Cape Suckling area of Alaska, Sheppard and Jacoby (1989) determined that the 1964 Alaska earthquake (Ms 8.4) was recorded in the annual rings of Sitka spruce (*Picea sitchensis*), about 240 km from the earthquake's epicenter. Keefer (1984) found that an earthquake of this magnitude could trigger landslides as far as 500 km from the epicenter, whereas an earthquake of magnitude 6.0 should only be able to trigger landslides within about 40 km of the epicenter.

Since 1897, eight significant earthquakes, of magnitude or intensity 6.0 or greater have been recorded within about 200 km of the study area (Table 2). Some of these earthquakes appear to be recorded in the tree-ring records of the study sites (Table 2 and Fig. 5). In fact, those periods of movement indicated by the strongest signals (most trees) at an individual site occurred the year following several of these earthquakes. At the Bench Road site, three episodes of landslide movement occurred the year following a significant earthquake in the region: Borah Peak (1983), Hebgen Lake (1959), and Helena (1935). At the Cliff Lake site, two periods of landslide movement occurred the year following a significant earthquake: Hebgen Lake (1959) and Clarkson (1925). At the Freezeout Lake site, four periods of landslide movement occurred the year following a significant earthquake: Borah Peak (1983), Helena (1935), Clarkson (1925), and Virginia City (1908).

To test the relationship between significant earthquakes in the region and periods of disturbance in the tree-ring record that indicate landslide movement, the period 1890 to 1995 (Freezeout Lake) was divided into 2-year intervals to account for the time between an earthquake and its associated response in the tree-ring record. For instance, at the Freezeout Lake site, in the 52 2-year intervals there are eight disturbances in the tree-ring record that affected more than 30% of the trees (Table 1). Four of these tree-ring disturbances occurred the year following one of the eight significant earthquakes (Fig. 5). The estimated frequency of joint occurrences of two random, independent events, is equal to the product of their individual probabilities in any period (2-year intervals in this case) multiplied by the number of periods; (eight earthquakes divided by 52 2-year intervals = 0.154, and eight disturbances in the tree-ring record divided by 52 2-year intervals = 0.154; therefore, the estimated probability of joint occurrences is 0.154 x 0.154 x 52 = 1.2). Hence, the observed number of joint occurrences (4) is more than three times greater than that expected by chance. Note that in the following analyses the date of disturbance in the tree-ring record never preceded that of the associated earthquake within the 2-year intervals.

Each study site was then subjected to a two-way contingency analysis using a X^2 calculated from the observed and expected frequencies of joint occurrence and using the Yates correction for continuity due to small sample size (LaMarche and Hirschboeck 1984; Walpole and Myers 1992). At the Freezeout Lake site the relationship between the earthquakes and tree-ring disturbance is significant at greater than the 98% confidence level. At the Bench Road site; 1880 to 1994, 57 2-year intervals, eight earthquakes, six disturbances in the tree-ring record, and three joint occurrences; the relationship is significant at greater than the 95% confidence level.

Table 2 Year of initial disturbance in the tree-ring record in the study area compared to significant earthquakes in southwestern Montana (earthquake data after Pardee 1926; Scott 1936; Qamar and Stickney 1983; Doser 1985; Stover and Coffman 1993; and U.S. Geological Survey, unpublished data accessed Dec. 5, 2000, http://www.neic.cr.usgs.gov). Note; magnitudes, intensities, and distances prior to about 1960 may be prone to substantial errors

	Site[b]				Date				
Year of disturbance[a]	*BR*	*CL*	*FL*	Probable earthquake	year/month/da	Mag[c]/Inten[d]at epicenter	Intensity[d] in study area	Distance[e] (km)	Direction from study area[f]
1984	X	?	X	Borah Peak	1983/10/28	7.3 Ms/IX	V	200	SW
1976	–	–	–	Yellowstone	1975/06/30	5.9 Ms/VII	?	80	E
1960	X	X	?	Hebgen Lake	1959/08/18	7.5 Ms/X	VIII-IX	30	E
1948	–	–	–	Gravelly Range	1947/11/23	6.25 Ms/VIII	VI-VII	10	W
1936	X	?	X	Helena	1935/10/19	6.25 Ms/VIII	III-IV	205	N
1926	?	x	X	Clarkson	1925/06/28	6.75 Ms/VIII	V-VI	185	N
1909	?	–	X	Virginia City	1908/10/20	?/VI-VII	?	55	N
1898	–	–	?	Dillon	1897/11/04	6.4 Mfa/VI	?	100	W

X ≥50% of trees with useful record including this date show disturbance.
x 30-49% of trees with useful record including this date show disturbance.
? <30% of trees with useful record including this date show disturbance.
[a] Year disturbance would first be recorded in the tree-ring record if tree was damaged by listed probable earthquake.
[b] Site – BR, Bench Road; CL, Cliff Lake; FL, Freezeout Lake (see Fig. 1).
[c] Mag – Magnitude – primarily given as Ms (surface wave) except for Dillon given as Mfa (body-wave magnitude commonly computed from the felt area for earthquakes occurring before seismic instruments were in general use (Stover and Coffman 1993).
[d] Inten - Intensity - Modified Mercalli (after Pardee 1926; Scott 1936; and Stover and Coffman 1993).
[e] Distance from study area to earthquake epicenter.
[f] Direction from study area to earthquake epicenter.

Finally, at the Cliff Lake site; 1900 to 1995, 47 2-year intervals, seven earthquakes, six disturbances in the tree-ring record, and two joint occurrences, the relationship is not significant at the 95% confidence level.

6.2 Seismic Events Unrecorded in the Tree-Ring Record

Three of the eight significant earthquakes in the region were not recorded in the tree-ring record at any of the study sites, these are the Yellowstone earthquake of June 1975, the Gravelly Range earthquake of November 1947, and the Dillon earthquake of November 1897 (Table 2).

It is unclear as to why some earthquakes whose epicenters were as much as 200 km from the study area are recorded in the tree-ring record, whereas other nearby earthquakes of similar magnitude are not. It may be in part that the magnitudes, intensities, and distances from the epicenters listed on Table 2 prior to about 1960 may be prone to substantial errors, due to the lack of an extensive seismic network and sparse population in southwestern Montana at that time. Hence, these earthquakes may have been of smaller magnitudes and intensities or at greater distances from the study area.

The addition of more tree-ring sites on other nearby landslides may have yielded evidence of these earthquakes. None of the eight significant earthquakes that have occurred in the region are present in the tree-ring record at all three sites (Table 2). For instance, evidence of the 1959 Hebgen Lake earthquake, the largest among the eight earthquakes, is clearly recorded in the tree-ring record at the Bench Road and Cliff Lake sites, yet not at the Freezeout Lake site (Fig. 5).

The direction of wave propagation may not have been favorable for inducing landslide movement at the sites investigated. The epicenters of two of the three unrecorded earthquakes (Gravelly Range 1947 and Dillon 1897) were to the west of the study area (Table 2).

Soil moisture can influence an area's susceptibility to landslides, but does not appear to be a significant factor in the study area. The Palmer Drought Severity Index for southwestern Montana from 1895 to 1999 indicates that only two of the eight significant earthquakes in the region occurred during extremely wet years (National Climatological Data Center, unpublished data accessed April 12, 2000, http://www.ncdc.noaa.gov). The 1983 Borah Peak and 1908 Virginia City earthquakes occurred during years in which the Palmer Index was greater than +5. Other earthquakes occurred during years when the Palmer Index ranged from +2 (1975 Yellowstone) to –5 (1935 Helena). Hence, one of the earthquakes best recorded in this study, the 1935 Helena earthquake, occurred during a severe drought.

7 Conclusions

The tree-ring records from the three landslide sites indicate multiple periods of movement during the twentieth century. Landslide movement was commonly indicated by a marked reduction in annual ring width and/or the formation of reaction wood.

In many cases disturbance in the tree-ring record began in the growing season of the year following a large earthquake in the region. A significant correlation was found between regional seismic events and landslide movement at two of the three sites studied. Five of the eight significant earthquakes that occurred within 200 km of the study area appear to have caused movement on at least one of the three landslides. These five seismic events are the 1983 Borah Peak, 1959 Hebgen Lake, 1935 Helena, 1925 Clarkson, and the 1908 Virginia City earthquakes. Many of the earthquakes in the region are of magnitudes that should be capable of triggering landslides no farther than 50 km from their epicenter (Keefer 1984). The fact that the tree-ring record indicates movement coincident with earthquakes at distances as great as 200 km suggests that at times these landslides movements were generated by Modified Mercalli intensities as low as III or IV (Table 2). This study demonstrates the usefulness of tree-ring analysis to date landslide movements and suggests that small, incremental movement of these landslides may be induced by earthquake intensities lower than previously accepted..

Acknowledgments The authors thank L.W. Anderson, R.A. Crovelli, H.C. Fritts, T.C. Hanks, D.K. Keefer, and D.R. Lageson whose knowledge and ideas contributed to this paper. Previous versions of this manuscript benefited from reviews by F.C. Brunstein, D.R. Butler, J.R. Giardino, H.L. Goldstein, K.M. Haller, and J.S. Pigati, and an anonymous reviewer

References

Baum R, Fleming R (1996) Kinematic studies of the Slumgullion landslide, Hinsdale County, Colorado. In: Varnes D, Savage W (eds) The Slumgullion earth flow: a large-scale natural laboratory. US Geol Surv Bull 2130: 9–12

Bekker M (2004) Spatial variation in the response of tree rings to normal faulting during the Hebgen Lake earthquake, southwestern Montana, USA. Dendrochronologia 22(1):53–59

Brown P (1996) Oldlist: a database of maximum tree ages. In: Dean J, Meko D, Swetnam T (eds) Tree rings, environment, and humanity. Radiocarbon pp. 727–731

Carrara P (1979) The determination of snow avalanche frequency through tree-ring analysis and historical records at Ophir, Colorado. Geol Soc Am Bull 90(8):773–780

Carrara P (2002) Response of Douglas-firs along the fault scarp of the 1959 Hebgen Lake earthquake, southwestern Montana. Northwest Geol 32:54–65

Doser D (1985) Source parameters and faulting processes of the 1959 Hebgen Lake, Montana, earthquake sequence. J Geophys Res 90(B6): 4537–4555

Fritts H (1976) Tree rings and climate. Academic Press, New York

Fuller M (1912) The New Madrid earthquake. US Geol Surv Bull 494

Jacoby G Jr, Sheppard P, Sieh K (1988) Irregular reoccurrence of large earthquakes along the San Andreas fault: evidence from trees. Science 241(4862):196–199

Jensen J (1983) The Upper Gros Ventre landslide of Wyoming-A dendrochronology of landslide events and possible mechanics of failure. Geol Soc Am Abstr 15(5):387

Jibson R, Keefer D (1988) Landslides triggered by earthquakes in the central Mississippi Valley, Tennessee and Kentucky. US Geol Surv Prof Paper 1336-C: 1-24

Keefer D (1984) Landslides caused by earthquakes. Geol Soc Am Bull 95(4):406–421

LaMarche V Jr, Hirschboeck K (1984) Frost rings in trees as records of major volcanic eruptions. Nature 307(5947):121–126

Logan R, Schuster R (1991) Lakes divided – The origin of Lake Crescent and Lake Sutherland. Clallam County Washington Washington Geology 19:38–42
Luikart EJ (1997) Syn- and post-Laramide geology of the south-central Gravelly Range, southwestern Montana. Montana State University, M.Sc. Thesis
McGee W (1893) A fossil earthquake. Geol Soc Am Bull 4:411–414
Meisling K, Sieh K (1980) Disturbance of trees by the 1857 Fort Tejon earthquake, California. J Geophys Res 85(B6): 3225–3238
O'Neill J, LeRoy T, Carrara P (1994) Preliminary map showing Quaternary faults and landslides in the Cliff Lake Quadrangle, Madison County, Montana. US Geol Surv Open-File Rep 94-198, scale 1:24,000
Panshin A, de Zeeuw C (1970) Textbook of wood technology, 3rd edn. McGraw-Hill, New York
Pardee J (1926) The Montana earthquake of June 27, 1925. US Geol Surv Prof Paper 147-B
Qamar A, Stickney M (1983) Montana earthquakes 1869–1979, historical seismicity and earthquake hazard. Montana Bureau of Mines and Geology, Memoir 51
Reeder J (1979) The dating of landslides in Anchorage, Alaska – A case for earthquake-triggered movements. Geol Soc Am Abstr 11(7):501
Scott H (1936) The Montana earthquake of 1935. Montana Bureau of Mines and Geology, Memoir 16
Sheppard P, Jacoby G (1989) Application of tree-ring analysis to paleoseismology: two case studies. Geology 17(3):226–229
Shroder J Jr (1978) Dendrogeomorphological analysis of mass movement on Table Cliffs Plateau, Utah. Quat Res 9(2):168–185
Smith R, Sbar M (1974) Contemporary tectonics and seismicity of the Western United States with emphasis on the Intermountain seismic belt. Geol Soc Am Bull 85(8):1205–1218
Stickney M, Bartholomew M (1987) Seismicity and late Quaternary faulting of the northern Basin and Range Province, Montana and Idaho. Bull Seismol Soc Am 77(5):1602–1625
Stokes M, Smiley T (1968) An introduction to tree-ring dating. University of Chicago Press, Chicago
Stover C, Coffman J (1993) Seismicity of the United States, 1568-1989 (Revised). US Geol Surv Prof Pap 1527
Walpole R, Myers R (1992) Probability and statistics for engineers and scientists, 4th edn. MacMillan, New York
Williams P, Jacoby G, Buckley B (1992) Coincident ages of large landslides in Seattle's Lake Washington. Geol Soc Am Abstr 24(5):90
Witkind I, Stickney M (1987) The Hebgen Lake earthquake area. In: Beus S (ed) Centennial Field Guide, Rocky Mountain Section, Geol Soc Am, Boulder, pp 89–94

Seismic Damage in Conifers from Olympic and Yellowstone National Parks, United States

Wayne L. Hamilton

1 Introduction

Two Douglas-fir (*Pseudotsuga menziesii*) from Olympic NP exhibit signs of the M~9 Cascadia earthquake of 26 January, 1700 (Atwater et al. 2005) and associated after-shocks on nearby faults. One lodgepole pine (*Pinus contorta*), sampled at the Madison River in Yellowstone NP shows damage associated with the 17 August, 1959 M7.5 earthquake or aftershocks (USGS 2008), and another appears to record the large earthquakes felt by the Hayden expedition on 22 August, 1871 at the north shore of Yellowstone Lake (Hayden 1872). Other, such evidence was noted in Yellowstone samples, and younger damage events were seen in western hemlock (*Tsuga heterophilla*) samples from Heart of the Hills in Olympic NP. The common characteristic of productive samples in both parks was that they were taken 6–24 m above ground level where stem whiplash produced by ground motion would be more likely to occur. It appears that such evidence has the potential to reveal unrecorded events; and perhaps epicenter locations.

The obvious, observed macro-features are healed fracture and 'chevron' structures exemplified by one Douglas-fir from Olympic illustrated in Fig. 1. The AD 1700 ring (17.5–17.8 cm) appears normal except for lignin in the late wood. It was fractured in shear by whiplash; perhaps by an aftershock midway through the AD 1701 growth season as suggested by growth inhibition. The diameter of the tree in 1700 ~20 m above ground level was 0.35 m. Micro-features include disorganized cell structure as shown at the same fracture in Fig. 1b. Abnormal cell orientation is obvious in the 1701 earlywood at center and again in the 1702 wood on the extreme right. Approximately 20° around the tree from the fracture, numerous traumatic

W.L. Hamilton (✉)
Department of Conservation Biology, CICESE, Kilometro 107, Carretera Tijuana-Ensenada, 22860, México
e-mail: hamilton@cicese.mx

M. Stoffel et al. (eds.), *Tree Rings and Natural Hazards: A State-of-the-Art*, Advances in Global Change Research 41, DOI 10.1007/978-90-481-8736-2_40,

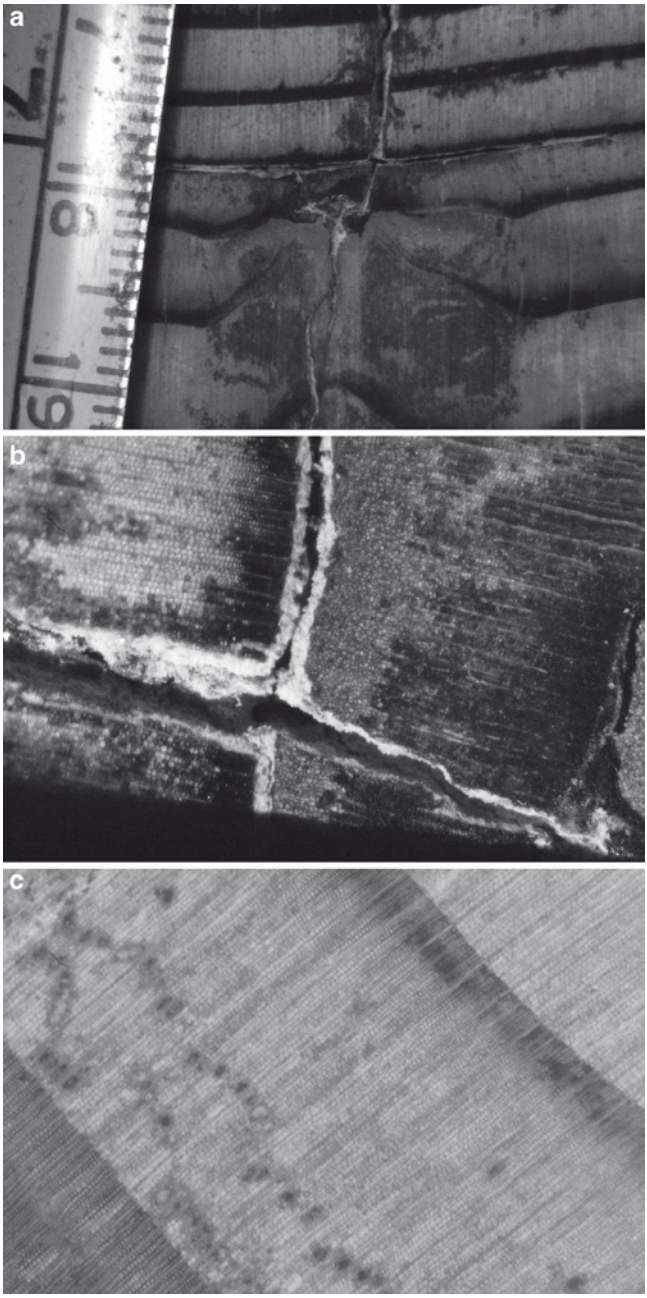

Fig. 1 Olympic Douglas-fir from Staircase Ranger Station: (**a**) shear macro-fracture and the start of a chevron; 1700 ring at 17.5–17.8 cm. 1701 growth reduction; (**b**) detail of the same shear fracture with 1700 on left and disorganized cells early in 1701; (**c**) detail of traumatic resin and lignin ducts in the 1701 ring

ducts (Stoffel and Bollschweiler 2008) are seen in the 1701 ring (Fig. 1c). Some ducts are filled with resin but others appear to be haloed or filled with lignin. In the lower left the 1,700 ring appears to have a false ring boundary in the latewood.

A second Douglas-fir exhibited numerous lignin-haloed traumatic ducts, mostly between 1698 and 1713 on the west (upwind) side. Largest numbers were in 1699, 1700, 1702, and 1704 through 1707. Only one such duct was found in 1701.

One Yellowstone lodgepole pine showed two structures similar to fire scars (lacking charcoal) with cessation of cambial growth at the end of 1960 (Fig. 2a). From left to right one sees the normal 1958 ring, a small chevron in the 1959 latewood, followed by a second chevron in 1960, cessation at a pitch pocket in 1961

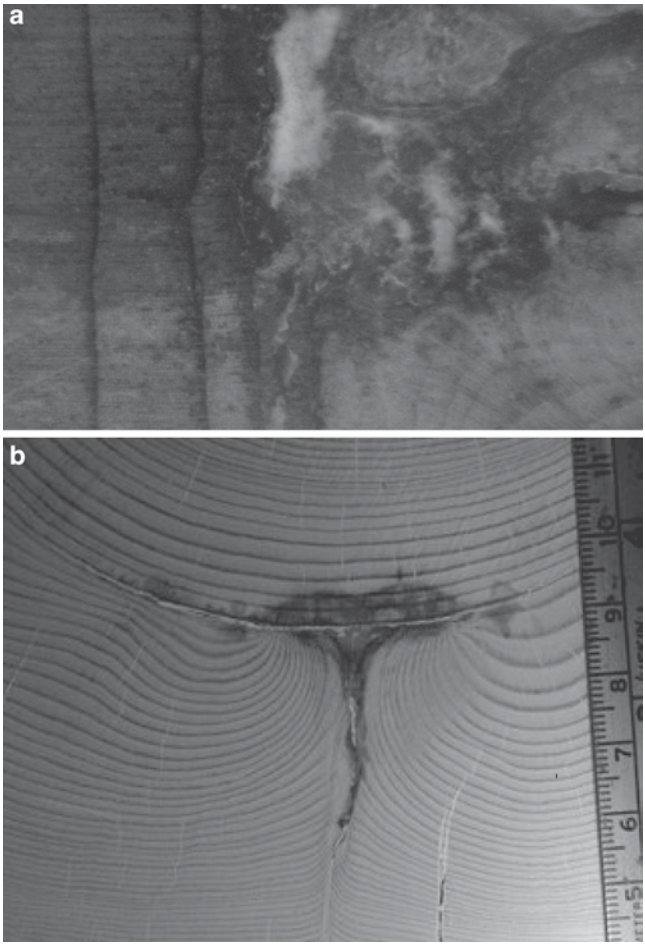

Fig. 2 Yellowstone Madison River lodgepole showing: (**a**) detail of chevron in 1959 latewood and cessation after 1960 and (**b**) another Madison River lodgepole with growth cessation and chevron development after 1873 following reported 1871 earthquakes

and misaligned rings at the right. The implied 1-year delay in growth cessation suggests that with the exception of chevrons most severe seismic whiplash damage occurred in the phloem and inner bark. Moreover, the evidence in this approximately-oriented tree suggests that the onset of chevron structures and growth-cessation structures were produced respectively by shear on the side of the tree ~75°, and by compression or tension ~15°, away from the direction of propagation of surface waves associated with the two largest 1959 seismic events. Inception of most chevron zones suggests micro-shear damage. Chevrons are present in all the samples discussed here. They are being assessed for their potential to record ground wave direction. Traumatic ducts in this sample began in 1959, were absent in 1960, then continued through 1967. The diameter of this tree in 1959 was 0.18 m at 6.2 m above ground level. Measurements show significant growth suppression in the 1960 ring, in agreement with findings of Bekker (2004).

The July, 1871 event was recorded in another nearby lodgepole 6 and 10 m above the ground by chevrons and at 6 m by growth cessation after 1872, suggesting that damage structure lag varies dependent on season of seismic events and on the portion of the phloem that is affected by whiplash (Fig. 2b). Structures tentatively suggest a ray path of 70° (or 250°). Two other nearby lodgepoles sampled at 6 and 7 m (not shown) also exhibited growth cessation after 1911 at 8° and 14°, suggesting close resolution of the ray path from an unrecorded event.

Acknowledgments The collaboration of Brian Atwater and Henry Heasler in sample selection and collection, respectively in Olympic and Yellowstone, and consultation with Frank Telewski are gratefully acknowledged. NPS Study OLYM-276.

References

Atwater BF, Satoko M-R, Kenji S, Yoshinobu T, Kazue, U Yamaguchi D (2005) The orphan tsunami of 1700. U S Geol Surv Prof Pap 1707

Bekker MF (2004) Spatial variation in the response of tree rings to normal faulting during the Hebgen Lake Earthquake, Southwestern Montana, USA. Dendrochronologia 22:53–59

Hayden FV (1872) Fifth annual report of progress. U.S Geological Survey of Montana and portions of adjacent territories. U.S. Government, Print. Off. Washington DC

Stoffel M, Bollschweiler M (2008) Tree-ring analysis in natural hazards research – an overview. Nat Haz Earth Syst Sci 8:187–202

USGS (2008) http://earthquake.usgs.gov/regional/states/events/1959_08_18.php

Part X
Volcanic Activity

Tree stumps buried by the White River tephra, ca. AD 820, Yukon, Canada (© J. J. Clague)

Studying Past Volcanic Activity with Tree Rings

Olga Solomina

1 Introduction

A volcano is an opening in the Earth's crust from which hot magma, ash, and gases escape to the surface. Volcanic eruptions produce numerous and dramatic environmental changes from very local to global scales. Strong explosive eruptions ejecting sulfur aerosols in the stratosphere can impact the Earth's radiation balance, and hence, surface temperature as well as atmospheric circulation patterns. The radiative effect and related cooling after explosive, especially tropical, eruptions is stronger in summer. In the cold season, on the contrary, eruptions generally lead to warming due to an enhanced pole-to-equator gradient and subsequent change in circulation mode. The maximum global cooling (0.1–0.2°C) occurs approximately one year after a strong tropical explosive eruption and the degree of this cooling follows the solar declination displaced toward the north. The eruptions occurring in the high latitudes (e.g. Laki in 1783), on the contrary, reduce the pole-to-equator temperature gradient and lead to the cooling even in winter. Another important effect of this type of eruption is the failure of the summer Indian monsoon (Robock 2000).

Annually resolved and temperature-sensitive tree rings provide a significant proxy for the climatic effects and dating of past volcanic eruptions. The first section of this paper briefly reviews the opportunities and limitations of tree-ring research for these large scale, often global, studies (see also Salzer and Hughes 2010, this volume). The second part of this paper plus three case studies (Pringle et al. 2010, this volume; Biondi and Estrada 2010, this volume; Solomina 2010, this volume)

O. Solomina (✉)
Department of Glaciology, Institute of Geography, Moscow, Russian Federation
e-mail: olgasolomina@yandex.ru

M. Stoffel et al. (eds.), *Tree Rings and Natural Hazards: A State-of-the-Art*,
Advances in Global Change Research 41, DOI 10.1007/978-90-481-8736-2_41,

deal with the local geomorphic impacts of eruptions. Due to the complexity and great diversity of these processes, I will only touch on tree-ring studies of pyroclastic flows and lahars in the following brief review. The information on the frequency and magnitude of these events can serve for the assessment of potential future activity of the volcano, related possible environmental destruction and risks.

The large volumes of gases, liquids and solid material ejected by volcanoes may produce strong geochemical environmental effects that potentially can be identified in vegetation, including wood. The third part of this paper will briefly mention some of the related issues in connection with dendrochemistry. These are also considered in the case study of the dendrochemical effects of the AD 1781 eruption of Mount Hood in Oregon by Sheppard et al. (2010, this volume).

2 Global Climatic Effects of Volcanic Eruptions and Tree Rings

Long temperature sensitive tree-ring chronologies and tree-ring networks are useful to explore the spatial patterns of climate responses to volcanic eruptions for periods prior to the instrumental climatic record. In 1984 LaMarche and Hirschboek demonstrated the correspondence of frost rings in the subalpine bristlecone pine chronology with major volcanic eruptions. Lough and Fritts (1987) further explored the spatial pattern of the regional climatic effect of the eruptions in USA in more detail. Filion et al. (1986), working at treeline sites in Quebec, introduced the idea of light rings (rings with very few latewood cells) as indicators of shortened growing seasons, often related to volcanic eruptions. Yamaguchi et al. (1993) later quantified the threshold May-September temperature for light ring formation in this region. Subsequently Jones et al. (1995) and Briffa et al. (1998) used a network of maximum density chronologies across North America and Eurasia to reconstruct cool summers since AD 1600, claiming that most of them coincided with the dates of major explosive volcanic eruptions. Following these pioneering works almost all new long chronologies are checked for the presence of volcanic footprints. In general the conclusion is that ring width, maximum density, missing, false, frost and light rings can be useful for studying the climatic effect of explosive volcanic eruptions and establishing their precise calendar dates. However, many problems still remain unresolved. Most are related to the complex response of the climate system to volcanic forcing, such as differences in the response time in different regions. Also the transformation of the initial signal by the global and regional atmospheric circulation processes may result in different level of cooling, warming or change in precipitation. It is also very difficult to distinguish the "volcanic" signal from other causes of narrow ring formation or low latewood density.

Ice cores also record the footprints of both local and distant volcanic eruptions. In both proxies – tree rings and ice cores - the location of the volcano responsible for the signal is unknown though the analyses of volcanic glass in ice core layers may provide some clues to identify the potential source. However, ice cores rarely

provide annually resolved dates for eruptions. The accuracy of ice core dating decreases with time and strongly depends on the accumulation rate and the quality of the ice flow model. In contrast, the accuracy of tree ring dating remains stable over time. Salzer and Hughes (2007) illustrate this effect by comparing the ice core and tree-ring chronologies over the last 5000 years. Consequently there have been several attempts to improve the precision of ice core dates for eruptions (and hence the ice core chronologies themselves) using the tree-ring record of growth suppressions potentially related to the ancient volcanic eruptions (e.g. Baillie 2008). However, the linkage between tree-ring extremes and volcanic effects should be treated cautiously as it involves several assumptions and potential errors (Sadler and Gratton 1999). Nevertheless, tree-ring records are of great value in developing the backbone of the chronology of eruptions although the potential ambiguity of the interpretation of the signal should be always taken into account.

3 Dating Volcanic Eruptions, Geomorphic Processes and Related Hazards

The landforms and sediments in volcanic areas that can usually be dated with the help of tree-rings are formed by ashfalls, pyroclastic density currents, landslides, and lahars. These processes are clearly significant environmental hazards and determining the history, magnitude and frequency of these events is a critical element in defining the hazards associated with individual volcanoes. Pyroclastic density currents are fast-moving currents of hot gas and pyroclastic material that travel down the volcano. The speed, tracks, deposition and potential danger of these currents depend on their origin and physical properties. Most pyroclastic currents consist of two parts: a basal flow of coarse fragments that moves along the ground, and a turbulent cloud of ash. The ground speed of the pyroclastic currents is typically greater than 80 km per hour. The temperature of rocks and gas inside a pyroclastic current is generally between 200°C and 700°C and deposited layers of loose rock fragments can be up to 200 m in thickness.

Landslides occur on the slopes of stratovolcanoes due to steepness and the weak consolidation of their constituent debris. These landslides often transition into "lahars" – volcanic mudflows – flows of water mixed with tephra moving downslope or in the river valleys. Lahars may also be generated by intense rainfall, rapid melting of ice and snow, or the outburst of crater lakes. These flows may erode the volcanic material over which they move and increase considerably in volume downslope. They may travel more than 100 km from their source and cover wide areas with cement-like sediments when they cease moving (Fig. 1).

Tree-ring approaches and procedures for dating these processes are similar to those used for other geomorphic hazards such as snow avalanches, landslides, mudflows and debris flows. The trees in the vicinity of the volcano can be affected by different mechanical, thermal and chemical damage and, hence, used as a tool to date the eruption or related geomorphic events. The vegetation at the volcano and

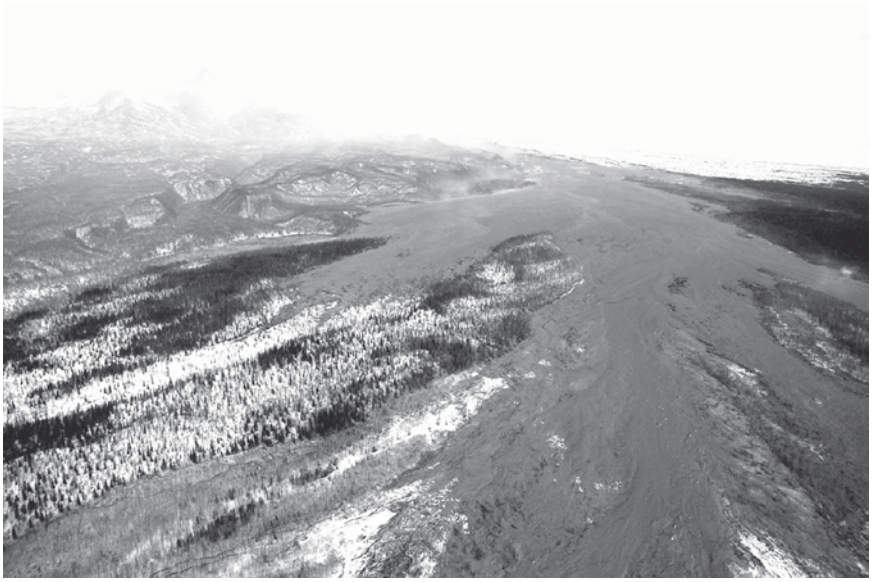

Fig. 1 Pyroclastic flow deposits at the Shiveluch volcano (27 February 2005, Photo courtesy Yu. Demianchuk)

in the immediate vicinity can be completely or partly destroyed and trees can be burned, carbonized (Fig. 2), partly or completely buried *in situ* by debris. They may also be uprooted and displaced kilometers away from their original location. Trees that survive, can be tilted, hit and scarred by boulders or by other objects transported by the flows, or suffer from chemical and thermal burns. They may also lose foliage, bark or roots, their lower stems can be buried by debris or photosynthesis reduced by the ashfall, etc. These damages affect the tree's productivity and the events can be later identified in ring width (and density) chronologies as a suppression lasting from one to a few years depending on the degree of damage. Volcanic activity can also produce positive growth anomalies due to soil fertilization from a thin layer of ash rich in mineral components or the removal of neighboring plants which reduces competition for sunlight and other resources. The comparison of the chronologies developed from potentially affected trees with a "normal" regional ring-width chronology can provide information on candidates for potential dates of eruptions, lahars and other events. However, such evidence is not, by itself conclusive and should be supported by the dates from directly affected trees (Bollschweiler et al. 2010).

It is not clear whether local volcanic eruptions can produce a signal detectable in the chronologies of the trees that do not have direct thermal, mechanical or chemical damage. Battipaglia et al. (2007) recently showed a significant decrease in ring width following each eruption of Vesuvius coinciding with the local temperature changes recorded by instrumental observations. However in these

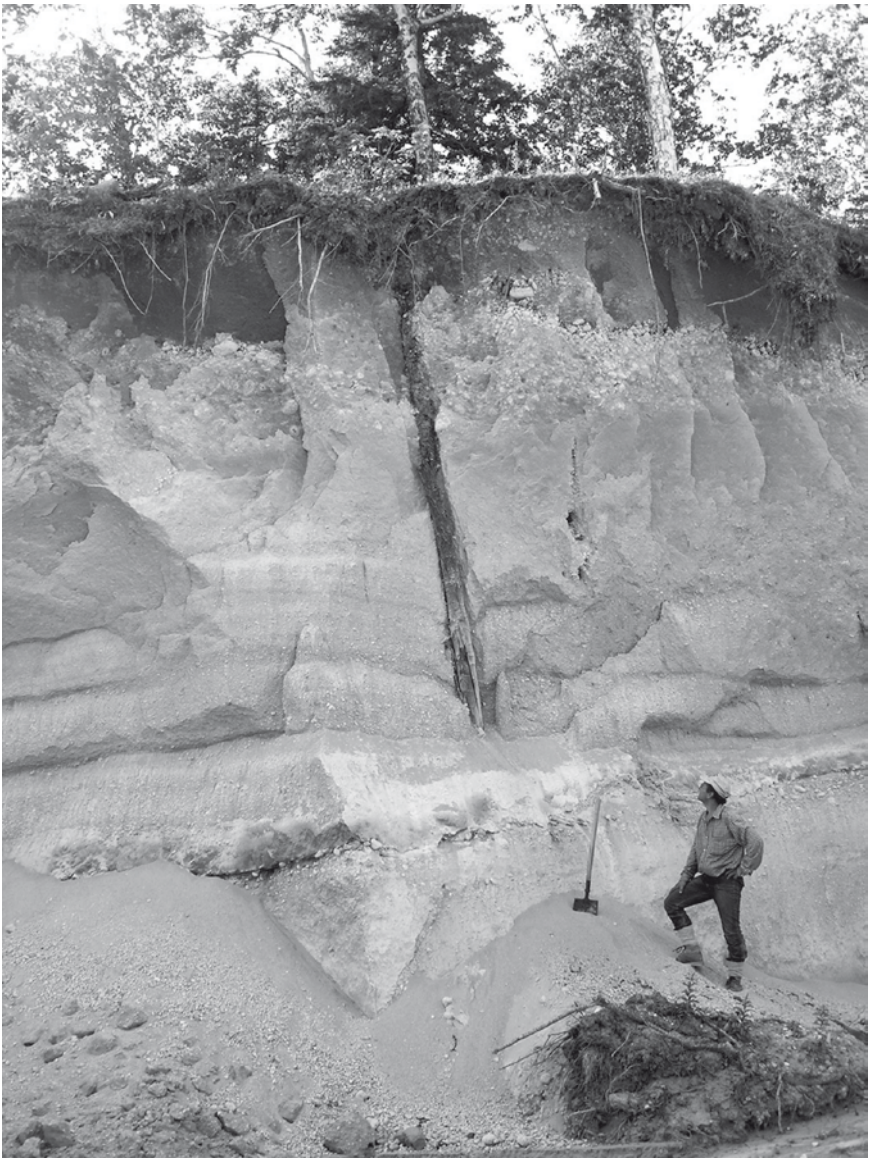

Fig. 2 Kamenskaya valley, Shiveluch volcano, Kamchatka. Carbonized wood buried in situ in the pyroclastic deposits

cases a clear mechanism should be proposed to explain the causal relationship between tree-ring growth suppression and local eruptions while their climatic effect is usually quite limited (Yamaguchi 1993).

The dates of eruptions detected from direct damage or tree mortality are less equivocal. The most reliable dates are from carbonized wood of trees buried *in situ*

in a standing position, killed by a hot pyroclastic flow (see Fig. 2). Their burial by hot fine-grained material results in instantaneous death related to an obvious source without any delay. The main problem is often the poor quality of fragile charcoal and the loss of external burned wood layers. These trees are often rooted in buried soils and help to distinguish pyroclastic deposits of different generations (Fig. 3).

In some cases the trees can survive for several years after a lahar if part of the cambium remains intact. Therefore the death of trees incorporated in lahar deposits may be from causes unrelated to the volcanic eruption and a careful stratigraphic analysis and sufficient samples are necessary (where possible) to avoid mistakes of this kind (Yamaguchi and Hoblitt 1995).

Sometimes lava, pyroclastic flow or lahar deposits cover many square kilometers and completely destroy the vegetation. A minimum date for the flow can be established by tree-ring dating of the oldest tree on the new surface with a correction for ecesis. The ecesis will vary depending on species, availability of seeds, climate and the properties of the lava flows or fine grained pyroclastic material on which the

Fig. 3 Kamenskaya valley, Shiveluch volcano, Kamchatka. The roots of the birch are located in the paleosol separating the deposits of the 500 BP debris avalanche (*lower unit*) and SH1 pyroclastic density current (250–300 BP, the *uppermost unit*). The bark is partly carbonized, the wood is unscathed (Photo courtesy M. Pevzner)

seedling grows. The ecesis may range up a century if the ash layer is thick enough and the new plant colonization is considered as a primary succession. Yamaguchi and Hoblitt (1995) believe that at Mount St Helens the minimum ages of deposits are underestimated by 10–30 years. Dates derived from dating of successive flows should be used as a measure of the period of volcano dormancy with care due to potentially local impacts of the eruptions. Even if the eruption is followed by great changes in the landscape (pyroclastic flow, lahars etc.) these dramatic changes usually happen in limited locations. Therefore although one valley has a pyroclastic flow several kilometers long and a few meters thick, an adjacent valley from the same volcano may have no record of the event. Attempts to reconstruct past eruption history must consider the evidence from many adjacent sites rather than relying on a single investigation.

The best strategy to reconstruct the past volcanic events would be to combine the direct dates of damaged or killed trees, indirect evidence (growth suppressions) from the ring width chronologies and historical records. However, historical records may also be misleading. In places where people live far away from active volcanoes, their descriptions can be rather ambiguous. "Smoke" that is often described in historical documents as evidence of an eruption, probably will not produce any direct effect on the trees growing several kilometers away from the crater. The historical dates for eruptions may also be poorly constrained having begun earlier and ended later than is recorded in the anecdotal stories. Therefore in some cases when the tree-ring records slightly pre-date or post-date the historical dates of volcanic event it is not possible to determine which dates are correct without additional information from further research or alternative approaches.

4 Dendrochemistry

The diagnosis of a chemical signature of past eruptions in tree-rings would be of great value for paleoreconstructions. Although the related geochemical and biological processes are very complex (Watt et al. 2007) some authors have found a chemical fingerprint in the tree rings. Hall, Yamaguchi and Rettberg (1990) report selected element concentrations in trees adjacent to Mount St. Helens marked two anomalous peaks at AD 1478 and 1490 that closely correlate with past eruptions. Sheppard et al. (2008) report an increase in sulphur and phosphorus content in rings from the first year of the eruption (AD 1943–1952) of Michoacan volcano in Mexico. Similar increases in P, S and K concentrations were reported by Cruz-Muñoz et al. (2008) for the Popocatépetl volcano. Pearson et al. (2005) identified dendrochemical footprints in a tree-ring growth anomaly associated with the Late Bronze Age eruption of Thera. They report an increase of sulfur, calcium, and rare earth elements, concentration spikes of zinc and hafnium in the first affected growth-ring.

However in general the dendrochemical results are far from being consistent and some researchers are skeptical about the possibility of a chemical identification

of the past eruptions either from local or distant volcanoes. Pearson et al. 2006 found no chemical signal of a strong Icelandic eruption of Askja (1875) in pine tree rings from central Sweden. Similarly, Watt et al. (2007) reported that there is no systematic correlation of the dendrochemistry from tree rings in pine on the flanks of Mount Etna with periods of effusive, explosive or increased degassing activity. They conclude that "dendrochemistry does not provide a record of persistent but fluctuating volcanic activity" (p. 48). Generally the elemental composition of tree rings shows significant compositional variability within and between trees as well as between species, and a great influence of soil and other environmentally specific conditions- all of which may mask any signal related to volcanic activity.

5 Concluding Remarks

Dendrochronology operates with a very limited number of variables (ring width, density, chemical composition), which can be affected by a multiplicity of causes. Therefore the interpretation of tree-ring records of specific phenomena requires imagination, but also care, common sense and sometimes support from other sources. This general caution is applicable to all branches of dendrochronology and specifically here to what we can conventionally call "dendrovolcanology".

Although the field of "dendrovolcanology" is successfully developing there are important problems which still require further investigation. A central problem is probably resolving disagreement between the ice-core and tree-ring records for ancient eruptions. Where the climatic effects are short term (1–2 years) the deterioration of the precision of the volcanic ice-core chronology with time is a critical limitation for the interpretation and modeling of volcano-climate interactions. The application of more sophisticated statistical methods may help to a certain extent to better match the two chronologies. The dendrochemistry of wood could also significantly contribute to the detection and precise dating of eruptions, but so far the results are promising but remain too ambiguous. As in other fields we also require more information from the Southern Hemisphere and the tropics to develop a truly global picture.

Tree-ring dating of individual eruptions is probably the greatest strength of dendrochronology. Recently a branch from an olive tree buried in tephra on Santorini was used to identify the age of the famous Santorini (Thera) eruption (Friedrich et al. 2006) which was discussed for decades by archeologists, geologists, ice-core scientists and dendrochronologists. Although direct cross-dating of the ring width was not possible in this case due to the irregularities in the olive rings, the tree-rings were dated by ^{14}C and wiggle-matched to the radiocarbon calibration curve. This example demonstrates that close cooperation with other research fields within geology, climatology, modeling, history and others that is essential for success in this complex field.

Acknowledgement I would like to thank Brian Luckman for valuable comments and improvements of my English.

References

Baillie M (2008) Proposed re-dating of the European ice core chronology by seven years prior to the 7th century AD. Geophys Res Lett 35:L15813

Battipaglia G, Cherubini P, Saurer M, Siegwolf R, Strumia S, Cotrufo F (2007) Volcanic explosive eruptions of the Vesuvio decrease tree-ring growth but not photosynthetic rates in the surrounding forests. Global Change Biol 13:1122–1137

Biondi F and Estrada I (2010) Tree-Ring Evidence for the 1913 Eruption of Volcán de Fuego de Colima, Mexico. In: Stoffel M, Bollschweiler M, Butler DR, Luckman BH (eds) Tree rings and natural hazards: A state-of-the-art. Springer, Berlin, Heidelberg, New York, this volume

Bollschweiler M, Stoffel M, Vazquez-Selem L, Palacios D (2010): Tree-ring reconstruction of past lahar activity at Popocatépetl volcano, Mexico. The Holocene 20:265–274

Briffa KR, Jones PD, Schweingruber FH, Osborn TJ (1998) Influence of volcanic eruptions on Northern Hemis-phere summer temperature over the past 600 years. Nature 393:450–455

Cruz-Muñoz AR, Rodríguez-Fernández L, Calva-Vázquez G, Ruvalcaba-Sil JL (2008) Effects due to Popocatepetl volcano eruptions on the elemental concentrations in tree growth rings. X-Ray Spectrometry 37 2:163–168

Filion L, Payette S, Gauthier L, Boutin Y (1986) Light rings in subarctic conifers a dendrochronological tool. Quat Res 26(2):272–279

Friedrich, Walter L, Kromer B, Friedrich M, Heinemeier J, Pfeiffer T, Talamo S (2006) Santorini eruption radiocarbon dated to 1627-1600 B.C. Science 312 5773:548

Hall G, Yamaguchi D, Rettberg T (1990) Multielemental analyses of tree rings by inductively coupled plasma mass spectrometry. J Radioanal Nuclear Chem 146(4):255–265

Jones P, Briffa K, Schweingruber F (1995) Tree-ring evidence of the widespread effects of explosive volcanic eruptions. J Geophys Res 22(11):1333–1336

LaMarche V Jr, Hirschboeck K (1984) Frost rings in trees as records of major volcanic eruptions. Nature 307(5946):121–126

Lough J, Fritts H (1987) An assessment of the possible effects of volcanic eruptions on North American climate using tree-ring data, 1602 to 1900 A.D. Clim Change 10:219–239

Pearson C, Dale D, Brewer P, Kuniholm P, Lipton J, Manning S (2005) Dendrochemical analysis of a tree-ring growth anomaly associated with the Late Bronze Age eruption of Thera. J Archaeol Sci 32(8):1265–1274

Pearson C, Manning S, Coleman M, Jarvis K (2006) A dendrochemical study of Pinus sylvestris from Siljansfors Experimental Forest, central Sweden. Appl Geochem 21(10):1681–1691

Pringle P, Pierson T, Cameron K, Sheppard P (2010) Late 18th century Old Maid eruption and lahars at Mount Hood, Oregon (USA) dated with tree rings and historical observations. In: Stoffel M, Bollschweiler M, Butler DR, Luckman BH (eds) Tree rings and natural hazards: A state-of-the-art. Springer, Berlin, Heidelberg, New York, this volume

Robock A (2000) Volcanic eruptions and climate. Rev Geophys 38:191–219

Sadler J, Gratton J (1999) Volcanoes as agents of past environmental changes. Global Planet Change 21:181–196

Salzer MW, Hughes MK (2007) Bristlecone pine tree rings and volcanic eruptions over the last 5000 yr. Quat Res 67:57–68

Salzer M, Hughes M (2010) Volcanic eruptions over the last 5,000 years from high elevation tree-ring widths and frost rings. In: Stoffel M, Bollschweiler M, Butler DR, Luckman BH (eds) Tree rings and natural hazards: A state-of-the-art. Springer, Berlin, Heidelberg, New York, this volume

Sheppard P, Ort M, Anderson K, Elson M, Vázquez-Selem L, Clemensi A, Little N, Speakman R (2008) Multiple dendrochronological signals indicate the eruption of Parícutin volcano, Michoacán, Mexico. Tree-Ring Res 64(2):97–108

Sheppard P, Weaver R, Pringle P, Kent A (2010) Dendrochemical evidence of the 1781 eruption of Mount Hood, Oregon. In: Stoffel M, Bollschweiler M, Butler DR, Luckman BH (eds) Tree rings and natural hazards: A state-of-the-art. Springer, Berlin, Heidelberg, New York, this volume

Solomina O (2010) Unknown eruption of Shiveluch volcano (Kamchatka, Russia) around AD1756 is identified by dendrochronology. In: Stoffel M, Bolschweiler M, Butler DR, Luckman BH (eds) Tree rings and natural hazards: A state-of-the-art. Springer, Berlin, Heidelberg, New York, this volume

Watt S, Pyle D, Mather T, Day J, Aiuppa A (2007) The use of tree-rings and foliage as an archive of volcanogenic cation deposition. Environ Poll 148(1):48–61

Yamaguchi D (1993) On tree-ring records of volcanic events in Kamchatka and elsewhere. Quat Res 40:262–263

Yamaguchi DK, Filion L, Savage M (1993) Relationship of temperature and light ring formation at subarctic treeline and implications for climate reconstruction. Quat Res 39:256–262

Yamaguchi D, Hoblitt R (1995) Tree-ring dating of pre-1980 volcanic flowage deposits at Mount St Helens, Washington. Geol Soc Am Bull 107(9):1077–1093

Tree-Ring Evidence for the 1913 Eruption of Volcán de Fuego de Colima, Mexico

Franco Biondi and Ignacio Galindo Estrada

1 Introduction

Dendrochronological records provide various types of evidence for the impact of volcanic activity, which can then be used to quantify the amount of risk associated with this environmental hazard. Major explosive volcanic eruptions that inject dust and aerosols into the stratosphere are capable of causing large-scale surface cooling (Minnis et al. 1993). Distant, large-scale networks of temperature sensitive tree-ring chronologies reflect those eruptions either in anatomical xylem features, such as frost damage (LaMarche and Hirschboeck 1984), or in measured annual growth parameters, especially maximum latewood density (Briffa et al. 1998). Trees growing close enough to the volcano to be covered with tephra may either be killed or survive depending on tephra layer thickness and coarseness (Yamaguchi 1985). Surviving trees experience abrupt suppression of radial growth (Druce 1966; Hinckley et al. 1984), including locally absent rings (Yamaguchi 1983). Such initial response can generate prolonged periods of reduced radial increment (Segura et al. 1995b; Smiley 1958), or be followed by greater than normal growth rates (Abrams et al. 1999; Hinckley et al. 1998; Segura et al. 1995a).

Despite the presence of many active volcanoes in the North American tropics, little or no information is available on forest species as biological archives of past eruptions in that heavily populated region. Early work (Eggler 1967) conducted near the apex of Volcán Paricutín used a total of nine relatively young trees belonging to three different pine species. Abnormal wood growth was associated with the aftermath of volcanic activity, but the absence of crossdating among ring patterns, the limited number of samples, and the below-treeline elevation of the sites cast doubts on the reliability of dates assigned to xylem layers (Biondi and Fessenden

F. Biondi (✉)
DendroLab, Department of Geography, University of Nevada, Reno, NV 89557, USA
e-mail: franco.biondi@gmail.com

I.G. Estrada
Ciencias del Ambiente, Universidad de Colima, Colima, Mexico

M. Stoffel et al. (eds.), *Tree Rings and Natural Hazards: A State-of-the-Art*,
Advances in Global Change Research 41, DOI 10.1007/978-90-481-8736-2_42,

1999). Based on a recently developed, 400-year tree-ring chronology from tropical North America (Biondi 2001a), we present here the impact of tephra fallout from the January 1913 Plinian eruption of Volcán de Fuego de Colima on the Hartweg's pine (*Pinus hartwegii*) timberline found near the top of the nearby Nevado de Colima. Our objective was to investigate changes in annual growth of forest trees following the deposition of volcanic tephra, as well as to test if tree growth response was organized spatially within that upper elevation forest.

2 Study Area

Volcán de Fuego de Colima is one of the most active volcanoes in the North American continent (Bretón Gonzáles et al. 2002; Martin del Pozzo and Sheridan 1993; Medina Martinez 1983). Located at the western end of the Trans-Mexican Neovolcanic Belt, Volcán de Fuego rises almost 4,000 m above sea level, and lies about 5.5 km south of the older, higher (ca. 4,300 m), and larger Nevado de Colima, an andesitic volcano long extinct and covered by abundant vegetation (Fig. 1). Both peaks are part of the Colima Volcanic Complex, although some confusion has been generated by authors who have used such names as synonyms (e.g., Simkin and Siebert 1994, p. 267). Volcán de Fuego is a typical composite volcano characterized by periods of reduced activity separated by short, cataclysmic eruptions (Martin del Pozzo et al. 1995). One such event occurred in January 1913, and lasted a few days, causing widespread damage (Saucedo Girón 1997; Saucedo Girón and Macías Vázquez 1999). The 1913 event featured a volcanic explosivity index (Newhall and Self 1982) of 4, and is included among the largest explosive eruptions since A.D. 1500. After the emission of a tall vertical eruptive column, pyroclastic flows descended following major canyons towards the south, southeast, and southwest sides of the cone, reaching as far as 15 km from the crater (Robin et al. 1991). Repeated photographs taken before and after the eruption show that the summit crater lost nearly 100 m in height, while changing from a nicely rounded shape to a jagged, irregular rim (Luhr 1981; Waitz 1914). Ash and pumice fallout extended to the northeast, covering Nevado de Colima with tephra deposits reaching and sometime exceeding 50 cm in depth (Saucedo Girón 1997). Wind measurements performed from 1994 to 1997 at 3,500 m elevation on the Volcán in a locality called "El Volcancito", just a few hundred meters below the summit, indicate that in January predominant wind directions are from W-WNW and S-SSE (Galindo Estrada et al. 1998). By adding wind vectors together, it is therefore expected that ashfall and ash clouds will be most abundant in the resulting direction of NE-ENE. Upper-level winds, which in this region are driven mainly by the strong Hadley circulation system (Waliser et al. 1999), are also expected to point northeastward. In fact, ashfall reached as far as northern Mexico: it was reported in the states of San Luis Potosí (400 km to the northeast) and Coahuila (700 km northward).

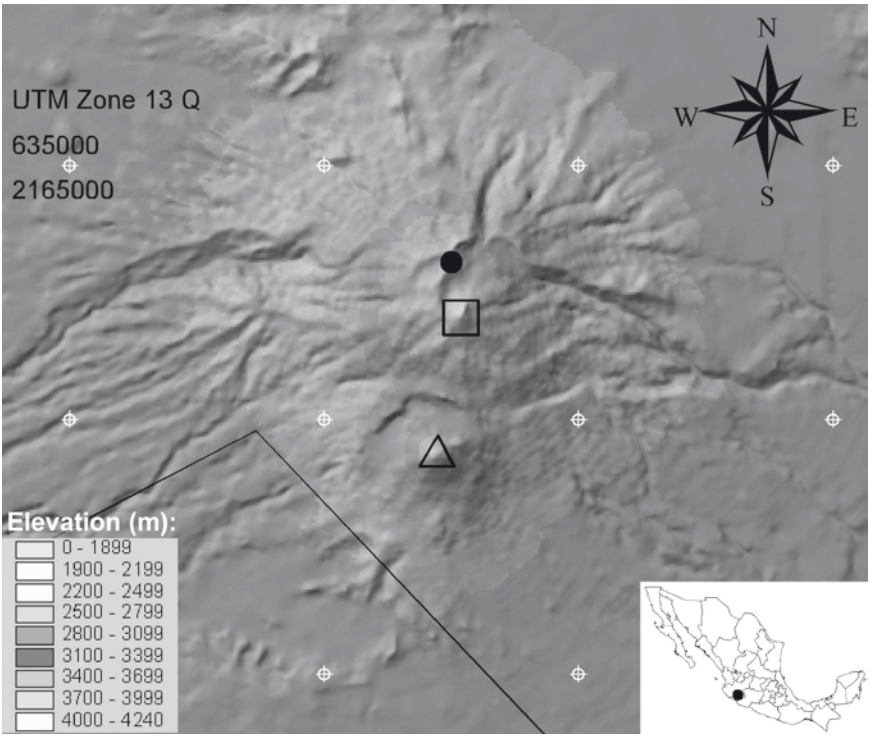

Fig. 1 Shaded relief map of the Colima Volcanic Complex. Grid nodes (white crosshairs) at 10 km intervals are shown for reference, together with Universal Transverse Mercator (UTM) coordinates of the upper left grid node. Volcán de Fuego (**V**) is about 5.5 km south of Nevado (**N**), and both peaks rise 2,000 m above the surrounding landscape. Our study area (□) was covered by 15–30 cm of tephra following the 1913 eruption of Volcán de Fuego

While volcanic activity maintains the slopes of Volcán de Fuego free of forests, abundant vegetation is found on Nevado de Colima, especially on its northern side (Madrigal Sánchez 1970). The southern aspects of Nevado have frequently been disturbed from Volcán de Fuego historic eruptions. For instance, there are reports of fires burning on the southern flanks of Nevado de Colima shortly after the start of the 1913 eruption (Saucedo Girón 1997). Tree species found on Nevado can be grouped and classified according to elevational zones that change along gradients of temperature and precipitation (McVaugh 1992). Near the top, up to about 4,000 m elevation, the dominant species is *P. hartwegii*, which forms open, uneven-aged stands, and endures daily temperature ranges as large as the annual range, approaching 20°C (Galindo Estrada et al. 1998). While *P. hartwegii* treelines on Pico de Orizaba (Lauer 1978) and on the twin peaks Iztaccihuatl and Popocatepetl (Beaman 1962), all mountains that exceed 5,200 m elevation, have already been investigated, the Nevado de Colima treeline has not been studied in detail, not even after the 1936 creation of the Parque Nacional Volcán-Nevado de Colima.

Field observations on forest structure and dynamics were recorded during extended trips in April 1998, May 2000, and May 2001. A total of 50 dominant trees were dendrochronologically sampled, and used to develop the first multi-century tree-ring chronology in the Americas between 20°N and the equator (Biondi 2001a). Sampled trees ranged from 0.5 to 1.3 m in diameter at breast height (dbh), reached ages in excess of 500 years, and were located within or near a site called Puerto La Calle, north of Nevado (Fig. 1). The site covers about 2 km^2, and is relatively protected against strong winds by nearby ridges, but it received a tephra fallout with a thickness of 15–30 cm from the 1913 eruption (Saucedo Girón 1997).

3 Materials and Methods

Crossdated tree-ring records were combined by tree to obtain a representation of growth damage caused by the 1913 eruption. Dates were assigned to individual xylem layers by visually matching ring patterns among core samples underneath a stereo-zoom binocular microscope with 7–35x magnification (Fig. 2). Ring width was measured to the nearest micron, and numerical verification of dating accuracy was performed using the COFECHA software (Grissino-Mayer 2001; Holmes 1983). A total of 63 samples from 26 trees included years 1913–1914, and were used to investigate the impact of the 1913 eruption on the *P. hartwegii* forest. Ring–width patterns of 51 core samples that included years from 1910 to 1920 were digitally captured using an image analysis system, and combined into a web-accessible animation (Biondi 2001b). To minimize growth effects related to tree age and size, standardized ring indices were computed as follows (Biondi 1993, 1999):

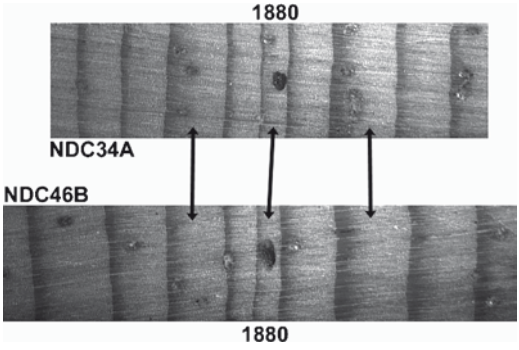

Fig. 2 Example of crossdating two *Pinus hartwegii* core samples from Nevado de Colima, Mexico. Identification codes are formed by three letters for the site (NDC), two digits for the tree (34 and 36), and a letter for the increment core (**A** and **B**). Time is from right to left, and a pencil dot marks year 1880. Inter-annual growth variability and degree of replication across samples are high enough to allow for matching ring patterns both visually (*arrows*) and numerically Biondi 2001a

$$i_{it} = \log (w_{it} + k) - y_{it}$$

with i_{it} = ring-index of sample i on year t; w = crossdated ring width (μm); k = constant added to avoid taking the logarithm (log) of zero; y = modified negative exponential or straight line with slope ≤0. Tree summaries were produced by averaging ring indices, and mean ring-index in 1913–1914 ($I_{13–14}$) was compared to the mean of ring indices in 5 previous years (1908–1912) and five following years (1915–1919). Tree growth reduction ($gr_{13–14}$, %) was then computed for each tree, as follows:

$$gr_{13–14} = (1–\mathrm{I}_{13–14}/\ \mathrm{I}_{08–12,\ 15–19}) \times 100$$

with $I_{08–12,\ 15–19}$ = arithmetic average of ring indices in 1908–1912, 1915–1919.

The main climatic signal recorded by *P. hartwegii* annual wood increment on Nevado de Colima is June rainfall (Biondi 2001a), which corresponds to the onset of summer monsoon precipitation. To test for potential interactions between volcanic activity and climate as factors influencing tree growth in 1913–1914, monthly precipitation data for the 1900–1998 period were obtained from global datasets gridded at 2.5° latitude by 3.75° longitude resolution (Hulme 1992; Hulme 1999; Hulme et al. 1998). We used the average of grid boxes 4149 and 4150, which include our study area as they cover 18°45'N–21°15'N latitude and 106°52.5'W–99°22.5'W longitude. The total summer (June-August) rainfall was computed to represent monsoon precipitation.

Coordinates of sampled trees were obtained in the field using handheld global positioning systems (GPSs). Geostatistical techniques (Isaaks and Srivastava 1989) were used to investigate spatial patterns of growth reduction. In particular, variogram analysis was used to test for spatial dependence, and block kriging was used to produce a map of tree response to the 1913 eruption (Biondi et al. 1994). It should be noted that the Nevado de Colima tree-ring chronology shows extreme reduction of tree growth not only in 1913–1914, but also in 1816–1917 and in 1655 (Biondi 2001a). We decided to focus on the twentieth century events because in 1655 the chronology is based on a very small sample (6 trees only), and in 1816–1917 tree-ring records could not be compared with climatic records.

4 Results

Comparison among different radii and trees shows that the 1913 eruption resulted in a sudden reduction of stem growth (e.g., Fig. 3). All 63 measured ring-width series decreased 20% or more in 1913 compared to 1912. In addition, 22 samples had no visible ring in 1913, and 8 were missing the 1914 ring as well. Growth reduction ($gr_{13–14}$) of individual pines reached a maximum of 83%, with a mean of 43% and a standard deviation of 23%. Only three individuals suffered less than 10% reduction; 73% of the trees showed a reduction ≥30%. Based on measured in

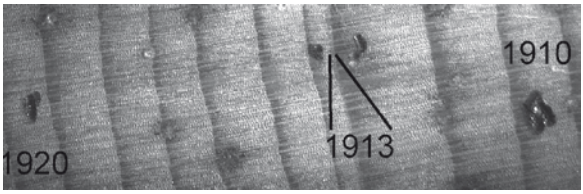

Fig. 3 A representative sample of tree growth response to the 1913 eruption. In this core, the 1913 ring is barely visible (0.092 mm wide). The amount of radial growth suppression in 1913–1914 ($gr_{13\text{-}14}$) was 52%

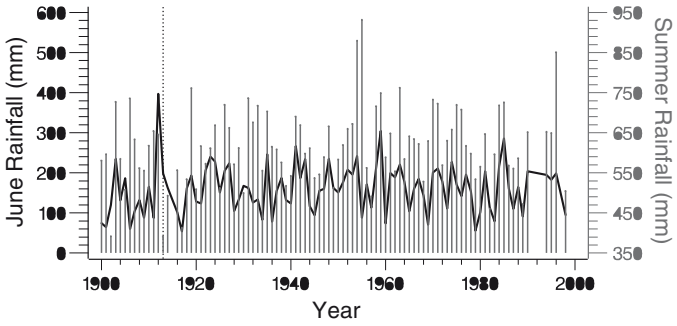

Fig. 4 Time series plot of June rainfall (solid line) and summer (June–August) total precipitation (needles) from 1900 to 1998 (see text for details). The summer of 1913 (dotted line) was very dry. The wettest June on record occurred in 1912. Values were missing in 1915 and in a few years after 1990

1998 and on collected tree-ring specimens, at coring height (1–1.3 m above ground) all trees were older than 50 years in 1913, and 85% exceeded 100 years.

June and summer (June–August) precipitation from 1900 to 1998 is shown in Fig. 4. In 1913, even though summer rainfall was very low (about 390 mm *vs.* the long-term average of 616 mm), June rainfall was above normal (198 mm *vs.* the long-term average of 161 mm). In addition, the June of the year before the eruption, 1912, was the wettest June on record (397 mm, or 2.5 times the long-term average). June rainfall in 1914 was slightly more than normal (163 vs. 161 mm).

Variogram analysis of tree response to the 1913 eruption revealed no spatial dependence. The isotropic semivariogram of 1913–1914 growth reduction could best be modeled as a pure nugget effect, indicating a lack of spatial autocorrelation. This derived from the presence of highly variable amounts of growth reduction at either short or long distances (Fig. 5).

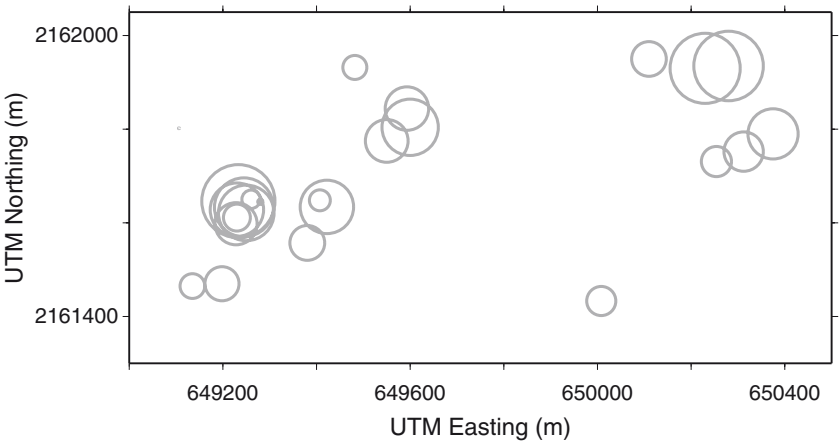

Fig. 5 Map of 1913–1914 radial growth reduction in 26 *Pinus hartwegii* trees sampled on Nevado de Colima. Circle diameter is directly proportional to growth reduction ($gr_{13\text{-}14}$), and center of circle is drawn at the tree location. For scale, the largest circle corresponds to an 83% reduction

5 Discussion

In 1913, access to our study area was possible only by foot, horseback, or burro, the latter being the most common form of transportation in those areas until the late 1900s. Although stumps and other indicators of selective logging are scattered within the study area, together with evidence of cattle grazing and low-intensity fires, the overall synchronicity of wood growth among samples indicates that large-scale, mostly climatic factors have controlled tree ring formation over the past few centuries. As the 1913–14 growth reduction is widespread among sampled trees, but unique over the 1900s, it cannot be related to intermittent and repeated disturbance events. Furthermore, the absence of frost damage in every tree-ring sequence rules out a potential influence of distant volcanic activity (LaMarche and Hirschboeck, 1984), such as the 1912 Novarupta eruptions in what is now Katmai National Park on the Alaska Peninsula (Fierstein and Hildreth 1992).

Given the climate data we have for the study area, it is unlikely that the 1913–1914 extreme growth reduction experienced by *P. hartwegii* trees was caused by climatic factors alone. Nevertheless, rainfall variability could have enhanced tree response to the 1913 eruption, either by increasing the size of the 1912 radial increment (see Fig. 3 for an example) or by further reducing wood formation during the 1913–1914 growing seasons. Even more plausibly, a lowering of summer rainfall delayed the removal of tephra deposited on pine crowns and on the soil surface, which, as explained in the following paragraph, was the most likely mechanism behind the observed tree growth suppression (see Hinckley et al. 1998).

Volcanic ashfall and tephra fallout reduce photosynthesis in multiple ways (Eggler 1967; Seymour et al. 1983; Yamaguchi 1985). First, mechanical damage to

foliage from lapilli and ash accumulation curtails the amount of photosynthetic tissue. Second, dust in the atmosphere and deposited on tree crowns lowers photosynthetically active radiation reaching pine needles. Third, dust layers plug stomata, impeding gas exchange between plant epidermis and atmosphere. Fourth, besides hampering the supply of photosynthate, crown damage and metabolic malfunction also hinder auxin production and transport to the lower stem, so that wood growth is delayed, asymmetric, and even absent at coring height. Fifth, the mantle of ash (and mud as soon as rain begins to fall) covering the ground decreases aeration of roots and changes soil chemistry, which in turn may affect absorption of water and nutrients. Because of the processes that drive growth suppression, trees on Nevado de Colima that survived the 1913 eruption could recover after monsoon rainfall had washed away the accumulated tephra. The dry summer of 1913 exacerbated the negative impact of the eruption on pine growth, which did not return to normal until 1915 (Biondi 2001a).

Other abnormal wood increment patterns have also been associated with the aftermath of tephra deposition, such as increased growth rates following an initial reduction of tree radial increment (Abrams et al. 1999; Eggler 1967; Hinckley et al. 1998). That 'rebound' effect is typical of areas where tree growth is limited by lack of soil nutrients and/or by competition with surrounding individuals. Ash-driven fertilization, mulching, and partial stand mortality favor wood increment of surviving trees after an initial growth decline (Mahler and Fosberg 1983; Segura et al. 1995a). The openness of *P. hartwegii* stands, and the deep volcanic soils they can exploit on Nevado de Colima, are consistent with the lack of a rebound effect, which was also absent in Ponderosa pine (*Pinus ponderosa*) from northern Arizona (Smiley 1958).

Because no spatial structure existed in the data, block kriging values provided no improvement over inverse distance weighting interpolation (Isaaks and Srivastava 1989). The lack of distance-dependent growth reduction within the forest provides useful information. In particular, it shows that tree response to the 1913 eruption did not follow a spatially coherent pattern, presumably because of the stochastic nature of ashfall and tephra deposition on irregular terrain and crown forms. Although the study area is relatively small, with maximum inter-tree distances of about 1.3 km, the number of pairs in 100-m distance intervals ranged between 11 and 50, hence it should not have biased our results. In a previous study, post-1980 tree-ring reductions in trees and saplings of four coniferous species growing northeast of Mt. St. Helens were found to be largely a function of distance from the volcano (Hinckley et al. 1984). However, subsequent research using old-growth Pacific Silver fir (*Abies amabilis*) (Segura et al. 1994) found no spatial structure in tree growth reductions following tephra deposition from the 1980 eruption of Mount St. Helens, mostly because of the interaction with other factors (elevation, competition, etc.) affecting radial growth.

As mentioned in the Materials and Methods section, we focused on the 1913 eruption because in the early 1800s the tree-ring evidence is not clear enough to argue in favor of a volcanic effect, from either a local or a remote eruption. Indeed, the 1816–1817 negative peak of *P. hartwegii* tree growth was preceded, in 1813, by widespread frost damage (Biondi 2001a). The 1816–1817 suppression follows the

1815 Tambora eruption (Harrington 1992), and Volcán de Fuego de Colima also erupted in February 1818 with a volcanic explosivity index of 4 (Newhall and Self 1982). Considering that the 1913 and 1818 volcanic events should have had similar magnitude, occurred prior to the growing season, and had similar geographical axes of tephra fallout, it would then be tempting to postulate that tree-ring dates should be changed by 2 years, so that 1813 could become 1815, and the growth suppression could coincide with the years 1818–19. In reality, tree rings differ from any other kind of paleoenvironmental record because their dating is *independent* and *internally consistent*. More than 50 samples were visually and numerically crossdated back to 1800,[1] and it is unlikely that all samples included two false rings, although that possibility cannot be excluded *a priori*.

False rings, or intra-annual growth bands (Fritts 1976; Kuo and McGinnes 1973), are associated with a temporary cessation of apical growth followed by growth resumption during the same year (Larson 1962; Panshin and de Zeeuw 1980). Storm and frost damage, drought, insect defoliation, fire, etc., can induce the formation of false rings (Glock and Agerter 1963; Kramer and Kozlowski 1979). Anatomical features of tree-ring series used in this study demonstrate that transition from one ring to another is sharp and well defined (see for example Figs. 3 and 4). Stem increment of *P. hartwegii* on Nevado de Colima during the 2001–2002 growing seasons has been measured at half-hour intervals (Biondi 2002) and shows no evidence of intra-seasonal cessation and resumption of growth (Biondi et al. 2005). Therefore, one would have to assume that the two double rings were formed because of the volcanic eruptions themselves, in 1913 and 1818. In other words, rings considered missing would not be, and what was considered a micro-ring (such as 1913 in Fig. 3) would instead be an intra-annual band. While the development of additional dendrochronological records from *P. hartwegii* sites in other parts of Mexico and Central America should provide a test of this hypothesis, currently available evidence does not seem to warrant a revision of Nevado de Colima tree-ring dates.

In conclusion, we were able to demonstrate that *P. hartwegii* trees growing near treeline on Nevado de Colima were negatively affected by the impact of the January 1913 eruption from the nearby Volcán de Fuego. Exactly dated, annually resolved tree-ring records uncovered a sudden growth reduction in 1913, often extending into 1914 as well. Such 2-year response was strengthened by summer drought. Given that little information has been available to date on forest species as biological archives of past environments in the North American tropics, it appears that treeline tropical sites hold valuable records of environmental phenomena, including volcanic eruptions.

Acknowledgments The authors thank the Parque Nacional Volcán-Nevado de Colima and El Patronato del Nevado de Colima y Cuencas Adyacentes A.C. for permission to conduct fieldwork. Drs. Andrew Burton and Shirley Imsand helped with field collections. Juan Carlos Gavilanes Ruiz and Alejandro Elizalde Torres provided local support and information. Robin J. Burnham reviewed an earlier draft. The comments of Alan Gillespie, Katherine K. Hirschboeck, Thomas M. Hinckley, Christopher Newhall, and one anonymous reviewer are gratefully acknowledged. F. Biondi was supported by the Paleoclimate Program of the National Science Foundation under

[1] Dates reported by Biondi 2001a, were independently verified at the Laboratory of Tree-Ring Research, University of Arizona, Tucson.

Grant No. 0096316, and by the Climate and Atmospheric Research Program of the National Oceanic and Atmospheric Administration under Grant NA06GP0690. Permission to reproduce previously published text and figures was kindly provided by Elsevier's Copyright Clearance Center.

References

Abrams MD, Copenheaver CA, Terazawa K, Umeki K, Takiya M, Akashi N (1999) A 370-year dendroecological history of an old-growth *Abies-Acer-Quercus* forest in Hokkaido, northern Japan. Can J Forest Res 29:1891–1899

Beaman JH (1962) The timberlines of Iztaccihuatl and Popocatepetl, Mexico. Ecology 43:377–385

Biondi F (1993) Climatic signals in tree-rings of Fagus sylvatica L. from the central Apennines, Italy. Acta Oecologica 14:57–71

Biondi F (1999) Comparing tree-ring chronologies and repeated timber inventories as forest monitoring tools. Ecol Appl 9:216–227

Biondi F (2001a) A 400-year tree-ring chronology from the tropical treeline of North America. Ambio 30:162–166

Biondi F (2001b) http://wolfweb.unr.edu/homepage/fbiondi/NDC_AN.GIF

Biondi F (2002) Treeline dendroclimatology in the north American tropics. PAGES News 10:9–10

Biondi F, Fessenden JE (1999) Radiocarbon analysis of *Pinus lagunae* tree rings: Implications for tropical dendrochronology. Radiocarbon 41:241–249

Biondi F, Hartsough PC, Galindo Estrada I (2005) Daily weather and tree growth at the tropical treeline of North America. Arct Antarc Alp Res 37:16–24

Biondi F, Myers DE, Avery CC (1994) Geostatistically modeling stem size and increment in an old-growth forest. Can J Forest Res 24:1354–1368

Bretón Gonzáles M, Ramírez JJ, Navarro C (2002) Summary of the historical eruptive activity of Volcán de Colima, Mexico 1519-2000. J Volcanol Geothermal Res 117:21–46

Briffa KR, Jones PD, Schweingruber FH, Osborn TJ (1998) Influence of volcanic eruptions on Northern Hemisphere summer temperature over the past 600 years. Nature 393:450–454

Druce AP (1966) Tree-ring dating of recent volcanic ash and lapilli, Mt Egmont. NZ J Bot 4:3–41

Eggler WA (1967) Influence of volcanic eruptions on xylem growth patterns. Ecology 48:644–647

Fierstein J, Hildreth W (1992) The plinian eruptions of 1912 at Novarupta, Katmai National Park, Alaska. Bull Volcanol 54:646–684

Fritts HC (1976) Tree rings and climate. Academic Press, London

Galindo Estrada I, Elizalde Torres A, Solano Barajas R, Cruz Calvario M (1998) Climatología del Volcán de Fuego de Colima. Universidad de Colima, Colima, Col. (Mexico).

Glock WS, Agerter SR (1963) Anomalous patterns in tree rings. Endeavour 22:9–13

Grissino-Mayer HD (2001) Evaluating crossdating accuracy: a manual and tutorial for the computer program COFECHA. Tree-Ring Res 57:205–221

Harrington CR (ed) (1992) The year without a summer? World climate in 1816. Canadian Museum of Nature, Ottawa

Hinckley TM et al (1984) Impact of tephra deposition on growth in conifers: the year of the eruption. Can J Forest Res 14:731–739

Hinckley TM et al (1998) Scaling and integration in trees. In: Peterson DL, Parker VT (eds) Ecological scale: theory and applications. Columbia University Press, New York, pp 309–337

Holmes RL (1983) Computer-assisted quality control in tree-ring dating and measurement. Tree-Ring Bull 43:69–78

Hulme M (1992) A 1951-80 global land precipitation climatology for the evaluation of General Circulation Models. Clim Dyn 7:57–72
Hulme M (1999) 'gu23wld0098.dat', Version 1.0. University of East Anglia, Norwich
Hulme M, Osborn TJ, Johns TC (1998) Precipitation sensitivity to global warming: Comparison of observations with HadCM2 simulations. Geophys Res Lett 25:3379–3382
Isaaks EH, Srivastava RM (1989) An introduction to applied geostatistics. Oxford University Press, New York
Kramer PJ, Kozlowski TT (1979) Physiology of woody plants. Academic Press, Orlando
Kuo M-L, McGinnes EA Jr (1973) Variation of anatomical structure of false rings in eastern redcedar. Wood Sci 5:205–210
LaMarche VC Jr, Hirschboeck KK (1984) Frost rings in trees as records of major volcanic eruptions. Nature 307:121–126
Larson PR (1962) Auxin gradients and the regulation of cambial activity. In: Kozlowski TT (ed) Tree growth. Ronald Press, New York, pp 87–117
Lauer W (1978) Timberline studies in central Mexico. Arct Alp Res 10:383–396
Luhr J (1981) Colima: history and cyclicity of eruptions. Volcano News 7:1–3
Madrigal Sánchez X (1970) Caracterizacion Fito-ecologica Preliminar de los Volcanes de Fuego y Nevado de Colima (Mexico). In: Instituto Nacional de Investigaciones Forestales, Mexico City, p 32
Mahler RL, Fosberg MA (1983) The influence of Mount St. Helens volcanic ash on plant growth and nutrient uptake. Soil Sci 135:197–201
Martin del Pozzo AL, Sheridan M (1993) Volcán de Colima. Geofísica Internacional 32:541–542
Martin del Pozzo AL, Sheridan M, Barrera D, Lugo Hubp J, Vázquez Selem L (1995) Potential hazards from Colima volcano, Mexico. Geofísica Internacional 34:363–376
McVaugh R (1992) Flora Novo-Galiciana. The University of Michigan Herbarium, Ann Arbor
Medina Martinez F (1983) Analysis of the eruptive history of the Volcan de Colima, Mexico (1560-1980). Geofísica Internacional 22:157–178
Minnis P et al (1993) Radiative climate forcing by the Mount-Pinatubo Eruption. Science 259:1411–1415
Newhall CG, Self S (1982) The Volcanic Explosivity Index (VEI): an estimate of explosive magnitude for historical volcanism. J Geophys Res 87:1231–1238
Panshin AJ, de Zeeuw C (1980) Textbook of wood technology, 4th edn. McGraw-Hill, New York
Robin C, Camus G, Gourgaud A (1991) Eruptive and magmatic cycles at Fuego de Colima volcano (Mexico). J Volcanol Geothermal Res 45:209–225
Saucedo Girón R (1997) Reconstruccion de la Erupción de 1913 del Volcan de Colima. In: Instituto de Geofisica. Universidad Nacional Autonoma de Mexico, Mexico City, p 190.
Saucedo Girón R, Macías Vázquez JL (1999) La historia del Volcán de Colima. Tierra Adentro 98:8–14
Segura G, Brubaker LB, Franklin JF, Hinckley TM, Maguire DA, Wright G (1994) Recent mortality and decline in mature Abies amabilis: the interaction between site factors and tephra deposition from Mount St Helens. Can J Forest Res 24:1112–1122
Segura G, Hinckley TM, Brubaker LB (1995a) Variations in radial growth of declining old-growth stands of *Abies amabilis* after tephra deposition from Mount St Helens. Can J Forest Res 25:1484–1492
Segura G, Hinckley TM, Oliver CD (1995b) Stem growth responses of declining mature *Abies amabilis* trees after tephra deposition from Mount St Helens. Can J Forest Res 25:1493–1502
Seymour VA, Hinckley TM, Morikawa Y, Franklin JF (1983) Foliage damage in coniferous trees following volcanic ashfall from Mt. St. Helens [Washington State]. Oecologia 59:339–343
Simkin T, Siebert L (1994) Volcanoes of the world: a regional directory, gazetteer, and chronology of volcanism during the last 10,000 years, 2nd edn. Geoscience Press, Tucson

Smiley TL (1958) The geology and dating of Sunset Crater, Flagstaff, Arizona. In: Anderson RY, Harshberger JW (eds) Guidebook of the Black Mesa Basin Northeastern Arizona. New Mexico Geological Society, Socorro, pp 186–190

Waitz P (1914) Der gegenwärtige Stand der Mexikanischen Vulkane und die letzte Eruption des Vulkans von Colima (1913). Z Vulkanol 1:247–274

Waliser DE, Shi Z, Lanzante JR, Oort AH (1999) The Hadley circulation: assessing NCEP/NCAR reanalysis and sparse in situ estimates. Clim Dyn 15:719–735

Yamaguchi DK (1983) New tree-ring dates for recent eruptions of Mount St Helens. Quat Res 20:246–250

Yamaguchi DK (1985) Tree-ring evidence for a two-year interval between recent prehistoric explosive eruptions of Mount St Helens. Geology 13:554–557

Dendrochemical Evidence of the 1781 Eruption of Mount Hood, Oregon

Paul R. Sheppard, Russ Weaver, Patrick T. Pringle, and Adam J.R. Kent

Dendrochronological responses to an eruption of Mount Hood, Oregon, including new dendrochemical evidence, are documented here. Mount Hood, a stratovolcano of the Cascade Volcanic Arc (Fig. 1a), is thought to have erupted in AD 1781, as determined from tree death dates (Pringle et al. 2008), ring-width reductions (Sheppard et al., 2008a), and historical documents (Cameron and Pringle 1986, 1987). Ring-width evidence alone can indicate past volcanic eruptions (Yamaguchi and Lawrence 1993), but elemental concentrations in tree rings also reflect environmental changes brought about by eruptions (Hughes 1988). Dendrochemistry has been useful in past research of eruptions (Pearson et al. 2005; Sheppard et al., 2008b), so it was tried on Mount Hood and its 1781 eruption.

Three tree-ring sites were sampled. Site 1 is high up on Mount Hood itself (Fig. 1c) and has Engelmann spruce (*Picea engelmannii*). Site 1 received at least 10 cm of ash fall during the 1781 eruption, and its trees were expected to show dendrochemical evidence of that event. Site 2 is down low on Mount Hood (Fig. 1c) and has Douglas-fir (*Pseudotsuga menziesii*). The ash fall deposit from the 1781 eruption at Site 2 is only 1 cm at most, so its trees were not expected to show dendrochemical evidence of that event. Site 3 is 80 km north of Mount Hood (Fig. 1b) and has western red cedar (*Thuja plicata*). Site 3 is well away from ash fall from the 1781 eruption, so its trees were not expected to show dendrochemical evidence of that event.

Samples were visually crossdated by matching patterns of wide and narrow rings across trees (Douglass 1941). Short portions of these cores were measured

P.R. Sheppard (✉)
Laboratory of Tree-Ring Research, University of Arizona, Tucson AZ 85721, USA
e-mail: sheppard@ltrr.arizona.edu

R. Weaver
Heritage High School, Vancouver, WA 98682, Canada

P.T. Pringle
Science Department, Centralia College, Centralia, WA 98531, USA

A.J.R. Kent
Department of Geosciences, Oregon State University, Corvallis, OR 97331, USA

M. Stoffel et al. (eds.), *Tree Rings and Natural Hazards: A State-of-the-Art*,
Advances in Global Change Research 41, DOI 10.1007/978-90-481-8736-2_43,

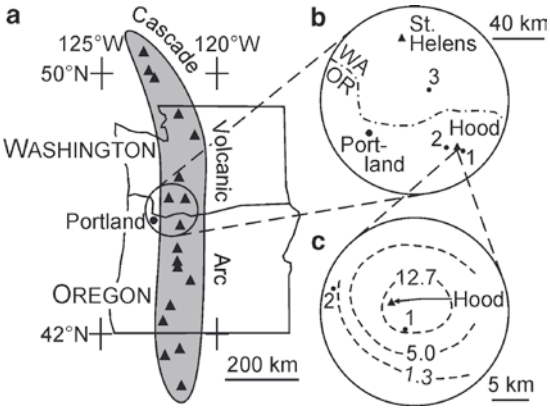

Fig. 1 Maps showing Mount Hood and tree-ring sites (1-3) sampled there. Contour lines of C are isopachs of ash fall (cm) from the 1781 eruption

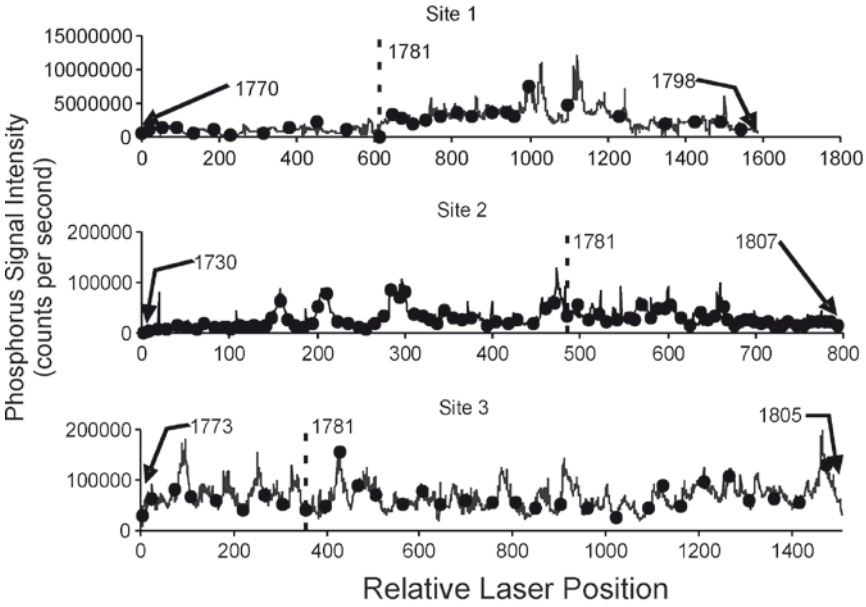

Fig. 2 Dendrochemistry data for phosphorus for three trees on or near Mount Hood. Start and end years are given, dots indicate years, and vertical dashed lines mark AD 1781

chemically using laser ablation inductively-coupled plasma, mass spectroscopy (Watmough et al. 1998). This method provides data with sub-annual resolution, and the data were marked off in annual ring time by measuring ring widths along the laser tracks on each sample. No calibration was done for absolute elemental concentrations, so results will be in relative intensity (counts per second), with higher values indicating higher elemental concentrations and vice versa.

From Site 1, within ash fall of the 1781 eruption of Mount Hood, a tree shows a clear increase in ring phosphorus beginning in AD 1781 and lasting for many years (Fig. 2). By contrast, trees from Sites 2 and 3, outside the ash fall from the 1781 eruption, do not show any clear changes in ring phosphorus at or near that time period (Fig. 2). The absolute values of phosphorus intensity are also much higher for Site 1 than for Sites 2 and 3. This pattern for ring phosphorus, an increase in a tree within ash fall areas versus no increase outside of ash fall, is similar to dendrochemical responses demonstrated for cinder-cone eruptions (Sheppard et al. 2008b).

Other elements measured show no relevant changes through time in any of these three trees, making phosphorus distinctive by comparison. More trees still need dendrochemical measuring in order to improve the replication of these results to be certain that a true dendrochemical signal exists from this eruption.

Dendrochemistry appears to have excellent potential for research on past eruptions of stratovolcanoes, and laser ablation appears to be a functional method for dendrochemistry. Further development and testing is needed, but combining dendrochemistry with ring-width dendrochronology could improve the identification and analysis of eruptions of the past few centuries to perhaps a millennium or two.

Acknowledgements Laser ablation measurement work was done by the WM Keck Collaboratory for Plasma Spectrometry at Oregon State University.

References

Cameron KA, Pringle PT (1986) Post-glacial lahars of the Sandy River basin, Mount Hood, Oregon. Northwest Sci 60:225–237

Cameron KA, Pringle PT (1987) A detailed chronology of the most recent major eruptive period at Mount Hood, Oregon. Geol Soc Am Bull 99:845–851

Douglass AE (1941) Crossdating in dendrochronology. J Forest 39(10):825–831

Hughes MK (1988) Ice-layer dating of the eruption at Santorini. Nature 335:211–212

Pearson C, Manning SW, Coleman M, Jarvis K (2005) Can tree-ring chemistry reveal absolute dates for past volcanic eruptions? J Archaeol Sci 32:1265–1274

Pringle PT, Pierson TC, Cameron KA, Sheppard PR (2008a) Late 18th century Old Maid eruption and lahars at Mount Hood, Oregon–evidence from tree-ring dating and from observations of Lewis and Clark in 1805-6. 1st AmeriDendro Conference, June 23–27, 2008, Vancouver, British Columbia, Canada

Sheppard PR, Ort MH, Anderson KC, Elson MD, Vázquez-Selem L, Clemens AW, Little NC, Speakman RJ (2008) Multiple dendrochronological signals indicate the eruption of Parícutin Volcano, Michoacán, Mexico. Tree-Ring Res 64:97–108

Sheppard PR, Weaver R, Pringle PT, Kent A (2008b) Dendrochemical evidence of the 1780s Old Maid Eruption of Mount Hood, Oregon. 1st AmeriDendro Conference, June 23–27 (2008) Vancouver. British Columbia, Canada

Watmough SA, Hutchinson TC, Evans RD (1998) The quantitative analysis of sugar maple tree rings by laser ablation in conjunction with ICP-MS. J Environ Quality 27:1087–1094

Yamaguchi DK, Lawrence DB (1993) Tree-ring evidence for 1842-1843 eruptive activity at the Goat Rocks dome, Mount St. Helens, Washington. Bull Volcanol 55:264–272

Volcanic Eruptions over the Last 5,000 Years from High Elevation Tree-Ring Widths and Frost Rings

Matthew W. Salzer and Malcolm K. Hughes

1 Introduction

Some tree-ring records, due to their great age, the annual resolution of their dates, and their sensitivity to the climatic effects of large volcanic eruptions, are useful in understanding the magnitude and frequency of large globally-effective volcanic eruptions. Two primary factors are thought to have forced much of late Holocene variation in climate prior to industrialization: solar output and volcanic eruptions (Free and Robock 1999; Crowley 2000; Shindell et al. 2001). While there is some debate regarding which of these forcings has played the dominant role (Shindell et al. 2003), there is little doubt that volcanism affects climate. Large explosive eruptions inject great quantities of sulfur compounds into the stratosphere, which combine with water to produce sulfuric acid aerosol (Rampino and Self 1982). This injection changes the radiative balance by increasing absorption and reflection of incoming short wave radiation by stratospheric aerosols, and generally has a cooling effect on climate (Lacis et al. 1992; Minnis et al. 1993; McMormick et al. 1995). Volcanism has also been reported to cause winter warming in the extratropical Northern Hemisphere due to cold season shifts in the Arctic Oscillation (Robock and Mao 1992; Kelly et al. 1996). However, radiative forcing dominates the net surface temperature changes from very large eruptions and leads to significant cooling (Shindell et al. 2003). There is some evidence that volcanic eruptions have played a major role in forcing past global temperatures. Pulses of volcanic activity, for example, contributed substantially to the decadal-scale climate variability of the Little Ice Age (LIA) interval (AD 1400–1850) (Porter 1986; Mann et al. 1998; Crowley 2000). Yet the climatic impact of past eruptions varies spatially and appears to be partly dependent on eruption frequency, size, location, seasonal timing, sulfur content, and the state of the climate system at the time of the eruption.

M.W. Salzer (✉) and M.K. Hughes
Laboratory of Tree-Ring Research, University of Arizona, Tucson, AZ 85721, USA
e-mail: msalzer@ltrr.arizona.edu

M. Stoffel et al. (eds.), *Tree Rings and Natural Hazards: A State-of-the-Art*,
Advances in Global Change Research 41, DOI 10.1007/978-90-481-8736-2_44,

At the upper forest border in the western conterminous United States, tree-ring growth processes are often limited by warm-season temperature (Fritts 1991). It has long been suspected that upper-treeline ring-widths are recording variability in temperature or a temperature-related variable such as growing season length (LaMarche 1974; LaMarche and Stockton 1974). Prior to the mid-nineteenth century, narrow and frost-damaged growth rings in ancient pines (*Pinus longaeva, Pinus aristata*, *Pinus balfouriana*) at upper forest border (3,200–3,500 m), where the ecological context promotes sensitivity to warm-season temperature, have been shown to be associated with lowered temperature and with large explosive volcanic eruptions (LaMarche and Hirschboeck 1984; Scuderi 1990; Salzer and Kipfmueller 2005). While an eruption is not required to generate the cool climatic conditions that lead to narrow and/or frost-damaged rings at high elevation, narrow rings or frost rings and explosive eruptions do tend to coincide more often than would be expected by chance. Very small rings (Hughes et al. 1999) and rings with low maximum latewood density (Jones et al. 1995; Briffa et al. 1998) from tree-ring chronologies near circumboreal tree limit have also been shown to be coincident with major volcanic eruptions.

It is possible that factors other than temperature may be involved in the local tree-ring growth-response to distant volcanoes. For example, the reduced atmospheric transparency associated with the dust veil may affect photosynthesis (Gu et al. 2003) and Scuderi (1992) demonstrated an association with atmospheric opacity/solar radiation receipts at high elevation in the Sierra Nevada. Furthermore, Shindell et al. (2003) have suggested that continental proxies sensitive to warm-season temperatures, such as some tree-ring chronologies, tend to emphasize the enhanced continental summer cooling associated with the radiative response to volcanic forcing, but not the winter warming climatic response In either case, however, continental proxies sensitive to atmospheric transparency and/or warm-season temperatures are well suited for our purposes here: the identification of past volcanic events.

Electrical conductivity and sulphate measurement data from ice cores have been used successfully to reconstruct volcanic histories for much of the Holocene at near-annual resolution (Hammer et al. 1980; Crowley et al. 1993; Zielinski et al. 1994; Langway et al. 1995; Zielinski 1995; Clausen et al. 1997; Cole-Dai et al. 1997; Budner and Cole-Dai 2003). However, these studies do not address the degree to which a large past eruption may have influenced the climate system and thus the biosphere. Here, we analyze growth responses of climatically-sensitive trees to volcanic eruptions. We present a western North American chronology of annually resolved high-elevation tree-ring growth minima over the past five millennia and compare this to the record of volcanic deposition in ice cores and to ring-width minima in two other high latitude non-North American tree-ring chronologies. The aims of the study are to use these tree-ring data to augment the ice-core record in a number of ways: by providing confirmation from an alternative proxy record for volcanic signals in ice-cores, by suggesting alternative dates for ice core dated eruptions, and by adding to the list of years when volcanic events were likely.

2 Study Sites, Materials, and Methods

2.1 Chronology Development and Standardization

Five upper forest border bristlecone pine tree-ring chronologies (4 *P. longaeva* and 1 *P. aristata*) from four mountain ranges in western North America (Fig. 1, Table 1) were developed from temperature-sensitive upper forest border trees. The ring-width series that make up these chronologies were all crossdated to the calendar year, measured to the nearest 0.01 mm, and conservatively standardized to remove age and size related trends. Crossdating quality was checked using COFECHA12K (Holmes 1983).

Standardization is a basic procedure in dendrochronology that is designed to remove long-term non-climatic factors associated with increasing tree age and tree size from individual time series of ring-width measurements (Fritts 1976). The standardization procedure involved the fitting of a line or curve to the individual sample ring-width series using ARSTANL (Cook 1985), and dividing the raw data by the fitted curve. Due to the open non-competitive nature of these high elevation stands, a modified negative exponential curve, a straight line of negative slope, or a horizontal line were used in the standardization. To create a mean site chronology, the annual standardized indices of tree growth were averaged. This process was repeated for each of the five upper forest border chronologies used in the study. Mean segment length was 492 years, so that this standardization procedure should retain variability on time scales up to 164 years (Cook et al. 1995), but as time scales lengthen beyond 164 years the proportion of variability retained declines.

The variances of the chronologies were adjusted to remove variance bias as a result of sample size (Osborn et al. 1997; pp. 90–92, equations 4–6) and the chronologies

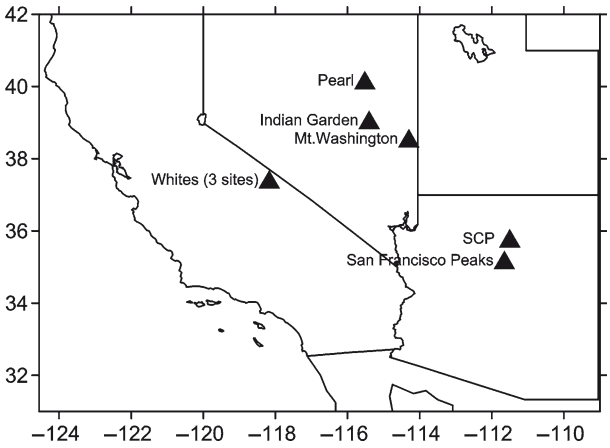

Fig. 1 Western USA tree ring site locations. Upper forest border sites used in HI5 chronology include: Whites (2 sites Sheep Mtn. and Campito Mtn), Pearl, Mt. Washington, and San FranciscoPeaks. Lower forest border drought-sensitive chronologies include Whites (1 site-Methuselah), Indian Garden, and SCP

Table 1 Tree-ring chronologies used in analyses

CRN[a]	Elev. m	N.LatW.Lon	Species[b]	Timespan	Trees/radii	Meanseries length	Meanseries intercor
High	Elev.			BC AD			
CAM	3400	37/118	PILO	3000–1983	92/188	472	0.68
SHP	3555	37/118	PILO	3000–1990	156/259	501	0.64
MTW	3450	39/114	PILO	2032–2002	109/175	456	0.63
PRL	3275	40/115	PILO	1242–2002	70/107	648	0.61
SFP	3580	35/112	PIAR	250–1997	139/233	384	0.54
Low	Elev.						
MWK	2800	37/118	PILO	3000–1979	100/285	748	0.76
IND	2900	39/115	PILO	2370–1980	112/112	766	0.54
SCP[c]	2290-1890	35/112	PIPOPIED PSME	AD570–1997	107/239	261	0.79

[a] Chronologies: CAM=Campito; SHP=Sheep Mtn.; MTW=Mt. Washington; PRL= Pearl Peak; SFP=San Francisco Peaks; MWK=Methuselah Walk; IND=Indian Garden

[b] Species: PILO=*Pinus longaeva*; PIAR=*Pinus aristata*; *PIPO=Pinus Ponderosa*; *PIED=Pinus edulis*; *PSME= Pseudotsuga menziesii*

[c] Southern Colorado Plateau Precipitation Reconstruction (see Salzer and Kipfmueller 2005)

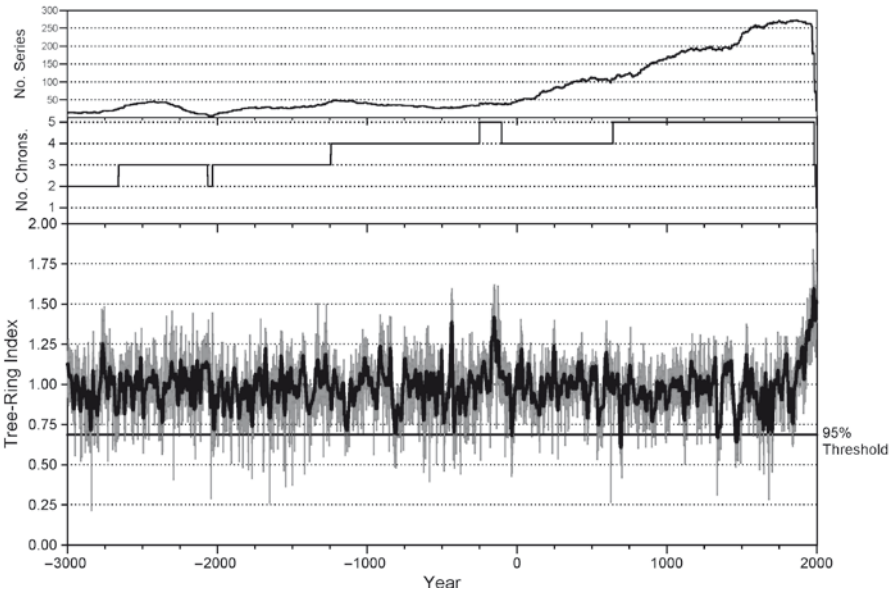

Fig. 2 Time-series plot of regional high elevation tree-ring index from 3000 BC to AD 2002 (HI5 chronology – variance-adjusted normalized mean of five subalpine bristlecone pine chronologies). Dark thicker line smoothed with a 20-year spline. Upper panel is total number of series in the chronology; middle panel is total number of chronologies through time

normalized using the mean and standard deviation. The resulting normalized index chronologies consist of a variance-adjusted average of many individual samples from living trees and from dead remnant material. The average correlation between the five chronologies over their common intervals is 0.41 ($n > 2{,}230$ years, all significant at $p<0.0001$) despite an average distance between sites of over 440 km. The five chronologies were then averaged to form a single time series. This series was also adjusted to remove variance bias (Osborn et al. 1997) and normalized. The resulting regional tree growth time-series is a high elevation chronology of upper forest border tree growth from 3000 BC to AD 2002 with a variance that does not depend on the size of the sample. The chronology minimizes any single site idiosyncrasies and maximizes the signal common to all five sites (Fig. 2) (hereafter referred to as the HI5 chronology). It should be noted that due to the nature of chronology building, particularly the use of overlapping series with a mean length of approximately 500 years, millennial-scale variability would not be retained in the HI5 chronology.

2.2 Isolating the Volcanic Signal in Tree Rings

To identify potentially volcanically influenced growth years, we first determined those years when extreme low growth occurred at the upper forest border.

The normalized values of the HI5 chronology were ranked and the narrowest 250 years (5%) identified. To eliminate a potential drought effect, we then compared the values of the narrowest 5% years of the HI5 chronology with the normalized index values for the same years with several long tree-ring chronologies from the region known to be drought sensitive (Methuselah Walk and Indian Garden *P. longaeva*, on file at the Laboratory of Tree-Ring Research) and the southern Colorado Plateau precipitation reconstruction (Salzer and Kipfmueller 2005) (Fig. 1). The normalized values of the chronologies were compared. Years in which growth was more limited at lower elevation than at upper treeline were considered drought years and were removed from the analyses. In a relatively small number of cases, growth was severely suppressed both at high and low elevations in the same year. In these cases, when other evidence for volcanism such as a frost-damaged ring existed, these years were included in the analysis. When such evidence was absent the year was eliminated. The process of comparing high elevation and low elevation chronologies resulted in the removal of 85 years from the pool of 250 years thought to have high potential for volcanic forcing of low growth. The resulting pool contains 165 years of extreme low growth in upper forest border trees over the last 5,000 years.

In addition, during the crossdating process, years in which the cellular structure of the ring was damaged by freezing events during the growing season (frost-ring years) were tabulated (Table 2). Frost rings have been previously shown to be associated with explosive eruptions, primarily as a result of late growing-season polar air outbreaks in years with extended growth seasons (LaMarche and Hirschboeck 1984). In order to emphasize large-scale events we included for consideration those years with frost rings at two or more sites or years with frost rings in three or more trees at a single site.

Table 2 Ring-width minima and frost-ring signals for the past 50 centuries

BC	Year(s)
30th	**2951[a], 2911[a],** 2906**[*a], 2905*[a]**; (*2906*)
29th	2885, 2879, 2872, 2862, 2853, 2841*, 2821, 2800; (*2841*)
28th	2794, 2732*; (*2731*)
27th	2699, 2685, 2677, 2670
26th	None
25th	**2495[a]**
24th	None
23rd	**2294[a]**
22nd	2173, 2157, **2148[a]**, 2131
21st	**2036[*a], 2035*[a]** 2028, 2027, 2023; (*2036*)
20th	**1996[a], 1962[b], 1921[a], 1909[b,c], 1908[b,c], 1907[b,c]**
19th	1857, 1831; (*1815*)
18th	1771
17th	**1693[a]**, 1652*, **1649[c], 1626*[a,c];** (*1653, 1627*)
16th	**1597[a]**, 1544, 1524
15th	1418*; (*1419*)
14th	1386, 1385, 1373; (*1359*)
13th	None (*1297*)
12th	1150, 1147, 1135*, 1134*, **1133[a], 1132[a]**; (*1187, 1138, 1135*)

(continued)

Table 2 (continued)

BC	Year(s)
11th	None; (*1089, 1031*)
10th	None; (*973, 953, 952*)
9th	854, 826, 811
8th	**776**[a]; (*737, 711*)
7th	**624**[a]; (*655*)
6th	**586**[a], (*570, 551*)
5th	476*[a], **472**[a], **425***[b], **424***[b], **421***[b], **420**[b], **419**[b], **406***[a]; (*480, 476, 474, 424, 422, 407*)
4th	None; (*355*)
3rd	**294**[a], 282, 281, 280, **245***[b]; (*275, 244, 206*)
2nd	**180**[a]; 139, 125, (*194, 161, 140, 123*)
1st	61, **42***[a], 38, 37, 36; (*90, 43*)
AD	*Year(s)*
1st	None
2nd	137; (*119, 140, 188*)
3rd	274*; (*227, 230, 251, 268, 273, 282*)
4th	344; (*310, 337, 389, 390, 393*)
5th	451, **472**[a]; (*411, 421, 438, 469, 479, 484*)
6th	**536***[b,c], **537***[b,c], 542*, 543, 545, 547, **569**[b,c]; (*522, 532, 536, 541, 574*)
7th	**627***[b], 681*, **687***[a], **688***[a], **690**[a], **691**[a]*, **692***[a], **693***[a], **694***[a], **695***[a], **696**[a], **697**[a], **698**[a]; (*627, 674, 681, 684, 687, 692, 694*)
8th	**743**[b,c]; (*715, 789*)
9th	860, **899***[a,b,c]; (*816, 822, 835, 884, 889, 899*)
10th	**900***[a,b,c], **902**[a,b,e], **903**[a,b,e], 990*; (*909, 934, 959, 985, 989*)
11th	None; (*1003, 1008, 1015, 1029, 1057, 1066, 1076*)
12th	**1114**[e], 1121; (*1109, 1118, 1134, 1139, 1142, 1171, 1190*)
13th	**1201***[a], **1204**[a], **1230**[a,b,c,d], **1288***[a,d,e], (*1200, 1225, 1257, 1259, 1275, 1277, 1280, 1287*)
14th	**1332***[a], **1334**[d], **1336**[d], **1342**[a,d,e], **1348**[a,d], **1349**[a,d], **1350**[a,d,e], **1355**[c], **1357**[c], **1360**[c]; (*1329, 1331*)
15th	**1458***[a,c,d,f], **1459**[a,c,d,e,f], **1460**[a,c,d,e,f], **1461**[a,c,d,f], **1462**[c,d,f], **1464d, 1466**[a,d], **1468**[d], 1471*, **1472**[b], **1473**[a,b,c], **1474**[a,b,c], **1480**[a,b,c], (*1443, 1453, 1455, 1457, 1470*)
16th	1578*; (*1546, 1557, 1577, 1596*)
BC	*Year(s)*
17th	**1602***[a,b,e,f,g], **1606**[a,f,g], **1618**[e,f,g], **1624**[f,g], 1641*[a,b,c,e,f,g], **1644**[a,b,c,f,g], 1645[a,b,c,f,g], **1646**[a,b,c,g], **1647**[a,b,c,g], **1672**[a,b,c,e,f,g], **1675**[f,g], **1677**[f,g], **1681***[g]; (*1601, 1640, 1680, 1699*)
18th	1702*, 1703*, 1704, 1705; (*1702, 1725, 1732, 1761*)
19th	**1836**[a,d,e,f,g], **1838**[d,e,f,g], **1840**[d,e,f,g], **1842**[e,f,g]; (*1809, 1810, 1828, 1848, 1882, 1884*)
20th	None; (*1941, 1965*)

Non-italic years are ring-width minima signals.
(*Italic years in parentheses*) are frost-ring signals.
* indicate ring-width minima year that corresponds with a frost damaged ring (frost-rings ±1 year of minima).
Bold years indicate ring-width minima year that corresponds with a volcanic signal in an ice-core (ice-core signals ±5 years of ring-width minima). Underlined years indicate exact-year match between ring-width minima year and GISP2 signal
[a]GISP2 Signal (Zielinski et al. 1994; Zielinski 1995)
[b]GRIP Signal (Clausen et al. 1997)
[c]DYE Signal (Clausen et al. 1997)
[d] BIPOLAR Signal (Langway et al. 1995)
[e]Antarctic Signal (Budner and Cole-Dai, 2003)
[f]Antarctic Signal (Cole-Dai et al. 1997)
[g]CRETE Signal (Crowley et al. 1993)

2.3 Comparison with Ice-Core Records of Volcanism

We tested the statistical significance of the association between the HI5 ring-width minima and volcanic signals reported in the Greenland Ice Sheet Project (GISP2) ice core (Zielinski et al. 1994) in several ways. First we treated the ice core as an annually dated time series and only allowed for exact year matches between the two data sets. We also used a Monte Carlo simulation to test the statistical significance of the apparent association. However, due to local depositional effects, up to a third of the known volcanic event signals can be missing from a single ice core (Zielinski et al. 1994). For this reason we expanded the analysis to include data from a number of ice cores from both poles (Robock and Free 1996; Ammann and Naveau 2003). To allow for some uncertainty in the ice core dates, and to account for seasonality and lag effects in the processes from eruption to deposition and from eruption to climatic effect(s) to tree growth response, we allowed for matches between ring-width minima years and ice core years within a range of ±5 years of the ring-width minima date.

2.4 Comparison with High Latitude Tree-Ring Chronologies

Large-scale explosive volcanic events may influence tree-ring growth not only at high altitude but also in high latitude locations. The argument that ring-width minima signals are the result of past hemispheric- or global-scale events is strengthened through comparison of the HI5 minima years with minima years from remote high latitude tree-ring chronologies. These comparisons improve our ability to subsequently identify past eruptions, because years with extremely narrow tree rings in multiple locations are stronger candidates for past large-scale events. Two existing high latitude chronologies were investigated: The 4,000-year Yamal Peninsula Siberian larch (*Larix sibirica*) chronology (Hantemirov and Shiyatov 2002) (data from IGBP PAGES/World Data Center for Paleoclimatology # 2003-029) and the 7,000-year Scots pine (*Pinus sylvestris*) chronology from Finnish Lapland (Eronen et al. 2002; Helama et al. 2002). The Yamal chronology is from northwestern Siberia (approximately 67°30’ N, 70 °E) and has been used as the basis for a multimillennial summer temperature reconstruction. The *P. sylvestris* chronology, from the forest-tundra ecotone region of northern Finnish Lapland (approximately 68°–70° N, 21°–29°E) has also been used to generate a long midsummer temperature reconstruction. We sorted the annual tree-ring index values for each chronology to ascertain the narrowest 5% of years as we did earlier with the HI5 chronology. A total of 204 Yamal *L. sibirica* minima years were identified (2067 BC–AD 1996) and compared with 141 HI5 minima years; 250 Finnish *P. sylvestris* (3000 BC–AD 2004) minima years were identified and compared with the 165 HI5 minima years identified over that same period.

The correspondence between the minima series was tested with two techniques to determine statistical significance: joint probability (described above)

and Monte Carlo simulation. The effects of some volcanoes may take a couple of years to impact around the globe. With the Monte Carlo technique we expanded the analysis to allow for significance tests of not only "direct hit" matches, but also matches between ring-width minima years with an uncertainty range of ±1 year (3-year window) and ±2 years (5-year window). In the simulation an ARMA (1, 1) model was fit to the HI5 time series (truncated at AD 1900), and 1,000 synthetic time series conforming to this model were created. The 'dates' of the N smallest values of each of these synthetic time series were compared with those for marker years in the GISP2, Finland tree-ring and Yamal tree-ring time series, and the following recorded – direct matches, matches within a 3-year window centered on a year with one of the N smallest rings in HI5, and matches within a 5-year window of this. From the number of matches obtained in the Monte Carlo analyses it was possible to calculate 1-tailed critical values for the 95% and 99% probability levels.

3 Results

Many of the narrowest years in the HI5 chronology coincide with known large explosive volcanic eruptions and/or ice core signals of past eruptions (Table 2). If these were spread out evenly across the length of the record it would equate to one event every 30.3 years. The inclusion of frost-rings increases the pool of event years to 264 out of 5,000 or one every 18.9 years.

The expected frequency of joint occurrences of events in two random independent series is equal to the product of their individual probabilities. Joint occurrences between ring-with minima and GISP2 volcanic signals would be expected with a frequency of 0.0011, or 5.5 times over 5,000 years. The observed number of joint occurrences of over this time is 16 (years underlined in Table 2), almost three times that expected by chance (x^2=20.05, p<0.0001). With the Monte Carlo simulation technique, the 16 joint occurrences between the HI5 and GISP2 were also found to be significant (p<0.01).

When using the expanded ice-core data set and the longer temporal window the agreement is high between the HI5 tree-ring data and volcano/ice-core data over the last millennium. Ring-width minima years can be matched with known volcanoes or ice-core volcanic signals in 44 of 51 cases (86%) (ice-core signals ±5 years of ring-width minima, with many within 1 year). In previous millennia, although there are still many matches, the agreement decreases. While all matches between tree-ring characteristics and volcanic eruptions are tentative, the following well dated eruptions appear to be linked with decreased tree-ring width: Coseguina 1835; Tongkoko 1680; Gamkonora 1674; Parker/Komagatake 1641; Colima/Raul 1622; Unknown 1619; Huynaputina 1600; Kelut 1463; and Pele, 1459.

In all cases the correspondence between the HI5 chronology and the high latitude tree-ring time series is higher than would be expected by chance. Between Yamal *L. sibirica* and HI5 we found 13 exact matches. Joint probability expects only half that many by chance (x^2=4.87, p<0.05). With the Monte Carlo

Table 3 Results of Monte Carlo simulation comparing matches of HI5 ring-width minima to minima from high latitude tree-ring chronologies and ice-core signals over three different windows

	A. Direct hits	B. 3-year window		C. 5-year window					
Vs. Hi5	Actual	95%	99%	Actual	95%	99%	Actual	95%	99%
GISP 2	16	8	10	19	18.5	21	28	27	32
Finland	22	10	12.5	34	20	24	43	30	35
Yamal	13	9	11	26	20	20.5	35	29	34

Bold – actual greater than 99% critical value
Italic – actual greater than 95% critical value
The simulation was conducted for the following periods for the comparisons with GISP2, Finland and Yamal respectively:
GISP2 –3000 to 1900, N = 144 events (2.94%)
Finland – 3000 to 1900, N = 165 events (3.37%)
Yamal – 2067 to 1900, N = 141 events (3.55%)

technique the correspondence was significant ($p<0.01$) for direct hits, the 3-year window and the 5-year window (Table 3). Between Finnish *P. sylvestris* and HI5 we found 22 exact matches, whereas fewer than nine would be expected by chance ($x^2= 20.06$, $p<0.0001$) using joint probability. Higher than expected correspondence between Finnish pine and HI5 was also found using the Monte Carlo simulation ($p<0.01$) (Table 3).

4 Discussion and Conclusions

The results of the comparisons with ice cores indicates that the observed number of joint occurrences of upper forest border ring-width minima and volcanic signals in the GISP2 ice core is very unlikely to have arisen by chance and that there is some non-random association between major volcanic eruptions, as recorded in ice cores, and ring-width minima signals at the upper forest border. Lack of agreement between the tree rings and ice cores at any given time might be due to the differential impacts of atmospheric circulation following volcanism or simply forcings that differ between the southwestern USA and high latitudes. The pattern of diminishing agreement between the records in earlier millennia may be the result of more cool years forced by non-volcanic means in the first part of the record, but this decrease is more likely the result of fewer available ice-core records and decreased ice-core dating accuracy in the earlier time period. Thus, we suggest that the early years identified in the tree-ring data are strong candidates for previously undated or misdated eruptions.

There are many instances when extreme low growth occurred simultaneously at high altitude in the western USA and at high latitude on the Yamal Peninsula and/or Finnish Lapland. The correspondence of these years with potential ice-core signals and/or volcanic eruptions suggest years when events have influenced

hemispheric-scale climate and have caused severe growth suppressions of two different species of trees on two different continents (Salzer and Hughes 2007). Unlike the pattern of matches between HI5 minima and volcanic signals in ice cores, the number of matches between the HI5 minima and high-latitude minima does not display a pattern of diminishing agreement in previous millennia. This further supports our claim that the pattern of diminishing agreement between the ice-core and tree-ring records is the result of fewer available ice-core records and decreased ice-core dating accuracy in the earlier time period. The early years identified in the tree-ring data, particularly those in more than one tree-ring data set, are strong candidates for previously undated or misdated eruptions.

There is also some early historical evidence for large eruptions noted in the Mediterranean region that can be linked with tree-ring evidence for cool conditions in AD 627, 536, and 472 and in 44 BC (Stothers and Rampino 1983; Stothers 1984). There was some suggestion that the AD 536 dust-veil event might be the result of a comet impact (Baillie 1994); however, this event has now been linked with volcanism (Larsen et al. 2008). Recently, Baillie (2008), has questioned the attribution of dates by Larsen et al. (2008), in part by pointing out that their dates for eruptions would be consistent with the frost-ring dates we report for the sixth century AD (AD 522, 532, 536, 541 and 574) and several other lines of evidence if shifted forward by 7 years, rather than the 4.5–5 years shift they adopted. The AD 536–547 environmental disruption has been observed in multiple proxies and has been characterized as a widespread catastrophic event (D'Arrigo et al. 2001).

The well known eruptions of Laki in 1783, Tambora in 1815, and the Alaskan eruption of Katmai in 1912, were not identified by this tree-ring technique. Although there was substantial ring-width decrease following the eruptions of Tambora and Katmai, the decline was not enough to include those years in the narrowest 5% of years. There is also no ring-width minimum signal from the 1883 Krakatoa eruption, despite a frost-damaged ring in 1884. This suggests that Krakatoa may have erupted during a period when the volcanic forcing of the climate system was not sufficient to adversely impact ring-width.

We have established a temporal association between narrow growth rings in subalpine pines and large explosive volcanic eruptions as recorded in the historical volcano record and in polar ice cores. This association suggests that these eruptions produced mid-latitude warm-season cooling with potential effects across the northern hemisphere or globe. Of those years identified in the BC period (Table 2) there is especially strong evidence for climatically-effective eruptions in or just before 2906/2905, 2036, 1626, 1524, 476, 425/424, 421, 406, 245, and 42 BC. These growth-minima years can be matched with both ice-core signals of eruptions (ice-core signals ±5 years of ring-width minima) and with frost-damaged rings (frost rings ±1 year of minima). Similar circumstances supporting climatically-effective eruptions can be seen in or immediately preceding the following years AD: 536, 627, 687/688, 691–695, 899/900, 1201, 1288, 1458, 1602, 1641, and 1681. Additional support for many of these past volcanic eruptions is provided by decreased tree-ring growth in years both at upper forest border in western North America and at high latitude in Eurasia and/or Fennoscandia.

In addition to the individual years that can be matched with volcanic eruptions, there is some evidence for extended periods of cooling. These low-growth intervals may be a result of several eruptions closely spaced in time, as appears to be the case in the mid-sixth, late-seventh, early tenth, mid-fifteenth, and seventeenth centuries AD. Intervals of low growth resulting from two or more eruptions are in agreement with prior suggestions that the effects on the climate system of multiple eruptions spaced within a short interval are cumulative, and thus the episode of volcanic influence increased (Robock 1978; Hammer et al. 1980; Porter 1986; Bradley 1988; Briffa et al. 1998) Alternatively, these low-growth periods could be the result of extended growth responses to single events. Eruptions that coincide with intervals when the climate system is sensitive, or the trees are particularly vulnerable to volcanic forcing might be expected to generate such sustained periods of low growth.

Our study has improved the volcanic chronology beyond what tree-rings and ice-cores alone could accomplish. Future research on volcanic histories could benefit from an extension of what we have done here. A synthesis of tree-ring, ice core, solar, geologic, archaeological, and historic records to inform scenarios of past volcanism, would help create a more accurate and complete volcanic chronology.

Acknowledgments This article is an abridged and slightly modified version of a paper previously published in Quaternary Research: (Salzer and Hughes 2007). It was supported by the National Science Foundation under Grant NSF-ATM 0213962 from the Earth System History program and by The Institute for Aegean Prehistory. We were also supported by the Laboratory of Tree-Ring Research at The University of Arizona. Mauri Timonen kindly made the Finnish data available in a convenient form. We appreciate the help of Thomas Harlan, Fenbiao Ni, Dave Meko, Rex Adams, Jim Parks, and Chris McPhee.

References

Ammann CM, Naveau P (2003) Statistical analysis of tropical explosive volcanism occurrences over the last 6 centuries. Geophys Res Lett 30:L16388

Baillie MGL (2008) Proposed re-dating of the European ice core chronology by seven years prior to the 7th century AD. Geophys Res Lett 35:L15813

Baillie MGL (1994) Dendrochronology raises questions about the nature of the AD 536 dust-veil event. Holocene 4:212–217

Bradley RS (1988) The explosive volcanic eruption signal in Northern Hemisphere continental temperature records. Clim Change 12:221–243

Briffa KR, Jones PD, Schweingruber FH, Osborn TJ (1998) Influence of volcanic eruptions on Northern Hemisphere summer temperature over the past 600 years. Nature 393:450–455

Budner D, Cole-Dai J (2003) The number and magnitude of explosive volcanic eruptions between 904 and 1865 AD: Quantitative evidence from a new South Pole ice core. In: A Robock and C Oppenheimer (eds) Volcanism and the earth's atmosphere. American Geophysical Union, Washington DC, pp 165–176

Clausen HB, Hammer CU, Hvidberg CS, Dahl-Jensen D, Steffensen JP, Kipfstuhl J, Legrand M (1997) A comparison of volcanic records over the past 4000 years from the Greenland Ice Core Project and Dye 3 Greenland ice cores. J Geophys Res 102:26707–26723

Cole-Dai J, Mosley-Thompson E, Thompson LG (1997) Annually resolved southern hemisphere volcanic history from two Antarctic ice cores. J Geophys Res 102:16761–16771

Cook ER (1985) A Time Series Approach to Tree-Ring Standardization. Ph.D. Dissertation Laboratory of Tree-Ring Research University of Arizona, Tucson: version 6.04P: http://www.ltrr.arizona.edu/software.html.

Cook ER, Briffa KR, Shiyatov S, Mazepa V (1990) Tree-ring standardization and growth-trend estimation. In: Cook ER, Kairiukstis LA (eds) Methods of dendrochronology: applications in the environmental sciences. International Institute for Applied Systems Analysis. Kluwer, Boston, pp 104–123

Cook ER, Briffa KR, Meko DM, Graybill DA, Funkhouser G (1995) The segment length curse in long tree-ring chronology development for paleoclimatic studies. Holocene 5: 229–235

Crowley TJ (2000) Causes of climate change over the past 1000 years. Science 289:270–277

Crowley TJ, Criste TA, Smith NR (1993) Reassessment of Crete (Greenland) ice core acidity/volcanism link to climate change. Geophys Res Lett 20:209–212

D'Arrigo R, Jacoby G, Frank D, Pederson N, Cook ER, Buckley B, Nachin B, Mijiddorj R, Dugarav C (2001) 1738 years of Mongolian temperature variability inferred from a tree-ring width chronology of Siberian Pine. Geophys Res Lett 28:543–546

Eronen M, Zetterberg P, Briffa KR, Lindholm M, Merilainen J, Timonen M (2002) The supra-long Scots pine tree-ring record for Finnish Lapland: Part 1, chronology construction and initial references. Holocene 12:673–680

Free M, Robock A (1999) Global warming in the context of the Little Ice Age. Geophys Res Lett 104:19057–19070

Fritts HC (1976) Tree-rings and climate. Academic Press, New York

Fritts HC (1991) Reconstructing large-scale climatic patterns from tree-ring data. University of Arizona Press, Tucson

Gu L, Baldocchi DB, Wofsy SC, Munger JW, Michalsky JJ, Urbanski SP, Boden TA (2003) Response of a deciduous forest to the Mt Pinatubo eruption: enhanced photosynthesis. Science 299:2035–2038

Hammer CU, Clausen HB, Dansgaard W (1980) Greenland ice sheet evidence of post-glacial volcanism and its climatic impact. Nature 288:230–235

Hantemirov RM, Shiyatov SG (2002) A continuous multimillennial ring-width chronology in Yamal, northwestern Siberia. Holocene 12:717–726

Helama S, Lindholm M, Timonen M, Meriläinen J, Eronen M (2002) The supra-long Scots pine tree-ring record for Finnish Lapland: Part 2, interannual to centennial variability in summer temperatures for 7500 years. Holocene 12:681–687

Holmes RL (1983) Computer-assisted quality control in tree-ring dating and measuring. Tree-Ring Bulletin 43:69-78. Version 6.06P: http://www.ltrr.arizona.edu/software.html.

Hughes MK, Vaganov EA, Shiyatov S, Touchan R, Funkhouser G (1999) Twentieth-century summer warmth in northern Yakutia in a 600 year context. Holocene 9:603–608

Jones PD, Briffa KR, Schweingruber FH (1995) Tree-ring evidence of the widespread effects of explosive volcanic eruptions. Geophys Res Lett 22:1333–1336

Kelly PM, Jones PD, Pengqun J (1996) The spatial response of the climate system to explosive volcanic eruptions. Int J Climatol 16:537–550

Lacis A, Hansen J, Sato M (1992) Climate forcing by stratospheric aerosols. Geophys Res Lett 19:1607–1610

LaMarche VC Jr (1974) Paleoclimatic inferences from long tree-ring records. Science 183:1043–1048

LaMarche VC Jr, Stockton CW (1974) Chronologies from temperature-sensitive bristlecone pines at upper treeline in western United States. Tree-Ring Bull 34:21–45

LaMarche VC Jr, Hirschboeck KK (1984) Frost rings in trees as records of major volcanic eruptions. Nature 307:121–126

Langway CC, Osada K, Clausen HB, Hammer CU, Shoji H (1995) A 10-century comparison of prominent bipolar volcanic events in ice cores. J Geophys Res 100:16241–16247

Larsen LB et al (2008) New ice core evidence for a volcanic cause of the A.D. 536 dust veil. Geophys Res Lett 35:L04708

Mann ME, Bradley RS, Hughes MK (1998) Global-scale temperature patterns and climate forcing over the past six centuries. Nature 392:779–787

McMormick MP, Thomason LW, Trepte CR (1995) Atmospheric effects of the Mount Pinatubo eruption. Nature 373:399–404

Minnis P, Harrison EF, Stowe LL, Gibson GG, Denn FM, Doelling DR, Smith WL Jr (1993) Radiative climate forcing by the Mount Pinatubo eruption. Science 259:1411–1415

Osborn TJ, Briffa KR, Jones PD (1997) Adjusting variance for sample size in tree-ring chronologies and other regional-mean timeseries. Dendrochronologia 15:89–99

Porter SC (1986) Pattern and forcing of Northern Hemisphere glacier variations during the last millennium. Quat Res 26:27–48

Rampino MR, Self S (1982) Historic eruptions of Tambora (1815), Krakatau (1883), and Agung (1963), their stratospheric aerosols, and climatic impact. Quat Res 18:127–143

Robock A (1978) Internally and externally caused climate change. J Atm Sci 35:1111–1122

Robock A, Free MP (1996) The volcanic record in ice cores for the past 2000 years. In: Jones PD, Bradley RS, Jouzel J (eds) Climatic variations and forcing mechanisms of the last 2000 years. Springer, New York, pp 533–546

Robock A, Mao J (1992) Winter warming from large volcanic eruptions. Geophys Res Lett 19:2405–2408

Salzer MW, Kipfmueller KF (2005) Reconstructed temperature and precipitation on a millennial timescale from tree-rings in the southern Colorado Plateau, USA. Clim Change 70:465–487

Salzer MW, Hughes MK (2007) Bristlecone pine tree rings and volcanic eruptions over the last 5000 yr. Quat Res 67:57–68

Scuderi LA (1990) Tree-ring evidence for climatically effective volcanic eruptions. Quat Res 34:67–85

Scuderi LA (1992) Climatically effective volcanism. Quat Res 37:130–135

Shindell D, Schmidt GA, Mann ME, Rind D, Waple A (2001) Solar forcing of regional climate change during the Maunder Minimum. Science 294:2149–2152

Shindell D, Schmidt GA, Miller RL, Mann ME (2003) Volcanic and solar forcing of climate change during the Preindustrial Era. J Clim 16:4094–4107

Stothers RB (1984) Mystery cloud of AD 536. Nature 307:344–345

Stothers RB, Rampino MR (1983) Volcanic eruptions in the Mediterranean before A.D. 630 from written and archaeological sources. J Geophys Res 88:6357–6371

Zielinski GA (1995) Stratospheric loading and optical depth estimates of explosive volcanism over the last 2100 years derived from the Greenland Ice Sheet Project 2 ice core. J Geophys Res 100:20937–20955

Zielinski GA, Mayewski PA, Meeker LD, Whitlow S, Twickler MS, Morrison M, Meese DA, Gow AJ, Alley RB (1994) Record of volcanism since 7000 B.C. from the GISP2 Greenland ice core and implications for the volcano-climate system. Science 264:948–952

Unknown Eruption of Shiveluch Volcano (Kamchatka, Russia) Around AD 1756 Identified by Dendrochronology

Olga Solomina

Shiveluch (N 56°38', E 161°19') is one of the most active volcanoes in Kamchatka. The eruptions of this volcano result in environmental damage caused by debris avalanches, hot pyroclastic flows, tephra falls and lahars. The last major eruption of Shiveluch occurred in 2005; it was accompanied by a pumice fall and a large pyroclastic flow.

According to tephrochronological data, one of the largest Shiveluch eruptions of the last millennium (SH_1) occurred ca 250+/–40 ^{14}C years BP (AD 1641(1652) 1663) (Braitseva et al. 1997; Ponomareva et al. 1998, 2007). This very large explosive eruption took place about 50 years earlier than the arrival of the first Russian cossacks in Kamchatka, explaining its absence from historical chronicles. The eruption produced pumice fall and voluminous ignimbrite more than 22 km long, and caused extensive debris flows (lahars) down all the valleys. Tephrochronologists identified the footprints of this eruption in many places on the southern flank of the volcano. However using tree ring analyses we found that the story was more complex. In fact there were two different eruptions separated by one century. They deposited very similar pyroclastic flow units.

In 2005 we found eight carbonized logs buried in a 2–10 m thick pyroclastic flow deposit recently exposed in an almost vertical outcrop in the Baidarnaia valley. They were in a standing position and clearly were killed and buried by the pyroclastic event and carbonized *in situ*. We cross-dated the logs against our regional larch (*Larix cajanderi*) chronology (KAM). The latest date of the outer rings, AD 1756 (Table 1), indicates the date of the eruption responsible for the pyroclastic flow emplacement that killed and buried these trees under fine-grained pyroclastic products. Although the bark was not preserved, we believe that no more than a very few rings could be lost due to rather smooth surface of the log. Other samples show similar, but slightly older dates (AD1752, AD1748, AD1741) and generally support the dating by these minimum age estimates. Three of the six dated trees indicate

O. Solomina (✉)
Institute of Geography, Department of Glaciology, Moscow, Russian Federation
e-mail: olgasolomina@yandex.ru

M. Stoffel et al. (eds.), *Tree Rings and Natural Hazards: A State-of-the-Art*,
Advances in Global Change Research 41, DOI 10.1007/978-90-481-8736-2_45,

Table 1 Cross-dated charcoal samples in Baidarnaia valley

Tree	Measured interval		Measured number of rings	Estimated additional outer rings	Inner year	Outer year
1a	1648	1683	36	~30	~1645	~1713
1b	1648	1680	33		~1645	
2a	1649	1707	59	~20-25	~1640	~1730
2b	1650	1686	37		~1640	
3	1697	1747	51	~5	~1680	~1752
6	1650	1688	39	~20	~1640	~1708
7a	1664	1738	75			
7b	1660	1737	78			
7c	1660	1756	97	0	1660	1756
8a	1671	1734	64	~10?	1668	1751
8b	1671	1738	68	~10?		

innermost ring dates varying from AD1640 to AD1645. These dates limit the age of previous eruptions (accompanied by pyroclastic flow) in the Baidarnaia valley. The oldest spruce tree found on the surface of this pyroclastic flow in the mixed forest (site SHE) dates back to AD1793. This allows 37 years for flow colonization by woody vegetation and therefore does not contradict the AD1756 deposition date.

Did this eruption leave any signature in the trees now growing on the slopes of the Shiveluch volcano? In fact, we found such evidence in the chronologies (SHI, PKAM) of mature larch trees growing in the Baidarnaia and Pravaia Kamenskaia valleys. These trees have survived many eruptions. If we compare these chronologies with one from an undisturbed site elsewhere in Kamchatka (KAM chronology) we will see that all chronologies agree well except for the period between AD1757 and 1763 when the Shiveluch chronologies (SHI, PKAM) demonstrate a very strong growth suppression (Fig. 1).

The question arises: does this finding mean that the age of the Sh-1 eruption should be re-assessed and did the eruption in fact happen a century later? Three burned trees buried *in situ* in the Kamenskaia valley pyroclastic flow, which looks very similar to the one in the Baidarnaya valley, show that the answer is negative. The buried samples yielded tentative tree-ring dates of AD1646, AD1649 and AD1649. As there is no bark preserved for these samples, these are only minimum dates. Due to the age limit of the reference chronology (AD1632–2005) and its short overlap with the sample chronology in the Kamenskaia valley, the dates of these deposits are very preliminary. This date is, however, in close agreement with the previously obtained radiocarbon date of these sediments to AD1641(1652)1663.

Despite the uncertainty of the tree-ring dating of the 17th century eruption, we determined through tree-ring analyses that the AD1756–1758 eruption that emplaced pyroclastic flows in the Baidarnaia valley was distinct from the canonic

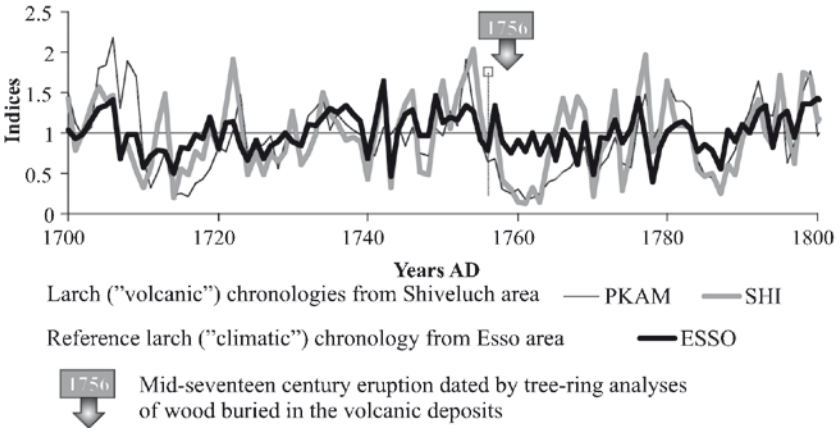

Fig. 1 Larch chronologies in Esso (non-volcanic region), Shiveluch. The deviation of Shiveluch chronologies in the Baidarnaia (SHI) and Kamenskaia (PKAM) valleys from the reference ESSO chronology in 1756(57)-1763 supports the tree-ring date (AD1756 or very shortly after this date) of the trees killed by pyroclastic flow in the Baidarnaia valley

Shiveluch 1, which occurred a century earlier. This information is important for estimating the cycles of Shiveluch volcanic activity and forecasting its future behavior.

References

Braitseva OA, Sulerzhitsky LD, Ponomareva VV, Melekestsev IV (1997) Geochronology of the greatest Holocene explosive eruptions in Kamchatka and their imprint on the Greenland glacier shield. Transactions (Doklady) of the Russian Academy of Sciences. Earth science sections 352(1):138–140 (in Russian)

Ponomareva VV, Pevzner MM, Melekestsev IV (1998) Large debris avalanches and associated eruptions in the Holocene eruptive history of Shiveluch volcano, Kamchatka Russia. Bull Volcanol 59:490–505 (in Russian)

Ponomareva VV, Kyle PR, Pevzner MM, Sulerzhitsky LD, Hartman M (2007) Holocene eruptive history of Shiveluch volcano, Kamchatka Peninsula. In: Eichelberger J, Gordeev E, Kasahara M, Izbekov P, Lees J (eds) Volcanism and tectonics of the Kamchatka Peninsula and adjacent arcs. Am Geophys Union, Geophysl Monogr Series 172:263–282

Late Eighteenth Century Old Maid Eruption and Lahars at Mount Hood, Oregon (USA) Dated with Tree Rings and Historical Observations

Patrick T. Pringle, Thomas C. Pierson, Kenneth A. Cameron, and Paul R. Sheppard

1 Introduction

Tree rings of subfossil trees buried by lahars and lahar-derived sediments along the Sandy and Zigzag Rivers record the onset of a late eighteenth century eruption at Mount Hood, Oregon, USA (Figs. 1–2). Crandell (1980) described and named this eruptive activity the 'Old Maid eruptive period' and estimated its age at about "200–300 year" using radiocarbon ages of trees killed by lahars. Cameron and Pringle (1986, 1987, 1991) used dendrochronology to constrain the major eruptive events to several decades in the late 1700s. Precise dating of the Old Maid eruption using tree rings, however, has been complicated by the inconsistent wood quality and scarcity of victim subfossil trees. A lack of nearby master chronologies, diverse physiography and microclimates of the region, and the generally low sensitreivity of local tree-ring series to climate variation also create problems with interpretation.

Mount Hood is a composite volcano about 75 km east of Portland, Oregon USA, and 35 km south of the Columbia River (Fig. 1). The Sandy River and its tributaries, the Zigzag and Salmon Rivers, drain much of the southwest flank of Mount Hood including the southwest-facing debris fan, which was largely formed about 1500 years ago when a partial flank collapse of the volcano was followed by repeated collapses of a growing lava dome (Crandell 1980; Cameron and Pringle 1987).

P.T. Pringle (✉)
Science Department, Centralia College, Centralia, WA 98531, USA
e-mail: ppringle@centralia.edu

T.C. Pierson
U.S. Geologic Survey, Cascades Volcano Observatory, Vancouver, WA 98683-9589, USA

K.A. Cameron
Milwaukie, OR 97267, USA

P.R. Sheppard
Laboratory of Tree-Ring Research, University of Arizona, Tucson, AZ 85721, USA

M. Stoffel et al. (eds.), *Tree Rings and Natural Hazards: A State-of-the-Art*,
Advances in Global Change Research 41, DOI 10.1007/978-90-481-8736-2_46,

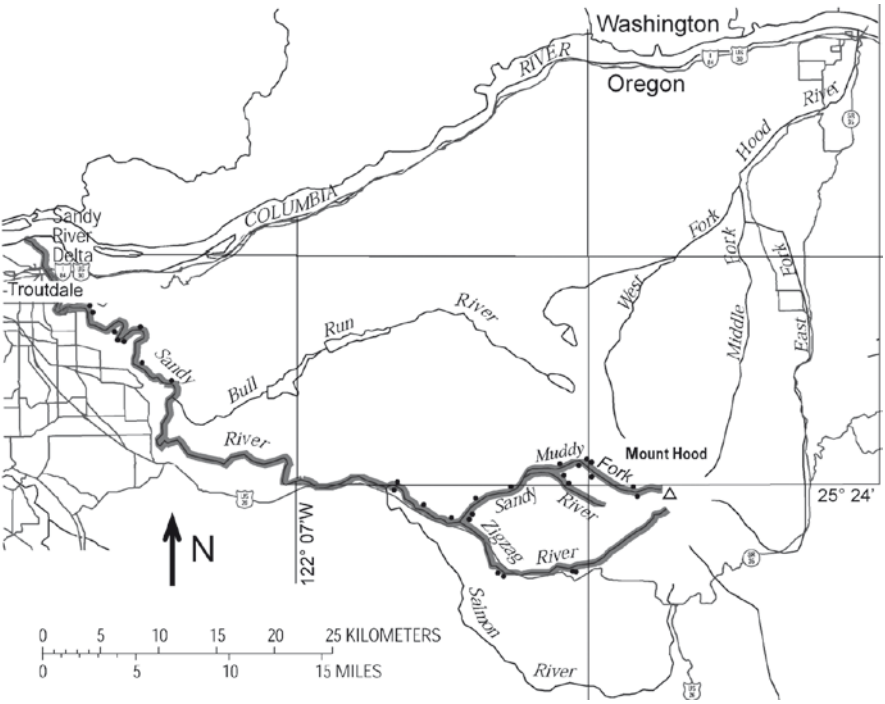

Fig. 1 Location map of the Mount Hood area in northwest Oregon USA. Small black dots show main locations of subfossil trees buried by lahars and lahar-derived sediments (*gray shading*) of the Old Maid eruptive period along the Sandy and Zigzag Rivers

Lawrence (1948) and Lawrence and Lawrence (1959) obtained the first radiocarbon ages for a buried tree and used dendrochronology in a "ghost forest" near treeline that they attributed to an eruption in about AD 1800 in which trees were killed by fallout of volcanic ash. Cameron and Pringle (1986, 1987, 1991) determined that the ghost forest trees had been scorched by a pyroclastic surge of Old Maid age in the upper White River, which drains the crater to the south and east.

Light rings are very consistent in upper-elevation Douglas-fir (*Pseudotsuga menziesii*) and western redcedar (*Thuja plicata*) trees across the region and have been therefore used to cross-date subfossil trees at Mount Rainier about 150 km to the north (Pringle 2008).

Cross-dating of two bark-bearing subfossil trees, one Douglas-fir and a western redcedar buried by lahars in the Sandy and Zigzag River valleys (460 and 1115 m a.s.l.) shows they died near the end of, or after the AD 1781 growing season but before the 1782 growing season (Pringle et al. 2002). Damaged survivor Douglas-firs along the south bank of the Sandy River at Old Maid Flat and near the mouth of Lost Creek (Fig. 2) show growth suppression starting in 1782 (and also 1791?) possibly owing to abrasion or burial trauma (Fig. 3). An abrupt growth release begins in both trees in 1801 probably because of the removal of competitors by lahars (Fig. 3).

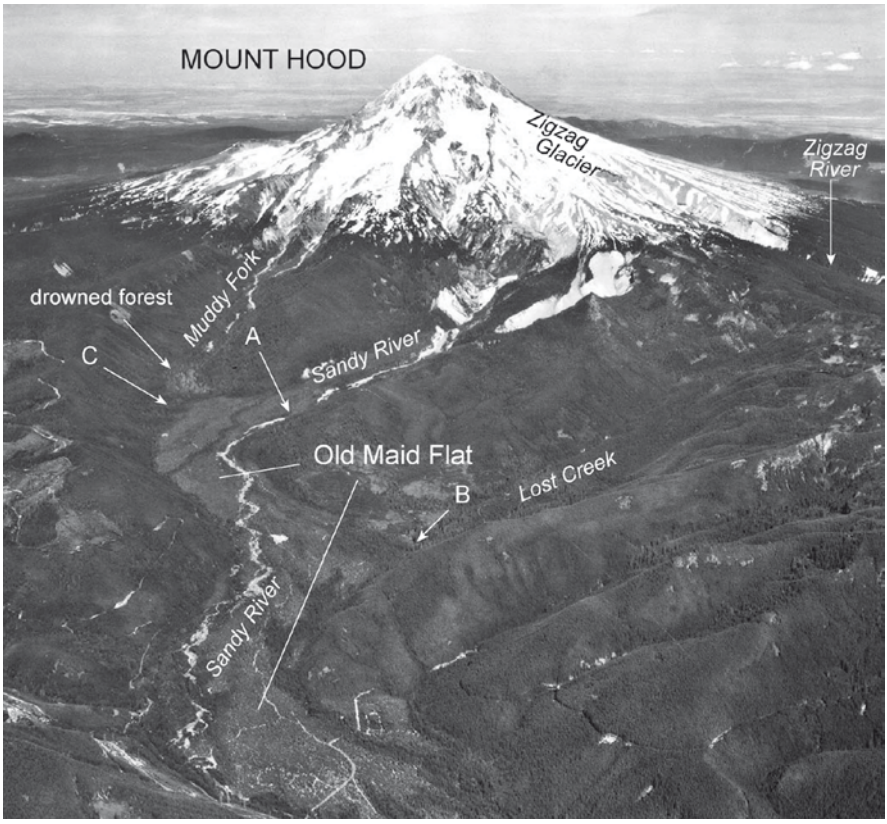

Fig. 2 Aerial-oblique photograph of Mount Hood and upper Sandy River valley at Old Maid Flat, which is veneered by lahar deposits of the Old Maid eruptive period from AD 1781–1801(?). Standing snags in Muddy Fork drainage were likely drowned by an ephemeral lake created by the lahar damming the river. Locations of subfossil trees are shown by arrows **A** and **B** (Fig. 3) and **c** (Fig. 4). US Geological Survey photo by Austin Post, 1980; view is to the east

The living tree along the south valley margin noted above (C in Fig. 2) shows a dense line of traumatic resin canals that cut the 1801 latewood and likely indicates severe cambial injury (Stoffel and Bollschweiler 2008), possibly from a lahar that occurred during that year. Cross-dating of a scarred western redcedar along the Muddy Fork of the Sandy River reveals missing rings and dramatically decreased growth for several years after 1787 (Figs. 2, 4). The tree evidently was damaged when a lake impounded by the 1781 lahar breached catastrophically.

Thus deposits and impacted trees in the upper reaches of the Sandy River record at least one post-1781 flood and significant lahar(s?) that impacted the "Quicksand River" before the arrival of Lewis and Clark in 1805. Dendrochemical evidence from living trees in areas that received Old Maid tephra fallout suggests that the Old Maid eruptive activity began in 1781 at least early enough to be detected in that annual growth ring (Sheppard et al. 2010, this volume).

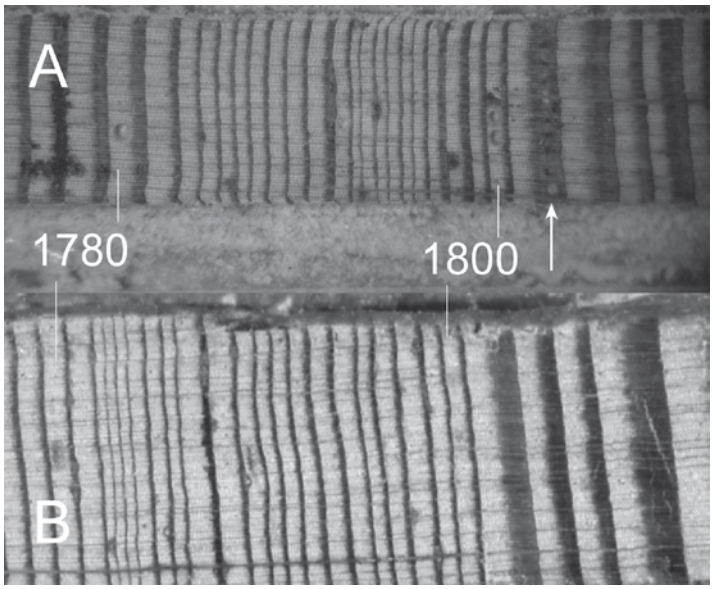

Fig. 3 Photomicrographs of tree rings from cores of two living Douglas-firs (**A**) along the valley margin of the Sandy River at Old Maid Flat and (**B**) at Lost Creek (Fig. 2) show the onset of a narrow ring sequence about 1782 and possibly again in 1791 and onset of larger rings in 1800. Note the dense line of traumatic resin canals (*arrow*) that cuts the latewood in 1801 in (**A**) and that likely indicates severe cambial injury (Stoffel and Bollschweiler 2008)

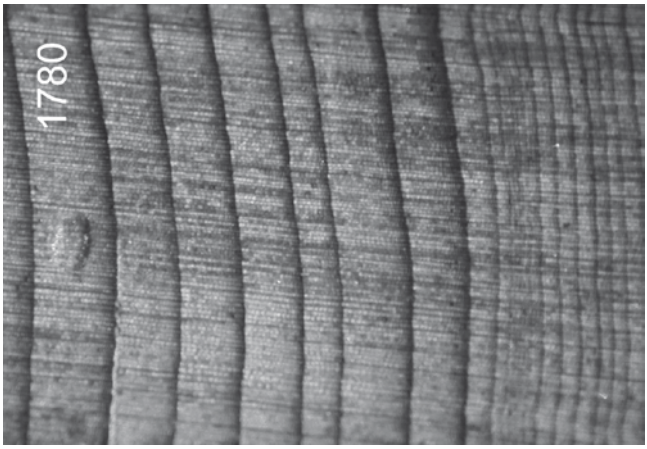

Fig. 4 Photomicrograph of rings in a living western redcedar adjacent to the channel of the Muddy Fork Sandy River (**C** in Fig. 2). This tributary was dammed by the initial Old Maid lahar, and the tree shown was scarred by breaching of the lahar-dammed lake about 7 years later. Note the response to scarring expressed as suppressed growth beginning in 1788

Our investigations using several dendrochronologic techniques show that the first major lahar of the Old Maid eruption (possibly the largest) originated from the upper southwest flank of Mount Hood, probably late in 1781 or early in 1782. A lahar-derived flood continued more than 80 km farther to the Columbia River extensively burying riparian forests. Narrow-, and large-ring sequences and traumatic resin canals in upper elevation trees that survived the 1781 Old Maid lahar record responses to geomorphic and/or eruptive events over the next 2 decades to 1800 and possibly 1801, within 5 years of the Lewis and Clark visits in 1805–1806. The explorers' accounts of the "Quicksand River" aptly describe how such a volcanic disturbance must have looked, based on the great thickness of sediment that aggraded following onset of volcanic activity.

Acknowledgments In 1997, Blythe Underwood Creek, an amateur geologist, found additional buried trees, including a key bark-bearing western redcedar snag, and assisted us in sampling these.

References

Cameron KA, Pringle PT (1986) Postglacial lahars of the Sandy River basin, Mount Hood, Oregon. Northwest Sci 60(4):225–237

Cameron KA, Pringle PT (1987) A detailed chronology of the most recent major eruptive period at Mount Hood, Oregon. Geol Soc Am Bull 99(6):845–851

Cameron KA, Pringle PT (1991) Prehistoric buried forests of Mount Hood. Oregon Geol 53(2):34–41

Crandell DR (1980) Recent eruptive history of Mount Hood, Oregon, and potential hazards from future eruptions. US Geol Surv Bull 1492, p 81

Lawrence DB (1948) Mount Hood's latest eruption and glacier advances. Mazama 30(13):22–29

Lawrence DB, Lawrence EG (1959) Radiocarbon dating of some events on Mount Hood and Mount St Helens. Mazama 41(13):10–18

Pringle PT (2008) Roadside geology of Mount Rainier National Park and vicinity. Washington Division of Geology and Earth Resources Information Circular 107, p 191. [http://www.dnr.wa.gov/ResearchScience/Topics/GeologyPublicationsLibrary/Pages/pub_ic107.aspx]

Pringle PT, Pierson TC, Cameron KA (2002) A circa A.D. 1781 eruption and lahars at Mount Hood, Oregon—Evidence from tree-ring dating and from observations of Lewis and Clark in 1805-6. Geol Soc Am Abstr 34:6

Sheppard PR, Weaver R, Pringle PT, Kent A (2010) Dendrochemical evidence of the 1780s Old Maid eruption of Mount Hood, Oregon. In: Stoffel M, Bollschweiler M, Butler DR, Luckman BH (eds) Tree rings and natural hazards: A state-of-the-art. Springer, Berlin, Heidelberg, New York, this volume

Stoffel M, Bollschweiler M (2008) Tree-ring analysis in natural hazards research – an overview. Nat Haz Earth Syst Sci 8:187–202

Part XI
Overall Conclusion and Outlook

Multiple rockfall scars on stem surface of a freshly cut European larch (*Larix decidua*) tree, Swiss Alps (© M. Stoffel)

Whither Dendrogeomorphology?

Markus Stoffel, Michelle Bollschweiler, David R. Butler, and Brian H. Luckman

1 Introduction

The initial employment of tree rings in natural hazard studies was simply as a dating tool and rarely exploited other environmental information that could be derived from studies of ring-width variations and records of damage contained within the tree. However, these unique, annually resolved, tree-ring records preserve potentially valuable archives of past geomorphic events on timescales of decades to centuries. As many of these processes are significant natural hazards, understanding their distribution, timing and controls provides valuable information that can assist in the prediction, mitigation and defence against these hazards and their effects on society. This book has provided many illustrations of these themes, demonstrating the application of tree rings to studies of snow avalanches, rockfalls, landslides, debris flows, floods, earthquakes, wildfires and several other processes. Some of these papers are

M. Stoffel (✉) and M. Bollschweiler
Laboratory of Dendrogeomorphology, Institute of Geological Sciences, University of Bern, CH-3012 Bern, Switzerland
and
Chair for Climatic Change and Climate Impacts, Institute for Environmental Sciences, University of Geneva, CH-1227 Carouge-Geneva, Switzerland
e-mail: markus.stoffel@dendrolab.ch

D.R. Butler
Department of Geography, Texas State University-San Marcos, San Marcos, TX 78666-4616, USA

B.H. Luckman
Department of Geography, University of Western Ontario, London ON N6A 5 C2, Canada

M. Stoffel et al. (eds.), *Tree Rings and Natural Hazards: A State-of-the-Art*, Advances in Global Change Research 41, DOI 10.1007/978-90-481-8736-2_47,

"classic studies", others represent more recent applications using previously unpublished material. They illustrate the breadth and diverse applications of contemporary dendrogeomorphology and underline the growing potential to expand these studies, possibly leading to the establishment of a range of techniques and approaches that may become standard practice in the analysis of specific hazards. In this brief concluding chapter, we will identify some growing research needs and possible future applications for tree rings in natural hazard studies.

2 Need for Methodological Improvement of Existing Approaches

As in most fields of dendrogeomorphology, the application of tree rings in natural hazard research began with relatively simple dendrochronological investigations that largely involved increment ring counting, dating of individual events, or minimum age dating of disturbed surfaces (Alestalo 1971). Subsequently the importance of crossdating and verification has been recognized and studies have expanded to develop event–response–chronologies and other data for a variety of scales. One of the central problems with such chronologies involves sampling and replication. In dendroclimatology techniques have been developed to assess signal strength and the fidelity of the common signal as sample replication decreases back in time. In the building of event chronologies it is important to develop similar techniques and criteria that can be applied to assess the quality of these records. Two issues are apparent here, one is the selection of criteria to identify the events of interest from "noise", and the other is to provide reasonable estimates of the frequency of past events from a sample population that is increasingly censored as one goes back in time.

Many different processes can produce disturbance in tree-ring series and the problem is to identify and isolate the signal related to the process under study from other potential sources of disturbance. One significant approach is to develop measures such as the "tree-ring response index" suggested by Butler et al. (1987) to distinguish snow avalanche events from "noise" in the chronologies developed. This approach is applicable to processes with a strong spatial footprint such as floods or wildfires, and accurate dating of past occurrences can be done with reasonable confidence based on the temporal synchronicity of signals across samples. However, more studies are needed to determine threshold levels for the reconstruction of processes and phenomena which are point-based and cover limited areas where spatial replication of events is rarely possible. Rockfalls, for example, often occur as single or small-scale events with local rather than areal impacts, rendering a determination of frequencies problematic (Moya et al. 2010, this volume). One might therefore ask if the probability of a rockfall hitting ten 10-cm diameter trees is the same as hitting one 1-m diameter tree. We need more experimental studies focusing on point-based earth-surface processes and the reconstruction and analysis of these hazards in greater detail.

We are fully aware that the nature of tree-ring approaches and the detail of results will probably continue to being dictated by the nature and geographical extent of the specific hazard under study. Nevertheless, we would like to see the development of more general guidelines about sampling strategies and sample depth in the way, for example, that dendroclimate studies have developed techniques for establishing signal strength in a chronology. Will it become possible to develop similar robust measures for dendrogeomorphic event chronologies that would allow for more solid statistical inferences to be made about future probabilities?

Similarly, future research should take account of process dynamics in time and space. Landslides, for example, are often singular events and their reconstruction is essentially retrospective. Other processes might be expected to recur on a regular (or irregular) basis at the same site and require a different sampling program more akin to continuous monitoring and prediction. The sampling goal here may be to estimate past frequency to determine hazard and hazard zoning. Several past studies have involved the development of frequency or magnitude data, without necessarily addressing problems of sampling (e.g. sample depth, spatial distribution of trees on the affected surface, etc.) or the representative nature of the analyses undertaken. In many cases with repeated hazard in a specific locality, the process under study may damage or remove the record of past activities, thus truncating or censoring the population available for sampling and "eliminating" the record of moderate and smaller events back in time. In such cases a risk exists that the observed frequencies can be biased: the full range of activity in the recent record is probably better preserved than for earlier periods. There is a need, therefore, for more fundamental research focusing on dating accuracy and uncertainty, magnitude–frequency relationships as well as for new ways of approaching and quantifying incompleteness of records.

3 Need for Fundamental Research on Tree Reactions to Geomorphic Disturbance

Besides the methodological problems originating from the nature of the different earth-surface processes and the clearing of forests by catastrophic events, dendrogeomorphic studies also face uncertainties resulting from biological and tree physiological causes. One of the more common problems in many dating studies is an inadequate estimate of the time taken for colonization of a disturbed surface (ecesis) and there is a clear need for more ecesis studies in different environments and dealing with different natural hazard processes. Other dating limitations are more related to the fact that – although ring series develop continuously – trees are not equally sensitive responders to geomorphic disturbance over their lifetimes. As a consequence, the response and likelihood of recording an event may vary over time – and may vary differently for different locations (i.e. trees) within the sampled network. In this sense, it appears trivial that tilting a younger tree is certainly easier than an older tree, but when does a tree become rigid enough to resist unilateral pressure? Uncertainties and limitations of this kind attain key relevance especially

when recurrence intervals or changes in frequency are assessed over time based on observing systems that may have differential responses over time. We therefore need experimental research to determine the optimal size and age (or range of ages) for sampling different species. Is it necessary perhaps to specify a restricted size range of "sample responders" to avoid compromising our results?

The classic dendrogeomorphic work has usually been based on conifers but there is excellent scope and need for the development of studies using deciduous and perhaps tropical species. Research performed with new species or parts of trees (e.g. roots, branches) needs to go beyond simple ring counting and has to include more rigorous statistical comparisons of ring chronologies or event–response replications to avoid spurious errors. The dendrogeomorphic research community should focus on wood anatomy and explicitly look for and exploit new lines of physiological evidence from tree rings. First results on wood-anatomical changes following flooding exist for several broad-leaved species (e.g., Astrade and Bégin 1997; St. George and Nielsen 2003; Tardif et al. 2010, this volume), and future research should continue to investigate these research lines, including more tree species as well as shrubs or perennial herbs. The effects of wounding and the subsequent formation of tangential rows of traumatic resin ducts (TRD) have been analyzed for *Larix decidua* and *Picea abies* (Bollschweiler et al. 2008; Stoffel and Hitz 2008; Schneuwly et al. 2009a, b) following debris-flow, rockfall or snow avalanche activity. More fundamental studies are needed to understand which other, non-European species produce TRD as a result of geomorphic activity, and how TRD intensity, and distribution vary in species and in response to different earth-surface processes. A better understanding of tree reactions following geomorphic activity will facilitate identification of responses in tree-ring series and avoid abundant destructive sampling in the future.

4 Development and Application of New Tree-Ring Based Approaches

There are many unresolved questions relating to the response of trees to disturbance by geomorphic processes. For example, we still do not know whether the intensity of an impact or the duration of an event will influence the nature and intensity of the reaction: What is the lag between an event and the evidence of reaction to that event that is visible in the tree ring? Does response time differ for different types of responses (e.g. reaction wood, TRD) or differ between tree species? Geomorphologists and natural hazard specialists are usually not wood anatomists or biologists. More, preferably collaborative research is needed with tree phytologists and physiologists to improve understanding of how bio-chemical agents initiate tree response to disturbance and how and when the actual formation of reaction wood, flood rings or TRD become visible in the tree ring and for what reasons. This extra knowledge could be very beneficial to improve intra-ring dating and seasonal dating accuracy. New insights could be generated relatively easily through artificially inflicting wounds, burial of stems,

root exposure or destabilization (tilting) of trees. Alternatively, it would be feasible to analyze trees that have been damaged during well documented events in the past (Bollschweiler et al. 2008; Ballesteros et al. 2010; Kaczka et al. 2010, this volume).

We also call for the experimental investigation of additional, alternative "dendrogeomorphic" techniques in natural hazard research. Several promising approaches have been illustrated in this book. For example, dendrochemical analyses have been shown to be a promising tool for the analysis of past volcanic activity (Sheppard et al. 2010, this volume) and progress could be made in paleo-hurricane dating through the study of oxygen isotope ratios of tree-ring α-cellulose (Gentry et al. 2010, this volume; Grissino-Mayer et al. 2010, this volume). Further future progress could be expected through the use of densitometric, resistograph (Lopez et al. 2010) or computer tomography (CT) analyses in dendrogeomorphic research, mainly for the identification of tension wood in broadleaved trees or the identification of hidden injuries in cross sections.

5 New Thematic and Geographic Fields

The vast majority of hazard-related, dendrogeomorphic research has focused on snow avalanches, landslides, flooding, debris flows and wildfires. In this book, we have demonstrated the application of tree-ring studies to other processes e.g., rock-falls or volcanic lahars. Additional processes have been analyzed only occasionally using dendrogeomorphic methods and we see potential for more tree-ring based studies of glacier-lake outburst floods, ice avalanches, thermokarst phenomena (e.g. Burn and Friele 1989; Burn and Smith 1988), pyroclastic flows, movements of and processes from rock-glacier bodies (Shroder 1978; Bachrach et al. 2004), flash floods (Ruiz-Villanueva et al. 2010) or strong winds (Hamilton 2005). In addition, dendrogeomorphic analyses have largely focused on mountain regions in general and the North American cordillera and European Alps in particular. We therefore call for more dendrogeomorphic research in Latin America, the Indian subcontinent, Africa, Northern and Eastern Europe or Russia.

6 Application of Tree-Ring Data in Other Fields

In addition to the simple reconstruction of event chronologies or magnitude–frequency relationships of natural hazard processes, efforts should be made towards a better understanding of climatic triggers and endogenic causes of hazardous processes and related disasters (Solomina 2002).

Most tree-ring analyses of natural hazards have primarily focused on isolated case studies, e.g. on debris flows at specific sites, and/or the demonstration of the utility and potential of the techniques. Single site studies are important but, in some cases, a regional study may be more significant. In an alpine valley, the recurrence

interval of debris flows at a particular site may be about once every 20–40 years. However the entire valley may have several potential sites with different histories and patterns of flow activity (Bollschweiler and Stoffel, 2007, 2010). Although the occurrence of a debris flow is difficult to be predicted at any specific site, studies from a site network might demonstrate with greater confidence that there will be a debris flow somewhere in the valley every 3–5 years (although we cannot specifically say where). Such information might be particularly useful in deciding whether it would be practical to put in place a regional emergency response system to deal with events likely to occur once in three years, rather than having to initiate a new response every time there is a debris flow.

In this sense, and particularly for mountain areas, we call for the establishment and comparison of regional or supra-regional event chronologies and for the development of databases for natural hazards similar to those existing in dendroclimatology. Perhaps some of our unique event chronologies could be archived in existing international data repositories, such as the Global Resources Information Database (GRID) of the United Nations Environmental Program (UNEP). In addition, there is also a need for our databases to be compared with (dendro-) climatological networks (Briffa et al. 1992, 2001) so as to better understand climate–natural hazard interactions.

Another promising approach is the use of tree-ring based data for an accuracy assessment or calibration of models of different geomorphic processes. Dendrogeomorphic data have been used sporadically in the past for the testing of rockfall (Stoffel et al. 2006), snow avalanche (Casteller et al. 2008) and debris-flow models (Graf et al. 2009) and results clearly pinpoint the high value-added to model verification and improvement with true field data.

One of the primary motivations for paleoclimate studies is the need to extend instrumental climate records to document climate variability at longer timescales and therefore better understand the present and model future climates. Examination of the past nature, occurrence and distribution of natural hazards using dendrogeomorphology fulfills a similar role. The evidence preserved in trees represents a unique source of information on many types of natural hazard. In many parts of the world it is the only available source of information to document changing process dynamics over time and space, and therefore a vital tool to showing the influence of past and current conditions on a range of natural hazards. It is hoped that the studies presented herein demonstrate the contribution that tree rings can make to these studies, advancing the case for their employment as an integral part of future studies of hazard assessment and management at suitable sites.

References

Alestalo J (1971) Dendrochronological interpretation of geomorphic processes. Fennia 105:1–139

Astrade L, Bégin Y (1997) Tree-ring response of *Populus tremula* L. and *Quercus robur* L. to recent spring floods of the Saône river, France. Ecoscience 4:232–239

Bachrach T, Jakobsen K, Kinney J, Nishimura P, Reyes A, Laroque CP, Smith DJ (2004) Dendrogeomorphological assessment of movement at Hilda rock glacier, Banff National Park, Canadian Rocky Mountains. Geogr Ann 86A:1–9

Ballesteros-Canovas JA, Stoffel M, Bodoque del Pozo JM, Bollschweiler M, Hitz OM, Diez-Herrero A (2010) Changes in wood anatomy in tree rings of Pinus pinaster Ait. following wounding by flash floods. Tree-Ring Res, in press

Bollschweiler M, Stoffel M (2010) Trends and changes in debris-flow frequency since 1850 – results from eight torrents in the Zermatt valley. Global Planet Change, in press

Bollschweiler M, Stoffel M (2007) Debris flows on forested cones – reconstruction and comparison of frequencies in two catchments in Val Ferret, Switzerland. Nat Haz Earth Syst Sci 7:207–218

Bollschweiler M, Stoffel M, Schneuwly DM, Bourqui K (2008) Traumatic resin ducts in *Larix decidua* trees impacted by debris flows. Tree Physiol 28:255–263

Briffa KR, Osborn TJ, Schweingruber FH, Harris IC, Jones PD, Shiyatov SG, Vaganov EA (2001) Low-frequency temperature variations from a northern tree ring density network. J Geophys Res 106:2929–2942

Briffa KR, Jones PD, Schweingruber FH (1992) Tree-Ring Density Reconstructions of Summer Temperature Patterns across Western North America since 1600. J Climatol 5(7):735–754

Burn CR, Friele PA (1989) Geomorphology, vegetational succession, soil characteristics and permafrost in retrogressive thaw slumps near Mayo, Yukon Territory. Arctic 33:31–40

Burn CR, Smith MW (1988) Thermokarst lakes at Mayo, Yukon Territory. Proc. 5th International Permafrost Conference, Trondheim, Tapir Publishers, Trondheim, pp 700–705

Butler DR, Malanson GM, Oelfke JG (1987) Tree-ring analysis and natural hazard chronologies: minimum sample sizes and index values. Prof Geogr 39:41–47

Casteller A, Christen M, Villalba R, Martínez H, Stöckli V, Leiva J, Bartelt P (2008) Validating numerical simulations of snow avalanches using dendrochronology: The Cerro Ventana event in Northern Patagonia, Argentina. Natural Hazards Earth Syst Sci 8:433–443

Gentry CM, Lewis D, Speer JH (2010) Dendroecology of hurricanes and the potential for isotopic reconstructions in Southeastern Texas. In: Stoffel M, Bollschweiler M, Butler DR, Luckman BH (eds) Tree rings and natural hazards: A state-of-the-art. Springer, Berlin, Heidelberg, New York, this volume

Graf C, Stoffel M, Grêt-Regamey A (2009) Enhancing debris flow modeling parameters integrating Bayesian networks. Geophys Res Abstr 11:10725

Grissino-Mayer HD, Miller DL, Mora CL (2010) Dendrotempestology and the Isotopic Record of Tropical Cyclones in Tree Rings of the Southeastern United States. In: Stoffel M, Bollschweiler M, Butler DR, Luckman BH (eds) Tree rings and natural hazards: A state-of-the-art. Springer, Berlin, Heidelberg, New York, this volume

Hamilton W (2005) Correlation of wind records and proxy wind history from tree rings at Port Angeles, Washington with sodium concentration at Summit, Greenland, and linkages with Gulf of Alaska sea level pressure forcing. Polar Geogr 29:253–290

Kaczka RJ, Deslauriers A, Morin H (2010) High-precision dating of debris-flow events within the growing season. In: Stoffel M, Bollschweiler M, Butler DR, Luckman BH (eds) Tree rings and natural hazards: A state-of-the-art. Springer, Berlin, Heidelberg, New York, this volume

Lopez Saez J, Corona C, Berger F, Stoffel M (2010) L'utilisation de la résistographie en dendrogéomorphologie: retour d'expériences. In: Astrade L, Miramont C (eds) Panorama de la dendrochronologie en France. Collection EDYTEM, Cahiers de Géographie, in press

Moya J, Corominas J, Pérez Arcas J (2010) Assessment of the rockfall frequency for hazard analysis at Solà d'Andorra (Eastern Pyrenees). In: Stoffel M, Bollschweiler M, Butler DR, Luckman BH (eds) Tree rings and natural hazards: A state-of-the-art. Springer, Berlin, Heidelberg, New York, this volume

Ruiz-Villanueva V, Díez-Herrero A, Stoffel M, Bollschweiler M, Bodoque JM, Ballesteros JA (2010) Dating flash flood events by means of dendrogeomorphic analysis in a small ungauged mountain catchment (Spanish Central System). Geomorphology, doi:10.1016/j.geomorph.2010.02.006

Schneuwly DM, Stoffel M, Bollschweiler M (2009a) Formation and spread of callus tissue and tangential rows of resin ducts in Larix decidua and Picea abies following rockfall impacts. Tree Physiol 29:281–289

Schneuwly DM, Stoffel M, Dorren LKA, Berger F (2009b) Three-dimensional analysis of the anatomical growth response of European conifers to mechanical disturbance. Tree Physiol 29:1247–1257

Sheppard PR, Weaver R, Pringle PT, Kent AJ (2010) Dendrochemical evidence of the 1781 eruption of Mount Hood, Oregon. In: Stoffel M, Bollschweiler M, Butler DR, Luckman BH (eds) Tree rings and natural hazards: A state-of-the-art. Springer, Berlin, Heidelberg, New York, this volume

Shroder JF (1978) Dendrogeomorphological analysis of mass movement on Table Cliffs Plateau, Utah. Quat Res 9:168–185

Solomina O (2002) Dendrogeomorphology: research requirements. Dendrochronologia 20:233–245

St. George S, Nielsen E (2003) Palaeoflood records for the Red River, Manitoba, Canada, derived from anatomical tree-ring signatures. Holocene 13:547–555

Stoffel M, Hitz OM (2008) Snow avalanche and rockfall impacts leave different anatomical signatures in tree rings of Larix decidua. Tree Physiol 28:1713–1720

Stoffel M, Wehrli A, Kühne R, Dorren LKA, Perret S, Kienholz H (2006) Assessing the protective effect of mountain forests using a 3D model. Forest Ecol Manage 225:113–122

Tardif J, Kames S, Bergeron Y (2010) Spring water levels reconstructed from ice-scarred trees and cross-sectional area of the earlywood vessels in tree rings from eastern boreal Canada. In: Stoffel M, Bollschweiler M, Butler DR, Luckman BH (eds) Tree rings and natural hazards. Springer, Berlin, Heidelberg, New York, this volume

ERRATUM

Chapter 40
Seismic Damage in Conifers from Olympic and Yellowstone Parks, United States

Wayne L. Hamilton

Erratum to: DOI 10.1007/978-90-481-8736-2_40

Page 437 paragraph 1, line 3, after-shocks, should read: fore- and after-shocks.

Page 437 paragraph 2, page 438 figure caption and page 439 paragraph 1, All dates are changed 22 years earlier, e.g., 1700 is changed to 1678.

The online version of the original chapter can be found under DOI 10.1007/978-90-481-8736-2_40

M. Stoffel et al. (eds.), *Tree Rings and Natural Hazards: A State-of-the-Art*, Advances in Global Change Research 41, DOI 10.1007/978-90-481-8736-2_48,

Index

M. Stoffel et al. (eds.), *Tree Rings and Natural Hazards: A State-of-the-Art*,
Advances in Global Change Research 41, DOI 10.1007/978-90-481-8736-2,